THE LITHOSTRATIGRAPHY
AND
PETROGENESIS
OF THE
ŃSUZE GROUP
NORTHWEST OF ŃKANDLA,
ŃATAL

by

Peter Bruce Groenewald.

Submitted in partial fulfilment of the requirements
for the degree of Master of Science in the
Department of Geology, University of Natal,
Pietermaritzburg, South Africa.

I, PETER BRUCE GROENEWALD, hereby declare that this thesis is my own original work, that all assistance and sources of information have been acknowledged, and that this work has not been presented to any other University for the purpose of a higher degree.

Groenewald
....

ABSTRACT

The volcanic and sedimentary Nsuze Group constitutes the lower part of the 3.0 Ga Pongola Supergroup which is exposed sporadically in southeastern Transvaal, Swaziland and northern Natal.

The pre-Nsuze basement in the area studied consists of the Nondweni Group, a typical Archaean volcanic and sedimentary sequence, and gneissic tonalite. This basement was deformed and denuded prior to deposition of the Nsuze Group which rests upon greenstones to the north and south of the study area and on tonalite in the east.

The 4 000 m thick Nsuze Group consists of five formational units. The lowest unit in the north of the study area, the Ndikwe Formation is a 1 200 m thick assemblage of sediments, pyroclastics and lavas. Turbidites, BIF and shallow marine siliciclastic sediments interdigitate with ash-flow and ash-fall tuffs. Rare, thin lava flows of basaltic andesite are also present. This sequence reflects a complex history of synchronous sedimentation and volcanism which is interpreted as precursory to the main development of the Nsuze depository.

This unit interdigitates with, or is overlain unconformably southwards by the Mdlelanga Formation, a thick ($\sim$ 1 200 m) sequence of arenaceous and argillaceous rock-types. Biogenic carbonates occur sporadically at the base of the unit. Debris flow deposits high up in the formation contain large blocks of locally derived quartz-arenite and smaller fragments of tuff and banded iron formation.

The Qudeni Formation, a 40 - 600 m thick sequence of andesites and basaltic andesites, overlies the lower two stratigraphic units, apparently conformably. This formation becomes significantly thinner north of its type area in the Nsuze River Valley. Lava flows are rarely recognizable and extensive silicification, chloritization and epidotization is present. Plagioclase

phenocrysts are commonly present in these lavas which are predominantly composed of tremolite, chlorite, untwinned albite and quartz.

Overlying this is the Vutshini Formation, a 600 - 1 000 m sequence of arenaceous and argillaceous sediments. These sediments are heterogeneous with alternations of argillites, ferruginous argillites and mature arenites on a variety of scales. Immature arenites occur in the basal and upper parts of the formation.

The overlying Ekombe Formation has a limited outcrop area with a residual thickness of only 60 m. It consists of andesitic lavas.

Preliminary sedimentological analysis of the Nsuze Group suggests that shallow marine sediments are dominant. Facies associations similar to those of intertidal prograding, transgressive tidal and proximal to distal shelf models are recognized. More rare are sequences ascribed to braided stream depositional environments. Palaeocurrent data indicate that flow towards the south and southeast was most common. A more distal setting than that observed elsewhere in the Nsuze Group is inferred.

The geochemistry of the Nsuze volcanics is as yet poorly understood because many of the samples analysed display aberrant chemistry as a result of pervasive alteration. In some cases this alteration is attributed to interaction with sea water soon after extrusion. Tholeiitic and calc-alkalic affinities are present, but the available data do not allow a more definite classification of the magma type. Major and trace element abundances differ slightly for the two volcanic units analysed. The data are inadequate for petrogenetic modelling of the volcanics.

Deformation of the Archaean sequences is dominated by tight to isoclinal folding possibly related to the 1 000 m Natal Thrust Front. An earlier folding event is recognized and a younger weak deformation is locally distinguishable.

Faulting associated with the dominant folding event produced crestal and wrench displacements. Younger block faulting of two generations is also present.

Metabasites are characterized by the presence of tremolite-chlorite-albite-clinozoisite/epidote. Biotite and muscovite co-exist in metapelites, an assemblage which is taken to indicate upper greenschist facies metamorphic conditions. More than one metamorphism cannot be discounted as early phyllonitic cleavages are present, and post-folding, unfoliated dykes also have greenschist facies mineral assemblages.

Numerous intrusions of mafic and ultramafic rock-types are present in the study area and include the pre-metamorphic sills of the Hlagothi Complex, and metapyroxenite and metagabbro dykes. The Hlagothi sills are conformable with the Nsuze Group which they intrude close to its stratigraphic base. The age of the complex is equivocal, but it does predate the main penetrative deformation. The form of the sills suggests intrusion at depths shallower than the inferred maximum thickness of the Nsuze Group. The sills consist of peridotites, pyroxenites, olivine gabbronorites and gabbros which define a threefold macro-layering of each body. Smaller-scale layering of olivine-rich and -poor lithologies occurs locally. The upper marginal rocks of the sills have a skeletal texture identical to the spinifex textures of extrusive komatiites. Geochemistry of the complex indicates that fractionation of olivine, orthopyroxene and clinopyroxene has occurred. Estimated bulk compositions derived from quench-textured marginal rocks are consistent with the inferred crystallization history of the body and, significantly, conform to criteria for the recognition of basaltic komatiites of the Barberton type. The composition is similar to spinifex-textured rock-types from the Nondweni Group in its type area.

Ultramafic units within the Nsuze Group appear to be locally transgressive and represent either intrusions or intersliced sheets of the pre-Nsuze basement. These bodies have chemical similarities to komatiites. If they represent intrusions, they provide further evidence of a post-Pongola resurgence of komatiitic magmatism. Other pre-tectonic intrusions show petrographic similarities to the complex, but there is little geochemical evidence for this.

Most of the area studied consists of Phanerozoic cover sequences. The Natal Group comprises conglomerates, immature arenites and argillites which locally attain thicknesses of 60 - 100 m. These are interpreted as alluvial fan deposits. Karoo Sequence sediments of the Dwyka and Ecca Groups are present. These are glaciogenic diamictites and sandstones, and pelagic argillites respectively. High ground in much of the area consists of post-Karoo dolerite in the form of 10 - 150 m thick sills of wide lateral extent.

CONTENTS

---oooooo---

CHAPTER 1

INTRODUCTION

1. General

The Archaean Pongola Supergroup occurs in isolated, but locally extensive exposures in northern Natal, southeastern Transvaal and southern Swaziland (Fig. 1.1). The Supergroup overlies granitoid basement and greenstones unconformably. It is commonly obscured by younger cover of the Natal Group and Karoo Sequence.

The Pongola sequence is subdivided into a lower, predominantly volcanic Nsuze Group and an upper, mostly sedimentary Mozaan Group. The type areas for these groups are in the extensive outcrops in the Vryheid - Piet Retief area. The Nsuze Group in this northern area consists of a lower volcanic-sedimentary unit 800 m thick, overlain by 7 500 m of volcanics which, in turn, are overlain by a volcaniclastic-sedimentary unit locally attaining a thickness of 600 m (Armstrong *et al.*, 1982). There is an upward transition from this unit into the Mozaan Group which comprises 3 000 m of alternating argillites and arenites with a subordinate, upper volcanic zone (Watchorn, 1978).

In the southern inliers of the Mhlatuze, Nsuze, Buffalo and White Mfolozi Rivers, the stratigraphy is somewhat different (Fig. 1.2). The Nsuze Group has a residual thickness of, at most, 4 500 m. It consists of alternating sedimentary and volcanic units with considerable lateral variations in thickness and lithology. The Mozaan Group is present only in the White Mfolozi inlier (Matthews, 1967), where it is lithostratigraphically similar to the type area described by Watchorn (1978). It is separated from the Nsuze Group by an angular unconformity inclined to the southeast. The Mozaan Group is not present in the inliers around Nkandla.

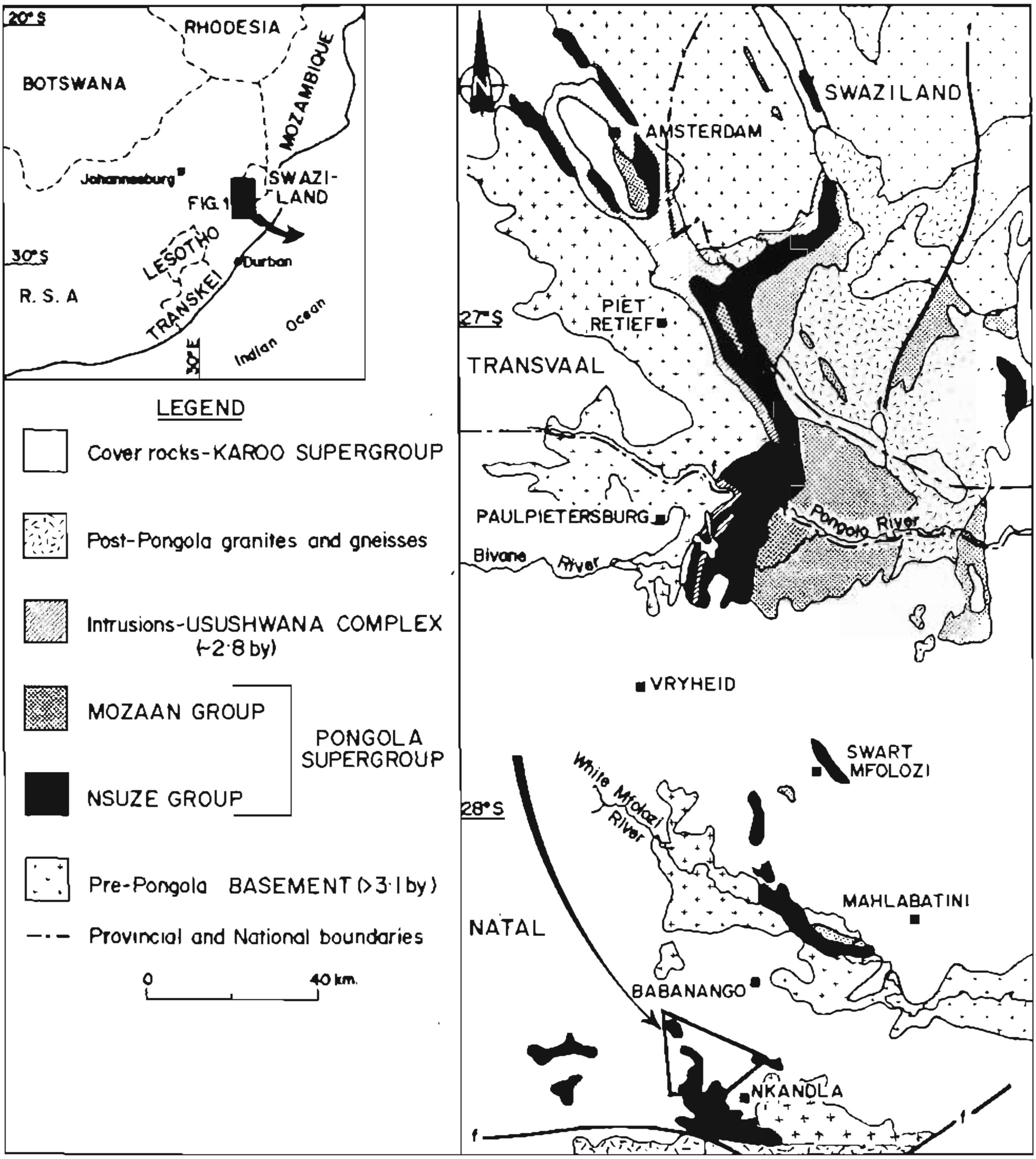

Figure 1.1 Locality map showing distribution of Pongola Supergroup inliers. Study area is indicated by the arrow in lower centre of map.

The present study is concerned with several inliers northwest of Nkandla (Fig. 1.2). The Nsuze Group in this area is exposed in two major synclines. These trend east-west with opposed plunges. The Central Nsuze Syncline plunges west, whereas the more northerly Gem Syncline plunges east. The intervening anticline has been disrupted by diabase intrusion and faulting. Discontinuous outcrop from the highest exposed stratigraphic level in the Vutshini Syncline to the inliers in the upper Mhlatuze Valley in the northeast of the study area provides a section through most of the stratigraphic thickness of the Nsuze Group. North of the Gem Syncline is an area of tight, small-scale folding. This peters out northwestwards in the headwaters of the Nsuze Valley. Here dips are consistently southwards, except where local deformation related to the intrusion of major gabbro sills has occurred.

2. Location and Extent of the Study Area

The study area is situated northwest of Nkandla and covers some 280 square kilometres (Map 1). Rocks of the Nsuze Group occur in several isolated windows in the Phanerozoic cover sequences which in total cover just over 30% of the area.

Access is by way of gravel roads between Nkandla, Qudeni, Fort Louis and Babanango. Minor tracks traverse the areas between the roads and may be negotiated to within easy walking distance of remoter parts of the area. The topography is generally rugged, with most of the outcrops in deeply-incised valleys. This is especially true in the southern part of the area where valleys 300 m deep have been incised. Fresh outcrop is most common in these actively eroding river valleys which provide good vertical and lateral sections through the rock sequences.

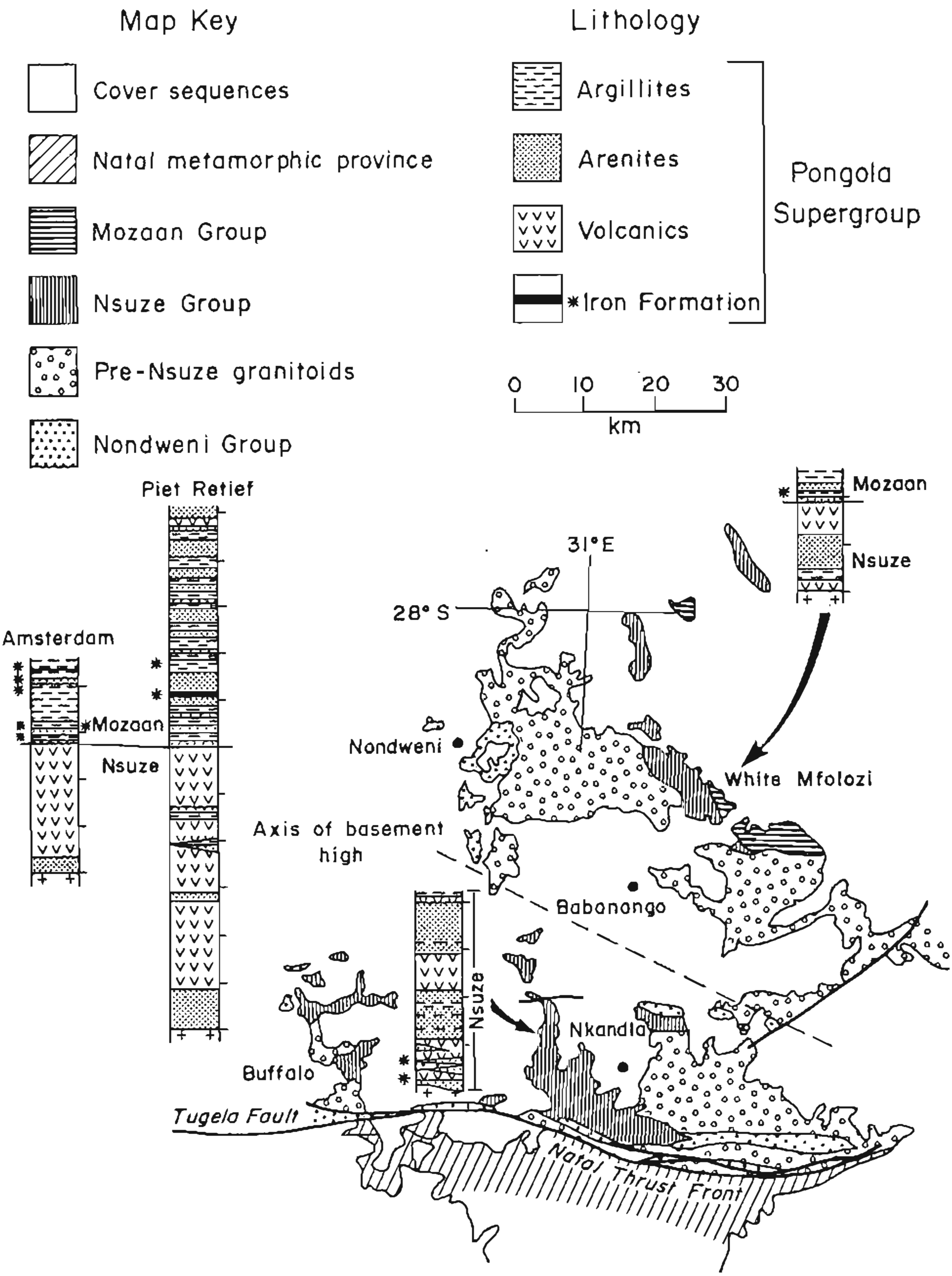

Figure 1.2 Distribution and stratigraphy of the southern part of the Pongola depository. Intervals of 1 000 m indicated on stratigraphic columns. (Modified after Matthews, 1967).

3. Objectives and Methods

This study is intended to establish the lithostratigraphy, depositional palaeoenvironment and petrogenesis of Nsuze Group sediments and volcanics in the southern part of the Pongola basin. The area is of particular interest in that no detailed work has been done since the pioneering mapping carried out by A.L. du Toit (1931).* Recognition of the antiquity of the sequence dates back to Hatch (1911) who used the name "Insuzi** Series", a term subsequently applied to the lower division of the Pongola Supergroup in other areas.

Mapping of the area was done directly onto 1 : 10 000 aerial photographs. Various marker horizons were identified and used to provide lateral correlation in areas of discontinuous outcrop. A formal stratigraphic subdivision was defined in an attempt to conform with the stratigraphy given by Matthews (1979, cited by SACS, 1980). Subdivision presented serious problems in that the area is complexly deformed and rapid lateral changes in thickness and lithology are characteristic of the Nsuze Group in this area.

Sedimentological analysis of measured sections was undertaken and this enabled identification of the dominant environments of deposition. Diagenetic and metamorphic effects have obscured primary sedimentary textures and structures in parts of the area. This has rendered very detailed sedimentological work impracticable.

The petrography of the volcanic rocks and various diabasic and layered gabbroic intrusions was studied. Fifty samples were analysed by X-ray fluorescence spectroscopy for eleven major and minor elements and thirteen trace elements. The trace elements are: Sc, V, Cr, Ni, Cu, Zn, Ba, Rb, Sr, Y, Nb, Zr and La. These data provide the basis for discussion of magma type, tectonic setting and petrogenesis. The analytical methodology is described in Appendix 4.

* This mapping was completed in 1918 but not published until 1931.

** The spelling of "Insuzi" has been changed to "Nsuze", SACS (1980) in order to conform with accepted usage in the vernacular language.

The effects of metamorphism on the rocks were investigated using petrographic sections. Although the age of the metamorphism is not precisely known, the pre- or post-metamorphic age of various intrusions was established petrographically. The deformational history of the area has been partly elucidated using numerous measurements of S surfaces. At least two folding events are discernible locally, but appear to be coaxial and indistinguishable on a regional scale. The age relationships of block faulting and thrusting were investigated where the exposures permitted this.

4. Previous Work

Previous work on the Nsuze Group inliers around Nkandla is limited to a few publications and the unpublished mapping of Matthews (1979). The emphasis thus far has been on elucidating the regional stratigraphy and structural geology; hence little is known about the detailed lithostratigraphy, sedimentology and deformational history of the area.

Du Toit (1931) proposed a six-fold subdivision of the Nsuze Group into alternating quartzite and volcanic units (Table 1.1). He proposed a correlation of these units with the lower Pongola series recognized by Humphreys (1912, p. 99) in the Vryheid - Utrecht area.

Matthews (1979, unpublished work cited in SACS, 1980) proposed a formal nine-fold subdivision of the group. The lower five formations (Table 1.1) correspond to the units of Du Toit (1931), whereas the upper four define a stratigraphy which is apparently unique to the Central Nsuze Syncline. Matthews (1979) could not correlate these units beyond the limits of this syncline due to shearing in the anticlines separating it from the adjacent structures.

TABLE 1.1: LITHOSTRATIGRAPHIC SUBDIVISIONS OF THE NSUZE GROUP

DU TOIT (1931)	MATTHEWS (1959)	MATTHEWS (1979)	THIS STUDY
6 Third volcanic (> 60 m)		9 Mankane (> 200 m)	
		8 Vutshini (1030 m)	
5 Central Nsuze Quartzite (650 m)			5 Ekombe (Msukane?) (> 60 m)
		7 Qudeni (580 m)	
4 Second volcanic (500 m)		6 Mdlelanga (1475 m)	
		TECTONIC CONTACT	4 Vutshini (1000 m)
3 Mdlelanga Quartzite (> 500 m)	NSELENI GRANITE	5 Msukane (1130 m)	3 Qudeni (750 m)
		4 Dlabe (1510 m)	
2 Lower volcanic (300 m)	3 Lower volcanic	3 Mome (1680 m)	
	2 Nomanci	2 Mabaleni---? (910 m)	1/2 Mdlelanga/Ndikwe (1200 m)
1 Nomanci Quartzite (200 m)	1 Nkandla	1 Hlathini---? (300 m)	
~~	UNCONFORMITY	~~~~~~~~	~~~~~~~~
NSELINI GRANITE		NSELINI GRANITE	NSELINI GRANITE
NKANDLA		NKANDLA	NKANDLA/NONDWENI
NONDWENI		NONDWENI	
MFONGOSI			

The relationship of the granitoids east of Nkandla to the Nsuze Group has been the subject of some dispute. Du Toit (1931, p. 53) considered two phases of intrusion to be present, one predating and the other postdating the Nsuze. Matthews (1959) found that all the granitoids postdated the Nsuze Group because they intrude what he considered to be the lowest sedimentary unit of the Nsuze Group. Subsequently (Matthews, 1979, cited SACS, 1980) correlated the sediments intruded by the granites with the Nondweni Group, and acknowledged a normal sedimentary contact between stratigraphically higher sediments and the granitoids, thus demonstrating that intrusion occurred prior to accumulation of the Nsuze sequence.

A series of mafic-ultramafic sills intrusive into the lower Nsuze sediments in the north of the area was recognized by Du Toit (1931). He named these intrusions the Hlagothi Complex in view of their lithological variability and substantial extent from the upper Mhlatuze Valley in the east to west of the Nsuze River, and possibly as far as the Buffalo River. No work has been done on the Hlagothi Complex since Du Toit's (1931) study.

5. Age and Chronostratigraphic Relationship of the Nsuze Group to the Archaean of southern Africa

Direct radiometric age determinations have not yet given a precise age for the Nsuze Group. An age of 3.090 ± 0.090 Ga (U-Pb) for lavas from the Nsuze River inlier was obtained by Burger and Coertze (1973), who considered the age reliable. Nsuze Group lavas from southwestern Swaziland give a Rb-Sr whole rock age of 2.900 ± 0.060 Ga (Allsopp, unpublished data, cited by Barton, 1983, p. 76). (All Rb-Sr ages have been recalculated using a decay constant of $1.42 \times 10^{-11} yr^{-1}$).

Near Amsterdam in the southeastern Transvaal the Pongola Supergroup rests unconformably on the Lochiel Granite which is dated at 3.028 ± 0.014 Ga (Rb-Sr whole rock) (Barton *et al.*, 1983). Pre-Nsuze Group granitoids in the

Vryheid - Piet Reitef area have yielded two ages, 3.160 ± 0.080 Ga (Allsopp, unpublished data, quoted in Burger and Coertze, 1973, p. 18; Rb-Sr whole rock) and 2.980 ± 0.070 Ga (Burger and Coertze, 1973; U-Pb). The maximum age of the Pongola Supergroup is thus close to ∿ 3.0 Ga.

A minimum age is provided by the Usushwana Complex which intrudes Pongola rocks in the northern outcrop areas. The complex has been dated at 2.813 ± 0.059 Ga (Rb-Sr whole rock, Davies *et al.*, 1970).

The Pongola Supergroup has considerable chronostratigraphic significance for the evolution of the Kaapvaal craton because it is different in every respect from typical Archaean sedimentary-volcanic assemblages emplaced synchronously, notably those of Zimbabwe (Hawkesworth *et al.*, 1979), North America (Peterman, 1979) and Australia (reviewed by Windley, 1977, p. 29). Most important is the evidence for accumulation of the Pongola sediments and volcanics in a stable, epicratonic environment at about 3.0 Ga.

CHAPTER 2

TECTONIC AND STRATIGRAPHIC FRAMEWORK

1. General

Diverse lithologies of various ages occur in and around the study area. Although this study is mainly concerned with the Nsuze Group, the regional tectonic and chronostratigraphic setting is considered an essential part of the study. The description which follows extends beyond the limits of the actual study area; where data sources have not been indicated the information is based on unpublished data accumulated by the writer in 1980-1981 during a mineral exploration project in the region. A simplified stratigraphic column is shown in Figure 2.1.

The regional geology is dominated by two tectonic features: (i) the thrust belt which defines the southern limit of the Kaapvaal craton and (ii) the basement high extending from east of Nkandla to Nondweni (Fig. 1.2).

Volcanics with intercalated sediments of the Nondweni Group occur as a discontinuous belt within the basement high. They have been intensely deformed, and were intruded by tonalitic granitoids prior to initiation of the Pongola depository. The Nsuze Group rests unconformably on the granite-greenstone terrane. The residual thickness of the group increases progressively southwards from the basement high. Individual units also increase in thickness in the same direction. The Nsuze sequence is terminated abruptly by the Natal Thrust Front, which marks the northern limit of the Natal high-grade metamorphic province. The north-verging imbricate thrusts of the Thrust Front reflect the orientation of the compressive forces responsible for deformation of the Nsuze Group. This major tectono-thermal event (∿ 1 000 Ma) obliterated most of the evidence of an early deformational history and resulted in tight to isoclinal folding of the Nsuze Group about east-west trending axes.

SUPERGROUP/ SEQUENCE	GROUP	FORMATION	INTRUSIONS
			Dolerite sills and dykes
	Ecca		
Karoo			
	Dwyka		
Cape (?)	Natal		
			Monzogabbros/Gabbros/ Syenites/Pyroxenites/ Diorite/Porphyry Hlagothi Complex
		Ekombe	
		Vutshini	
Pongola	Nsuze	Qudeni	
		Mdlelanga	
		Ndikwe	
			Gneissic Tonalite
	Nondweni		

Figure 2.1 Simplified stratigraphic sequence for the area northwest of Nkandla.

Much of the area is now overlain by the undeformed Phanerozoic Natal Group and Karoo Sequence. These sedimentary successions occupy a rugged palaeotopography which reflects pre-Natal downwarping to the southeast of the present Natal coastline (Hobday and von Brunn, 1979). Numerous post-Karoo dolerite sills are present in the area.

A prominent lineament strikes east-southeast across the northern part of the study area. This feature has been the locus of several episodes of intrusion, notably pre-metamorphic gabbros of the Hlagothi Complex, syn- or late-tectonic syenites and monzogabbros and post-Karoo dolerites. As is demonstrated in Chapter 7, the Hlagothi Complex is of basaltic komatiite composition possibly reflecting tapping of upper mantle sources by deep fracturing. Alkaline rocks are also characteristic of rift settings. Thus, a long-lived, deep-seated fracture or rift feature is probably present. However, the significance and implications of the lineament are not yet understood fully and considerable further work is required.

2. The Nondweni Group

The most extensive outcrops of this volcanic and sedimentary sequence lie in an arcuate belt of inliers north of the study area (Fig. 1.2). Another linear belt southeast of Nkandla has also been correlated with the Nondweni Group (Du Toit, 1931, p. 29). The name of the group is derived from the area surrounding Nondweni where the similarity of the succession to the Barberton Sequence was first recognized by Du Toit (1931).

The age of the group is not known with any degree of precision as direct radiometric age determinations have yet to be reported. It predates tonalitic basement which yields ages of 3.138 ± 0.038 Ga (U-Pb on zircons, A. Burger, pers. comm.) to 3.160 ± 0.080 Ga (Rb-Sr, Allsopp, unpublished data quoted by Burger and Coertze, 1973, p. 18).

A formal stratigraphic subdivision of the Nondweni Group has not yet been published. Work still in progress in the Nondweni area suggests that a substantial thickness of komatiites, basalts, rhyolites, cherts and clastic sediments is present (J.A. Versfeld, pers. comm., 1983).

Metamorphosed ultramafic rocks ascribed to the Nondweni Group are present at one locality in the study area. Field relations are equivocal, but there is other evidence to substantiate the correlation. The occurrence is situated in a structurally low, fault-controlled site close to the stratigraphic base of the Nsuze Group. In addition, the rocks may be defined as ultramafic komatiites (on chemical criteria), rock types which have not yet been reported from the Nsuze Group. Metamorphic textures and structural features of the rocks do not clarify the age relationships.

The exposure of the Nondweni Group rocks at the confluence of the Mdlelanga and Welendhlovu Rivers lies within the core of the anticline separating the Gem and Central Nsuze Synclines (Map 2). The dark greenish-grey, tremolite-talc-chlorite schists are highly sheared and their exact relationship to overlying Nsuze sediments cannot be established. This is due to the presence of a cross-cutting diabase dyke and to shearing at the interface between the schists and the quartzites (Fig. 2.2). Grain size within the schists is highly variable with tremolite laths ranging from barely discernible to several millimetres in length. The rock has a well-developed tectonic fabric. Planar zones of interlayered schists and secondary quartz demarcate faint changes in lithology and are thought to represent sheared primary bedding features, possibly flow top breccias. An irregular 1 m long amygdaloidal zone is present below one of these zones.

In thin section, the rock is seen to have variable composition and grain size (BG112, 122, 123, 124, Appendix 1). The minerals present are: tremolite (45 - 90%); chlorite (5 - 50%); and talc ($\sim$ 5%).

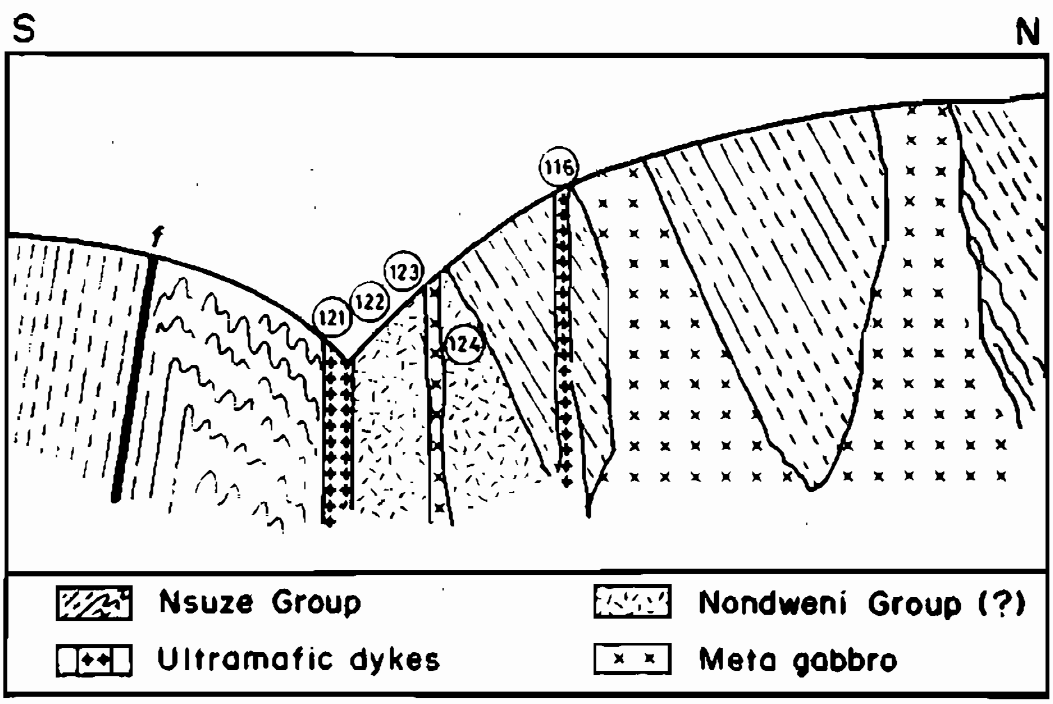

Figure 2.2 Schematic section through the area between the Gem and Central Nsuze Synclines at the confluence of the Welendhlovu and Mdlelanga Rivers. : Sample localities (cf. Chapter 6).

The tremolite laths, which occur as well-defined aggregates, have acicular, branching terminations (Fig. 2.3). These needles are commonly bent, rotated or kinked. Ragged flakes of chlorite are either evenly dispersed or concentrated in cleavage planes. This cleavage is crenulated, indicating more than one deformational event. Microfracturing of some tremolite laths also indicates that deformation has occurred after the main metamorphic event. Euhedral chrome-spinel is present locally, as are ragged patches of an opaque mineral, possible magnetite.

Another occurrence of ultramafic rocks is situated west of Ndikwe (Map 2). Here ultramafic schists have been caught up in the sole of a thrust fault and lie within the Nsuze sequence. The mineral assemblages in these schists range from talc-chlorite to talc-tremolite and talc-magnesite-tremolite.

Several analyses of the two ultramafic units were undertaken in order to assess the possibility that they are related to the Nsuze volcanics. This geochemistry is discussed in a later chapter, but it is worth noting that trace element data indicate similarities to the Nondweni rather than to the Nsuze volcanics.

3. Gneissic Tonalite

A small outcrop of gneissic tonalite is present in the upper reaches of the Mhlatuze River on the farm Driefontein 336 (Maps 1 and 4). Tonalitic gneisses are also present east of Nkandla(Matthews and Charlesworth, 1981).

In outcrop the tonalite is a pinkish-grey, medium-grained, foliated, leucocratic rock. In thin section the rock is seen to consist of 60% plagioclase, 26% quartz, 10% microcline, 3% chloritized biotite and 1% white mica (point count analysis). Trace amounts of chlorite, epidote, sphene and apatite are also present. The seriate, granular rock has very large, elongated quartz grains (4 - 8 mm long) which display minor strain-

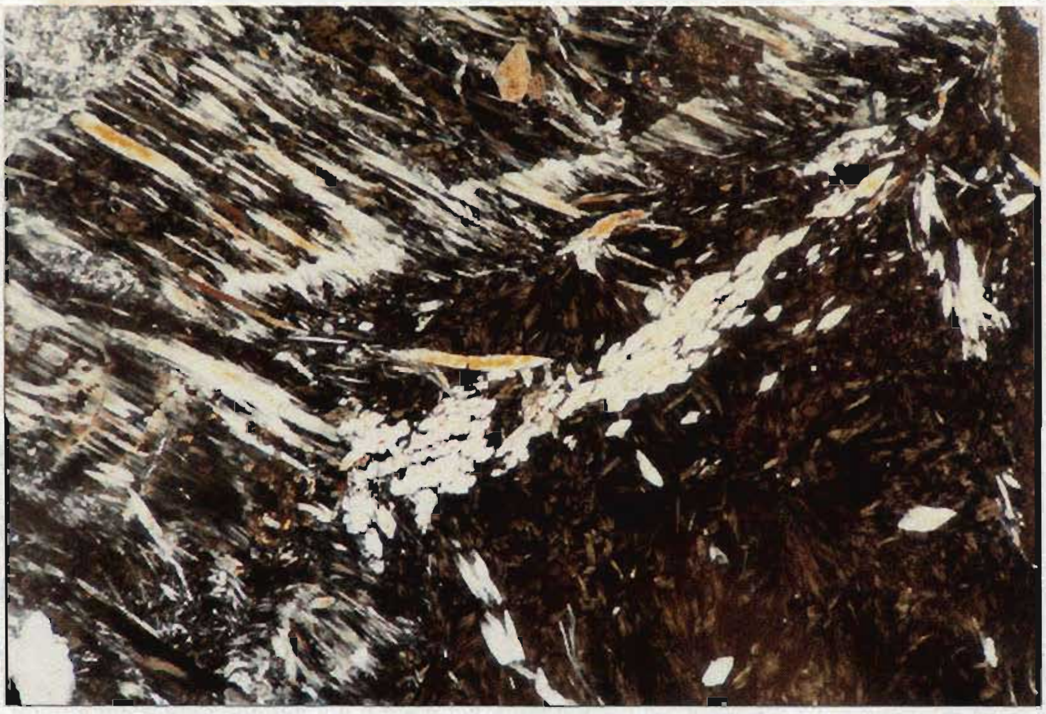

Figure 2.3 Photomicrograph of tremolite-chlorite schist from the Welendhlovu-Mdlelanga confluence (60x magnification).

Figure 2.4 Photomicrograph of tonalite form the Nkungumathe inlier. Note deformed quartz and large plagioclase primocrysts with smaller late plagioclase crystals along margins (centre right). Saussuritization of plagioclase is also visible (25x magnification).

induced wavy extinction. Large (3 - 4 mm) equant grains of oligoclase-andesine have abundant small grains of albite along their boundaries. This texture is reminiscent of a mortar texture that has been partly obscured by recrystallization (Fig. 2.4). It appears that the feldspar in the rock has undergone brittle deformation, whereas the quartz deformed ductilely. Small microcline grains are present interstitially. Myrmekitic texture is sparsely present in the plagioclase grains where they abut against microcline. Alteration is indicated by the chloritization of ragged patches of biotite and the extensive saussuritization of the larger plagioclase grains.

The tonalites are intrusive into the Nondweni Group east of Nkandla (Du Toit, 1931, p. 55) and contain large xenoliths of amphibolite southeast of the study area. They are overlain unconformably by the Nsuze Group, and in the exposure mentioned above, conglomerates of this group may be observed to occupy palaeochannels scoured in the underlying tonalite. Direct radiometric age determinations of the tonalitic gneisses have not yet been reported. However, Charlesworth and Matthews (1981, p. 34) cite a personal communication (T. Elworthy, E. Barton and R. Harmer) of preliminary Rb-Sr isochron data which indicate ages of 3.177 to 3.199 Ga for granitoids along the southern limit of the Kaapvaal craton.

4. The Nsuze Group

The Nsuze Group has been mapped in greater detail than the other units and its stratigraphy is the subject of a later chapter. The erection of a formal lithostratigraphy for the group poses problems in that it is structurally complex, has considerable lateral variability in thickness and lithology, and occurs in several discrete inliers. The stratigraphic subdivision proposed by Matthews (1979, cited SACS, 1980, p. 73) has been used, with the addition of one new formational name. The Nsuze Group is subdivided as follows:

(i) Ndikwe Formation: a sequence of intercalated volcaniclastic and epiclastic sediments up to 1 000 m thick, but wedging out southwards, at the base of the group. This formational unit has not previously been recognized.

(ii) Mdlelanga Formation: a 1 200 m thick unit of quartz wackes and quartz arenites at the base of the Nsuze Group. It attains maximum thickness in the south of the study area and wedges out or interfingers with the Ndikwe Formation to the north.

(iii) Qudeni Formation: a basaltic andesite, andesite and dacite unit overlying the lower two formations. It increases in thickness from 50 m in the north to 750 m in the south of the area.

(iv) Vutshini Formation: an argillaceous and arenaceous sedimentary unit 1 000 m thick.

(v) Ekombe Formation: this is stratigraphically the highest unit of the Nsuze Group in the study area and comprises at least 60 m of andesitic volcanics. It is present only in the core of the Vutshini Syncline. This unit was previously termed the Mankane Formation (Matthews, 1979, cited SACS, 1980).

5. The Natal Group

Sediments of the Natal group are exposed in the Mdlelanga, Nsuze and Mhlatuze River valleys. They overlie the Nsuze Group on a rugged palaeotopography which represents a major erosional episode. The Natal Group comprises, in order of abundance, conglomerates, arkosic arenites and argillites. Clasts in the conglomerates are predominantly boulder-size, but decrease in size upwards. The clasts are well-rounded to subrounded and reflect the lithology of the basement with Nsuze quartzite and vein quartz being the dominant clast types. Rare gneiss and jaspilite clasts are also present. The conglomerates display moderate to good sorting and are clast-supported. Clast imbrication indicates a southeastward palaeocurrent direction.

Arkosic sandstones overlie boulder conglomerates either gradationally in upward-fining sequences, or abruptly. These typically medium- or coarse-grained immature sediments contain rare mudstone intercalations. The mudstone units may occur as drapes over primary structures, as discrete layers or as a more regular interlayering with the arkose. Sedimentary structures are commonly obscured by weathering. Where present, the sedimentary structures observed are planar, angular based cross-stratification or trough cross-stratification.

Maroon, micaceous silty mudstones occur in the Mhlatuze and Mdlelanga River exposures (Map 1). At the former locality they overlie arkoses within palaeo-valleys and contain minor intercalations of arkosic sandstone. The mudstones extend beyond the limits of these valleys and rest directly on basement rocks to the north.

At the Mdlelanga locality mudstones appear to have accumulated prior to the deposition of boulder conglomerates which occupy an incised palaeovalley cut into the mudstones.

A synthesis of Natal Group sedimentology (Hobday and von Brunn, 1979) has demonstrated that the association of boulder conglomerates and arkosic sands most probably resulted from aggradation of a humid alluvial fan. These authors considered the high flow competence, evidenced by the clast size of the conglomerates, to have resulted from the confinement of flow in steep intermontane valleys. As aggradation occurred a more distal, braided stream environment became dominant. The maroon silts represent abandoned channel deposits, or perhaps suspension deposits resulting from waning high water episodes in areas removed from the aggrading fans.

The Natal Group sediments were correlated with the Table Mountain Group of the Cape Supergroup for many years (e.g. Du Toit, 1931). This correlation is no longer considered tenable, instead an approximate lateral time equivalence with either the Table Mountain or Witteberg groups is accepted (SACS, 1980).

6. The Karoo Sequence

Much of the higher ground in the study area is underlain by sediments of the Karoo Sequence. These are predominantly glaciogenic sediments of the Dwyka Group, with shales of the Ecca Group preserved in topographically higher areas.

(a) The Dwyka Formation

Glaciogenic sediments of the Dwyka Formation overlie all the older sequences unconformably. The presence of these sediments in areas up to 100 m below the general topographic level of the Nsuze Group rocks indicates that considerable pre-Dwyka incision occurred. The best exposures of these rocks occur in the upper reaches of the Mankane River and in a belt north of Itala Mountain in the valleys of the Gozweni and Nsuze Rivers (Map 1). At the first-mentioned locality, the lower part of the sequence consists of 20 m of blue tillite. The tillite has a clay-dominated matrix which supports scattered angular clasts up to 2 m in diameter. The clasts are mainly gneisses or granite with quartzite, chert, pyroxenite and jaspilite as less frequently observed compositions. Overlying the tillite is a thick unit (> 40 m) of diamictite. This is distinguished from the tillite by its darker colour and sandier nature. Clasts are generally smaller than those in the tillite. The diamictite is overlain by a fine-grained massive sandstone unit about 19 m thick. Sedimentary structures are not recognizable because this unit has ubiquitous leisegang banding. The sandstone is overlain by an unknown thickness of diamictite.

In the valley of the Nsuze River, immediately north of Hlagothi (Map 1) diamictites, identical to those described above, crop out in a palaeovalley more than 100 m deep. These deposits have a crude stratification indicating a pulsatory depositional mechanism (Fig. 2.5). Farther to the north, these diamictites are overlain by a massive sandstone unit. This is similar to that in the Mankane Valley described above. When traced eastwards along the

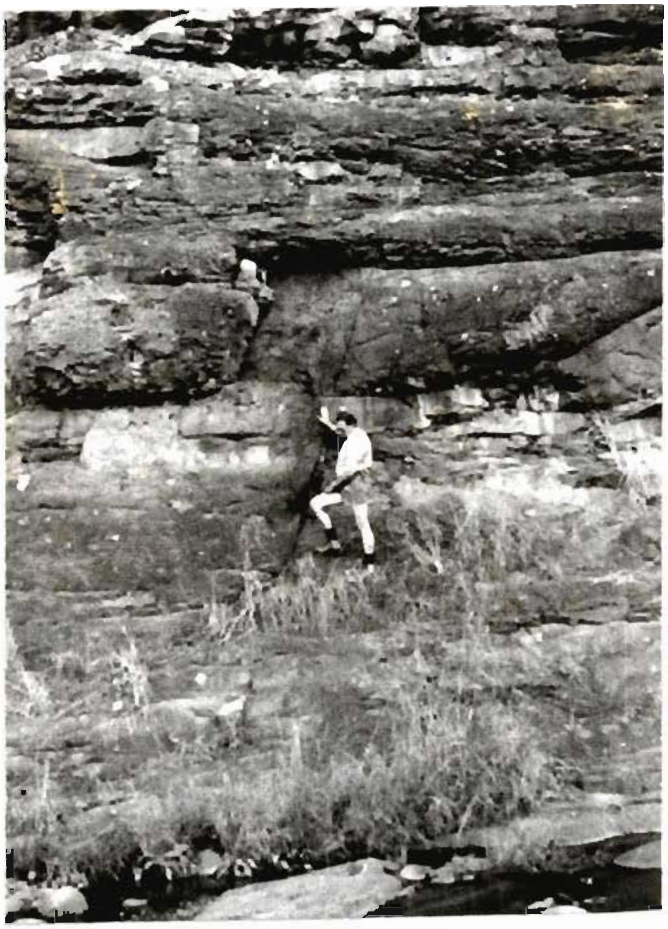

Figure 2.5 Crudely stratified diamictites in the Dwyka Group north of Hlagothi Mountain. These deposits are interpreted as debris flows.

flanks of Itala Mountain, the sandstone unit bifurcates. The lower sandstone is inclined southwards at 5° and may be traced for two kilometres south along the Mhlatuze River valley on the farm Riversmeet. The upper sandstone is horizontal. The two units are separated by a great wedge of diamictite.

The deposition of the Dwyka tillites and diamictites occurred in a glacially-dominated environment. After a period of erosion by southward-moving glaciers, the ice sheets receded, leaving behind basal tills in the deeper valleys. Debris deposited on the higher ground slumped down into the valleys as gravity flows. Periods of submergence also occurred as indicated by the presence of sandstone deposits. These processes may have been repeated, although the later ice sheets were probably not grounded. The diamictites filled the topographic depressions to form a virtually horizontal surface, on which sediments of the Ecca Group were deposited.

Nsuze Group outcrops at the base of the Dwyka Group reveal several glacial pavements. *Roche moutonées* are also recognizable at some localities. The direction of ice movement may be inferred from the striations which result from clasts embedded in the sole of the ice sheet scraping across the underlying rock. Several of these striated surfaces were measured and indicate a dominant movement towards N130°, with variations of up to 90° noted locally where the direction of movement has been influenced by elevated parts of the palaeotopography.

(b) *The Ecca Group*

Outliers of the lowest shales of the Ecca Group, the Pietermaritzburg Formation, occur only in the topographically highest areas. Outcrop of the shales is rare and consequently little can be said about them. They are dark bluish-grey where fresh and weather to pale yellow, beige or grey. They are locally micaceous or ferruginous. An origin as pelagic suspension deposits is considered likely.

7. Intrusions

Post-Nsuze intrusions of several types and ages are present within the area. Lithological differences between the intrusions are generally sufficiently marked to enable recognition of the various dykes and sills as belonging to different episodes. The episodes of intrusion may be subdivided into post- or pre-deformational on petrographic grounds. Where intrusions belonging to different episodes are juxtaposed the field relations allow recognition of relative ages within the pre- or post-tectonic groups.

The petrography, geochemistry and petrogenetic aspects of the pre-tectonic intrusions are the subject of Chapter 7. For this reason the description below is restricted to a brief introduction to the relative ages and distribution of the intrusions.

(a) *The Hlagothi Complex*

This group of differentiated sheet-like bodies intrudes the lower part of the Nsuze Group in the northern part of the study area. Peridotitic, pyroxenitic and gabbroic cumulates make up the major part of each sheet. The uppermost unit of each sheet is a non-cumulate gabbro or granophyric quartz gabbro. Estimated bulk compositions for the complex fall in the basaltic komatiite-high magnesium tholeiite range as defined by Jensen (1976). Individual sheets are 50 - 300 m in thickness, with substantial lateral variation in some areas. The peridotitic cumulates have been totally serpentinitized. The primary mineralogy is largely preserved in the pyroxenites and gabbros, but the uppermost gabbros have undergone deuteric and metamorphic alteration.

The complex predates the main metamorphic and deformational event as evidenced by the tectonic fabric of the serpentinites. Greenschist facies mineral parageneses have been recognized in the gabbros.

(b) Other Pre-Tectonic Mafic Intrusions

Sills and dykes of metagabbro and metapyroxenite 10 - 100 m thick are common in the area between the Gem and Central Nsuze Synclines and in the area north of the Mhlazi River (Map 2). The metagabbros are typically albite-tremolite/actinolite-epidote rocks. The meta-pyroxenites are now composed mainly of tremolite. Du Toit (1931) considered these rocks to be coeval with the Hlagothi Complex. This hypothesis is considered in Chapter 7. Dykes of plagioclase porphyry 10 - 40 m wide occur as remarkably linear and persistent intrusions in the area south and east of Hlagothi. They are intrusive into the Hlagothi Complex, but predate a greenschist facies metamorphic event. These dykes were intruded along pre-existing fault planes which form part of a north-south trending block faulting episode.

(c) Syenite, Monzogabbro and Albitite Intrusions

Syenite and monzogabbro occur in the northeastern part of the study area in the valleys of the Mbizwe, Gozweni and Mhlatuze Rivers (Map 1). These occurrences are the westward extension of a larger syenite body in the Mhlatuze Valley which extends as far east as the farm Naauwkloof. Fresh outcrops of the syenite are not present in the study area due to the proximity of the pre-Dwyka erosion surface at the present level of exposure. For this reason it is difficult to assess the relationship between the syenites and monzogabbros. The monzogabbros are exposed in the Igozwe River valley where reasonably fresh outcrop extends for nearly a kilometre along the river bed. These rocks are separated from pyroxenites of the Hlagothi Complex by a thin remnant of Nsuze Group sediments. At the northern limit of this exposure a gabbro, which has many characteristics in common with the gabbros of the Hlagothi Complex,is in contact with the monzogabbros. The field relations are equivocal and it is not possible to establish the relative ages of the two intrusions.

A narrow (10 m wide) dyke in the lower Mankane River valley (Map 2) consisting of albite (70%) and secondary carbonate (30%) is thought to be an albitite. The dyke is conformable with the general strike of the Nsuze Group volcanics which it intrudes. Its relative age, chemistry and origins are obscure.

A dark, fine-grained dyke (< 1 m wide) of syenitic composition is intrusive into Nsuze Group lavas in the Welendhlovu Valley (Map 2). The dyke is highly irregular in thickness and orientation. For this reason it was initially thought to be contemporaneous with the Nsuze magmatism, but its geochemistry is not consistent with this interpretation (Chapter 6).

(d) Post-Tectonic Dolerite Intrusions

Dolerite of post-Karoo age occurs as narrow dykes (10 - 50 m wide) and sills which are generally more substantial (10 - 100 m thick). Dykes are rarely observed in the area, except just south of Ndikwe Store where several have been recognized (Map 2). The Dwyka Formation is virtually devoid of dolerite intrusions. The most common loci of sill intrusion are at the Ecca-Dwyka contact and within the overlying Ecca shales. Most of the higher ground in the area is underlain by about equal proportions of the Ecca Group and dolerite.

Dolerite dykes are typically fine-grained, dark, grey-black rocks. The sills are medium-grained and are variable in composition. They range from dark, feldspar-poor rocks to light grey, quartz dolerites with a high plagioclase content. The dark mineral in all the dolerites is augite, with minor amounts of olivine present in the more mafic rock types.

CHAPTER 3

NSUZE GROUP - LITHOSTRATIGRAPHY

1. The Ndikwe Formation

General

The type area for this formation is the Nsuze River valley north of its confluence with the Ndikwe River. Continuous outcrops extend for several kilometres upstream from this area, but they are generally weathered. Other outcrops of the formation are situated between the Gem and Central Nsuze Synclines and in the valleys of Nsongeni, Gozweni, Mbizwe and Mhlatuze Rivers (Map 1).

The thickness of the formation is difficult to estimate accurately owing to deformation, lack of continuous vertical exposure, disruption of the sequence by gabbroic intrusions of the Hlagothi Complex, and lateral variation in thickness and lithology of individual units. A further complexity is introduced by the possibility that sediments of the Mdlelanga Formation, which occurs farther south, interfinger northwards with the Ndikwe Formation. A maximum thickness of 1 000 - 1 500 m is probably present in the type area. The thickness diminishes considerably farther south in the Welendhlovu-Mdlelanga inlier where the upper and lower contacts of the formation can be located. Here the sequence is disturbed by gabbro intrusions, but an estimate of 500 m is reasonable (Map 1). This southwards-thinning is ascribed to either the initial morphology of the basin or pre-Mdlelanga northwards tilting and consequent erosion to form a low-angle, angular unconformity which truncates the sequence southwards.

The dominant lithologiesare pyroclastics, volcanogenic sediments, arenites and argillites. Subordinate intercalations of lava and banded iron formation are also present (Fig. 3.1). This diversity within a formational unit results

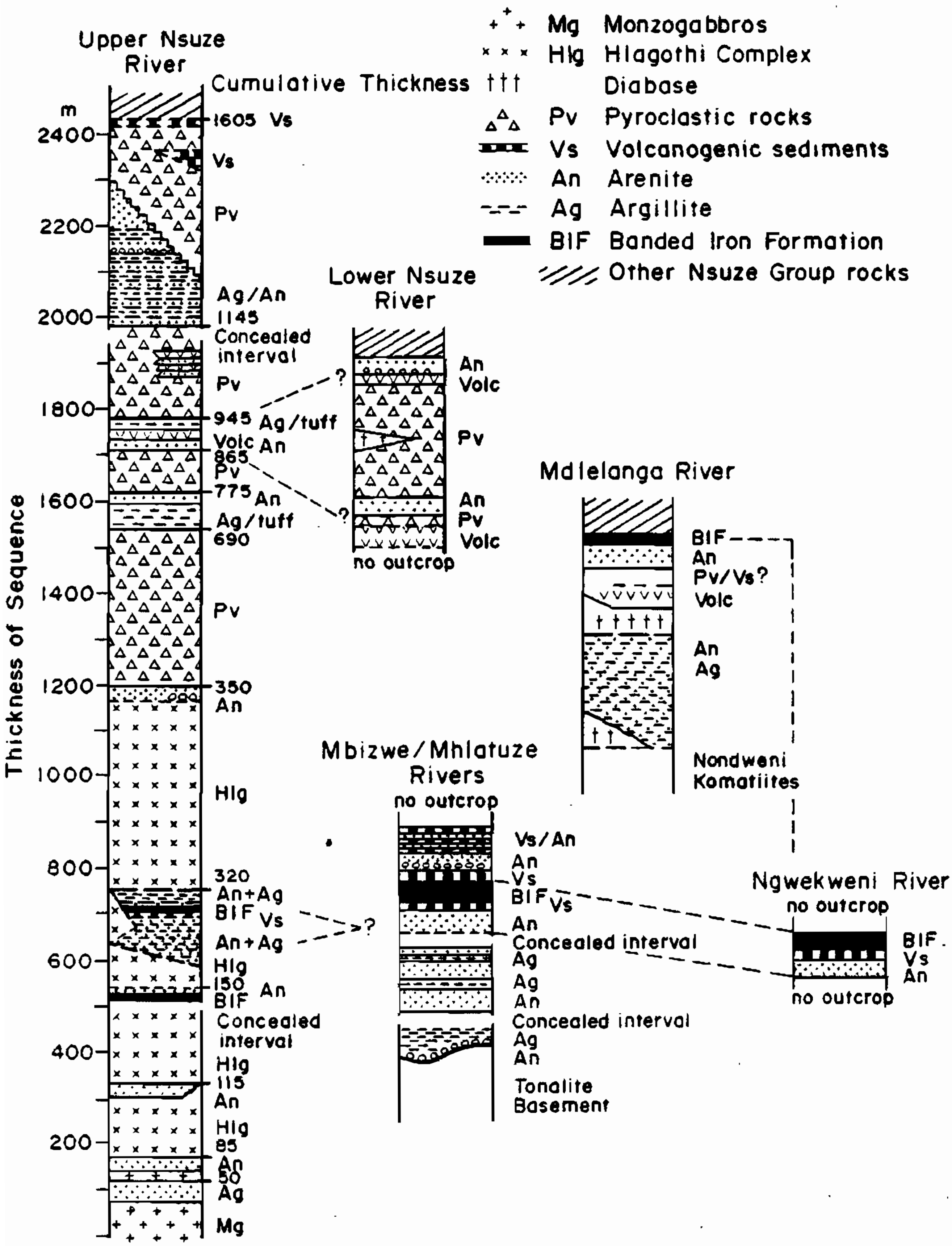

Figure 3.1 Stratigraphy of the Ndikwe Formation in its various outcrop areas.

from the complexity of internal lithological relationships which makes subdivision into smaller, more homogeneous formational units impracticable.

Lithology

(a) Volcaniclastites

Although volcaniclastites dominate the lithostratigraphy of the Ndikwe Formation, the paucity of fresh outcrops and the sheared nature of the rocks prevent detailed subdivision and description such as that presented by Armstrong (1980) for the Vryheid - Piet retief area. Several varieties of volcaniclastite can be distinguished locally, but cannot be correlated laterally for any distance.

Pyroclastic rock types make up about 65% of the formation in the type area. Bomb, lapilli and ash tuffs are most common. Crystal tuffs are present as minor constituents of the sequence, but most of the pyroclastics contain some crystals or crystal fragments.

In outcrop, the pyroclastics are greenish-grey chloritic rocks composed of very fine - grained angular or flattened volcanic fragments set in a fine, heterogeneous groundmass. Most of the volcanic fragments are of identical composition; grey or light grey dacite. Accidental fragments of amygdaloidal basalt, quartzite, chert and banded iron formation have also been recognized. These probably originated by explosive fragmentation from the sequence through which the conduits passed.

Lapilli tuffs are the most common pyroclastics. The lapilli are usually 5 - 10 mm in diameter, but range from 2 - 32 mm. Bombs up to 30 cm in diameter are relatively common in the lapilli tuffs (Fig. 3.2). The lava fragments are flattened parallel to the stratification, a feature which is conspicuous only where the angle between the primary and tectonic fabric is high (Fig. 3.3). In rocks where the angle between S_0 and S_1 is small, it is difficult to detect whether the lapilli are flattened parallel to the tectonic cleavage or the primary layering.

Figure 3.2 Lapilli tuff in the Ndikwe Formation, Nsuze Valley southwest of Ndikwe Store. Note compositional similarity of lapilli, bombs and groundmass. Accidental quartzite fragment indicated by arrow. Pen is 15 cm long.

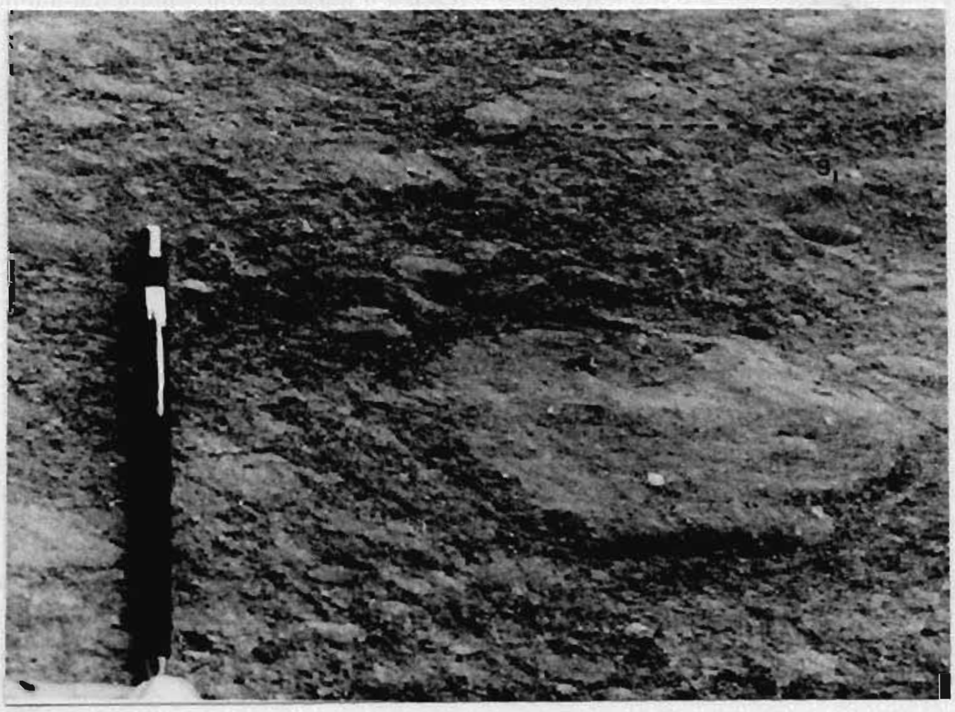

Figure 3.3 Lapilli tuff, Ndikwe Formation, showing flattening of fragments in bedding plane. Tectonic fabric, S_1, is oblique to S_0. Note amygdales in bomb-sized fragment. Nsuze Valley, south of Ndikwe Store. Pen is 15 cm long.

The primary mineralogy of the lithic fragments is not preserved. Two varieties may be distinguished in thin section. The first is a microcrystalline mica, untwinned albite and quartz assemblage which probably represents recrystallized volcanic glass (Fig. 3.4). The second is a coarser-grained, chlorite - albite - quartz - mica volcanic rock which was probably very fine-grained dacite or andesite (Fig. 3.4). Larger fragments of this type may be amygdaloidal, but are considered to be juvenile ejecta because of their rounded shape (Fig. 3.3).

Crystal tuffs and crystal-bearing lapilli tuffs are common, particularly in the lowest pyroclastics on the southern flanks of Hlagothi Mountain (Map 1). Rounded to extremely angular broken crystal fragments are the dominant form. Euhedral crystals are rare. Resorption features are commonly present (Fig. 3.5). About 95% of the crystals are of quartz, the remainder being plagioclase. The quartz crystals are typically strained, 1 - 2 mm in diameter and locally contain fluid inclusions. Plagioclase crystals are generally untwinned and virtually indistinguishable from the quartz grains except for a biaxial positive optic figure and slightly higher birefringence. Glide twinning is present in some grains. The untwinned and glide twinned grains have been strained; in the case of the former, the wavy extinction pattern is identical to that of adjacent quartz grains. Apparently undeformed albite-twinned grains are rare. These plagioclase crystals have the composition of andesine using the Michel-Levy method for extinction on albite twins.

Volcanogenic sediments are rarely present at the basal and upper contacts of the pyroclastic units. An agglomerate which may have been reworked is present at the base of the third pyroclastic unit. This rock is composed of a wide variety of juvenile and accidental clast types and is sporadically developed along the contact with the underlying quartz arenite (Fig. 3.6). The agglomerate probably represents airborne ejecta which landed in water as

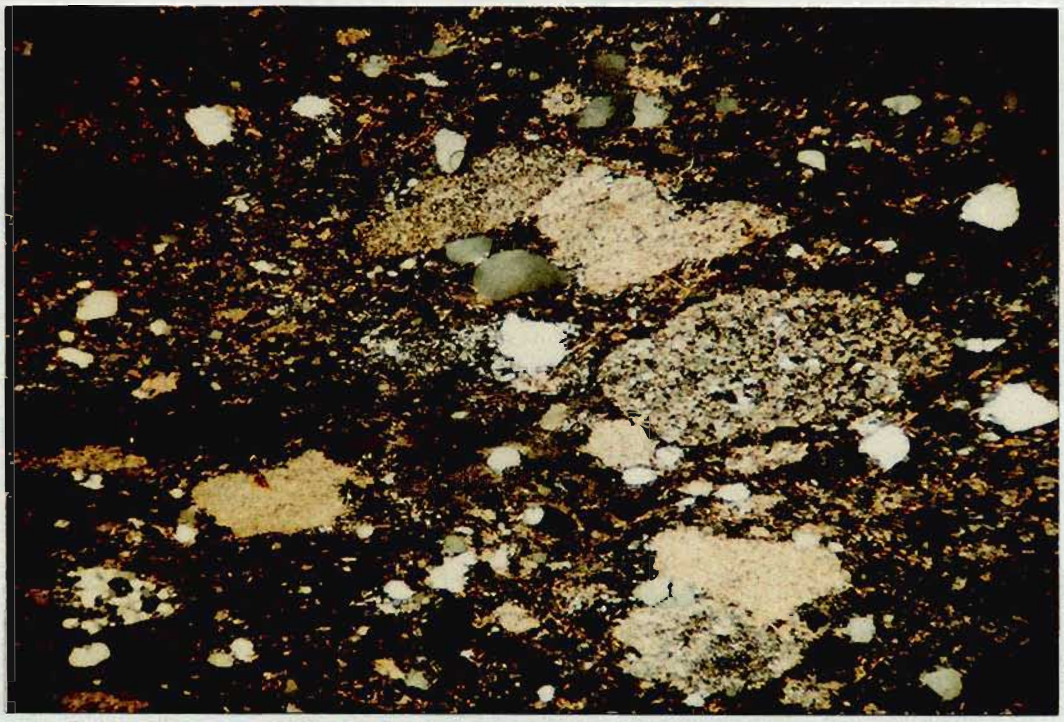

Figure 3.4 Photomicrograph of lapilli tuff shown in Figure 3.3. Coarser-grained fragment (centre right) is thought to be altered lava whereas very fine-grained fragment (below left centre) was probably volcanic glass. Groundmass is predominantly chlorite. Lapilli composed of mica, talc, chlorite and albite. Quartz crystals show reaction boundaries in unrecrystallized examples. (10x magnification, crossed nicols).

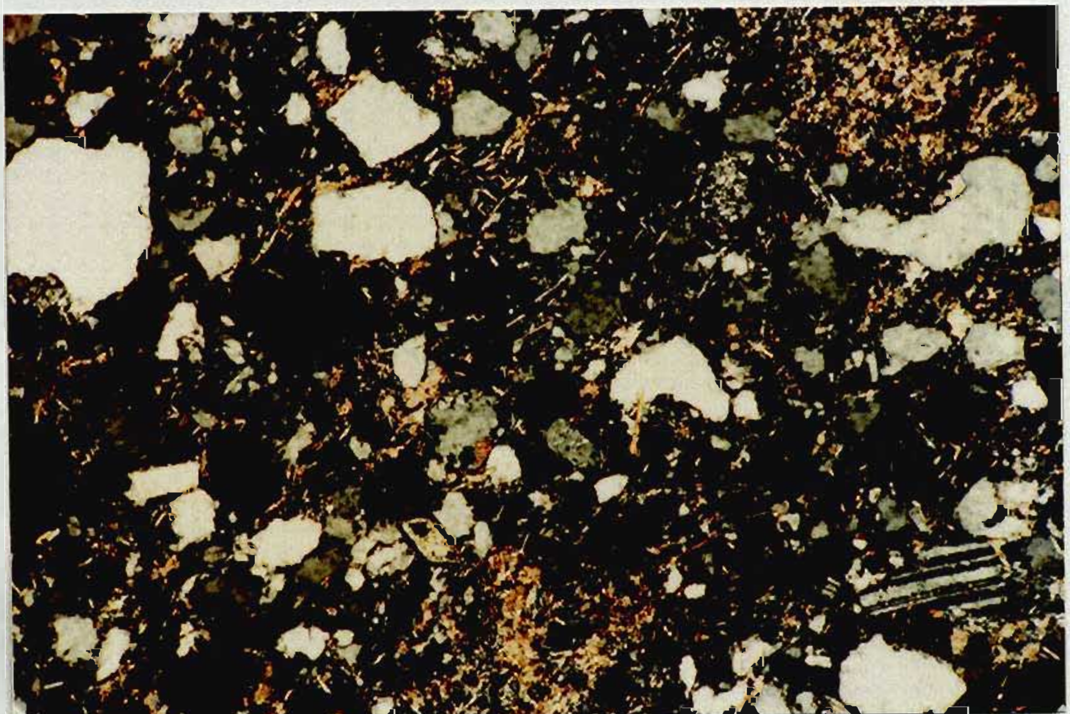

Figure 3.5 Crystal tuff from the Ndikwe Formation, south slope of Hlagothi Mountain. Note partial resorption of quartz and plagioclase crystals. (63x magnification, crossed nicols).

suggested by the preservation of bedforms on the upper contact of the quartz arenite. The agglomerate apparently grades upwards into lapilli tuff.

A 20-m thick unit of tuffaceous greywacke is present near the top of the highest pyroclastic unit (Fig. 3.1). It is composed of rounded volcanic clasts, 5 - 20 mm in diameter, in a sandy immature matrix. This rock type is thought to represent partially reworked debris flows or laharic breccias. This unit is overlain, with a gradational contact, by typical Ndikwe Formation lapilli tuffs. These become finer grained upwards and grade into ash tuffs. A gradual upward change in these ash tuffs to tuffaceous siltstones is observable in the area around the confluence of the Nsuze and Ndikwe Rivers. An X-ray diffraction analysis of the tuffaceous siltstones reveals that they are composed predominantly of chlorite with subordinate geothite and quartz.

The upper epiclastites contain rare dacitic lava bombs up to 25 cm in diameter. These are rounded and tapered clasts with some fractures or scalloped boundaries resembling conchoidal fractures. One bomb, weighing about 4 kg, was extracted and analysed (Chapter 6).

(b) Lavas

Although lava flows constitute a small percentage of the Ndikwe Formation, dark greenish-gray basalt and lighter grey andesite and dacite have been recognized. These fine-grained rocks have weakly to well-developed tectonic foliation. Amygdales and vesicles are frequently present, but primary textural features such as flow top breccias, pillows or pahoehoe surfaces have not been positively identified.

The lavas cropping out along the Malunga, Ndikwe, Mankane and Mamba Rivers are dark grey to greenish-grey chloritic, vesicular basaltic andesites (Maps 2 and 3). They consist of chlorite, limpid albite and tremolite in variable proportions. Minor amounts of epidote, biotite and quartz are present.

Figure 3.6 Basal contact of third pyroclastic unit of the Ndikwe Formation north of Ndikwe Store. Note agglomerate includes wide variety of clast lithologies and that underlying bedform has been preserved. There is no evidence for basal scour. Agglomerate overlain by lapilli tuff. Pen is 15 cm long.

White mica, sphene, leucoxene, opaques and carbonate occur in trace amounts. The carbonate, most probably calcite, and quartz become major constituents in carbonated and silicified zones respectively. Phenocrysts, or pseudomorphs after phenocrysts, are 1 - 3 mm long plagioclase crystals.

The amygdaloidal lavas in outcrops along the Welendhlovu and Mdlelanga Rivers are fresher and less sheared than those described above. Compositionally, the rocks range from basaltic andesite to dacite. The basaltic andesites are green, medium-grained rocks made up of saussuritized andesine (40%), tremolite (30%), epidote (20%) and quartz (5%). Chlorite, sphene and opaques are present in accessory or trace amounts.

The andesites are dark green-grey, very fine-grained, vesicular, porphyritic rocks composed of tremolite and plagioclase laths, anhedral epidote and flakes of chlorite. The andesine phenocrysts show albite twinning and are surrounded by a thin rim of biotite-enriched groundmass (Fig. 3.7). The amygdales consist of recrystallized quartz with subordinate chlorite, biotite and epidote.

Some of the dacites have features resembling those found in welded tuffs. These include the presence of flattened, barely distinguishable lapilli, and a very fine lamination. The very fine-grained groundmass consists of actinolite, albite, quartz and epidote. Phenocrysts of quartz and oligoclase up to 3 mm in length display resorption textures. The boundaries of the flattened and welded fragments are narrow, irregular zones defined by higher concentrations of chlorite and opaques than in the rest of the groundmass (Fig. 3.8).

A basaltic andesite flow is present in the upper pyroclastic unit west of Ndikwe Store. The flow is less than a metre thick and has an irregular base thought to have resulted from disruption and compaction of the underlying, unconsolidated pyroclastic debris (Fig. 3.9).

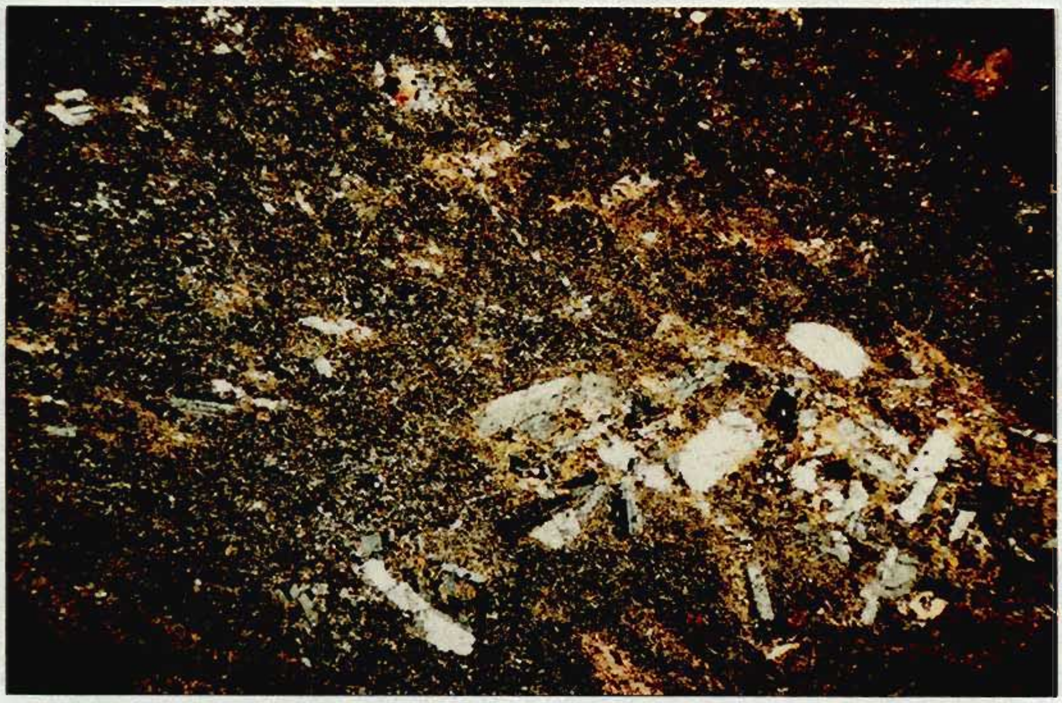

Figure 3.7 Photomicrograph of andesite from Welendhlovu River outcrop of Ndikwe Formation. Plagioclase phenocrysts, locally glomeroporphyritic, show twinning according to albite and Carlsbad laws. Groundmass is chlorite and albite with local concentrations of biotite. Epidote at top left. (10x magnification, crossed nicols).

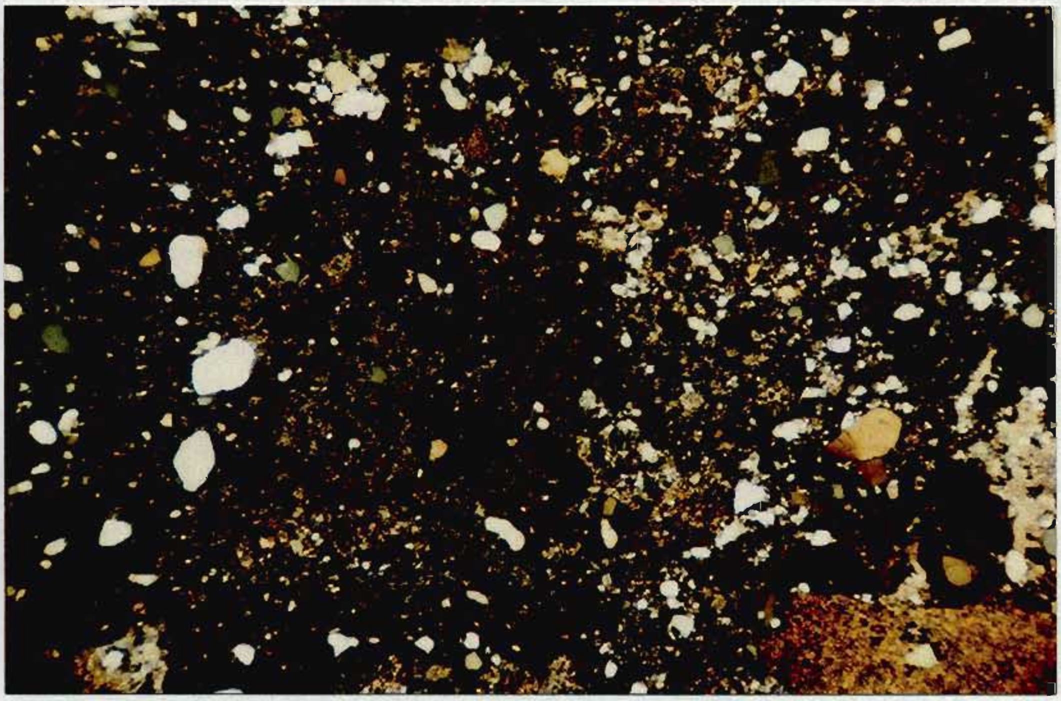

Figure 3.8 Photomicrograph of welded tuff from Welendhlovu River outcrop of Ndikwe Formation. Boundary of devitrified glassy fragment aligned vertically in centre of field. Note the abundant crystals. (10x magnification, crossed nicols).

(c) Sediments

Arenites and argillites make up over 90% of the sedimentary sequences of the Ndikwe Formation. Arenite is used as a broad term here since the quartzose rocks include quartz arenites, quartz wackes and lithic wackes. The quartz arenites are coarse- to fine-grained rocks composed of rounded to subangular quartz grains set in a sericitic or chloritic matrix which constitutes 5 - 20% of the rock. The quartz wackes are medium- to very fine-grained rocks consisting of subangular to angular quartz grains in a clayey matrix (up to 30% of the rock). The quartz arenites are generally lighter coloured than the quartz wackes. Colours range from off-white to tan and apple green for the arenites, whereas the wackes are a duller green or grey colour. The quartz grains are commonly recrystallized and have metamorphic overgrowths, although the original grain shapes have been well-preserved locally.

The argillites are quite variable mineralogically. Light brown pelites composed of white mica, quartz and plagioclase represent one end member of a continuum. At the other extreme is a dark grey phyllitic rock with a mineralogy dominated by chlorite. Other argillaceous sediments contain a high proportion of iron and may have centimetre-scale layering similar to that in the banded iron formation. Another variety of argillite is a massive black mudstone containing blocks of carbonate or siltstone. The carbonate has fine laminations reminiscent of algal mat deposits.

In the lower part of the Ndikwe Formation (Fig. 3.1) in the outcrops along the Nsuze, Gozweni, Mbizwe and Mhlatuze Rivers the arenites have been recrystallized more intensely than elsewhere due to the proximity to the intrusions of the Hlagothi Complex. In these outcrops, the arenites fine upwards into a heterolithic unit, which, in turn, is overlain by argillite.

In the outcrop on the Mhlatuze River close to Nkungumathe (Map 4), the basal arenite rests with a sedimentary contact on gneissic tonalite. Conglomerate lenses are present in channels scoured into the underlying tonalite. The medium pebble, polymictic, clast-supported conglomerate consists of subrounded quartzite and quartz clasts. The matrix has an apple green colouration due to the presence of Cr or Ni illites (recognized by XRD). These are thought to reflect high proportions of ultramafic rock types in the provenance. A 50 m-thick banded iron formation occurs in association with tuffaceous wackes about 300 m above the base in the Mbizwe River valley. The banded iron formation (BIF) comprises alternating micro- or mesobands of magnetite-rich, haematite-rich and iron-poor chert (Fig. 3.10). The BIF is laterally extensive and is recognized in the headwaters of the Gozweni and Ngwekwene Rivers (Map 4). At the former locality chert-rich bands are less abundant than elsewhere and silt is a significant component (Fig. 3.11). In the Ngwekwene inlier it is virtually devoid of light-coloured chert bands.

An arenite unit is present about 50 m above the BIF in the Mbizwe River outcrops. This unit is significant because it contains a unique internal conglomerate horizon. This is a matrix-supported, oligomictic, medium pebble conglomerate with disc-shaped clasts of haematitic cherty iron formation. Further comment on this unit is deferred to the section on debris flows (Chapter 5).

A debris flow, situated at the base of an arenite unit 1 200 m from the base of the sequence (Fig. 3.1), consists of scattered clasts up to 30 cm in diameter in a quartz wacke matrix. The clasts consist of rhyolite, black chert and fine-grained quartzite. The arenite unit overlying this debris flow is 30 m thick and is, in turn, overlain by a pyroclastic sequence in excess of 300 m thick. The volcaniclastites are overlain by a 60 m-thick unit of dark grey, glossy phyllitic argillite composed of chlorite (70%), quartz (20%) and white mica (10%). This unit probably represents a reworked ash tuff.

Figure 3.9 Thin basaltic andesite flows in pyroclastics of the Ndikwe Formation west of Ndikwe Store. The irregular basal contact is interpreted as a product of loading of the underlying lapilli tuff. Scale is 15 cm long.

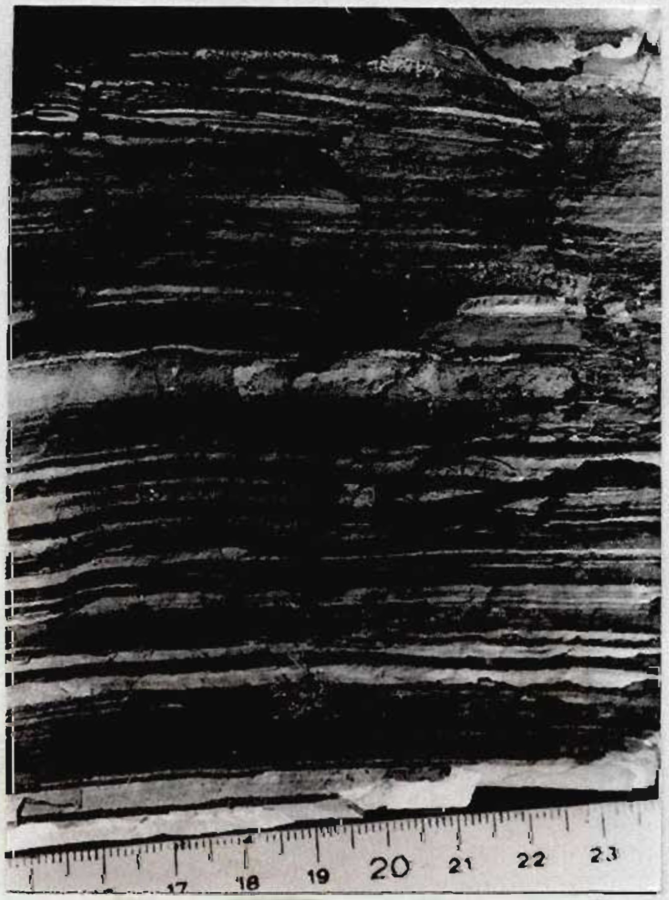

Figure 3.10 Cherty banded iron formation, Ndikwe Formation, Ngwekweni Valley. Scale in centimetres.

Figure 3.11 Cherty banded iron formation showing quartzose lenses and argillaceous horizons. Ndikwe Formation, Upper Gozweni Valley. Scale is 15 cm long.

The uppermost sediments of the formation are found in the Nsuze and Mhlazi River valleys (Map 2) north of the Gem Syncline. These comprise alternating arenites and ferruginous argillites in which sedimentary structures and textures are well-preserved (Chapter 5). The sequence consists of several thin (29 - 40 m) alternating layers in the lower part, with two much thicker (199 m) arenaceous units in the upper part. The sequence is overlain, apparently with a slight angular unconformity, by a thick sequence of pyroclastics.

2. The Mdlelanga Formation

General

The type section for the Mdlelanga Formation is situated in the valley of the Mdlelanga River in the southern part of the map area (Map 1). The name was first applied by Du Toit (1931) who referred to the formation as the Mdlelanga Quartzite. Matthews (1979, cited SACS, 1980) changed the term "quartzite" to Formation in order to conform with accepted lithostratigraphic nomenclature.

Rocks of this formation are present in the Central Nsuze Syncline and on the south limb of the Gem Syncline. They are not recognized north of the latter fold because of northward interdigitation of the Mdlelanga and Ndikwe Formations. Alternatively, the Mdlelanga Formation may have been deposited as a southward-thickening wedge as a result of differential subsidence of the depository.

The formation comprises 1 200 m of dominantly arenaceous sediments in its type area. Farther north, in the area around Vuleka, the sediments are more heterogeneous and have a total thickness of 800 m. In the Mankane River the sequence has been partly eliminated by faulting, but is at least 500 m thick.

Lithology

In the type area the Mdlelanga Formation consists almost exclusively of recrystallized quartzose rocks. These are very pure quartz arenites with intercalations of quartz wackes. Minor intercalations of argillite and volcanogenic sediments have been recognized. The domination of the sequence by arenites may be an illusion resulting from the extensive recrystallization of the rocks in the type area, which to some extent discourages detailed study of the sequence.

Good outcrops of the sediments are present upstream of the type area on the south limb of the Gem Syncline. The sequence in this area consists of alternating quartz arenites, siltstones and mudstones. The quartz arenite units, which are up to 30 m thick, show both upward-fining and coarsening cycles. The coarser-grained parts are mature, matrix-poor sandstones consisting of well-rounded quartz grains. These grade into finer-grained, mature quartz arenites which, in turn, grade into siltstones or mudstones. Not all the graded sequences include all of the lithologies and some abrupt changes from arenite to mudstone, for example, occur over a distance of a few centimetres. Whereas complete graded sequences range in thickness from 10 - 30 m, some incomplete sequences are thinner than 10 m and some homolithic units exceed 30 m. The various configurations and associated sedimentary structures are the result of a dynamic depositional environment as discussed in Chapter 5.

A diamictite layer cuts across a part of the sequence described above. The layer is $\sim$ 40 m thick at its eastern extremity, but becomes considerably thinner westwards. It is composed of large blocks of quartz arenite chaotically distributed in a lithic greywacke matrix. This lithology is considered to be the product of large-scale sediment gravity flow (Chapter 5).

The basal unit of the Mdlelanga Formation is a 40 m zone of calc-arenite in which carbonate lenses are present The carbonates commonly exhibit crinkle lamination of inferred biogenic origin. Stromatolites have been recognized in this unit to the south of the study area (cf. Chapter 5).

3. The Qudeni Formation

General

The Qudeni Formation overlies the Mdlelanga Formation conformably in the Gem and Central Nsuze Synclines. The formation was called the "second volcanic group" by Du Toit (1931) and named the Qudeni Formation by Matthews (1979 cited SACS 1980) The type area according to SACS (1980) is situated south of the study area on the farm Qudeni

The formation is 580 m thick in the type area (Matthews. 1979, cited SACS. 1980) but becomes much thinner northwards. In the Gem Syncline it is 40 - 60 m thick. The correlation between the thick lava sequence of the Central Nsuze Syncline and the thinner sequence in the Gem Syncline has not previously been recognized. However, overlying sediments and the lavas themselves are lithologically similar enough to substantiate the correlation. In addition the chemistries of the correlated lavas are reasonably similar (Chapter 6). The problems of correlation stem from the structural relationship of the two synclines which brings laterally distant parts of the sequence into closer proximity with one another.

Lithology

The Qudeni Formation comprises volcanics which range in composition from basaltic andesite to dacite. The lavas commonly contain quartz-, calcite-, chlorite- or epidote-bearing amygdales. The amygdales range from minute spherical or elongate bodies to large (20 cm) irregular bodies (Fig. 3.12). Very large tunnel-like cavities (up to 1 m in diameter) also occur. No pillow structures have been observed.

Flow top textures are rare, and, even where two flows of markedly different lithology are seen in juxtaposition, the contact is not usually characterized by any textural change. Exceptions do occur, as can be seen in the Nsuze River outcrops close to the upper contact of the Qudeni Formation. At this locality a light-coloured andesite overlies a darker basaltic andesite, in which small, spherical amygdales become more concentrated towards its highly irregular upper contact (Fig. 3.13). In the Nsuze River valley on the north limb of the Gem Syncline, flow tops are typified by networks of siliceous, light-coloured material separating angular fragments of darker-coloured rock. This texture probably represents a flow top breccia cemented by secondary quartz.

Silicification of the volcanics has occurred in some areas. This results in patchy and lenticular leucocratic zones in the lava flows. On the north limb of the Gem Syncline these silicified zones are spatially associated with the amygdales (Fig. 3.12). The introduction of silica was apparently controlled by the location of microfractures, which were probably more dilated close to voids left by gas bubbles. Alternatively, the silica-filled amygdales may have had different thermal expansion-contraction behaviour from the enclosing lava, resulting in a higher density of microfractures in their immediate area.

Another form of silicification is present on the north limb of the Vutshini Syncline. Here, angular, curved, elongate patches of silicified lava are present within unsilicified volcanics (Fig. 3.14). These leucocratic patches possibly represent autoclastic breccia ripped from the top of the flow underlying the one in which they occur. Subaerial leaching or weathering may have produced the change in composition in this detritus prior to its inclusion in the later flow.

The quality and lateral continuity of outcrop are seldom sufficient to enable the measurement of flow dimensions. Where observed, flow thickness ranges from 1 - 16 m, with an average of 2 - 4 m. The lateral extent of flows is unknown, although one flow containing large amygdales and phenocrysts is tentatively correlated across the Gem Syncline, a distance of about 3 km.

The mineralogy of the lavas is not always easy to ascertain accurately due to the fine grain size of the rocks. In addition, very little of the original mineralogy has survived the greenschist-facies regional metamorphism.

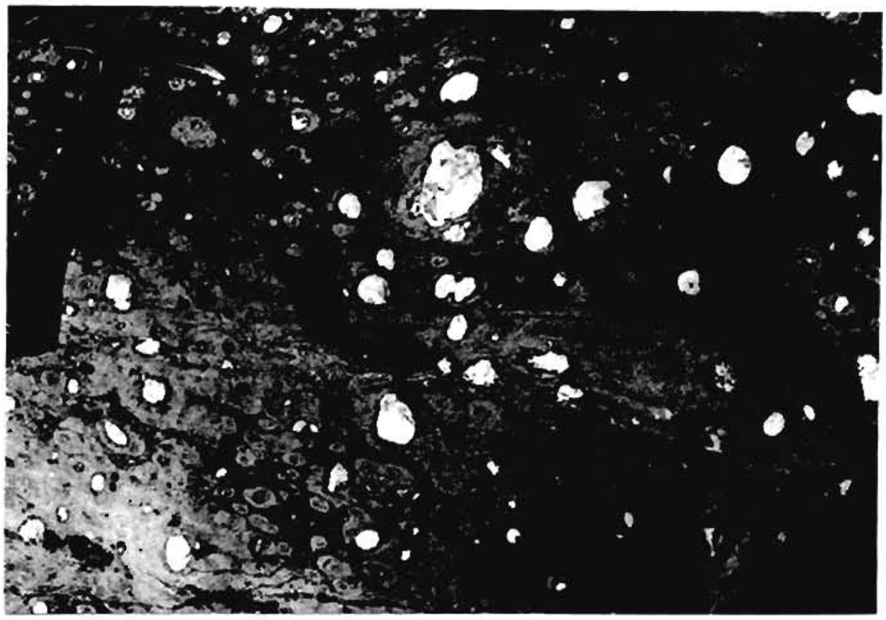

Figure 3.12 Amygdaloidal basaltic andesite, Qudeni Formation, north limb of Gem Syncline, Nsuze River valley. Silicification in zones surrounding quartz - calcite - chlorite-filled amygdales.

Figure 3.13 Contact between basaltic andesite and andesite (upper) flows, Qudeni Formation, north limb of Central Nsuze Syncline.

Figure 3.14 Irregular patches of silicification on upper contact of basaltic andesite flow. Locality as for Figure 3.13. See text for further discussion.

The basaltic andesites are texturally and mineralogically diverse. One example, (BG22, Appendix 1), is a very fine-grained, phenocryst-free amygdaloidal rock composed of xenocrystic biotite (20%), epidote (20%), saussuritized plagioclase (55%), leucoxene/sphene (5%), and traces of tremolite, chlorite and calcite. There is no recognizable twinned plagioclase, possibly as a result of metamorphic transformation to untwinned albite. Quartz and epidote occupy a cross-cutting microfracture. More typical basaltic andesites have an intergranular to hyaloophitic texture with small, partially saussuritized laths of plagioclase (well-orientated in some specimens) surrounded by wisps of xenocrystic chlorite or biotite (Fig. 3.15). Plagioclase phenocrysts (1 - 5 mm in length) occur singly or as glomeroporphyritic clusters. Typical mineral abundances are presented in Table 3.1.

The andesites are also variable in mineralogy and show the same tendency to either biotite- or chlorite-rich parageneses. The rocks lack primary igneous textures, although some ghost phenocryst outlines may be recognized. Sparse 2 - 20 mm amygdales are zoned. The core is filled with light green, isotropic chlorite. Surrounding this is a ring of granular biotite with a few euhedral zoned epidote crystals. The biotite is surrounded by a ring of calcite, which is surrounded by a thin rim of epidote (Fig. 3.16). The mineralogy of the andesites is summarized in Table 3.1.

In the basaltic andesites and andesites there is some remnant andesine although most of the plagioclase has undergone metamorphic transformation to albite. Epidote is present either as 0,5 mm equant, zoned grains or as fine-grained aggregates (Fig. 3.16). The biotite is a light brown to dark brown pleochroic variety and occurs in ragged to euhedral flakes. Chlorite is present as minute to large (5 mm) irregular flakes. It is a dark green, pleochroic variety, most probably prochlorite.

TABLE 3.1: MINERALOGY OF THE QUDENI FORMATION VOLCANICS

	Basaltic Andesites	Andesites	Dacites
Plagioclase	30 - 60	30 - 50	50 - 60
Chlorite	0 - 40[1]	0 - 20[1]	5 - 15
Biotite	0 - 25	0 - 30	Trace
Tremolite/Actinolite	0 - 30	0 - 15	Trace
Epidote	5 - 25	8 - 30	5 - 10
Muscovite	0 - 5	0 - 5	Trace
Calcite	0 - 10	0 - 8	0 - 20
Quartz	1 - 10	2 - 20[2]	2 - 30
Sphene/Leucoxene	1 - 3	1 - 5	Trace
Opaques	1 - 3	1	Trace
Kaolinite	-	-	Trace

[1] - Biotite seldom co-exists with chlorite

[2] - Higher quartz contents in silicified rocks.

Figure 3.15 Photomicrograph of basaltic andesite, Qudeni Formation, locality as for Figure 3.12. Plagioclase phenocrysts are surrounded by very fine-grained xenocrystic chlorite groundmass possibly representing original hyalo-ophitic texture. Epidote and sphene present as accessory minerals. (63x magnification, crossed nicols).

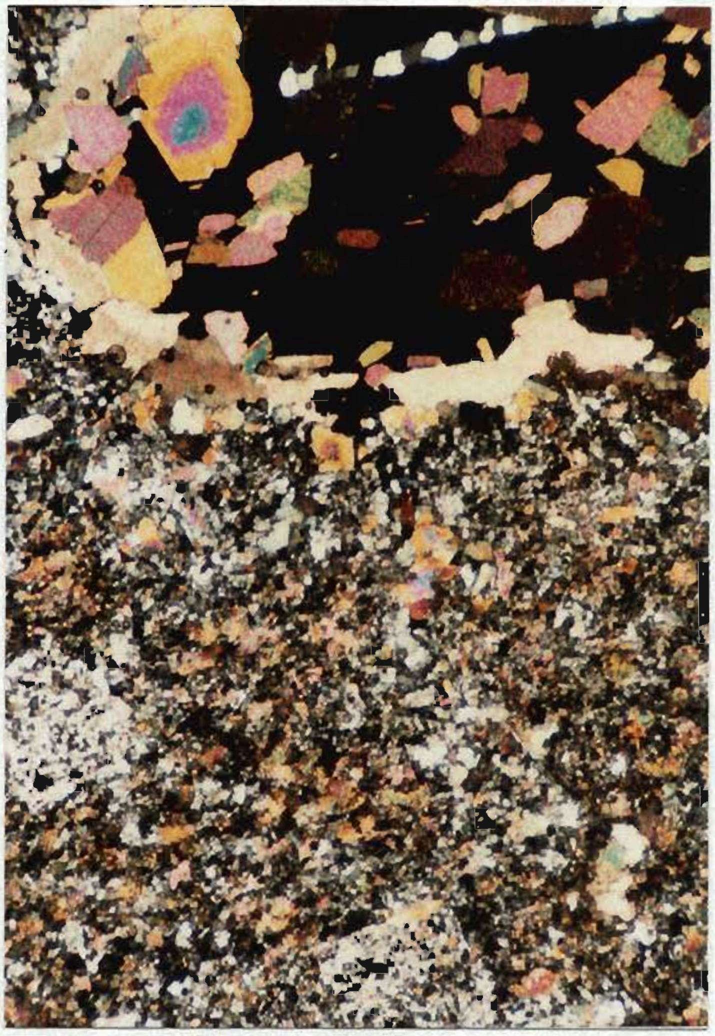

Figure 3.16 Photomicrograph of amydaloidal andesite from the Qudeni Formation, north limb, central syncline in the Nsuze River valley. Fine-grained biotite, albite and saussurite (epidote - zoisite - clinozoisite - white mica) make up the host rock. The amygdale has a central core of chlorite (at extinction). This is surrounded by an irregular layer of granular biotite with some epidote crystals. A thin calcite layer overlies the biotite and this, in turn, is rimmed by epidote. (25x magnification, crossed nicols).

The dacites are similar in appearance to the andesites except for a lower content of the mafic minerals. They are generally partly carbonated or silicified. The range in mineralogy for rocks considered to be dacites is given in Table 3.1.

The relative proportions of plagioclase and quartz are not always easy to ascertain because the former is invariably untwinned albite. The fine grain size compounds this problem and discrimination is possible only where traces of alteration products are present within the plagioclase.

The proportions of the various lithologies in the formation are difficult to estimate. Available outcrops indicate a greater content of andesitic lavas than basaltic andesites and dacites.

4. The Vutshini Formation

General

The type area of the Vutshini Formation is situated in the valley of the river of that name in the southern limb of the Central Nsuze Syncline (Matthews, 1979, cited SACS, 1980, p. 73). The formation is restricted to the cores of the two major synclines and the best outcrops are to be found where the Nsuze River cuts through these structures (Maps 1 and 2).

A total thickness of 1 000 m is present in the south, whereas a residual thickness of 350 m is preserved in the Gem Syncline.

Lithology

The Vutshini Formation comprises arenaceous and argillaceous sediments in three slightly different sequences. The lower 350 m of the formation in the Vutshini Syncline consists of a sequence of alternating argillite and quartz arenite units 2 - 25 m thick. This is overlain by a substantial thickness of immature arenites with rare argillite intercalations. The lower sequence comprises at least twenty alternations of the two main lithologies on the north limb of the syncline, whereas on the south limb only three cycles are present. This reflects a southward-thinning of the lower sequence and a concomitant increase in the thickness of the upper arenaceous sequence.

The sediments of the Vutshini Formation in the Gem Syncline are the equivalent of the lower sequence in the Central Nsuze Syncline. They comprise a similar alternation of arenites and argillites, but differ in that the arenites are the dominant lithology, whereas the southern occurrence has about equal amounts of each lithology.

Limited recrystallization and the excellent preservation of primary sedimentary structures are features of the Vutshini Formation sediments.

5. The Ekombe Formation

General

The Ekombe Formation is restricted to the core of the Vutshini Syncline. The exposed area is very small (8 000 m^2) owing to overlap of the Phanerozoic cover sequence. Matthews (1979, cited SACS, 1980) termed this formation the "Mankane Formation", a name which is not retained in this study because no rocks which may be correlated with this formation occur in the Mankane River valley. Similar lithologies do occur in the Mankane Valley, but their stratigraphic position precludes correlation with the outcrops ascribed to the Ekombe Formation. It is hoped that the change will prevent confusion between the two stratigraphic levels at which the volcanics occur.

A residual thickness of 60 m is present in the exposed area.

Lithology

The Ekombe Formation consists of fine-grained, amygdaloidal andesites. These lavas are always highly weathered and have a weakly developed tectonic fabric. Pipe amygdales are recognizable, as are very small, zoned spherical amygdales. The filling of the larger amygdales is quartz, whereas the small ones have a chlorite core surrounded by quartz. The quartz is not the microcrystalline variety typical of amygdales, but consists of coarse grains with well-defined triple junctions.

In the only thin section available (NZ-1, Appendix 1), the groundmass consists of white mica (40%), quartz or albite (not distinguishable, 55%), and sphene (5%). Du Toit (1931, p. 51) reports a groundmass of quartz, pale chlorite and some feldspar.

6. Discussion

Correlation

The critical aspect of the lithostratigraphy presented above is the correlation between areas separated by either younger cover sequences or structural breaks. The former situation may even include major structural features which are obscured by the Phanerozoic cover. Adequate marker horizons are usually present to enable correlation between the inliers, but there are two important exceptions.

The first is the correlation between various inliers of rocks attributed to the Ndikwe Formation. In this case, correlation between the various outcrops in the valleys of the Mhlatuze, Gozweni and Mbizwe Rivers can be achieved using the presence of the banded iron formation horizon and associated sediments (Fig. 3.1 and Map 1). The relationship between these inliers and the major outcrop area in the Nsuze River valley is not so easily resolved and remains uncertain. Likewise, precise correlation between the outcrops of Ndikwe Formation sediments in the Welendhlovu and Mdlelanga River valleys and those north of the Gem Syncline is not possible. The grounds for the correlation are a general similarity in lithologic sequence which in each case consists of alternating arenites and banded, ferruginous argillites. One of the upper units in the Welendhlovu Valley has been traced laterally under the Karoo cover, to the Ngwekweni River inlier using geophysical methods (Esterhuizen and Groenewald, 1980). This banded iron formation is correlated with one near the base of the Ndikwe Formation in the Gozweni River valley on lithological grounds. This apparent lateral continuity of sedimentary units in the lower part of the formation is not displayed by the upper volcaniclastic units as these are absent in the southern part of the map area as noted earlier.

The second correlation, which is fundamental to the lithostratigraphic subdivision, is the one between the sequences in the two major synclines. Matthews (1979, unpublished mapping) recognized the Mdlelanga, Qudeni and Vutshini Formations in the Central Nsuze Syncline but ascribed the sequence in the Gem Syncline to the Dlabe, Mome and Mankane Formations (Table 1.1). The present study has revealed that the basal part of the Mdlelanga Formation is lithologically unique within the Nsuze Group, and that correlation between the two synclines is possible. The lithology in question is the calcareous arenite containing biogenic carbonates mentioned earlier. Since biogenic carbonates are rare in the Nsuze Group, it seems reasonable to correlate the three occurrences of the calc-arenite unit in the field area. Two of the outcrops are situated at the base of the Mdlelanga Formation on the north limb of the Vutshini Syncline in the Mdlelanga and Nsuze River valleys. The third occurrence is only a few hundred metres north of the Mdlelanga River outcrop, but is northward facing, that is, on the south limb of the Gem Syncline (Map 2).

Lithostratigraphic Relationship to the Pongola Supergroup

In the foregoing presentation of the local lithostratigraphy there has been no mention of the regional correlation of the sequence in the study area with the Nsuze Group elsewhere in the Pongola depository. The situation is not as simple as that implied by Du Toit (1931, p. 38): " ... the Insuzi Series can without any doubt be correlated with Humphrey's (1912, 1913) 'Lower Pongola Beds', a great succession of quartzites, amygdaloids and slates, that crop out in the Vryheid and Utrecht districts ...". Armstrong (1980, p. 65) reports that the Nsuze Group in the Vryheid - Piet Retief area comprises three subunits: a lower sedimentary-volcanic unit ($\sim$ 800 m), a middle, predominantly volcanic unit (7 500 m), and an upper volcaniclastic sedimentary unit (500 m).

In the White Mfolozi inlier (Fig. 1.1), the stratigraphy of the Nsuze Group as described by Matthews (1967; 1979, cited SACS, 1980) comprises six formational units. The formations and their lithologies (SACS, 1980, p.76) are given in Table 3.2.

TABLE 3.2: LITHOSTRATIGRAPHY OF THE NSUZE GROUP, WHITE MFOLOZI INLIER (SACS, 1980, p. 76).

Formation	Lithology	Thickness
Taka	quartzites and shales	> 530 m
Bivane	lavas	> 2 050 m
Chobeni	sandstones, mudstones, breccias and dolomites with stromatolites	760 m
Thembeni	banded shales with sandy and pebbly intercalations	60 - 240 m
Nhlebela	lavas	0 - 120 m
Bomvu	quartzitic sandstone with arkosic layer near base	0 - 60 m

From the above, it is apparent that the sequences in the various outcrop areas of the Nsuze Group differ substantially. The proportion of volcanics in the sequence is a good indicator of the variation. In the northern areas 90% of the group is of volcanic origin (Armstrong, 1980, p. 65; SACS, 1980, p. 75), but in the White Mfolozi and Nkandla areas the proportions are 57% and 38% respectively. The proportion of fragmental volcanics in the same areas is 5%, 0% and 22% in the order given above. Although there is a systematic increase in the volume of sediment in the group southwards, there is apparently no consistant variation in the volcaniclastic content.

On the basis of chronostratigraphic position and general lithology, it is reasonable to correlate the Nsuze Group in the study area with the outcrop areas mentioned above. It is also clear that correlation of individual units or erosion surfaces between the various areas is not possible. This is not unexpected, given the necessarily complex tectonic, magmatic and sedimentological evolution of an Archaean depository. In fact, it is more surprising that the Pongola Supergroup is as undeformed and lithologically uniform as it appears to be.

CHAPTER 4

STRUCTURE AND METAMORPHISM

1. Introduction

The study area is situated close to the southern margin of the Kaapvaal province and consequently its structure is influenced by the high-grade tectonic front marking this boundary. Intense deformation in the basement sequence adjacent to the Natal Thrust Front has been described by Clark (1983), Brown (1982) and Matthews (1959). The deformation and metamorphic grade diminishes northwards and most outcrops of the Nsuze Group north of Nkandla have undergone tight to isoclinal folding and greenschist facies metamorphism. Several deformational episodes have affected the Nsuze group in the Vryheid - Piet Retief area (Armstrong, 1980), but these are relatively less intense than the dominant folding event recognized in the study area. The geometry of these folds suggests that they resulted from northwards compression along the Natal Thrust Front and are thus synchronous with the $\sim$ 1 000 Ma Namaqua-Natal orogenic province. Later deformation is restricted to two episodes of block faulting.

2. Structure

The earliest structural element recognized in the study area is a faint cleavage which is virtually obliterated by later refoliation. The cleavage, which is crenulated by the younger foliation (Fig. 4.1), is defined by orientated phyllosilicates and occurs rarely in tuffaceous and argillaceous rock types. This S_1 fabric is observed only in thin section, consequently no field data are available for its orientation. Only microscopic folding has been recognized in association with S_1 (Fig. 4.2).

Figure 4.1 S_1 cleavage in Vutshini Formation argillite, from northern limb of Central Nsuze Syncline. Note crenulation by S_2 cleavage. 63x magnification - crossed nicols.

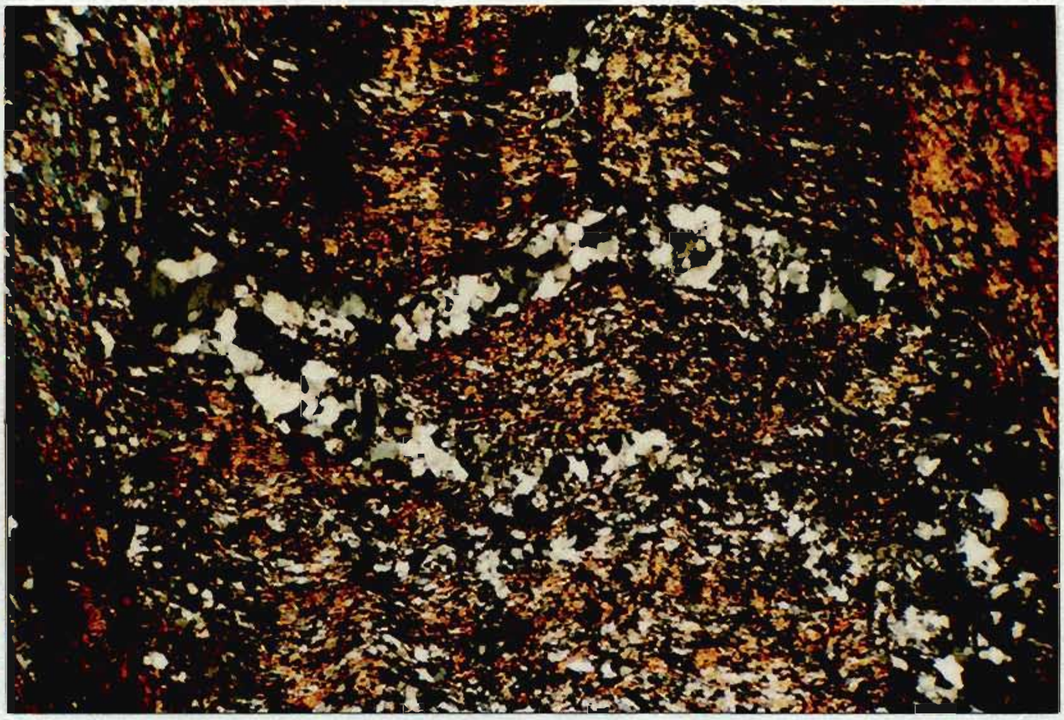

Figure 4.2 Micro folding in argillite shown in Figure 4.1. 10x magnification - crossed nicols.

The dominant deformation, D_2, is tight to isoclinal folding related to the 1 000 Ma Natal belt episode. This event resulted in the three large synclinal structures in the Nsuze River Valley, of which only the northern two fall within the study area. These folds have wavelengths of 3 - 5 km with numerous associated smaller parasitic folds. A pervasive axial planar foliation is developed in all the fine-grained rocks and is faintly visible in arenaceous rock types. A grain shape lineation is developed on S_0 surfaces in the arenites. Several measurements of S_0 surfaces were taken on many of the smaller folds. S_2 surfaces were also measured where visible, as were L_2 lineations. A typical Schmidt net plot of these data for a single fold is shown in Figure 4.3, the remainder of the data being presented in Appendix 2, also as Schmidt net plots. In general; the poles to S_0 define a girdle indicative of cylindrical folding. All fold axes are inclined at less than 40° and are in a broadly east-west orientation. L_2 lineations commonly lie close to the fold axes, although in some plots there is considerable dispersion. S_2 surfaces are steep, although south and north dipping fabrics are common within a single fold. This is a result of cleavage refraction and obscures the axial planar nature of the S_2 cleavage. Most of the axial surfaces dip southwards at 70 - 85°.

Dislocations recognized as being related to D_2 are equivocal, but at least three examples are thought to exist. A large part of the stratigraphy is absent from the north limb of the anticline separating the Central Nsuze and Gem Synclines. The Mdlelanga Formation is obliquely truncated by a linear feature along this limb which marks the contact with the underlying volcanics of the Ndikwe Formation. As this fault is orientated parallel to the fold axis and occurs at the contact between rock types of very different rheology, it is thought to represent a large lag structure within the limb of the fold (Fig. 4.4). North of the Gem Syncline steep overthrusts occur within the northern limb of the main syncline itself and adjacent isoclinal anticlines

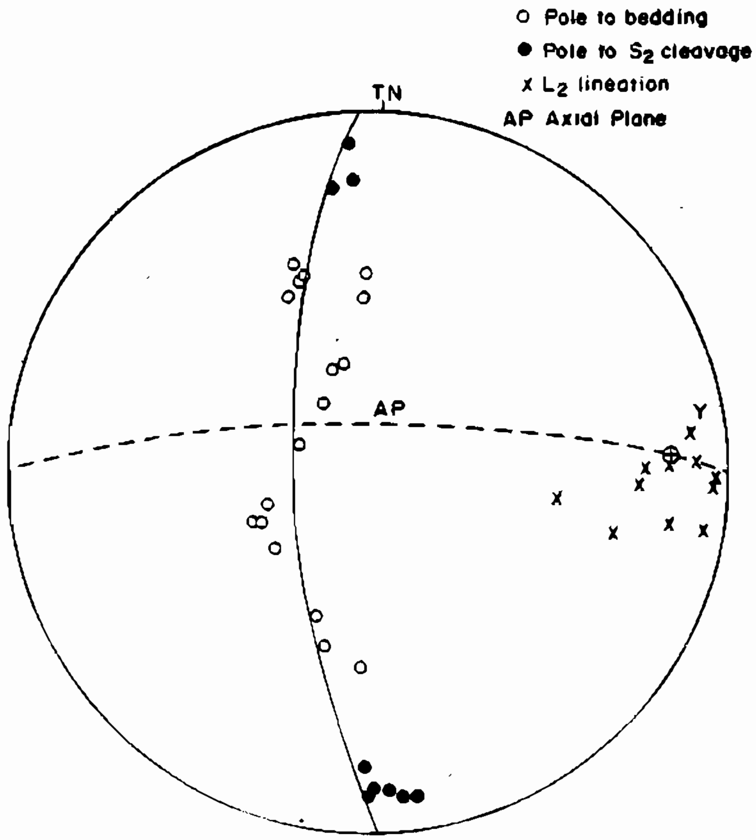

Figure 4.3 Schmidt net plot for D_2 small-scale fold south of Vuleka.

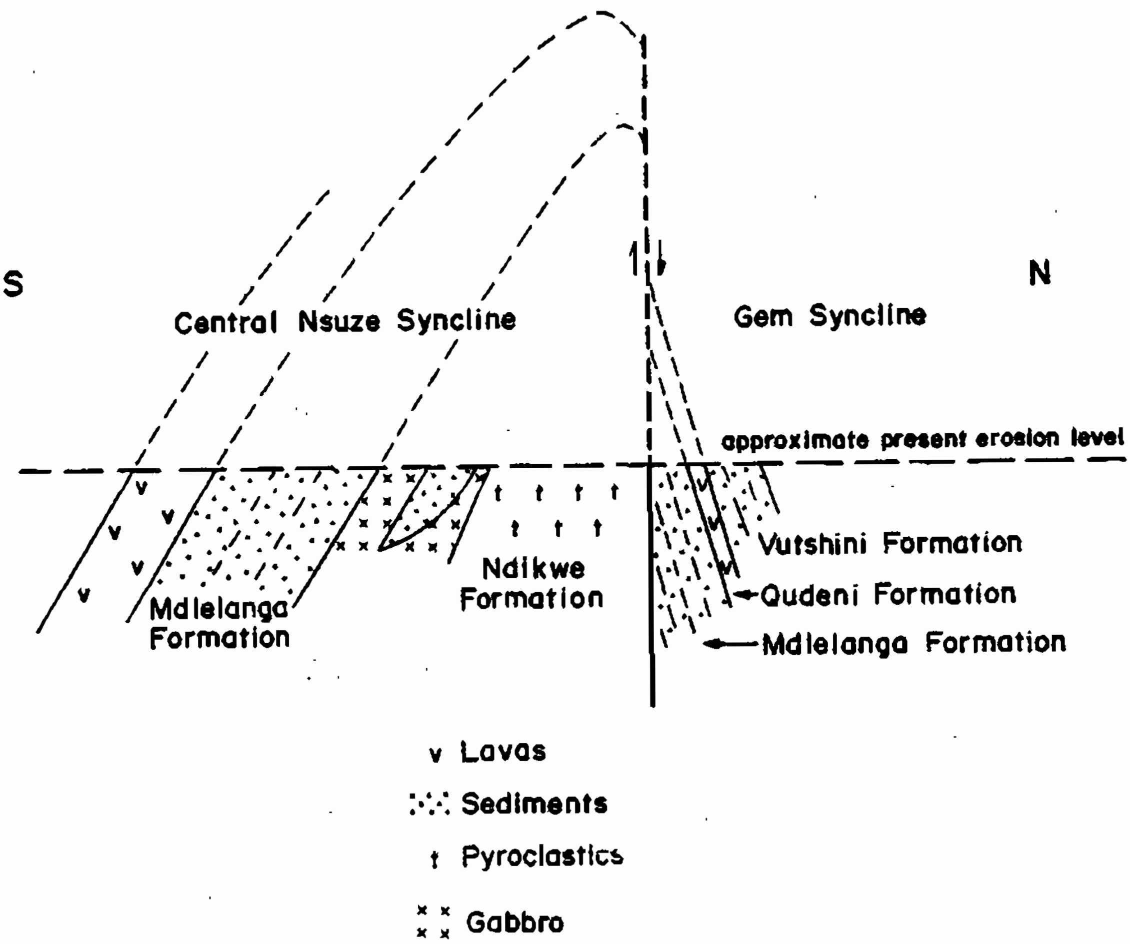

Figure 4.4 Section through the anticline separating the Gem and Central Nsuze Synclines. Note the oblique truncation of the Mdlelanga Formation by faulting. Not to scale.

(Map 2, Mhlazi River area and west of Ndikwe Store). These thrusts result in local duplication of incompetent arenite units along curved fault planes. Although the actual fault planes are not exposed, the sense of movement is inferred from displaced markers. The throw on these faults is of the order of 20 - 80 m (Fig. 4.5).

Faults orientated normal to the axial surface of the Gem Syncline are recognized in the area between the Mankane and Nsuze Rivers and farther west close to the limit of the inlier. These have almost vertical fault planes and downthrow to the west. They resemble the cross and wrench faults described by De Sitter (1964), who considers them a consequence of longitudinal stretching in cylindrical folds.

Boudinaging has occurred locally where thin quartz arenite beds are present within a thick sequence of phyllitic pyroclastics. The boudins are 5 - 10 m thick and 10 - 50 m long and are spaced at intervals of several hundred metres. Internal sedimentary structures are well preserved within the boudins, but extension and brecciation is marked towards their extremities.

There is little evidence for post-D_2 folding although local crenulation and kink folding of the S_2 fabric has been observed (Fig. 4.7). The kink folding is limited to ash tuffs in the area north of Ndikwe Store and comprises 1 cm wide kink bands spaced at 10 - 30 cm intervals. The banding is sub-parallel and forms an anastomosing network on some exposed S_2 surfaces. Ramsay (1967, p. 440) considers this type of folding to be a product of flexural slip as a result of compressive stress acting along the layering.

Plots of S_2 and L_2 measurements have been prepared in an attempt to identify post-D_2 folding. These diagrams (Fig. 4.8) show some dispersion of L_2 lineations, but do not define clearly any arc or cone segments which may be ascribed to D_3 folding.

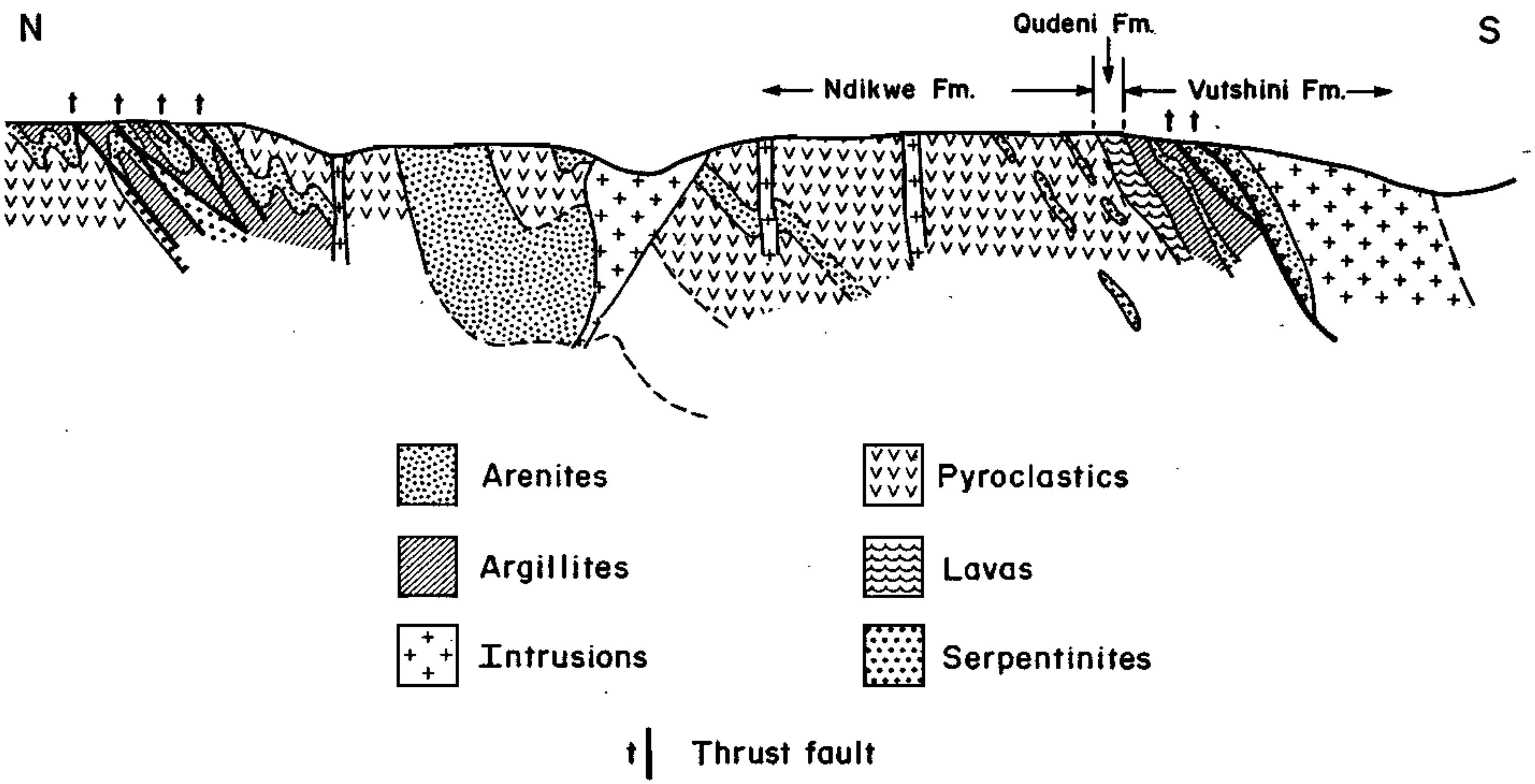

Figure 4.5 Cross-section through the north limb of the Gem Syncline showing thrusting within the Vutshini and Ndikwe Formations. Not to scale.

Post-D_2 faulting is common within the study area and consists essentially of east-west and north-south trending generations of normal dip-slip faults. The north-south faults are commonly displaced by the east-west generation. Several of the north-south faults in the upper Nsuze Valley have been the locus of plagioclase porphyry dyke intrusion, after the main displacement occurred but prior to the later east-west faulting event. The throw on these faults is seldom greater than 10 m, with the exception of the fault along the Nsuze River east of Hlagothi Mountain, which has a downthrow of at least 150 m to the west.

The east-west trending faults are of post-Karoo age in at least two examples although there are other cases where the displacement cannot be traced into Karoo strata. The two definitely post-Karoo examples are situated north of the Ndikwe Store and north of Hlagothi Mountain. The downthrow on these faults is to the south and north respectively, resulting in a horst-type structure now represented by Itala Mountain. There is some evidence that these faults were active prior to Karoo times in that they are the locus of intrusion of diabase and syenite in the upper Mhlatuze and Igozweni Valleys.

3. Metamorphism

The Nsuze Group, Nondweni ultramafics, Hlagothi Complex and the pre-Natal Group dykes have all been subjected to regional greenschist facies metamorphism.

Minerals recognized in the various rock types are detailed in Table 4.1. The major parageneses are all unequivocally of low grade of greenschist facies origin. According to Winkler (1974, p. 73), the beginning of low grade is defined by the paragenesis:

Chlorite + zoisite/clinozoisite ± actinolite ± quartz

This paragenesis is common in the Nsuze Group sediments and volcanics, as well as in the metagabbros of the Hlagothi Complex and post-Nsuze dykes. Meta-ultramafic rocks of the Hlagothi Complex and Nondweni Group have the paragenesis:

Chlorite + tremolite + talc ± magnesite ± serpentine

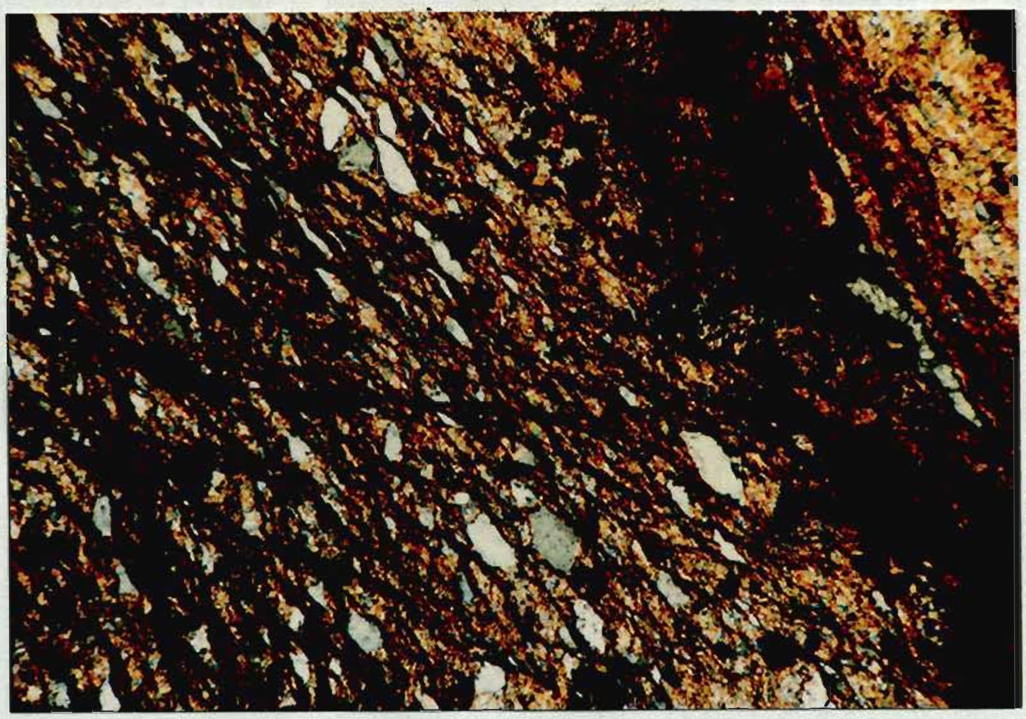

Figure 4.6 Photomicrograph of post-D_2 cleavage (horizontal) cutting across S_2 fabric. Metapelite of the Ndikwe Formation south of Ndikwe River. 63x magnification

Figure 4.7 Photomicrograph of kinking of S_2 foliation in tuff from the Ndikwe Formation north of Ndikwe Store. 10x magnification.

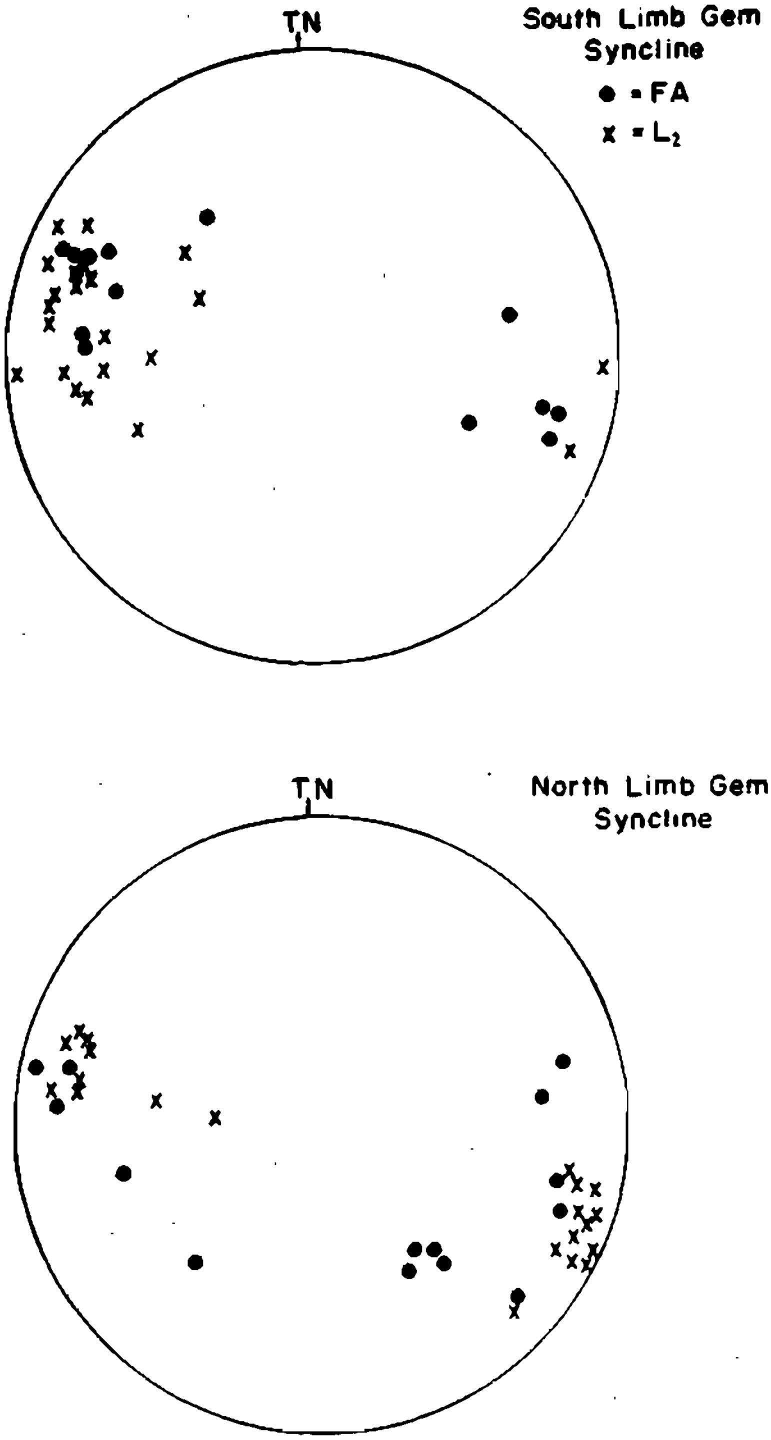

Figure 4.8 Schmidt net plots of L_2 lineations and F_2 fold axes for the north and south limbs of the Gem Syncline.

The upper limit of low grade, greenschist facies metamorphism may be defined on the basis of appearance of hornblende, oligoclase, almandine and cordierite. None of these minerals is present in the study area, although garnet is present in a sample of metapelite from Vuleka. The small, colourless, subhedral crystals are probably manganiferous pyralspitic garnet. Garnet of this composition may form at relatively low temperatures and pressures within low grade metamorphic terranes (Winkler, 1974, p. 209). Miyashiro (1973) considers the lower limit of spessartine stability to be about 400°C. Stilpnomelane has not been recognized within the study area. Several likely samples were examined by X-ray diffraction methods, but in all cases the mineral thought to be stilpnomelane was identified as biotite. Tainton (1977) and Bühmann (1983, pers. comm.) have found stilpnomelane in Nsuze Group metapelites east of the study area. The metamorphic grade of the study area is, therefore, considered to exceed the isograd:

(Stilpnomelane + muscovite). out/(biotite + muscovite). in

The timing of the metamorphism is not readily determined although there is evidence for several episodes. Muscovite is present in the earliest recognized cleavage in pelitic rock types. There is, however, no other evidence for pre-D_2 metamorphism. The main development of greenschist facies mineralogy probably accompanied D_2 folding in which a strong penetrative foliation developed. This fabric is defined by orientated phyllosilicates and tremolite.

That this metamorphism has also affected the Hlagothi Complex is demonstrated by the local development of an S_2 fabric in serpentinitized and talcified parts of the complex. In the unfoliated gabbros the tremolite - saussurite - chlorite mineral assemblage (Chapter 7) predates the growth of very fine tremolite crystals which display a preferred orientation. The earlier mineral assemblage may reflect a metamorphic event prior to D_2 deformation. Another possibility is that deuteric alteration and metamorphism have combined to produce the observed mineralogy (Chapter 7).

TABLE 4.1 METAMORPHIC PARAGENESES AND OTHER MINERALS IN ROCKS OF THE NONDWENI, NSUZE GROUP AND PRETECTONIC INTRUSIONS

	Chlorite	Tremolite/ Actinolite	Biotite	Clino zoisite	Epidote	Calcite	Quartz	Muscovite	Albite	Talc	Serpentine	Magnesite
Nsuze Group:												
Pelites[1]	xx	x	x	xxx	xxx	xx	*	xxx	x	-	-	-
Tuffs	xxx	xx	xx	x	xx	x	*	x	x	-	-	-
Arenites[2]	x	-	x	xxx	xxx	x	*	xx	-	r	-	-
Volcanics	xxx	xx	xx	xx	xxx	x	xxx	x	xxx	-	-	-
Nondweni Group:												
Ultramafics	xxx	xxx	-	-	-	-	-	-	-	xxx	x	xx
Hlagothi Complex:												
Metaperidotites	xxx	xxx	x	-	-	-	-	-	-	xx	xx	-
Metapyroxenites	xxx	xxx	x	-	r	-	-	-	x	x	x	-
Metagabbros	xxx	xxx	x	xx	xxx	-	r	r	xx	r	-	-
Intrusions:												
Plag porphyry	x	xxx	x	x	x	-	x	xx	xxx	-	-	-
Gabbros	xx	xxx	x	r	x	-	r	-	xx	-	-	-
Pyroxenites	xx	xxx	-	-	r	-	-	-	-	xx	x	-

Key to *Abundances*:

r = rare

x = present in 25 - 50% of samples examined

xx = present in 51 - 75% of samples examined

xxx = present in 76 - 100% of samples examined

* = present in all samples

NOTES: 1. Garnet (spessartine) recognized in one sample.

2. Calcite present in all metacarbonates and calc-arenites.

A relatively young metamorphic event may also have occurred. Plagioclase porphyry dykes which intrude along post-D_2 fault planes (thus post-dating the main greenschist facies metamorphism) have the mineral assemblage:

Albite + zoisite + epidote + actinolite + chlorite

This paragenesis is typical for greenschist facies metabasites. However, this metamorphism was not accompanied by penetrative deformation, for there is a total lack of foliation in these dykes. Thus, the possibility of a third greenschist facies metamorphism cannot be discounted.

CHAPTER 5

SEDIMENTOLOGY OF THE NSUZE GROUP

1. General

Sedimentary rocks account for over 60% of the stratigraphic thickness of the Nsuze Group in the study area. An attempt has been made to identify the dominant sedimentary facies and facies assemblages in order to provide an insight into the geological evolution of this southern part of the Pongola depository.

Several measured sections were described in detail for areas where the preservation of sedimentary structures and textures has been adequate. The sections are limited to areas of continuous outcrop where tectonic deformation has not been excessive. Their localities are shown on maps 2, 3 and 4. In the Ndikwe Formation, the considerable disruption of the sequence by intrusions of the Hlagothi Complex prevents the investigation of continuous sequences. This necessitated the use of numerous short sections for which the relative stratigraphic position in the formation is not well established. Few data were collected for the Mdlelanga Formation in the Central Nsuze Syncline as diagenetic and metamorphic effects have obliterated most of the primary textural characteristics of the sequence.

Detailed facies definitions are avoided below, partly because the facies vary slightly in different facies associations, but also because of poor lateral control of facies interrelationships which precludes detailed sedimentological analysis in the present study.

2. Dominant Sedimentary Facies

(a) Medium-scale Cross-stratified Sandstone (S_A)

Sandstone units thicker than 1 m with planar and trough cross-stratification are ascribed to facies S_A. The sandstones range from extremely pure quartz arenites to quartz wackes and quartz arkoses. Grain sizes vary from very fine to very coarse, but are most commonly fine to medium. Facies S_A ranges in thickness from 1 to 50 m, and cross-strata set heights range from 5 cm to 1.20 m. Upper and lower boundaries of the facies are of several types including planar or irregular scour surfaces, gradational or abrupt non-erosive transitions.

The planar cross-stratification is either angular or tangentially based. Angular based cross-stratification (Fig. 5.1) occurs in individual, compound or multiple sets. Individual sets are of tabular form and diminish in thickness laterally over several metres at low angles. The foresets are rarely graded and more typically consist of alternations of slightly different grain sizes. Regressive ripples are uncommon. Tangentially based cross-strata are generally ungraded. They display characteristic changes in foreset slope angle within single sets (Fig. 5.2). Reactivation surfaces may be present in either type of planar cross-stratification (Figs 5.1 and 5.2).

Trough cross-stratification is present in many facies S_A units. There is a continuum of widths and depths, ranging from very broad, shallow troughs to narrower features of much smaller radius of curvature. The depth of individual troughs is generally between 2 and 30 cm. Evidence for both lateral and vertical accretion is present, and adjacent troughs may show accretion in opposing directions. Small current or oscillation ripples are commonly observed in the troughs where bedding surfaces are exposed (Fig. 5.3).

All three of the above cross-stratification types are found commonly in a single sandstone body. The planar cross-strata in many outcrops show opposed directions of transport, both in immediately adjacent sets (as herringbone cross-stratification) and in sets separated by trough or horizontal stratification (Fig. 5.4).

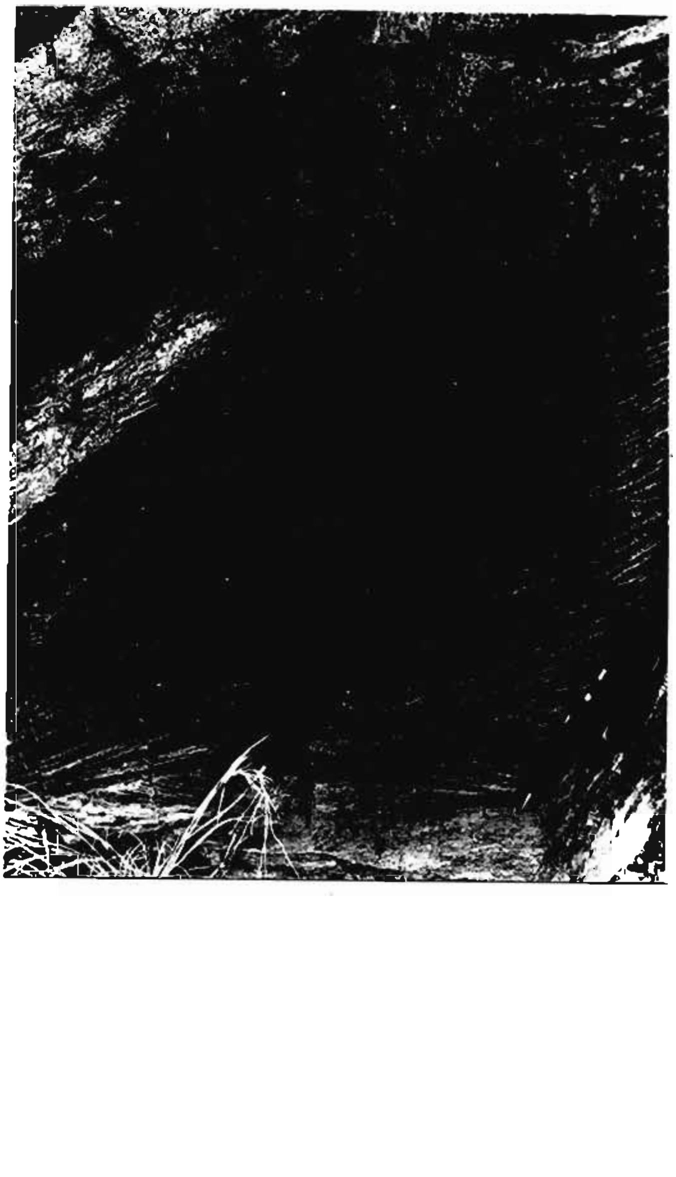

Figure 5.1 Angular based planar cross-stratification (centre) of facies S_A. Note reactivation surface below centre, recumbent foresets in upper half. Ndikwe Formation east of Hlagothi Mountain. Pen is 15 cm long.

Recumbent foresets and water escape structures are common in these sandstones. The former are either smooth overturns of the upper parts of the foresets in a downcurrent direction (Fig. 5.1), or a more irregular but generally continuous folding of the foresets (Fig. 5.5). Water escape structures are present as vertically orientated disruptions of the stratification by small pipe-like channelways or more diffuse disturbances (Fig. 5.6). Some of these structures may be traced upwards for several metres in the sandstone.

Interpretation

Medium-scale cross-stratification results from the migration of bedforms of appropriate size in response to hydraulic conditions encountered in several environments. On its own cross-stratification is not diagnostic of specific depositional settings, but associations of different types of cross-strata are of greater significance.

Planar cross-stratification forms as a result of dune, megaripple or sand bar migration in fluvial, marine or aeolian environments. The accretionary foresets result from flow separation in the lee of the bedform, with flow reversal moving sediment up the lee face. Higher current velocities lead to deposition farther from the lee fall and favours tangentially-based cross-stratification. Graded, avalanche foresets result from migration of smaller superimposed bedforms across the upper surface of the large body. As the small bedforms migrate over the brink point of the sandwave, the coarser detritus from interripple troughs cascades down the lee face first, followed by the finer sand making up the body of the ripples. This process occurs in both fluvial and marine environments.

Reactivation surfaces imply interruption of the migration of a bedform owing to changes in hydraulic regime. In fluvial settings this results from a change in flow direction or depth for a period, during which the shape of the bedform is modified, followed by a resumption of normal conditions

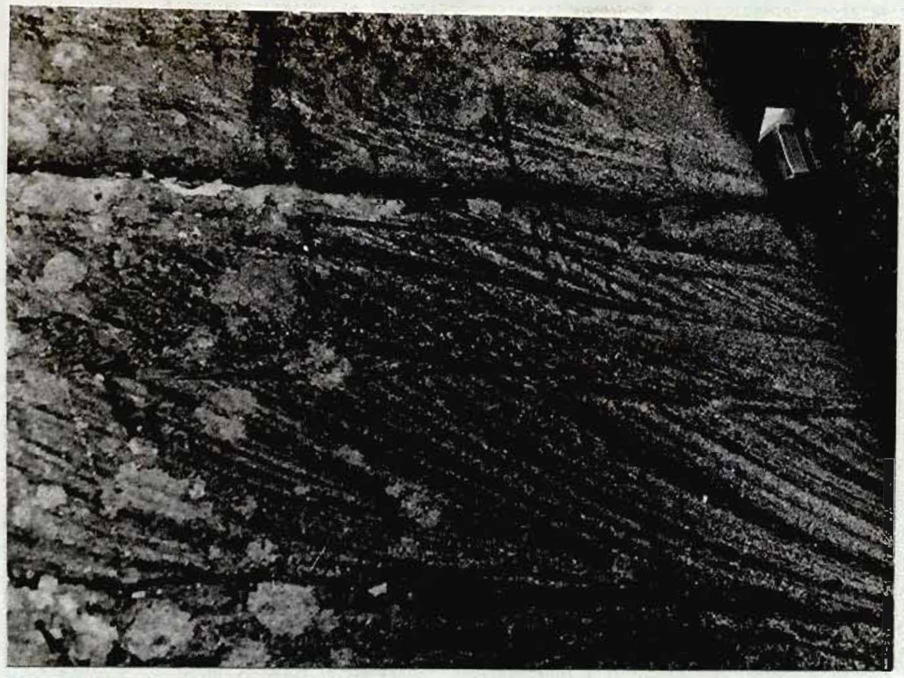

Figure 5.2 Tangentially-based cross-stratification in facies S_A, Mdlelanga Formation, due west of Vuleka. Note current reversals in centre and reactivation surface, arrowed. Box is 35 mm long.

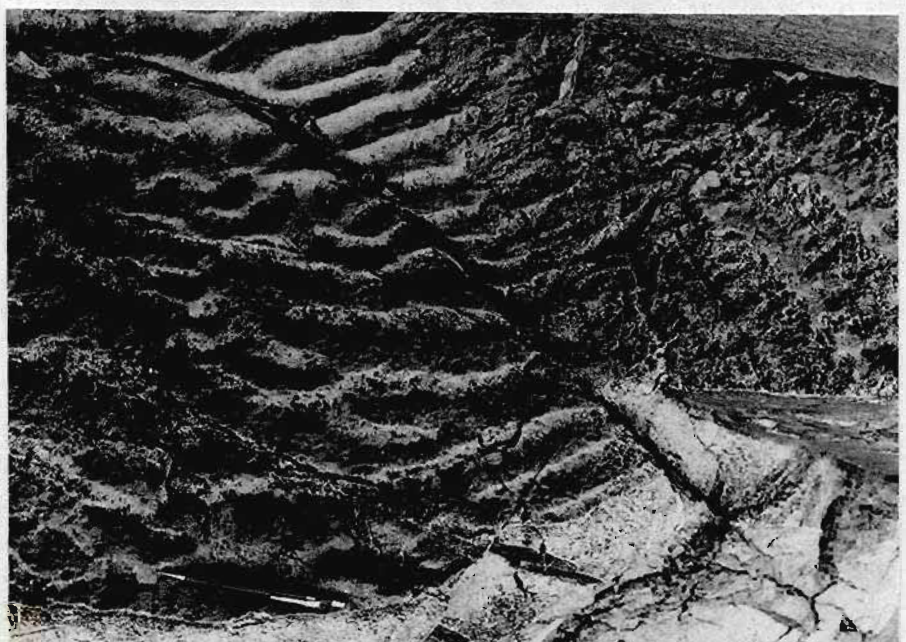

Figure 5.3 Bedding surface exposure of shallow trough in facies S_A, Ndikwe Formation south of Hlagothi Mountain. Note ripples superimposed on trough surface. Pen is 15 cm long.

Figure 5.4 Herringbone cross-stratification showing sharp set boundaries and reversed palaeocurrent directions. Mdlelanga Formation, west of Vuleka. Pen is 15 cm long.

(Collinson, 1970). In a marine environment, tidal flow reversals can produce reactivation surfaces (Klein, 1977a, b). Similarly, herringbone cross-stratification reflects switches in flow direction which are most common in tidal settings (Klein, 1977a, b).

Recumbent foresets are the result of either liquefaction of the sand (Allen, 1970) or an increase in drag at the interface of the water and bedform (Reineck and Singh, 1980). In this facies, the former case is supported by the presence of water escape structures, whereas the alternative process finds support in the presence of sedimentary structures indicative of high sediment load. These are horizontal, and climbing-ripple laminations which commonly overlie recumbent foresets in the study area (Fig. 5.1). The crenulated foresets are probably a result of compaction.

(b) Sandstones with Low-angle Cross-stratification and Horizontal Lamination (S_B)

This facies consists of fine- to medium-grained mature sandstones, 0.5 to 20 m thick, in which low-angle, planar cross-stratification and horizontal lamination are the dominant structures. Thin clay drapes are commonly present as are rip-up clasts and thin coarse-grained sandstone lenses.

The horizontal laminae are 1 mm to 1 cm thick, laterally continuous units which are parallel in planar or slightly sinuous configurations (Fig. 5.7). Grading from medium to very fine grain sizes characterizes some units of this facies. Horizontal lamination has been observed to change laterally to inclined or planar cross-stratification.

The low-angle planar cross-stratification occurs in sets up to 2 m thick. Foreset-bedding angles are typically 5 to 10° but may be variable within a single set. Very small-scale planar or trough cross-stratification is common within the foresets. The small planar foresets are overturned in many places. Set boundaries are defined typically by very low-angle truncations by the overlying set, reflecting slight changes in three-dimensional orientation of the foresets.

Figure 5.5 Overturned foresets in facies S_A, Vutshini Formation, Mhlazi Valley south of Ndikwe. Hammer is 40 cm long

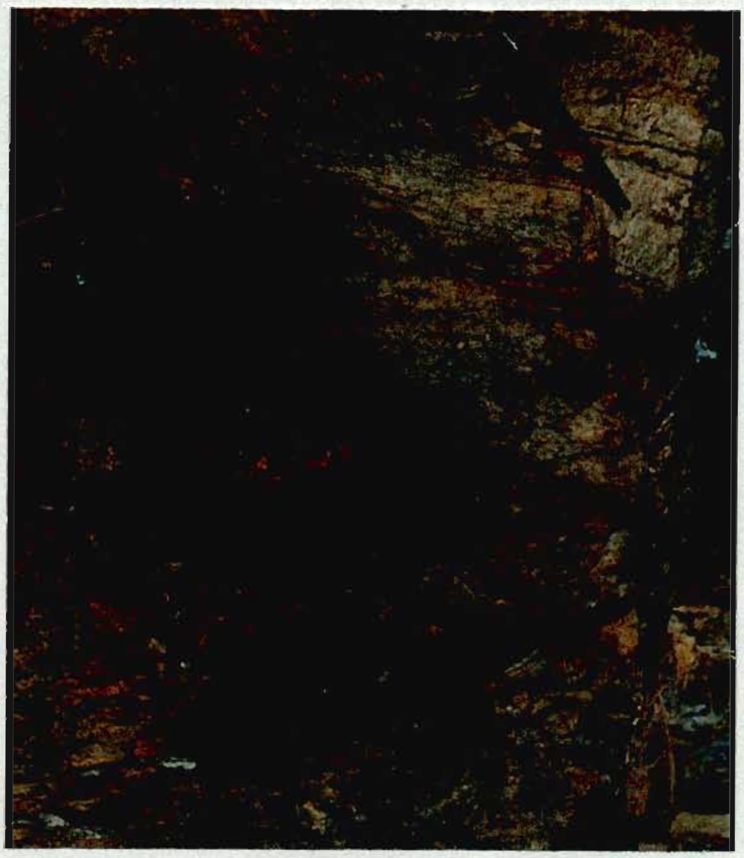

Figure 5.6 Water-escape structure, facies S_A arenites, Vutshini Formation, Mankane Valley. Pen is 15 cm long.

Facies S_B commonly has gradational upward transitions into facies S_C (Fig. 5.8). The basal contacts are generally sharp or erosive with development of thin pebble lags (Fig. 5.7).

Interpretation

Horizontal lamination and low-angle planar cross-stratification are generally considered the products of different processes. Reineck and Singh (1980) recommended that the structures be distinguished wherever possible. However, in the study area, they are commonly in close association which suggests a related origin. Furthermore, the two structures are not readily distinguished from each other in small or poor outcrops.

Horizontal lamination is formed under both upper and lower flow regime conditions. Lower flow regime plane bedding or lamination is not favoured because it is restricted to sediments coarser than 0.6 mm mean grain size and results in very low rates of accumulation of sediments of low survival potential (Harmes *et al.*, 1975). However, Klein (1977a) included lower flow regime plane bedding in his tidal bedload process-response model. Horizontal lamination occurs in ephemeral stream deposits (Pickard and High, 1973; Tunbridge, 1981). Middleton and Hampton (1973) suggested an association of this structure with turbidites, and more specifically, with migration of long wavelength antidunes. Smith (1971) observed horizontal lamination developing from low-angle sand waves in very shallow water under lower or transitional flow regime conditions. A generally accepted, single mode of origin for these structures does not exist, although the most commonly cited mechanism is deposition from sediment-laden water at high flow velocities on plane beds in water depths deep enough to prevent the formation of in-phase waves (Harms *et al.*, 1975).

Large, low-angle planar cross-stratification has been ascribed to various sedimentary processes. Beach and longshore bar cross-bedding are probably the most commonly recognized low-angle planar cross-strata. Beach surfaces

Figure 5.7A Planar bedding in arenites of the Vutshini Formation, central Nsuze Syncline. Note local low-angle attenuation.

B Plane bedding in Mdlelanga Formation, Nsuze River valley. Note structureless basal part with numerous intraformational mud clasts. Lamination becomes progressively clearer upwards. Pen is 15 cm long in both figures.

characteristically dip seawards at 2 to 10° and are laterally continuous, planar surfaces. The internal structure of beach deposits consists of evenly laminated sand, analogous in most respects to horizontal lamination. Seawards-dipping faces of longshore bars are similar and consist of low-angle (4 - 5°) cross-strata in tabular, wedge-shaped units (Reineck and Singh, 1980).

Ancient low-angle cross-stratification of the Beaufort Group has been related to a high sinuosity fluvial environment by Turner (1981). He postulated high velocity, sediment-laden currents in which the settling rates of saltating grains are considerably reduced. This results in suppression of sand wave relief, which produced long wavelength, low-angle bedforms. Parallel-laminated sand-dominated deposits have been interpreted as products of ephemeral stream flooding (Tunbridge, 1981).

Hummocky cross-stratification, according to Harms (1975), is characterized by low-angle, erosional lower bounding surfaces overlain by nearly parallel laminae. Scattered dip directions and low-angle truncation are noteworthy features of this type of bedding. Harms (1975) recognized a shoreline origin for these structures where deposition on low swales and hummocks is related to fluctuations in tidal energy.

(c) Cross-laminated Sandstone Facies (S_C)

Very fine-grained and fine-grained sandstones characterized by ubiquitous micro-cross-stratification are ascribed to facies S_C. These sandstones, which are probably quartz arenites, are typically 20 - 100 cm thick and less commonly several metres thick. Recrystallization has obscured most of the original textures. Thin drapes of green clay are commonly present on the ripples.

Sedimentary structures present include climbing-ripples, wave-ripples and current ripple cross-laminations. In and out of phase climbing-ripple

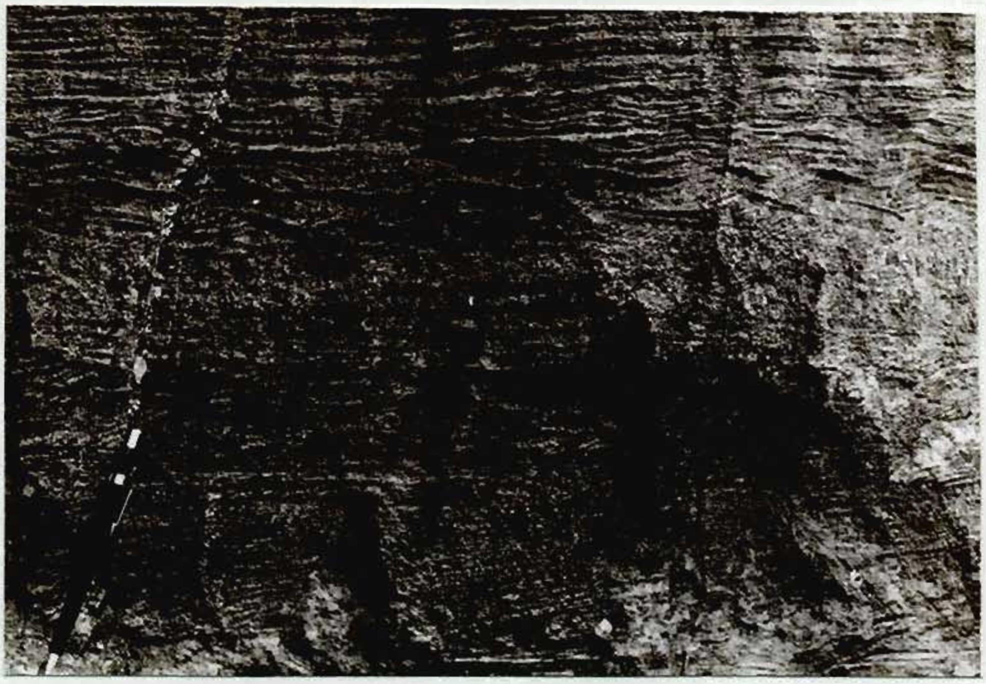

Figure 5.8 Ripple cross-lamination in facies S_C, Ndikwe Formation east slope of Hlagothi Mountain. Note climbing ripples (in phase) in upper part of photograph. Plane lamination is also present. Pen is 15 cm long.

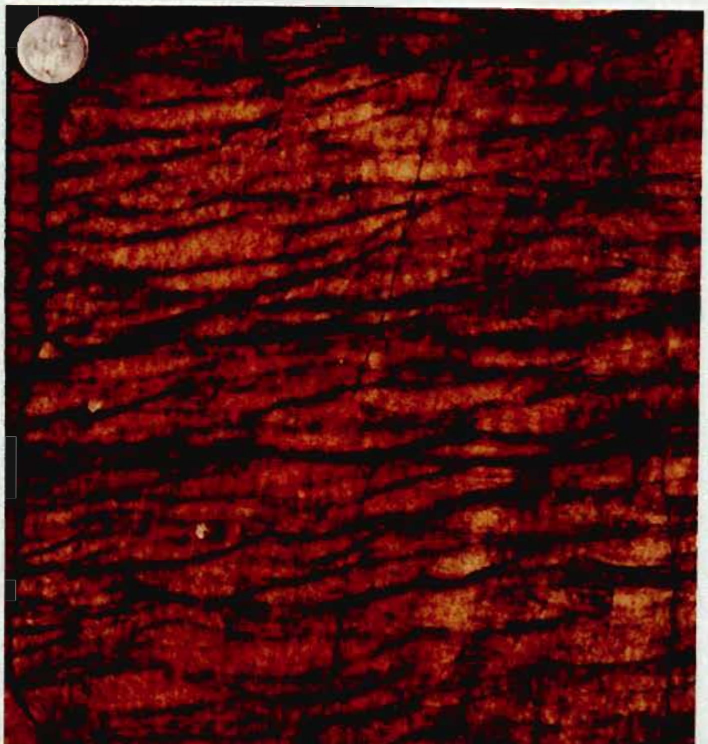

Figure 5.9 Wave ripple cross-lamination in facies S_C, Ndikwe Formation, Nsuze Valley west of Ndikwe Store. Coin is 20 mm in diameter.

lamination is present, commonly in association with horizontal lamination. Intricately interwoven trough lamination is common (Fig. 5.9) and closely resembles the wave-ripple lamination described by Boersma (1970, cited in Johnson, 1978). Planar cross-lamination is also present in many units of this facies. Interference ripples are common on bedding surfaces and display a variety of forms. These are described in more detail below.

Interpretation

Ripple cross-lamination is the product of deposition in small bedforms typically generated by currents of low Froud number in the lower flow regime. Oscillatory currents produce symmetrical ripples which result in wave-ripple cross-lamination. However, wave-ripples or symmetrical ripples can also develop from unidirectional current action.

Climbing-ripples result from simultaneous vertical accretion and lateral migration of current ripples. In-phase climbing-ripples may represent high rates of sediment fall-out in either flowing or oscillating water. The change from in-phase to out-of-phase climbing-ripples results from increased current velocities and rates of deposition (Harms *et al.*, 1975). These structures have been recognized in several sedimentary environments, especially overbank and flood plain deposits (McKee, 1966), deltaic settings (Coleman and Gagliano, 1965) and in turbidite sequences (Walker, 1969). They may be locally important in tidal settings (Wunderlich, 1970) but are not always present.

The interference ripples are worthy of further comment. Most examples in the study area display two prominent directions of ripples which intersect at 70 - 90°. The small size of many of the interference ripples on horizontal planar surfaces probably implies an origin in very shallow water. The change in direction of oscillation responsible for interference wave ripples could be a result of either changes in direction of winds blowing over shallow ponds or of different ebb and flow tidal paths. Within a tidal setting, small waves may be propagated in different directions by the breaking of large waves at different points along a curved foreshore. Where small ripples are superimposed on linear mega-wave-ripples with orientations at close to 90° "ladderback" ripples are produced (Fig. 5.10). These reflect wave generation of the larger ripples, whereas the smaller, superimposed ones result from drainage currents moving nearly parallel to the shoreline (Davis, 1978).

(d) Large-scale Cross-stratified Sandstones (S_D)

Sandstones characterized by large-scale planar or sigmoidal cross-stratification belong to facies S_D. Although rare, this facies is recognized in all three of the formations comprising sedimentary rock types.

The sigmoidal cross-strata are up to 3 m in height (Fig. 5.11) in their only occurrence which is in the lower part of the Ndikwe Formation. The sandstones in which they occur are extensively recrystallized which prevents recognition of grain size and grain shape parameters. Internal structures are poorly defined, but small-scale planar and trough cross-stratification and ripple lamination are recognized.

Large-scale, angular-based planar cross-stratification is present at several localities. These sandstones are mature medium-grained quartz arenites and have frequent pebbly and very coarse-grained horizons close to the base. Normal grading is apparent in the lower parts of the foresets. Small-scale internal structures are generally avalanche planar cross-beds and small scour troughs.

Interpretation

Large-scale composite bedforms occur in several environments of which fluvial and shallow marine settings are the most important. Sigmoidal cross-strata may result from the lateral migration of point bars in fluvial and tidal channels. In the present instance there are insufficient data to distinguish between these possibilities, although the association of the sigmoidal cross-

Figure 5.10 Ladderback ripples with local infill of clay. Mdlelanga Formation west of Vuleka. The relief has been accentuated by tectonic shortening. Pen is 15 cm long.

Figure 5.11 Large-scale, sigmoidal cross-stratification of facies S_D, Ndikwe Formation, Nsuze River valley southeast of Hlagothi Mountain. Person at far left is 1,7 m tall.

strata with sediments interpreted as tidal deposits indicates an origin in relatively high sinuosity tidal channels.

The large-scale planar cross-strata also represent composite bedforms, either transverse bars in a fluvial setting or shallow marine sand bars. They may also represent delta foresets. No realistic interpretation can be made on the basis of available data, although this facies occurs exclusively in sequences interpreted as proximal shelf deposits.

(e) Heterolithic Facies - H_A, H_B and H_C

Units in which an appreciable amount of clay-size material is present are classified as heterolithic. Facies H_A has between 75 and 90% sand-sized material which forms beds less than 1 m thick. These alternate with 1 to 10 cm thick argillite units. The facies is usually thinner than 3 m, but locally may attain 10 or 15 m in thickness. The internal structure of the sandstone units may be horizontal or ripple lamination, planar or trough cross-stratification. Basal scour surfaces are rarely present. Clay drapes are commonly present on ripple surfaces. The arenite-argillite contacts are either abrupt or gradational with flaser, wavy or lenticular bedding in the transition zone (Figs. 5.12 and 5.13).

Facies H_B differs from H_A in that sand content is in the range of 50 to 70%. The sandstone beds are thinner than those of facies H_A. Lenticular, flaser and wavy bedding are common (Fig. 5.14), especially the first-mentioned which may make up several metres of this facies within its normal 5 to 20 m thickness.

Heterolithic units having a sand content of 10 to 50% are assigned to facies H_C. This facies occurs as 1 to 10 m thick units consisting of laminated argillites which contain 5 to 20 cm thick, isolated, tabular beds of sandstone. Lenticular bedding is very common, but flaser bedding is less common than in the other heterolithic facies. The same internal structures observed in facies H_A are also present in facies H_B and H_C.

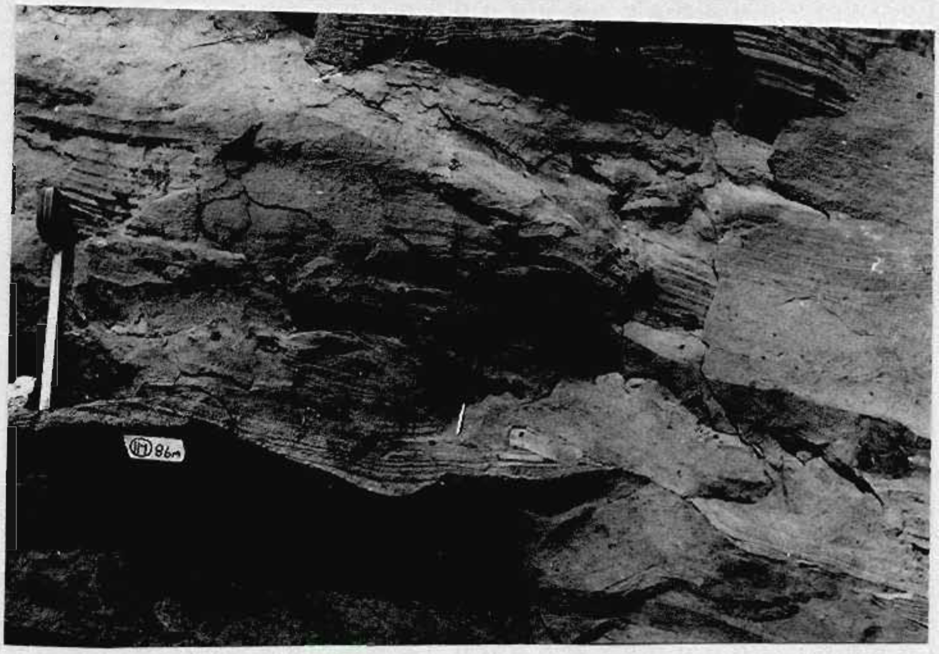

Figure 5.12 Facies H_C and S_B contact in the Vutshini Formation, Central Nsuze Syncline. Note scoured nature of contact and mudclasts (MC) in the arenite. Ruler is 20 cm long.

Figure 5.13 Facies H_A and S_A contact, showing transitional nature with lenticular bedding in the lower part of the arenite (arrowed). Locality as for Figure 5.12.

A notable variant of facies H_b consists of laterally continuous, horizontal or slightly undulose, alternating arenite and argillite laminae. The individual lamina are 3 to 5 mm thick and commonly have normal grading from fine sand to mud (Fig. 5.15). These sediments, which fit the definition of rhythmites (Reineck and Singh, 1980, p. 123), attain a substantial thickness ($\sim$ 50 m) in the Mdelanga Formation in the Central Nsuze Syncline.

Interpretation

Sand and mud accumulation require substantially different hydraulic regimes in that the former is transported as bedload and the latter as suspended load. The intimate association of these two lithologies in the heterolithic facies thus reflects an environment in which variable periods of alternating current or wave activity and slack water occur. The lengths of these periods and the survival potential of their deposits determines the relative proportion of each sediment type in the facies. In the latter regard, water depth can also be assumed to have an influence as deeper water is less likely to be affected by traction currents than shallow water.

Various environmental settings are thought to favour deposition of heterolithic sequences. Lower delta front environments have been invoked for similar sediments of the Ecca Group in the Tugela Valley (Hobday, 1973). Ephemeral streams deposit similar sediments locally (Pickard and High, 1973), but not to any great extent. The tidal environment is, however, the setting most commonly invoked to account for heterolithic sequences (Klein, 1977a, b; Johnson, 1978). In this environment, bedload transport occurs during tidal ebb and flow, with periods of slack water occurring at high and low tides. This model is favoured for all occurrences in this study in view of the considerable vertical and lateral extent of units of this facies.

The alternating sand-mud laminated variant of facies H_C resembles the longitudinal bedding of Reineck and Singh (1980) and the tidal "pinstripe" bedding of Wunderlich (1970). Its association with the other heterolithic

Figure 5.14 Lenticular bedding in facies H_B, Mdlelanga Formation east of Vuleka. The sequence, although distorted by loading or tectonic deformation, shows excellent preservation of planar micro cross-stratification within the arenaceous layers. Pen is 15 cm long.

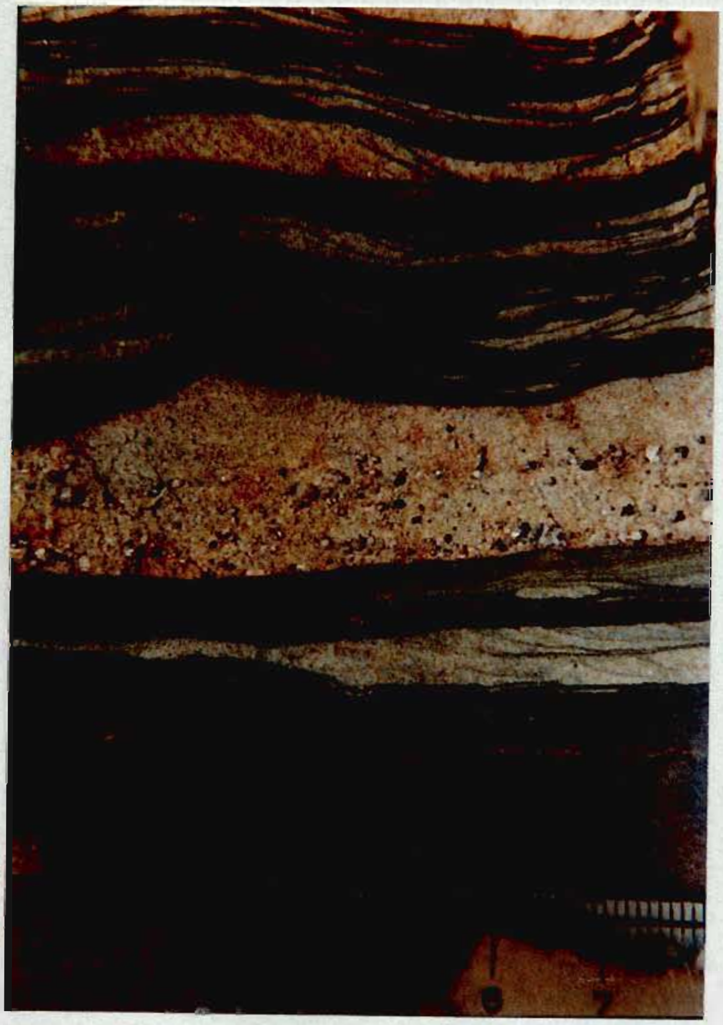

Figure 5.15

Lenticular, wavy and flaser bedding in facies H_B, Vutshini Formation, north limb of Central Nsuze Syncline. Note the high degree of rounding and sphericity of coarse sediment layer interpreted as a product of storm surge. Scale in millimetres.

facies, which are inferred to be tidal in origin, favours alternating bedload and suspension load deposition in a mid-tidal setting (Wunderlich, 1970; Klein, 1977a).

(f) Massive (M_M), Laminated (M_L) and Ferruginous (M_F) Argillite Facies

Argillaceous rock-types constitute a minor but significant part of the Nsuze Group. Several facies may be defined on the basis of internal structure and composition as set out below. However, in weathered outcrops, the variations are not easily recognized and for argillites of indeterminant type, the symbol M is used without a subscript.

Massive dark grey or black mudstones (M_M) occur as units 1 - 30 m thick. Although rare silty or sandy laminae are present, these rocks are largely featureless. A tuffaceous massive mudstone is present in the Ndikwe Formation and is characterized by an extremely high chlorite content.

The laminated argillites (M_L) consist of alternating silt and mud layers on a variety of scales. Graded beds 1 - 3 cm thick are commonly upward-fining but inverse grading has been observed. Compactional slumping of these units has resulted in the frequent occurrence of complex deformation structures. At some localities chaotic slump units contain intraformational, angular, deformed blocks of argillite or carbonate.

The massive and laminated mudstones are pyritic in some areas. Pyrite occurs as poorly-defined, lenticular stringers of closely-packed millimetre-sized cubes of secondary origin. Locally, sulphides may constitute as much as 25% of the rock.

Ferruginous argillites (M_F) are the most common fine-grained rocks in the Ndikwe Formation but are also present in the other sedimentary sequences. They consist of regular alternations of 1 cm argillite and cherty, ferruginous sediment. These rocks have, in the past, been mapped as banded iron formations (Tunnington, 1981), but their high content of fine clastic material is not in accordance with the definition of cherty banded iron formation.

Interpretation

In modern environments significant mud deposits accumulate in high sinuosity fluvial systems, along muddy prograding shorelines, and in distal shelf and abyssal marine settings (Harms *et al.*, 1975). The interpretation of these modern mud sequences rests largely upon observed environmental conditions, but in ancient deposits the characteristics of associated clastic sediments and the overall geometry of the sequence must be considered before reliable conclusions may be drawn.

The thickest massive mudstones in the study area overlie coarse- to fine-grained sandstones and have ferruginous argillites in their upper parts. Identification of pelagic or abyssal deposits in Archaean rocks is difficult (cf. Selley, 1970) because of the lack of faunal remains and other definitive indicators of water depth. In the present instance the thick, massive mudstones may represent pelagic sediments, but there is some evidence to support a slightly less distal environment. In particular, the vertical association of these sediments with proximal shelf sediments which occur in repeated cyclical sequences indicates a shelf setting. Rare, coarser-grained zones within the argillites suggest that deposition by traction currents or suspension generated by storm turbulence also occurred. Thus a distal to middle shelf setting is favoured for the deposition of these sediments.

The laminated mudstones (M_L) with thin graded units may be ascribed to distal shelf processes of two types with a continuous background suspension deposition superimposed on these effects. Firstly, graded beds of silt and mud may result from periodic high-energy storms producing traction currents at depths where these are not usually present. Coarser sediment than usual may also be held in suspension by turbulence and current activity during these storms. Abatement of the storm results in lower energies, and suspension settling in accordance with Stokes' law produces graded laminae.

Secondly, distal turbidite deposits are characterized by silt to mud-graded units. These have been recognized in several ancient and modern distal delta front and distal shelf sequences (Rupke, 1978) and the graded units may represent deposition of suspension loads or low density turbidity flows.

Interpretation of the ferruginous argillite facies is deferred to the section on facies BIF below.

(g) Banded Iron Formation (BIF)

Facies BIF is common in the Ndikwe Formation, but virtually absent from the remainder of the Nsuze Group. A single occurrence at the base of the Mdlelanga Formation is laterally equivalent to a BIF unit in the Ndikwe Formation and reflects the interfingering of these formations.

This facies is typically 10 - 15 m thick and may be traced for several kilometres along strike. It consists of alternating thin ($\sim$ 2 cm) layers of three different chert types. These are: reddish, haematitic chert, black, magnetite-bearing chert, and white iron-poor chert. The layers are variable in thickness; they may be of equal thickness or of very different thickness. Two scales of layering may be observed in a single specimen, usually consisting of centimetre-scale bands of the three lithologies interspersed with layers which consist of microscopic laminae. The micro-banded layers typically have specularite on parting surfaces.

The cherty BIF may change laterally or vertically to ferruginous argillite with a transition zone characterized by alternating argillite and chert-dominated layers.

Deformation of the banding is common and is typically tight angular and cylindrical intrastratal folding (Fig. 5.16). This deformation is similar to that produced by compaction or slumping in semi-consolidated sediments except for the distribution of the deformation. In areas where the Nsuze Group as a

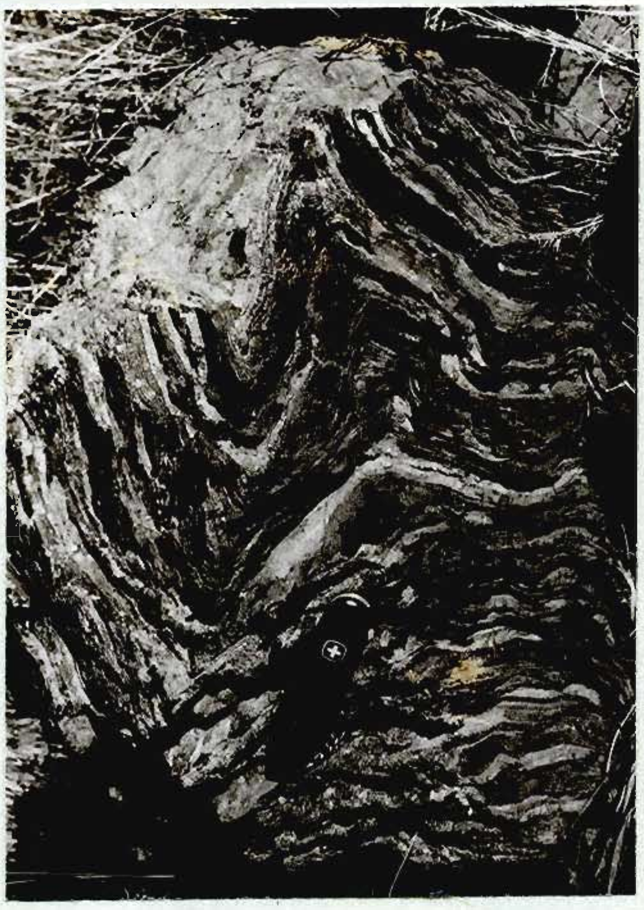

Figure 5.16 Banded iron formation consisting of alternating magnetite-rich and poor cherty banding. Ndikwe Formation, Mbizwe River valley. Penknife is 7 cm long.

whole has undergone tight folding, the BIF shows intense internal deformation. Elsewhere, such as the area north of Itala Mountain, the BIF is relatively undeformed, as is the remainder of the sequence. For this reason, the intrastratal deformation is ascribed to tectonic rather than penecontemporaneous processes.

Interpretation

Argillites in which cherty iron formation occupies the upper, fine-grained part of normally graded units has already been described. Dimroth (1975) observed a similar association in Canadian Archaean sequences. He ascribed the ferruginous cherts to a continuous background precipitation of chemical sediments, interrupted periodically by an influx of clastic material as low density turbidity flows. Thus, a continuum of distal shelf environments may be envisaged for the deposition of facies M_F and BIF. In areas devoid of clastic input, pure cherty banded iron formation forms. The same processes of precipitation occur in more proximal areas, but in these, the volume of clastic input prevents the development of BIF.

This is in general agreement with the conclusion of Watchorn (1978) that banded iron formation and associated argillites of the Mozaan Group were deposited in a distal shelf environment. In contrast, von Brunn and Hobday (1974) demonstrated a high tidal flat depositional environment for jaspilitic iron formations of the Mozaan Group. Thus, the development of banded iron formations in the Pongola Supergroup does not appear to be controlled by the bathymetry of the basin. In this respect and in their haematitic component these sediments have some features in common with Superior type banded iron formation. However, the Ndikwe Formation occurrences are spatially associated with volcanics, are lenticular and are volumetrically not very substantial. These features are more similar to Algoma type iron formation as defined by Gross (1966). It may be that two distinct types of BIF occur in the Pongola Supergroup, but too little is known at present to allow resolution of this problem.

(h) Conglomerate Facies (G_{MS} and G_L)

Two conglomerate facies are recognized primarily on the basis of their sorting and packing characteristics. Facies G_L consists of poorly- to well-packed clasts in a medium- to coarse-grained arenaceous matrix. The conglomerates of facies G_L may be matrix-supported where the matrix is coarse-grained and has primary sedimentary structures indicative of emplacement through current action. Facies G_{MS} consists of clasts of highly variable sizes and compositions scattered in a heterogeneous, largely argillaceous matrix. This facies is described in detail in the section on debris flow and is not discussed further here.

G_L facies conglomerates occur as laterally-extensive, thin (2 - 30 cm) beds, lenticular bodies in troughs, sporadic pebble accumulations on planar erosion surfaces, and as local, thicker bodies. The thickest conglomerates in the study area are those on Driefontein in the Mhlatuze Valley (Map 4). At this locality the base of the Ndikwe Formation is marked by a basal conglomerate between 10 cm and 1 m thick. It consists of subrounded, moderately spherical clasts of white or clear quartz, white granular quartzite and, more rarely, chert. Sorting is apparently good with the development of bimodal clast size distributions. The dominant clast size range is 15 - 40 mm with less common, well-rounded clasts about 1 cm in diameter in the matrix. Granular, siliceous, coarse-grained quartz arenite forms the matrix. This is highly recrystallized which obscures most of the primary textures. Green mica, probably fuchsite, and pyrite are present as accessory minerals. Stylolitic surfaces mark bedding planes and clast-clast interfaces, representative of differential dissolution during diagenesis. At the basal contact with the gneissic tonalite, only the upper parts of the clasts are preserved.

The basal conglomerate is overlain by an upward-fining quartz arenite sequence in which three other conglomerate units occur. These are similar in textural characteristics except that a systematic upward decrease in clast size and bed thickness occurs.

Two laterally-extensive planar units of well-sorted, clast-supported conglomerates 5 - 20 cm thick occur in the Gem syncline area. These are situated at the lower contact of the Vutshini Formation and about 80 m above the base. The conglomerates consist of clasts 0,5 - 3 cm in diameter of white quartzite, striped chert, vein quartz and clear greyish quartz. The clasts are commonly well-rounded and moderately spherical (Fig. 5.17). The matrix is medium-grained, mature quartz arenite in which well-rounded, highly spherical quartz grains are dominant. Heavy mineral lenses are locally present and consist predominantly of ilmenite.

An extensive, but discontinuous conglomerate sheet 0,1 - 1 m thick is present at the base of the Vutshini Formation in the Central Nsuze syncline. This variant of facies G_L is less well packed than that described above. The same clast types are present, but these are subangular and the matrix is generally less mature. Trough-shaped scours are common in this unit and contain more mature conglomerates than the remainder of the sheet. The conglomerate is split into several thinner horizons locally by quartz arenite units of facies S_A.

Thin, sporadic conglomerates are common in the arenites of the Vutshini Formation. These layers are typically one or two clasts thick. The pebbles are smaller than those in the other conglomerates and range from 3 - 10 mm in diameter. They consist of blue, grey or colourless quartz or, rarely, fine-grained granular quartzite. Although locally well packed, these units of facies G_L consist predominantly of dispersed clasts on planar erosion surfaces or shallow trough-shaped scour surfaces.

Figure 5.17 Conglomerate of facies G_L at base of the Vutshini Formation north of Vuleka. Matchbox is 52 mm long.

Interpretation

Rudaceous sediments of the Nsuze group have been ascribed to fluvial processes (Watchorn and Armstrong, 1980) and transgressive marine reworking of fluvial sediments (von Brunn and Hobday, 1974). Within the context of the portion of the Pongola depository under discussion, these two modes of origin require careful evaluation. The basal conglomerates of the Ndikwe Formation show a strong association with trough cross-bedded arenites of facies S_A. This association is also found at the base of the Vutshini Formation in the Central Nsuze Syncline. In the more northerly Gem Syncline the major conglomerates rest on essentially planar erosion surfaces. The sediments overlying the conglomerates are interpreted as marine deposits (see Facies Associations, below), which provides an insight to the origin of facies G_L sheets. Hydrodynamic factors make the deposition of extensive lags in marine settings unlikely unless a transgressive phase occurs. Transgression is essentially an erosive process and results in reworking of the existing sediments at the transgressive boundary. Thus, the facies G_L deposits are possibly fluvial sediments which have been reworked by marine processes. The cases where scour troughs containing conglomerates are present may represent unreworked deposits or tidal channels within the transgressive sequence.

(i) Carbonate Rocks

Carbonates and their silicified equivalents are present near the base of the Mdlelanga Formation. Clasts of carbonate and porous calc-arenite are present in rare, sporadically-developed horizons in both the Mdlelanga and Ndikwe Formations.

The main occurrence is south of the study area in the south limb of the Central Nsuze Syncline and was recognized during regional mapping prior to the start of the present investigation. It consists of a 40 m unit in which chert and limestone occur in a variety of forms. Most of the sequence consists of silicified or cherty, massive limestones except for a 10 m thick unit near the top of the sequence. The lower 8 m of this unit consists of crenulated laminae of alternating cherty and arenaceous sediment. In thin section calcite is observed to form fine stringers along the boundary between the two lithologies. It is recrystallized and is probably a relict of somewhat thicker laminae which have been silicified. This unit bears considerable resemblance to algal mat deposits identified in the Malmani Dolomite (Eriksson, 1977) and Bulawayan rocks in southern Zimbabwe (Martin *et al.*, 1980). The latter authors refer to this structure as "crinkle lamination".

The uppermost 2 m consist of well-defined undulating laminae, which, where observed in plan view, define domical structures. These domes, which are 20 - 25 cm in diameter have superimposed smaller domical structures a few centimetres in diameter. The overall structure, which is persistent for as much as 20 cm vertically in the lamination, is identical to stromatolites from the Nsuze Group described by Mason and von Brunn (1977).

Although no exposures as extensive as the one described above have been found within the study area, carbonate beds and clast horizons are always present at the base of the Mdlelanga Formation. On the north limb of the Central Nsuze Syncline, numerous 10 - 20 cm thick carbonate layers are present in the basal 40 m of the sequence. These layers commonly display crinkle lamination (Fig. 5.18). On the south limb of the Gem Syncline in the Mdlelanga Valley similar, although thinner (2 - 3 cm thick) units are present.

Angular blocks of crinkle laminated impure limestone occur in argillites northeast of Hlagothi Mountain. The blocks are commonly 10 - 20 cm in diameter, but attain 50 cm in some cases. They are scattered through a sequence of chaotically-disrupted banded black and grey argillites interpreted as a submarine slump.

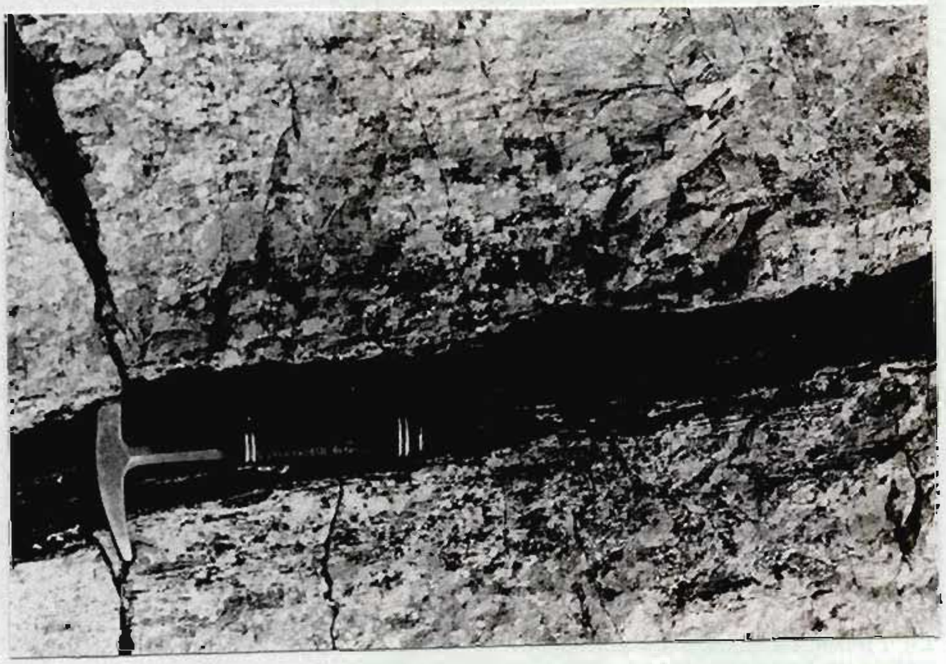

Figure 5.18 Carbonate layer in basal unit of Mdlelanga Formation north limb of the Central Nsuze Syncline, Nsuze River valley.

Interpretation

Stromatolitic limestones in Archaean sequences are usually associated with subtidal or intertidal sedimentary sequences (Martin *et al.*, 1980, Mason and von Brunn, 1977). The same situation applies in the present study where the sediments enclosing limestones are interpreted as being of shallow marine or intertidal origin.

Stromatolites and crinkle lamination result from an accumulation of clastic and carbonate sediment over colonies of blue-green algae in modern rocks. There is evidence to suggest a different form of algae in early Proterozoic and Archaean time (Walter, 1977) but the general principles remain the same. The close spatial association between all Archaean stromatolitic limestones and volcanic rock types (Martin *et al.*, 1980; Mason and von Brunn, 1977), and evident in the present study, is thought to be of fundamental importance to the existence of the early life forms. Mineral nutrients and warmth generated by submarine volcanic activity may have been essential for the existence of the algae which presumably survived by some form of photosynthesis.

The existence of these oxygen-generating organisms during the essentially anaeorobic Archaean has significant implications. The scale on which oxygen production took place was probably insufficient to have any effect on the composition of the atmosphere. It is more likely that this free oxygen was fixed by the precipitation of ferric oxides in the form of haematitic banded iron formation (Cloud, 1973).

As noted above, the carbonates are dominantly limestone rather than dolomite. This fact has been demonstrated using X-ray diffraction analysis and the identification of calcite as by far the dominant carbonate species is unequivocal (Fig. 5.19). This is in agreement with the findings of Martin *et al.* (1980) that the Belingwe greenstone belt stromatolites occur in limestones rather than dolomites.

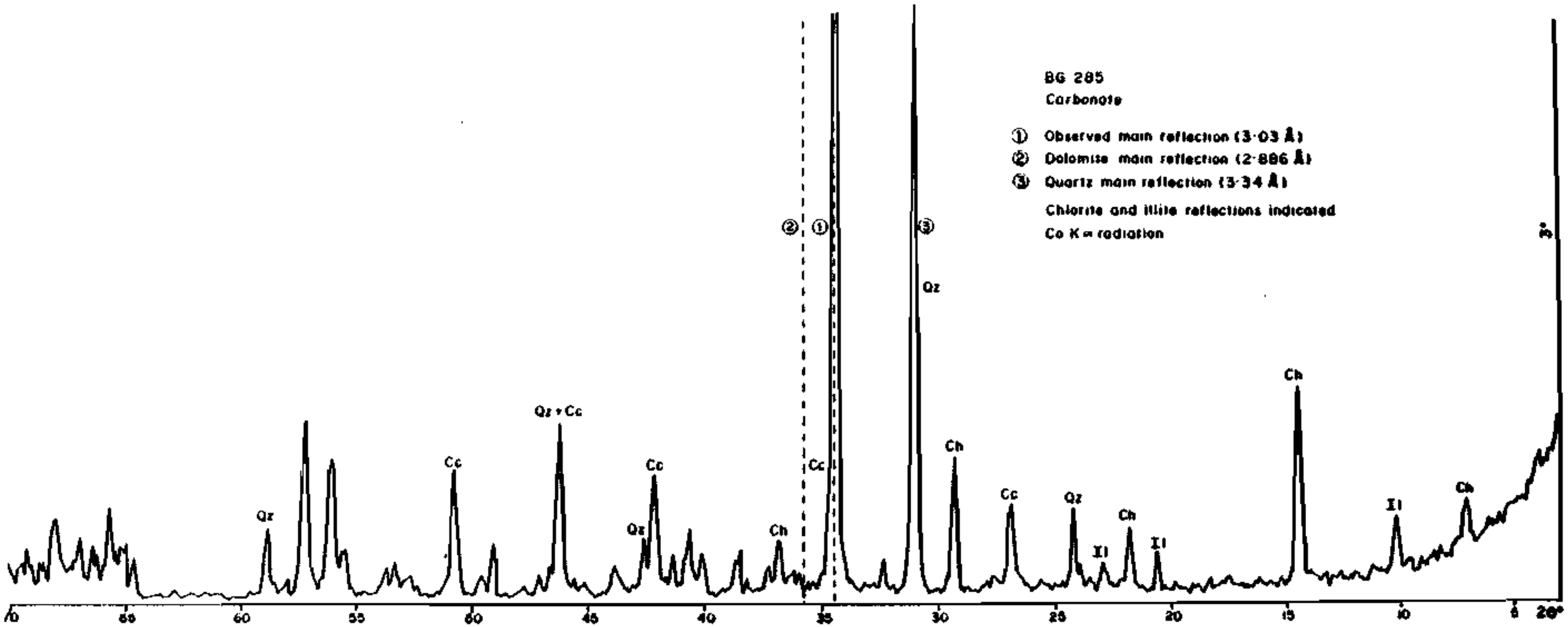

Figure 5.19 X-ray diffractogram for cherty carbonate from the Mdlelanga Formation, locality as for Figure 5.18. The dominant carbonate species is unequivocally calcite as indicated by the position of the main reflection as compared with the peak position shown for dolomite. Main reflection for quartz indicated as reference peak.

3. <u>Sediment Gravity Flow Deposits</u>

Sediment gravity flow encompasses a variety of depositional systems in which sediment transport is achieved by one or more of several support mechanisms rather than simple entrainment of grains by moving fluids. The different support mechanisms, notably dispersion by grain-grain interaction, escaping pore fluids, turbulence or matrix strength, result in different rheologic behaviour and thus produce deposits which vary in parameters such as sorting, stratification and packing. Although multiple support mechanisms commonly occur in a single flow, the dominant process can usually be recognized from the nature of the deposit. The nomenclature and understanding of these sedimentary processes is not yet thoroughly established, although substantial advances have been made recently (Lowe, 1979, 1982; Cook, 1979; Middleton and Hampton, 1973, 1976.) The classification used below is largely after Lowe (1979) and the summary of Weimer (1976).

(a) Turbidites and Slumps: Ndikwe Formation

Sediments with the characteristics of turbidity current deposits are present within quartz arenites and ferruginous and black argillites northeast of Hlagothi Mountain in the Nsuze Valley (Map 4). Within the black muddy argillite, normally-graded silt to mud units are present in sequences 1 - 4 cm thick These are thought to represent distal, low density turbidity flow deposits. This argillite unit is overlain by medium-grained quartz arenite of a subtidal facies association (see later). Within this unit are several incomplete Bouma sequences which typically consist of small-scale planar cross-stratification overlain by climbing ripple and then plane bedding. These units, which are 20 - 30 cm thick, could be interpreted differently but, because of their similarity to the upper part of Bouma sequences and their presence in sediments interpreted as of shallow marine origin, a genesis by low density turbidity flow mechanisms is favoured. Walker (1978) indicated that partial Bouma sequences beginning at the B (plane parallel laminated) or C (ripple or wavy bedded) units occur in intermediate to distal parts of submarne fans. Levees within proximal turbidite environments may also show partial Bouma sequences.

A 1 m thick chaotic slump or cohesive debris flow deposit cuts across the argillite unit containing the graded units. This unit cannot be traced laterally for more than 6 m due to poor outcrop. It consists of randomly orientated, deformed blocks of the banded argillite set in a homogeneous silty mudstone matrix. Carbonate clasts, showing crinkle lamination, are also present. These were probably introduced from a more proximal environment by mass transport mechanisms.

(b) Volcanogenic Sediments: Ndikwe Formation

Resedimented pyroclastic rocks occur in the upper part of the Ndikwe Formation adjacent to the Ndikwe River (Map 2). The sequence, the boundaries of which are obscured, is at least 30 m thick. It consists of crudely stratified 20 - 50 cm thick units of volcanic clasts set in a generally massive, immature sandy matrix. This contrasts with the adjacent lapilli tuffs, which have a chloritic matrix, presumably derived from volcanic ash.

Ash flow emplacement generally takes place by gravity processes analogous to cohesive debris flow and grain flow (Lajoie, 1979). In this sense it is difficult to distinguish, on a process-response basis, between the resedimented pyroclastic rocks and the more normal pyroclastic rock types described in Chapter 3. The distinction made here is based largely upon the difference in matrix composition. A possible interpretation is that progressive winnowing of pyroclastic ash occurred on the flanks of the volcanic pile by traction currents. Periodic oversteepening of the residual pyroclastic debris resulted in slumping, especially when water saturated to produce the crudely stratified units. Earthquakes or tremors may have been the triggering mechanism.

(c) Slumps and Cohesive Debris Flows: Mdlelanga Formation

Lithology

A sequence of matrix-supported conglomerates, greywackes and resedimented ferruginous argillites in the Mdlelanga Formation at Vuleka (Map 2) is attributed to sediment gravity flow processes. The sequence is at least 40 m thick at the eastern extremity of the Vuleka exposures and tapers to about 5 m towards the western limit, along a strike length of 1,5 km.

The sequence is situated in a core of a synclinal structure which, combined with discontinuous outcrop, makes recognition of lateral lithological variations and thicknesses difficult. A crude three-fold subdivision of the sequence is, nevertheless, possible.

The base of the sequence is discordant and transgresses southeastwards across 40 m of tidal sedimentary rocks. Where the contact is exposed, the sedimentary structures in the underlying sediments display considerable deformation. The basal unit is 5 - 20 m thick and is present over the observed strike length of the sequence. It consists of quartz arenite boulders up to 7 m in diameter set in a pebbly, tuffaceous mudstone matrix (Fig. 5.20A). The boulders are rarely in contact with one another and are generally separated by several metres of matrix. Internal sedimentary structures of the boulders are commonly distorted by plastic deformation. In one occurrence the bedding surfaces are folded through nearly 360°. Despite this deformation, the assemblage of sedimentary structures is recognized as including planar, trough and herringbone cross-stratification with rare micro-cross-lamination, clay drapes and plane bedding. These structures, in addition to compositional features, are identical to those of the quartz arenites truncated by the basal contact of the mass-flow sequence. This suggests that the boulders were locally derived, were relatively ductile and only partially consolidated at the time of emplacement.

Figure 5.20A

Block of quartz arenite in debris flow of the Mdlèlanga Formation southwest of Vuleka. The block is 1,7 m in length. It rests in a greywacke matrix. Note the disturbance of internal sedimentary structures.

Figure 5.20B

Tabular clasts of banded chert and cherty iron formation in uppermost unit of Mdelanga Formation debris flow sequence, southeast of Vuleka. The clasts are commonly plastically deformed. Lichen covering at left and top of photograph. Lens cap is 5,5 cm in diameter.

The matrix containing the boulders is extremely poorly sorted and inhomogeneous. Rounded quartz pebbles 1 - 5 cm in diameter occur sparsely throughout the unit, but are locally more concentrated. Sandy and gritty patches are present, but have diffuse boundaries. Dark chloritic particles 1 - 2 cm in length are locally common. Their shape suggests that they represent rip-up clasts. Light grey tuffaceous fragments up to 1 cm in diameter are common near the base of the unit. The remainder of the matrix is a fine-grained greywacke consisting of fine- to medium-grained sand ($\sim$ 40%) and chloritic argillite.

The second or middle unit is a discontinuous graywacke up to 20 m thick, which is compositionally identical to the matrix of the underlying unit. It is distinguished by an absence of clasts exceeding 5 cm in diameter and a local crude stratification. Rare trough cross-stratification is present towards the top of this unit. A single, 15 m long quartz arenite body is present near the upper contact. This body is intensely deformed as indicated by small-scale tight folding along its margins.

The uppermost unit is a clast-supported conglomerate up to 8 m thick, which may be traced for about 150 m along strike. The clasts are angular, elongate or tabular fragments of banded iron formation consisting of alternating haematitic and cherty layers 1 - 5 mm thick (Fig. 5.20B). Clast sizes range from 1 - 15 cm in length and are 0.6 - 5 cm thick. The matrix consists of a poorly-sorted mixture of ferruginous argillite and grains of chert, haematite and subordinate quartz. Lenses of specular haematite 2 mm thick occur locally. A vague horizontal alignment of clasts is apparent locally. Elsewhere the clasts are randomly orientated.

Inferred Mode of Origin

The sequence described above has several characteristics which can be attributed to a combination of three gravity-driven depositional mechanisms.

The variety of clast sizes and lithologies and paucity of bedforms and grading in the basal unit suggest deposition by cohesive debris flow as defined by Lowe (1982). The principal support mechanism in cohesive debris flow is the yield strength of the matrix. Buoyant lift is provided by the high density of interstitial mud which provides considerable support for the larger clasts in debris flows. Boulders as large as those in the basal unit are unlikely to be transported as suspended material unless the matrix had very high viscosity and hence yield strength. Lowe (1972) found that blocks 50 cm in diameter exceed the yield strength and buoyant support in debris flows of the Great Valley Sequence, California. Lowe (1972) concluded that some larger blocks are moved as bedload and are thus likely to be confined to the base of a debris flow. He does, however, document transport of discrete blocks up to 10 m in diameter at the top of flow units in the same sequence, a feature ascribed to buoyant support provided by the mudflows. High sediment cohesion is another critical aspect of cohesive debris flows in that it prevents particle size-segregation (Enos, 1977). In the Vuleka deposits local concentrations of pebbles or coarse sand may reflect local zones of poor cohesion and lower viscosity which allowed some sorting to occur. Alternatively, these pebbles or sandy zones may represent reworking of the debris flow deposits by traction currents.

The middle unit is also interpreted as the product of debris flow sedimentation, although a slightly different mechanism must be invoked to explain the lack of clasts greater than 5 cm in diameter. These debris flows are probably more distal than those observed at the base. Cook (1979) documented variations in debris flow sequences whereby lateral change in dominant transport and support mechanisms may be recognized. "Many flows probably undergo a secular evolution involving changes in the relative effectiveness of a number of support mechanisms. A mass of sediment may fail as a slump, liquify, accelerate and become a turbulent high density turbidity current, and finally slow and resediment as a liquified flow." (Lowe, 1979, p. 180).

Pure laminae or non-turbulent flow of liquified sediment masses is probably a relatively uncommon transport mechanism in flows other than those consisting of cohesionless silt or sand (Lowe, 1979). The middle Vuleka unit has a high mud content and thus may have originated as a series of high density turbidity flows or mud flows.

The upper agglomeratic unit is thought to have formed as normal banded iron formation by processes discussed above. Partial lithification occurred during deposition. This was followed by disruption as a result of pore water overpressures to form the flattened, angular clasts and local resedimentation. Cook (1979) illustrated a similar rock type in which tabular clasts of laminated lime mudstone and greywackes occur in a micritic matrix. He interpreted these deposits as the product of submarine sliding in which the yield strength of an initially plastic flow was exceeded, resulting in fragmentation and deposition by debris flow mechanisms. The conglomerates illustrated by Cook (1979, p. 299) are clast-supported and have a matrix of identical composition to the clasts. These two features are typical of the Mdlelanga Formation agglomerate, suggesting a possibly similar mode of origin.

The probable sequence of events responsible for the Mdlelanga Formation sediment gravity flow deposits is summarized in Figure 5.20C. The available field data are insufficient to allow formulation of a definite depositional model and collection of such data is precluded by the nature and extent of the outcrops.

4. Facies Associations and Sequences

For the purposes of this section a facies association is defined as a recognizably consistent co-existence of several facies. Facies sequences consist of a preferred vertical order in which facies occur. The associations and sequences described below are defined on the basis of several measured vertical

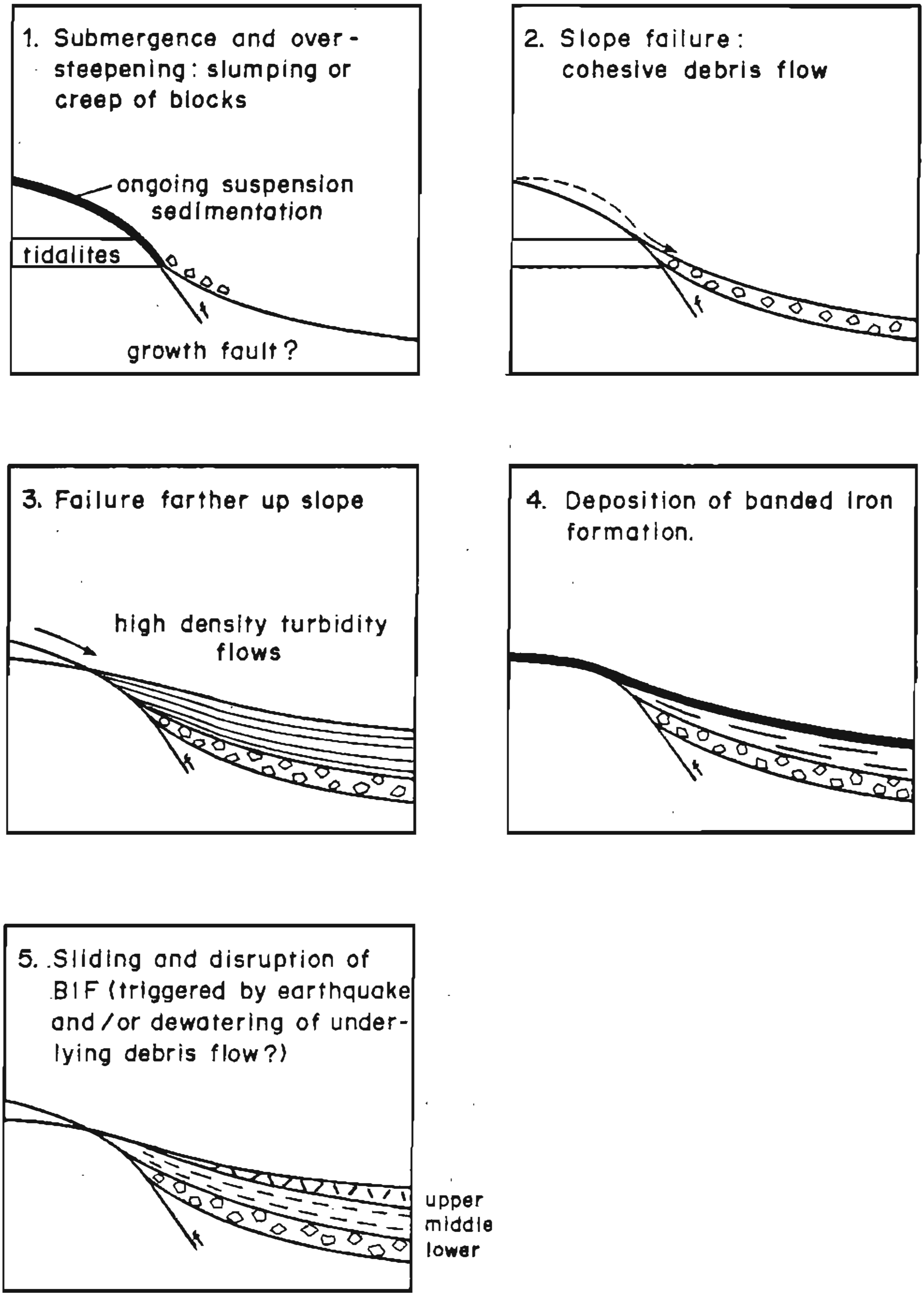

Figure 5.20C Schematic representation of the five stages in the development of the debris flow sequence, Mdlelanga Formation south of Vuleka.

sections through the Nsuze Group. This may be open to considerable subjectivity since the definition of the facies themselves is somewhat subjective. This is one of several points argued by Reading (1978) against the use of statistical methods in defining facies models. Although Markov analysis has been used below, the conclusions reached are not well constrained and must be considered tentative. Nonetheless, the facies associations recognized resemble well-documented depositional models.

The four most prominent facies associations and their areas of occurrence are as follows:

(a) Upwards-fining sequences in all Vutshini Formation outcrops in the Gem Syncline area and the lowest part of the Central Nsuze Syncline consist predominantly of facies S_A and S_B with subordinate occurrences of G_L basal to the sequences (Figs. 5.21 and 5.22). Facies G_L is laterally extensive and ranges from 2 - 25cm in thickness. It is best developed in low relief channels, 0 - 3 mm deep and 10 - 20 m wide, but is continuous over the intervening areas. The overlying S_A facies (5 - 80 m thick) has abundant trough and planar cross-bedding as well as shallow, low relief channels in which thin (1 pebble thick), sporadic, small pebble lags are present. Soft sediment deformation structures are common, generally as recumbent foresets and rarely as water-escape structures. Planar or gently undulating surfaces marked by a 1 - 5 cm thick green argillite unit are common. Facies S_B (0 - 15 m thick) is commonly fine-grained to very fine-grained and is characterized by plane lamination and low-angle, large-scale planar cross-stratification in this facies association. Small-scale cross-lamination is rarely observed, as are wave ripples on bedding surfaces. This facies is not always present. All three of the facies are present in several of the sequences in the order $G_L \rightarrow S_A \rightarrow S_B \rightarrow G_L$. The sequence $G_L \rightarrow S_A \rightarrow G_L \rightarrow S_A \rightarrow S_B \rightarrow S_A$ is not uncommon.

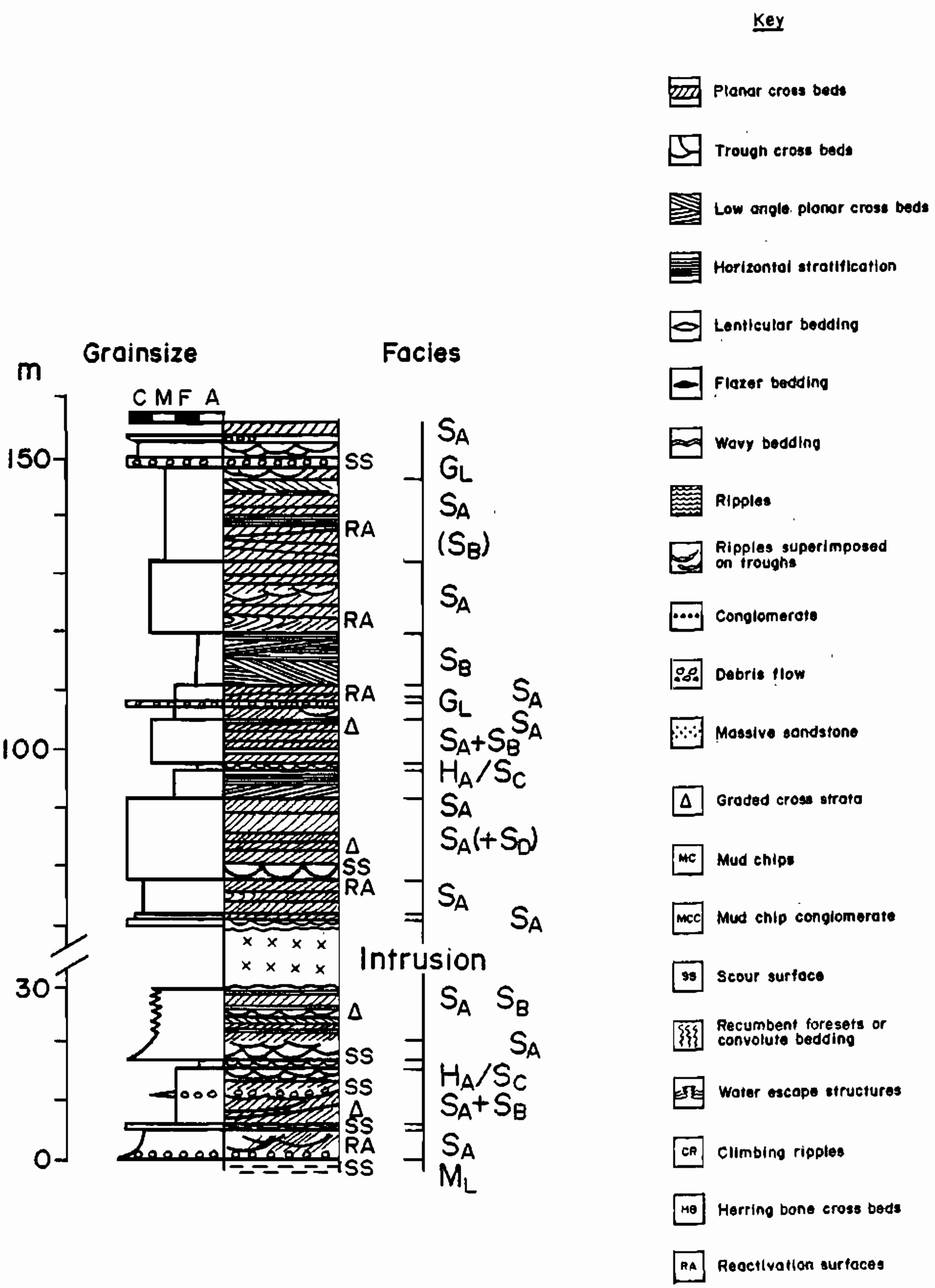

Figure 5.21 Measured section showing vertical facies relationships in the lower part of the Vutshini Formation in the Gem Syncline north of Vuleka.

This facies association and sequence is broadly similar to the prograding tidalite model proposed by von Brunn (1974), von Brunn and Hobday (1976) and Watchorn (1978) in other parts of the Pongola depository. Several major differences exist, including the substantially greater thickness of the cycles, the virtual absence of true mudstones and a complete absence of features such as mudclasts, mud cracks and herringbone cross-stratification. For this reason an upwards-fining, prograding tidalite model is considered inapplicable. The sequence does have many characteristics of shallow marine sediments. In particular, the thin laterally extensive gravel lags are probably best explained by marine transgression, whereas the overlying sandstones may represent migration and aggradation of subtidal sand bodies (cf. Johnston, 1978). This model would require a high rate of accumulation, continuous, slow subsidence and rapid delivery of clastic sediment to the shelf. Some tidal activity probably occurred to account for the shallow channels. A more detailed comparison with existing depositional models cannot be made on the basis of available data.

(b) An association of several arenaceous, heterolithic and mudstone facies is recognized in the Mdlelanga and Vutshini Formations. Two different types of sequence may be distinguished. The first comprises upwards-fining sequences with strong evidence for periodic emergence; the second being essentially random or upwards-coarsening sequences lacking evidence for emergence.

The upwards-fining sequences are present at the base of the Vutshini and within the Mdlelanga Formations in the Central Nsuze Syncline and south of Vuleka respectively (Figs. 5.22 and 5.23). Typically, the sequence has arenaceous facies S_A and S_C at the base with minor sporadic occurrences of facies G_L along or close to the basal contact. Facies S_A has, in addition to the cross-bedding noted in the facies definitions, rare herringbone cross-stratification and ubiquitous reactivation surfaces. An upwards decrease in grain size over

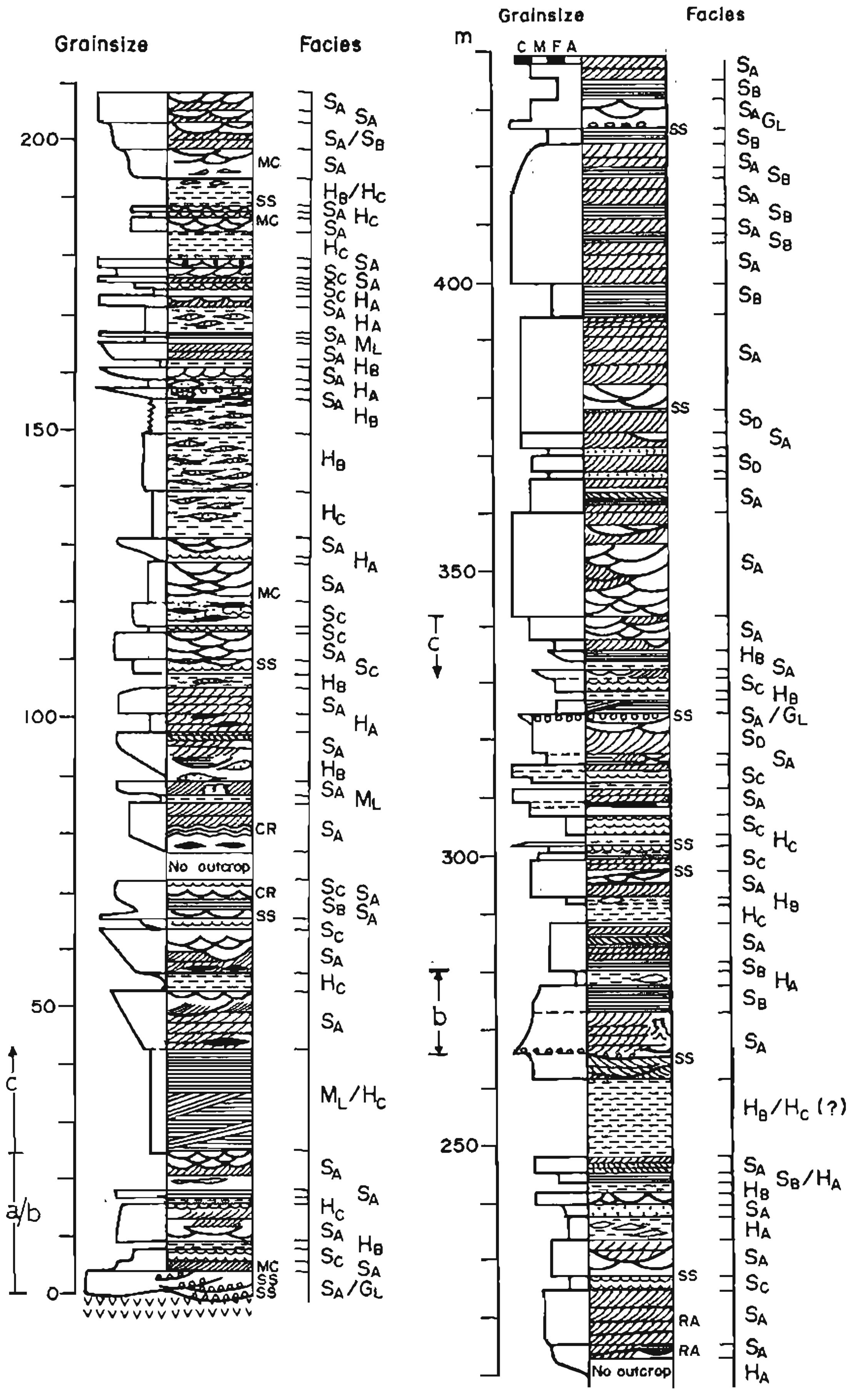

Figure 5.22 Measured section showing occurrence of various facies in the Vutshini Formation, Central Nsuze Syncline. Symbols and ornamentation as in Figure 5.21.

several metres is accompanied by a gradual reduction in the size of the cross-stratification. Facies S_C overlies this unit transitionally as a 1 - 5 m thick micro-cross laminated bed. In the upper part, thin mud drapes are present on the ripple laminae. Superimposed sedimentary structures are common, generally as small wave ripples on troughs or megaripples. The orientation of the ripples is generally oblique or normal to that of the larger bedform. Thicker mud layers are not common, but, where present, may rarely exhibit mudcracks. These mud units are commonly disrupted or scoured (Fig. 5.15). Beds containing mudclasts are common. The remainder of the facies sequence is: $H_A \rightarrow H_B \rightarrow H_C \rightarrow M_L$ in the rare complete vertical sequences. More commonly one or more of the facies is absent.

The upwards-fining facies sequence described above is identical in many respects to the tidal circulation model defined by Klein (1971, 1977a, b) on the basis of numerous modern and ancient sequences interpreted to be products of deposition in prograding epeiric and mioclinal shelf seas. Klein (1977a, b) defines nine groups of sedimentary features and inferred processes which form the basis of the prograding tidal sedimentation model. The characteristics of the Nsuze Group facies association are compared with these groups in Table 5.1. It is apparent that the Nsuze sediments conform to many of the criteria for all of the subenvironments defined by Klein (1977a, b). This alone does not prove a tidal origin, but supports strongly the inference that this facies association represents tidalite deposition. Von Brunn and Hobday (1976) and von Brunn (1974) related sediments from the upper Nsuze Group in areas to the northeast of the study area to prograding macrotidal shorelines on the basis of the Klein (1977a, b) model. Watchorn (1978) recognized an identical facies association in the Mozaan Group in southeastern Transvaal and northern Natal.

(c) The facies association S_A, S_B, S_C, H_A, H_B, H_C and G_L occurs in the Vutshini Formation in the Central Syncline and the lower Mdlelanga and Ndikwe Formations

TABLE 5.1: CLASTIC TIDALITE PROCESS-RESPONSE MODELS (After Klein, 1971, 1977)

TRANSPORT PROCESSES	CRITERIA	OCCURS IN: NDIKWE	MOLELANGA	VUTSHINI	COMMENT
A. Tidal current bedload transport with bipolar-bimodal reversals of flow direction	1. Cross stratification with sharp set boundaries	√	√	√	
	2. Herringbone cross-stratification	-	√	√	Uncommon
	3. Bimodal-bipolar palaeocurrent directions	√	√	√	
	4. Parallel lamination	√	√	√	
	5. Complex internal organization of dune and sand waves	√	?	?	
	6. Supermature rounding of quartz grains	?	?	√	Obscured by recrystallization
B. Time velocity assymetry of tidal current bedload transport	7. Reactivation surfaces	√	√	√	
	8. Bimodal or multimodal frequency distribution of set thickness of cross-strata	?	?	?	Suspected but not measured
	9. Bimodal frequency distribution of dip angle cross-strata	√	√	√	
	10. Unimodal palaeocurrent directions of planar cross-strata	?	-	-	
	11. Orientation of cross-strata parallel sand body trend and basinal topographic strike.	?	?	?	Insufficient data
	Also 5 and 6 above.				
C. Late-stage emergence ebb out-flow and emergence with sudden changes in flow direction at shallow water depths (2.0 m).	12. Trimodal distribution of palaeocurrent directions of planar cross-strata	-	-	-	Insufficient data
	13. Quadrimodal distribution of palaeocurrent data	-	-	-	Insufficient data
	14. Small current ripples superimposed at 90° of obliquely on larger current ripples	√	√	√	
	15. Interference ripples				
	16. Double crested ripples	-	?	-	One occurrence
	17. Flat topped ripples	-	-	-	
	18. Current ripples superimposed at 90° and 180° on crest and slip faces of dunes and sand waves, and cross-strata	?	-	-	One occurrence
	19. "B-C" sequence of cross-stratification overlain by micro-cross-laminae	√	√	√	
	20. Symmetrical ripples	-	-	-	
	21. Etchmarks on slip faces of cross-strata	√	√	?	
	22. Wash out structures				
D. Alternation of tidal current bedload transport with suspension settling during slack water periods	23. Cross-stratification with flasers	√	√	√	
	24. Flaser bedding	√	√	√	
	25. Wavy bedding	√	√	√	
	26. Lenticular bedding	√	√	√	
	27. Tidal bedding	√	√	?	
	28. Convolute bedding	√	√	√	
	29. Current ripples with muddy troughs	√	√	√	
E. Tidal slack water mud	30. As 23 above	√	√	√	

TABLE 5.1 continued

TRANSPORT PROCESSES	CRITERIA	OCCURS IN: NDIKWE	MDLELANGA	VUTSHINI	COMMENT
F. Tidal Scour	31. Mud chip agglomerates at base of wash outs and channels	√	√	√	
	32. Shell lag conglomerates at base of wash outs and channels	-	-	-	
	33. Ilots	?	-	-	One possible example in dip surface exposure at Wonderdraai
	34. Intraformational conglomerates	√	√	√	
	35. Flutes	-	-	-	
	36. Rills	-	-	-	
G. Exposure and evaporation	37. Mudcracks	?	√	√	
	38. Runzelmarks	-	?	-	
	(Also 34 above and rip-up clasts)	√	√	√	
H. Burrowing and organic diagenesis	39. Depth of burrowing	-	-	-	(Stromatolites at base (of Mdlelanga are (products of shallow (water or intertidal (biogenic activity
	40. Tracks and trails	-	-	-	
	41. Drifted plant remains	-	-	-	
	42. Impoverished fauna	-	-	-	
I. Differential compaction, loading and hydroplastic readjustment	43. Load casts	√	√	√	
	44. Pseudonodules	-	√	?	
	(Also 28 above)				
J. High rates of sedimentation combined with regressive sedimentation	45. Graded, fining upwards sequence	√	√	√	

KEY: √ = Present
- = Absent
? = Recognition not positive

in the area of the Mdlelanga and Nkonisa River confluence and the lower Welendhlovu River valley. Measured vertical sections through these areas reveal that the facies occur either in upwards-coarsening cycles or in a random sequence (Figs. 5.22 and 5.24). In order to test the relationship between the facies, Markov chain statistics were calculated for a part of the Vutshini Formation between the clearly upwards-fining basal unit and the predominantly arenaceous lithologies present in the upper half of the formation (Fig. 5.25, Table 5.2). These data indicate a strong tendency for upwards transitions to occur in the order: $H_C \rightarrow H_B \rightarrow H_A \rightarrow S_A$ with less probable transitions $S_B \rightarrow S_C$ and $S_B \rightarrow S_A$. In addition, field observations indicate that the basal part of each facies H_C unit is highly ferruginous and locally may be classified as banded iron formation.

This upwards- coarsening facies sequence is similar to deposits described by Watchorn (1978) who related this sequence to prograding shelf or delta front sedimentation. Hobday (1973) documented stacked, upwards-coarsening facies sequences in Phanerozoic sediments which resulted from deltaic progradation into a gradually subsiding basin. The cyclicity reflected lateral migration of delta lobes in this occurrence. The sequences of the Vutshini Formation differ from those of the Phanerozoic example in that they are seldom complete and have a considerable range in thickness (1 - 10 m, Fig. 5.22). As mentioned above, the Vutshini Formation comprises upwards-fining marine sequences in the Gem Syncline at an equivalent stratigraphic level to the sequence under discussion. As there is some evidence for the Vutshini upwards-fining sequences being of subtidal origin, any palaeoenvironmental interpretation must account for the lateral equivalence of substantially different facies assemblages. Taking folding of the sequence into account, the two localities were originally no more than 10 km apart. Thus a fundamental geographical control must have existed, such as a major change in the topography of the coastline. Possibly the difference between the sequences is related to the proximity of a fluvial entry point to the basin.

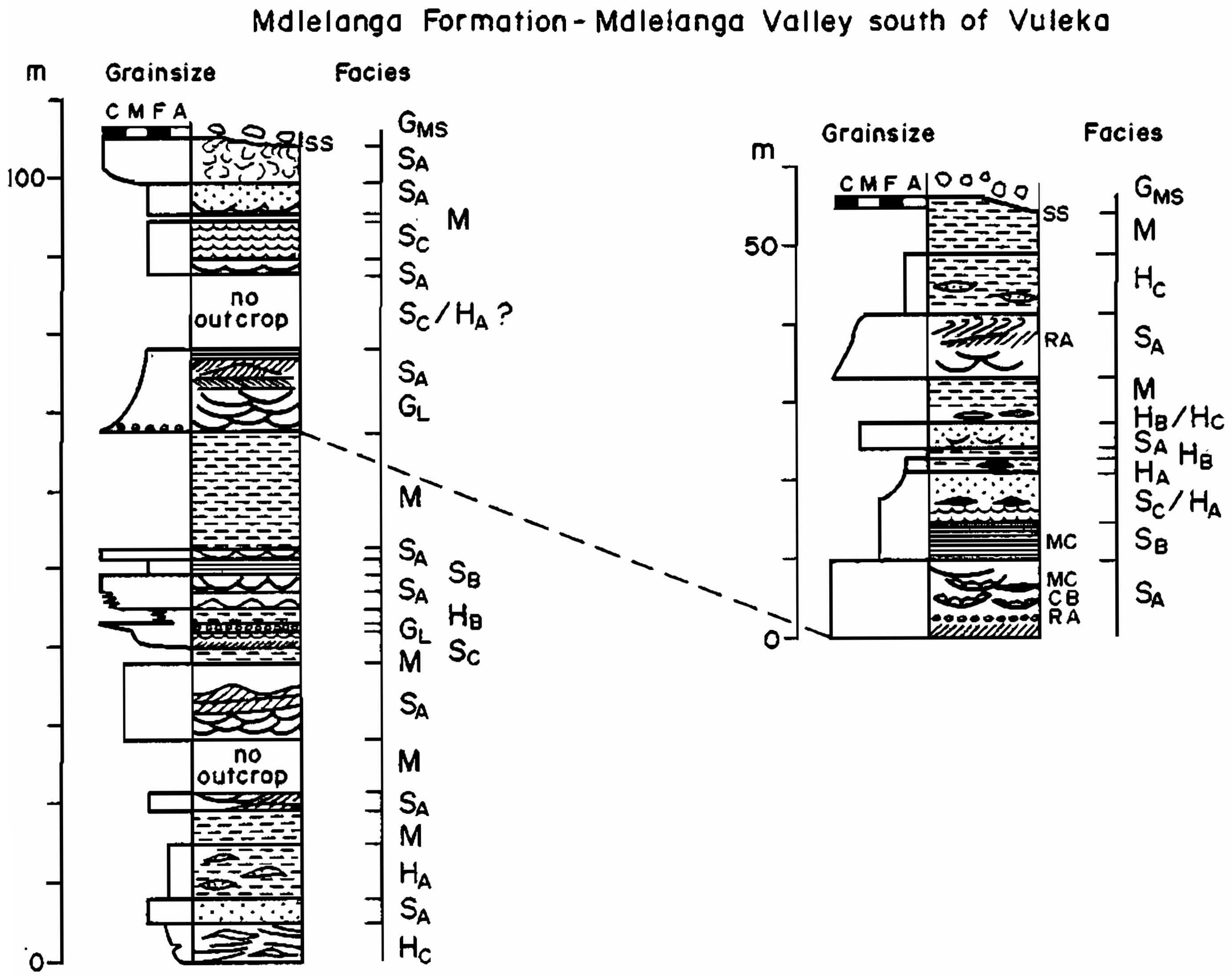

Figure 5.23 Measured section through the Mdlelanga Formation south of Vuleka in the Mdlelanga River valley. Symbols and ornamentation as in Figure 5.21.

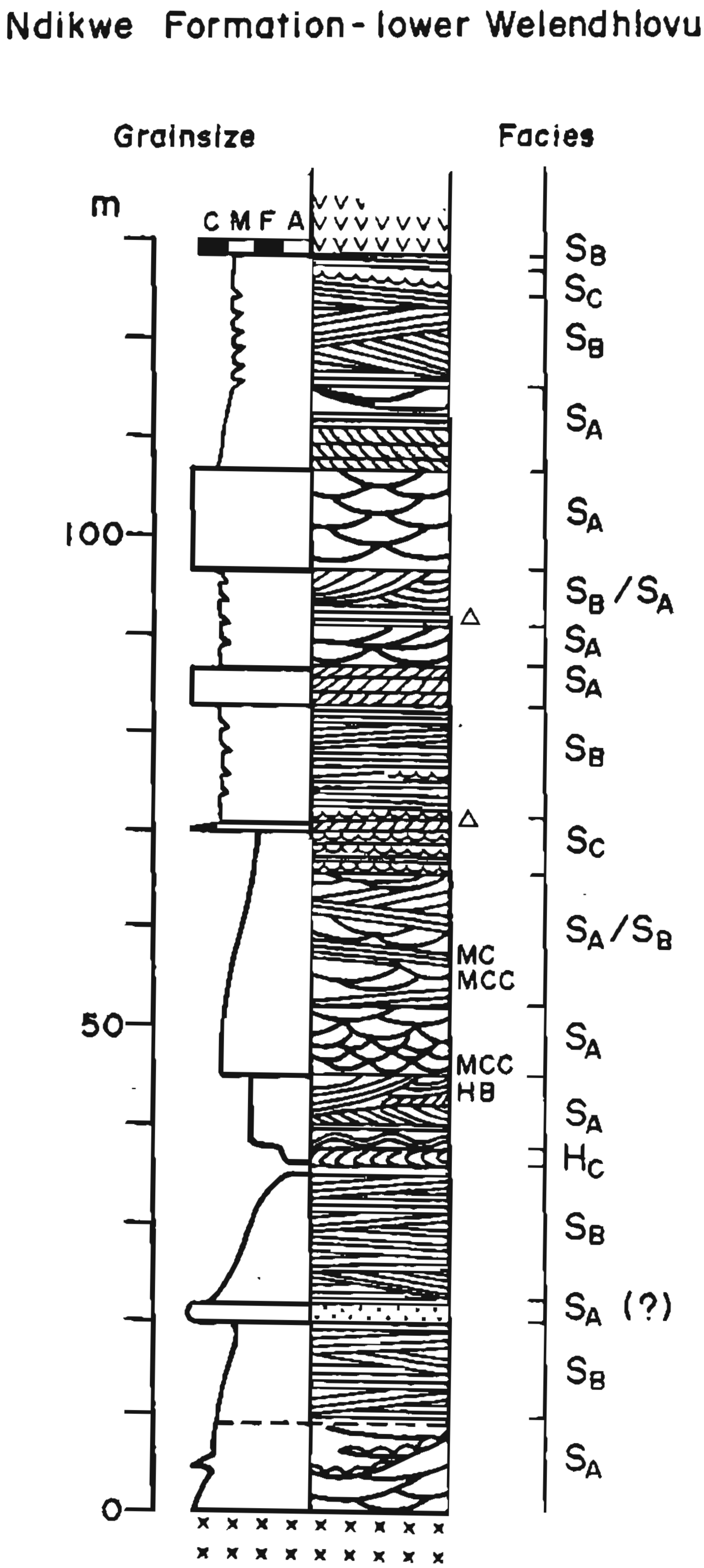

Figure 5.24 Measured vertical sections through parts of the Ndikwe Formation, lower Welendhlovu River valley. Key to ornamentation as in Figure 5.21.

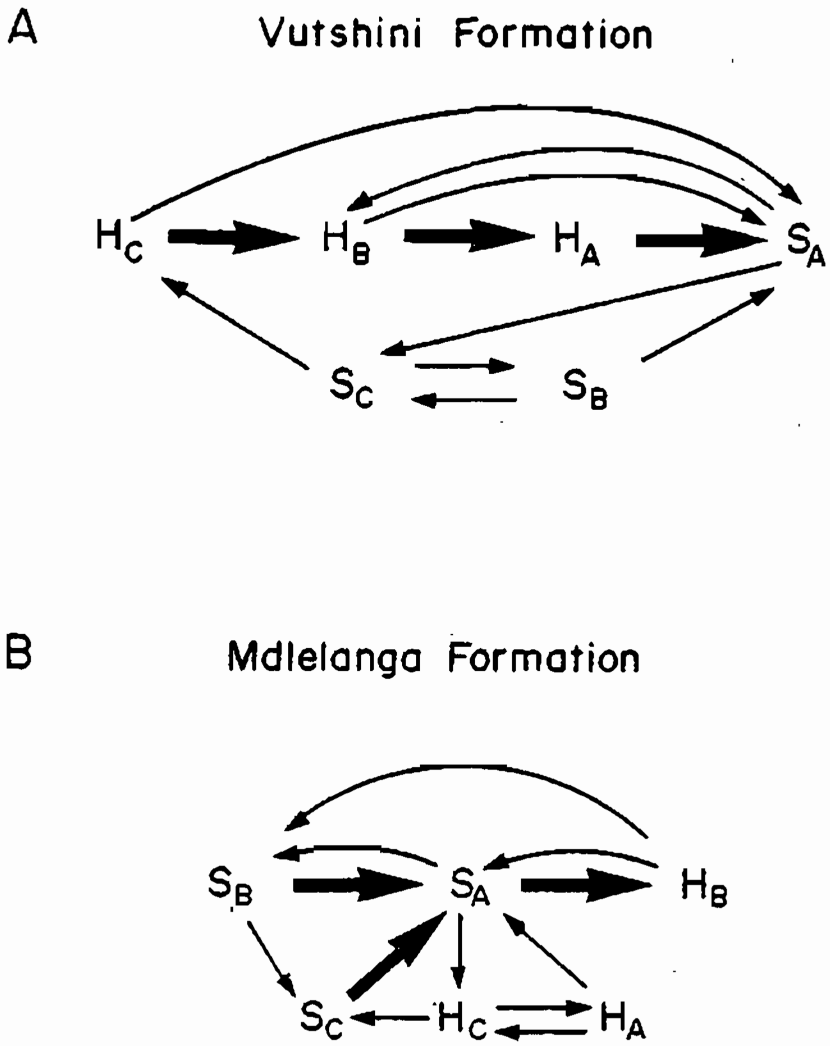

Figure 5.25 Markov chain showing facies transitions which are encountered more frequently than is statistically probable.

TABLE 5.2 : MARKOV CHAIN STATISTICS FOR UPWARDS FACIES TRANSITIONS, VUTSHINI FORMATION

(a) Observed Transition Matrix

	S_A	S_B	S_C	H_A	H_B	H_C
S_A	-	2	4	5	8	4
S_B	3	-	1	0	0	0
S_C	1	2	-	0	1	1
H_A	11	0	0	-	1	1
H_B	6	0	0	6	-	1
H_C	3	0	0	1	3	-

(b) Difference Matrix: Observed Minus Calculated Probabilities

	S_A	S_B	S_C	H_A	H_B	H_C
S_A	-	-0.01	0.05	-0.09	0.04	0
S_B	0.36	-	0.13	-0.21	-0.21	-0.11
S_C	-0.19	0.32	-	-0.21	-0.01	0.09
H_A	0.40	-0.08	-0.09	-	-0.17	-0.05
H_B	0.01	-0.08	-0.09	0.21	-	-0.05
H_C	0.02	-0.07	-0.08	-0.08	0.21	-

TABLE 5.3 : MARKOV CHAIN ANALYSIS FOR UPWARDS FACIES TRANSITIONS MDLELANGA FORMATION

(a) Observed Transition Matrix

	S_A	S_B	S_C	H_A	H_B	H_C
S_A	-	1	1	1	2	3
S_B	2	-	1	0	0	0
S_C	2	0	-	0	0	1
H_A	1	0	0	-	0	1
H_B	1	1	0	0	-	0
H_C	2	1	1	1	0	-

(b) Difference Matrix: Observed Minus Calculated Probabilities

	S_A	S_B	S_C	H_A	H_B	H_C
S_A	-	-0.07	-0.07	0.1	0.12	0.05
S_B	0.24	-	0.19	-0.10	-0.10	-0.24
S_C	0.24	-0.14	-	-0.10	-0.10	0.09
H_A	0.09	-0.14	-0.14	-	-0.09	0.27
H_B	0.09	0.36	-0.14	-0.09	-	-0.23
H_C	-0.07	0.04	0.04	0.09	0.09	-

Other occurrences of the heterolithic and arenaceous facies association (S_A, S_B, S_C, H_A, H_B, H_C, M) are in the lower parts of the Mdlelanga and Ndikwe Formations,, south of Vuleka (Map 2) and east of Hlagothi Mountain (Map 3) respectively. The measured sections through these parts of the stratigraphy are short owing to a paucity of outcrop and do not provide evidence for cyclicity or preferred sequences of occurrence (Fig. 5.26). They display considerable evidence for a subtidal origin (wave ripples, flaser, lenticular and wavy bedding, polymodal cross-bed orientation, reactivation surfaces). The absence of sequential ordering is ascribed to a complex interplay between subsidence through epeirogenic movement, transgression and progradation. Markov analyses (Table 5.3) for the Mdlelanga sequences suggest the order $H_B \rightarrow S_B \rightarrow S_A$ is most common with $H_B \rightarrow S_B \rightarrow S_C \rightarrow S_A$ being slightly less probable. The significance of this is not readily apparent.

(d) Several sections measured in the field cannot yet be ascribed to facies associations or sequences because of the constraints placed on interpretation by discontinuous outcrop and a resultant lack of data regarding the lateral and vertical relationship between the facies.

Figure 5.27 shows the vertical section through a part of the Ndikwe Formation west of Ndikwe Store. This sequence has trough and planar cross-stratification (S_A facies) at the base. The upper half of the 30 m section consists only of facies S_B (parallel laminated) and S_C (microcross-laminated, always with climbing ripples) in alternating units 30 - 100 cm thick. This alternation reflects an environment in which cycles of high energy and high sediment load preceded periods of lower energy flow and high rates of sediment fall-out. There is no visible difference in grain size between the two facies, possibly as a result of complete recrystallization. Facies S_B rests with a sharp or slightly scoured contact upon facies S_C. The S_B - S_C transition

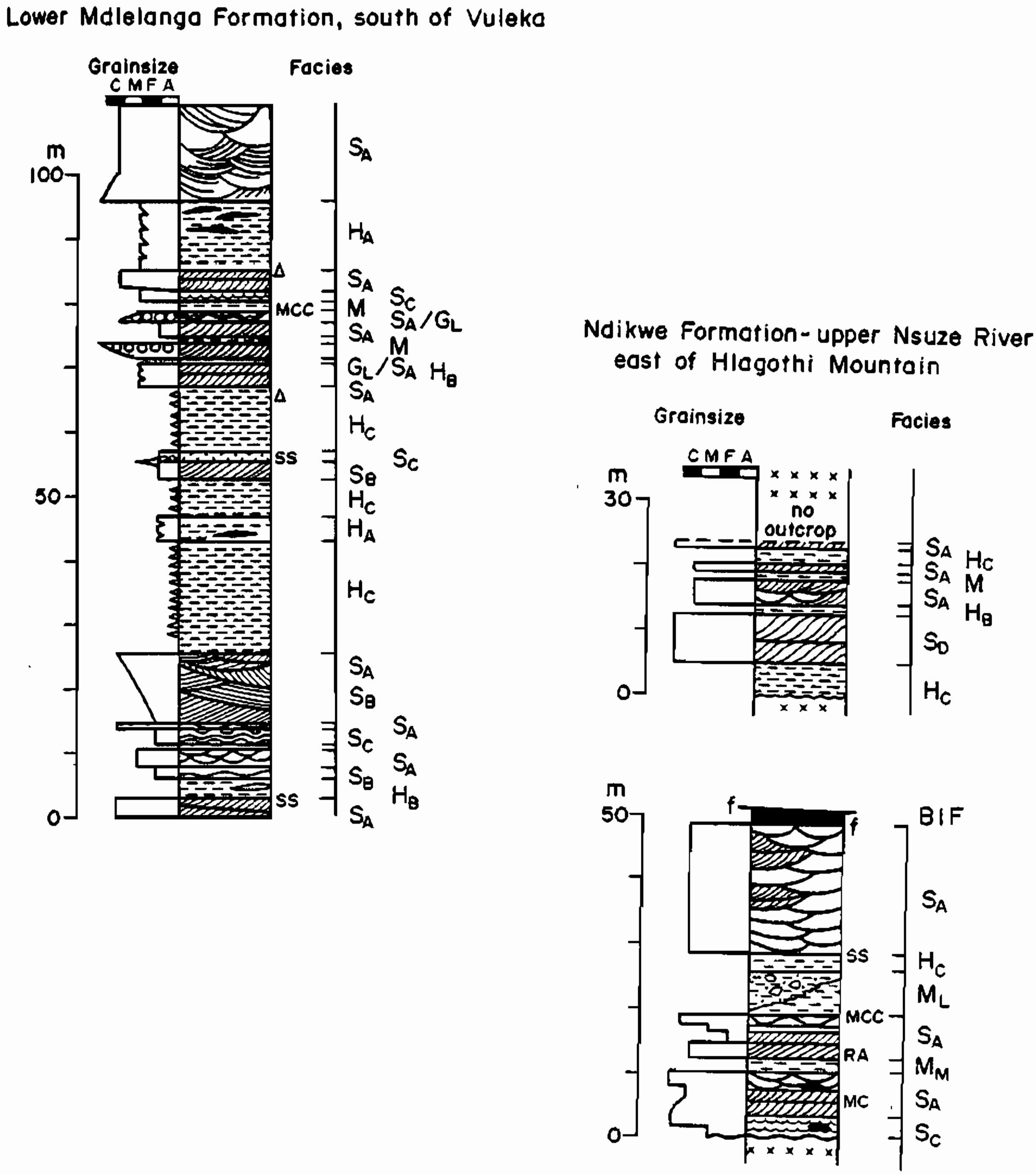

Figure 5.26 Measured vertical sections through parts of the Ndikwe Formation in the area around Hlagothi Mountain and the Mdlelanga Formation south of Vuleka. Symbols and ornamentation as in Figure 5.21.

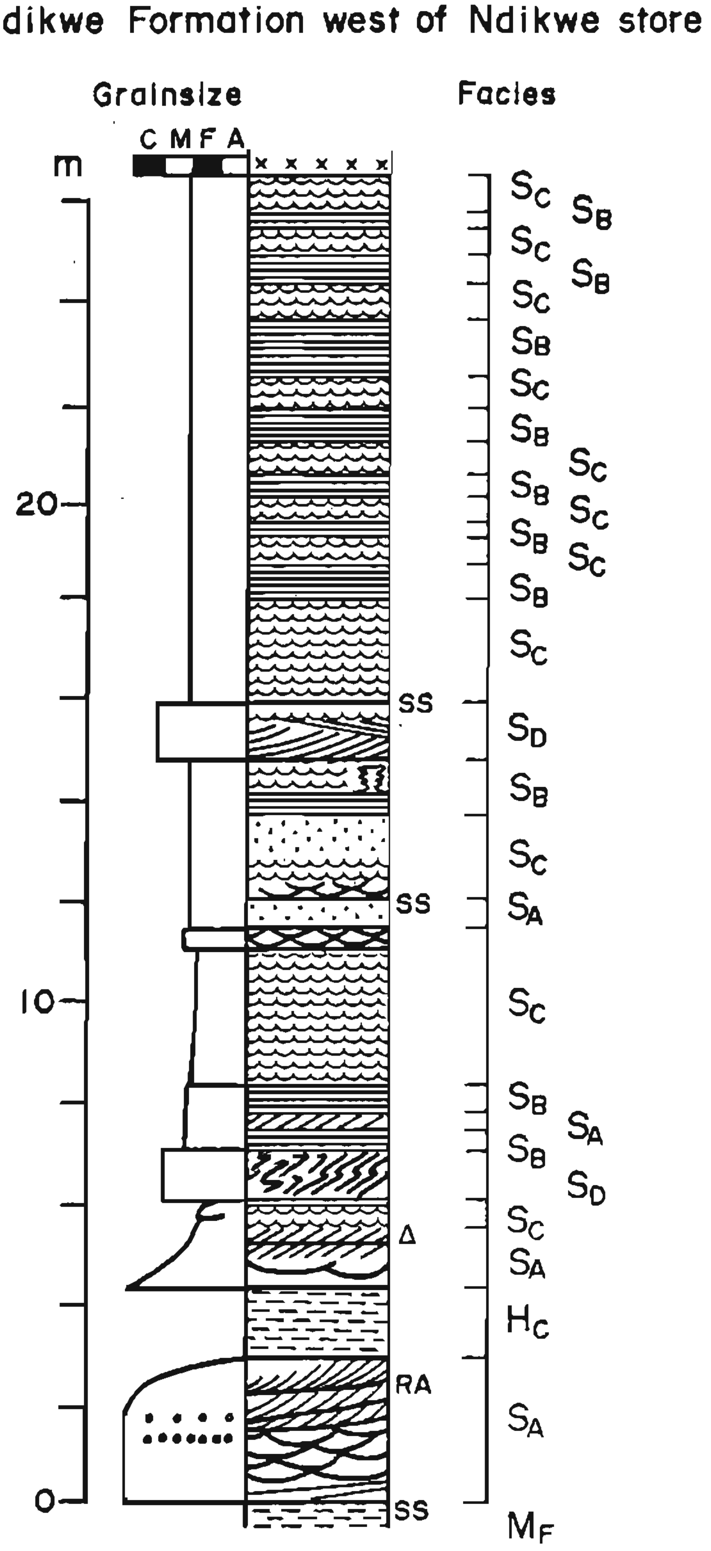

Figure 5.27 Measured vertical section through a portion of the Ndikwe Formation due west of Ndikwe Store. Symbols and ornamentation as in Figure 5.21.

occurs over a few centimetres in which in-phase climbing ripple cross-lamination is common. The sequence resembles high-energy flood deposits described by Tunbridge (1981) as the product of an ephemeral stream environment. However, the observed sequence lacks the rip-up clasts and evidence for exposure considered to be essential criteria for recognition of ancient ephemeral stream deposits (Tunbridge, 1981). It is difficult to envisage a shallow marine environment for these sediments because there are few features indicative of normal marine conditions.

5. Palaeocurrent Direction

The palaeocurrent directions measured in the Nsuze Group have been plotted as rose diagrams for each formation and the whole sequence (Figs. 5.28, 5.29, 5.30 and 5.31). The number of measurements within individual facies sequences is too small to make meaningful interpretations with regard to local sedimentary environments.

Within the Ndikwe Formation trough cross beds indicate a range between southwest and northwest (Fig. 5.28). Planar foreset measurements indicate a bimodal population with south and southeasterly directions being dominant. Wave ripple strikes range between northeast and north, whereas current ripples indicate a southeasterly flow direction. These data represent mixing of populations from different depositional environments which may account for the apparently contradictory evidence. The common factor in the groups is that south to southeast and west to southwest palaeocurrent directions are most common.

The Mdlelanga Formation trough cross-stratification data are weakly bimodal with dominantly south-southeast trends (Fig. 5.29). A weak westwards trend is also present. Planar cross-stratification yields generally southwards flow directions with no well-defined maximum. Wave ripple strikes display a strong northeast-southwest mode, normal to the flow direction inferred from the trough

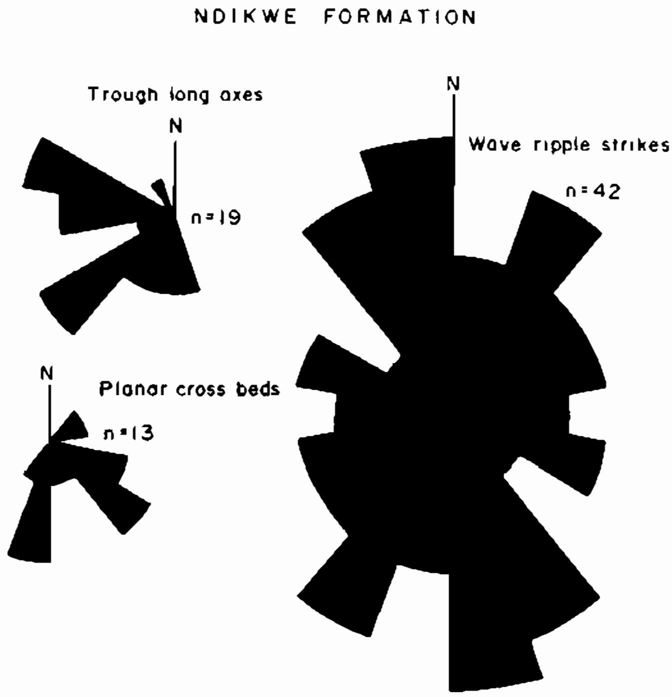

Figure 5.28 Palaeocurrent rose diagrams for the Ndikwe Formation.

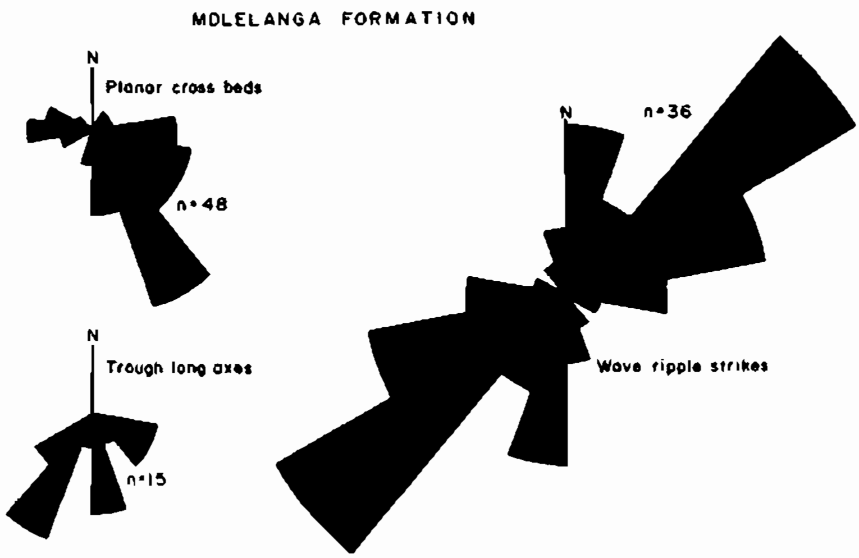

Figure 5.29 Palaeocurrent rose diagrams for the Mdlelanga Formation.

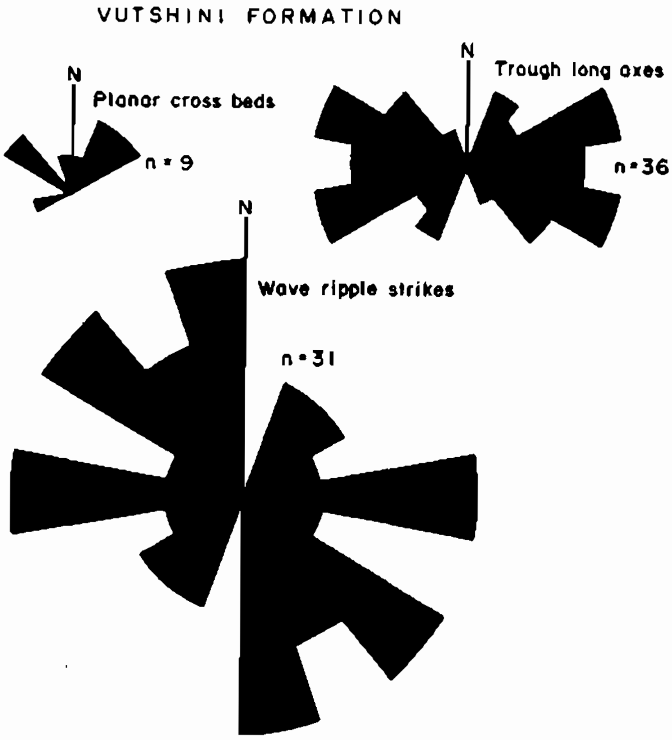

Figure 5.30 Palaeocurrent rose diagrams for the Vutshini Formation.

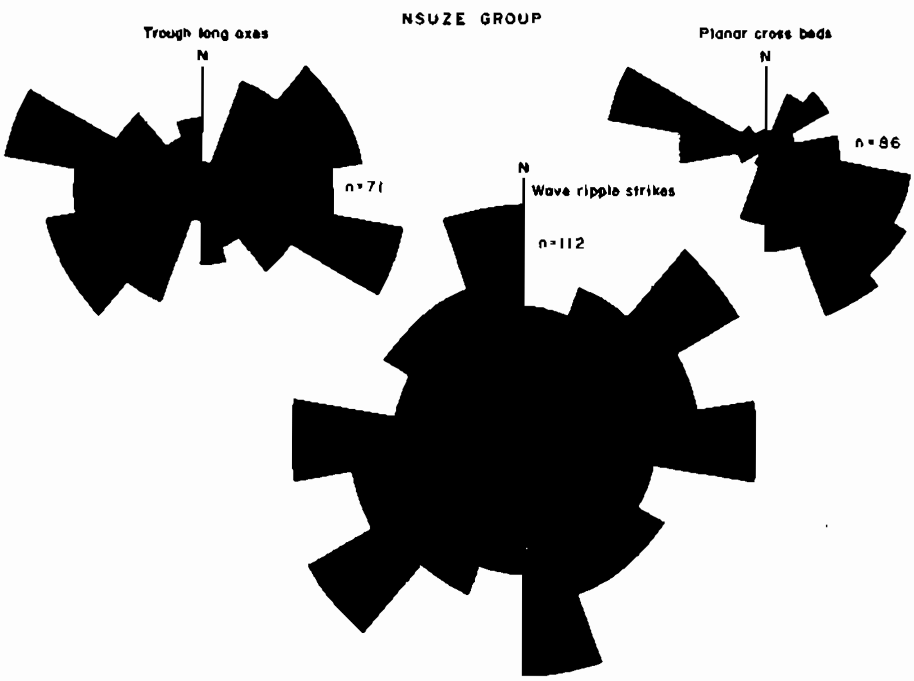

Figure 5.31 Palaeocurrent rose diagrams for the Nsuze Group.

and planar cross-stratification. This group of measurements is reasonably consistent and indicates a palaeoslope towards the south or southeast.

The data for the Vutshini Formation are more contradictory. Troughs could be measured most commonly on dip surfaces where they are exposed as shallow scoops. The recrystallization and maturity of the sandstones generally prevents recognition of the actual foresets and direction of movement. For this reason the trough long axes were measured and plotted, which provides an orientation but not a sense of movement. On the rose diagram the troughs display a dominant east-west trend (Fig. 5.30). The few instances where actual cross-strata could be measured indicate eastwards palaeocurrent directions. Planar cross-beds are equally uninformative, although weak northeasterly and northwesterly maxima are present. Wave ripple strikes are dispersed between north and west with a weakly trimodal distribution. A more detailed study might permit recognition of several subgroups, perhaps related to different facies assemblages. The Vutshini Formation overlies the Qudeni Formation volcanics which diminish substantially in thickness northwards (Chapter 3). Extrusion of this volcanic pile may have reversed the palaeoslope locally.

The combined data for the Nsuze Group are shown in Figure 5.31. Troughs in this population are dominated by those measured in the Vutshini Formation (36 out of 71 measurements), therefore the data are shown as strike azimuths. The dominant orientation of the troughs is east-west. No well-defined maximum is present in the ripple strike data, although three weak maxima are present: N-S, NE-SW and E-W. Planar cross beds show a bimodal, bipolar distribution. The dominant mode is towards the south and southeast; a moderately strong northwest trend also being present.

The palaeocurrent data are thus reasonably consistent with a predominantly souteastwards palaeoslope, but reflect the influences of shifting depositional environments. The Qudeni Formation volcanics may have changed the local basin morphology prior to deposition of the Vutshini Formation, resulting in a temporary northwards palaeoslope.

6. Summary of Sedimentological Data and Interpretations

Although the sedimentological data presented in this study are as yet inadequate for detailed facies modelling, several inferences can be made. The arenaceous and argillaceous sediments may be divided into several facies on the basis of sedimentary structures and petrographic associations. The sequence in which the facies occur allows comparison with established facies models. Thus far the Nsuze Group appears to be predominantly marine in origin, particularly in areas where cycles of arenaceous and argillaceous deposits have the characteristics of shoreline, proximal shelf and distal shelf sequences. Fluvial sediments are rarer but are probably locally developed. In the upper part of the Vutshini Formation poorly-exposed sediments seem likely to represent distal alluvial fan deposits.

Available palaeocurrent data are not particularly useful except that a dominant south to southeast palaeoslope is indicated. The manner in which cycles of shallow and deeper water deposits are in juxtaposition and the vertical and lateral variation in the sequence suggest a complex tectonic history for the depositional basin. Repeated transgression and regression must have occurred in response to isostatic adjustment or crustal flexing caused by deepseated magmatism or variations in regional stress field. The occurrence of volcanics at various levels within the sequence is evidence for repeated resurgence of magmatism. A feature common to the Vutshini and Mdlelanga Formations is a southwards thickening. Whether this represents a shift in position of the depocentre or progressive uplift of the Nondweni-Nkandla basement high cannot be inferred at this stage. If the latter is the case, then the area studied may lie within an embayment or trough separate from the remainder of the Pongola Supergroup. This may have significant implications for crustal evolution of the Kaapvaal province in terms of proximity to the original boundary of the early crustal fragment.

CHAPTER 6

GEOCHEMISTRY OF THE NSUZE LAVAS AND SOME ULTRAMAFIC ROCK-TYPES

1. Introduction

Sixteen Nsuze Group lavas and eight ultramafic rock-types of intrusive or extrusive origin have been analysed for major and minor elements as well as thirteen trace elements. The data provide a basis for comparison with analyses from other areas and some indication as to magmatic affinity and possible fractionation trends. In addition, data from Tunnington (1981) and Brown (1982) are used in discussion of the geochemistry of the Nsuze Group lavas.

Relevant information concerning the sample localities, stratigraphic position, petrography and alteration of the samples is provided in Appendix 1. A description of the analytical methodology is given in Appendix 4.

2. Alteration

In addition to devitrification, metamorphism and deformation, the lavas have undergone considerable alteration. As it is not always possible to obtain samples free of all alteration, it is considered important to review available data pertaining to chemical variations stemming from calcitization, silicification, epidotization and chloritization.

Condie *et al.* (1977) indicated that considerable mobilization of many elements occurs during intense alteration although at levels less than 10% calcitization and 60% epidotization the elements Ti, Y, Nb, Zr, Cr and Ni are effectively immobile. Other changes are summarised in Table 6.1.

TABLE 6.1: CHANGE IN CHEMISTRY RELATED TO TRANSFORMATION AND ALTERATION OF PRIMARY MINERALOGY IN VOLCANIC ROCKS

Mineralogical Change	Si	Al	Mg	Fe^{3+}	Fe^{2+}	Ca	Na	K	Ti
Augite to chlorite[1]	-	+	0	0	0	-	0	0	
Labradorite to albite[1]	+	-	0	0	0	-	+	-	
Calcitization/chloritization[2]				-	+	-	-		+
Epidotization[2]	-		-	+	-	+		-	-

[1] - Hughes (1982, p. 476) [2] - Condie *et al.* (1977)

\- = depletion + = enrichment 0 = unchanged

For these reasons it is essential to attempt to identify samples which have undergone significant alteration before proceeding to a discussion of the chemical data. The Nsuze group samples retain little of their primary mineralogy. For this reason it has been necessary to classify them on the basis of their chemistry. As sodium and potassium abundances strongly influence classification, it is important to identify samples which have been subjected to alkali enrichment or depletion. Hughes (1972) suggests the plot: $K_2O + Na_2O$ versus $K_2O/(K_2O + Na_2O)$ for this purpose. A large proportion of the analyses fall outside of the igneous spectrum of Hughes (1972) (Fig. 6.1). Most of the same samples are also aberrant on a plot of total alkalies against differentiation index (D.I.) (Fig. 6.2). A plot of normative diopside and corundum versus silica may also be used to identify alteration (Chayes, 1969) although the presence of normative corundum, considered in isolation, need not necessarily indicate alteration. Armstrong (1980, p. 216) considers corundum normative Nsuze lavas to be products of normal petrologic processes in rocks with D.I. > 60. Cawthorn *et al.* (1976) maintain that some corundum normative lavas result from amphibole fractionation in calc-alkaline

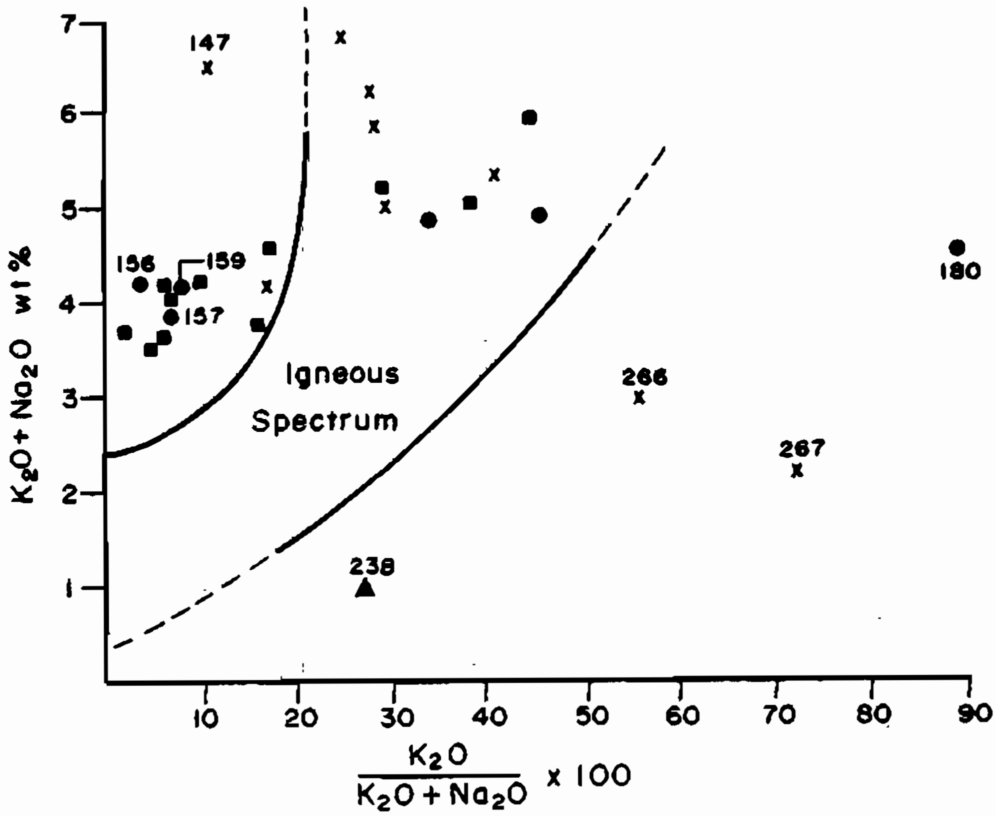

Figure 6.1 $K_2O + Na_2O$ vs $K_2O/(K_2O + Na_2O)$ variation for the Nsuze Group samples. Analyses which plot outside of the Hughes (1972) "igneous spectrum" are assumed to be altered. Ornamentation: ● - Qudeni Formation; x - Ndikwe Formation lavas; ▲ - Ndikwe Formation pyroclastics; ■ - Analyses from Tunnington (1981) and Brown (1982).

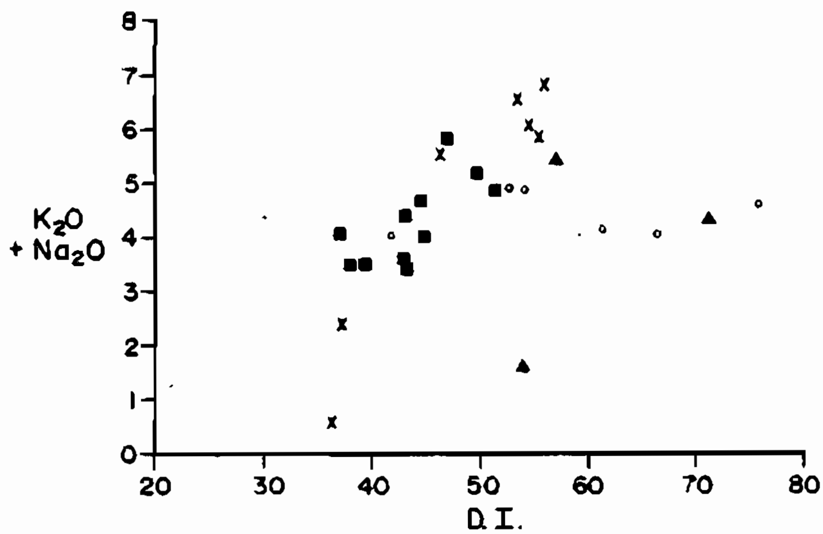

Figure 6.2 Plot of $K_2O + Na_2O$ against D.I. for the Nsuze Group lavas. Samples which plot away from the main trend are probably altered, leached or have been affected by alkali metasomatism. Ornamentation as for Figure 6.1.

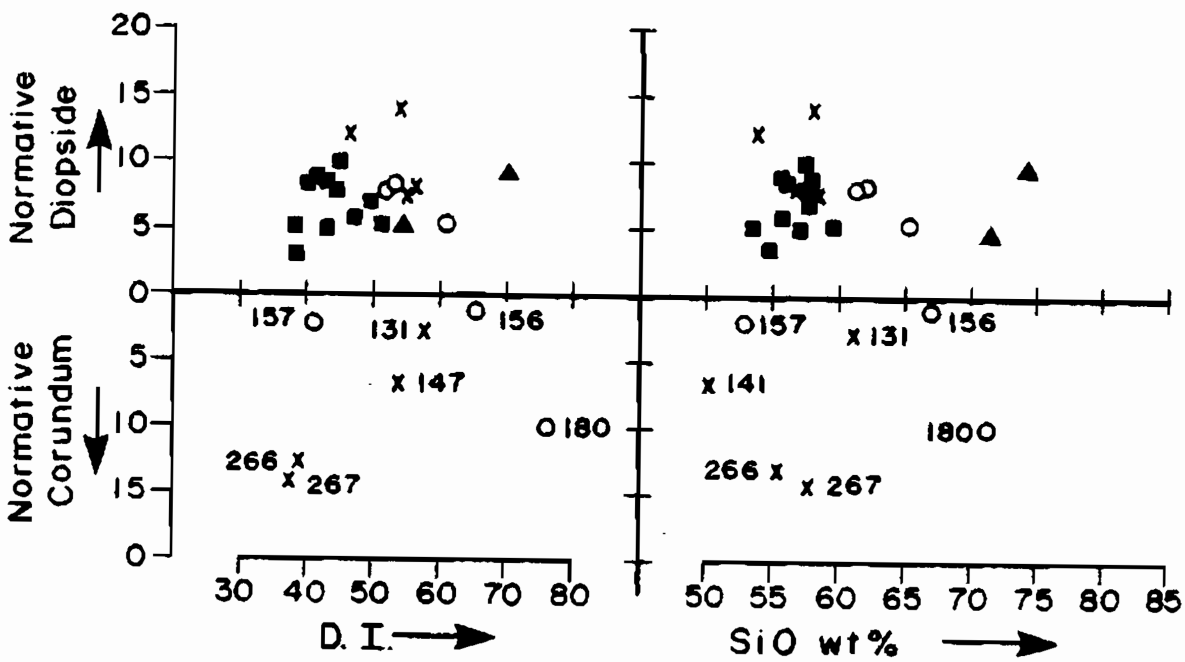

Figure 6.3 Variation diagrams showing the relationship between normative diopside, normative corundum, D.I. and SiO_2. Samples containing normative corundum at D.I. < 65 and SiO_2 < 65 wt. % are considered to be altered. Ornamentation as for Figure 6.1.

suites. Nsuze Group samples which plot well away from the amphibole fractionation trend and have normative corundum at D.I. values < 60 (Fig. 6.3) are considered to be altered.

3. Oxidation State of Iron

Analysis by XRF yields a value for the concentration of iron metal irrespective of the oxidation state. In the present case the lavas analysed are extensively altered and unlikely to have iron oxidation ratios resembling the original values. Wet chemical methods have therefore not been used

Several methods have been proposed for estimating Fe^{3+}/Fe^{2+} ratios of altered volcanic rocks (Table 6.2). In spite of detailed investigation of the problem, the validity of any estimate for a particular rock is difficult to prove. It is generally agreed that Fe^{2+} is the dominant species in basaltic rocks. Although use of a single value for the oxidation ratio in these rocks has been suggested (e.g. Kay *et al.*, 1970; Flower, 1973), this practice is questionable because oxidation ratios are dependent on bulk composition, pressure, temperature and oxygen fugacity.

The accurate estimation of iron oxidation is particularly important in computing the normative mineralogy. Hughes and Hussey (1976) and Le Maitre (1976) stress this in connection with methods of classification based on normative mineralogy. The presence or absence of normative quartz is critical in many classification schemes, yet quartz in the norm depends largely on the oxidation ratio used. Equal amounts of FeO and Fe_2O_3 are allocated to magnetite, and in the event of ferric iron being overestimated, reduced amounts of ferrous iron are available to form diopside, hypersthene and olivine. This results in an excess of SiO_2 which is reflected as normative quartz.

Le Maitre's (1976) statistical evaluation of a large number of analyses indicates that the oxidation ratio may be calculated thus:

$$FeO/(FeO + Fe_2O_3) = 0.88 - 0.0016.SiO_2 - 0.022.(K_2O + Na_2O).$$

TABLE 6.2: METHODS OF ESTIMATING FERRIC/FERROUS RATIOS FOR VOLCANIC ROCKS.

ESTIMATED OXIDATION STATE OR RATIO	VALUE OR FUNCTION	AUTHOR
Fe_2O_3	1.5%	Kay *et al.* (1970)
	2.0%	Flower (1973)
	1.5% + wt % TiO_2	Irvine and Baragar (1971)
	1.5% if (K_2O + Na_2O) < 4%	) Thompson
	2.0% if (K_2O + Na_2O) < 7%	) *et al.*
	2.5% if (K_2O + Na_2O) > 7%	) (1972)
Fe_2O_3/FeO	0.15	Green *et al.* (1974)
	0.25	Stice (1968)
$Fe^{3+}/(Fe^{2+} + Fe^{3+})$	0.1	Pyke *et al.* (1973)
	0.2	O'Hara (1973)
	0.25	Baker *et al.* (1974)
$Fe_2O_3/(Fe_2O_3 + FeO)$	0.2 (basic rocks only)	Hughes and Hussey (1976)
$FeO/(FeO + Fe_2O_3)$	0.88 − 0.0016 SiO_2 − 0.022 (Na_2O + K_2O)	Le Maitre (1976)

For most of the lavas analysed this equation gives values between 0.75 and 0.85, equivalent to an Fe_2O_3/FeO ratio of 0.20 to 0.25. However, in order to facilitate comparison with data presented in other studies, the following values for Fe_2O_3 are used: komatiites, 0.1; basalts, 0.2; basaltic andesites, 0.3; andesites and dacites, 0.4; and rhyolites, 0.5.

4. The Nsuze Group

Major and minor element abundances for the ten Ndikwe Formation and six Qudeni Formation rocks analysed are presented in Tables 6.3, 6.4 and 6.5. Additional samples from Tunnington (1981) and Brown (1982) are also used in this section. The samples of Ndikwe lavas are from thin flows intercalated in the pyroclastic succession in the south limb of the Gem Syncline (BG128, 129, 131, 147 and 152), and a thin flow northwest of Ndikwe (BG266 and 267). A volcanic bomb from due west of Ndikwe (BG257), a crystal tuff from just south of Hlagothi (BG238) and a welded lapilli tuff from south of Vuleka (BG130) have also been analysed. Samples BG180, 183 and 184 are from the Qudeni Formation on the north limb of the Central Nsuze Syncline. BG156, BG157 and BG159 are from the same unit on the north limb of the Gem Syncline. The Tunnington (1981) samples were taken from the Qudeni Formation immediately south of the study area, but Brown's (1982) data are from uncorrelated lavas from an area some 12 km to the southeast.

Chemically the rocks show evidence for alteration and disturbance of alkali contents. Only ten of the analyses fall within the criteria for unaltered rocks discussed in part two of this chapter (above) despite the absence of obvious weathering or alteration in hand specimen. In thin section minor epidotization, calcitization and silicification are recognized, particularly in the Ndikwe Formation lavas. On the variation diagrams the altered samples are identified but not excluded because the ten relatively fresh samples are compositionally too similar to define any meaningful trends.

TABLE 6.3: CHEMICAL DATA FOR THE NDIKWE FORMATION VOLCANICS

	BG128	BG129	BG130	BG131	BG147	BG152	BG266	BG267	BG238	BG257
SiO_2	58.14	57.94	54.43	60.98	50.16	57.26	55.28	57.73	71.57	74.04
Al_2O_3	13.93	13.87	25.43	13.55	19.37	14.53	15.97	14.96	8.51	8.76
Fe_2O_3	3.50	3.53	2.96	3.38	2.51	3.32	4.73	3.96	2.06	1.07
FeO	7.88	7.95	8.88	7.61	11.28	7.47	10.63	8.91	4.64	2.42
MnO	0.15	0.16	0.15	0.14	0.08	0.13	0.21	0.04	0.10	0.07
MgO	3.91	3.67	2.89	5.62	6.68	4.94	9.39	11.95	7.18	5.38
CaO	4.96	6.33	7.51	2.31	1.51	4.68	1.05	0.28	4.59	3.53
Na_2O	4.22	4.43	3.18	1.88	5.94	5.12	0.24	0.06	0.98	3.39
K_2O	1.61	1.73	2.33	3.57	0.55	1.68	1.24	0.59	0.68	0.90
TiO_2	1.42	1.44	1.63	1.50	1.59	0.97	1.69	1.55	0.28	0.34
P_2O_5	0.19	0.22	0.22	0.24	0.27	0.20	0.23	0.21	0.03	0.00
TOTAL*	99.92	101.17	99.61	100.78	99.94	100.37	100.66	100.24	100.62	99.92
Sc	20	20	21	15	49	30	29	28	21	23
V	201	203	219	197	383	205	242	239	116	112
Cr	63	57	62	68	65	193	216	69	1239	496
Ni	51	48	49	50	112	84	99	112	199	126
Cu	45	45	12	22	56	16	102	0	38	78
Zn	115	99	102	105	122	86	182	76	48	35
Y	31	33	33	35	26	12	32	32	29	16
Zr	201	209	225	222	240	162	228	214	92	61
Nb	12	12	12	12	9	8	11	12	4	6
Rb	57	62	79	102	9	57	36	18	20	17
Sr	177	273	391	129	150	134	0	0	63	87
Ba	364	402	493	642	184	517	126	1	493	263
La	16	19	18	19	25	20	18	16	12	14

Loss on ignition not determined for any of the samples analysed.

TABLE 6.4: CHEMICAL DATA FOR THE QUDENI FORMATION VOLCANICS

	BG180	BG183	BG184	BG156	BG157	BG159
SiO_2	71.49	61.60	62.34	66.78	53.29	65.51
Al_2O_3	15.52	14.73	15.03	12.54	16.00	12.42
Fe_2O_3	2.40	2.46	2.36	3.31	4.36	3.41
FeO	4.31	5.52	5.32	7.45	13.09	7.67
MnO	0.11	0.13	0.12	0.15	0.20	0.18
MgO	1.12	3.47	3.30	1.07	2.78	1.13
CaO	0.25	6.67	6.66	3.17	5.12	5.09
Na_2O	0.18	2.43	3.24	3.93	3.34	3.75
K_2O	4.42	2.51	1.71	0.16	0.36	0.40
TiO_2	1.03	0.76	0.78	1.02	1.30	1.05
P_2O_5	0.05	0.20	0.19	0.50	0.63	0.52
TOTAL	100.88	100.47	101.05	100.08	100.47	101.13
Sc	34	19	17	19	24	22
V	217	134	126	7	11	7
Cr	41	84	96	38	12	2
Ni	19	32	33	5	0	0
Cu	7	19	18	3	2	13
Zn	38	82	83	172	275	175
Y	35	25	24	47	47	46
Zr	200	193	195	235	278	236
Nb	10	8	9	12	14	13
Rb	91	36	28	4	12	15
Sr	6	514	638	220	218	275
Ba	256	840	474	149	172	218
La	21	26	24	37	45	44

TABLE 6.5: CHEMICAL ANALYSES OF QUDENI FORMATION VOLCANICS FROM TUNNINGTON (1981) AND BROWN (1982)

	NZ7-4	NZ7-5	NZ7-7	NZ7-9	NZ7-10	NZ7-11	NZ7-12	NZ7-13	NK81-1	NK81-2	NK81-6
SiO_2	56.07	54.65	56.88	53.52	54.32	57.60	55.73	57.30	57.64	55.39	57.62
Al_2O_3	13.69	13.06	15.55	14.96	14.87	14.23	14.74	14.44	14.54	15.11	15.14
FeO	3.66	3.28	3.46	2.99	3.67	3.26	3.46	3.23	3.29	3.50	2.69
Fe_2O_3	8.24	7.39	7.78	8.98	8.26	7.33	7.79	7.25	7.40	7.87	6.05
MnO	0.20	0.18	0.15	0.18	0.16	0.16	0.18	0.16	0.13	0.17	0.14
MgO	6.12	5.01	3.80	6.65	6.45	4.96	5.06	4.55	4.61	5.17	6.10
CaO	7.11	5.22	7.32	6.55	6.50	7.46	7.08	7.49	6.00	5.63	6.89
Na_2O	3.34	2.92	2.83	3.78	3.49	3.50	3.85	3.77	3.51	3.23	3.72
K_2O	0.22	2.00	0.79	0.28	0.17	0.13	0.43	0.27	1.69	2.59	0.78
TiO_2	0.99	0.94	1.04	1.10	1.16	1.02	1.00	1.00	0.88	0.97	0.59
P_2O_5	0.43	0.40	0.45	0.48	0.49	0.47	0.46	0.44	0.32	0.20	0.29
TOTAL	100.08	100.05	100.06	99.47	100.04	100.11	99.79	99.90	100.01	99.83	100.02

NZ7 Samples - Tunnington (1981)

NK81 Samples - Brown (1982)

Each element has been plotted against differentiation index and MgO content (Figs. 6.4, 6.5 and 6.6). The former, (D.I.), is the sum of normative quartz, albite and orthoclase. Although it represents the extent of evolution of the magma and provides good separation of data, it has the disadvantage of being sensitive to ferric/ferrous iron ratio inaccuracy. It is also too complex to provide petrologically meaningful trends. MgO is independent of iron ratio and is more easily related to magmatic processes, but provides little separation of low magnesium rock-types. The trends identified by Armstrong (1980) for the Nsuze Group volcanics have been superimposed on the diagrams to facilitate comparison between the lavas in the two areas studied.

MgO abundances of the Ndikwe Formation samples are slightly higher overall than for the Qudeni lavas. This produces a displacement of the trends for the two groups of samples on the MgO variation diagrams, but not on the D.I. Plots. The differences between the groups are discussed in more detail below.

Silica, K_2O and total alkalies increase with D.I. and decrease with MgO, as would be expected. The Ndikwe Formation lavas have slightly higher alkali contents than those from the Qudeni Formation. Na_2O and Al_2O_3 show little variation over the range of compositions with the exception of pyroclastic and altered samples which have spuriously high or low values. CaO, FeO* and MnO decrease with increasing D.I., but show no systematic variation on the MgO diagram. Altered samples have extremely low CaO contents. Samples from the Ndikwe Formation have slightly higher FeO* than the remainder of the samples. TiO_2 and P_2O_5 are more or less constant but provide separation of the Ndikwe and Qudeni Formation samples. The Ndikwe lavas have higher TiO_2 but lower P_2O_5 than those from the Qudeni Formation. The pyroclastic rocks have very low abundances of these elements.

On all of the plots data for the unaltered samples lie within or close to the trends defined by Armstrong (1980).

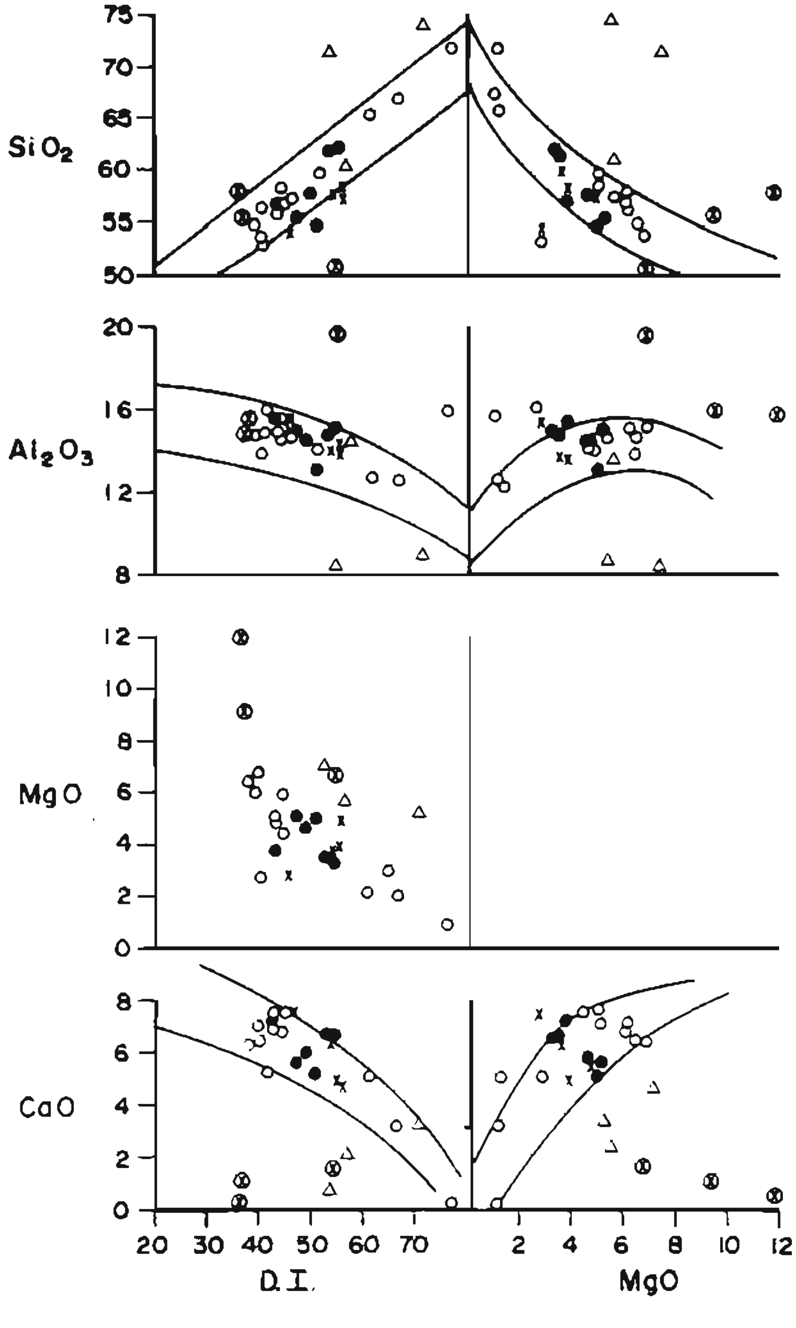

Figure 6.4 D.I. and MgO variation diagrams for SiO_2, Al_2O_3, MgO and CaO in the Nsuze lavas. Ornamentation: ○ - Qudeni Formation (unaltered); • - Qudeni Formation (altered); X - Ndikwe Formation (unaltered); ⊗ - Ndikwe Formation (altered); △ - Ndikwe pyroclastics. (All oxides as weight percentages). Trends determined by Armstrong (1980) lie within the solid lines on each diagram.

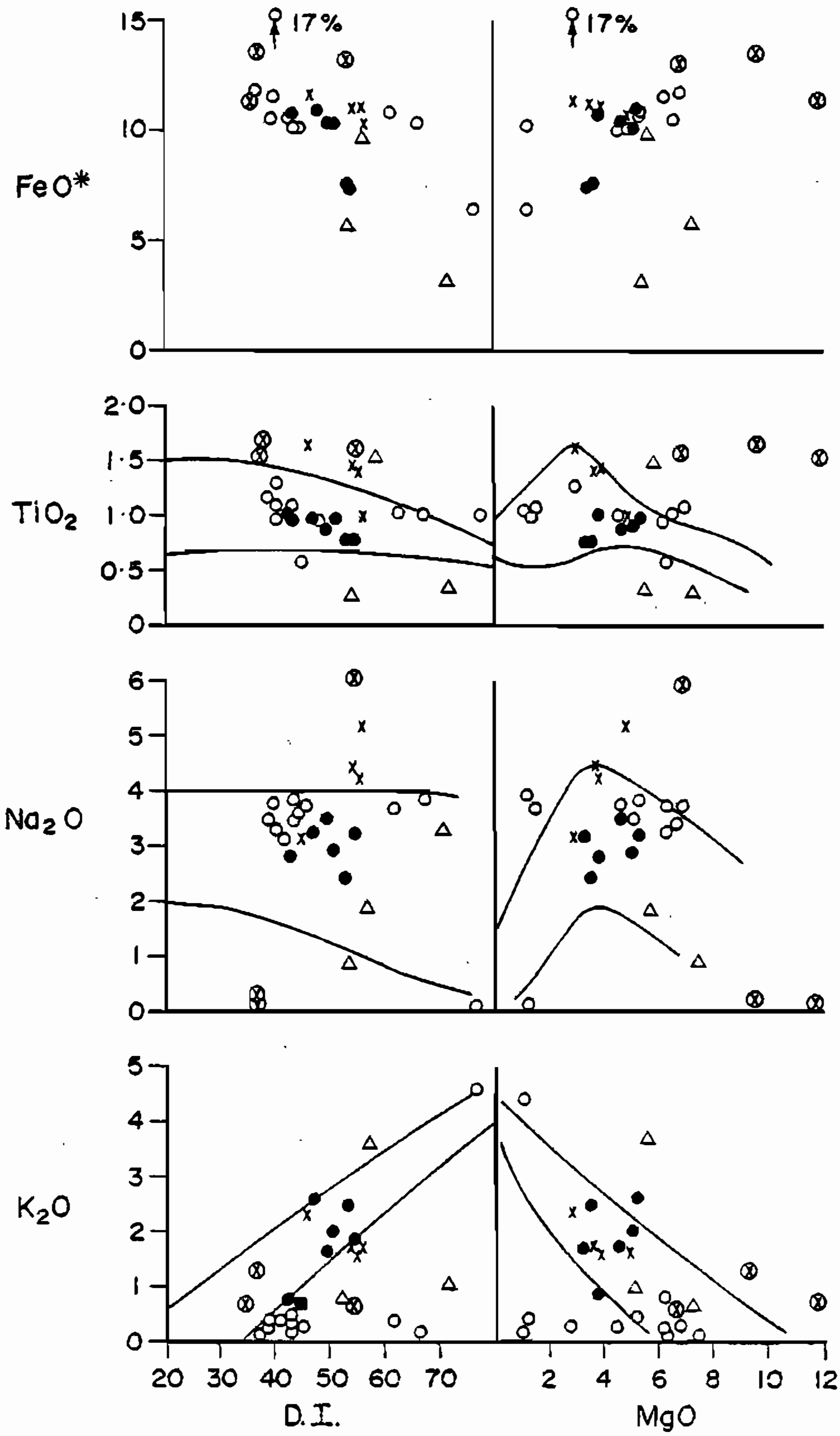

Figure 6.5 D.I. and MgO variation diagrams for FeO*, TiO_2, Na_2O and K_2O. Ornamentation as for Figure 6.4. All oxides as weight percentages.

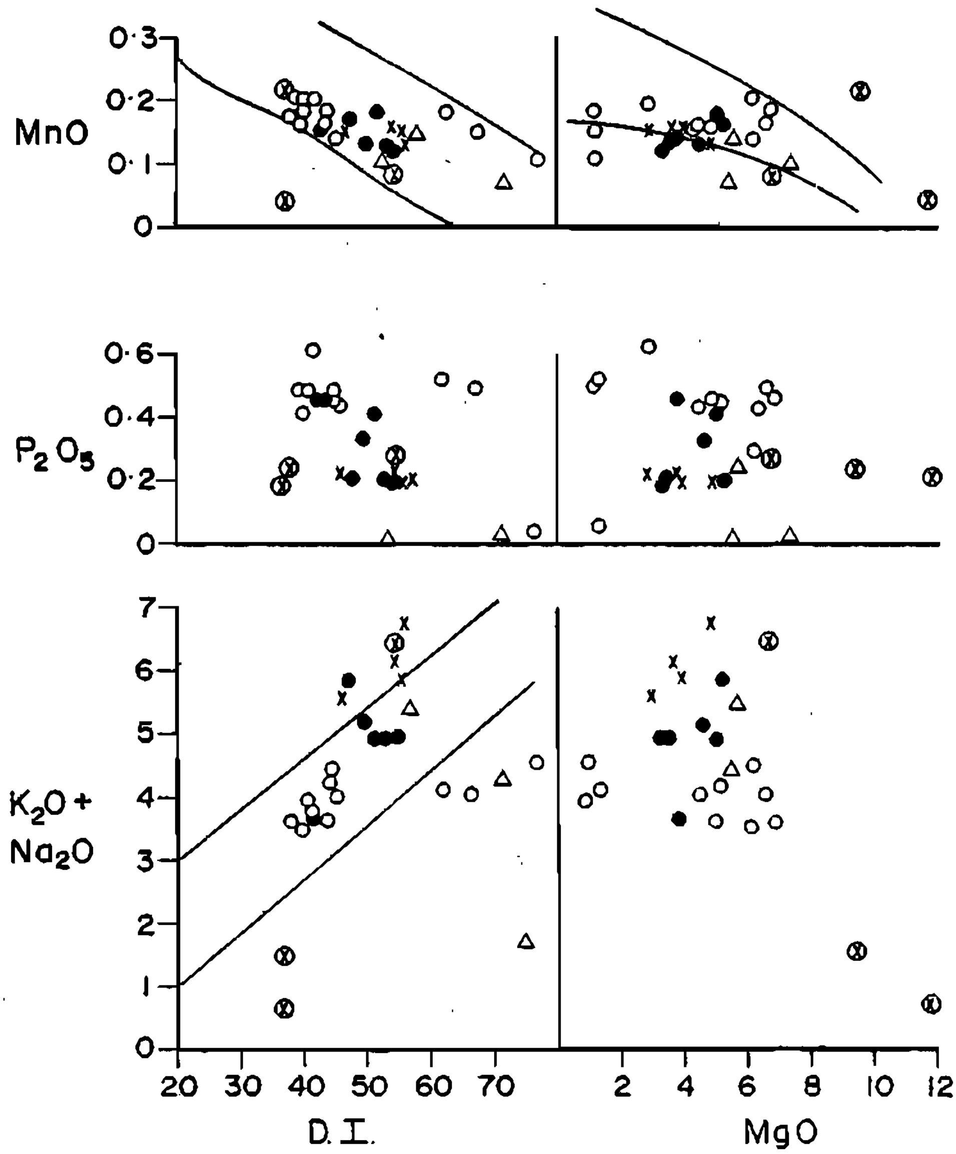

Figure 6.6 D.I. and MgO variation diagrams for MnO, P_2O_5 and total alkalies. Ornamentation as for Figure 6.4. All oxides as weight percentages.

The trace elements are shown on D.I., MgO and Ti variation diagrams (Figs. 6.7, 6.8 and 6.9). Ti is used because it is essentially immobile and was shown to provide reasonable separation of the data in the major element plots.

Nb, Y, Sc and Zr have no apparent covariance with D.I. and MgO. On the titania plot, positive trends are poorly defined, but do show enrichment of these elements at higher Ti values. Y/Ti, Zr/Ti and Nb/Ti ratios for Qudeni Formation lavas show enrichment relative to chondritic values. The Ndikwe lavas have similarly high Nb/Ti and Zr/Ti ratios but chondritic Y/Ti ratios. Sc shows no systematic variation on any of the plots. On the Sc/Ti plot Sc seems to be nearly constant between 20 and 30 ppm except for two or three samples. The chondritic ratio for Sc/Ti (1/78, which is off the scale of the plot used), is very much higher than the observed values. Extreme Sc depletion is thus recognized for the Nsuze lavas.

V for the Ndikwe samples decreases systematically with increasing D.I. and MgO and decreasing Ti. These samples define a linear trend passing through the origin, with a slope considerably lower than chondritic V/Ti ratios, suggesting that the Ndikwe lavas were derived from a source which was either depleted in vanadium or enriched in zirconium. In contrast, the plots for the Qudeni lavas show no systematic trends against D.I., MgO or Ti.

Cr shows no systematic variation on any of the plots, although Cr abundances in two samples from the Ndikwe Formation are significantly higher than the remainder.

Ba, La and Zn do not vary systematically with D.I. The Ndikwe samples show decreasing Ba contents at higher MgO values. Contents of La and Zn in the Ndikwe lavas show little variation with increasing MgO content. However, these lavas lie in fields discrete from those of the Qudeni samples on the La/Ti and Zn/Ti diagrams. On the Ti diagram samples from the Qudeni Formation have a negative slope for Ba, whereas La and Zn lie on trends of positive slope. The La/Ti ratios are higher than that of chondrites for both sample groups.

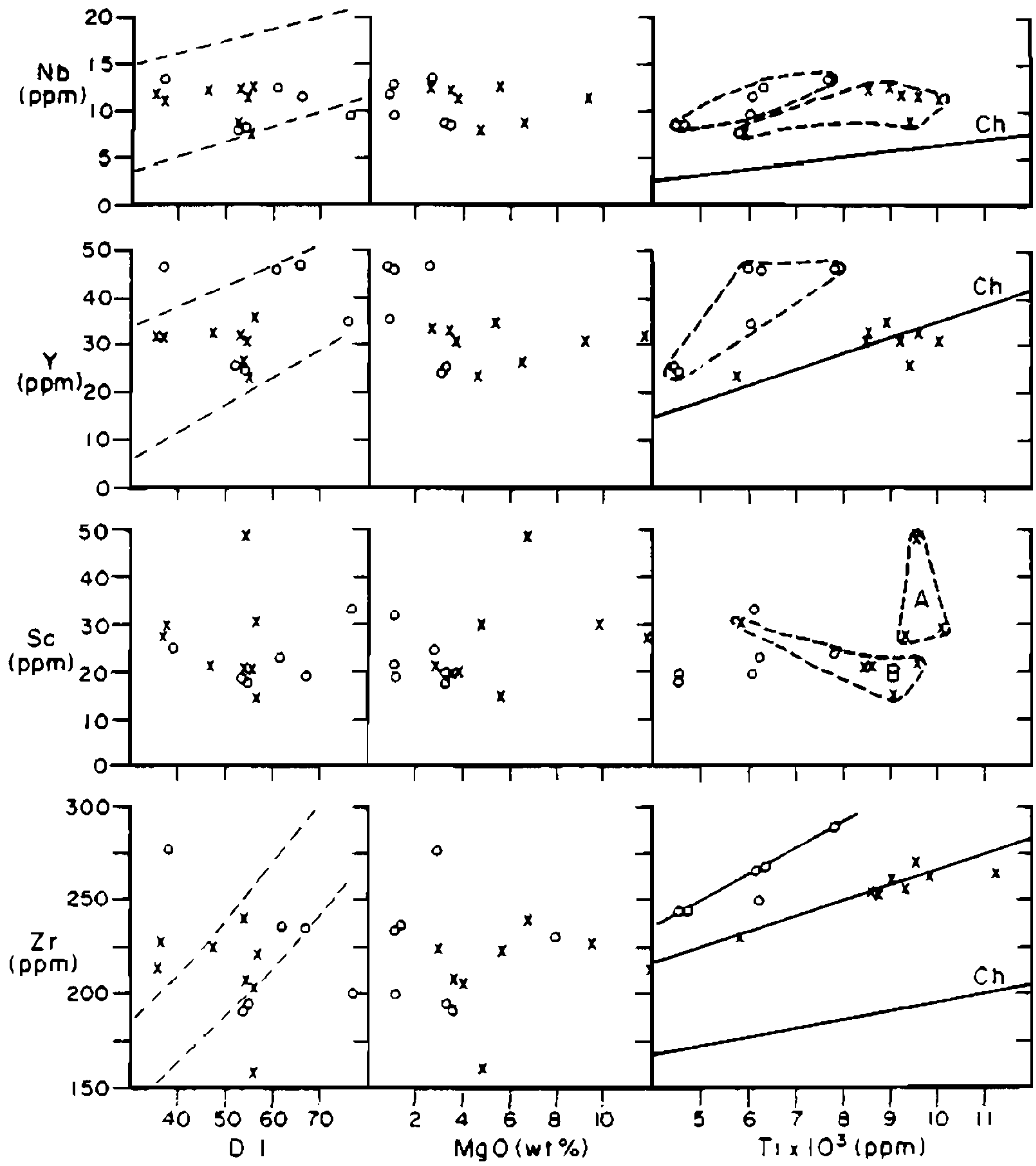

Figure 6.7 D.I., MgO and Ti variation diagrams for Nb, Y, Sc and Zr in the Nsuze lavas. Ornamentation: o - Qudeni Formation; x - Ndikwe Formation. In these and subsequent variation diagrams the pyroclastic samples are excluded.
Ch - chondrite ratio for elements concerned;
A - field for lower Ndikwe lavas;
B - upper Ndikwe;
C - (where shown) field for the Qudeni lavas.

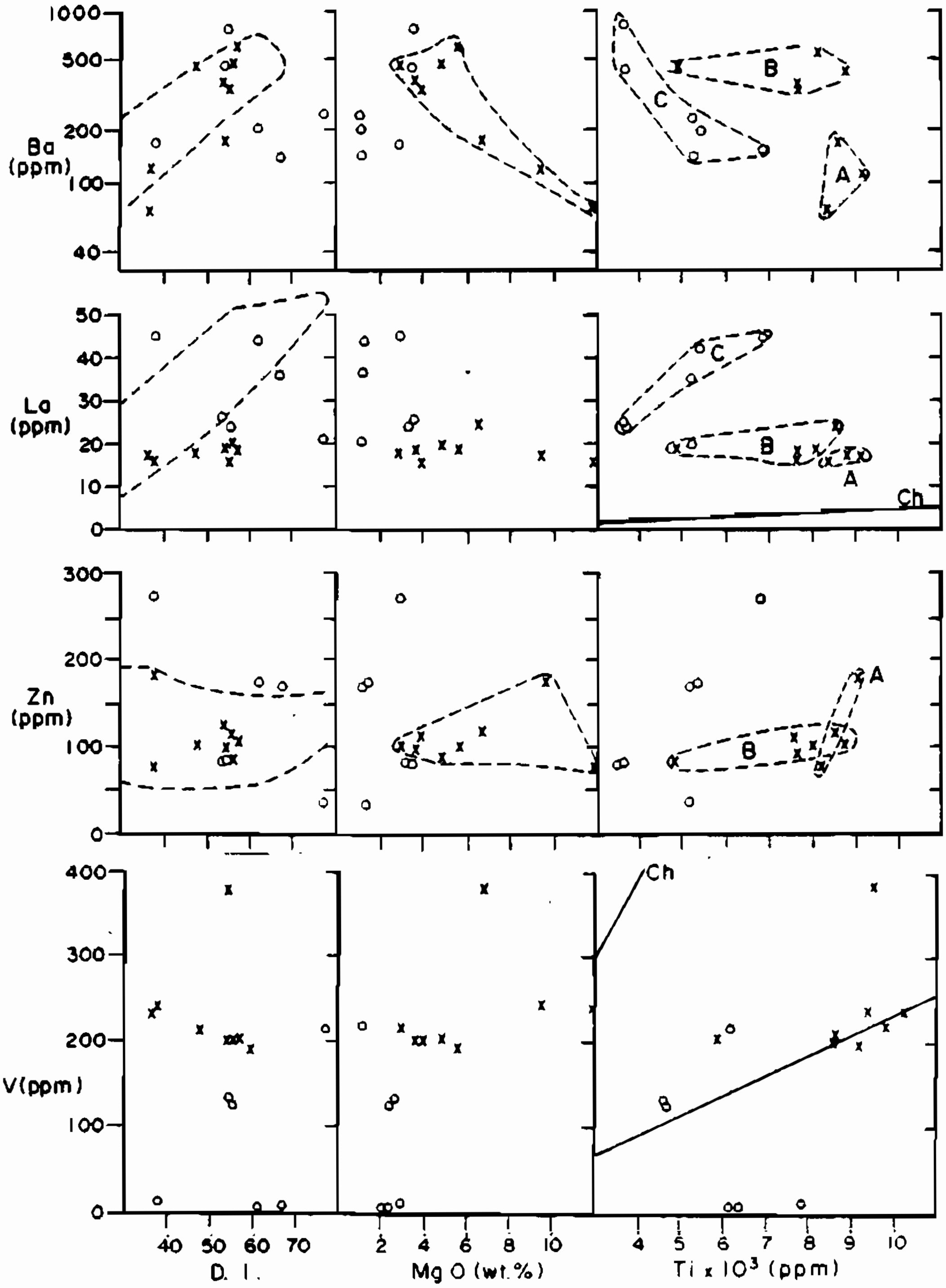

Figure 6.8 D.I., MgO and Ti variation diagrams for Ba, La, Zn and V in the Nsuze lavas. Ornamentation as for Figure 6.7.

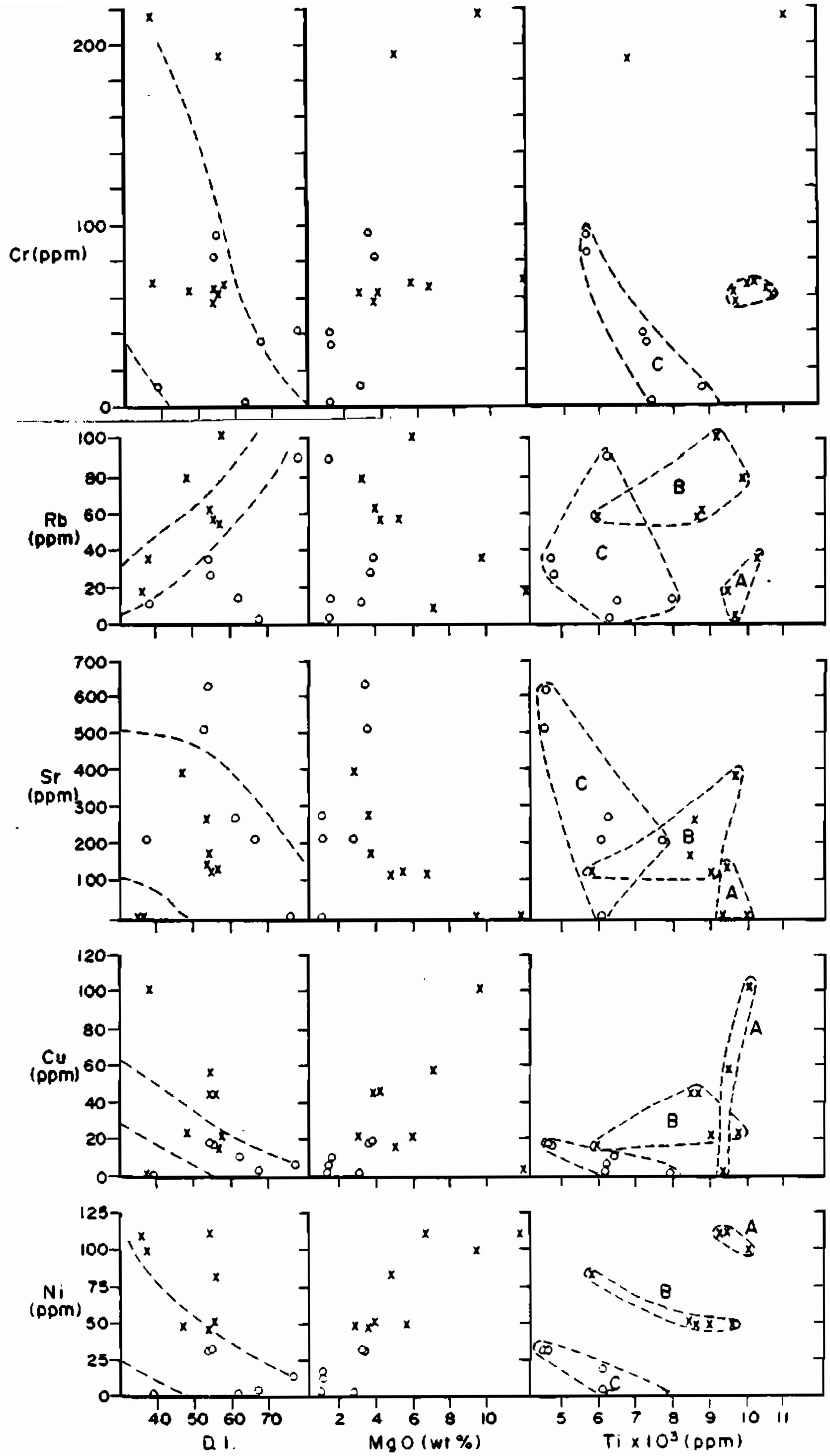

Figure 6.9 D.I., MgO and Ti variation diagram for Cr, Rb, Sr, Cu and Ni in the Nsuze lavas. Ornamentation as for Figure 6.7.

Rb and Sr values for the Qudeni lavas show no systematic variation when plotted against D.I., MgO or Ti. In contrast, the Ndikwe samples decrease in Rb and Sr contents with increasing MgO with the exception of two apparently aberrant plots on the Rb-MgO diagram.

Cu decreases with increasing D.I. and decreasing MgO along a dispersed trend which includes the samples from both of the units. For the Qudeni Formation, a decrease of Cu with increasing Ti occurs, whereas the Ndikwe Formation shows no correlation between Ti and Cu. Ni-D.I. reveals no systematic variation. On the Ni-MgO plot the combined sample populations show a sympathetic increase in Ni with MgO. There is no correlation between Ni and Ti abundances of the Ndikwe lavas, but there is an antipathetic increase in Ni with decreasing Ti in the Qudeni samples.

Fields in which samples from the lower and upper parts of the Ndikwe Formation fall (fields A and B respectively on Figs. 6.7, 6.8 and 6.9) are shown on the trace element plots. There is an apparent difference between the two sub-populations, but this may be spurious because all of the samples from the lower group are altered. Additional data are required to confirm that the Qudeni Formation and upper and lower lava sequences in the Ndikwe Formation do have distinctive geochemical signatures with respect to trace elements. The fact that the distinction can be made with respect to minor and trace elements that are believed to be relatively immobile during alteration suggests that there are real differences between the three lava sequences.

5. Ultramafic Rocks

Chemical analyses of eight ultramafic rocks of uncertain correlation are presented in Table 6.6. Samples BG122, BG123 and BG124 are from talc - tremolite - chlorite schists interpreted as lavas because of the presence of features resembling sheared out flow-top textures, amygdaloidal zones and local

TABLE 6.6: CHEMISTRY OF ULTRAMAFIC ROCKS

	EXTRUSIVE ROCKS			SERPENTINITES		ULTRAMAFIC DYKES		
	BG122	BG123	BG124	BG173	BG175	BG116	BG121	BG158
SiO_2	50.79	44.94	48.14	47.65	51.04	50.72	50.18	50.34
Al_2O_3	5.69	9.37	6.59	8.21	7.45	5.03	4.78	5.93
Fe_2O_3	1.25	1.45	1.42	1.05	0.99	1.34	1.29	1.21
FeO	11.23	13.01	12.75	9.42	8.92	12.09	11.58	10.93
MnO	0.27	0.23	0.18	0.23	0.16	0.19	0.19	0.20
MgO	20.64	22.60	21.36	24.01	25.95	19.28	21.99	20.87
CaO	9.92	6.64	8.37	8.03	4.34	10.22	8.99	9.47
Na_2O	0.00	0.29	0.08	0.24	0.00	0.28	0.00	0.10
K_2O	0.02	0.01	0.00	0.00	0.00	0.00	0.00	0.00
TiO_2	0.61	0.39	0.51	0.21	0.19	0.52	0.35	0.83
P_2O_5	0.09	0.07	0.09	0.03	0.04	0.09	0.08	0.11
Cr_2O_3	0.42	0.70	0.44	0.82	0.77	0.24	0.66	0.31
TOTAL	100.93	99.70	99.93	99.90	99.85	100.00	100.09	100.30
				Trace elements (ppm)				
Sc	47	19	42	31	22	27	13	20
V	259	168	272	172	142	166	116	160
Cr	3580	4804	3887	5627	6207	1611	4620	2680
Ni	899	1623	1090	1058	1348	540	1779	1399
Cu	-	3	3	-	97	205	184	13
Zn	122	98	109	116	80	106	77	100
Y	14.6	4.8	11.2	4.4	6.0	13.4	6.0	12.7
Zr	72.1	43.3	62.3	26.1	27.6	62.5	52.3	83.3
Nb	1.9	0.6	2.4	0.2	1.0	2.6	1.4	4.6
Rb	0.9	1.6	0	1.3	0.3	-	-	-
Sr	31.9	37.2	35.7	127	9.5	3	7.9	18
Ba	-	12	-	-	-	-	-	2
La	14	-	9	-	-	7	-	6

compositional heterogeneity. The rocks now consist of relatively coarse-grained secondary mineralogy and no relict textures are present. These samples are from the anticline separating the Central and Gem Synclines in the Mdlelanga Valley. Two samples, BG116 and BG121, from sub-vertical, conformable intrusions in the same area are included in this group because of their petrographic similarity. Two samples from a sheared serpentinite body in the sole of a thrust west of Ndikwe are also included (BG173 and BG175). The serpentinite may represent part of the pre-Nsuze basement "squeezed" along the fault. A sample (BG158) from a conformable sill intruded along the contact of the Ndikwe and Qudeni Formations 1 km south of Ndikwe is included as it is petrographically identical to the other ultramafic dyke samples.

The major elements are shown on MgO variation diagrams (Fig. 6.10). The three samples believed to be extrusive show increasing SiO_2, TiO_2, CaO and CaO/Al_2O_3 with decreasing MgO, with FeO*, Al_2O_3 and Cr_2O_3 decreasing synpathetically. As these trends are defined by only three samples they cannot be assumed to have any significance. The samples from the intrusions are scattered on all of the plots except SiO_2 and CaO on which an apparent linear increase in these elements accompanies decreasing MgO. The two serpentinites plot at higher MgO values and are not obviously related to the other two sample groups. Combined data for all three groups are scattered on the SiO_2, Al_2O_3 and FeO* plots, but show apparently systematically increasing TiO_2, CaO and CaO/Al_2O_3 and decreasing Cr_2O_3 trends with decreasing MgO. All of the samples have similar alkali contents, but these are close to the detection limits of the analytical methods used.

Plots of trace element contents against MgO (Fig. 6.11) reveal increases in Zr, Sc, Y and Nb with decreasing MgO. V is nearly constant with only a poorly-defined negative slope. Nickel decreases with decreasing MgO contents. These trends are not particularly useful as Zr, Sc and Y are incompatible in most

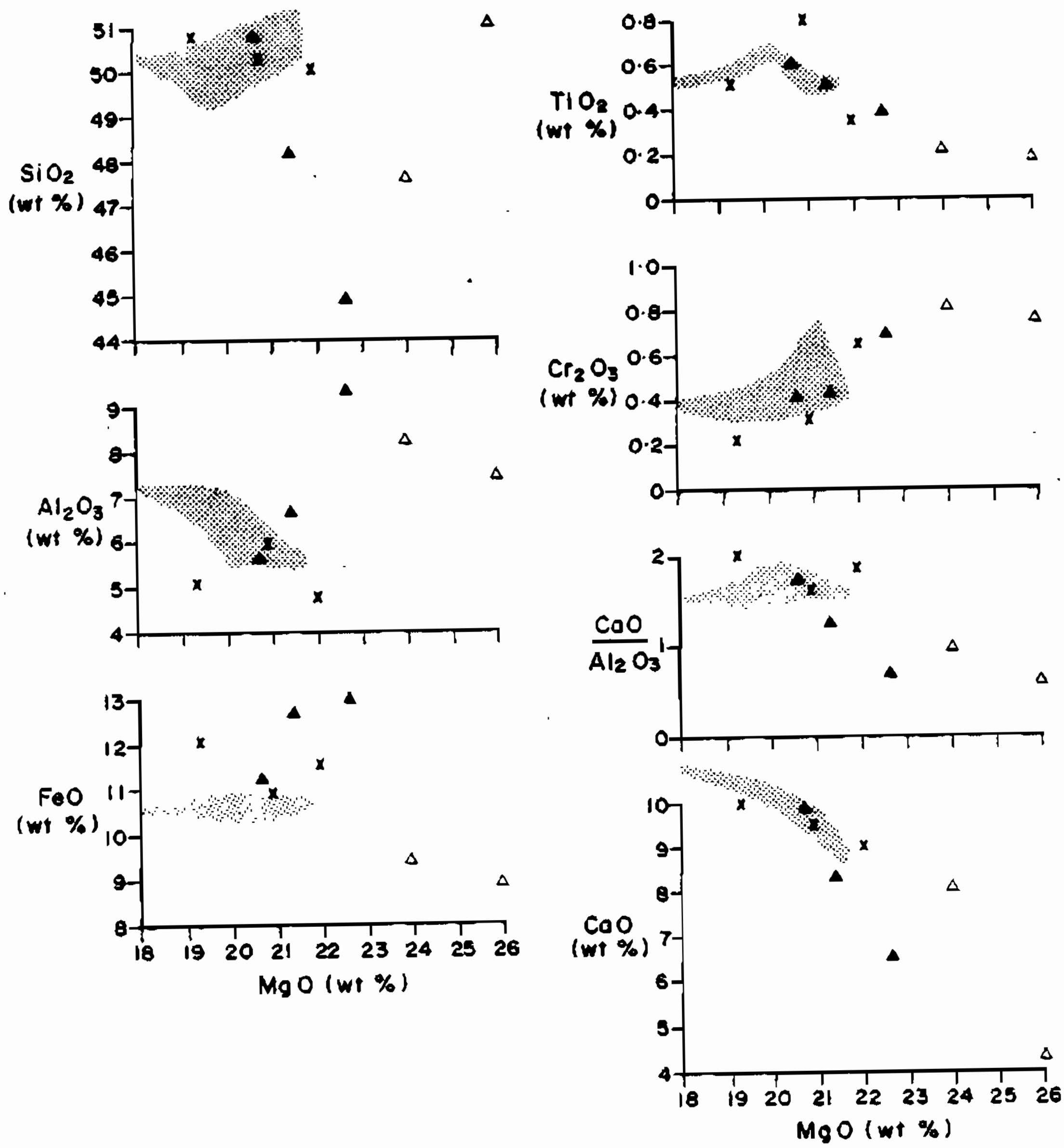

Figure 6.10 MgO variation diagrams for SiO_2, Al_2O_3, FeO*, TiO_2, Cr_2O_3, CaO/Al_2O_3 and CaO in extrusive (?) - (solid triangles) and intrusive - (crosses) ultramafic rocks. Serpentinites - (open triangles) are included. Shaded fields are for komatiitic lavas in the Nondweni type area (after Wilson *et al.*, in preparation).

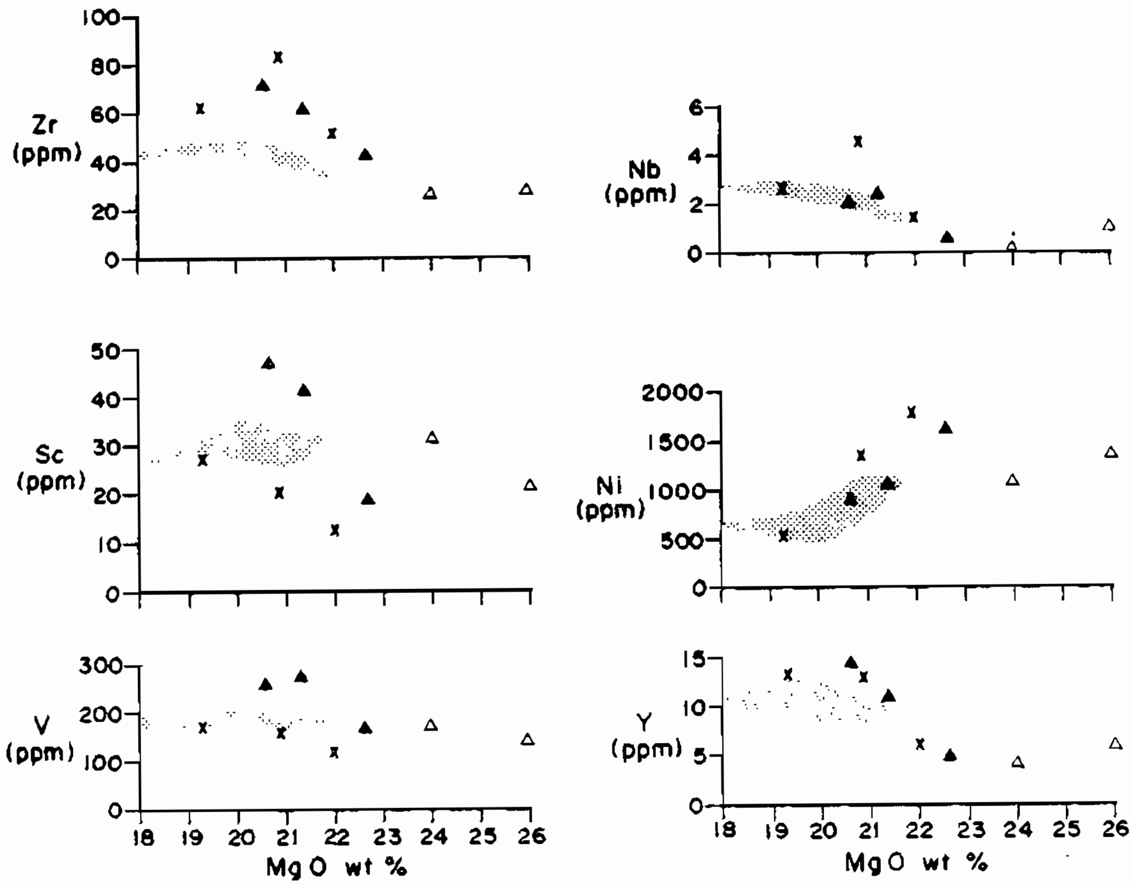

Figure 6.11 MgO variation diagrams for selected trace elements in the ultramafic rocks. Ornamentation and shaded field as in Figure 6.10.

mafic phases. Likewise, the behaviour of Ni and Cr could indicate olivine or pyroxene fractionation.

Selected trace elemnts are plotted against Zr (Fig. 6.12). The fields of the lavas and intrusive rock-types are generally coherent. The rocks have Y/Zr Ti/Zr, Nb/Zr, V/Zr and Sc/Zr ratios slightly lower than chondritic values for the same ratios. Although the Y/Zr, Ti/Zr and Nb/Zr show linear distributions which extrapolate close to the origin, V and Sc plot in scattered fields. V/Sc and Sc/Y ratios are approximately chondritic, whereas the Nb/Y ratio is slightly higher than chondrite (diagrams for these relationships are not presented) A phase in which these elements are compatible, or at least less incompatible than Zr must have been involved either as a fractionating phase or as a residual phase during partial melting. This suggests the involvement of garnet at some stage as Sc is partitioned into this mineral. Significantly, these plots show considerable similarity between the trace element values and ratios and those reported from the Nondweni type area (Wilson *et al.*, in prep.).

6. Discussion

The Nsuze lavas and associated ultramafic rock-types have a wide range in chemistry which shows few consistent trends. There is no apparent relationship between the two groups of samples which must, therefore, be discussed separately.

Data for the Nsuze volcanics plot close to the trends identified by Armstrong (1980), indicating some geochemical similarity between lavas from the Vryheid - Piet Retief inlier and the study area. The altered samples commonly plot beyond the limits of these trends as might be expected.

On the basis of the few samples considered to be unaltered, there are few differences between the Ndikwe and the Qudeni lavas. The former do have slightly higher Al_2O_3, FeO* and TiO_2 contents and lower CaO than the latter. It is clear

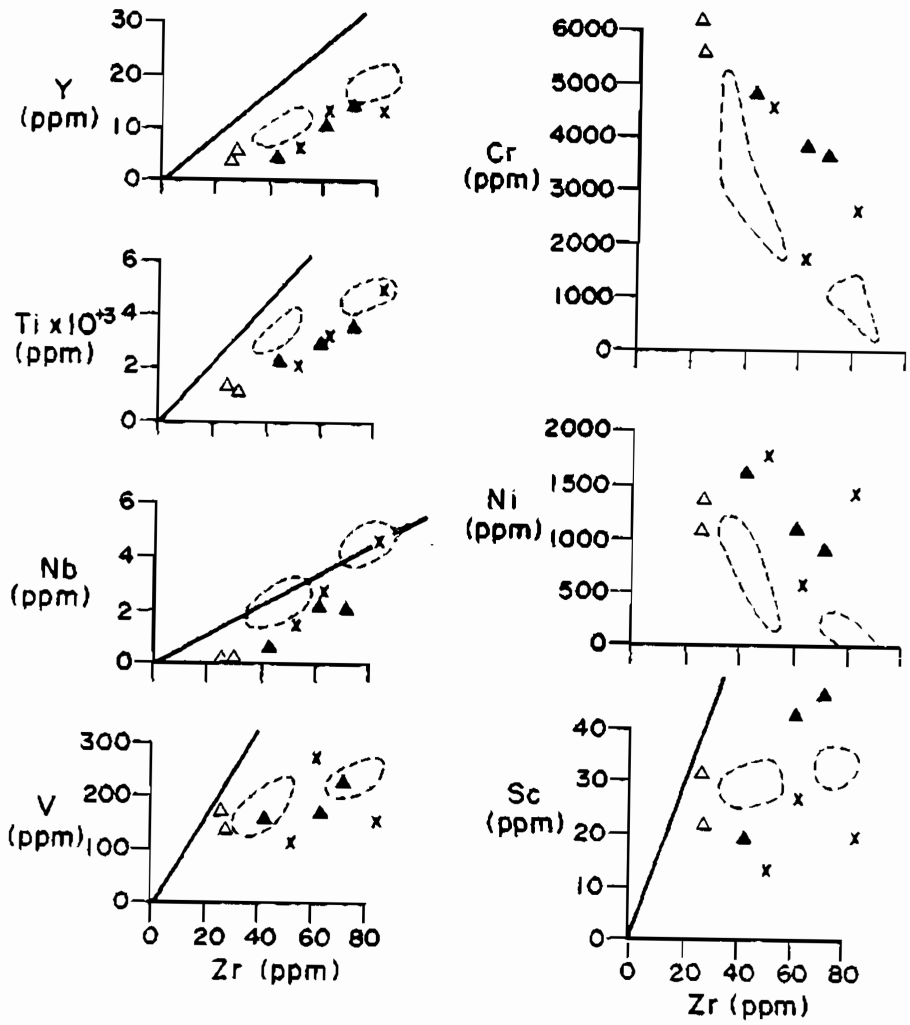

Figure 6.12 Diagram showing selected trace element concentrations plotted against Zr. Ornamentation as in Figure 6.10. Fields are for komatiites (lower Zr values) and high magnesium basalts in the Nondweni type area (after Wilson *et al.*, in preparation). Slope of heavy line is the chondrite ratio for the elements involved.

that the sampling of the different volcanic units has been inadequate to allow modelling of their petrogenesis, either as a group or as separate units.

Several samples show extreme depletion of CaO and excessively high MgO contents for their silica, alumina and iron abundances. Alteration by interaction with seawater may be the cause of this. Mottle and Holland (1978) and Seyfried and Mottle (1982) documented experimental studies of Ca-Mg ion exchange during submarine alteration of basalt. Substitution of Mg for Ca can lead to extreme depletion of the latter element. Despite the lack of primary textural evidence for extrusion of the lavas subaqueously, their stratigraphic association with shallow marine sediments presumes that the lavas were submerged at some stage. If submarine alteration did affect the lavas displaying aberrant chemistry, then the possibility exists that other rocks sampled may have been affected,albeit to a lesser degree. This implies that any variation involving Mg, Ca and perhaps the alkali elements cannot be related unequivocally to primary igneous processes.

The trace element data, although showing considerable scatter on the variation diagrams, provide some discrimination between the various lava units sampled. The three fields shown on the trace element plots as A, B and C represent sample groups from the lower and upper Ndikwe and the Qudeni Formation in the order given. The general alteration of the volcanics means that the slight separation of the fields for the lower and upper Ndikwe volcanics is probably not meaningful, particularly as this separation is least pronounced on plots of the immobile elements. There is, however, good evidence for separation of the Ndikwe and Qudeni lavas on the basis of their Nb, Y, Zr, Ni, La and Cr abundances. As noted in section 2 of this chapter (above), these are the elements least likely to be disturbed by the effects of alteration.

The magmatic affinity of the Nsuze Group lavas may be assessed using various parameters. On the basis of a total alkalies - silica diagram, the lavas are classified as sub-alkaline (Fig. 6.13) according to the parameters defined by

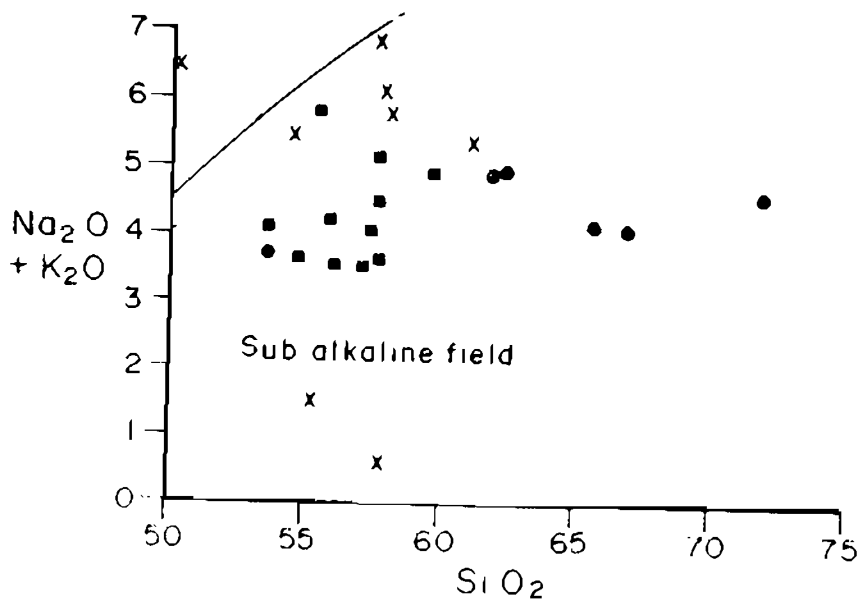

Figure 6.13 Plot of total alkalies vs silica. Field of the subalkaline rocks after Irvine and Baragar (1971). Solid line defines boundary between alkaline and subalkaline magma suites after Irvine and Baragar (1971). Ornamentation as in Figure 6.1.

Irvine and Baragar (1971). Sub-alkaline rocks may be separated into calc-alkaline and tholeiitic using other discrimination diagrams. On the ternary plot of $Na_2 + K_2O$ - FeO* - MgO (AFM) (Fig. 6.14A) the plots of the data overlap both calc-alkaline and tholeiite fields as defined by Irvine and Baragar (1971). If only the unaltered samples are considered (Fig. 6.14B), most of the points lie within the calc-alkaline field and well away from the tholeiite trend defined by Armstrong (1980) for the northern area of the Nsuze group. On the ternary plot of Al_2O_3 - FeO + Fe_2O_3 + TiO_2 - MgO the data plot close to the boundary of the high Fe, high-Mg tholeiitic basalts and the calc-alkalic basalt fields (Fig. 6.15) as defined by Jensen (1976). If the altered samples are excluded, the data plot predominantly within the calc-alkalic field. This apparent variation from the dominantly tholeiitic trend identified by Armstrong (1980) requires careful evaluation. Several parameters based on FeO*, MgO, V and Cr may also be used to distinguish calc-alkalic from tholeiitic suites (Miyashiro and Shido, 1975). On the FeO* : FeO*/MgO diagram the lavas plot predominantly in the tholeiitic field (Fig. 6.16), but on the Cr/V diagram, they plot in the transitional field (Fig. 6.17). According to the parameters defined by Irvine and Baragar (1971) for discriminating between calc-alkaline and tholeiitic suites using the relationship of alumina content to normative plagioclase content all of the samples except BG147, which is altered, may be classified as tholeiites (Fig. 6.18). The Nsuze lavas from the study area thus have some characteristics of both tholeiitic and calc-alkalic magma suites. This is in agreement with the findings of Armstrong (1980), who reported that no discriminant diagram provided an unequivocally calc-alkaline classification of the Nsuze Group lavas in the Vryheid - Piet Retief area. He also reported that not all of the major and trace element data indicated a wholly tholeiitic character for these lavas.

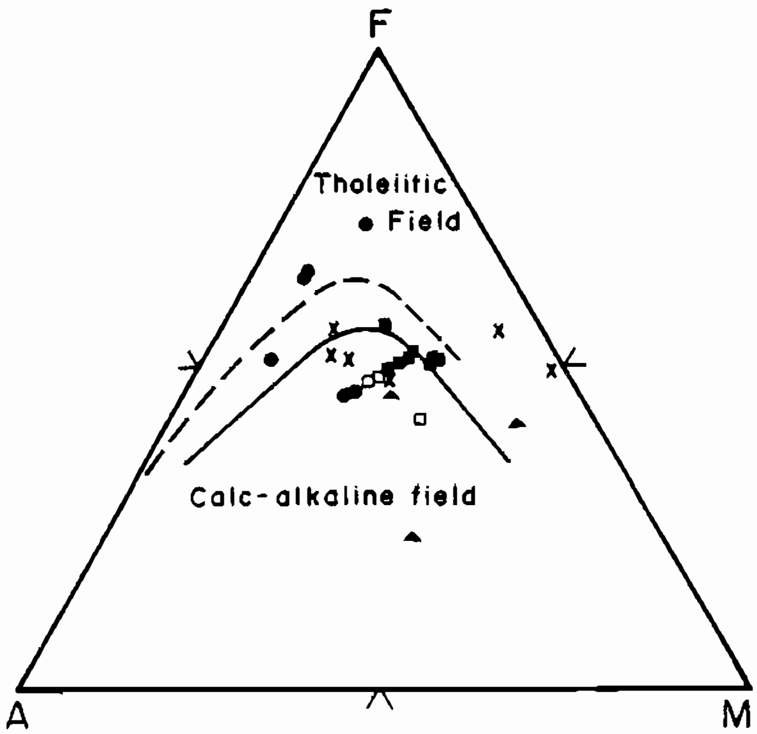

Figure 6.14A The ternary plot ($Na_2O + K_2O$) - FeO^* - MgO for the Nsuze Group volcanics. Ornamentation as for Figure 6.1. —— = boundary of tholeiitic field (after Irvine and Baragar, 1971).
— —- = dominant Nsuze trend (after Armstrong, 1980).

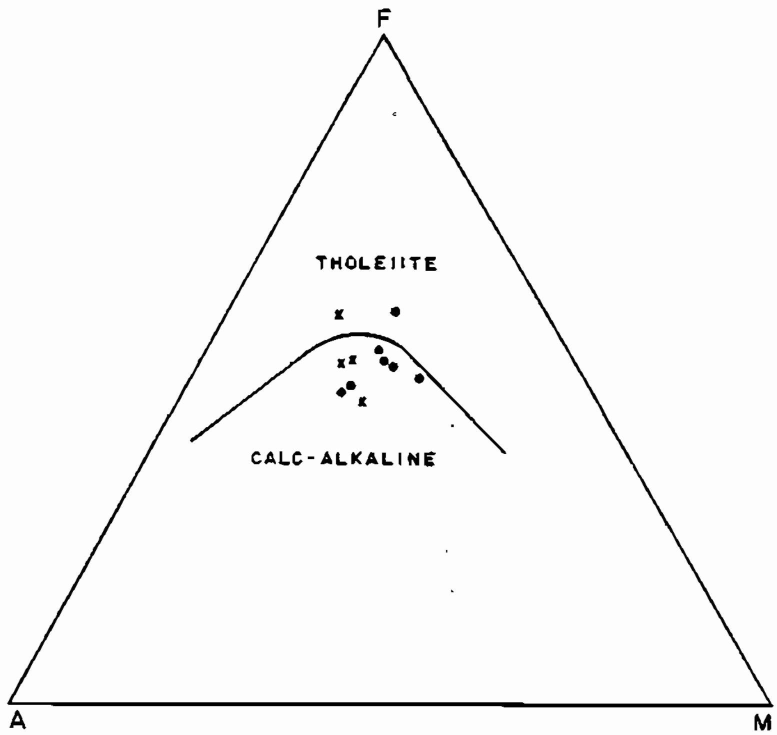

Figure 6.14B AFM diagram showing only unaltered Nsuze Group lavas. Circles - Qudeni Formation; crosses - Ndikwe Formation.

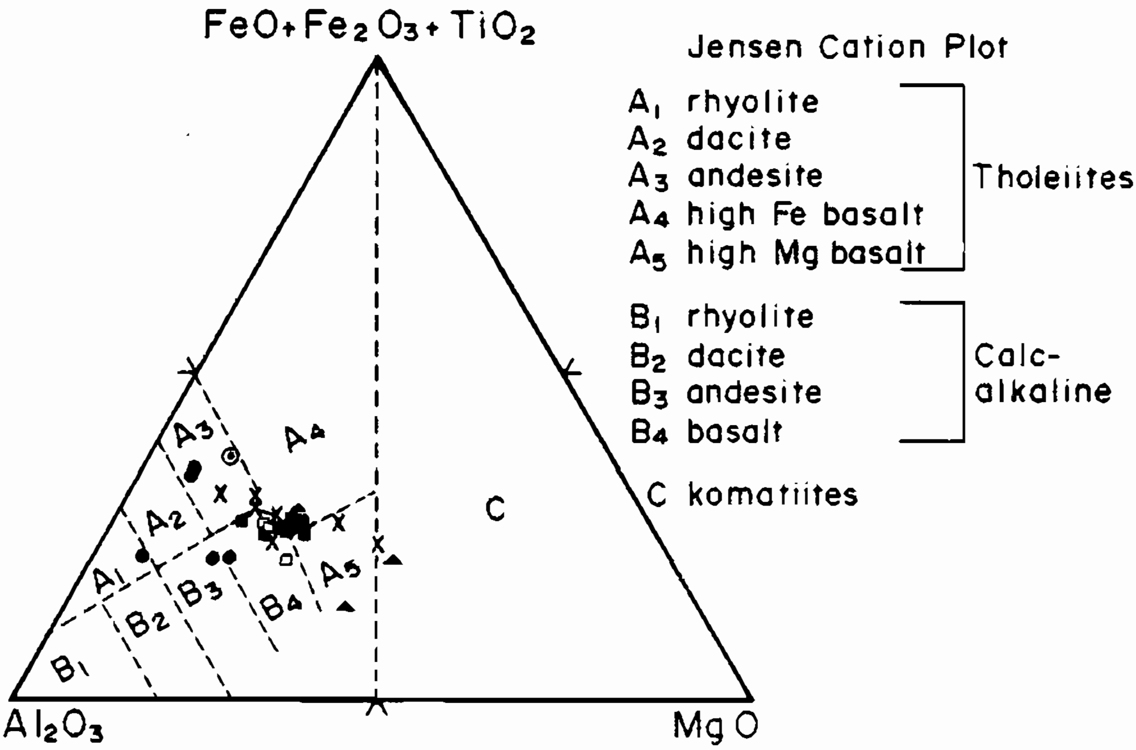

Figure 6.15 Jensen diagram for the Nsuze Group volcanics. Ornamentation as for Figure 6.1. (Boundaries after Jensen, 1976).

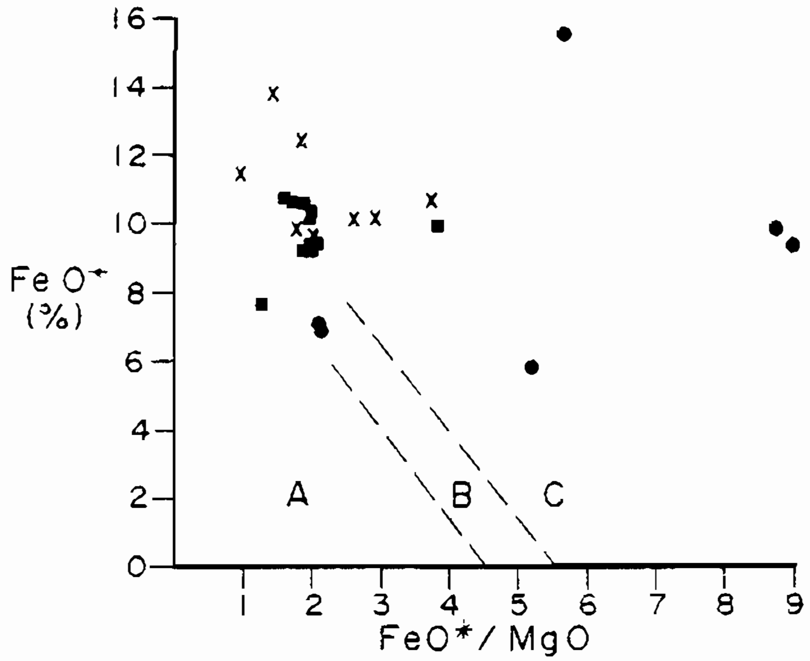

Figure 6.16 Diagram showing variation of FeO* with FeO*/MgO for the Nsuze Group lavas. Fields A, B and C represent calc-alkaline, transitional and tholeiitic suites respectively. Fields after Miyashiro and Shido (1975). Ornamentation as for Figure 6.1.

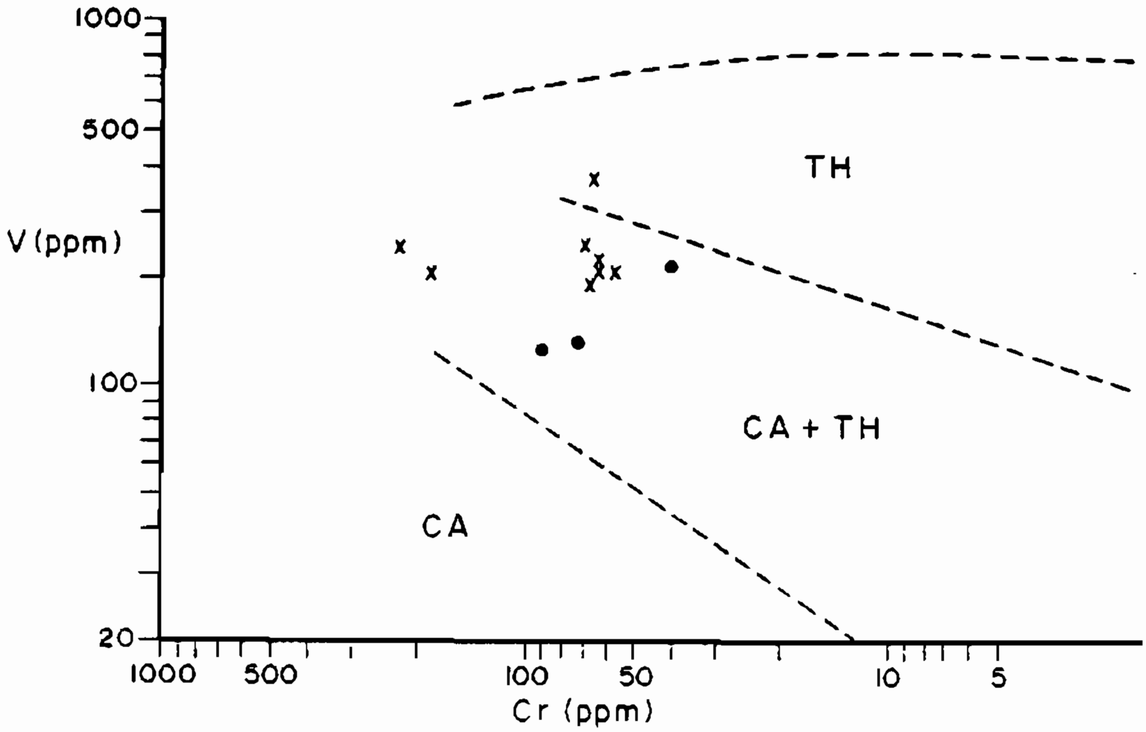

Figure 6.17 Cr-V discrimination diagram showing Nsuze Group lavas in relation to calc-alkaline, transitional and tholeiitic fields as defined by Miyashiro and Shido (1975). Ornamentation as in Figure 6.1. Pyroclastics and rhyolites excluded.

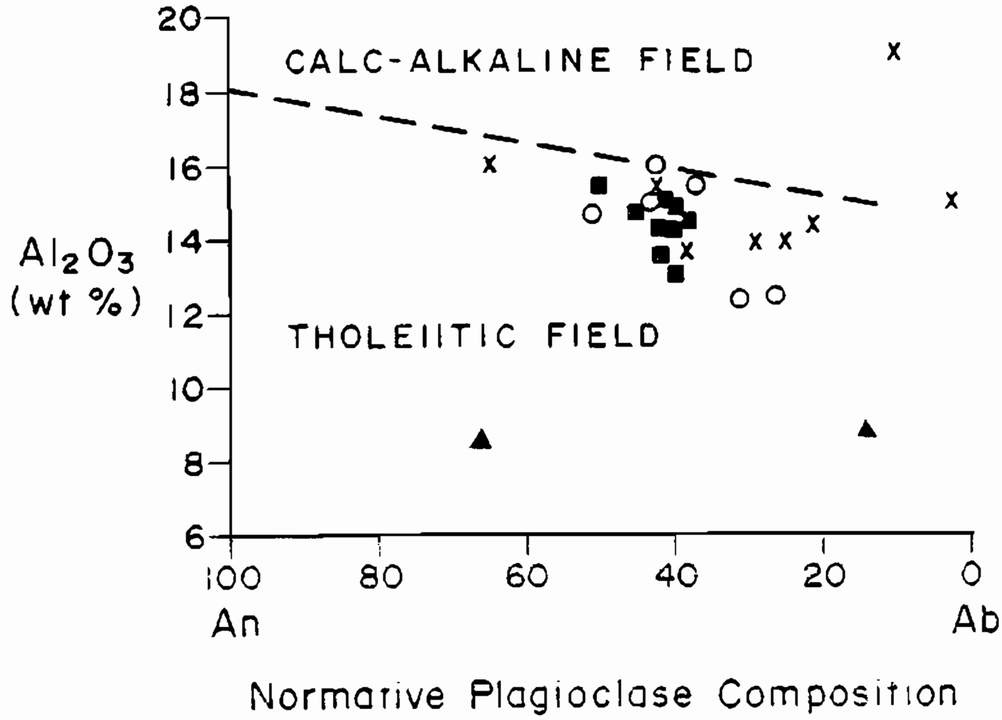

Figure 6.18 Plot of AL_2O_3 against normative plagioclase content for the Nsuze Group lavas. Fields of tholeiitic and calc-alkaline rocks after Irvine and Baragar (1971). Ornamentation as for Figure 6.1.

The tectonic setting within which lavas are generated is thought to influence their chemistry and several discrimination diagrams have been devised for the recognition of these settings (Pearce *et al.*, 1977; Floyd and Winchester, 1976 and Pearce and Cann, 1973). These schemes of discrimination were devised for Mesozoic volcanics erupted in known plate tectonic settings. Their application to the Nsuze lavas requires the equivocal supposition that similar plate motions were operative during the Archaean. Furthermore, the plots were devised for rocks of basaltic composition which are rare in the study area. On the ternary plot of MgO - FeO* - Al_2O_3 presented by Pearce *et al.* (1977) for sub-alkaline rocks having SiO_2 contents of 51 - 56% magmas generated in a number of settings may be distinguished. The eight Nsuze lavas which meet the above criteria plot predominantly within the field of continental volcanic (Fig. 6.19). However, only two of the samples are unaltered on chemical criteria and one of these plots in the oceanic island field and the other in the field of continental volcanics. This evidence for an intraplate setting is tenuous, but is in agreement with Armstrong's (1980) conclusion in this regard for the Nsuze volcanics.

Rocks of ultramafic composition are found as dykes, sills and, possibly, interbedded flows in the stratigraphically lowest parts of the Nsuze Group. The possibility cannot be excluded that those ultramafic rocks interpreted as flows and sills could represent members of the pre-Nsuze Nondweni Group tectonically intersliced with the Nsuze rocks. The sheared nature of the rocks, together with the lack of laterally extensive outcrop could obscure such interslicing.

Alternatively, the marked difference in chemistry between these rocks and the more typical Nsuze volcanics does not preclude a chronostratigraphic relationship between these rock-types. Chemically distinct and apparently unrelated tholeiitic and komatiitic lavas commonly occur together in typical Archaean sequences (Wilson, *et al.*, in prep., Smith and Erlank, 1983; Jahn *et al.*, 1980). Even the sub-vertical intrusions, here referred to as dykes, are

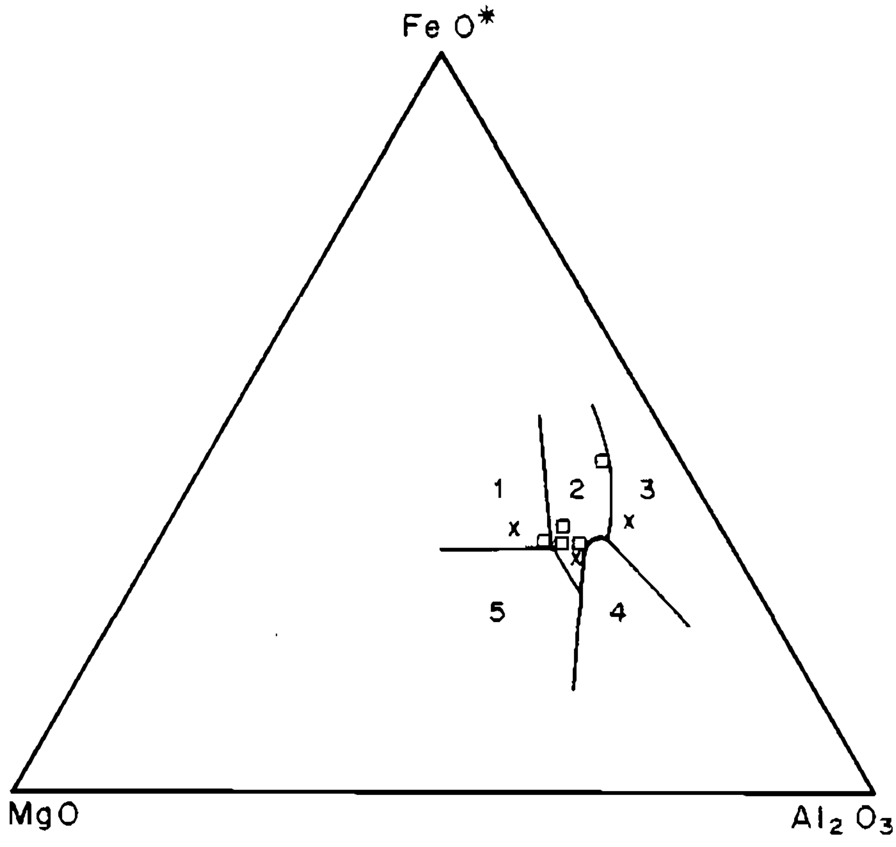

Figure 6.19 Ternary plot of MgO-FeO*-Al_2O_3 showing fields of tectonic setting as defined by Pearce *et al.* (1977). Nsuze Group lavas having SiO_2 between 51 and 56% plotted.

□ = Qudeni Formation X = Ndikwe Formation

1. Oceanic island
2. Continental
3. Spreading centre island.
4. Orogenic.
5. Ocean ridge and floor.

conformable to the enclosing Nsuze rocks. Thus there is no unequivocal evidence to support a post-Nsuze age for these rocks. It may be significant that these sub-vertical intrusions are restricted to the stratigraphically lowest parts of the Nsuze Group. This relationship could be interpreted in two ways. If tectonic interslicing had occurred it might be reasonable to assume that it would manifest itself most commonly at or near the base of the Nsuze pile. An alternative argument could be that this komatiitic magmatism was limited to the earliest evolutionary stage of the Nsuze basin. Evidence will be presented in Chapter 8 that there was indeed a period of post-Nsuze magmatism of komatiitic affinity. The komatiitic rocks described above might, therefore, herald this later magmatic event.

Rocks of komatiitic affinity have yet to be found in other areas where the Pongola Supergroup crops out. The only exception is the classification of the Thole sills near Amsterdam as komatiitic by Hammerbeck (1977). This author believes these sills to be related to the Usushwana Complex. That these rocks may represent cumulates cannot be excluded at this time. If such were the case, they would not, of course, represent a primary magmatic composition. A similar argument could apply in the present case despite the obviously komatiitic character of the ultramafic rocks on a Jensen plot (Fig. 6.20).

A more detailed investigation of these poorly-exposed rocks is necessary before this enigma can be adequately resolved.

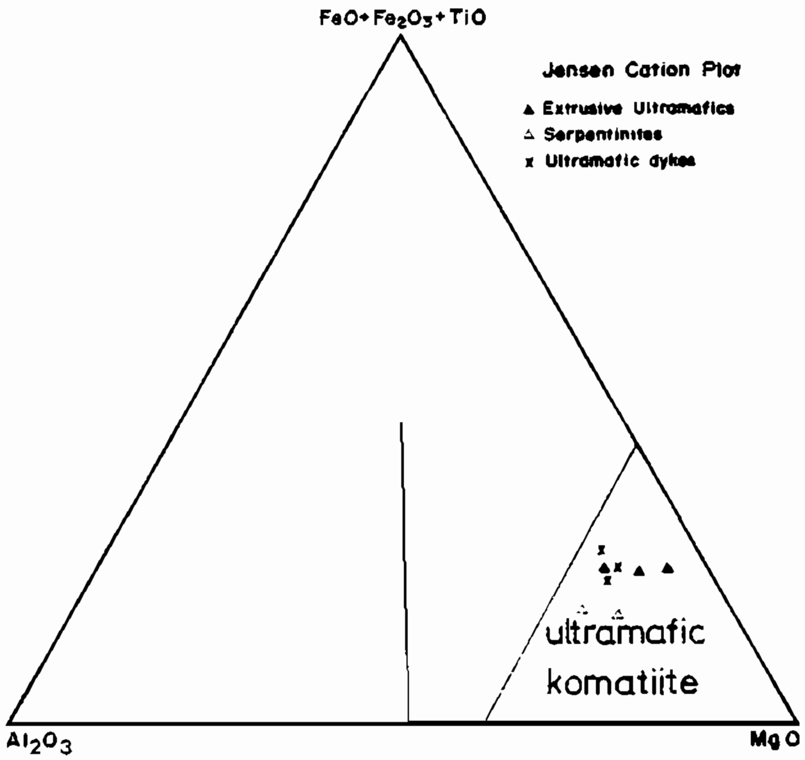

Figure 6.20 Ternary plot of Al_2O_3 - (FeO + Fe_2O_3 + TiO_2) - MgO for the ultramafic rocks. Ornamentation as for Figure 6.10. Field boundaries from Jensen (1976).

CHAPTER 7

THE HLAGOTHI COMPLEX

1. Introduction

A series of layered mafic to ultramafic sills intrudes the Nsuze Group in the northern part of the study area (Map 1). These bodies were first recognized by Du Toit (1931), who termed them the Hlagothi Igneous Complex. Du Toit (1931) noted that the intrusions comprised alternating layers of peridotite, gabbro and diorite, representing "the differentiated products of a single reservoir." He also mentioned the extensive alteration of most of the rock types.

Preliminary geochemical and petrographic studies have been carried out in order to identify the broad characteristics, magmatic affinity and crystallization history of the Complex.

2. Field Relationships and Extent of the Complex

Intrusions regarded as being associated with the Complex are located in an 18 km belt from the farm Wonderdraai in the east to west of the Nsuze River (Map 1). A maximum north-south extent for the complex is 8 km, measured along the Nsongeni and Nsuze Rivers. The most extensive occurrence is along the above-mentioned rivers where at least five layered sills are recognized. The sills are generally conformable with the Nsuze Group country rocks, which dip south at 10 -20°, but transgress and disrupt the sequence locally (Fig. 7.1). The combined observed thickness of the sheets is in excess of 500 m, with the thickest individual body being about 200 m thick. For the purposes of the ensuing discussion, the northern, stratigraphically lower sills are collectively known as the Nsongeni sheets. The southern, stratigraphically higher sheets are referred to as the main Hlagothi sheets.

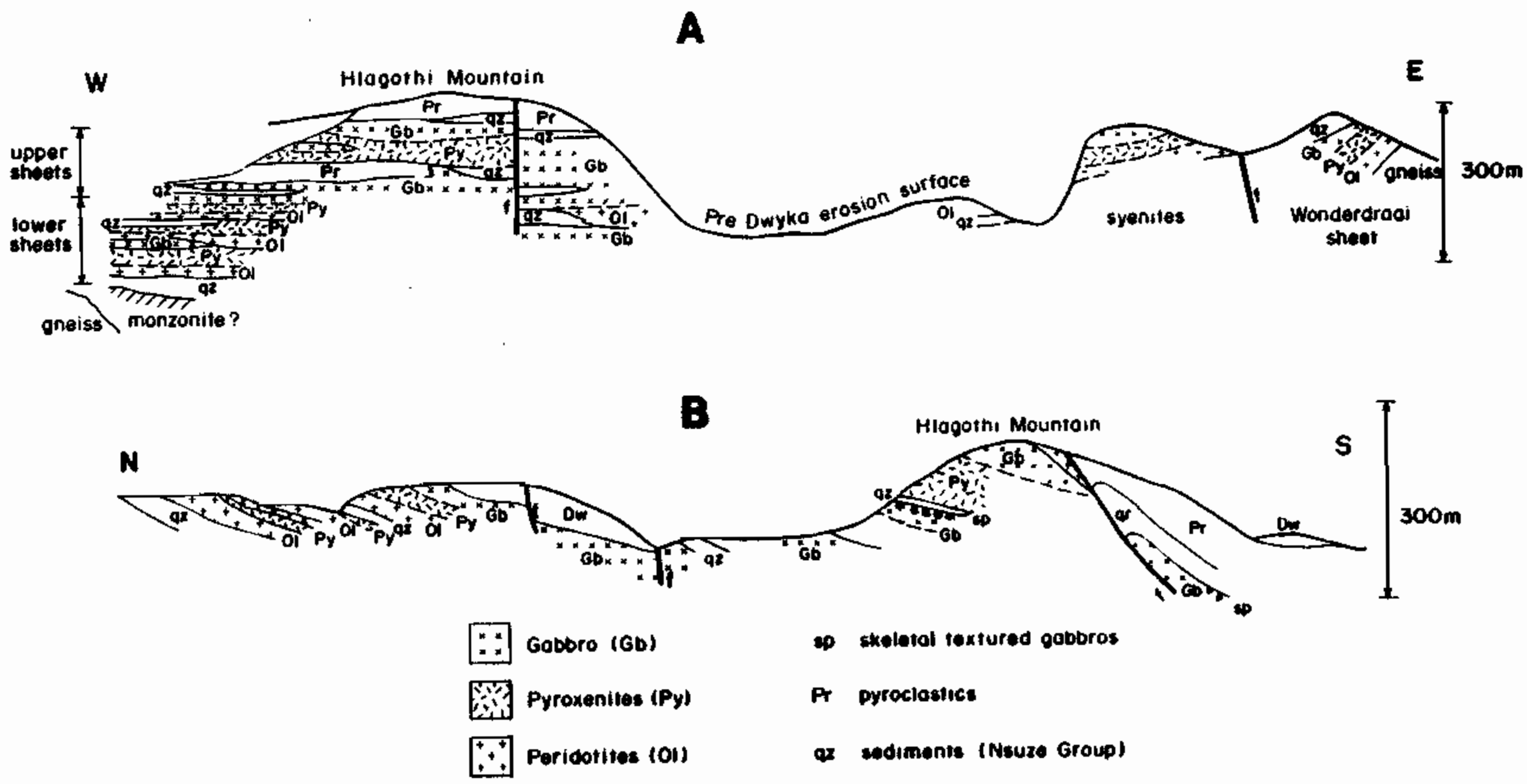

Figure 7.1 Simplified E-W and N-S cross-section through the Hlagothi Complex (not to scale). E-W section represents 18 km long section from Wonderdraai to the headwaters of the Nsuze River. The N-S section shows the 8 km long outcrop area along the upper Nsuze Valley.

Eastward extensions of the complex are situated in the valleys of the Mbizwe, Gozweni and Mhlatuze Rivers (Map 4). These sills are poorly exposed and their thickness and lateral extent are not well known. A minimum total thickness of 200 m is probable. The eastern sills, in particular the Wonderdraai sheet in the Mhlatuze Valley, dip conformably with the Nsuze Group to the southwest (Fig. 7.1). Their correlation with specific sheets in the western outcrops is not known.

The complex is intruded by porphyritic dykes which predate the Natal Group sediments of Ordovician age. Much of the complex is obscured by the overlying Dwyka Group sediments. The complex predates deformation and metamorphism thought to be related to the 1 000 Ma Natal-Namaqua orogenic event (Chapter 6), as it is locally deformed by folding and faulting of the main tectonic episode.

3. Petrography

General

A broad four-fold subdivision of the complex is possible on petrographic grounds. Individual sheets may not include all of the petrographic subdivisions but at least two may be recognized in each body. The lower portion of each sheet is feldspathic wehrlite, olivine websterite or lherzolite (the IUGS nomenclature presented by Streckeisen, 1973 is used). Rock types characterized by a dominance of two pyroxenes overlie the olivine-rich lithologies and are generally devoid of olivine. These rocks are either gabbronorites or websterites. The upper part of most of the sheets is gabbroic. Fine-grained marginal rocks containing skeletal minerals are present in some of the sills.

Olivine-bearing Rocks

The lower half of the Wonderdraai and the Nsongweni sheets consist of olivine-bearing rock types. Clino- and orthopyroxene are the other major constituent minerals, with minor amounts of plagioclase. These rocks are mostly completely altered to tremolite, chlorite, talc and serpentine, but retain relict textures.

Unaltered and partly altered olivine gabbronorites and lherzolites are present in the Wonderdraai sheet. These are locally layered on a 20 - 100 cm scale with alternating olivine-rich and olivine-poor zones. Outcrop is insufficient to allow more detailed observation of the layering and only broad mineralogical characteristics have been documented here. In relatively unaltered lherzolites and gabbronorites the following range in mineralogy is observed: olivine (40 - 60% by volume); clinopyroxene (10 - 30%); orthopyroxene (10 - 40%) and plagioclase (0 - 15%). The subhedral to euhedral olivine grains are 1 - 5 mm in diameter (Fig. 7.2). The pyroxenes are subhedral to anhedral, 0.1 - 7 mm in diameter and generally enclose the olivine crystals. Plagioclase occurs as interstitial anhedra up to 3 mm long. Reaction and textural relationships between the crystals indicate the crystallization sequence: olivine - orthopyroxene/ clinopyroxene - plagioclase. A rarely observed reaction boundary between the pyroxenes may indicate earlier crystallization of orthopyroxene than clinopyroxene in some rock specimens. Biotite, chromite and magnetite occur in roughly equal amounts as accessory minerals. The biotite, which is a deep orange variety, occurs as minute flakes adjacent to the ore minerals. Incipient chloritization and serpentinization are present in even the freshest samples from this body.

Completely altered ultramafic rocks make up the lower parts of the Nsongeni sheets (Fig. 7.1). Two lithologies are present: resistant tremolite-chlorite schists lacking relict textures; and talc-chlorite-tremolite-antigorite rocks in which relict olivine crystal shapes are easily recognized.

The tremolite-chlorite schists are green, medium-grained and consist of intergrown coarse fibrous tremolite and fine ragged flakes of chlorite. Magnetite occurs as sparse, minute, irregular grains.

The talc-chlorite-tremolite-antigorite rocks are massive and dark grey-green to black. In thin section, the original olivine crystals are defined by concentrations of fine magnetite and chromite along grain boundaries and fractures within the grains (Fig. 7.3). The olivine has been replaced by talc, antigorite and chlorite. The finely intergrown talc-chlorite-tremolite groundmass may reflect the presence of ortho- and clinopyroxene in the original mineral assemblages.

A lens of fresh wehrlite is present at the upper, southwestern contact of the main Hlagothi sheets with the Nsuze Group. The rock is dark green-brown or black, coarse-grained and massive. Olivine and clinopyroxene constitute about 30 and 65% of the rock respectively. The olivine crystals are 1 - 3 mm in diameter and are euhedral or subhedral (Fig. 7.4). The clinopyroxene is of similar grain size and ranges from subhedral to anhedral. A small amount of interstitial plagioclase is present. Accessory chromite and magnetite are present.

Pyroxenites

Pyroxene-dominated lithologies occur as 10 m thick layers between the peridotites and gabbros of the Nsongeni sheets. Although extensively altered, relict textures have been well preserved. Original large euhedral clinopyroxenes have been pseudomorphed by amphibole. The surrounding finer-grained tremolite and chlorite probably represents altered clino- and orthopyroxene. These rocks were probably websterites.

The basal 80 m of the 150 m thick sheet on Hlagothi Mountain consists of pyroxenite. Gabbro constitutes the upper part of this sheet. The pyroxenite appears to be rather homogeneous and consists of ortho- and clinopyroxene with minor amounts of plagioclase. Incipient alteration to tremolite and chlorite is pervasive, but does not obscure the original mineralogy. Orthopyroxene is by far the dominant mineral (60 - 70%) and occurs as small, equant, subhedral

Figure 7.2 Olivine websterite from lower part of Wonderdraai sheet, Mhlatuze Valley. Note olivine - hypersthene - augite zonation. (63x).

Figure 7.3 Altered harzburgite from lower ultramafic unit, near Nsongeni Valley. Talc-antigorite replacement of olivine crystals whose form is defined by fine opaques. Pale green chlorite after orthopyroxene in the groundmass. (25x).

grains. Clinopyroxene (25 - 30%) occurs rarely as small euhedral grains, and more commonly as large, elongated crystals (Fig. 7.5). The latter have reacted strongly with the orthopyroxene crystals which are often enclosed poikilitically. Magnetite and chromite occur as accessory minerals.

Gabbros

Gabbro constitutes a major proportion of the complex. It occurs as thin ($\sim$ 10 m) units in the Nsongeni sheets, but as much thicker layers (up to 70 m) in the main Hlagothi and Wonderdraai sheets. They are greenish-grey, medium-grained unfoliated rocks composed almost entirely of secondary replacement minerals.

Amphibole (30 - 60%), plagioclase (0 - 25%) granular aggregates of epidote - zoisite - clinozoisite - mica (5 - 40%), epidote (5%), leucoxene (trace - 5%), quartz (0 - 20%) and chlorite (0 - 15%) are present in variable proportions. Prior to alteration the rock probably consisted of plagioclase and pyroxene.

The amphibole, a pale green to colourless tremolitic hornblende, occurs as single and polycrystalline pseudomorphs after clinopyroxene in equant to elongate subhedral grains 1 - 15 mm long (Fig. 7.6). Plagioclase, which is seldom unaltered, occurs as anhedral interstitial grains of labradorite composition. In general, it has been extensively saussuritized to produce fine-grained, brownish aggregates of zoisite - clinozoisite and white mica. It is also present as micrographic intergrowths with quartz (Fig. 7.7). These intergrowths have also been subjected to saussuritization and probably represent a primary, late-stage eutectic crystallization. Epidote is present as 0.2 - 2 mm equant, zoned grains which do not seem related to the alteration of plagioclase, but do have a spatial relationship to rounded quartz-rich patches (Fig. 7.8) Biotite is commonly associated with these patches which represent segregations of late-stage fluids. Leucoxene is present as large

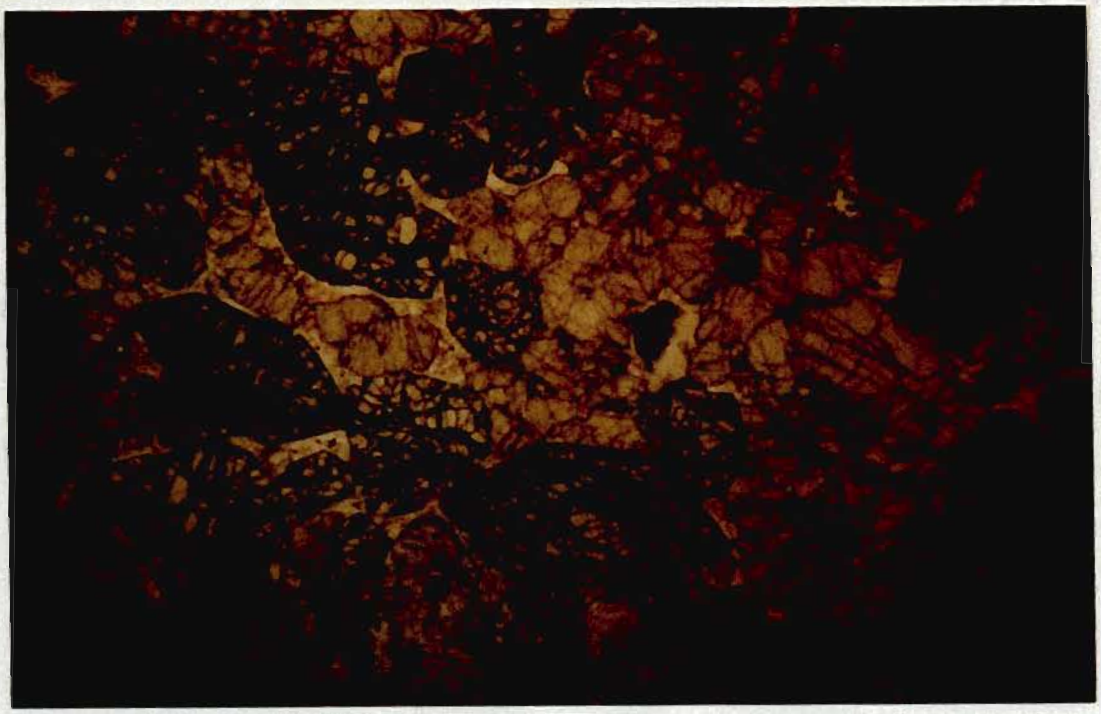

Figure 7.4 Felspathic wehrlite, upper sheet on Hlagothi Mountain, east of Jubilee Store (Map 3). Olivine (highest relief) as euhedral to subhedral crystals. Augite (intermediate relief) is subhedral to anhedral. Interstitial plagioclase has lowest relief (10x).

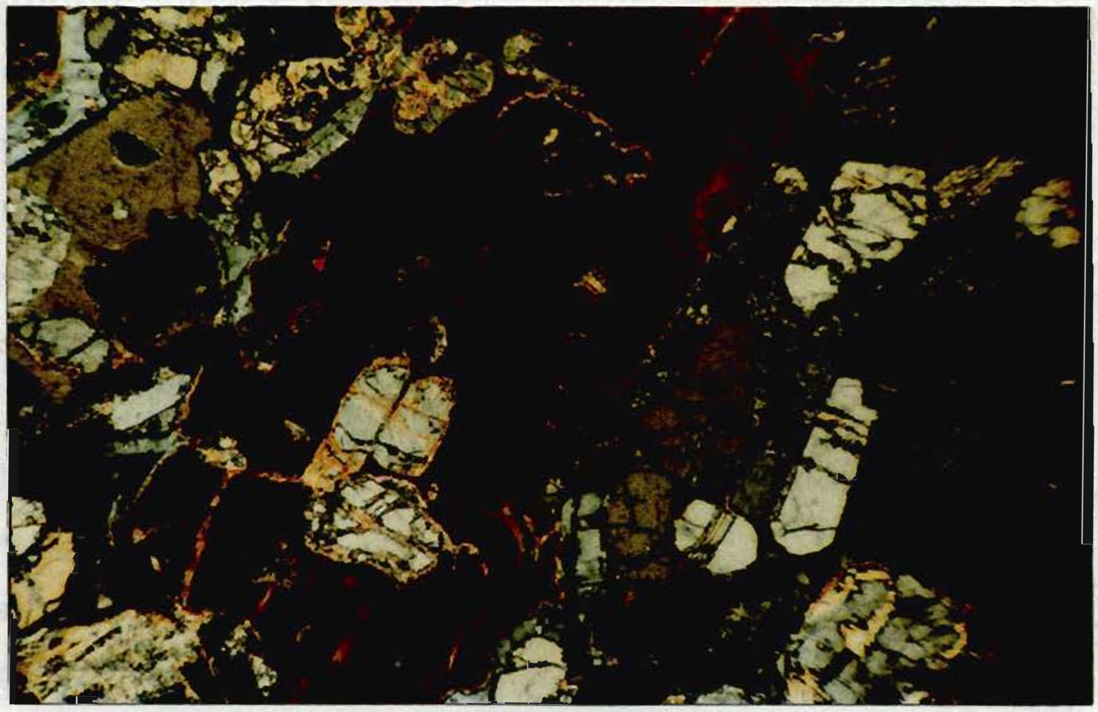

Figure 7.5 Clinopyroxene-orthopyroxenite, upper sheet on north slope of Hlagothi Mountain. Large augite lath in reaction relationship with earlier orthopyroxene cyrstals (63x).

irregular grains (Fig. 7.7) as well as trellis-textured pseudomorphs after ilmeno-magnetite (Fig. 7.9). Chlorite occurs in irregular blebs within the amphibole crystals and as well-defined, interstitial anhedra associated with the biotite, quartz and epidote segregations mentioned above. Biotite, chromite and magnetite are present in trace amounts.

The gabbros are not observed in direct contact with the underlying more mafic rock types although the transition may be located to within a few metres. These contacts are likely to be sharp as there is no gradual change in the mineralogy of either rock-type near mutual boundaries. In the main Hlagothi sheets the gabbros grade upwards into the marginal zones described below. Elsewhere, the upper contacts have not been observed.

Marginal Rocks

Two types of marginal rock sequences are recognizable: (a) a 1 - 10 m thick zone at the top of each of the three upper main Hlagothi gabbro units contains skeletal pyroxene and variolitic textures and (b) a chilled margin is present in the lower Nsongeni sheet and comprises skeletal olivine and plagioclase crystals in a devitrified glassy groundmass.

(a) Skeletal-pyroxene-textured marginal sequence

The skeletal-textured and variolitic marginal rocks are best developed at the upper contact of the second highest gabbro sheet east of Hlagothi Mountain (Map 3 and Fig. 7.1). A complex variation in textures and grain sizes is present (Fig. 7.10), which is considered important to an understanding of the complex and is therefore described in detail below.

The varioles are leucocratic, spherical bodies (Figs. 7.11 and 7.12) which consist of very fine-grained quartz, epidote, chlorite and white mica. They are typically 1 - 10 mm in diameter, although rarely as large as 10 cm. The contacts of the varioles are sharp although there is no marked mineralogical difference

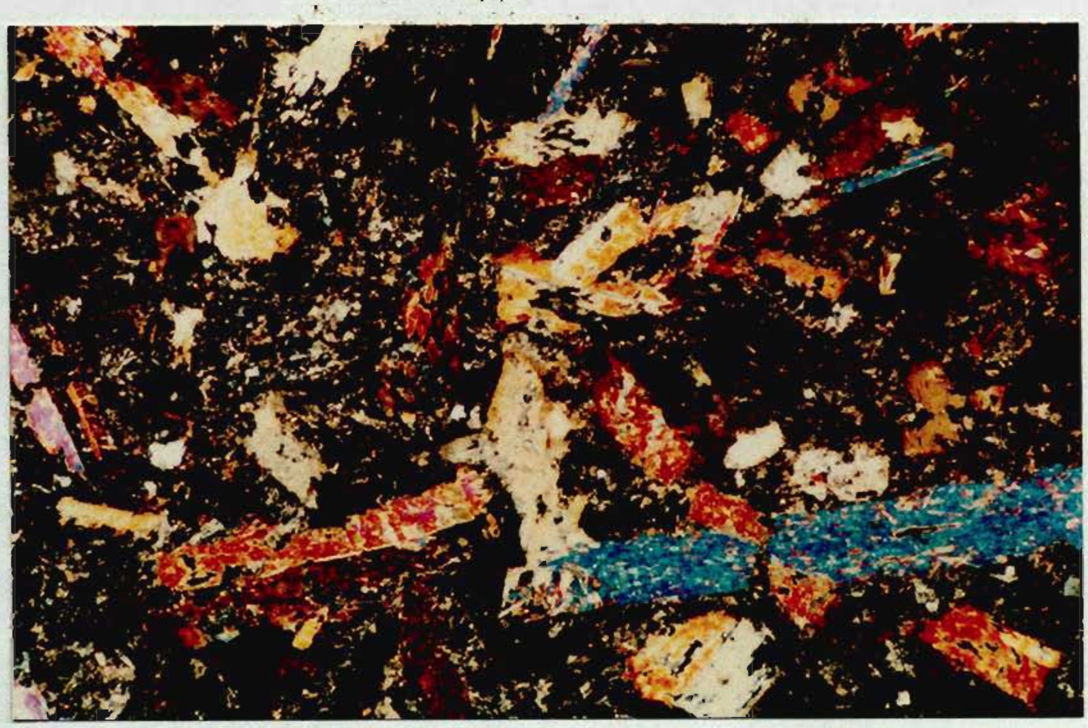

Figure 7.6 Typical gabbro from Hlagothi Complex. Amphibole (high birefringence) is partly pseudomorphic after pyroxene. Fine-grained groundmass consists of epidote - zoisite - clinozoisite - white mica, produced by saussuritization of felspar, and minor chlorite. Lower gabbro unit, Nsongeni Valley. (25x).

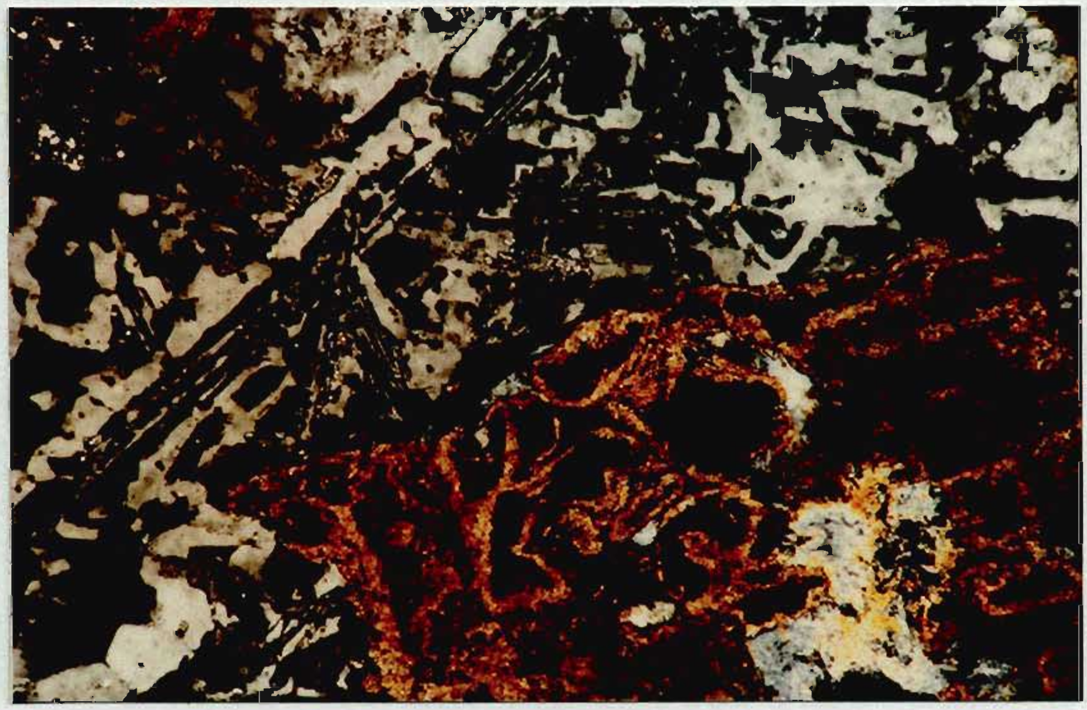

Figure 7.7 Micrographic intergrowth of quartz and plagioclase in gabbro of the Hlagothi Complex. Note leucoxene and sphene produced by breakdown of ilmeno-magnetite. Lower gabbro unit, Nsongeni Valley. (160x).

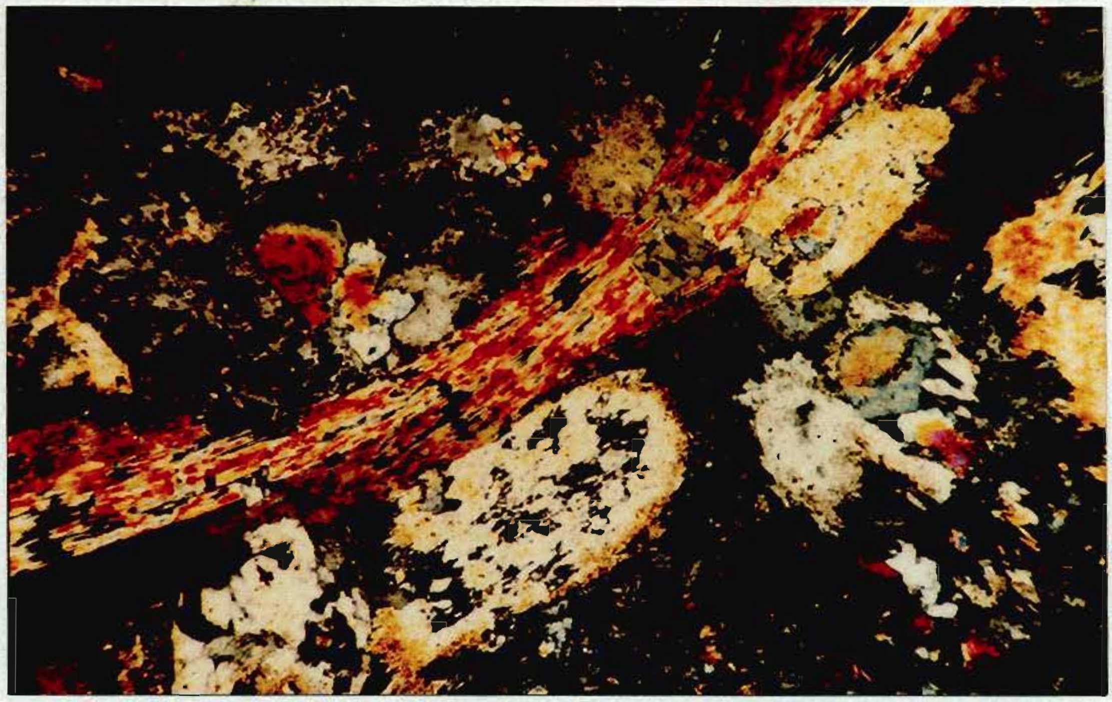

Figure 7.8 Zoned epidotes, quartz patches and large curved amphibole crystal possibly pseudomorphic after original augite. Upper gabbro unit, Hlagothi Mountain. (63x).

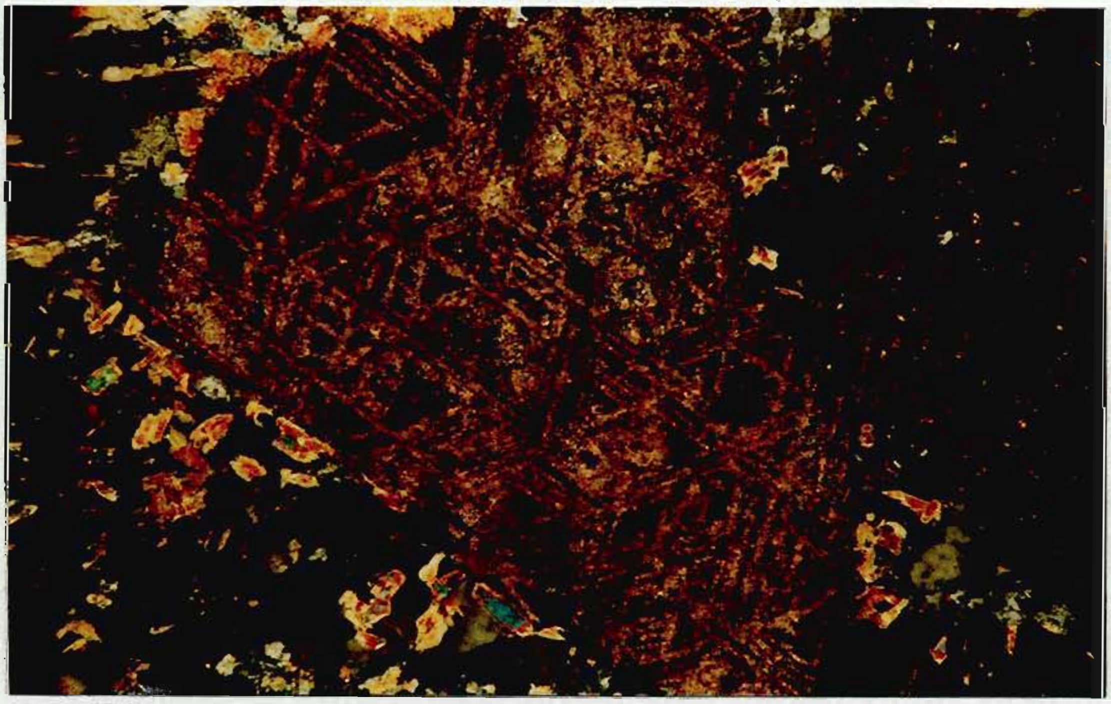

Figure 7.9 Trellis texture, leucoxene after exsolved ilmeno-magnetite. Upper gabbro unit, Hlagothi Mountain. (160x).

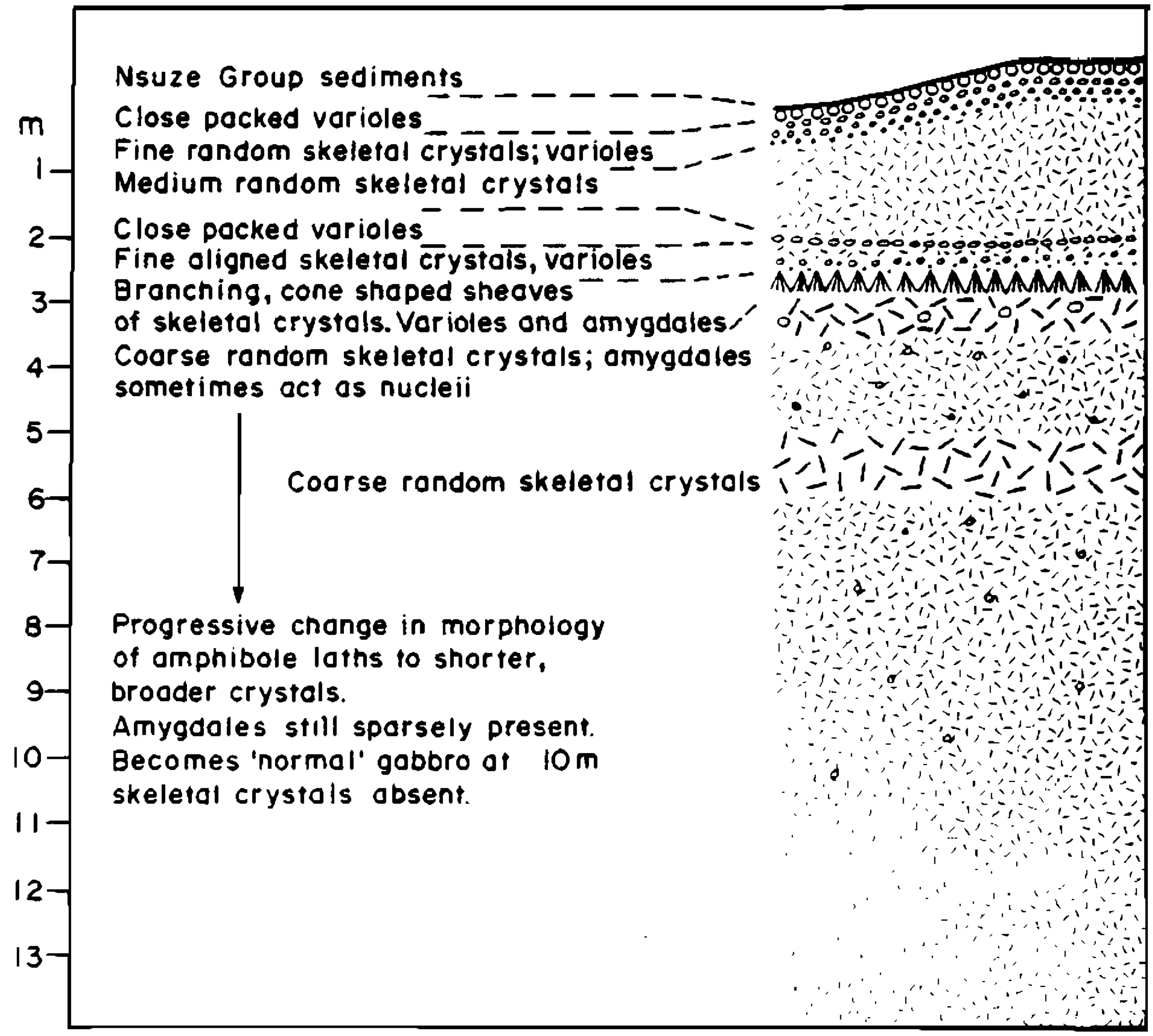

Figure 7.10 Textural relationships of upper marginal sequence, uppermost gabbro unit, due east of Hlagothi Mountain.

between them and the groundmass of the surrounding gabbro. The varioles are concentrated along the upper contact and rest in a very fine-grained chloritic groundmass.

Similar structures are common in metavolcanics of the Barberton (Ferguson and Currie, 1972), Canadian (Gêlinas *et al.*, 1976) and Nondweni (Wilson *et al.*, in prep.) Archaean sequences. Philpotts (1977) reports similar structures in lamprophyric dykes in eastern Canada. Armstrong (1980) reports several varieties of spheroid from the Nsuze Group lavas, some of which resemble those in the Hlagothi Complex. The origin of the varioles, ocelli, or spherulites is a contentious issue. Liquid immiscibility has been invoked by numerous authors (Gêlinas *et al.*, 1976, 1977; Ferguson and Currie, 1972; Philpotts, 1977), but it has been argued that only liquids of extreme composition can exsolve a second liquid phase. Alternative hypotheses have been proposed that envisage the structures being formed by metasomatic and metamorphic alteration (Hughes, 1977). Roedder (1978) reviewed evidence for liquid immiscibility in lunar and Hawaiian basaltic glasses. He concluded that there is unequivocal evidence for silicate liquid immiscibility over a limited range of composition.

Available data for the Hlagothi Complex varioles do not allow speculation as to their origin. In addition to the possibility of silicate liquid immiscibility, processes such as local silicification, assimilation of siliceous country rock or the effects of intrusion into hydrous sediments may be involved.

With progressive distance from the upper contact, varioles become sparser and the groundmass grades into a skeletal-textured gabbro. This texture consists of randomly orientated, ($\sim$ 1 cm long) skeletal amphibole crystals (Fig. 7.13A), which represent pseudomorphic replacement of pyroxene. In the description below the term '"pyroxene" crystals' is used throughout to identify these pseudomorphs. Evidence for the replacement is presented below. The

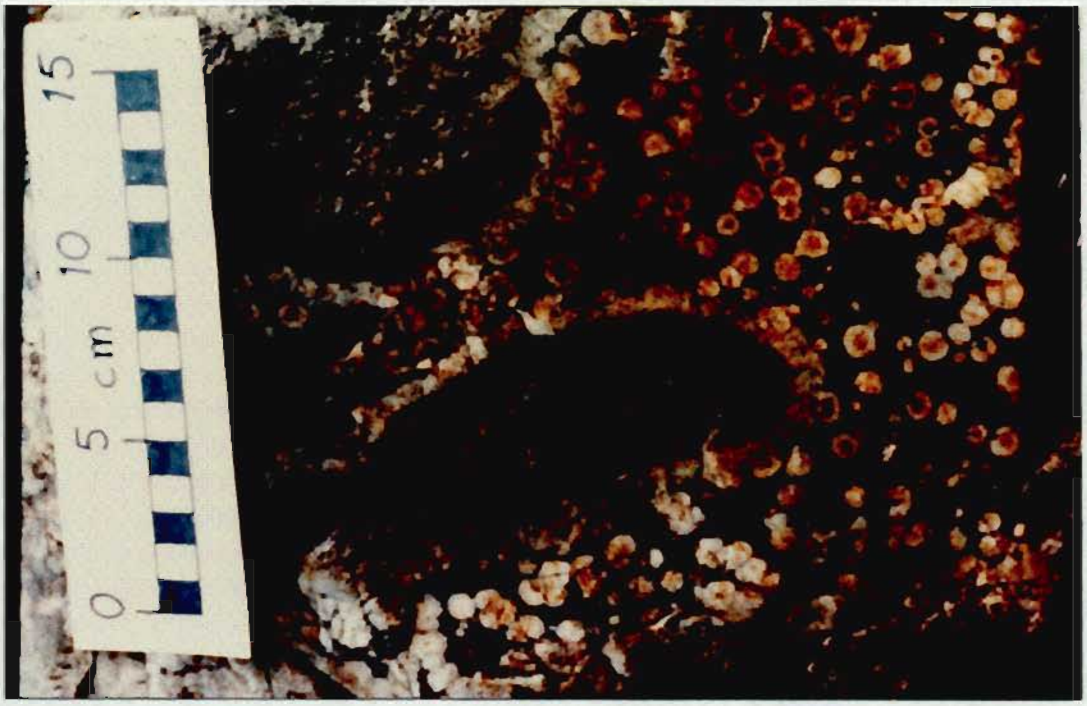

Figure 7.11 Siliceous varioles in gabbroic marginal sequence, uppermost gabbro unit, due east of Hlagothi Mountain.

Figure 7.12 Dip surface view of felsic varioles, upper marginal sequence due east of Hlagothi Mountain. Lens cap is 55 mm in diameter.

amphibole is colourless to very pale green under plane light and resembles tremolite. In sections cut parallel to long axes, the individual crystals consist of several parallel laths, in optical continuity, separated by narrow cores of chlorite (Fig. 7.13B). Sections cut normal to the long axes reveal that the crystals have polygonal outlines resembling the sector growth patterns (Fig. 7.14) illustrated by Arndt and Fleet (1979). The proportion of these "pyroxene" crystals in the rock is very variable, ranging from 10 - 50%.

The groundmass consists of very fine-grained chlorite, tremolite and epidote-clinozoisite. Delicate fan-like sprays are visible locally and may reflect devitrification of glass. Amygdales 1 - 5 mm in diameter are present locally, and are composed of quartz, biotite, epidote and chlorite (Fig. 7.15) There is little variation in the groundmass mineralogy throughout the marginal sequence.

The skeletal-textured gabbro becomes coarser downwards with 2 - 3 cm long "pyroxene" crystals common in the zone 1 - 2 m below the upper contact. About 2 m from the upper contact, is another variolitic layer. This has sharp upper and diffuse lower boundaries. The upper 20 cm has closely packed 5 - 10 mm varioles which decrease in size and abundance downards. Sparse varioles are present in the underlying 30 cm (Fig. 7.10). The gabbro below the variolitic unit consists of up to 50% by volume of skeletal amphibole crystals about 2 cm long, in the groundmass described above. These crystals are crudely aligned (Fig. 7.16) parallel to the contact.

At the base of the aligned crystal unit is a 40 cm thick gabbro unit consisting of downward-branching skeketal "pyroxene" crystals arranged in conical sheaves. The sheaves originate at a point source on the upper contact and spread downwards (Fig. 7.17). Individual crystals become more robust downwards. The cones are typically 30 - 40 cm in height and have an estimated basal diameter of 20 - 30 cm. The observed growth of megacrysts probably indicates very low

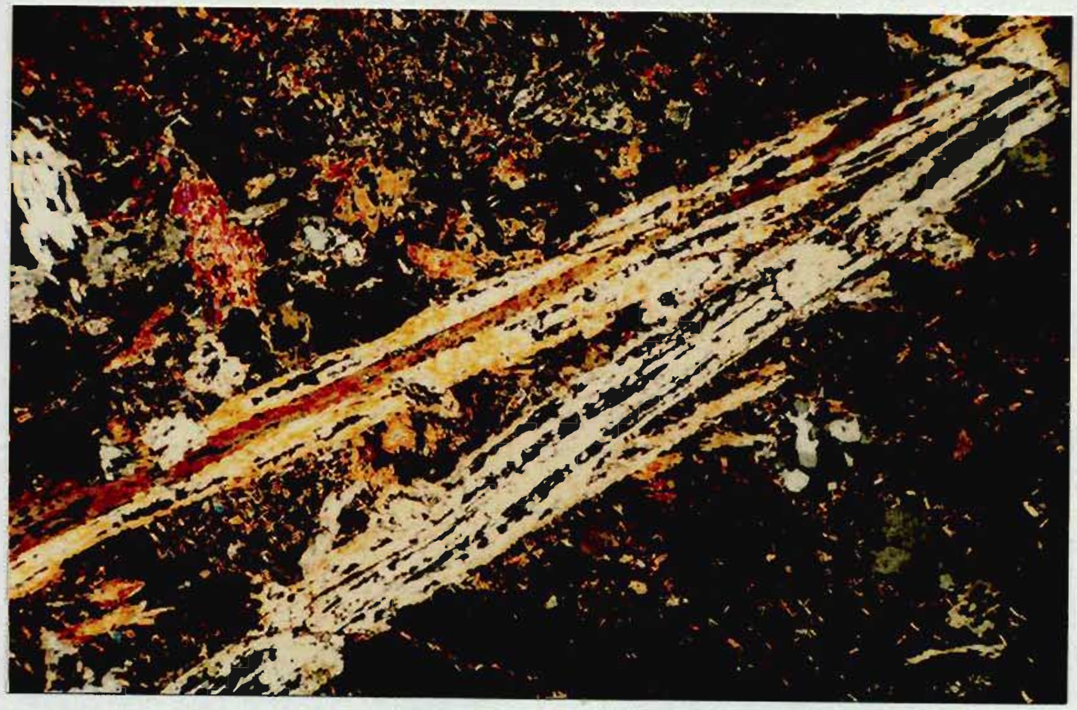

Figure 7.13 A. Amphibole pseudomorph after skeletal pyroxene crystals, upper marginal sequence due east of Hlagothi Mountain. Note the presence of quartz amygdales in lower right-hand quadrant. (10x).

B. Detail of composite structure of crystal in A. Note the chlorite in the core surrounded by amphibole. (160x).

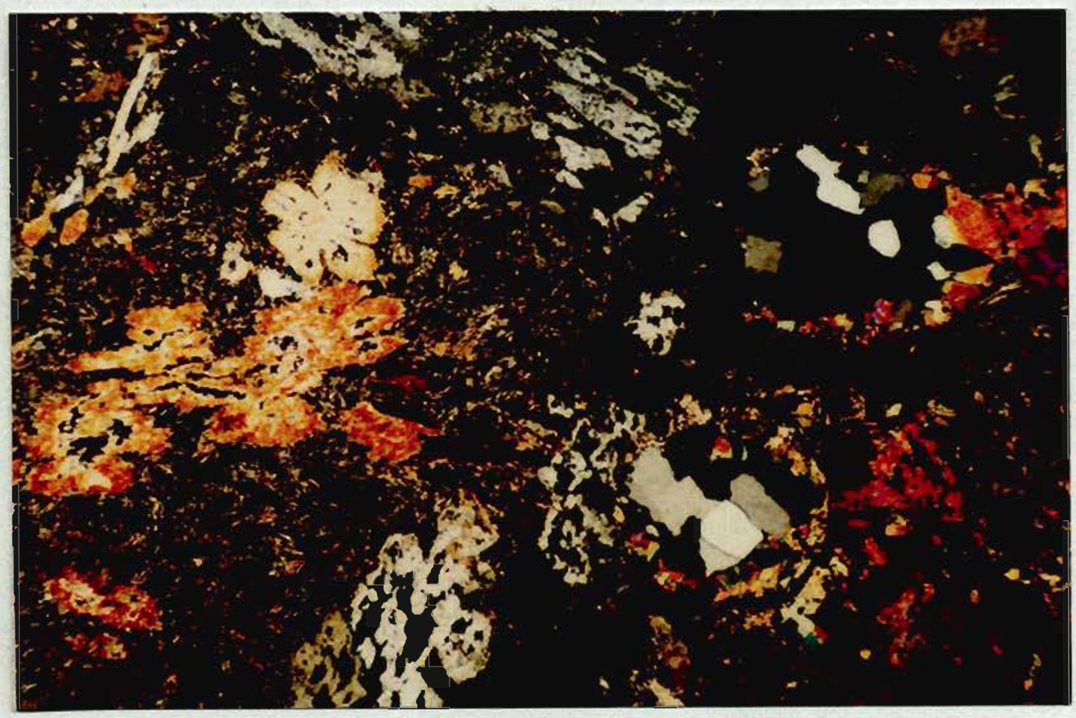

Figure 7.14 Section cut normal to long axis of skeletal pyroxene texture in Figure 7.15. Note sector growth in crystal at centre left. Crystals from a single sheaf in optical continuity indicated by arrows. Quartz-epidote amygdales in right-hand half of field. (25x).

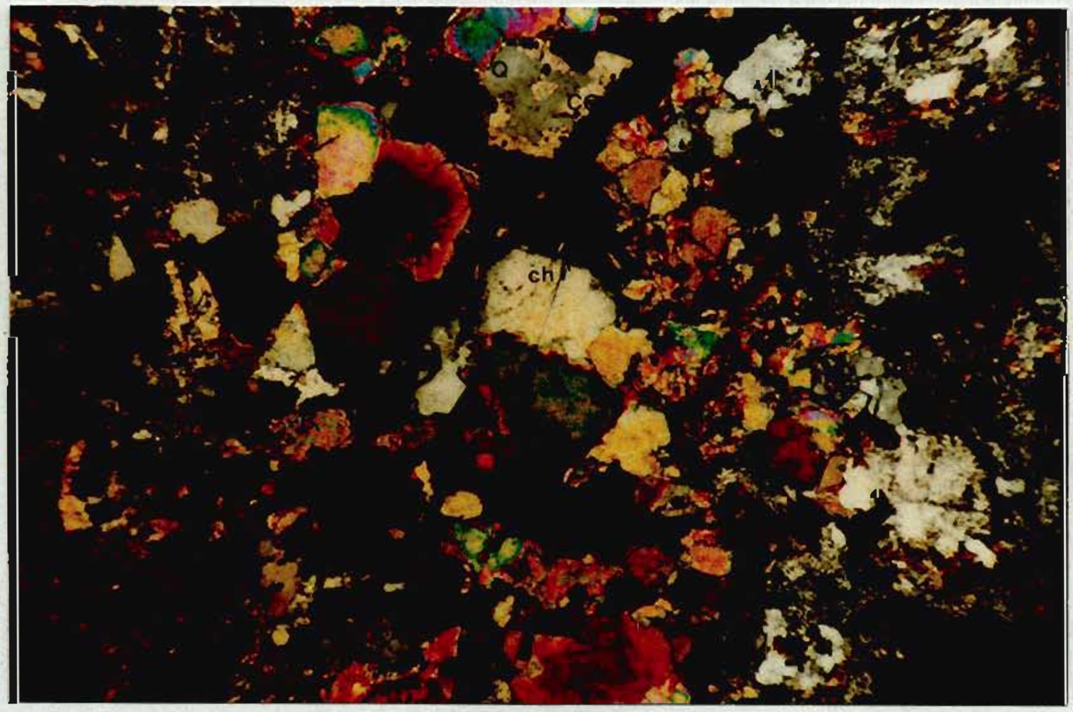

Figure 7.15 Detail of segregation (amygdale?) in skeletal pyroxene-textured gabbro, upper marginal sequence. (63x).
Q = quartz; ep = epidote; ch = chlorite; Cc = calcite;
B = biotite.

Figure 7.16 Aligned skeletal pyroxene crystals pseudomorphed by amphibole, upper marginal sequence. Scale in centimetres.

Figure 7.17 Downwards branching conical sheaves of skeletal pyroxene crystals, upper marginal sequence, due east of Hlagothi Mountain. Pen is 15 cm long.

nuclei density. In thin section crystals belonging to individual cones are in optical continuity (Fig. 7.14). They commonly have a core of chlorite and are less commonly twinned parallel to their long axes.

Below the unit of branching crystals is a zone of coarse-grained gabbro containing randomly orientated skeletal "pyroxene" crystals. These crystals have a shorter, thicker habit than the "pyroxenes" described above, a feature which becomes more marked downwards until the gabbro is indistinguishable from typical Hlagothi gabbros. Within this coarse unit are rare incompletely transformed pyroxene crystals in which the core zone consists of pigeonite (Fig. 7.18). Most of the composite crystals have undergone transformation to a core of chlorite and a margin of colourless amphibole identical to those higher up in the marginal sequence. Electron microprobe analysis of the amphibole provides a composition equivalent to tremolitic hornblende as defined by Leake (1968). Recalculation of the analysis using 6 oxygen atoms yields an augite of sub-calcic stochiometry (Table 7.4). This is in agreement with the chemistry reported for spinifex texture pyroxenes and experimentally produced quenched pyroxenes (Arndt and Fleet, 1979).

The similarity of petrological and chemical aspects of the skeletal-textured rocks to spinifex textures in effusive komatiites has considerable significance for petrogenetic interpretation. For this reason a discussion of their origin is deferred to a later section.

(b) Chilled Margin, Nsongeni Sheet

The chill phase recognized from the Nsongeni sheets is in an equivocal relationship with the upper contact of the lowest sheet and the margin of a feeder dyke to an overlying sheet. It is part of the Hlagothi Complex, but cannot be ascribed with any certainty, due to poor outcrop, to a particular sill. The chill phase is a thin (20 cm), sporadically developed, very fine-grained, black, massive rock-type. Small olivine phenocrysts are visible in hand specimen.

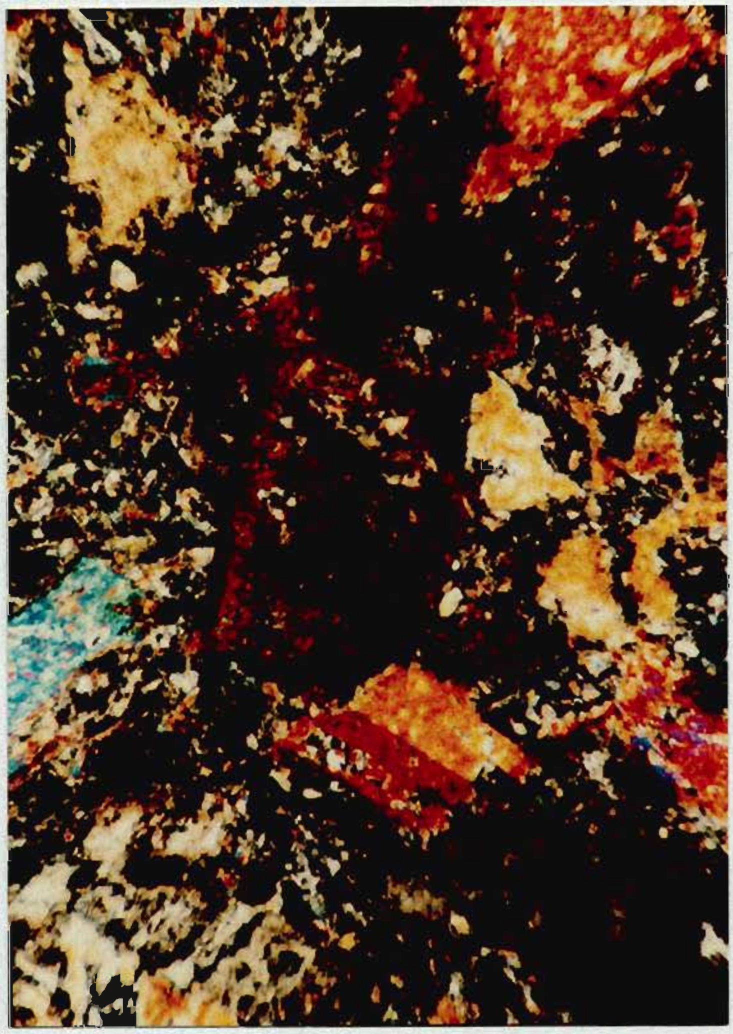

Figure 7.18 Relict pigeonite core surrounded by amphibole in gabbro 8 m below upper contact of the upper marginal sequence due east of Hlagothi Mountain. (63x).

In section, the rock consists of skeletal olivine (5%) and plagioclase (10%) crystals set in a devitrified glassy groundmass. The olivine crystals are generally 0.1 - 0.3 mm across, but some slender elongate crystals 3 mm long are present. Most of the crystals are euhedral in external form, but contain irregular or rounded voids filled with fine-grained groundmass material (Fig. 7.19). The skeletal forms are similar to those recognized in experimental quenching of high Mg-basalts by Donaldson (1976). Plagioclase crystals occur as very thin, up to 5 mm long needles which have a central core of groundmass material. In cross-section the crystals are rectangular with a rounded core. They appear to radiate from olivine megacrysts, perhaps indicating that nucleation of the plagioclase occurred in the proximity of olivine grains where a local depletion of iron and magnesium resulted from diffusion to the olivine. The groundmass consists of sub-microscopic brownish crystallites in radiating fans which appear to start at the terminations of the plagioclase crystals. Some very small orthopyroxene grains are recognizable. Accessory chromite and magnetite occur as small euhedra and anhedra respectively.

Feeder Dykes

Dykes which penetrate lower sills but not the upper ones have been recognized in the Nsongeni and main Hlagothi sheets. These are typically altered but at least one has retained its primary mineralogy. This dyke, which intruded the lowermost ultramafic portion of a sheet near the confluence of the Nsongeni and Nsuze Rivers (Map 3), cannot be traced into the overlying sill. The dyke is a thin (< 10 m), fine-grained, olivine gabbronorite body which trends parallel to the strike of the sills. The rock consists of plagioclase (40%), augite (25%), olivine (20%) and orthopyroxene (10%) with accessory biotite and magnetite. In general, the rock is granular but some radiating plagioclase-augite intergrowths are present. This texture has been described by Mackenzie *et al.* (1982, p. 57) who considered it to be allied to skeletal growth of pyroxene. The olivine grains are typically subhedral or euhedral but embayed by reaction with the augite. The augite occurs in angular, elongate anhedral crystals, whereas the orthpyroxene generally occurs as equant subhedra. Exsolved pigeonite is present within some of the larger augite and orthopyroxene grains. Plagioclase, which occurs as large, elongate crystals, encloses the mafic minerals poikilitically in parts of the rock. Alteration to chlorite and talc is restricted to small angular patches, suggesting that the alteration may be related to fractures. Undulatory extinction of the plagioclase indicates that the rock has undergone some deformation.

Summary

Mafic and ultramafic rock types of the Hlagothi Complex, although rarely unaltered, are recognized as consisting predominantly of olivine, two pyroxenes and plagioclase prior to alteration. Pigeonite, ilmeno-magnetite, biotite and chromite are the most commonly encountered minor phases.

The lower ultramafic rocks of the Nsongeni sheets consisted of olivine-orthopyroxene-(clinopyroxene) cumulates before alteration. In the Wonderdraai sheet olivine websterites are the most common ultramafic rocks, whereas in the main Hlagothi sheets feldspathic wehrlites and clinopyroxene-orthopyroxenites are the most mafic rock types recognized. Within these lithologies, the following sequences of crystallization are apparent:

Olivine → orthopyroxene → clinopyroxene (Upper Wonderdraai and lower Nsongeni ultramafics)

Olivine → orthopyroxene + clinopyroxene → plagioclase (Wonderdraai sheet, olivine websterite)

Olivine → clinopyroxene → plagioclase (main Hlagothi sheet, feldspathic wehrlite)

Orthopyroxene → clinopyroxene → plagioclase (main Hlagothi sheet, clinopyroxene orthopyroxenites)

Pigeonite → clinopyroxene (skeletal-textured marginal sequence)

Olivine → plagioclase (chill phase, Nsongeni feeder dyke)

The gabbroic rocks have undergone total alteration (with rare exceptions) to an amphibole - chlorite - epidote assemblage, which may represent a metamorphic transformation related to the regional greenschist facies metamorphism. However, this metamorphic event was accompanied by strong northwards directed stress where it has affected Nsuze Group volcanics close to the Complex, a feature which is not apparent in the altered gabbros. Additional evidence in favour of possibly late or magmatic or autometasomatic alteration is provided by other textures and structures in the gabbros. The vesicles in the upper parts of the gabbro sheets, trellis-textured sphene pseudomorphs after ilmeno-magnetite, quartz-plagioclase micrographic intergrowths and the chlorite-biotite-zoned epidote patches are interpreted as reflecting originally high water contents of the gabbroic magma. If the primary magma had a relatively high water content, a progressive crystallization of anhydrous phases would have resulted in a concomitant concentration of water in the higher parts of the body. This progressive increase in water activity may have caused early, anhydrous phases to become unstable and out of equilibrium with interstitial late-stage liquids. The alteration of the gabbros pre-dates the growth of small, aligned fibrous tremolite crystals which transgress the original mineral boundaries. It is considered probably that this later generation of amphibole grew during the regional greenschist facies episode and associated deformation.

The petrographic data and field relationships place certain constraints on a model for the development of the Hlagothi Complex. Cross-cutting relationships between the sills imply that repeated sill intrusion occurred along the same general locus. The presence of amygdales and late-stage deuteric/hydration effects indicates a relatively shallow depth of intrusion. High magmatic water contents probably applied, particularly towards the top of the complex, and the exsolution of a hydrous phase was possible because of low confining pressure at the time of intrusion.

Significantly, the sills were intruded close to the base of the 4 km-thick Nsuze Group prior to deformation.

The optimum depths at which sill emplacement occurs has been discussed by Roberts (1970) in terms of the stress field applicable at the time of intrusion. He considers an initial state of stress such that $\sigma_x = \sigma_y = n.\sigma_z$ where σ_x, σ_y and σ_z are the principal stresses and n is a constant less than unity. Where n = 1, the initial state is one of hydrostatic stress and sill emplacement can occur at any depth. However, if n = 1/3 the initial state is one of complete lateral restraint, and sill emplacement would be restricted to within 1 - 2 km of the surface. Mudge (1968) concluded that minor sills are intruded at depths between 0.5 and 2 km. Some major sills appear to have been emplaced at somewhat greater depths (Bradley, 1965).

The fact that the Hlagothi Complex predates deformation of the Nsuze Group, coupled with the above conclusions, suggests that the Hlagothi sills might have been emplaced at shallow depths soon after or nearly synchronously with the accumulation of the Nsuze Group.

4. Geochemistry

Geochemical Variation

The nineteen samples analysed were selected so as to provide a broad characterization of individual sheets. Similar fractionation histories for the sills are likely, and therefore the combined data are considered to provide broad geochemical characteristics of the whole complex. The sampling is not considered adequate for petrogenetic modelling.

The analyses for the major, minor and trace elements were done by XRF spectroscopy according to the methodology outlined in Chapter 6 and Appendix 2 Chemical abundances and distribution of the samples are presented in Tables 7.1 - 7.3. Comprehensive listings of normative data and computed phase diagram projections are presented in Appendix 5. In the following discussion, the olivine- and pyroxene-dominated rock types are referred to as peridotites and pyroxenites respectively for ease of reference. It is recognized that the terms are not strictly applicable but the common factor in each group is not easily expressed by other terminology.

The major elements have been plotted on MgO variation diagrams (Fig. 7.20). SiO_2 abundances show little variation with all of the gabbroic and pyroxenitic rocks falling in the range 53 - 56%. These rocks have MgO contents of less than 23%, but a large compositional gap in the range 11 - 18% MgO separates the gabbroic and pyroxenitic rocks. The peridotites, which have MgO > 23%, all have SiO_2 in the range 46 - 49%.

Alumina decreases from 23% for the gabbros to $\sim$ 6% in the peridotite range along a reasonably coherent trend (Fig. 7.20). There is a slight inflection at the change from olivine-poor to olivine-rich lithologies. The skeletal-textured samples have lower Al_2O_3 than gabbros of similar MgO content. Low alumina values are to be expected in the ultramafic rocks as they are dominated by pyroxene and olivine, neither of which contains appreciable alumina. Total iron, as FeO, shows little variation with changing magnesia except for a slight increase in the peridotitic rocks. Iron-magnesia ratios thus increase with decreasing MgO. CaO abundances decrease systematically with increasing MgO. Values of 11% CaO are typical of the gabbros, falling to 4% in the ultramafic rocks.

No clear or coherent relationships exist between Na_2O or K_2O and MgO. The alkalies are more abundant in the gabbros than in the ultramafic rocks.

TABLE 7.1: CHEMICAL ANALYSES OF GABBROIC[a] AND SKELETAL-TEXTURED[b] ROCKS

	BG192[a]	BG220[a]	BG222[a]	BG223[a]	BG231[a]	BG237[a]	BG232[b]	BG239[b]	BG242[b]
SiO_2	53.49	57.17	55.43	54.97	56.32	56.03	55.98	54.69	54.75
Al_2O_3	15.64	15.00	15.03	12.98	14.96	14.21	12.15	11.92	11.50
Fe_2O_3	0.71	0.95	0.90	0.83	0.91	1.05	0.96	0.96	0.98
FeO	6.39	8.55	8.12	7.47	8.23	9.49	8.64	8.60	8.84
MnO	0.15	0.17	0.16	0.16	0.17	0.19	0.17	0.19	0.18
MgO	8.97	5.94	6.65	10.57	6.56	5.35	8.53	9.75	10.01
CaO	11.69	8.47	10.52	9.20	10.74	10.74	9.73	9.25	9.30
Na_2O	1.76	3.76	2.19	2.77	2.16	2.15	1.89	2.86	2.10
K_2O	0.83	0.66	0.74	0.85	0.78	0.58	1.35	0.73	0.96
TiO_2	0.34	0.65	0.55	0.46	0.37	0.45	0.67	0.64	0.64
P_2O_5	0.06	0.13	0.10	0.09	0.06	0.07	0.10	0.11	0.10
Cr_2O_3	0.11	0.01	0.01	0.08	0.01	0.00	0.11	0.13	0.18
TOTAL	100.14	101.46	100.40	100.43	101.27	100.31	100.28	99.83	99.54
Trace elements (ppm)									
Sc	28		36	32	44	47	34	31	30
V	170	233	217	199	221	245	222	213	216
Cr	740	44	57	568	89	23	741	893	1247
Ni	225	129	132	276	121	86	157	200	236
Cu	26	52	42	36	60	43	79	105	72
Zn	70	68	62	59	72	91	68	76	77
Y	14	24	20	18	14	16	23	20	21
Zr	55	103	84	69	60	71	91	90	88
Nb	3.9	5.5	4.7	4.1	2.9	4.0	4.4	5.3	4.8
Rb	33	26	26	32	19	12	32	17	21
Sr	213	277	240	251	110	129	463	106	103
Ba	138		136	467	206	200	476	268	394
La	8	13	9	6	11	4	12	5	7

BG192 - Wonderdraai Sheet.

BG220 - BG223 - Nsongeni Sheet.

BG231 - BG242 - Main Hlagothi Sheets

TABLE 7.2: CHEMISTRY OF THE PERIDOTITES[c] AND PYROXENITES[d]

	BG193[c]	BG196[c]	BG212[c]	BG216[c]	BG226[c]	BG228[c]	BG224[d]	BG227[d]	BG 229[d]	BG236[d]
SiO_2	50.06	47.76	47.60	47.59	46.26	49.14	54.86	55.75	55.58	55.33
Al_2O_3	7.00	6.74	6.44	8.64	5.83	5.85	8.23	8.02	6.80	6.49
Fe_2O_3	1.09	1.14	1.08	1.10	1.18	1.16	0.99	0.94	0.92	0.94
FeO	9.80	10.25	9.71	9.88	10.61	10.40	8.88	8.49	8.32	8.50
MnO	0.20	0.20	0.19	0.22	0.19	0.20	0.23	0.19	0.21	0.21
MgO	25.51	27.57	26.93	23.42	30.97	26.22	18.00	18.45	20.00	21.52
CaO	5.38	5.13	5.91	8.04	3.85	5.11	7.65	7.47	6.64	5.63
Na_2O	0.68	1.12	0.04	0.37	0.00	0.43	0.85	0.61	0.32	0.63
K_2O	0.24	0.31	0.40	0.02	0.13	0.36	0.03	0.04	0.59	0.23
TiO_2	0.23	0.29	0.29	0.35	0.24	0.31	0.37	0.35	0.22	0.17
P_2O_5	0.05	0.07	0.05	0.06	0.04	0.07	0.06	0.06	0.03	0.02
Cr_2O_3	0.55	0.64	0.56	0.57	0.77	0.56	0.29	0.35	0.38	0.62
TOTAL	100.79	101.21	99.20	100.26	100.07	99.81	100.44	100.72	100.01	100.29
Trace elements (ppm)										
Sc	19	17	36	21	18	20		31	32	34
V	115	119	129	149	104	131	164		160	153
Cr	3785	4420	3834	4352	4429	3775	2391	2748	2591	4241
Ni	1280	1632	2088	1298	1909	1375	635	596	469	811
Cu	24	29	0	0	0	15	13	8	6	36
Zn	68	69	64	78	76	55	72	65	68	60
Y	8	8	7	13	17	9	13	9	10	6
Zr	36	44	41	49	37	45	55	46	37	26
Nb	1.9	1.9	1.0	1.9	1.0	2.0	1.8	1.1	1.4	1.3
Rb	12	14	27	0	12	27	1	1	37	9
Sr	79	78	49	6	17	48	24	12	13	40
Ba	50	78	22	1	5	14		8	29	43
La	2	4	3	4	1	1	3.5	7	5	0

BG193 + BG196 - Wonderdraai Sheet. BG212, BG216, BG224, BG226, BG227, BG228 - Nsongeni Sheets
BG229, BG236 - Main Hlagothi Sheet.

TABLE 7.3: GROUP MEANS AND COMPARATIVE DATA

	Peridotites		Pyroxenites		Gabbros		Skeletal-textured Gabbros		A
	n=6 $\bar{x}$	σ	n= 4 $\bar{x}$	σ	n=6 $\bar{x}$	σ	n=3 $\bar{x}$	σ	
SiO_2	48.07	1.21	55.38	0.34	55.57	1.16	55.14	0.73	53.75
Al_2O_3	6.75	0.95	7.39	0.75	14.64	0.85	11.86	0.27	10.02
Fe_2O_3	1.13	0.04	0.95	0.03	0.89	0.10	0.97	0.01	
FeO	10.11	0.33	8.55	0.20	8.04	0.95	8.69	0.10	11.02
MnO	0.20	0.01	0.21	0.01	0.17	0.01	0.18	0.01	0.22
MgO	26.77	2.51	19.49	1.39	7.34	1.83	9.43	0.65	10.30
CaO	5.57	1.27	6.85	0.80	10.23	1.07	9.43	0.11	10.18
Na_2O	0.44	0.38	0.60	0.19	2.47	0.65	2.28	0.42	0.47
K_2O	0.24	0.13	0.22	0.23	0.74	0.09	1.01	0.26	0.87
TiO_2	0.29	0.04	0.28	0.08	0.47	0.11	0.65	0.01	-
P_2O_5	0.06	0.01	0.04	0.02	0.09	0.03	0.10	0.00	-
Cr_2O_3	0.61	0.08	0.41	0.13	0.04	0.04	0.14	0.03	-
	100.24		100.37		100.69		99.88		99.53

A = Average basaltic komatiite, Barberton type, Barberton greenstone belt (Viljoen and Viljoen, 1969, p. 80). Total iron as FeO.

TABLE 7.4: MINERAL CHEMISTRY

	1	2	3	4	5	6
SiO_2	52.50	38.57	54.55	56.80	55.00	51.90
Al_2O_3	2.42	0.03	1.79	1.44	3.05	4.60
FeO*	6.70	20.65	7.84	11.18	12.64	7.70
MnO	0.17	0.16	0.20	0.30	-	0.25
MgO	17.67	39.60	16.08	27.39	14.98	17.80
CaO	19.71	0.19	19.30	2.23	12.99	17.30
Na_2O	-		0.16	0.01	0.23	0.14
K_2O	-		0.03	0.03	0.08	-
TiO_2	0.26		0.27	0.06	0.03	0.37
Cr_2O_3	-		-	0.17	-	0.23
NiO	0.60	0.50	0.03	0.10		-
TOTAL	100.02	99.69	100.24	99.69	99.00	99.80

1. BG292 clinopyroxene
2. BG292 olivine
3. BG235 clinopyroxene
4. BG235 orthopyroxene
5. Tremolitic hornblende pseudomorph of clinopyroxene.
6. Augite from composite needle. Arndt and Fleet (1979, p. 859, analysis # 3).

The plot of TiO_2 vs MgO shows discrete fields for the three rock-types. The peridotites lie on a linear trend of low negative slope indicating a slight enrichment of Ti with increasing fractionation. Pyroxenitic rock-types define a trend of steeper negative slope. Gabbroic rock-types plot as a dispersed field although the three skeletal-textured samples plot close together.

MnO shows very little variation over the entire range of MgO contents.

Trace element contents of the Hlagothi Complex are presented in Tables 7.1 and 7.2. These values have not been used in the discussion below because they do not contribute significantly to an understanding of the Complex. An attempt to model parental magma composition and origin on the basis of trace element geochemistry is considered premature in view of the limited number of analyses available at present.

Figure 7.19 Chilled margin of feeder dyke to second lowest sill, Nsongeni River valley. Hopper olivine and acicular, skeletal plagioclase crystals are set in devitrified groundmass. (25x).

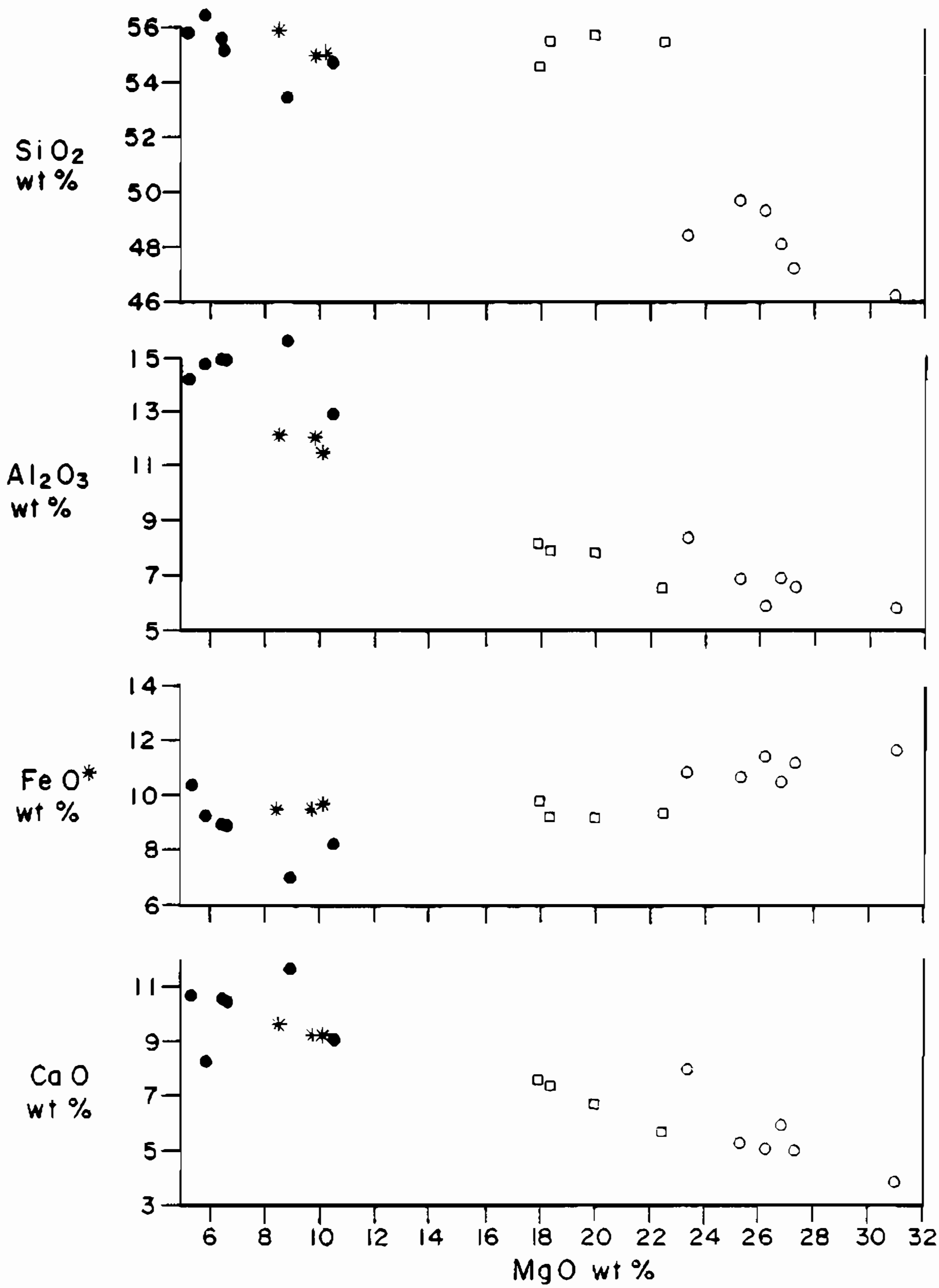

Figure 7.20 Variation diagrams for major and minor elements plotted against MgO. All values as weight percentages. Solid circles - gabbros; stars - skeletal-textured gabbros; hollow circles - peridotites; squares - pyroxenites and gabbronorites. Continued overleaf.

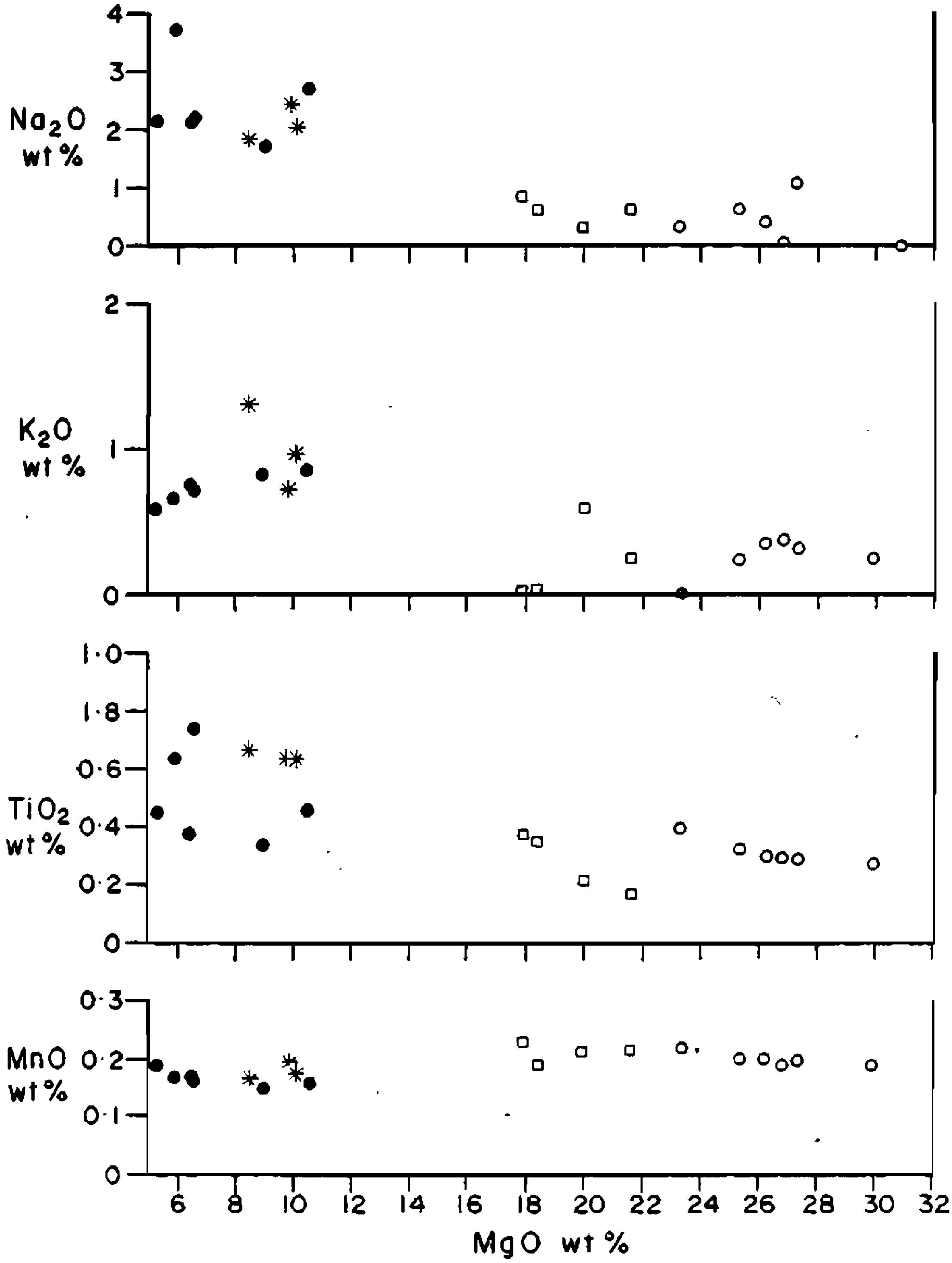

Figure 7.20 continued

Molecular Proportion Ratios

The principal behind the use of molecular proportion ratio (MPR) plots has been given by Pearce (1968). Pearce (1970) and Beswisk (1982) have shown that these ratios may be used to identify fractionating phases in layered intrusions and volcanic sequences respectively. MPR plots may also be used to identify open system behaviour since only closed system fractionation produces coherent chemical variation trends (Beswick, 1982).

Petrographic evidence for olivine, clinopyroxene and orthopyroxene fractional crystallization has been indicated above. The object of this section is to demonstrate the relative importance of these phases in the crystallization of the various rock types. As Zr is incompatible over the range of compositions present, its abundance is used to compute the oxide molecular proportion ratios.

In order to recognize olivine, orthopyroxene and clinopyroxene fractionation the covariation of MgO/Zr, FeO*/Zr and (MgO + FeO*)/Zr with SiO_2/Zr is investigated. The MPR slopes required for fractionation of the minerals analysed by electron-microprobe are given in Table 7.5. The peridotitic rock-types plot on a linear trend with a slope midway between those predicted for olivine and orthopyroxene fractionation (Fig. 7.21). The pyroxenites fall on a linear trend of slope within the range predicted by clinopyroxene and orthopyroxene fractionation. Data points for the gabbroic rocks plot with some scatter on a line, the slope of which is close to that expected for clinopyroxene fractionation.

The involvement of clinopyroxene and plagioclase in fractionation is tested using Al_2O_3/Zr and CaO/Zr versus SiO_2/Zr MPR plots (Fig. 7.22). On the Al_2O_3/Zr : SiO_2/Zr plot, the slope of the line defined by the gabbro analyses is close to that predicted for fractionation of plagioclase of composition An_{75}. The other rock types plot on a linear, horizontal trend which indicates that alumina is not a component of any of the fractionating phases in these rocks.

TABLE 7.5: SLOPES FOR MPR FRACTIONATION TRENDS PREDICTED FROM OBSERVED MINERAL COMPOSITIONS

Sample No.	Phase	MgO/ SiO_2	FeO/ SiO_2	(FeO+MgO)/ SiO_2	Al_2O_3/ SiO_2	CaO/ SiO_2	CaO/ (FeO+MgO)
BG292	01	1.54	0.46	2.0	-	-	-
	Cpx	0.49	0.11	0.6	<0.1	0.40	0.66
BG235	Opx	0.77	0.18	0.95	-	-	-
	Cpx	0.47	0.13	0.60	<0.1	0.40	0.66

TABLE 7.6: CATION FORMULAE FOR MEGACRYSTIC AMPHIBOLE (No. 4 in Table 7.4).

	Amphibole (22 oxygens/formula unit)	Pyroxene (6 oxygens/formula unit)
Si	7.44	2.03
Al	0.49	0.13
Fe	1.43	0.39
Mg	3.02	0.82
Ca	1.88	0.51
Na	0.06	0.06
K	0.01	0.00
Total	14.33	3.90

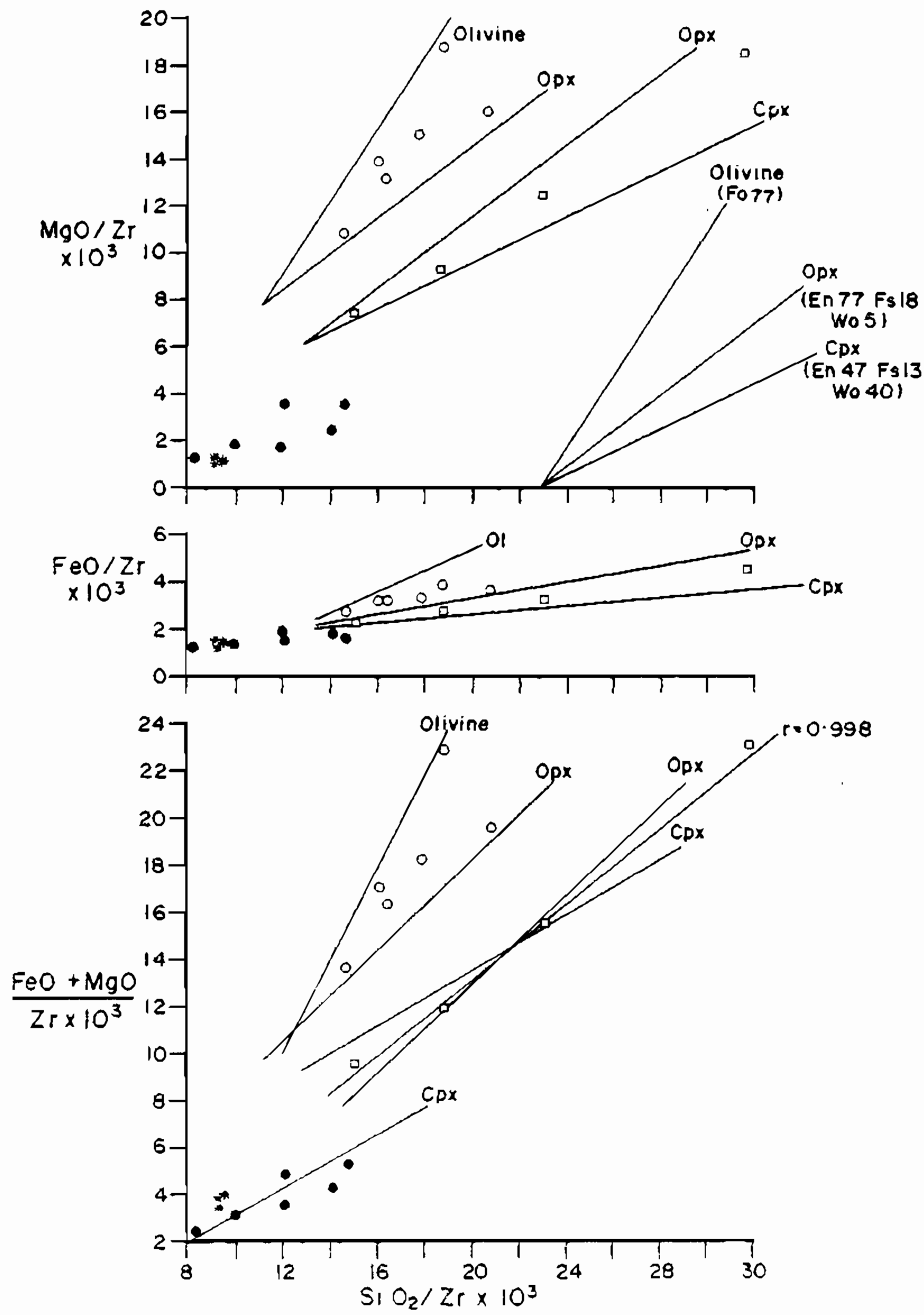

Figure 7.21 Molecular proportion ratio (MPR) plots showing the relationships MgO/Zr, FeO*/Zr and (FeO* + MgO)/Zr versus SiO_2/Zr. All ratios computed using molecular proportions. Lines of predicted slope calculated from minerals analysed by electron microprobe (Table 7.5). Symbols as for Figure 7.20. See text for explanation.

On the CaO/Zr : SiO_2/Zr plot (Fig. 7.22), the gabbros plot on a trend whose slope is midway between predicted slopes for An_{75} and An_{100} and close to that expected for clinopyroxene fractionation. The pyroxenites plot on a line of very low positive slope, indicating that the covariance of calcium and silica is influenced by the presence of a calcium-free fractionating phase in addition to the clinopyroxene postulated earlier. Peridotites plot on a horizontal trend indicating the absence of calcium-bearing phases as fractionating components in these rocks.

In order to test for clinopyroxene fractionation in the gabbros, a plot of CaO/Zr : $(FeO^* + MgO)/Zr$ is used (Fig. 7.23). The gabbros plot close to or on the line predicted for clinopyroxene fractionation, whereas the pyroxenitic rock-types plot on a subhorizontal trend. As expected, the peridotites plot on a trend of zero or negative slope.

From the preceding, it is clear that crystallization of the olivine-bearing rock-types was dominated by olivine and orthopyroxene fractionation. The pyroxenites were dominated by orthopyroxene crystallization, although minor clinopyroxene fractionation, probably as an interstitial phase, must have occurred to account for the CaO - SiO_2 and CaO - $(FeO^* + MgO)$ covariance. The gabbros evolved through fractionation of clinopyroxene and plagioclase in about equal amounts. Clinopyroxenes and plagioclase did not crystallize during the formation of the olivine-bearing rock-types as evidenced by a lack of variation in CaO and Al_2O_3 molecular proportion ratios. Plagioclase was almost certainly unimportant in the crystallization of the pyroxenites as shown by a lack of Al_2O_3 variation.

Phase Diagram Considerations

The crystallization history of layered complexes in which olivine, pyroxene and plagioclase are dominant crystal phases may be examined in terms of the

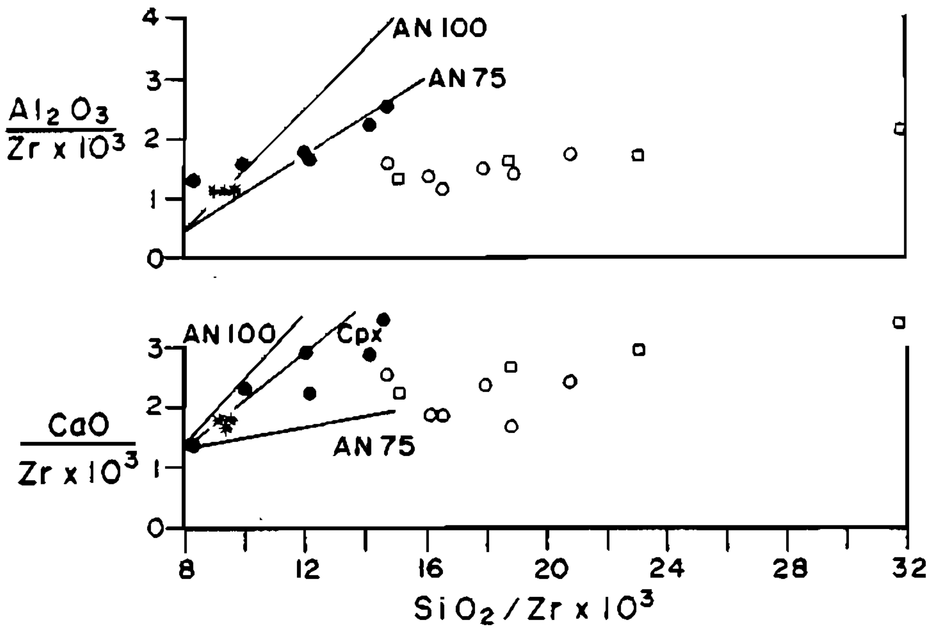

Figure 7.22 MPR plots of Al_2O_3/Zr and CaO/Zr versus SiO_2/Zr. The clinopyroxene slope is given for Wo_{40} En_{48} Fs_{12}. Symbols as for Figure 7.20.

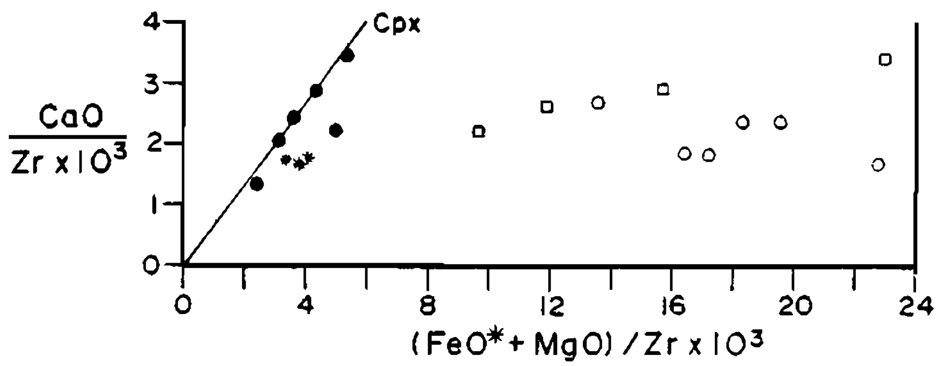

Figure 7.23 MPR plot of CaO/Zr versus (FeO* + MgO/Zr). Clinopyroxene slope is given for Wo_{40} En_{48} Fs_{12}. Symbols as for Figure 7.20.

simple system olivine - clinopyroxene - plagioclase - quartz developed by Irvine (1970, 1979). Orthopyroxene may be plotted on the olivine - quartz edge of the tetrahedron at a point determined by the equation:

$$SiO_2 + (Mg,Fe)_2\ SiO_2 = 2(Mg,Fe)\ SiO_2$$

The system is a gross simplification of the complex chemistry of the magma but has been used to model crystallization sequences for the Bushveld, Muskox, Stillwater and Skaergaard intrusions (Irvine, 1970). Calculation of the projection of the composition for the Hlagothi Complex through the clinopyroxene, olivine and plagioclase apices has been done according to the method of Irvine (1970). The numerical data are given in Appendix 5.

Petrographic data and MPR plots for the complex dictate that any proposed bulk composition must be capable of crystallizing extensive olivine, orthopyroxene, clinopyroxene and plagioclase in that order. Final crystallization must occur at the quartz - plagioclase eutectic in order to account for micrographic intergrowths of these minerals observed in the gabbros. Wehrlites present a problem (see later section).

The system and the three projections used are shown in Figure 7.24. As noted above, the main parental liquid must plot within the olivine field (shaded area in Figure 7.24A). The projected skeletal-textured gabbro compositions project close to the orthopyroxene end of the predicted bulk composition field. Their projected compositions would, however, change if the apportioning of iron to Fe^{3+} has been incorrect, as indicated by the scale bar shown for reduction in FeO content. For the purposes of this discussion, the skeletal-textured gabbros are considered a first order approximation of the initial liquid composition although the rationale behind this is deferred to a later section. Before discussing the proposed liquid path, mention must be made of the reaction boundary separating the olivine and orthopyroxene volumes. A liquid, crystallizing olivine, upon reaching this boundary begins forming enstatite, but at the same time, olivine reacts with the liquid as follows:

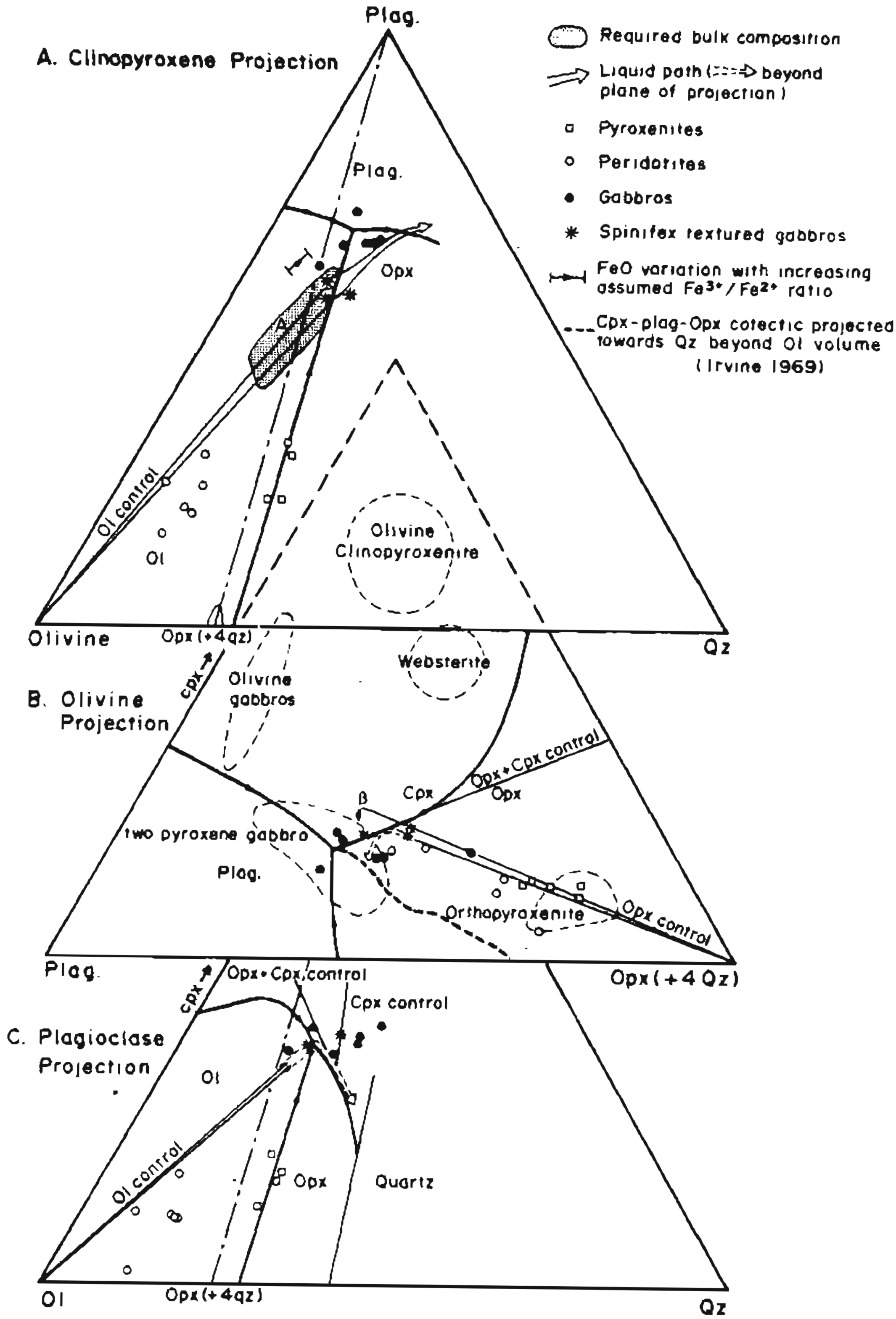

Figure 7.24 The system plagioclase - clinopyroxene - olivine - quartz.
A. Projection from clinopyroxene apex.
B. Projection from olivine apex.
C. Plagioclase projection.

System after Irvine (1970, 1979). Symbols as in Figure 7.20.
See text for further discussion.

$(Mg,Fe)\ 2SiO_4 + SiO_2 \rightarrow (MgFe)\ SiO_3$
olivine liquid enstatite

Once all the olivine is consumed or mantled by orthopyroxene, the liquid composition is free to move across the boundary into the orthopyroxene field. If the olivine is not consumed or removed from the system, the liquid path is constrained to the olivine - orthopyroxene peritectic boundary and moves towards the clinopyroxene - orthopyroxene - olivine cotectic line.

If the skeletal-textured gabbro is a first order approximation of the bulk composition, then olivine would begin crystallizing, with the result that the liquid composition moves to the olivine - orthopyroxene peritectic boundary plane (orthopyroxene - plagioclase line on clinopyroxene projection, Fig. 7.24A). The olivine-bearing rocks plot towards the olivine apex of the clinopyroxene projection which is in general agreement with this initial stage of crystallization. As crystallization was unlikely to be in an equilibrium situation, the removal by crystal settling or isolation of the olivine as noted above would allow the liquid composition to move out of the olivine volume before all olivine was consumed by reaction.

The liquid composition reaches the clinopyroxene - orthopyroxene cotectic plane before the plagioclase - orthopyroxene boundary (Fig. 7.24B). Crystallization of both clinopyroxene and orthopyroxene would then occur, driving the liquid composition towards a more felsic composition beyond the plane of observation in Fig. 7.24B. The rocks formed during this stage of crystallization would be the clinopyroxene orthopyroxenites which plot astride the olivine - orthopyroxene cotectic in Fig. 7.24A and on the orthopyroxene control line in Fig. 7.24B. The liquid path beyond the olivine volume is not easily illustrated, but the clinopyroxene-plagioclase-orthopyroxene cotectic line, towards which the liquid moves, is shown (Fig. 7.24B). Upon reaching the three phase cotectic, the liquid may move along the line, or across it into the plagioclase-clinopyroxene plane. In either case, the final liquid composition must be on a quartz-plagioclase volume boundary or a quartz-plagioclase-clinopyroxene cotectic line (Fig. 7.24C) in order to account for the plagioclase - quartz - micrographic intergrowth observed in the gabbroic rocks.

Feldspathic wehrlite (BG292 - not analysed) occurs near the top of the main Hlagothi sill and presents a minor problem in that the observed modal composition of 30% olivine, 65% clinopyroxene and 5% plagioclase cannot be achieved along the equilibrium crystallization path proposed above. Two possible explanations exist. First, a different bulk composition may have existed such that the olivine control line could reach the clinopyroxene - olivine cotectic directly (without reaching the orthopyroxene peritectic boundary). Second, and more probable, a combination of relatively rapid cooling and low nuclei concentration could have resulted in metastable crystallization of clinopyroxene. This is shown as line B in Fig. 7.24B.

5. Comparison of Skeletal Pyroxene and True Spinifex Textures and Implications for Petrogenesis.

The skeletal pyroxene texture of the upper marginal sequence has been described in an earlier section. The term "spinifex" has not been applied to the texture as an origin by extrusion and resultant quenching is generally associated with this usage. Although the rocks in which the texture occurs are clearly intrusive, the texture conforms well with the definition of pyroxene spinifex agreed upon at the Penrose Conference on komatiites (Arndt and Nisbet, 1982, p. 211): "pyroxene spinifex texture consists of pigeonite and augite or both pyroxenes in complex skeletal megacrysts that are arranged in sheaths perpendicular to flow margins. The pyroxene needles typically are 1 - 5 cm long but only 0.5 cm wide, and lie in a matrix of fine augite and devitrified glass, or augite, plagioclase and quartz. Usually the primary phases are replaced by hydrous phases." The example under discussion differs from this definition only in that the "sheaves" are found to be cones radiating downwards from point sources (recognized elsewhere prior to this study by A.H. Wilson, *et al.*, in preparation), the megacrysts may exceed the given dimensions, and that the aligned-skeletal crystals are parallel to the upper contact of the cooling unit (also recognized in Barberton komatiites, Viljoen *et al.*, 1983).

The structure of the megacrysts is also typical of pyroxene spinifex as described by Arndt and Fleet (1979) who point out that the pyroxene megacrysts are typically composite. Pigeonite occurs as the core of the grains described by these authors and is surrounded by subcalcic augite. In the Hlagothi Complex pyroxene megacrysts, the usual form consists of a central core of chlorite surrounded by amphibole, which are the common hydrous replacement products of pigeonite and augite respectively. Pigeonite has been found in the cores of some of the grains but unaltered augite has not yet been recognized. The pseudomorphism of amphibole after the clinopyroxene has been excellent and the morphology in sections cut normal to the long axis of the crystals is identical to that recognized by Arndt and Fleet (1979) in unaltered samples.

Spinifex textures are commonly attributed to supercooling of high magnesium rocks (Viljoen *et al.*, 1983; Donaldson, 1983; Arndt and Fleet, 1979) and show evidence for metastable crystallization of pyroxenes in that these commonly have compositions not found in rocks crystallized under equilibrium conditions. Arndt and Fleet (1979) report pigeonite cores surrounded by subcalcic augite as the typical form of pyroxene spinifex.

In order to test the similarity of the chemistry of skeletal crystals from the Hlagothi Complex with that of pyroxene spinifex in extrusive rocks, microprobe analysis of the crystals was attempted. Owing to difficulties with the instrument used, only a single analysis of the outer part of a skeletal crystal was obtained. No satisfactory results were obtained on the cores of the crystals. The analysis is presented as an amphibole composition (calculated using 22 oxygens) and as a pyroxene (calculated using 6 oxygens) (Table 7.5, p.197). This requires the equivocal assumption that little bulk chemical change occurred during hydration of the original pyroxene. Nonetheless, the analysis compares well with the data presented by Arndt and Fleet (1979). Thus, a common crystallization mechanism may be applicable to the Hlagothi marginal sequence and to normal spinifex-textured extrusive rock-types.

Available data do not allow identification of this mechanism, although the following factors are probably involved: (i) skeletal crystals are typical of rapid cooling and large degrees of supercooling. This condition is easily envisaged for extrusive high magnesium rocks of high liquidus temperature, but not for an intrusive body of the observed composition (MgO of skeletal-textured rocks = 8 - 10%); (ii) megacrystic growth is favoured by high water contents (Hughes, 1982) and by low nuclei density (Donaldson, 1982). Both these conditions may have been operative in the Hlagothi Complex since a high water content is postulated for the complex (see above) and the conical sheaves radiate downwards from point sources at the base of the variolitic unit. If the varioles are a product of liquid immiscibility, which is favoured by high water concentrations (Philpotts and Doyle, 1983), they may have formed at temperatures above the liquidus. In this case, heterogeneous nucleation may have occurred once the magma cooled to the pyroxene liquidus temperature. High water contents reduce magma viscosity and enhance diffusion to nuclei (Donaldson, 1979).

Spinifex-textured komatiites have been used to estimate the bulk composition of the cooling units. However, recent work (Viljoen *et al.*, 1983; Wilson *et al.*, in prep.) indicates that considerable fractionation occurs through flows having these textures. Fractionation almost certainly occurred within the marginal sequence of the Hlagothi Complex, but may not have been of the same order of magnitude as in the remainder of the intrusion.

This is substantiated by the chemical similarity of the three skeletal-textured rocks analysed in this study (Fig. 7.20). For this reason the skeletal-textured rocks may be used as a first order approximation of the bulk composition of the complex.

6. Magmatic Affinity

The chemical data presented above display reasonable consistency and coherence and may, therefore, be used to identify the magmatic affinity of the complex. When plotted on an AFM ternary diagram (Fig. 7.25), the plots with one exception lie in the tholeiitic field as defined by Irvine and Baragar (1971).

Jensen (1976) presented a ternary diagram of Al_2O_3 - (FeO + Fe_2O_3 + TiO_2) - MgO on which tholeiitic, calc-alkalic and komatiitic rock series may be discriminated. The analyses plot in the high Mg-tholeiite, basaltic komatiite and ultramafic komatiite fields (Fig. 7.26). The skeletal-textured rocks plot astride the boundary of the basaltic komatiite field. These rocks have been compared with all of the chemical parameters used by Viljoen *et al.* (1982) to characterize the different classes of komatiite and have been found to lie within the limits of "Barberton" type basaltic komatiites in most respects.

The recognition of komatiitic affinities of the Hlagothi Complex and the ultramafic dykes (cf. Chapter 6) is significant in that a resurgence of typically Archaean magmatism is indicated. No evidence for the existence of komatiites in the Pongola Supergroup has been reported as yet. This absence, in conjunction with the sedimentological evidence for the deposition of the Pongola on a stable craton, has been interpreted as evidence for cratonisation of the Kaapvaal crustal fragment at about 3.0 Ga when large volumes of potassic granite are known to have been emplaced (Hunter, 1974a). The emplacement of

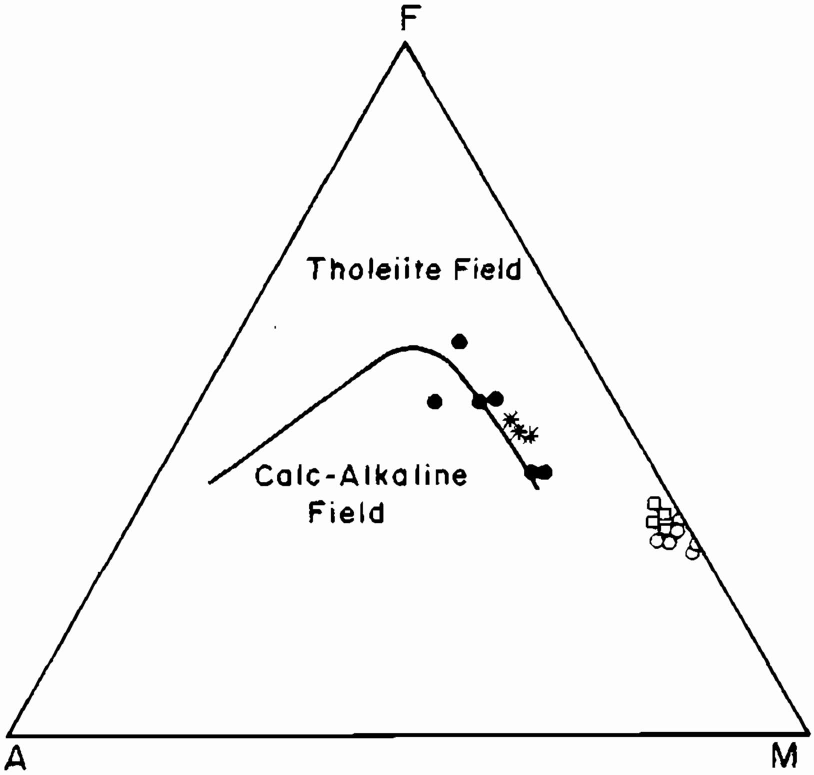

Figure 7.25 AFM diagram showing positions of Hlagothi Complex rock types. Boundary between tholeiitic and calc-alkaline fields after Irvine and Baragar (1971).
Symbols as in Figure 7.20.

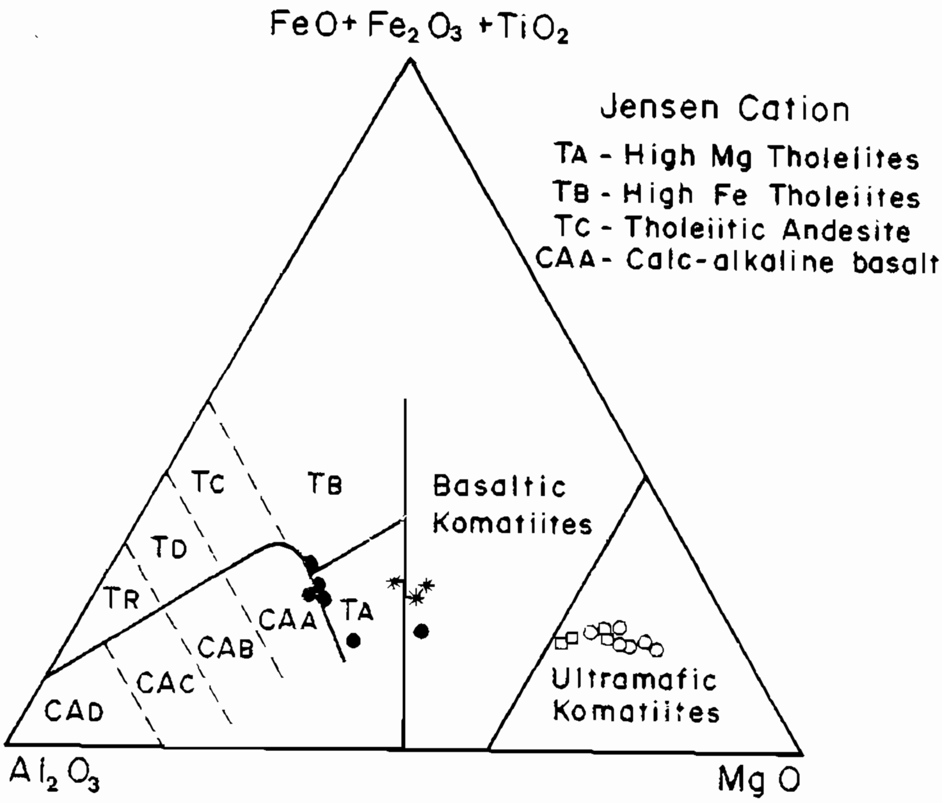

Figure 7.26 Jensen cation plot of Hlagothi Complex rock-types. Boundaries after Jensen (1976). See text for further discussion.
Symbols as in Figure 7.20.

komatiitic magmas as dykes rather than eruptive rocks could be expected if crustal thickening through underplating by thick granitic sheets caused reduced geothermal gradients and also provided a physical impediment to the upwards passage of the magmas except where deep fractures are present. An analogous situation has been proposed for the Great Dyke of Zimbabwe which was emplaced at about 2.5 Ga shortly after cratonization of the Zimbabwean region (Wilson *et al.*, 1978). The probable bulk composition of the Great Dyke contains about 15% MgO (Wilson, 1982) and falls within the komatiitic basalt field defined by Jensen (1976). It has been proposed that the Great Dyke represents an aborted greenstone belt and that the initial stages of rifting resulted in mantle-tapping fractures through which komatiitic liquids were emplaced to high crustal levels (Wilson, *et al.*, 1978). According to this model, the factors which prevented the magmas from being erupted are very similar to those mentioned above for the Kaapvaal structural province. Clearly, a great deal more research is required to resolve the problems introduced by the recognition of komatiitic dykes in the southern part of the Pongola Basin. In particular, geochronological data are essential in order to establish the duration of Archaean style magmatism in areas marginal to the Kaapvaal crustal fragment.

7. The Relationship of the Complex to Pretectonic Dykes

Several pretectonic dykes are present in the study area. The samples analysed (Table 7.7) are distributed as follows: BG84 is from an irregular body which intrudes the Ndikwe pyroclastics west of Ndikwe Store; BG125 and BG126 are from gabbroic dykes on the south limb of the Gem Syncline; BG141 is a thin irregular dark-coloured, aphyric dyke in the Welendhlovu Valley; BG208 is a gabbro from a sill close to the base of the complex; BG164 is from a narrow dyke which is truncated by the erosional base of the debris flow sequence south of Vuleka.

TABLE 7.7: GEOCHEMISTRY OF DYKES

	BG84	BG125	BG126	BG141	BG164	BG208
SiO_2	54.26	52.00	50.72	52.76	61.79	50.98
Al_2O_3	5.09	14.97	16.78	18.85	13.43	13.81
Fe_2O_3	1.08	0.91	0.78	0.93	1.57	1.63
FeO	9.73	8.20	6.99	8.40	14.14	13.20
MnO	0.18	0.17	0.13	0.20	0.27	0.25
MgO	13.35	9.81	9.20	7.60	5.13	5.38
CaO	13.28	10.73	10.63	2.94	9.14	8.77
Na_2O	1.55	1.81	2.52	0.78	2.59	2.43
K_2O	0.23	1.02	1.14	6.01	0.48	1.06
TiO_2	0.78	0.48	0.39	1.01	1.89	1.52
P_2O_5	0.11	0.08	0.07	0.15	0.24	0.16
Cr_2O_3	0.38	0.09	0.12	-	-	-
TOTAL	100.02	100.27	99.47	99.63	100.62	99.19
			Trace elements (ppm)			
Sc	28.3	32.5	19.7	32.2	51.4	46.2
V	148	165	118	253	360	455
Cr	2571	583	818	536	98	79
Ni	436	286	435	105	42	94
Cu	149	50	-	55	45	241
Zn	90	74	69	25	105	113
Y	13	23	11	20	33	42
Zr	85	92	56	88	111	125
Nb	7.4	6.0	4.4	5.0	4.4	4.7
Rb	5	27	26	297	26	40
Sr	164	148	260	233	262	130
Ba	112	476	507	2203	62	205
La	4.7	5.0	-	3.7	1.8	8.4

Petrographically only BG125 and BG126 resemble the Hlagothi gabbros. BG141, BG164 and BG208 are dissimilar and cannot be related to any specific group of intrusions. BG84 is probably related to the gabbroic dykes, but is very coarse-grained and may be of cumulate origin. In addition, the ultramafic dykes described in Chapter 6 are examined here with a view to establishing any possible relationship to the Hlagothi Complex.

The chemical variation of the dykes is shown in Figure 7.27. It is immediately clear that the dykes have no definite chemical similarity to the Hlagothi rock-types on the basis of major and minor element chemistry. There is also no obvious geochemical relationship between the dyke samples which suggests that they may not be from a single magmatic event. The ultramafic rock-types discussed in Chapter 6 are also shown on these plot and show some broad similarities to the peridotites of the complex.

Whilst it is not intended to attempt a detailed examination of the differences between the various groups of samples on the basis of the limited data available, some evidence for an absence of a genetic relationship is presentec When plotted on a Jensen cation diagram, the dyke samples fall predominantly within the tholeiite field with samples BG125 and BG126 plotting close to the Hlagothi gabbros (Fig. 7.28). The remainder of the samples are somewhat removed from the Hlagothi trend, although the observed differences are not very significant. On a plot of MgO versus SiO_2 (Fig. 7.29) the different sample populations fall into overlapping fields, but small displacements of the fields may be significant. The same feature is evident on plots of the incompatible elements Y and Nb versus Zr (Fig. 7.30). Most significant on the plots is the large displacement between the Nsuze group lavas and the intrusive rock-types. The latter samples plot close to the chondritic ratio on the Nb/Zr diagram. The Nsuze lavas are highly enriched in Zr or depleted in Y relative to chondrite. This would support the hypothesis that the Nsuze Group magmatism is distinct from the later intrusive events.

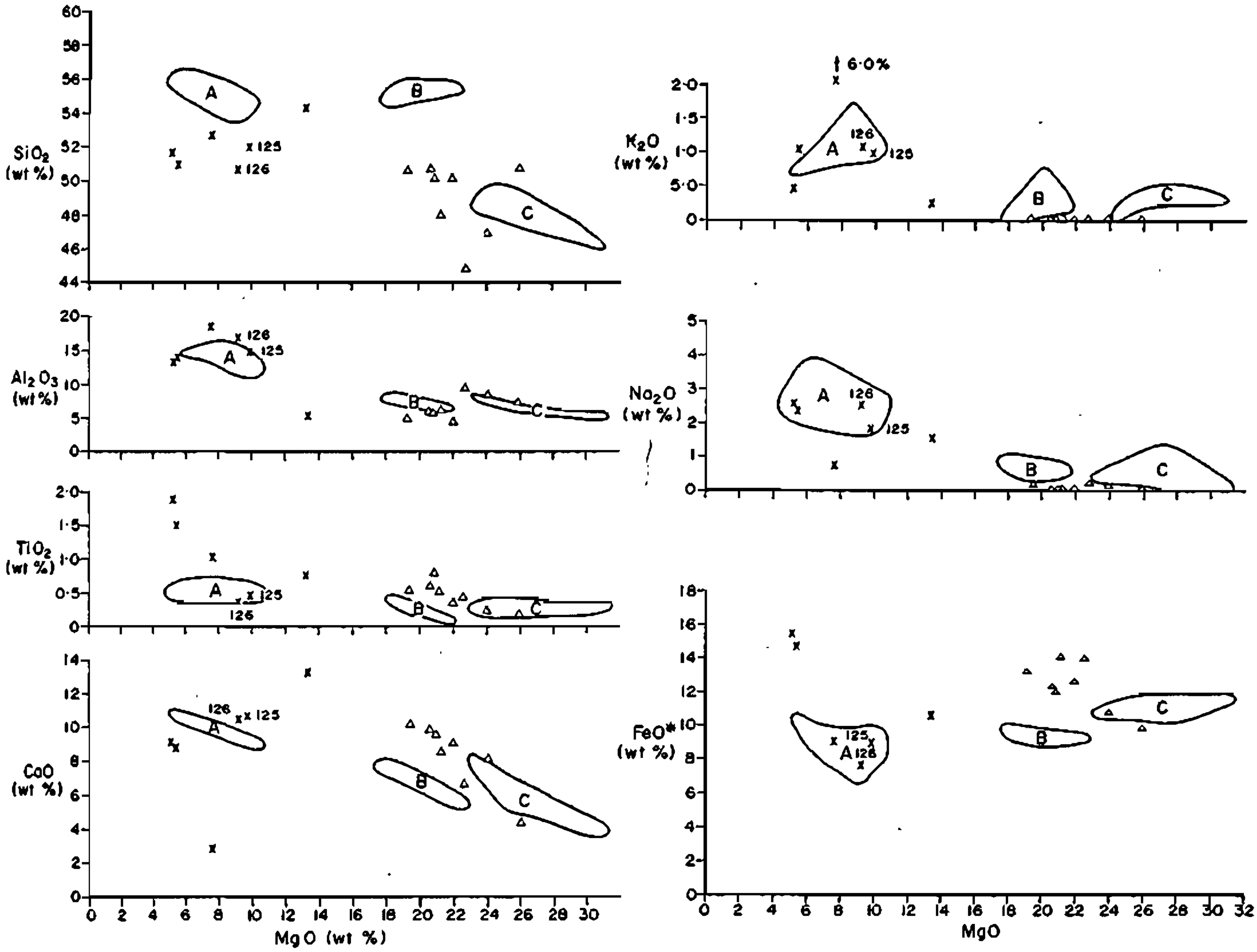

Figure 7.27 Geochemical variation for the pre-tectonic dykes (crosses), ultramafic dykes (triangles) and Hlagothi Complex gabbros (A), pyroxenites (B) and peridotites (C).

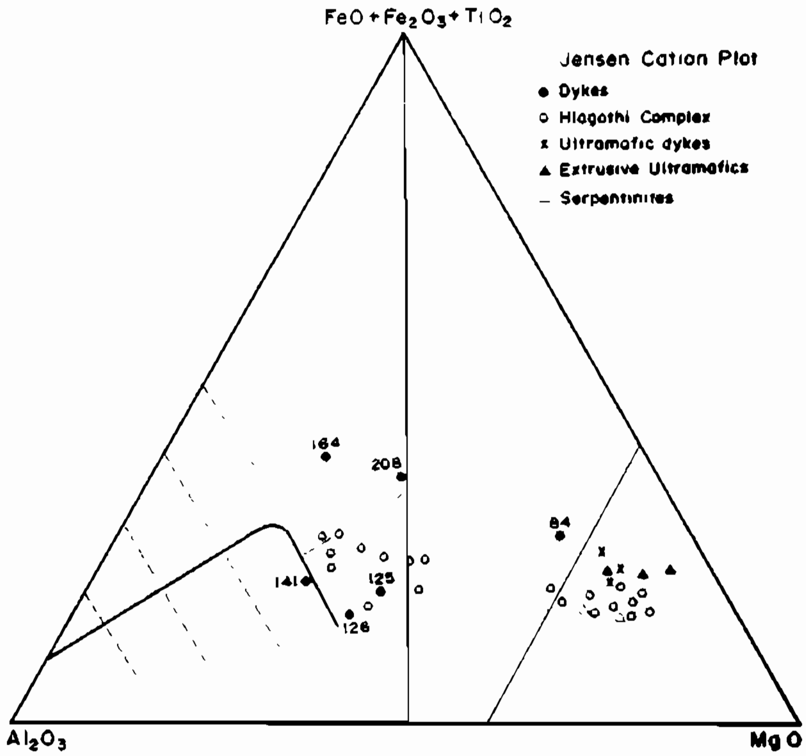

Figure 7.28 Jensen cation diagram for the pre-tectonic dykes (solid circles). Hlagothi Complex samples shown as open circles. Ultramafic rocks also shown.

In order to test the possibility that some of the dykes may be related to the complex, the CMAS system of O'Hara (1968) is used. This system has the benefit of allowing fractionation trends to be evaluated, and magmas of the same origin should be related by their trends to a common starting composition. Inspection of Figure 7.31 reveals that the Hlagothi peridotites and pyroxenites fall on control lines equivalent to 70% olivine, 30% enstatite and 90% enstatite, 10% diopside respectively. This serves to confirm the MPR and phase diagram conclusions reached above. Also noteworthy is the displacement of the ultramafic rocks away from the Hlagothi trends which suggests an unrelated origin for these rocks. The various gabbroic dyke rocks are not obviously related to any of the other groups and may thus be considered unrelated magmatic events. The exceptions are BG125 and BG126 which are chemically similar to the Hlagothi gabbros. The field for the Nsuze volcanics is superimposed on the CMAS projections and shows clearly that these cannot be related genetically to the other suites.

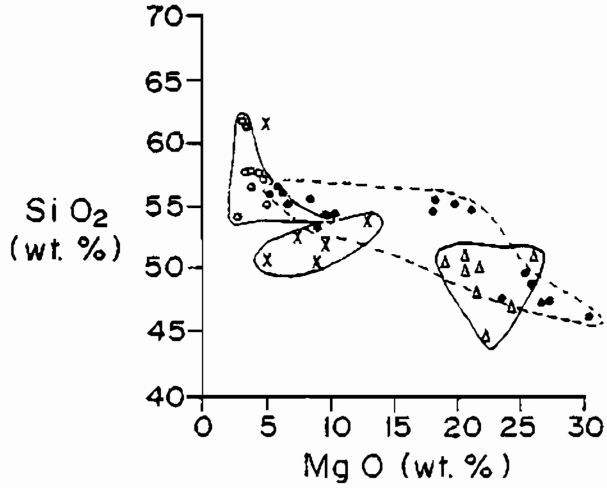

Figure 7.29 Plot of MgO vs SiO_2 for the various groups of samples analysed. See text for discussion.

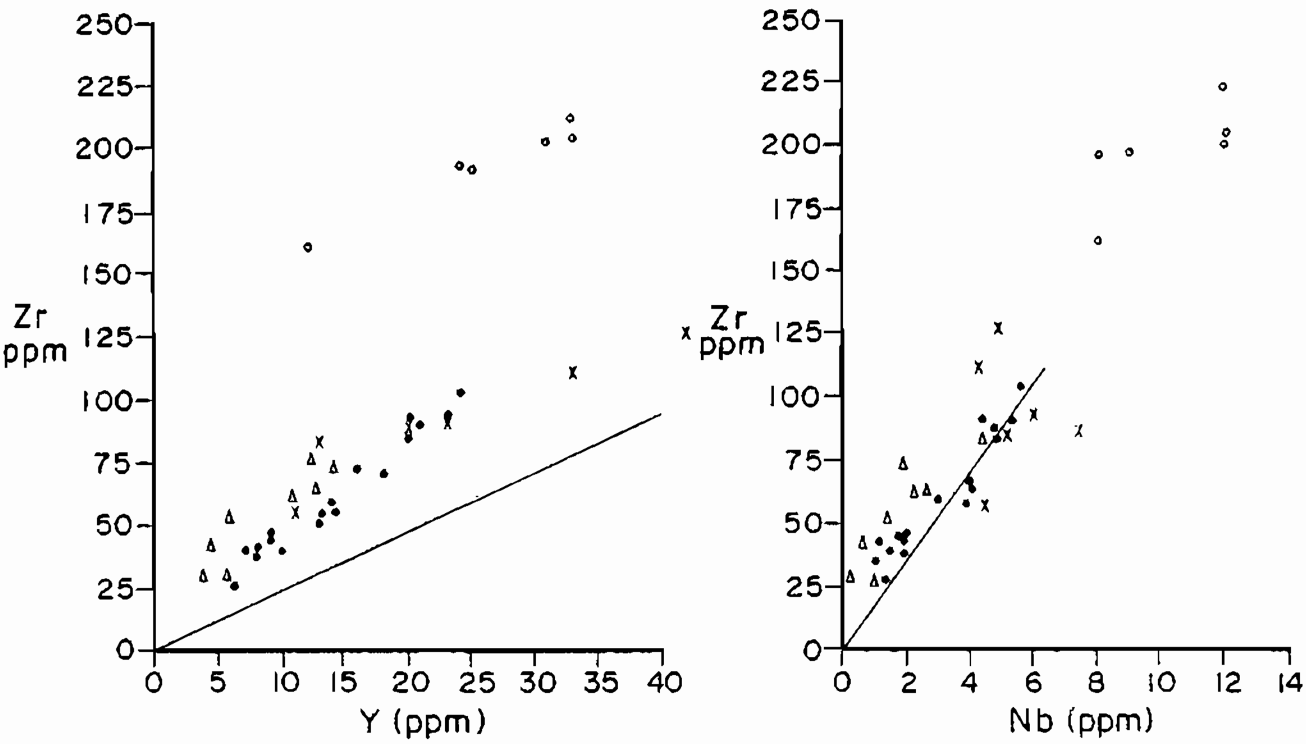

Figure 7.30 Y/Zr and Nb/Zr plots for the intrusive rocks and the Nsuze volcanics. Note displacement of Nsuze Group volcanics from the remainder of the samples on Y/Zr diagram. Slope of line is chondritic ratio in each case. Ornamentation as for Figure 7.29.

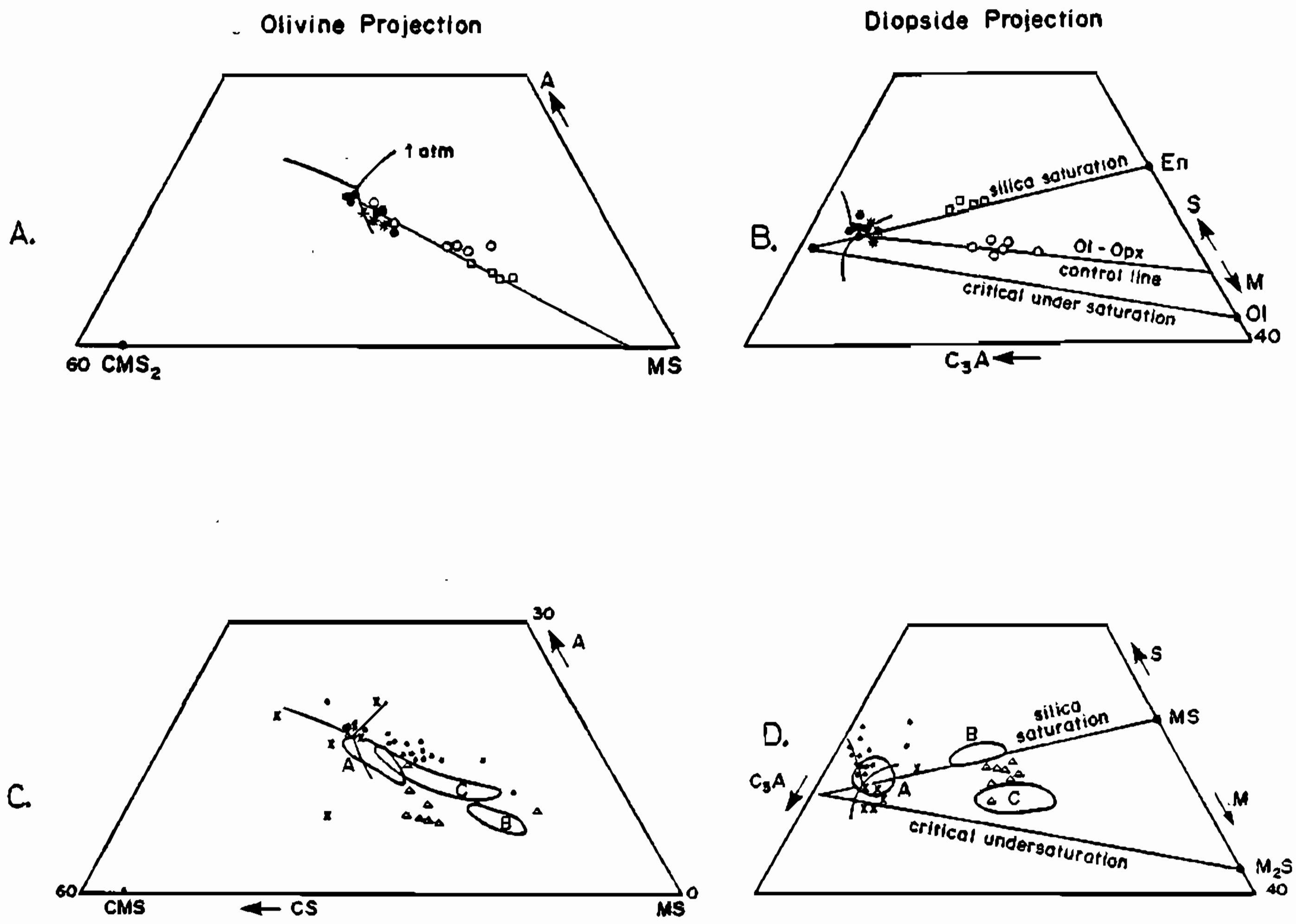

Figure 7.31 Olivine and diopside projections in the system CMAS after O'Hara (1968). A and B are for the Hlagothi Complex and show the control lines for peridotites (70% olivine, 30% enstatite) and pyroxenites (90% enstatite, 10% diopside). C and D show the plots of the other sample groups. Note the dispersion of the post-Nsuze, pre-tectonic dykes (crosses) and displacement of the trends for ultramafic dykes (triangles) and Nsuze Group volcanics (circles). Ornamentation for Hlagothi Complex samples as in Figure 7.31. Invariant point and cotectic boundaries for 1 atm.

CHAPTER 8

DISCUSSION AND CONCLUSIONS

1. The Pre-Nsuze

The earliest geological evolution of the study area is obscure, although it is known that a substantial sequence of komatiitic, high-magnesium and tholeiitic lavas with intercalated sediments constituting the Archaean Nondweni Group accumulated during this time. In the type area around Nondweni the thickness of the sequence is substantial (of the order of several thousand metres), but in the Nkandla area thickness and precise correlation of this group are as yet equivocal. The Nondweni komatiites have many characteristics in common with the Barberton examples, especially very high Ca/Al ratios and a compositional gap between komatiite and high-magnesium basalt compositions (Wilson *et al.*, in prep.). Sedimentary rock-types are subordinate and as yet poorly understood. In the study area the only rock-types that can be correlated tentatively with the Nondweni Group are tremolite - chlorite - talc schists in which poorly-defined relict volcanic textures are recognized. These rock-types have chemical compositions similar to the ultramafic komatiites in the Nondweni type area reported by Wilson *et al.* (in prep.).

This sequence was intruded by tonalitic granitoids and subjected to folding and erosion prior to the start of the Nsuze deposition. As a result the Nsuze Group rests unconformably upon Nondweni in the south and to the far north of the study area, but directly on gneissic tonalites in the northeast at Nkungumathe.

The crustal fragment upon which the Nsuze Group accumulated is considered to have achieved a substantial degree of stability by about 3.0 Ga, at which time large volumes of potassic granite were emplaced in the area to the north of the study area. The Nsuze Group rests with a sedimentary contact on this granite in the vicinity of Amsterdam (Fig. 1.1). The accumulation of the group was contemporaneous with active komatiitic and tholeiitic volcanism in Zimbabwe; where cratonization of the early Precambrian crust occurred at about 2.6 Ga. The Nsuze Group thus records a period of crustal evolution that is apparently unique to southern Africa. The study area is also significant in that it is situated close to the boundary between the Kaapvaal and Natal-Namaqua structural provinces.

2. The Nsuze Group

Nsuze Group deposition began with the accumulation of the 1 200 m-thick Ndikwe Formation in the north of the study area. The Ndikwe Formation is dominated by pyroclastic rock-types in which thin lava flows occur. It also contains substantial arenaceous and argillaceous sediments as well as subordinate banded iron formation. This sequence becomes thinner southwards and interdigitates with the 1 200 m-thick, sedimentary Mdlelanga Formation which consists of arenites, argillites and greywackes. Carbonates are present near the base of the sequence. A lateral time equivalence between the formations is envisaged as quartz arenite units within the Ndikwe may be correlated with the lower units of the Mdlelanga.

The Qudeni Formation, a lava sequence consisting predominantly of basaltic-andesites, overlies the Mdlelanga and Ndikwe Formations. This unit is 580 m thick in the south, but only 50 m is present in the north. As there is little evidence for an angular unconformity the variation in thickness of the formation is thought to reflect an original depositional feature.

The Vutshini Formation, which has much in common with the Mdlelanga Formation, is a 1 000 m-thick sequence of quartz-arenites, argillites and heterolithic sediments. However, it lacks carbonate rock-types and has a thin unit of fluvial and transgressive marine conglomerate and arenite at the base.

The uppermost part of the formation comprises relatively immature quartz arenites which may represent a fluvial fan which prograded over the shelf sequence.

A thin volcanic unit termed the Ekombe Formation overlies the Vutshini Formation. It consists of andesites about which little is known as the unit is poorly exposed and has a residual thickness of only 60 m.

The sedimentology of the group is not thoroughly established, although several facies associations and probable depositional environments are recognized. A large proportion of the sediments is thought to have been deposited in environments ranging from tidal to distal shelf. Fluvial sediments are not common in the area, although a large part of the sequence has not yet been defined in terms of depositional environment. Palaeocurrent data indicate predominantly south- and southeastwards palaeoslopes with considerable local variation. This is consistent with a northeast-southwest trending shoreline.

The geochemistry of the lavas is poorly constrained and shows considerable variation which is neither consistent nor readily explained. The lavas are heterogeneous in addition to being altered. The small number of samples analysed does not provide adequate data to represent these variations. The chemistry does allow discrimination between samples from the Qudeni and Ndikwe Formations, particularly in terms of Ti, Mn and Zr concentrations. The data are considered inadequate for modelling of petrogenesis, but resemble the data for the Nsuze type area presented by Armstrong (1980) sufficiently to allow the assumption that the volcanics in both areas share similar sources and fractionation histories. Characterization of the magma type is inconclusive, but it appears to have both tholeiitic and calc-alkalic affinities. Neither an oceanic nor a continental origin is clearly indicated for these volcanics, but they do show some characteristics of intra-plate magmatism using criteria established by Winchester and Floyd (1976).

The broad inferred depositional setting of the Nsuze Group is little different from that proposed for the Pongola Supergroup by Watchorn (1978) and Armstrong (1980). However, the Ndikwe Formation has some features more typical of Archaean volcanic - sedimentary sequences than the rest of the Nsuze Group. These are specifically the presence of Algoma-type banded iron formation of the oxide facies and the admittedly rare turbidite deposits. Turbidite deposits have been interpreted as the result of prograding submarine fans in Archaean sequences (Eriksson, 1980) which is consistent with the deep water, tectonically active depositories envisaged for Archaean terranes. The chemistry of the Ndikwe volcanics also differs subtly from that of the remainder of the Nsuze Group, especially in trace element abundances. The implications of this are not yet clear and more samples are required to determine whether the differences are due to alteration, metasomatism or a primary petrogenetic control. The absence of komatiitic volcanics is significant in this regard and is the major difference between this formation and typically Archaean sequences.

Sedimentological differences between this area and the type area are also significant. This study has shown that a considerable part of the Nsuze Group consists of shallow marine sediments in contrast to the fluvial deposits reported from the northern areas by Watchorn and Armstrong (1981). Furthermore, the arenaceous rocks in the southern area are considerably more mature than those documented by these authors. A more distal setting is thus indicated for the southern part of the Nsuze basin.

The lateral facies changes in the sedimentary formations and the repetition of volcanics within the group are evidence for some degree of instability of this part of the basin. It is unfortunate that no studies of the Pongola Supergroup have attempted to document the lateral facies variation in other areas, so it is impossible to assess probable variation in tectonic stability of different areas in the Pongola depositional basin.

3. Early Post-Nsuze Intrusions

Several episodes of intrusion post-date the deposition of the Nsuze Group These are the ultramafic dykes, the layered sheets of the Hlagothi Complex, diabases and porphyry dykes. All predate the main tectonic and metamorphic events which have affected the Nsuze Group. The ultramafic dykes are high-magnesium rocks which are characterized by high Ca/Al ratios and trace element ratios close to chondritic values. Chemically they conform to established criteria for the recognition of komatiitic lavas and are thus considered to be an intrusive equivalent to these rock-types. The narrow widths of the bodies appear to preclude an origin as cumulates. Dykes of similar chemistry have not been reported from other outcrops of the Nsuze Group.

The Hlagothi Complex consists of ultramafic and mafic rock-types intruded as differentiated sheet-like bodies in which altered harzburgites, olivine websterites and wehrlites are overlain by olivine gabbronorite and pyroxenites. The top of each sheet consists of gabbro and leucogabbro. Marginal rocks containing skeletal pyroxene crystals analogous to the spinifex texture of extrusive komatiites are present. Significantly these rocks have the chemical characteristics of komatiitic basalts. Field relationships indicate intrusion prior to the main deformational events in the area. The fact that the complex consists of sills suggests intrusion at depths less than a few kilometres. If this is valid, further work may provide evidence for a relationship between the complex and Nsuze magmatism. This would be important because of the apparent absence of komatiitic lavas from the Pongola Supergroup. Proposed parental magma compositions for the complex bear considerable resemblance to the least magnesium-rich spinifex-textured komatiites of the Nondweni Group as reported by Wilson *et al.*(in prep.). Therefore, a similar petrogenesis is envisaged for the Hlagothi Complex, that is, partial melting of upper mantle material followed by fractionation of olivine, clinopyroxene and perhaps orthopyroxene prior to intrusion.

The crystallization history of the complex in terms of the simple system Ol - Cpx - An - Qz suggests that olivine crystallized first in much of the complex. This was followed by orthopyroxene, ortho- and clinopyroxene together and finally plagioclase and possibly quartz. In the upper skeletal-textured marginal rocks initial metastable crystallization of pigeonite was followed by clinopyroxene as a result of supercooling and relatively high P_{H_2O}.

This recurrence of typical Archaean-type magmatism in late or post-Nsuze times, apparently restricted to the southernmost part of the Nsuze depositional basin adjacent to the Natal-Namaqua structural province, may have significant implications in understanding crustal evolution during the late Archaean in southern Africa. As noted above, komatiitic magmatism prevailed north of the Kaapvaal structural province in Zimbabwe until 2.6 Ga. It is tempting to speculate that this style of volcanism was a feature of the marginal areas of the Kaapvaal crustal fragment during late Archaean times. The komatiitic intrusions into the Nsuze Group in the southern part of this fragment could thus represent a manifestation of this volcanism, the komatiitic magmas being emplaced into the more stable plate as dykes rather than being extruded. Thickening of the Kaapvaal crustal fragment as a consequence of underplating by large volumes of granite as thick sheets may have prevented the rise and extrusion of mafic and ultramafic magmas except along deep crustal fracture systems. Clearly further research is required to resolve this matter.

Other pre-tectonic intrusions are of gabbroic, plagioclase porphyry and pyroxenitic composition and occur as cross-cutting irregular bodies and dykes. These intrusions are petrographically similar to the gabbros and pyroxenites of the Hlagothi Complex, but there is insufficient geochemical evidence to link the two episodes of intrusion. In any event, the plagioclase porphyry dykes are clearly younger than the complex. Syenites and monzogabbros in the northeastern corner of the study area have been afforded little attention, but appear worthy of more detailed study because their age relationship to the Hlagothi Complex is uncertain, although they are aligned parallel to the main locus of intrusion of the complex. This linear feature has apparently been active in Phanerozoic times as there is associated minor post-Karoo faulting and dolerite dyking.

4. Structural and Metamorphic History

The earliest D_1 fabric element, S_1, is a rarely recognized phyllonitic cleavage, which is deformed by the younger D_2 event. This D_2 episode dominates the area and has produced tight and isoclinal folding on various scales. These have axial planes dipping steeply southwards, with shallow eastwards or westwards plunging fold axes. S_2 cleavage is axial planar to the folds and is pervasive in all argillaceous and tuffaceous rock-types, but only faintly visible in the arenites and lavas. Kinking and crenulation of S_2 by a later, spaced cleavage is the only observed evidence for a third penetrative deformation.

Faulting of at least three ages is recognized. The first comprises slides (thrust and lag faulting), as well as crestal and wrench faulting associated with the D_2 folding event. North-south trending block faulting post-dates D_2, but pre-dates porphyry dykes and a group of east-west trending block faults, which may have been active in pre- and post-Karoo times.

Regional greenschist facies metamorphism has affected all pre-D_2 sequences and intrusions. The mica defining S_1 cleavages in Nsuze Group rocks represents the earliest metamorphic event. Subsequent metamorphism to upper greenschist facies probably occurred during D_2. This event is characterized by the co-existence of biotite and muscovite in pelitic rocks, in addition to the common diagnostic low-grade mineral parageneses. The absence of stilpnomelane in pelitic rocks indicates upper greenschist facies conditions. Post-D_2 dykes also have greenschist facies mineralogy, indicating a possible third regional metamorphism.

5. Conclusions

A. Ultramafic komatiites having features reminiscent of lava flows which occur in small structurally and stratigraphically low areas are tentatively assigned to the Nondweni Group. These rocks are chemically indistinguishable from unequivocally extrusive komatiites in the Nondweni type area and in the Barberton belt.

B. Intrusion of tonalite post-dates the Nondweni Group, but pre-dates deposition of the Nsuze Group.

C. Nsuze Group deposition began with the Ndikwe Formation, a clastic wedge up to 1 400 m thick which consists of pyroclastic, argillaceous, arenaceous and cherty ferruginous rock-types. Minor lava flows accompanied the pyroclastic volcanism which was dominated by Pelean or ash flow extrusion. The banded iron formation was deposited in a distal environment, in association with other ferruginous, clastic rock-types deposited by turbidity flows and suspension settling. Intertidal, proximal shelf and ephemeral stream environments existed during the deposition of this sequence. The wedge tapers southwards to less than 500 m, concomitantly, the overlying Mdlelanga increases in thickness to 1 200 m. This unit consists of quartz wackes and quartz arenites with subordinate argillaceous rock-types. It was deposited by shallow marine processes. A thin basal unit of silicified carbonates resulted from chemical and biogenic precipitation of calcite. Rare stromatolites and algal mats are recognized.

The Qudeni Formation is 60 - 580 m thick and comprises tholeiitic basaltic andesites, andesites and dacites. Textures such as flow top breccias are recognizable, but there are no unequivocal pillow structures.

The Vutshini Formation (up to 1 000 m thick) consists of arenites and argillites deposited by tidal and proximal shelf processes. Some arenite and conglomerates may be products of fluvial incursions into the predominantly marine depositional environment.

The stratigraphically highest formation of the Nsuze Group is the Ekombe Formation which comprises andesitic lavas with a maximum residual thickness of 60 m.

The geochemistry of the volcanics is similar to that reported from the northern parts of the Nsuze group by Armstrong (1980), although most of the samples analysed show evidence for alteration. Extreme CaO depletion and MgO enrichment in several samples is ascribed to submarine alteration. The magmas are sub-alkalic in character and show tholeiitic and calc-alkalic affinities. Available data do not allow modelling of the petrogenesis.

Palaeocurrent data from all sedimentary units indicate a palaeoslope towards the southeast, although there is considerable dispersion of the data. The dominance of sedimentary rocks of inferred tidal origin favours a broad shallow shelf sea. This part of the Pongola basin is probably more distal than the more northerly areas described in the literature.

D. A resurgence of magmatism occurred soon after deposition resulting in the intrusion of ultramafic dykes and the Hlagothi Complex. The latter consists of several layered sills in which cumulate rocks comprising olivine, ortho- and clinopyroxene are present in the lower part and gabbros and leuco-gabbros in the upper parts. These gabbros have been altered deuterically as a result of increasing water pressures with advancing fractionation. This alteration has also affected skeletal-pyroxene-textured marginal rocks, but has not obscured these textures. The skeletal textures are thought to reflect quenching. The estimated bulk composition of the Hlagothi Complex has the characteristics of a basaltic komatiite.

Ultramafic rock-types occur as dykes and sills which clearly intrude the lower part of the Nsuze Group. These are chemically similar to the komatiitic rocks ascribed to the Nondweni Group. This casts doubt on the recognition of the Nondweni Group in the study area, but confirms that a resurgence of komatiitic magmatism occurred in post-Nsuze time.

E. Several episodes of deformation and metamorphism are recognized. The folding is predominantly isoclinal with steep, southwards dipping, axial surfaces and subhorizontal fold axes. Regional low-grade metamorphism of greenschist facies has occurred repeatedly with three episodes being distinguishable.

ACKNOWLEDGEMENTS

I am indebted to Professor D.R. Hunter of the University of Natal, Pietermaritzburg for his guidance during this project. His geological insight and patience with an often wayward student have contributed substantially to this thesis. All errors and misinterpretations remain, of course, my own.

My thanks also to Dr A.H. Wilson for his guidance in the petrochemical procedures used. He also provided all computer software for calculating the XRF analyses, normative data and phase diagram projections.

I am grateful to the following people who have contributed to this study in many ways:

Professor V. von Brunn for accompanying me to the field and for maintaining my interest in sedimentology;

Geoff Grantham for many hours of useful disucssion;

Professor C.J. Talbot (University of Uppsala, Sweden) and Dr A.R. Allen for their contributions to my understanding of structural geology;

Dr D. Bühmann for his guidance in X-ray diffraction;

Roy Seyambu and Pat Suthan for assistance with photography, thin section preparation and other technical aspects;

Leslie le Roux for drafting the figures and maps;

Barbara Rimbault for typing the manuscript with considerable forbearance;

Anton Esterhuizen for many enjoyable days spent in the Nkandla area;

Gold Fields of South Africa for allowing me to use data accumulated whilst working in their mineral exploration programme in southern Zululand;

Anne and Don Balmer, Audrey and Des Pollock and Trish and Bob Turner for providing accommodation, entertainment and making my stay in Babanango memorable.

Finally, I thank Lisa, my wife, for her support in all things.

REFERENCES

ALLEN, J.R.L., 1970. *Physical Processes of Sedimentation.* Allen and Unwin, London. 248 pp.

ARMSTRONG, N.V., 1980. *Geology and Geochemistry of the Nsuze Group in northern Natal and southeastern Transvaal.* Unpub. Ph.D. thesis, Univ. of Natal. 386 pp.

ARMSTRONG, N.V., HUNTER, D.R. and WILSON, A.H., 1982. Stratigraphy and petrology of the Archaean Nsuze Group, northern Natal and southeastern Transvaal, South Africa. *Precambrian Res., 19,* 75-107.

ARNDT, N.T. and FLEET, M.G., 1979. Stable and metastable pyroxene in layered komatiite lava flows. *Am. Miner. 64,* 856-864.

ARNDT, N.T. and NISBET, E.G., 1982. Editorial Introduction to Part 3, 211-212. *Komatiites.* Allen and Unwin, London. 525 pp.

BAKER, P.E., BUCKLEY, F. and HOLLAND,J.G., 1974. Petrology and geochemistry of Easter Island. *Contr. Miner. Petrol., 44,* 85-100.

BARTON, J.M., Jr., 1983. Isotopic constraints on possible tectonic models for crustal evolution in the Barberton granite-greenstone terrane, Southern Africa. *Spec. Pub. Geol. Soc. S. Afr., 9,* 73-79.

BARTON, J.M., Jr., ROBB, L.J., ANHAEUSSER, C.R. and VAN NIEROP, D.A., 1983. Geochronological and Sr-isotopic studies of certain units of the Barberton granite-greenstone terrane, South Africa. *Spec. Pub. Geol. Soc. S. Afr., 9,*

BESWICK, A.E., 1982. Some geochemical aspects of alteration and genetic relations in komatiitic suites., 283-308. *In: Arndt, N.T. and Nisbet, E.G. (Eds). Komatiites.* Allen and Unwin, London. 525 pp.

BOERSMA, J.R., 1970. Distinguishing features of wave-ripple cross stratification and morphology. Doctoral thesis, Univ. of Utrecht. 65 pp.

BRADLEY, J., 1965. Intrusion of major dolerite sills. *Trans. R. Soc. N. Zealand, 3,* 27-55.

BROWN, G.J., 1982. The geology of the pre-Natal formations of the area to the west of the Nkandla forest reserve. Unpub. B.Sc. Hons. thesis, Univ. of Natal, Pietermaritzburg. pp.

BURGER, J.A. and COERTZE, F.J., 1973. Radiometric age measurements on rocks from Southern Africa to the end of 1971. *Geol. Surv., Pretoria, Bull. 58,* 46 pp.

CARMICHAEL, I.E.S., 1964. The petrology of Thingumuli, a Tertiary volcano in eastern Iceland. *J. Petrology, 5,* 435-460.

CAWTHORN, R.G., STRONG, D.G. and BROWN, P.A., 1976. Origin of corundum-normative intrusive and extrusive magmas. *Nature, 259,* 102-104.

CHARLESWORTH, E.G. and MATTHEWS, P.E., 1981. Archaean granulites along the southern margin of the Kaapvaal craton in eastern South Africa. *Geol. Soc. S. Afr. Abstracts of South African Geodynamics Symposium.* 34-35.

CHAYES, F., 1969. On the occurrence of corundum in the norms of the common volcanic rocks. *Carnegie Inst. Washington Yearbk. 64,* 179-182.

CLARK, S.M., 1983. The geology of an area southeast of Nkandla, particularly the Nkandla Formation. *Unpub. B.Sc. Hons. thesis, Univ. of Natal, Pietermaritzburg.* 64 pp.

CLOUD, P., 1973. Paleoecological significance of banded iron formation. *Econ. Geol., 68,* 1135-1143.

COLEMAN, J.M. and GAGLIANO, S.M., 1965. Sedimentary structures: Mississippi River deltaic plain. *In: Middleton, G.V. (Ed). Primary sedimentary structures and their hydrodynamic interpretation.* Soc. Econ. Paleontologists and Mineralogists, 12, 133-148.

COLLINSON, J.D., 1970. Bedforms of the Tana River, Norway. *Geogr. Annal. 52-A,* 31-56.

CONDIE, K.C., VILJOEN, M.J. and KABLE, E.J.D., 1977. Effects of alteration in element distributions in Archaean tholeiites from the Barberton greenstone belt, South Africa. *Contr. Miner. Petrol., 64,* 75-89.

COOK, H.E., 1979. Ancient continental slope sequences and their value in understanding modern slope development. *Soc. Econ. Paleontologists and Mineralogists Spec. Pub., 27,* 287-305.

DAVIES, R.D., ALLSOPP, H.L., ERLANK, A.J. and MENTON, W.I., 1970. Sr-isotope studies on various layered mafic intrusions in southern Africa. *In: Symposium on the Bushveld Complex and other Layered Intrusions, (D.J.L. Visser and G. von Gruenewaldt, eds).* Geol. Soc. S. Afr. Spec. Pub., 1, 576-593.

DAVIS, J.R., Jr. (Ed.)., 1978. *Coastal sedimentary environments.* Springer Verlag., New York. 420 pp.

DE SITTER, L.U., 1964. *Structural Geology.* 2nd Ed. McGraw-Hill, New York. 551 pp.

DIMROTH, E., 1975. Depositional environment of the iron-rich sedimentary rocks. *Geol. Rdsch., 64,* 751-767.

DONALDSON, C.H., 1976. An experimental investigation of olivine morphology. *Contr. Miner. Petrol., 57,* 187-213.

DONALDSON, C.H., 1979. An experimental investigation of the delay in nucleation of olivine in mafic magmas. *Contr. Miner. Petrol., 69,*

DONALDSON, C.H., 1982. Spinifex-textured komatiites: a review of textures, mineral compositions and layering, 213-244. *In: Arndt, N.T. and Nisbet, E.G. (Eds). Komatiites.* Allen and Unwin, London. 525 pp.

DU TOIT, A.L., 1931. Explanation of sheet 109 (Nkandla). Geol. Surv. S. Afr. *105 pp*

ELLIOT, T., 1978. Clastic Shorelines, 143-177. *In: Reading, H.G. (Ed). Sedimentary Environments and Facies.* Blackwell, London. 145-177.

ENOS, P., 1977. Flow regimes in debris flow. *Sedimentology, 24,* 144-142.

ERIKSSON, K.A., 1977. A palaeoenvironmental analysis of the Archaean Moodies Group, Barberton Mountain Land, South Africa. Unpub. Ph.D. thesis, Univ. of the Witwatersrand. 155 pp.

ERIKSSON, K.A., 1980. Hydrodynamic and paleogeographic interpretation of turbidite deposits from the Archean Fig Tree Group of Barberton Mountain Land, South Africa. *Geol. Soc. Am. Bull., 91,* 21-26.

ESTERHUIZEN, A. and GROENEWALD, P.B., 1980. Report on Magnetometer Traverses in the Nkandla District. Unpub. Company Repts. Gold Fields of South Africa Limited, Johannesburg.

FLOWER, M.J.F., 1973. Evolution of basaltic and differentiated lavas from Anjouan, Comores Archepelago. *Contr. Miner. Petrol., 38,* 237-260.

FLOYD, P.A. and WINCHESTER, J.A., 1975. Magma type and tectonic setting discrimination using immobile elements. *Earth Planet. Sc. Lett., 27,* 211-218.

FERGUSON, J. and CURRIE, K.L., 1972. Silicate immiscibility in the ancient "basalts" of the Barberton Mountain Land, Transvaal. *Nature, Phys. Sci., 235,* 86-89.

GELINAS, L., BROOKS, C., TRZCIENSKI, W.E., Jr., 1976. On Archaean variolites - quenched immiscible liquids. *Can. J. Earth Sc., 13,* 210-230.

GREEN, D.H., EDGAR, A.D., BEASLEY, P., KISS, E. and WARE, N.G., 1974. Upper mantle origin for some hawaiites, mugearites and benmorites. *Contr. Miner. Petrol., 48,* 33-43.

GROSS, G.A., 1968. Geology of iron deposits in Canada, Vol. 3. Iron ranges of Labrador Geosyncline. *Geol. Surv. Canada Econ. Geol. Dept., 22, Vol. 3,* 179 pp.

HAMMERBECK, E.C.O., 1977. The Usushwana Complex in the southeastern Transvaal with special reference to its economic mineral potential. *Unpub. D.Sc. thesis, Univ. Pretoria.* 226 pp.

HARMS, J.C., 1975. Stratification and sequence in prograding shoreline deposits. *Soc. Econ. Paleontologists and Mineralogists. Spec. Pub. 12,* 84-115.

HARMS, J.C., SOUTHARD, J., SPEARING, D.R. and WALKER, R.G., 1975. Depositional Environments as interpreted from Primary Sedimentary Structures and Stratification Sequences. Lecture Notes. *Soc. Econ. Paleontologists and Mineralogists. Short Course 2.* Dallas. 161 pp.

HATCH, F.H., 1910. Report on mines and minerals of Natal. Clay, London. 155 pp.

HAWKESWORTH, C.J., BICKLE, M.J., GLEDHILL, A.R, WILSON, J.F. and ORPEN, J.L., 1979. A 2.9 by event in the Rhodesian Archaean. *Earth Planet. Sc. Lett., 43,* 285-297.

HAWKESWORTH, C.J., MOORBATH, S. and O'NIONS, R.K., 1975. Age relationships between greenstone belts and "granites" in the Rhodesian Archaean craton. *Earth Planet. Sc. Lett., 25,* 251-262.

HOBDAY, D.K., 1973. Middle Ecca deltaic deposits in the Muden-Tugela Ferry area of Natal. *Trans. geol. Soc. S. Afr., 76,* 309-318.

HOBDAY, D.K. and VON BRUNN, V., 1979. Fluvial sedimentation and paleogeography of an early Paleozoic failed rift, southeastern margin of Africa. *Palaeogeography, Palaeoclimatology, Palaeogeography, 28,* 169-184.

HOLM, P.E., 1982. Non recognition of continental tholeiites using the Ti-Y-Zr Diagram. *Contr. Miner. Petrol., 79,* 308-310.

HUGHES, C.J., 1972. Spilites, keratophyres and the Igneous Spectrum. *Geol. Mag., 109,* 513-527.

HUGHES, C.J., 1977. Archaean variolites-quenched immiscible liquids: Discussion *Can. J. Earth Sci., 14,* 137-139.

HUGHES, C.J., 1982. *Igneous Petrology.* Developments in Petrology, Vol. 7. Elsevier. 551 pp.

HUGHES, C.J. and HUSSEY, E.M., 1976. M and Mg values in igneous rocks: proposed usage and a comment on currently employed Fe_2O_3 corrections. *Geochim. cosmochim. Acta., 40,* 485-486.

HUMPHREY, W.A., 1911. Notes on a traverse through parts of the Vryheid district and Zululand. *Ann. Rep. Geol. Surv., Union of S. Afr.*, 91-94.

HUMPHREY, W.A., 12. Geology of a portion of northern Natal between Vryheid and the Pongola River. *Ann. Rep. Geol. Surv., Union of S. Afr.* 99-124.

HUMPHREY, W.A. and KRIGE, L.J., 1931. The Geology of the country south of Piet Retief, an explanation of Sheet No. 68. Govt. Printer, Pretoria. 66 pp.

HUMPHREY, W.A. and KRIGE, L.J., 1932. The geology of the country surrounding Vryheid - an explanation of sheet No. 102. Govt. Printer, Pretoria. 59 pp.

HUNTER, D.R., 1974a. Crustal Development in the Kaapvaal Craton: I The Archaean. *Precam. Res.*, *1*, 259-294.

HUNTER, D.R., 1974b. Crustal Development in the Kaapvaal Craton: II The Proterozoic. *Precam. Res.*, *1*, 295-326.

IRVINE, T.N., 1970. Crystallization sequences in the Muskox intrusion and other layered intrusions, I. Olivine - pyroxene - plagioclase relations. *Spec. Pub. Geol. Soc. S. Afr.*, *1*. 441-476.

IRVINE, T.N., 1979. Rocks whose composition is determined by crystal accumulation and sorting, 245-306. *In: Yoder, H.S. (Ed). The evolution of Igneous Rocks.* Princeton Univ. Press.

IRVINE, T.N. and BARAGER, W.R.A., 1971. A Guide to the Chemical Classification of the Common volcanic rocks. *Can. J. Earth Sci.*, *8*, 523-548.

JAHN, B.M., AUVRAY, B., BLAIS, S., CAPDEVILA, R. CORNICHET, J. VIDAL, F. and HAMEURT, J., 1980. Trace element geochemistry and petrogeneis of Finnish greenstone belts. *J. Petrology*, *21*, 201-244.

JENSEN, L.S., 1976. A new cation plot for classifying sub-alkalic volcanic rocks *Ontario Division of Mines, Misc. Paper.* 66 pp.

JOHNSON, H.D., 1978. Shallow siliciclastic seas, 207-258. *In: Reading, G.E. (Ed), Sedimentary Environments and Facies.* Blackwell, London.

KAY, R., HUBBARD, N.J. and GAST, P.W., 1970. Chemical characteristics and origin of oceanic ridge basalts. *J. Geophys. Res.*, *75*, 1585-1613.

KLEIN, G. DE V., 1971. A sedimentary model for determining paleotidal range. *Bull. geol. Soc. A.*, *82*, 2585-2592.

KLEIN, G. DE V., 1977a. *Clastic Tidal Facies.* Cepco, Champaign, Illinois. 149 pp.

KLEIN, G. DE V., 1977b. Tidal circulation model for deposition of clastic sediment in epeiric and mioclinal shelf seas. *Sedim. Geol.*, *18*, 1-12.

LAJOIE, J., 1979. Volcaniclastic rocks, 191-200. *In: Walker, R.G. (Ed). Facies Models.* Geosci. Can. Reprint Series, 1.

LEAKE, B.E., 1968. A catalogue of analyzed calciferous and subcalciferous amphiboles together with their nomenclature and associated mineral. *Geol. Soc. Am. Spec. Paper 98.*

LE MAITRE, R.W., 1976. A new approach to the classification of Igneous rocks using the basalt-andesite-dacite suite as an example. *Contr. Miner. Petrol., 56,* 191-203.

LOWE, D.R., 1972. Implications of three submarine mass-movement deposits, Cretaceous, Sacremento Valley, California. *J. sedim. Petrol., 42,* 89-101.

LOWE, D.R., 1979. Sediment Gravity Flows: Their Classification and some problems of application to natural flows and deposits. *Soc. Econ. Paleontologists and Mineralogists, Spec. Pub. 27,* 75-88.

LOWE, D.R., 1982. Sediment gravity flows: II. Depositional models with special reference to the deposits of high-density turbidity cements. *J. sedim. Petrol., 52,* 279-297.

MACKENZIE, W.S., DONALDSON, C.H. and GUILDFORD, C., 1982. Atlas of Igneous Rocks and their Textures. Longman, London. 148 pp.

MARTIN, A., NISBET, E.G. and BICKLE, M.J., 1980. Archaean stromatolites of the Belingwe Greenstone Belt, Zimbabwe (Rhodesia). *Precam. Res., 13,* 337-362.

MASON, T.R. and VON BRUNN, V., 1977. 3 Gyr-old stromatolites from South Africa. *Nature, 266,* 47-49.

MATTHEWS, P.E., 1959. The metamorphism and tectonics of the Pre-Cape formations in the post-Ntingwe thrust belt, S.W. Zululand, Natal. *Trans. geol. Soc. S. Afr., 62,* 258-322.

MATTHEWS, P.E.,1967. The Pre-Karoo formations of the White Mfolozi Inlier, N. Natal. *Trans. geol. Soc. S. Afr., 70,* 39-64.

MATTHEWS, P.E., 1979. Unpublished mapping of the Nkandla district. Univ. Natal, Durban.

McKEE, E.D., 1966. Experiments on ripple lamination, 66-83. *In: Middleton, G.V. (Ed). Primary Sedimentary Structures and their Hydrodynamic Interpretation. Soc. Econ. Paleontologists and Mineralogists Spec. Pub., 12.*

MIALL, A.D., 1978. Lithofacies types and vertical profile models in braided river deposits: a summary, 597-604. *In: Miall, A.D. (Ed) Fluvial Sedimentology. Can. Soc. Petrol. Geol., Calgary.*

MIDDLETON, G.V. and HAMPTON, M.A., 1973. Sediment gravity flows: mechanics of flow and deposition, in Turbidites and deep water sedimentation. *Soc. Econ. Paleontologists and Mineralogists, Pacific Sect. Short Course Lecture Notes.*

MIDDLETON, G.V. and HAMPTON, M.A., 1976. Subaqueous sediment transport and deposition by sediment gravity flows, 197-218. *In: Stanley, D.J. and Swift, D.J.P., (Eds), Marine Sediment Transport and Environmental Management.* John Wiley, New York.

MIYASHIRO, A., 1973. *Metamorphism and Metamorphic Belts,* Allen and Unwin, London. 440 pp.

MIYASHIRO, A. and SHIDO, F., 1975. Tholeiitic and calc-alkaline series in relation to the behaviors of titanium, vanadium, chromium and nickel. *Am. J. Sc., 275,* 265-277.

MOTTL, M.J. and HOLLAND, H.D., 1978. Chemical exchange during hydrothermal alteration of basalt by sea-water - I. Experimental results for major and minor components of seawater. *Geochim. cosmochim. Acta, 42,* 1103-1115.

MUDGE, M.R., 1968. Depth control of some concordant intrusions. *Bull. Geol. Am. 79,* 315-331.

NESBITT, R.W., SUN, S.-S. and PAVES, A.C., 1979. Komatiites: geochemistry and genesis. *Can. Mineral., 17,* 155-186.

NORRISH, K. and HUTTON, J.T., 1969. An accurate X-ray spectrographic method for the analysis of a wide range of geological samples. *Geochim. cosmochim. Acta., 33,* 431-453.

O'HARA, M.J., 1968. The bearing of phase equilibria studies in synthetic and natural systems on the origin and evolution of basic and ultrabasic rocks. *Earth-sc. Rev., 4,* 69-133.

O'HARA, M.J., 1973. Non-primary magmas and dubious mantle plume beneath Iceland. *Nature, 243,* 507-508.

PARK, W.C. and SCHOT, E.H., 1968. Stylolites: their nature and origin. *J. sedim. Petrol., 38,* 175-191.

PEARCE, J.A. and CANN, J.R., 1973. Tectonic setting of basic volcanic rocks determined using trace element analysis. *Earth Planet Sc. Lett., 19,* 290-300.

PEARCE, T.H., 1968. A contribution to the theory of variation diagrams. *Contr. Miner. Petrol., 19,* 142-157.

PEARCE, T.H., 1970. Chemical variations in the Palisades sill. *J. Petrology, 11,* 15-32.

PEARCE, T.H., GORMAN, B.T. and BIRKET, T.L., 1977. The relationship between major element chemistry and tectonic environment of basic and intermediate volcanic rocks. *Earth Planet. Sc. Lett., 36,* 121-132.

PETERMAN, Z.E., 1979. Geochronology and the Archaean of the United States. *Econ. Geol., 74,* 1544-1562.

PHILPOTTS, A.R., 1976. Silicate liquid immiscibility, its probable extent and petrogenetic significance. *Am. J. Sc., 276,* 1147-1177.

PHILPOTTS, A.R., 1982. Compositions of immiscible liquids in volcanic rocks. *Contr. Miner. Petrol., 80,* 201-206.

PHILPOTTS, A.R. and DOYLE, C.D., 1983. Effect of magma oxidation state on the extent of silicate liquid immiscibility in a tholeiitic basalt. *Am. J. Sci., 283,* 967-986.

PICARD, M.D. and HIGH, L.R., Jr., 1973. Sedimentary structures of ephemeral streams. *Developments in Sedimentrology, 17,* 223. Elsevier, Amsterdam.

PYKE, D.R., NALDRETT, A.J. and ECKSTRAND, O.R., 1973. Archaean ultramafic flows in Munro Township, Ontario. *Bull. geo. Soc. Am., 84,* 955-978.

REINECK, H.-E. and SINGH, I.D., 1980. Depositional Seidmentary Environments (2nd Ed). Springer-Verlag, Berlin. 549 pp.

ROBERTS, J.L., 1970. The intrusion of magma into brittle rocks, 287-338. *In: Newall, S. and Rant, N. (Eds). Mechanism of Igneous Intrusion.* Gallery Press, Liverpool.

ROEDDER, E., 1979. Silicate liquid immiscibility in magmas, 15-57. *In: Yoder, H.S. (Ed). The Evolution of the Igneous Rocks.* Princeton Univ. Press.

RUPKE, N.A., 1978. Deep clastic seas, 372-415. *In: Reading, H.G. (Ed). Sedimentary Environments and Facies.*

SELLEY, R.C., 1970. *Ancient Sedimentary Environments.* Chapman and Hall, London. 237 pp.

SEYFRIED, W.E., Jr. and MOTTL, M.J., 1982. Hydrothermal alteration of basalt by seawater and under sea water dominated conditions. *Geochim. Cosmochim. Acta, 46,* 985-1002.

SMITH, H.S. and ERLANK, A.J., 1982. Geochemistry and petrogenesis of komatiites from the Barberton greenstone belt, South Africa, 347-397. *In: Arndt, N.T. and Nisbet, E.G. (Eds). Komatiites.* Allen and Unwin, London. 525 pp.

SMITH, N.D. , 1971. Transverse bars and braiding in the Lower Platte River, Nebraska. *Bull. geol. Soc. Am., 82,* 3407-3420.

SOUTH AFRICAN COMMITTEE FOR STRATIGRAPHY (SACS), 1980. Stratigraphy of South Africa. Part 1. (Comp. L.E. Kent). Lithostratigraphy of the Republic of South Africa, South West Africa/Namibia and the Republics of Bophuthatswana, Transkei and Venda. *Handb. Geol. Surv. S. Afr., 8.*

STICE, G.D., 1968. Petrography of Manua Islands, Somoa. *Contr. Miner. Petrol., 19,* 343-357.

TAINTON, S., 1977. An interpretation of the geology of the Mhlatuzi gorge, Nkandla-Mtonjaneni district, Zululand. Unpub. B.Sc. Hons thesis, Univ. Natal, Pietermaritzburg. 157 pp.

THOMPSON, R.N., ESSON, J. and DUNHAM, A.C., 1972. Major element chemical variation in the Eocene lavas of the Isle of Skye, Scotland. *J. Petrology, 13,* 219-252.

TUNBRIDGE, I.P., 1981. Sandy high-energy flood sedimentation - some criteria for recognition with an example from the Devonian of S.W. England. *Sedim. Geol., 28*, 79-95.

TUNNINGTON, D.P., 1981. The geology of the Central Nsuze Syncline. Unpub. B.Sc. Hons thesis, Univ. Natal, Pietermaritzburg. 58 pp.

TURNER, B.R., 1980. Palaeohydraulics of an Upper Triassic braided river system in the main Karoo Basin, South Africa. *Trans. geol. Soc. S. Afr., 83*, 425-431.

VILJOEN, M.J., VILJOEN, R.P. and PEARTON, T.N., 1982. The nature and distribution of Archaean komatiite volcanics in South Africa, 53-80. *In: Arndt, N.T. and Nisbet, E.D. (Eds), Komatiites.* Allen and Unwin, London. 525 pp.

VILJOEN, M.J., VILJOEN, R.P., SMITH, H.S. and ERLANK, A.J., 1983. Geological, textural and geochemical features of komatiitic flows from the Komati Formation, 1-20. *In: Anhaeusser, C.R. (Ed). Contributions to the geology of the Barberton Mountain Land.* Geol. soc. S. Afr. Spec. Pub. 9.

VON BRUNN, V., 1974. Tidalites of the Pongola Supergroup (Early Precambrian) in the Swart-Mfolozi area, Northern Natal, 107-122. *In: Kröner, A., (Ed), Contributions to the Precambrian geology of Southern Africa.* Precambrian Research Unit, U.C.T. Bull. 15.

VON BRUNN, V. and HOBDAY, D.K., 1976. Early precambrian tidal sedimentation in the Pongola Supergroup of South Africa. *J. sedim. Petrol., 46*, 670-679.

WALKER, R.G., 1969. Geometrical analysis of ripple-drift cross-lamination. *Can. J. Earth Sci., 6*, 383-391.

WALKER, R.G., 1978. Deep-water sandstone facies and ancient submarine facies: models for exploration for stratigraphic traps. *Amer. Assoc. Petrol. Geol., 62*, 932-966.

WALTER, M.R., 1977. Interpreting stromatolites. *Am. Sci., 65*, 563-571.

WATCHORN, M.B., 1978. Sedimentology of the Mozaan Group in the southeastern Transvaal and northern Natal. Unpub. M.Sc. thesis, Univ. Natal, Pietermaritzburg. 111 pp.

WATCHORN, M.B., 1980. A Reappraisal of the geology of the western Mozaan basin. *Trans. geol. Soc. Sc. Afr., 83,* 135-139.

WATCHORN, M.B. and ARMSTRONG, N.V., 1980. Contemporaneous sedimentation and volcanism at the base of the early Precambrian Nsuze Group, South Africa. *Trans. geol. Soc. S. Afr., 83,*

WEIMER, R.J., 1976. Deltaic and shallow marine sandstones: sedimentation, tectonics and petroleum occurrences. *A.A.P.G. Continuing Education Course Note Series No. 2.*

WILSON, A.H., 1982. The Geology of The Great "Dyke", Zimbabwe: the ultramafic rocks. *J. Petrology, 23,* 240-292.

WILSON, A.H., VERSFELD, J.A. and HUNTER, D.R. (in prep.). The petrology and geochemistry of spinifex-bearing komatiites and associated basalts of the Archaean Nondweni greenstone belt, South Africa.

WILSON, J.F., BICKLE, M.T., HAWKESWORTH, R.J., MARTIN, A., NISBET, E.G. and ORPEN, J.L., 1978. The granite-greenstone terrains of the Rhodesian Archaean craton. *Nature, 271,* 23-27.

WINCHESTER, J.A. and FLOYD, P.A., 1976. Geochemical magma type discrimination: application to altered and metamorphosed basic igneous rocks. *Earth Planet. Sc. Lett., 28,* 459-469.

WINCHESTER, J.A. and FLOYD, P.A. Geochemical discrimination of different magma series and their differentation products using immobile elements. *Chem. Geol., 20,* 325-343.

WINDLEY, B.F., 1977. *The Evolving Continents.* John Wiley, New York. 385 pp.

WINKLER, H.G.F., 1974. *Petrogenesis of metamorphic rocks.* (3rd Ed). Springer-Verlag, Berlin. 316 pp.

WUNDERLICH, F., 1970b. Schichtbänke, 48-55. *In: Reineck, H.-E. (Ed). Das Watt, Ablagerungs-und Lebensnaum.* Kramor, Frankfurt.

APPENDIX 1

Thin section descriptions

A. Nsuze Group Volcanics

B. Nsuze Group Sediments

C. Ultramafic Rocks

D. Hlagothi Complex

E. Pre-tectonic Dykes

In this appendix entries such as tremolite(50), plagioclase(10) etc. indicate the estimated mean content of the mineral in volume percent.

* indicates samples (or duplicates of samples) analysed.

NSUZE GROUP LAVAS AND PYROCLASTS

Ndikwe Formation

SAMPLE NO.	LOCALITY	ROCK-TYPE	TEXTURE	PHENOCRYSTS	CONSTITUENT MATRIX MINERALS	AMYGDALES	COMMENTS
*BG128	Ndikwe Formation Welendhlovu Valley	Andesite	Porphyritic, glomero-porphyritic with plagioclase phenocrysts set in fine-grained felspar, biotite, amphibole matrix.	Plagioclase	Plagioclase Biotite Tremolite/ Actinolite Epidote	Quartz	Quartz amygdales recrystallized. Untwinned albite in matrix (?).
*BG129	As above	Andesite	As above	As above	As above	Quartz, biotite	Phenocrysts sparser, otherwise identical to BG128.
*BG130	As above	Andesite	Very fine-grained, lacks phenocrysts.	Absent	Plagioclase Biotite Epidote/zoisite	Absent	Identical to matrix in BG129.
*BG131	As above	Welded dacitic tuff(?)	Consists of flattened irregular fragments with porphyritic zones.	Plagioclase Quartz	Plagioclase Quartz Epidote Saussuritized groundmass Biotite Chlorite	Absent	Partially reworked quartz crystals abundant. Chloritic zones define lapilli boundaries.
BG142	Ndikwe Formation, Mdlelanga Valley south of Vuleka.	Basalt	Fine- to medium-grained, short fibrous amphibole intergrown with plagioclase laths.	Absent	Actinolite Plagioclase Epidote	Quartz	
*BG147	Ndikwe lavas, Mankane River.	Basaltic andesite	Fine-grained intergrowth of chlorite and untwinned plagioclase.	Absent	Chlorite Actinolite Plagioclase Carbonate Epidote	Absent	Local calcitization. Rarely preserved albite twinning in plagioclase crystals.
BG148	As above	Basalt	Fine-grained intergrowth of amphibole, chlorite and plagioclase.	Plagioclase	Tremolite/actinolite Plagioclase Chlorite	Quartz	Local silicification.
*BG152	As above	Basaltic andesite	Fine-grained chlorite, plagioclase epidote intergrowth.	Absent	Chlorite Plagioclase Epidote	Chlorite	
BG266 and BG267	Ndikwe Formation, Malunga River south of Hlagothi Mountain	Basaltic-andesite	Very fine-grained, consists of felted mass of chlorite and tremolite with patches of plagioclase.	Chlorite after possible mafic crystals.	Chlorite Quartz Plagioclase Tremolite	Quartz	Locally carbonitized and silicified.

SAMPLE NO.	LOCALITY	ROCK-TYPE	TEXTURE	PHENOCRYSTS	CONSTITUENT MATRIX MINERALS	AMYGDALES	COMMENTS
BG19	Pyroclastic unit. Tuffs west of Ndikwe Store.	Lapilli tuff.	Extremely heterogeneous rock composed of crystalline and aphyric fragments in very fine-grained matrix. Has banding as a result of either flow or compaction.		Lapilli: 1. very fine-grained felted masses of tremolite/actinolite. 2. fine-grained inter-growths of chlorite, amphibole and plagioclase. Groundmass: Actinolite, chlorite, Plagioclase. Locally sericitic. Epidote/zoisite/clinozoisite as accessory minerals.		Abundant partially resorbed quartz crystals.
*BG238	Pyroclastic unit, south slope of Hlagothi Mountain.	Crystal tuff.	Abundant quartz and feldspar and ash fragments set in very fine-grained matrix.		Quartz } crystals (70% Plagioclase} of rock) Lapilli: chlorite and amphibole and plagioclase Groundmass: intergrown amphibole, chlorite and saussuritic material.		Quartz and plagioclase crystals 0.5 - 1.0 mm in diameter. Resorbed boundaries. Strained.
Qudeni Formation							
*BG156	Lava flows, north limb Gem Syncline, Nsuze River Valley.	Andesite	Recrystallized. Fine-grained Intergrown chlorite plagioclase with local carbonitization.		Plagioclase Chlorite Muscovite Magnetite Sphene Epidote	Calcite	
*BG157	As above	Basaltic andesite	Recrystallized except for local felted masses of short plagioclase laths.	Local angular con-centration of chlorite may represent mafic pheno-crysts.	Plagioclase Chlorite Actinolite Epidote Leucoxene Magnetite Sphene	Calcite Quartz	Abundant sphene. Local calcitization. Rare twinned plagioclase has composition An_{32}.
*BG159	As above	Andesite	As for BG156	-	As for BG156	Calcite Quartz	Abundant ragged magnetite grains.
*BG183	Upper flow. North limb of Central Nsuze Syncline, Nsuze River Valley.	Andesite	Remnants of plagioclase phenocrysts set in an allotriomorphic granular fine-grained groundmass of Plagioclase and biotite.	Plagioclase	Plagioclase Biotite Quartz Epidote Muscovite Leucoxene	Epidote	Locally carbonitized.
BG184	As above	Andesite	As above	Plagioclase	Plagioclase Biotite Epidote Actinolite Muscovite Quartz Sphene	Quartz	Texturally-identical to BG183, but contains more epidote.

B. NSUZE GROUP SEDIMENTS

SAMPLE NO. AND ROCK-TYPE	LOCALITY	MINERALOGY	TEXTURE	COMMENT
BG110 Ferruginous argillite	Upper part of debris flow sequence due east of Vuleka.	Quartz(70) Magnetite(30) Haematite(tr)	Alternating layers of opaques and cherty quartz 1 - 3 mm thick. Alteration of magnetite to haematite along margins of layers.	Very small local concentrations of epidote.
BG144 Meta calcarenite	Basal unit of Mdlelanga Formation south of Vuleka.	Quartz(40) as clasts Zoisite(30)* Calcite(25) Epidote(30)* Plagioclase(5)	Irregularly banded, immature poorly sorted arenite clasts and grains angular to subangular, 1 - 3 mm in diameter. Recrystallized quartz grains have overgrowths, but primary shape is preserved. Groundmass is dominantly epidote/zoisite. Carbonate as lenticular patches.	* Zoisite and epidote dominant in different parts of specimen. Proximal sands lacking in composite grains.
BG150 Greywacke	Matrix of debris flows south of Vuleka in upper Mdlelanga Formation.	Clasts-quartz Groundmass-quartz, Phengitic mica, Chlorite, Actinolite (Epidote) (Magnetite)	Poorly-sorted, matrix-supported sandstone. Clasts are generally single grains or recrystallized. Rare composite grains. Lenticular clasts composed of chlorite, tremolite and sericite. Very fine-grained groundmass.	Rounding of grains suggests resedimentation.
BG166 Pyritic argillite	Argillite unit below debris flow sequence south of Vuleka.	Quartz(60) Chlorite(30) Actinolite(tr) Epidote(tr) Pyrite($\sim$ 5) Garnet($\sim$ 1) Magnetite Muscovite(tr)	Very fine-grained, wholly recrystallized intergrowth of quartz and chlorite. Ubiquitous euhedral pyrite crystals. Garnet as 1 - 2 mm subhedral, poikiloblastic crystals.	Garnet is probably spessartine. Quartz is strained.

SAMPLE NO. AND ROCK-TYPE	LOCALITY	MINERALOGY	TEXTURE	COMMENT
BG189C Quartz arenite	Vutshini Formation, north limb, Central Nsuze Syncline.	Quartz(90) Mica Chlorite Epidote Magnetite/ haematite	Medium-grained, well-sorted and rounded quartz grains with minor interstitial material.	Quartz grains are strained but rarely recrystallized and lack overgrowths. Extremely well rounded. No composite grains.
BG200 Conglomerate	Basal unit of Ndikwe Formation at Nkungamathe	Quartz(80) Feldspar(10) Muscovite Detrital sphene and zircon	Clasts, up to 5 cm in diameter, (in this section < 4 mm) set in medium-grained immature matrix.	Clasts recrystallized, rarely composite quartz-feldspar masses (tonalitic).
BG285A Carbonate	Ndikwe Formation, east of Hlagothi Mountain in Nsuze River Valley.	Calcite(60) Quartz(20) Chlorite(10) Sericite Epidote Magnetite	Recrystallized calcite-quartz-chlorite in fine-grained mozaic. Fine irregular lamination defined by variations in quartz content.	Crinkle laminated carbonate from clast in debris flow unit. Contains rare angular plagioclase crystals.
BG185B Argillite	As above	Quartz(50) Calcite(20) Chlorite(10-20) Magnetite(10-20) Epidote	Finely laminated, recrystallized rock. Alternating magnetite- and chlorite-rich laminae. Calcite in lenticular stringers.	Magnetite is very fine-grained, irregular grains - possibly some graphite present.

C. ULTRAMAFIC ROCKS

SAMPLE NO.	LOCALITY	ROCK-TYPE	TEXTURE	MINERALOGY		RELICT IGNEOUS TEXTURE	COMMENTS
*BG23	Sill intrusive into base of Qudeni Formation, north limb Gem Syncline, Nsuze River Valley.	Meta ultramafic	Equant crystals of colourless amphibole 1-3 mm in diameter set in groundmass of fine ragged amphibole needles and flakes of chlorite.	Tremolite(70)	Epidote	Larger amphibole crystals may be pseudomorphic after pyroxene.	BG158 is a duplicate sample of BG23.
BG27	Same intrusion as above, 2 km farther west in Ndikwe River Valley.	Meta ultramafic	As above, patches of serpentine.	Tremolite(60) Chlorite(30) Antigorite(10)	Epidote Magnetite Quartz	Opaque minerals define vague banded texture (flow banding?)	Local concentrations of magnetite
*BG91	Wedge-shaped body of serpentinite due west of Ndikwe Store.	Serpentinite	Long fibrous amphibole needles set in fine-grained talc, chlorite serpentine groundmass.	Tremolite(30) Chlorite(30) Talc(20) Antigorite(15)	Magnetite (Quartz?)	None	Duplicate of BG175
*BG112	Central part of ultramafic body in core of anticline, at confluence of Mdlelanga and Welendhlovu Rivers.	Meta ultramafic	Coarse-grained, elongate tremolite crystals with acicular terminations set in groundmass of ragged chlorite. Local concentrations of chlorite define tectonic fabric.	Tremolite(60) Chlorite(30) Antigorite(10)	Magnetite (Sphene?)	None	Sample adjacent to amygdaloidal zone (duplicate of BG124). Ubiquitous anhedra of magnetite.
*B116	Dyke within Nsuze sediments 200 m north of BG112.	Meta ultramafic	Fractured and broken amphibole crystals up to 3 mm long set in fine felted mass of amphibole, chlorite and antigorite.	Tremolite(50) Chlorite(30) Antigorite(20)	Leucoxene Epidote	None	Chlorite and antigorite concentrated in fractures/ cleavage.
*BG173	Same locality as BG91 above.	Serpentinite	Fine-grained ragged intergrowth of talc, magnetite, antigorite, chlorite.	Talc(50) Magnetite(30) Chlorite(10) Antigorite(10)	Tremolite Magnetite Quartz	None	Tectonic fabric strongly developed.
*BG121	Dyke along northern contact of Mdlelanga sediments, south of BG112.	Meta ultramafic	As above, except antigorite absent.	Tremolite(60) Chlorite(40)	Magnetite	None	Ubiquitous anhedra of magnetite and fine "dusting" of opaques suggests originally medium-grained granular texture.
*BG173	Same locality as BG91 above.	Serpentinite	Fine-grained, ragged intergrowth of talc, magnetite, antigorite, chlorite.	Talc(50) Magnetite(30) Chlorite(10) Antigorite(10)	Tremolite Magnetite Quartz	None	Tectonic fabric strongly developed.

D. HLAGOTHI COMPLEX: Nsongeni (lower) sheets.

SAMPLE NO.	LOCALITY AND STRATIGRAPHIC POSITION	ROCK-TYPE	TEXTURE	CONSTITUENT MINERALS MAJOR	ACCESSORY	COMMENTS
BG209	Upper Nsongeni River, base of lowest sill.	Meta-peridotite	Randomly orientated sheaves of amphibole set in fine, xenocrystic chlorite and talc groundmass. No relict texture.	Tremolite(70) Chlorite(20) Talc(10)	Magnetite	Colourless amphibole and very pale green chlorite. No primary mineralogy. Faint tectonic fabric.
*BG212	5 m above BG209	Meta-peridotite	Fine tremolite and antigorite replace euhedral olivine grains defined by magnetite. Interstitial chlorite.	Tremolite(40) Chlorite(40) Serpentine(15)	Talc Magnetite	Olivine and pyroxene cumulate?
*BG216	Lower sill, Nsongeni River. Above BG212.	Meta-peridotite	Coarse amphibole grains prismatic to ragged. Coarse chlorite intergrowth.	Tremolite(75) Chlorite(25)		No relict texture. No magnetite or chromite.
BG217	Dyke cutting lower sill, but terminated by overlying gabbro sheet. Nsongeni River.	Olivine gabbronorite.	Medium-grained, granular. Radial intergrowths between zoned clinopyroxene and plagioclase.	Plagioclase(40) Augite(25) Olivine(20) Orthopyroxene(10)	Biotite Magnetite Epidote	Plagioclase is An_{54}. Incipient serpentinization and chloritization.
BG218	Chill zone of dyke of BG217.	Black, fine-grained rock with rare olivine phenocrysts, appears basaltic.	Skeletal olivines and plagioclase set in microcrystalline groundmass (devitrified?).	Olivine(10) Plagioclase(10) Groundmass(80) Orthopyroxene(?)	Magnetite Chromite(?)	Olivine brown, euhedra, skeletal. Plagioclase-acicular, skeletal, An_{45}(?)
*BG222	Nsongeni River, second Gabbro Sheet.	Meta-gabbro	Medium-grained, equigranular to intergranular relict igneous texture.	Amphibole(70) Plagioclase(20) Epidote(5)	Saussurite Leucoxene Magnetite	Micrographic intergrowths between plagioclase and quartz. Large leucoxene patches (5 mm).
*BG223	Contact zone between Gabbro and pyroxene, below BG222.	Meta-gabbro (?)	Medium-grained, equigranular relict texture.	Tremolite} Pargasite} (65) Chlorite(25) Epidote(5)	Magnetite Leucoxene	

D. HLAGOTHI COMPLEX: Nsongeni (lower) sheets continued

SAMPLE NO.	LOCALITY AND STRATIGRAPHIC POSITION	ROCK-TYPE	TEXTURE	CONSTITUENT MINERALS MAJOR	ACCESSORY	COMMENTS
*BG224	10 m below BG223 in meta-pyroxenite unit, Nsongeni River.	Metapyroxenite.	Medium-grained, equi-granular relict texture, euhedra and subhedra closely packed, cumulate.	Tremolite(60) Chlorite(40)	Chromite(?)	Tremolite contains zones of greenish-brown amphibole and is pseudomorphic after pyroxene.
*BG228	Lower peridotite unit, Nsongeni River.	Metaperidotite	Medium-grained relict texture, euhedral olivine (?) replaced by talc-antigorite. Chlorite and tremolite interstitial.	Tremolite(50) Talc(20) Chlorite(25) Antigorite(10)	Magnetite	Relict mineral shapes suggest ~ 60% olivine, 40% pyroxene cumulate rock.

D. HLAGOTHI COMPLEX: Hlagothi Mountain (main upper) sheets

SAMPLE NO.	LOCALITY AND STRATIGRAPHIC POSITION	ROCK-TYPE	TEXTURE	CONSTITUENT MINERALS MAJOR	ACCESSORY	COMMENTS
*BG229	Bottom of pyroxenite unit, north slope Hlagothi Mountain.	Metaperidotite	Bimodal grain size - large square or octagonal crystals (6 mm) amphibole surrounded by fine-grained groundmass.	Amphibole(60) Chlorite(30) Talc(10)	Leucoxene Magnetite (Quartz ?)	Amphibole is pale green tremolite/actinolite. Replaces original orthopyroxene or olivine grains. May represent cumulate.
*BG235	Above BG229, 25 m from base of sheet.	Pyroxenite	Closely packed subhedra and euhedra of pyroxene. Orthocumulate.	Hypersthene(50) Augite(35) Plagioclase(10)	Magnetite	Serpentinization up to 20% of rock. Augite is cumulate and post-cumulate in reaction relationship with hypersthene.
*BG236	25 m above BG225	Pyroxenite	Equigranular, closely-packed euhedra and subhedra of both pyroxenes. Also large orthocrysts of augite.	Hypersthene(50) Augite(40) Plagioclase(40)	Magnetite	Orthopyroxene predates augite. Cumulate rock.
*BG237	Upper part of Hlagothi Mountain, 50 m above BG236.	Metagabbro	Elongate or lath-like crystals of amphibole set in finer-grained matrix.	Tremolite(40) Epidote/Zoisite(40) Chlorite(10) Plagioclase(< 10)	Leucoxene	Large zoned epidotes and fine granular epidote-zoisite-white mica aggregates.
*BG230	West slope of Hlagothi Mountain. Approximately same level as BG237.	Metagabbro.	As above	Tremolite(40) Epidote/Zoisite(50) Chlorite (~ 5) Plagioclase(5) Quartz(2)	Leucoxene	Acicular plagioclase crystals, otherwise as for BG237. Single pigeonite core to amphibole lath. Quartz-plagioclase micrographic intergrowth.

SAMPLE NO.	LOCALITY AND STRATIGRAPHIC POSITION	ROCK-TYPE	TEXTURE	CONSTITUENT MINERALS MAJOR	ACCESSORY	COMMENTS
BG231	20 m above BG230	Metagabbro	Elongate or lath-like crystals of amphibole set in finer-grained matrix.	Tremolite(40) Saussurite groundmass(40) Chlorite(5) Plagioclase(5-10) Quartz(2-3)	Leucoxene	Texturally very similar to BG230, but amphibole crystals more slender.
BG275	South slope, Hlagothi Mountain, near top of uppermost gabbro.	Metagabbro	Medium-grained, bimodal with laths up to 3 mm of amphibole set in finer groundmass.	Tremolite(30) Saussurite(35) Epidote(<10) Chlorite(5) Leucoxene(5) (Plagioclase and quartz in rare patches)	Magnetite	Micrographic intergrowths of quartz and plagioclase. Tremolite (?) is pale green and has central zones of chlorite (see BG242 below).
*BG239	Upper marginal sequence of second highest gabbro unit, Nsuze Valley east of Hlagothi Mountain.	Metagabbro	Coarse-grained skeletal crystals set in fine groundmass. Skeletal crystals are amphibole pseudomorphic after pyroxene, contain chlorite cores. Arranged in downwards branching sheaves.	Tremolite(50) Remainder is very fine-grained groundmass. Quartz in amygdales (~5) Epidote-large zoned grains(2) Chlorite(-5a)	Leucoxene Magnetite Biotite	"Skeletal" texture is identical to spinifex texture of extrusive rocks. Amphibole laths up to 20 cm in length. Rounded amygdales and patches of biotite.
*BG242	2 m above BG239	Metagabbro	Finer-grained than BG239, consists of randomly orientated, 20 mm long skeletal crystals set in fine-grained groundmass.	Tremolite(60) Chlorite(10) Quartz(5) Epidote(5) Plagioclase(5) Saussuritic groundmass	Leucoxene Magnetite Sphene Sulphide	Quartz in amygdales. Some relict plagioclase.
BG283	Gabbro 10 m below marginal sequence.	Metagabbro	Medium-grained, inter-granular sub-ophitic relict texture.	Tremolite/ Actinolite(35) Plagioclase } Micrographic Intergrowth} (35) Biotite(3) Epidote(3) Saussuritic groundmass(20)		Plagioclase rarely unrecrystallized, also in micrographic intergrowths.

SAMPLE NO.	LOCALITY AND STRATIGRAPHIC POSITION	ROCK-TYPE	TEXTURE	CONSTITUENT MINERALS MAJOR	ACCESSORY	COMMENTS
BG302	Close to base of upper wehrlite sheet, Hlagothi Mountain.	Wehrlite (feldspathic)	Coarse-grained, equigranular.	Olivine(60) Augite(25) Plagioclase(10) Hypersthene(<5)	Magnetite (Chlorite) (Saussurite)	Euhedral olivines surrounded by anhedral post-cumulate augite. Local alteration.
BG304	Upper wehrlite sheet, Hlagothi Mountain.	Meta-wehrlite	Medium-grained and equigranular, millimetre scale layering defined by olivine and clinopyroxene.	Augite(40) Serpentine(40) (after olivine) Tremolite(8) Magnetite(2) Chlorite(10)		Relict olivine grain shape is euhedral. Microfracturing of pyroxenes post-dates magnetite stringers and alteration of olivines. Cumulate rock.
Wonderdraai Sheet						
BG11	Central part of sheet on east flank of Itala Mountain.	Olivine gabbronorite	Fine-grained. Equigrained except for local poikilitic enclosure of olivine by pyroxenes.	Olivine(30) Hypersthene(35) Augite(25) Plagioclase(10)	Biotite Magnetite Chromite	Partially altered to serpentine, chlorite and epidote. Pyroxenes in reaction relationship with olivine.
BG13	As above	Olivine gabbronorite	As above	As above		Orthopyroxene predates augite, reaction relationship.
BG28	Central part of sheet on southwest bank of Mhlatuze River near Wonderdraai farm.	Olivine gabbronorite	Medium-grained granular. Post-cumulate augite and plagioclase.	Olivine(25) Hypersthene(35) Augite(30) Plagioclase(10)	Biotite Magnetite	Serpentine and chlorite as alteration product locally. Euhedral olivine and orthopyroxene. Reaction of later augite with olivine and orthopyroxene.
*BG193	Upper part of sill, above BG28.	Olivine websterite	Medium-grained, equigranular, locally poikilitic with augite enclosing olivine.	Olivine(30) Hypersthene(45) Augite(20) Plagioclase(<5)	Magnetite	Incipient alteration to antigorite and chlorite. Olivine-euhedral, hypersthene, subhedral, plagioclase and augite interstitial/post-cumulate.
BG194	Central part of sill, below BG28.	Lherzolite	Medium-grained, equigranular.	Augite(40) Olivine(30) Hypserthene(25) Plagioclase (<5)	Magnetite Biotite	Olivine crystals, small and commonly enclosed by pyroxenes with a reaction relationship.

SAMPLE NO.	LOCALITY AND STRATIGRAPHIC POSITION	ROCK-TYPE	TEXTURE	CONSTITUENT MINERALS MAJOR	ACCESSORY	COMMENTS
BG195	Lower part of sill 50 m below BG194.	Lherzolite	Medium-grained, granular.	Augite(50) Olivine (5) Hypersthene(20) Plagioclase(<5)	Biotite Magnetite	Some secondary biotite replacing olivine. Has alteration to serpentine and chlorite.
*BG196	Lowest exposed part of sill, east bank of Mhlatuze River on farm Wonderdraai.	Lherzolite	Medium-grained, granular.	Olivine(55) Augite(25) Hypersthene(15) Plagioclase(~5)	Magnetite	Local veining of serpentine.

SAMPLE NO.	LOCALITY AND STRATIGRAPHIC POSITION	ROCK-TYPE	TEXTURE	CONSTITUENT MINERALS MAJOR	ACCESSORY	COMMENTS
BG17	Mbizwe River, small domical outcrop at base of Dwyka Formation	Syenite(?)	Coarse-grained, equi-granular, altered rock.	Orthoclase(60) Saussuritic patches (after plagioclase)(20) Riebeckite(15) Augite(3) Opaques(2)	Haematite	Weathered/altered. High content of opaque minerals.
BG66	Gozweni River, sill below Wonderdraai sheet of the Hlagothi Complex	Monzonite(?) (metamorphosed)	Coarse-grained, inter-granular, equigranular.	Plagioclase(60) Green Hornblende(30) Orthoclase(5) Quartz(3) Biotite(2)	Apatite Leucoxenes Opaques Epidote	Plagioclase extensively saussuritized. Highly pleo-chroic amphibole has a dark green rim.
*BG84	Sill(?) intrusive into Ndikwe Pyroclastics west of Ndikwe Store.	Metagabbro	Coarse-grained to very coarse-grained, granular. Elongate laths of amphibole form interlocking framework around smaller plagioclase crystals.	Plagioclase(50) Amphibole(50)	Epidote Leucoxene	Two generations of amphibole, both very pale green to colour less but the earlier has higher relief. (Paragasite replaced by tremolite?)
*BG125	Conformable intrusion immediately above base of Vutshini Formation in the Mankane River Valley.	Metagabbro	Medium-grained, granular.	Tremolite/ Actinolite(50) "Saussurite"(30) Epidote(5) Zoisite(Tr) Chlorite(5) Quartz(5)	Leucoxene	Irregular laths of amphibole surrounded by saussuritic "groundmass".
*BG126	Dyke identical to BG125 at confluence of Mdlelanga and Welendhlovu Rivers.	Metagabbro	As above	As above	As above	
*BG141	Narrow dyke in lavas, Ndikwe Formation, Welendhlovu River Valley.	Metagabbro(?)	Intergranular with large phenocrysts(tremolite after pyroxene?) set in very fine-grained plagioclase rich ground-mass.	Plagioclase(60) Tremolite(35) Chlorite(Tr) Quartz(2) Orthoclase(2)	Epidote Opaques Leucoxene	Although cross-cutting dykelets may be andesitic and of Nsuze
*BG164	Dyke west of Vuleka, cuts debris flow sequence in Mdlelanga River Valley.	Metagabbro	Fine-grained, granular.	Chlorite(45) Plagioclase(50) Epidote(5)	Calcite Ilmeno-magnetite Apatite	No relict igneous textures.

SAMPLE NO.	LOCALITY AND STRATIGRAPHIC POSITION	ROCK-TYPE	TEXTURE	CONSTITUENT MINERALS MAJOR	ACCESSORY	COMMENTS
BG187	Intrusion at confluence of Nsuze and Mankane Rivers.	Metagabbro/ monzonite	Sub-ophitic relict igneous texture.	Green Hornblende(30) Plagioclase(50) Orthoclase(10) Quartz(10)	Opaque, leucoxene	Very similar to BG66, BG208. Plagioclase almost entirely saussuritized. Trellis texture in magnetite crystals.
BG188	Conformable intrusion in Ndikwe Formation lavas, Mankane River Valley.	Carbonatized albitite.	Equigranular plagioclase laths cut across by carbonated patches.	Plagioclase(60) Calcite(35) Chlorite(5)	Magnetite	Glide twinning in plagioclase which is otherwise unaltered except where large "blebs" of carbonate occur.
BG198	Nkungumathe (Mhlatuze River Valley)	Tonalite	Coarse-grained, seriate granular, large elongate quartz grains (deformed) and fractured plagioclase crystals up to 4 mm long. Small microcline and biotite crystals.	Plagioclase(60) Quartz(26) Microcline(10) Biotite(3)	Chlorite Epidote Apatite	Biotite is chloritized. Local saussuritization of plagioclase.
*BG208	Sill at base of Hlagothi Complex in Nsongeni Valley.	Metagabbro/monzonite	Sub-ophitic.	Plagioclase(30) Green Hornblende/ Tremolite/ actinolite (50) Orthoclase(20) Quartz(10)	Epidote Leucoxene Magnetite	Cf. BG187, BG66

APPENDIX 2

Schmidt net plots for selected minor folds in the Nsuze Group which are considered representative of the F_2 folding event.

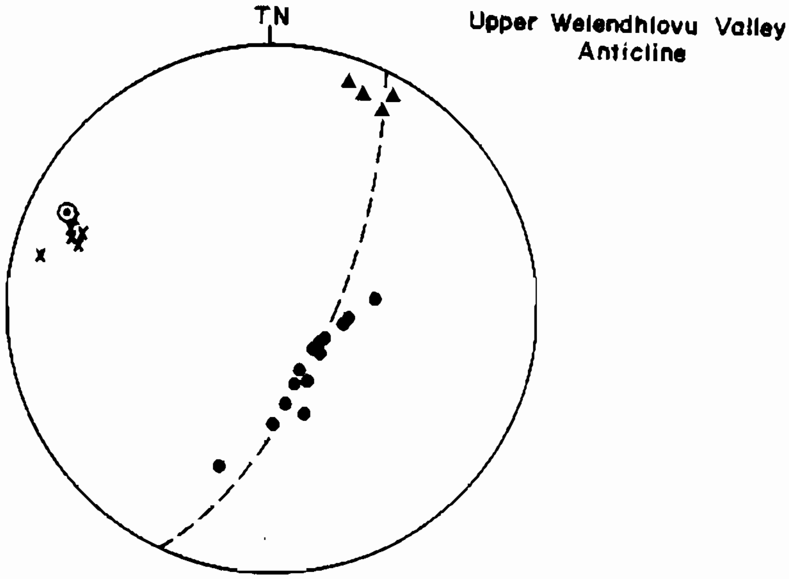

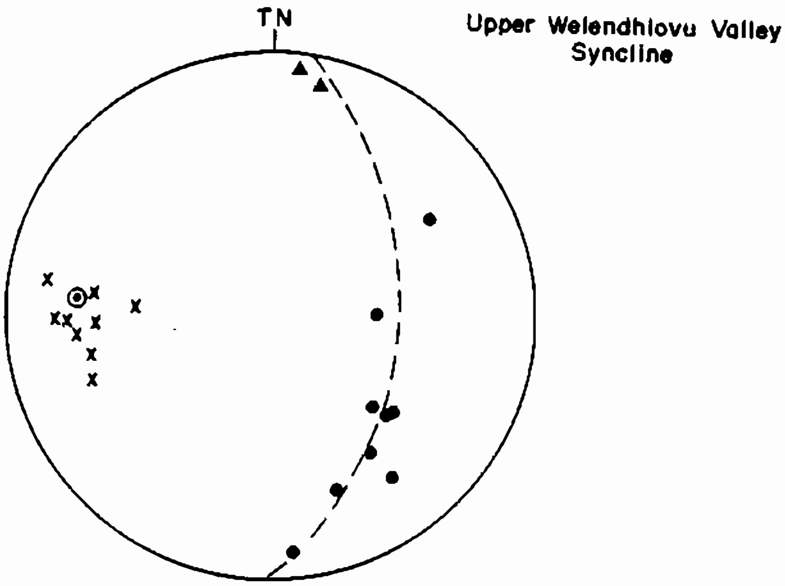

A2.1 Schmidt net plots of antiform and syncline in the upper Welendhlovu Valley. Poles to bedding (dots), S_2 cleavage (triangles) and L_2 lineations (crosses) indicated. Fold axes indicated by dot within circle.

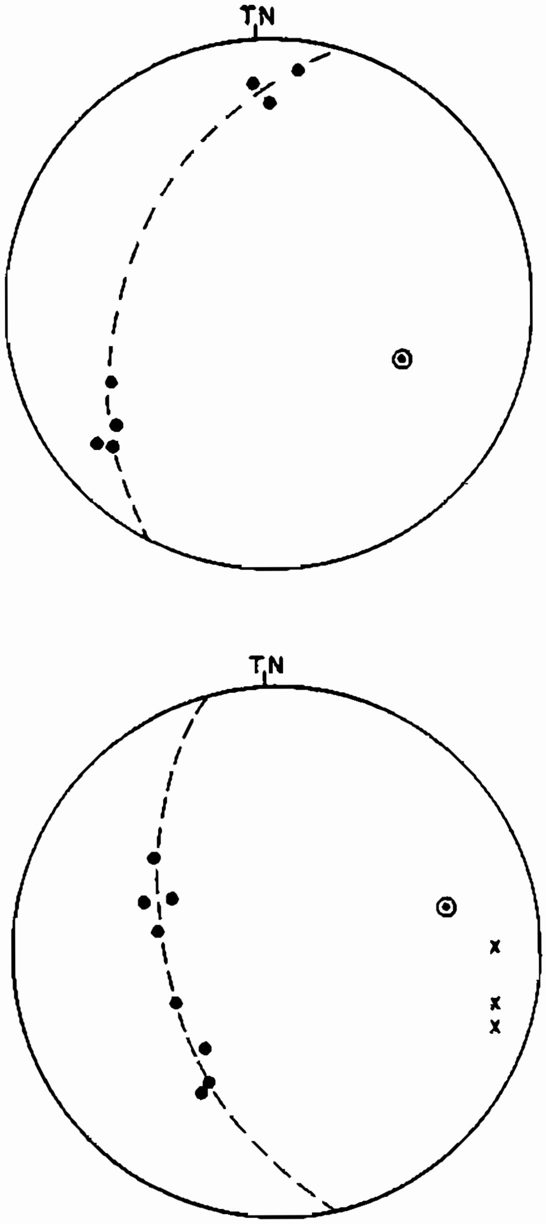

A2.2 Schmidt net plots of poles to bedding in folded quartz arenites west of Vuleka. Anticline (above) and syncline (below) show slightly different orientations. Ornamentation as in A2.1. No fabric or cleavages and very few lineations are recognizable.

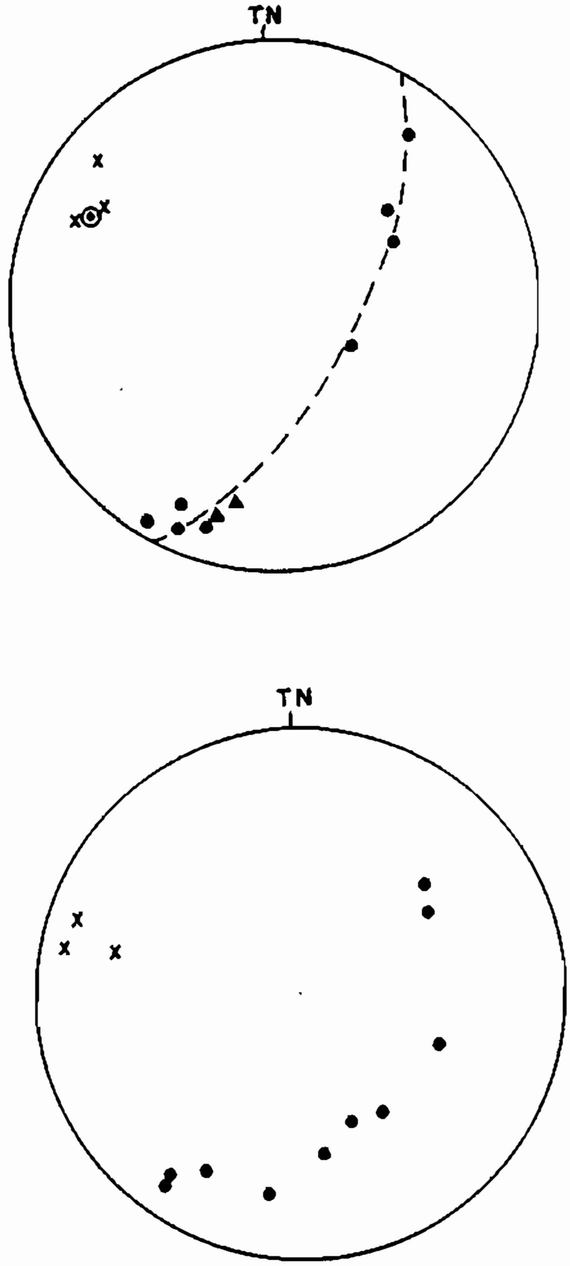

A2.3 Plots of poles to bedding and cleavage for anticline (upper) and syncline (lower) situated east of Vuleka.

APPENDIX 3

Palaeocurrent Data

UNCORRECTED PALAEOCURRENT DATA FOR NSUZE GROUP SEDIMENTS
(Values given as inclination and direction of inclination)

S_0	Planar Cross-Strata	Trough Cross-Strata	Ripples	Locality
70.012	68.046, 73.041, 72.019, 72.029 64.020, 62.023, 86.020, 79.034	 - - -	80.056A 86.340A 38.090A 66.080A	Mdlelanga Formation, Welendhlovu Vallue ($\mathfrak{L}_t$ = 26.066)'
79.012	69.024, 78.026	-	-	
79.014	78.358, 71.354 79.002, 70.030	- -	- 12.072B	
60.026	47.052, 49.056, 41.042, 47.058 53.354, 45.060 40.062, 42.056, 42.054, 32.052, 62.060, 62.058 64.042, 66.044	-		Mdlelanga Formation west of Vuleka ($\mathfrak{L}_t$ = 22.104)
20.157	-	-	10.160A 11.106A 18.170A 13.146A 18.146A	Ndikwe Formation northeast of Hlagothi Mountain in Nsuze River Valley.
28.145			16.186A 00.110A	(Fold axis assumed horizontal)
23.168			14.132A 23.186A 18.172A 21.168A 22.208A	
Flat-lying	Towards: 208, 198, 123, 80	Towards 217, 224, 239, 272, 296, 226, 252, 288, 336, 292, 178, 264, 213, 168, 232, 192, 190.	(Strikes) 014, 028, 012, 216, 230, 242, 192, 240, 230, 312	Wonderdraai Farm (Ndikwe Formation)
43.222	52.197, 67.212, 58.210	30.272A, 25.243A, 28.256A, 15.177A, 20.270A		Upper Gozweni Valley, Ndikwe Formation. (Fold axis assumed horizontal)
17.186	-	-	14.210, 9.262, 18.212, 12.260, 5.105, 17.230, 15.140, 00.268	Upper Nsongeni Valley, Ndikwe Formation. (Fold axis assumed horizontal)
19.023	14.140		25.060A	Mbizwe (Assumed horizontal fold axis)

UNCORRECTED PALAEOCURRENT DATA FOR NSUZE GROUP SEDIMENTS continued

S_0	Planar Cross-Strata	Trough Cross Strata	Ripples	Locality
34.230		00.130B		Vutshini Formation north limb, Central Syncline
30.249			20.274A 26.270A 09.156A 15.283A	(Fold axis: 20.290)
32.262			20.332A 05.132A 05.136A 12.288A	
30.230			14.167A 27.168A 20.270A	
34.240			18.276A	
66.030			37.318	Vutshini Formation, core of Gem Syncline
20.157			14.180	(Fold axis 20.100)
29.178			26.137	
08.163			05.225	
25.112	12.006			
19.168	20.040			
19.134	05.121			
10.121	10.024			
18.088	58.052			
36.066	56.068			
20.029	60.052			
06.050	41.026			

UNCORRECTED PALAEOCURRENT DATA FOR NSUZE GROUP SEDIMENTS continued

S_0	Planar Cross-Strata	Trough Cross-Strata	Ripples	Locality
64.009		69.342B		Vutshini Formation north of Vuleka
57.353	76.010	33.284B	31.050A	(Fold axis: 22.108)
		33.054B	04.079A	
		12.292A	30.300A	
		20.283A	18.288A	
		13.286B		
		12.256B		
		20.272B		
		22.076B		
		08.282B		
		68.308B		
		26.304B		
		19.284B		
		16.079B		
		06.069B		
		26.276B		
65.005		19.272B	67.030A	
		31.054B	40.054A	
		00.086B	22.066A	
		14.074B	33.290A	
		18.093B	05.274B	
		12.068B, 31.060B		
		00.088B, 08.080B		
		11.282B, 41.308B		
		14.276B, 39.296B		
		11.278B, 28.292B		
		19.066B, 19.066B		
		14.074, 44.059B		
		16.074, 06.090B		

1. A = Direction of flow; B = Orientation (no direction inferred).

2. A = Ripple Strike direction; B = Inferred flow direction.

3. $\bar{L}_2$ = Mean L_2 lineation as used in re-orientating these data.

APPENDIX 4

Analytical and sampling methodology

SAMPLING AND ANALYTICAL METHODOLOGY

Samples were taken from the freshest outcrops of the various rock units using normal hammer and cold chisel methods. At least 4 Kg of sample were taken from the volcanics and larger amounts from the coarser-grained units. All traces of weathering, alteration and old fracture surfaces were removed. The samples were then reduced to 5 cm chunks using an hydraulic splitter and the fragments examined under a hand-lens for traces of alteration which were then removed, if present. The fragments were scrubbed under running water with a nylon brush, then cleaned in an ultrasonic bath for a few minutes. After drying at 100°C for one hour, the samples were crushed to less than 1 cm diameter chips. The amygdaloidal lava samples were hand-picked under a low-power binocular microscope to remove all traces of amygdales. After cone and quartering to a residual mass of 100 g, the samples were ground to a very fine powder using a tungsten carbide swing mill. Fusion beads were prepared using the method of Norrich and Hutton (1969). These beads were used for major and minor element analyses. Pressed powder discs were also prepared by compressing 5 - 6 g of sample mixed with a polysynthetic binding agent in a stainless steel die at a pressure of 10 t. The pressed pellets were used for trace element analyses.

The chemical analyses were done using a Phillips PW 1410 X-ray fluorescence spectrometer. International, NIM and in-house rock standards were used to calibrate each analytical run. In-house synthetic standards were used to calibrate certain of the trace element runs, but these were checked against established whole rock standards in each case. Results were in good agreement with the standard values in all cases.

APPENDIX 5

Norms, Phase Diagram Projections and Other Petrologic Data

A. Nsuze Group Volcanics

B. Ultramafic Rocks

C. Hlagothi Complex

D. Pre-tectonic Dykes

NDIKWE FORMATION VOLCANICS

SAMPLE NUMBER BG 128

ORIGINAL WEIGHT PERCENT OXIDES

SIO2	AL2O3	FE2O3	FEO	MNO	MGO	CAO	NA2O	K2O	TIO2	P2O5	CR2O3	TOTAL
58.14	13.93	2.99	7.47	.15	3.91	4.96	4.22	1.61	1.42	.19	.00	98.99

WEIGHT PERCENT OXIDES RECALCULATED TO 100 PERCENT

SIO2	AL2O3	FE2O3	FEO	MNO	MGO	CAO	NA2O	K2O	TIO2	P2O5	CR2O3	TOTAL
58.73	14.07	3.02	7.55	.15	3.95	5.01	4.26	1.63	1.43	.19	.00	100.00

CATION PROPORTIONS IN ANALYSIS

SI	AL	FE(3)	FE(2)	MN	MG	CA	NA	K	TI	P	CR
54.96	15.52	2.13	5.91	.12	5.51	5.02	7.73	1.94	1.01	.15	.00

CIPW NORM

	QTZ	COR	OR	AB	AN	LC	NE	KP
WEIGHT PERCENT	9.381	.000	9.610	36.060	14.457	.000	.000	.000
MOLE PERCENT	29.653	.000	7.994	26.118	9.870	.000	.000	.000
CATION PERCENT	8.778	.000	9.708	38.665	14.610	.000	.000	.000

	AC	NS	KS	DI	WO	HY	OL	CS
WEIGHT PERCENT	.000	.000	.000	7.551	.000	15.386	.000	.000
MOLE PERCENT	.000	.000	.000	6.242	.000	12.864	.000	.000
CATION PERCENT	.000	.000	.000	7.392	.000	15.233	.000	.000

	MT	CM	IL	HM	TN	PF	RU	AP
WEIGHT PERCENT	4.379	.000	2.724	.000	.000	.000	.000	.455
MOLE PERCENT	3.592	.000	3.410	.000	.000	.000	.000	.257
CATION PERCENT	3.190	.000	2.019	.000	.000	.000	.000	.405

MAFIC INDEX = 30.495
NORM TOTAL = 100.003

OLIVINE COMPOSITION
FORSTERITE .000 FAYALITE .000

ORTHOPYROXENE COMPOSITION
ENSTATITE 51.451 FERROSILITE 48.549

CLINOPYROXENE COMPOSITION
WOLLASTONITE 50.562 ENSTATITE 25.436 FERROSILITE 24.002

FELDSPAR COMPOSITION
ORTHOCLASE 15.983 ALBITE 59.972 ANORTHITE 24.044
PLAGIOCLASE COMPOSITION (PERC AN) 28.619

THORNTON AND TUTTLE DIFFERENTIATION INDEX = 55.051
SOLIDIFICATION INDEX (100*MGO/(MGO+FEO+FE2O3+NA2O+K2O)) = 19.352
CRYSTALLIZATION INDEX (AN+MG DI+FO+FO EQIV OF EN) = 24.148
LARSEN INDEX (1/3SI+K)-(CA+MG) = 10.153
ALBITE RATIO (100*(AB+AB EQIV IN NE)/PLAG) = 71.381
IRON RATIO ((FE2+MN)*100/(FE2+MN+MG)) = 71.535
MG NUMBER AS CATIONS MG/CATIONS (FE+MG) = 48.245
OXIDATION RATIO ACCORDING TO LE MAITRE (FEO/FEO+FE2O3) = .784
DENSITY OF DRY LIQUID OF THIS COMPOSITION (AT 1050 DEG) = 2.567
AFM RATIO
TOTAL ALKALIS 29.29 TOTAL FE 51.07 MG 19.64

KOMATIITE PARAMETERS

FEO/(FEO+MGO)	CAO/AL2O3	SIO2/TIO2	AL2O3/TIO2	FEO*/TIO2	CAO/TIO2	NA2O/TIO2	K2O/TIO2
.7222	.36	40.94	9.81	7.16	3.49	2.972	1.134

JENSEN CATION AL2O3 - FEO+FE2O3+TIO2 - MGO
51.61 30.08 18.32

QUARTZ - FELDSPAR RATIOS

QUARTZ 13.50		ORTHOCLASE 13.83		PLAGIOCLASE 72.68			
QUARTZ 17.04		ORTHOCLASE 17.46		ALBITE 65.50			
CATION PROPORTIONS	CA	28.70	FE	39.83	MG	31.47	
	CA	7.67	MG	8.41	SI	83.92	
	SI	80.55	AL	11.37	MG	8.07	
	2MG	30.64	2FE	38.78	SI/5	30.57	
	CA	28.51	AL	44.04	NA+K	27.45	

COORDINATES IN THE SYSTEM PLAGIOCLASE - OLIVINE - CLINOPYROXENE - QUARTZ (IN MOLE PERCENT)

PROPORTION OF ANALYSIS IN BASALT TETRAHEDRON IS 84.68 MOLE PERCENT

BASALT TETRAHEDRON	OL	13.49	CPX	8.73	PLAG	62.91	QTZ	14.86
CLINOPYROXENE PROJECTION		14.78		0.0		68.93		16.29
QUARTZ PROJECTION		15.85		10.25		73.90		0.0
PLAGIOCLASE PROJECTION		36.38		23.54		0.0		40.08
OLIVINE PROJECTION		0.0		6.66		47.99	OPX+(4QTZ)	45.35

CMAS PROJECTIONS

TETRAHEDRON COORDINATES	C	17.01	M	12.40	A	17.27	S	53.32
DIOPSIDE PROJECTION	C3A	33.44	M	13.63	S	52.93		
OLIVINE PROJECTION	CS	20.19	M	61.81	S	18.00		
ENSTATITE PROJECTION	M2S	20.29	C2S3	34.15	A2S3	45.56		
QUARTZ PROJECTION	CAS2	*****	MS	*****	CMS2	*****		

NDIKWE FORMATION VOLCANICS

SAMPLE NUMBER BG 129

ORIGINAL WEIGHT PERCENT OXIDES

SIO2	AL2O3	FE2O3	FEO	MNO	MGO	CAO	NA2O	K2O	TIO2	P2O5	CR2O3	TOTAL
57.94	13.87	3.01	7.53	.16	3.57	6.33	4.43	1.73	1.44	.22	.00	100.24

WEIGHT PERCENT OXIDES RECALCULATED TO 100 PERCENT

SIO2	AL2O3	FE2O3	FEO	MNO	MGO	CAO	NA2O	K2O	TIO2	P2O5	CR2O3	TOTAL
57.80	13.84	3.01	7.52	.16	3.56	6.31	4.42	1.73	1.44	.22	.00	100.00

CATION PROPORTIONS IN ANALYSIS

SI	AL	FE(3)	FE(2)	MN	MG	CA	NA	K	TI	P	CR
54.07	15.26	2.12	5.88	.13	4.96	6.33	8.01	2.06	1.01	.17	.00

CIPW NORM

	QTZ	COR	OR	AB	AN	LC	NE	KP
WEIGHT PERCENT	6.752	.000	10.198	37.384	12.821	.000	.000	.000
MOLE PERCENT	22.751	.000	9.043	28.864	9.330	.000	.000	.000
CATION PERCENT	6.316	.000	10.298	40.071	12.951	.000	.000	.000

	AC	NS	KS	DI	WO	HY	OL	CS
WEIGHT PERCENT	.000	.000	.000	14.145	.000	11.096	.000	.000
MOLE PERCENT	.000	.000	.000	12.424	.000	9.823	.000	.000
CATION PERCENT	.000	.000	.000	13.797	.000	10.908	.000	.000

	MT	CM	IL	HM	TN	PF	RU	AP
WEIGHT PERCENT	4.360	.000	2.728	.000	.000	.000	.000	.520
MOLE PERCENT	3.812	.000	3.640	.000	.000	.000	.000	.313
CATION PERCENT	3.175	.000	2.021	.000	.000	.000	.000	.464

MAFIC INDEX = 32.849
NORM TOTAL = 100.004

OLIVINE COMPOSITION
FORSTERITE .000 FAYALITE .000

ORTHOPYROXENE COMPOSITION
ENSTATITE 48.970 FERROSILITE 51.030

CLINOPYROXENE COMPOSITION
WOLLASTONITE 50.394 ENSTATITE 24.292 FERROSILITE 25.314

FELDSPAR COMPOSITION
ORTHOCLASE 16.884 ALBITE 61.891 ANORTHITE 21.225
PLAGIOCLASE COMPOSITION (PERC AN) 25.537

THORNTON AND TUTTLE DIFFERENTIATION INDEX = 54.334
SOLIDIFICATION INDEX (100*MGO/(MGO+FEO+FE2O3+NA2O+K2O)) = 17.605
CRYSTALLIZATION INDEX (AN+MG DI+FO+FO EQIV OF EN) = 24.041
LARSEN INDEX (1/3SI+K)-(CA+MG) = 9.002
ALBITE RATIO (100*(AB+AB EQIV IN NE)/PLAG) = 74.463
IRON RATIO ((FE2=MN)*100/(FE2+MN+MG)) = 73.530
MG NUMBER AS CATIONS MG/CATIONS (FE+MG) = 45.779
OXIDATION RATIO ACCORDING TO LE MAITRE (FEO/FEO+FE2O3) = .780
DENSITY OF DRY LIQUID OF THIS COMPOSITION (AT 1050 DEG) = 2.575
AFM RATIO
TOTAL ALKALIS 30.84 TOTAL FE 51.29 MG 17.87

KOMATIITE PARAMETERS

FEO/(FEO+MGO)	CAO/AL2O3	SIO2/TIO2	AL2O3/TIO2	FEO*/TIO2	CAO/TIO2	NA2O/TIO2	K2O/TIO2
.7416	.46	40.24	9.63	7.12	4.40	3.076	1.201

JENSEN CATION AL2O3 - FEO+FE2O3+TIO2 - MGO
52.20 30.82 16.99

QUARTZ - FELDSPAR RATIOS
QUARTZ 10.05 ORTHOCLASE 15.19 PLAGIOCLASE 74.76
QUARTZ 12.43 ORTHOCLASE 18.77 ALBITE 68.80

CATION PROPORTIONS						
CA	34.71	FE	38.05	MG	27.24
CA	9.68	MG	7.60	SI	82.72
SI	81.11	AL	11.44	MG	7.45
2MG	28.69	2FE	40.08	SI/5	31.24
CA	33.32	AL	40.16	NA+K	26.52

COORDINATES IN THE SYSTEM PLAGIOCLASE - OLIVINE - CLINOPYROXENE - QUARTZ (IN MOLE PERCENT)

PROPORTION OF ANALYSIS IN BASALT TETRAHEDRON-IS 84.04 MOLE PERCENT

BASALT TETRAHEDRON	OL	9.73	CPX	16.42	PLAG	63.09	QTZ	10.76
CLINOPYROXENE PROJECTION		11.65		0.0		75.48		12.87
QUARTZ PROJECTION		10.91		19.40		70.70		0.0
PLAGIOCLASE PROJECTION		26.37		44.48		0.0		29.15
OLIVINE PROJECTION		0.0		13.40		51.48	OPX+(4QTZ)	35.12

CMAS PROJECTIONS

TETRAHEDRON COORDINATES	C	19.00	M	11.75	A	17.37	S	51.88
DIOPSIDE PROJECTION	C3A	34.52	M	13.30	S	52.19		
OLIVINE PROJECTION	CS	23.48	M	57.69	S	18.84		
ENSTATITE PROJECTION	M2S	24.92	C2S3	34.11	A2S3	40.97		
QUARTZ PROJECTION	CAS2	77.93	MS	16.38	CMS2	5.68		

SAMPLE NUMBER BG 130

ORIGINAL WEIGHT PERCENT OXIDES

SIO2	AL2O3	FE2O3	FEO	MNO	MGO	CAO	NA2O	K2O	TIO2	P2O5	CR2O3	TOTAL
54.43	15.43	2.96	8.48	.15	2.89	7.51	3.19	2.33	1.63	.22	.00	99.61

WEIGHT PERCENT OXIDES RECALCULATED TO 100 PERCENT

SIO2	AL2O3	FE2O3	FEO	MNO	MGO	CAO	NA2O	K2O	TIO2	P2O5	CR2O3	TOTAL
54.64	15.49	2.97	8.51	.15	2.90	7.54	3.19	2.34	1.64	.22	.00	100.00

CATION PROPORTIONS IN ANALYSIS

SI	AL	FE(3)	FE(2)	MN	MG	CA	NA	K	TI	P	CR
51.69	17.27	2.12	7.05	.12	4.09	7.64	5.85	2.82	1.16	.18	.00

CIPW NORM

	QTZ	COR	OR	AB	AN	LC	NE	KP
WEIGHT PERCENT	5.261	.000	13.822	27.005	21.029	.000	.000	.000
MOLE PERCENT	18.487	.000	12.780	21.742	15.957	.000	.000	.000
CATION PERCENT	4.977	.000	14.114	29.272	21.482	.000	.000	.000

	AC	NS	KS	DI	WO	HY	OL	CS
WEIGHT PERCENT	.000	.000	.000	12.548	.000	12.400	.000	.000
MOLE PERCENT	.000	.000	.000	11.329	.000	11.124	.000	.000
CATION PERCENT	.000	.000	.000	12.201	.000	11.950	.000	.000

	MT	CM	IL	HM	TN	PF	RU	AP
WEIGHT PERCENT	4.309	.000	3.108	.000	.000	.000	.000	.523
MOLE PERCENT	3.929	.000	4.324	.000	.000	.000	.000	.328
CATION PERCENT	3.173	.000	2.326	.000	.000	.000	.000	.472

MAFIC INDEX = 32.889
NORM TOTAL = 100.007

OLIVINE COMPOSITION
FORSTERITE .000 FAYALITE .000

ORTHOPYROXENE COMPOSITION
ENSTATITE 38.611 FERROSILITE 61.389

CLINOPYROXENE COMPOSITION
WOLLASTONITE 49.679 ENSTATITE 19.430 FERROSILITE 30.892

FELDSPAR COMPOSITION
ORTHOCLASE 22.346 ALBITE 43.658 ANORTHITE 33.996
PLAGIOCLASE COMPOSITION (PERC AN) 43.779

THORNTON AND TUTTLE DIFFERENTIATION INDEX	=	46.089
SOLIDIFICATION INDEX (100*MGO/(MGO+FEO+FE2O3+NA2O+K2O))	=	14.280
CRYSTALLIZATION INDEX (AN+MG.DI+FO+FO EQIV OF EN)	=	29.643
LARSEN INDEX (1/3SI+K)-(CA+MG)	=	8.047
ALBITE RATIO (100*(AB+AB EQIV IN NE)/PLAG)	=	56.221
IRON RATIO ((FE2+MN)*100/(FE2+MN+MG))	=	80.104
MG NUMBER AS CATIONS MG/CATIONS (FE+MG)	=	36.711
OXIDATION RATIO ACCORDING TO LE MAITRE (FEO/FEO+FE2O3)	=	.796
DENSITY OF DRY LIQUID OF THIS COMPOSITION (AT 1050 DEG)	=	2.617

AFM RATIO
TOTAL ALKALIS 27.63 TOTAL FE 57.88 MG 14.49

KOMATIITE PARAMETERS

FEO/(FEO+MGO)	CAO/AL2O3	SIO2/TIO2	AL2O3/TIO2	FEO*/TIO2	CAO/TIO2	NA2O/TIO2	K2O/TIO2
.7997	.49	33.39	9.47	7.08	4.61	1.951	1.429

JENSEN CATION

AL2O3	- FEO+FE2O3+TIO2	- MGO
54.50	32.60	12.91

QUARTZ - FELDSPAR RATIOS
QUARTZ 7.84 ORTHOCLASE 20.59 PLAGIOCLASE 71.57
QUARTZ 11.42 ORTHOCLASE 29.99 ALBITE 58.59

CATION PROPORTIONS						
	CA	38.51	FE	40.87	MG	20.62
	CA	12.05	MG	6.45	SI	81.50
	SI	80.25	AL	13.40	MG	6.35
	2MG	23.55	2FE	46.63	SI/5	29.76
	CA	37.07	AL	41.89	NA+K	21.05

COORDINATES IN THE SYSTEM PLAGIOCLASE - OLIVINE - CLINOPYROXENE - QUARTZ (IN MOLE PERCENT)

PROPORTION OF ANALYSIS IN BASALT TETRAHEDRON IS 79.91 MOLE PERCENT

BASALT TETRAHEDRON	OL	11.24	CPX	15.27	PLAG	63.51	QTZ	9.98
CLINOPYROXENE PROJECTION		13.27		0.0		74.96		11.77
QUARTZ PROJECTION		12.49		16.96		70.55		0.0
PLAGIOCLASE PROJECTION		30.81		41.84		0.0		27.34
OLIVINE PROJECTION		0.0		12.86		53.51	OPX+(4QTZ)	33.62

CMAS PROJECTIONS

TETRAHEDRON COORDINATES	C	19.00	M	11.97	A	18.02	S	51.01
DIOPSIDE PROJECTION	C3A	34.67	M	13.50	S	51.83		
OLIVINE PROJECTION	CS	23.81	M	56.37	S	19.82		
ENSTATITE PROJECTION	M2S	27.12	C2S3	32.45	A2S3	40.43		
QUARTZ PROJECTION	CAS2	79.20	MS	17.44	CMS2	3.36		

NDIKWE FORMATION VOLCANICS

SAMPLE NUMBER BG 131

ORIGINAL WEIGHT PERCENT OXIDES

SIO2	AL2O3	FE2O3	FEO	MNO	MGO	CAO	NA2O	K2O	TIO2	P2O5	CR2O3	TOTAL
60.98	13.55	2.89	7.21	.14	5.62	2.31	1.88	3.57	1.50	.24	.00	99.89

WEIGHT PERCENT OXIDES RECALCULATED TO 100 PERCENT

SIO2	AL2O3	FE2O3	FEO	MNO	MGO	CAO	NA2O	K2O	TIO2	P2O5	CR2O3	TOTAL
61.05	13.57	2.89	7.22	.14	5.63	2.31	1.88	3.57	1.50	.24	.00	100.00

CATION PROPORTIONS IN ANALYSIS

SI	AL	FE(3)	FE(2)	MN	MG	CA	NA	K	TI	P	CR
57.72	15.12	2.05	5.71	.11	7.93	2.34	3.45	4.31	1.07	.19	.00

CIPW NORM

	QTZ	COR	OR	AB	AN	LC	NE	KP
WEIGHT PERCENT	19.821	2.971	21.119	15.921	9.902	.000	.000	.000
MOLE PERCENT	47.881	4.229	13.424	8.812	5.166	.000	.000	.000
CATION PERCENT	18.739	3.311	21.553	17.247	10.110	.000	.000	.000

	AC	NS	KS	DI	WO	HY	OL	CS
WEIGHT PERCENT	.000	.000	.000	.000	.000	22.666	.000	.000
MOLE PERCENT	.000	.000	.000	.000	.000	14.888	.000	.000
CATION PERCENT	.000	.000	.000	.000	.000	23.308	.000	.000

	MT	CM	IL	HM	TN	PF	RU	AP
WEIGHT PERCENT	4.188	.000	2.852	.000	.000	.000	.000	.569
MOLE PERCENT	2.625	.000	2.728	.000	.000	.000	.000	.246
CATION PERCENT	3.082	.000	2.135	.000	.000	.000	.000	.513

MAFIC INDEX = 30.275
NORM TOTAL = 100.010

OLIVINE COMPOSITION
FORSTERITE .000 FAYALITE .000

ORTHOPYROXENE COMPOSITION
ENSTATITE 61.821 FERROSILITE 38.179

CLINOPYROXENE COMPOSITION
WOLLASTONITE .000 ENSTATITE .000 FERROSILITE .000

FELDSPAR COMPOSITION
ORTHOCLASE 44.990 ALBITE 33.915 ANORTHITE 21.095
PLAGIOCLASE COMPOSITION (PERC AN) 38.347

THORNTON AND TUTTLE DIFFERENTIATION INDEX = 56.861
SOLIDIFICATION INDEX (100*MGO/(MGO+FEO+FE2O3+NA2O+K2O)) = 26.549
CRYSTALLIZATION INDEX (AN+MG DI+FO+FO EQIV OF EN) = 19.723
LARSEN INDEX (1/3SI+K)-(CA+MG) = 12.722
ALBITE RATIO (100*(AB+AB EQIV IN NE)/PLAG) = 61.653
IRON RATIO ((FE2+MN)*100/(FE2+MN+MG)) = 62.772
MG NUMBER AS CATIONS MG/CATIONS (FE+MG) = 58.132
OXIDATION RATIO ACCORDING TO LE MAITRE (FEO/FEO+FE2O3) = .786
DENSITY OF DRY LIQUID OF THIS COMPOSITION (AT 1050 DEG) = 2.546
AFM RATIO
TOTAL ALKALIS 26.10 TOTAL FE 46.98 MG 26.92

KOMATIITE PARAMETERS

FEO/(FEO+MGO)	CAO/AL2O3	SIO2/TIO2	AL2O3/TIO2	FEO*/TIO2	CAO/TIO2	NA2O/TIO2	K2O/TIO2
.6357	.17	40.65	9.03	6.54	1.54	1.253	2.380

JENSEN CATION AL2O3 - FEO+FE2O3+TIO2 - MGO
47.42 27.71 24.87

QUARTZ - FELDSPAR RATIOS
QUARTZ 29.69 ORTHOCLASE 31.63 PLAGIOCLASE 38.68
QUARTZ 34.86 ORTHOCLASE 37.14 ALBITE 28.00

CATION PROPORTIONS

CA	13.77	FE	39.61	MG	46.62
CA	3.45	MG	11.66	SI	84.89
SI	78.85	AL	10.32	MG	10.83
2MG	38.80	2FE	32.96	SI/5	28.24
CA	17.00	AL	54.84	NA+K	28.16

COORDINATES IN THE SYSTEM PLAGIOCLASE - OLIVINE - CLINOPYROXENE - QUARTZ (IN MOLE PERCENT)

PROPORTION OF ANALYSIS IN BASALT TETRAHEDRON IS 69.41 MOLE PERCENT

BASALT TETRAHEDRON	OL	25.19	CPX	.00	PLAG	39.42	QTZ	35.40
CLINOPYROXENE PROJECTION		25.19		0.0		39.42		35.40
QUARTZ PROJECTION		38.99		.00		61.01		0.0
PLAGIOCLASE PROJECTION		41.57		.00		0.0		58.43
OLIVINE PROJECTION		0.0		.00		21.78	OPX+(4QTZ)	78.22

CMAS PROJECTIONS

TETRAHEDRON COORDINATES	C	11.38	M	14.75	A	15.74	S	58.12
DIOPSIDE PROJECTION	C3A	30.18	M	14.47	S	55.35		
OLIVINE PROJECTION	CS	12.20	M	72.98	S	14.82		
ENSTATITE PROJECTION	M2S	*****	C2S3	*****	A2S3	*****		
QUARTZ PROJECTION	CAS2	*****	MS	*****	CMS2	*****		

SAMPLE NUMBER   BG 147

ORIGINAL WEIGHT PERCENT OXIDES

SIO2	AL2O3	FE2O3	FEO	MNO	MGO	CAO	NA2O	K2O	TIO2	P2O5	CR2O3	TOTAL
50.16	19.37	2.51	11.28	.08	6.68	1.51	5.94	.55	1.59	.27	.00	99.94

WEIGHT PERCENT OXIDES RECALCULATED TO 100 PERCENT

SIO2	AL2O3	FE2O3	FEO	MNO	MGO	CAO	NA2O	K2O	TIO2	P2O5	CR2O3	TOTAL
50.19	19.38	2.51	11.29	.09	6.68	1.51	5.94	.55	1.59	.27	.00	100.00

CATION PROPORTIONS IN ANALYSIS

SI	AL	FE(3)	FE(2)	MN	MG	CA	NA	K	TI	P	CR
45.77	20.83	1.72	8.61	.06	9.08	1.48	10.51	.64	1.09	.21	.00

CIPW NORM

	QTZ	COR	OR	AB	AN	LC	NE	KP
WEIGHT PERCENT	.000	6.908	3.252	50.276	5.730	.000	.000	.000
MOLE PERCENT	.000	14.232	2.992	40.274	4.326	.000	.000	.000
CATION PERCENT	.000	7.426	3.201	52.536	5.643	.000	.000	.000

	AC	NS	KS	DI	WO	HY	OL	CS
WEIGHT PERCENT	.000	.000	.000	.000	.000	9.001	17.535	.000
MOLE PERCENT	.000	.000	.000	.000	.000	8.307	21.987	.000
CATION PERCENT	.000	.000	.000	.000	.000	8.667	17.205	.000

	MT	CM	IL	HM	TN	PF	RU	AP
WEIGHT PERCENT	3.639	.000	3.022	.000	.000	.000	.000	.640
MOLE PERCENT	3.301	.000	4.182	.000	.000	.000	.000	.400
CATION PERCENT	2.583	.000	2.192	.000	.000	.000	.000	.556

MAFIC INDEX = 33.836
NORM TOTAL = 100.003

OLIVINE COMPOSITION
FORSTERITE 48.285   FAYALITE 51.715

ORTHOPYROXENE COMPOSITION
ENSTATITE 50.713   FERROSILITE 49.287

CLINOPYROXENE COMPOSITION
WOLLASTONITE .000   ENSTATITE .000   FERROSILITE .000

FELDSPAR COMPOSITION
ORTHOCLASE 5.488   ALBITE 84.842   ANORTHITE 9.670
PLAGIOCLASE COMPOSITION (PERC AN) 10.231

THORNTON AND TUTTLE DIFFERENTIATION INDEX	=	53.523
SOLIDIFICATION INDEX (100*MGO/(MGO+FEO+FE2O3+NA2O+K2O))	=	24.777
CRYSTALLIZATION INDEX (AN+MG.DI+FO+FO EQIV OF EN)	=	17.396
LARSEN INDEX (1/3SI+K)-(CA+MG)	=	6.040
ALBITE RATIO (100*(AB+AB EQIV IN NE)/PLAG)	=	89.769
IRON RATIO ((FE2+MN)*100/(FE2+MN+MG))	=	68.675
MG NUMBER AS CATIONS MG/CATIONS (FE+MG)	=	31.338
OXIDATION RATIO ACCORDING TO LE MAITRE (FEO/FEO+FE2O3)	=	.759
DENSITY OF DRY LIQUID OF THIS COMPOSITION (AT 1050 DEG)	=	2.656

AFM RATIO
TOTAL ALKALIS 24.30   TOTAL FE 50.69   MG 25.01

KOMATIITE PARAMETERS

FEO/(FEO+MGO)	CAO/AL2O3	SIO2/TIO2	AL2O3/TIO2	FEO*/TIO2	CAO/TIO2	NA2O/TIO2	K2O/TIO2
.6696	.08	31.55	12.18	8.92	.95	3.736	.346

JENSEN CATION

AL2O3	FEO+FE2O3+TIO2	MGO
50.39	27.63	21.97

QUARTZ - FELDSPAR RATIOS

QUARTZ	.00		ORTHOCLASE	5.49		PLAGIOCLASE	94.51	
QUARTZ	.00		ORTHOCLASE	6.08		ALBITE	93.92	
CATION PROPORTIONS		CA	7.37	FE	47.28	MG	45.35	
		CA	2.62	MG	16.13	SI	81.25	
		SI	70.12	AL	15.96	MG	13.92	
		2MG	39.27	2FE	40.94	SI/5	19.79	
		CA	8.45	AL	59.63	NA+K	31.92	

COORDINATES IN THE SYSTEM PLAGIOCLASE - OLIVINE - CLINOPYROXENE - QUARTZ (IN MOLE PERCENT)

PROPORTION OF ANALYSIS IN BASALT TETRAHEDRON IS 84.05 MOLE PERCENT

BASALT TETRAHEDRON	OL	28.20	CPX	.00	PLAG	69.22	QTZ	2.58
CLINOPYROXENE PROJECTION		28.20		0.0		69.22		2.58
QUARTZ PROJECTION		28.95		.00		71.05		0.0
PLAGIOCLASE PROJECTION		91.63		.00		0.0		8.37
OLIVINE PROJECTION		0.0		.00		87.03	OPX+(4QTZ)	12.97

CMAS PROJECTIONS

TETRAHEDRON COORDINATES	C	15.06	M	20.45	A	22.01	S	42.48
DIOPSIDE PROJECTION	C3A	33.98	M	16.45	S	49.58		
OLIVINE PROJECTION	CS	23.50	M	46.37	S	30.13		
ENSTATITE PROJECTION	M2S	42.36	C2S3	19.74	A2S3	37.90		
QUARTZ PROJECTION	CAS2	*****	MS	*****	CMS2	*****		

NDIKWE FORMATION VOLCANICS

SAMPLE NUMBER BG 152

ORIGINAL WEIGHT PERCENT OXIDES

SIO2	AL2O3	FE2O3	FEO	MNO	MGO	CAO	NA2O	K2O	TIO2	P2O5	CR2O3	TOTAL
57.26	14.53	2.83	7.09	.13	4.94	4.68	5.12	1.68	.97	.20	.00	99.43

WEIGHT PERCENT OXIDES RECALCULATED TO 100 PERCENT

SIO2	AL2O3	FE2O3	FEO	MNO	MGO	CAO	NA2O	K2O	TIO2	P2O5	CR2O3	TOTAL
57.59	14.61	2.85	7.13	.13	4.97	4.71	5.15	1.69	.98	.20	.00	100.00

CATION PROPORTIONS IN ANALYSIS

SI	AL	FE(3)	FE(2)	MN	MG	CA	NA	K	TI	P	CR
53.07	15.87	1.98	5.49	.10	6.82	4.65	9.20	1.99	.68	.16	.00

CIPW NORM

	QTZ	COR	OR	AB	AN	LC	NE	KP
WEIGHT PERCENT	2.204	.000	9.984	43.558	11.770	.000	.000	.000
MOLE PERCENT	8.417	.000	10.032	38.111	9.706	.000	.000	.000
CATION PERCENT	2.031	.000	9.932	45.995	11.713	.000	.000	.000

	AC	NS	KS	DI	WO	HY	OL	CS
WEIGHT PERCENT	.000	.000	.000	8.416	.000	17.606	.000	.000
MOLE PERCENT	.000	.000	.000	8.466	.000	18.046	.000	.000
CATION PERCENT	.000	.000	.000	8.173	.000	17.420	.000	.000

	MT	CM	IL	HM	TN	PF	RU	AP
WEIGHT PERCENT	4.133	.000	1.853	.000	.000	.000	.000	.476
MOLE PERCENT	4.095	.000	2.801	.000	.000	.000	.000	.325
CATION PERCENT	2.965	.000	1.352	.000	.000	.000	.000	.418

MAFIC INDEX = 32.485
NORM TOTAL = 100.001

OLIVINE COMPOSITION
FORSTERITE .000 FAYALITE .000

ORTHOPYROXENE COMPOSITION
ENSTATITE 56.927 FERROSILITE 43.073

CLINOPYROXENE COMPOSITION
WOLLASTONITE 50.929 ENSTATITE 27.934 FERROSILITE 21.136

FELDSPAR COMPOSITION
ORTHOCLASE 15.287 ALBITE 66.693 ANORTHITE 18.021
PLAGIOCLASE COMPOSITION (PERC AN) 21.272

THORNTON AND TUTTLE DIFFERENTIATION INDEX = 55.747
SOLIDIFICATION INDEX (100*MGO/(MGO+FEO+FE2O3+NA2O+K2O)) = 22.807
CRYSTALLIZATION INDEX (AN+MG DI+FO+FO EQIV OF EN) = 23.865
LARSEN INDEX (1/3SI+K)-(CA+MG) = 8.445
ALBITE RATIO (100*(AB+AB EQIV IN NE)/PLAG) = 78.728
IRON RATIO ((FE2=MN)*100/(FE2+MN+MG)) = 65.307
MG NUMBER AS CATIONS MG/CATIONS (FE+MG) = 55.404
OXIDATION RATIO ACCORDING TO LE MAITRE (FEO/FEO+FE2O3) = .759
DENSITY OF DRY LIQUID OF THIS COMPOSITION (AT 1050 DEG) = 2.564
AFM RATIO
TOTAL ALKALIS 31.81 TOTAL FE 45.08 MG 23.11

KOMATIITE PARAMETERS

FEO/(FEO+MGO)	CAO/AL2O3	SIO2/TIO2	AL2O3/TIO2	FEO*/TIO2	CAO/TIO2	NA2O/TIO2	K2O/TIO2
.6611	.32	59.03	14.98	9.93	4.82	5.278	1.732

JENSEN CATION AL2O3 - FEO+FE2O3+TIO2 - MGO
51.47 26.41 22.12

QUARTZ - FELDSPAR RATIOS
QUARTZ 3.26 ORTHOCLASE 14.79 PLAGIOCLASE 81.95
QUARTZ 3.95 ORTHOCLASE 17.91 ALBITE 78.14

CATION PROPORTIONS	CA	25.89	FE	36.10	MG	38.02
	CA	7.20	MG	10.57	SI	82.23
	SI	78.24	AL	11.70	MG	10.06
	3MG	36.67	2FE	34.82	SI/5	28.52
	CA	25.57	AL	43.66	NA+K	30.77

COORDINATES IN THE SYSTEM PLAGIOCLASE - OLIVINE - CLINOPYROXENE - QUARTZ (IN MOLE PERCENT)

PROPORTION OF ANALYSIS IN BASALT TETRAHEDRON IS 85.33 MOLE PERCENT

BASALT TETRAHEDRON	OL	15.31	CPX	9.58	PLAG	67.63	QTZ	7.48
CLINOPYROXENE PROJECTION		16.93		0.0		74.79		8.28
QUARTZ PROJECTION		16.55		10.35		73.10		0.0
PLAGIOCLASE PROJECTION		47.30		29.58		0.0		23.12
OLIVINE PROJECTION		0.0		8.94		63.12	OPX+(4QTZ)	27.94

CMAS PROJECTIONS

TETRAHEDRON COORDINATES	C	18.45	M	13.91	A	18.00	S	49.63
DIOPSIDE PROJECTION	C3A	34.46	M	14.13	S	51.41		
OLIVINE PROJECTION	CS	24.24	M	55.01	S	20.75		
ENSTATITE PROJECTION	M2S	30.24	C2S3	30.57	A2S3	39.19		
QUARTZ PROJECTION	CAS2	77.56	MS	20.94	CMS2	1.51		

SAMPLE NUMBER BG 238

ORIGINAL WEIGHT PERCENT OXIDES

SIO2	AL2O3	FE2O3	FEO	MNO	MGO	CAO	NA2O	K2O	TIO2	P2O5	CR2O3	TOTAL
71.57	8.51	2.06	4.13	.10	7.18	4.59	.98	.68	.28	.03	.00	100.11

WEIGHT PERCENT OXIDES RECALCULATED TO 100 PERCENT

SIO2	AL2O3	FE2O3	FEO	MNO	MGO	CAO	NA2O	K2O	TIO2	P2O5	CR2O3	TOTAL
71.49	8.50	2.06	4.12	.10	7.17	4.58	.98	.68	.28	.03	.00	100.00

CATION PROPORTIONS IN ANALYSIS

SI	AL	FE(3)	FE(2)	MN	MG	CA	NA	K	TI	P	CR
67.96	9.52	1.47	3.28	.08	10.16	4.67	1.80	.82	.20	.02	.00

CIPW NORM

	QTZ	COR	OR	AB	AN	LC	NE	KP
WEIGHT PERCENT	41.466	.000	4.014	8.281	16.794	.000	.000	.000
MOLE PERCENT	73.673	.000	1.877	3.371	6.444	.000	.000	.000
CATION PERCENT	39.418	.000	4.119	9.020	17.241	.000	.000	.000

	AC	NS	KS	DI	WO	HY	OL	CS
WEIGHT PERCENT	.000	.000	.000	4.605	.000	21.250	.000	.000
MOLE PERCENT	.000	.000	.000	2.288	.000	10.654	.000	.000
CATION PERCENT	.000	.000	.000	4.726	.000	22.801	.000	.000

	MT	CM	IL	HM	TN	PF	RU	AP
WEIGHT PERCENT	2.989	.000	.531	.000	.000	.000	.000	.071
MOLE PERCENT	1.378	.000	.374	.000	.000	.000	.000	.023
CATION PERCENT	2.212	.000	.400	.000	.000	.000	.000	.064

MAFIC INDEX = 29.446
NORM TOTAL = 100.001

OLIVINE COMPOSITION
FORSTERITE .000 FAYALITE .000

ORTHOPYROXENE COMPOSITION
ENSTATITE 76.163 FERROSILITE 23.837

CLINOPYROXENE COMPOSITION
WOLLASTONITE 52.178 ENSTATITE 36.423 FERROSILITE 11.399

FELDSPAR COMPOSITION
ORTHOCLASE 13.798 ALBITE 28.467 ANORTHITE 57.734
PLAGIOCLASE COMPOSITION (PERC AN) 66.976

THORNTON AND TUTTLE DIFFERENTIATION INDEX = 53.761
SOLIDIFICATION INDEX (100*MGO/(MGO+FEO+FE2O3+NA2O+K2O)) = 47.770
CRYSTALLIZATION INDEX (AN+MG DI+FO+FO EQIV OF EN) = 31.755
LARSEN INDEX (1/3SI+K)-(CA+MG) = 8.838
ALBITE RATIO (100*(AB+AB EQIV IN NE)/PLAG) = 33.024
IRON RATIO ((FE2=MN)*100/(FE2+MN+MG)) = 43.140
MG NUMBER AS CATIONS MG/CATIONS (FE+MG) = 75.611
OXIDATION RATIO ACCORDING TO LE MAITRE (FEO/FEO+FE2O3) = .863
DENSITY OF DRY LIQUID OF THIS COMPOSITION (AT 1050 DEG) = 2.485
AFM RATIO
TOTAL ALKALIS 11.20 TOTAL FE 40.37 MG 48.44

KOMATIITE PARAMETERS

FEO/(FEO+MGO)	CAO/AL2O3	SIO2/TIO2	AL2O3/TIO2	FEO*/TIO2	CAO/TIO2	NA2O/TIO2	K2O/TIO2
.4546	.54	255.61	30.39	21.37	16.39	3.500	2.429

JENSEN CATION AL2O3 - FEO+FE2O3+TIO2 - MGO
38.66 20.10 41.24

QUARTZ - FELDSPAR RATIOS

QUARTZ	58.77		ORTHOCLASE 5.69		PLAGIOCLASE 35.54		
QUARTZ	77.13		ORTHOCLASE 7.47		ALBITE 15.40		
CATION PROPORTIONS	CA	24.78	FE	21.30	MG	53.92	
	CA	5.64	MG	12.27	SI	82.09	
	SI	81.99	AL	5.74	MG	12.26	
	2MG	48.45	2FE	19.14	SI/5	32.41	
	CA	43.46	AL	44.32	NA+K	12.23	

COORDINATES IN THE SYSTEM PLAGIOCLASE - OLIVINE - CLINOPYROXENE - QUARTZ (IN MOLE PERCENT)

PROPORTION OF ANALYSIS IN BASALT TETRAHEDRON IS 93.21 MOLE PERCENT

BASALT TETRAHEDRON	OL	18.35	CPX	5.07	PLAG	28.18	QTZ	48.41
CLINOPYROXENE PROJECTION		19.33		0.0		29.68		50.99
QUARTZ PROJECTION		35.56		[illegible].83		54.61		0.0
PLAGIOCLASE PROJECTION		25.54		7.06		0.0		67.40
OLIVINE PROJECTION		0.0		2.23		12.42	OPX+(4QTZ)	85.35

CMAS PROJECTIONS

TETRAHEDRON COORDINATES	C	7.81	M	14.33	A	7.55	S	70.31
DIOPSIDE PROJECTION	C3A	22.11	M	12.75	S	65.14		
OLIVINE PROJECTION	CS	7.09	M	86.89	S	6.02		
ENSTATITE PROJECTION	M2S	*****	C2S3	*****	A2S3	*****		
QUARTZ PROJECTION	CAS2	58.82	MS	39.58	CMS2	1.60		

SAMPLE NUMBER BG 257

ORIGINAL WEIGHT PERCENT OXIDES

SIO2	AL2O3	FE2O3	FEO	MNO	MGO	CAO	NA2O	K2O	TIO2	P2O5	CR2O3	TOTAL
74.04	8.76	1.07	2.15	.07	5.38	3.53	3.39	.90	.34	.00	.02	99.65

WEIGHT PERCENT OXIDES RECALCULATED TO 100 PERCENT

SIO2	AL2O3	FE2O3	FEO	MNO	MGO	CAO	NA2O	K2O	TIO2	P2O5	CR2O3	TOTAL
74.30	8.79	1.08	2.16	.07	5.40	3.54	3.40	.90	.34	.00	.02	100.00

CATION PROPORTIONS IN ANALYSIS

SI	AL	FE(3)	FE(2)	MN	MG	CA	NA	K	TI	P	CR
69.31	9.67	.76	1.68	.06	7.51	3.54	6.15	1.07	.24	.00	.01

CIPW NORM

	QTZ	COR	OR	AB	AN	LC	NE	KP
WEIGHT PERCENT	36.717	.000	5.337	28.776	6.049	.000	.000	.000
MOLE PERCENT	69.864	.000	2.672	12.546	2.486	.000	.000	.000
CATION PERCENT	34.253	.000	5.374	30.761	6.094	.000	.000	.000

	AC	NS	KS	DI	WO	HY	OL	CS
WEIGHT PERCENT	.000	.000	.000	9.139	.000	11.736	.000	.000
MOLE PERCENT	.000	.000	.000	4.735	.000	6.422	.000	.000
CATION PERCENT	.000	.000	.000	9.287	.000	12.594	.000	.000

	MT	CM	IL	HM	TN	PF	RU	AP
WEIGHT PERCENT	1.563	.030	.648	.000	.000	.000	.000	.000
MOLE PERCENT	.772	.015	.488	.000	.000	.000	.000	.000
CATION PERCENT	1.135	.022	.479	.000	.000	.000	.000	.000

MAFIC INDEX = 23.116
NORM TOTAL = 99.994

OLIVINE COMPOSITION
FORSTERITE .000 FAYALITE .000

ORTHOPYROXENE COMPOSITION
ENSTATITE 83.701 FERROSILITE 16.299

CLINOPYROXENE COMPOSITION
WOLLASTONITE 52.650 ENSTATITE 39.633 FERROSILITE 7.717

FELDSPAR COMPOSITION
ORTHOCLASE 13.288 ALBITE 71.651 ANORTHITE 15.061
PLAGIOCLASE COMPOSITION (PERC AN) 17.369

THORNTON AND TUTTLE DIFFERENTIATION INDEX = 70.829
SOLIDIFICATION INDEX (100*MGO/(MGO+FEO+FE2O3+NA2O+K2O)) = 41.728
CRYSTALLIZATION INDEX (AN+MG DI+FO+FO EQIV OF EN) = 20.746
LARSEN INDEX (1/3SI+K)-(CA+MG) = 13.015
ALBITE RATIO (100*(AB+AB EQIV IN NE)/PLAG) = 82.631
IRON RATIO ((FE2=MN)*100/(FE2+MN+MG)) = 34.702
MG NUMBER AS CATIONS MG/CATIONS (FE+MG) = 81.691
OXIDATION RATIO ACCORDING TO LE MAITRE (FEO/FEO+FE2O3) = .813
DENSITY OF DRY LIQUID OF THIS COMPOSITION (AT 1050 DEG) = 2.419
AFM RATIO
TOTAL ALKALIS 33.55 TOTAL FE 24.37 MG 42.08

KOMATIITE PARAMETERS

FEO/(FEO+MGO)	CAO/AL2O3	SIO2/TIO2	AL2O3/TIO2	FEO*/TIO2	CAO/TIO2	NA2O/TIO2	K2O/TIO2
.3667	.40	217.76	25.76	9.16	10.38	9.971	2.647

JENSEN CATION AL2O3 - FEO+FE2O3+TIO2 - MGO
48.69 13.49 37.81

QUARTZ - FELDSPAR RATIOS
QUARTZ 47.76 ORTHOCLASE 6.94 PLAGIOCLASE 45.30
QUARTZ 51.84 ORTHOCLASE 7.53 ALBITE 40.63

CATION PROPORTIONS

CA	27.01	FE	15.72	MG	57.27
CA	4.41	MG	9.34	SI	86.25
SI	84.89	AL	5.92	MG	9.19
2MG	45.50	2FE	12.49	SI/5	42.01
CA	29.54	AL	40.32	NA+K	30.15

COORDINATES IN THE SYSTEM PLAGIOCLASE - OLIVINE - CLINOPYROXENE - QUARTZ (IN MOLE PERCENT)

PROPORTION OF ANALYSIS IN BASALT TETRAHEDRON IS 92.99 MOLE PERCENT

	OL	CPX	PLAG	QTZ
BASALT TETRAHEDRON	10.16	9.99	39.63	40.22
CLINOPYROXENE PROJECTION	11.29	0.0	44.03	44.68
QUARTZ PROJECTION	16.99	16.71	66.30	0.0
PLAGIOCLASE PROJECTION	16.83	16.54	0.0	66.63
OLIVINE PROJECTION	0.0	4.74	18.83	OPX+(4QTZ) 76.43

CMAS PROJECTIONS

TETRAHEDRON COORDINATES	C	11.84	M	9.90	A	9.98	S	68.28
DIOPSIDE PROJECTION	C3A	26.69	M	11.17	S	62.14		
OLIVINE PROJECTION	CS	10.80	M	81.21	S	7.99		
ENSTATITE PROJECTION	M2S	*****	C2S3	*****	A2S3	*****		
QUARTZ PROJECTION	CAS2	69.62	MS	20.24	CMS2	10.14		

SAMPLE NUMBER BG 266

ORIGINAL WEIGHT PERCENT OXIDES

SIO2	AL2O3	FE2O3	FEO	MNO	MGO	CAO	NA2O	K2O	TIO2	P2O5	CR2O3	TOTA
55.28	15.97	4.03	10.08	.21	9.39	1.05	.24	1.24	1.69	.23	.00	99.4

WEIGHT PERCENT OXIDES RECALCULATED TO 100 PERCENT

SIO2	AL2O3	FE2O3	FEO	MNO	MGO	CAO	NA2O	K2O	TIO2	P2O5	CR2O3	TOTA
55.61	16.06	4.06	10.14	.21	9.45	1.06	.24	1.25	1.70	.23	.00	100.0

CATION PROPORTIONS IN ANALYSIS

SI	AL	FE(3)	FE(2)	MN	MG	CA	NA	K	TI	P	CR
52.96	18.03	2.91	8.08	.17	13.41	1.08	.45	1.52	1.22	.19	.00

CIPW NORM

	QTZ	COR	OR	AB	AN	LC	NE	KP
WEIGHT PERCENT	27.889	12.951	7.371	2.042	3.728	.000	.000	.000
MOLE PERCENT	54.048	14.789	3.259	.907	1.560	.000	.000	.000
CATION PERCENT	26.561	14.539	7.578	2.229	3.835	.000	.000	.000

	AC	NS	KS	DI	WO	HY	OL	CS
WEIGHT PERCENT	.000	.000	.000	.000	.000	36.376	.000	.000
MOLE PERCENT	.000	.000	.000	.000	.000	19.313	.000	.000
CATION PERCENT	.000	.000	.000	.000	.000	37.966	.000	.000

	MT	CM	IL	HM	TN	PF	RU	AP
WEIGHT PERCENT	5.880	.000	3.229	.000	.000	.000	.000	.548
MOLE PERCENT	2.957	.000	2.477	.000	.000	.000	.000	.190
CATION PERCENT	4.360	.000	2.435	.000	.000	.000	.000	.497

MAFIC INDEX = 46.033
NORM TOTAL = 100.014

OLIVINE COMPOSITION
FORSTERITE .000 FAYALITE .000

ORTHOPYROXENE COMPOSITION
ENSTATITE 64.669 FERROSILITE 35.331

CLINOPYROXENE COMPOSITION
WOLLASTONITE .000 ENSTATITE .000 FERROSILITE .000

FELDSPAR COMPOSITION
ORTHOCLASE 56.089 ALBITE 15.541 ANORTHITE 28.370
PLAGIOCLASE COMPOSITION (PERC AN) 64.609

THORNTON AND TUTTLE DIFFERENTIATION INDEX	=	37.302
SOLIDIFICATION INDEX (100*MGO/(MGO+FEO+FE2O3+NA2O+K2O))	=	37.588
CRYSTALLIZATION INDEX (AN+MG DI+FO+FO EQIV OF EN)	=	20.215
LARSEN INDEX (1/3SI+K)-(CA+MG)	=	4.438
ALBITE RATIO (100*(AB+AB EQIV IN NE)/PLAG)	=	35.391
IRON RATIO ((FE2=MN)*100/(FE2+MN+MG))	=	58.544
MG NUMBER AS CATIONS MG/CATIONS (FE+MG)	=	62.408
OXIDATION RATIO ACCORDING TO LE MAITRE (FEO/FEO+FE2O3)	=	.858
DENSITY OF DRY LIQUID OF THIS COMPOSITION (AT 1050 DEG)	=	2.656

AFM RATIO
TOTAL ALKALIS 6.02 TOTAL FE 55.77 MG 38.21

KOMATIITE PARAMETERS

FEO/(FEO+MGO)	CAO/AL2O3	SIO2/TIO2	AL2O3/TIO2	FEO*/TIO2	CAO/TIO2	NA2O/TIO2	K2O/TIO2
.5935	.07	32.71	9.45	8.11	.62	.142	.734

JENSEN CATION AL2O3 - FEO+FE2O3+TIO2 - MGO
41.32 27.96 30.72

QUARTZ - FELDSPAR RATIOS
QUARTZ 67.97 ORTHOCLASE 17.96 PLAGIOCLASE 14.06
QUARTZ 74.77 ORTHOCLASE 19.76 ALBITE 5.47

CATION PROPORTIONS	CA	4.49	FE	39.68	MG	55.84
	CA	1.60	MG	19.88	SI	78.52
	SI	70.25	AL	11.96	MG	17.79
	2MG CA	47.49 9.73	2FE AL	33.75 81.41	SI/5 NA+K	18.76 8.85

COORDINATES IN THE SYSTEM PLAGIOCLASE - OLIVINE - CLINOPYROXENE - QUARTZ (IN MOLE PERCENT)

PROPORTION OF ANALYSIS IN BASALT TETRAHEDRON IS 70.59 MOLE PERCENT

BASALT TETRAHEDRON	OL	40.34	CPX	.00	PLAG	8.59	QTZ	51.07
CLINOPYROXENE PROJECTION		40.34		0.0		8.59		51.07
QUARTZ PROJECTION		82.44		.00		17.56		0.0
PLAGIOCLASE PROJECTION		44.13		.00		0.0		55.87
OLIVINE PROJECTION		0.0		.00		4.03	OPX+(4QTZ)	95.97

CMAS PROJECTIONS

TETRAHEDRON COORDINATES	C	3.14	M	23.54	A	14.59	S	58.74
DIOPSIDE PROJECTION	C3A	26.38	M	17.31	S	56.30		
OLIVINE PROJECTION	CS	3.43	M	82.61	S	13.96		
ENSTATITE PROJECTION	M2S	*****	C2S3	*****	A2S3	*****		
QUARTZ PROJECTION	CAS2	*****	MS	*****	CMS2	*****		

SAMPLE NUMBER BG 267

ORIGINAL WEIGHT PERCENT OXIDES

SIO2	AL2O3	FE2O3	FEO	MNO	MGO	CAO	NA2O	K2O	TIO2	P2O5	CR2O3	TOTAL
57.73	14.96	3.38	8.45	.04	11.95	.28	.06	.59	1.55	.21	.00	99.19

WEIGHT PERCENT OXIDES RECALCULATED TO 100 PERCENT

SIO2	AL2O3	FE2O3	FEO	MNO	MGO	CAO	NA2O	K2O	TIO2	P2O5	CR2O3	TOTAL
58.20	15.08	3.41	8.51	.04	12.05	.28	.06	.59	1.56	.21	.00	100.00

CATION PROPORTIONS IN ANALYSIS

SI	AL	FE(3)	FE(2)	MN	MG	CA	NA	K	TI	P	CR
54.81	16.74	2.41	6.71	.03	16.91	.28	.11	.71	1.11	.17	.00

CIPW NORM

	QTZ	COR	OR	AB	AN	LC	NE	KP
WEIGHT PERCENT	32.911	14.332	3.515	.512	.017	.000	.000	.000
MOLE PERCENT	58.483	15.007	1.643	.208	.007	.000	.000	.000
CATION PERCENT	30.995	15.910	3.573	.552	.017	.000	.000	.000

	AC	NS	KS	DI	WO	HY	OL	CS
WEIGHT PERCENT	.000	.000	.000	.000	.000	40.318	.000	.000
MOLE PERCENT	.000	.000	.000	.000	.000	20.127	.000	.000
CATION PERCENT	.000	.000	.000	.000	.000	42.669	.000	.000

	MT	CM	IL	HM	TN	PF	RU	AP
WEIGHT PERCENT	4.938	.000	2.968	.000	.000	.000	.000	.501
MOLE PERCENT	2.277	.000	2.088	.000	.000	.000	.000	.159
CATION PERCENT	3.620	.000	2.213	.000	.000	.000	.000	.450

MAFIC INDEX = 48.725
NORM TOTAL = 100.011

OLIVINE COMPOSITION
FORSTERITE .000 FAYALITE .000

ORTHOPYROXENE COMPOSITION
ENSTATITE 74.416 FERROSILITE 25.584

CLINOPYROXENE COMPOSITION
WOLLASTONITE .000 ENSTATITE .000 FERROSILITE .000

FELDSPAR COMPOSITION
ORTHOCLASE 86.922 ALBITE 12.654 ANORTHITE .425
PLAGIOCLASE COMPOSITION (PERC AN) 3.246

THORNTON AND TUTTLE DIFFERENTIATION INDEX = 36.937
SOLIDIFICATION INDEX (100*MGO/(MGO+FEO+FE2O3+NA2O+K2O)) = 48.927
CRYSTALLIZATION INDEX (AN+MG DI+FO+FO EQIV OF EN) = 21.044
LARSEN INDEX (1/3SI+K)-(CA+MG) = 1.593
ALBITE RATIO (100*(AB+AB EQIV IN NE)/PLAG) = 96.754
IRON RATIO ((FE2+MN)*100/(FE2+MN+MG)) = 47.786
MG NUMBER AS CATIONS MG/CATIONS (FE+MG) = 71.602
OXIDATION RATIO ACCORDING TO LE MAITRE (FEO/FEO+FE2O3) = .865
DENSITY OF DRY LIQUID OF THIS COMPOSITION (AT 1050 DEG) = 2.632
AFM RATIO
TOTAL ALKALIS 2.70 TOTAL FE 47.69 MG 49.61

KOMATIITE PARAMETERS

FEO/(FEO+MGO)	CAO/AL2O3	SIO2/TIO2	AL2O3/TIO2	FEO*/TIO2	CAO/TIO2	NA2O/TIO2	K2O/TIO2
.4901	.02	37.25	9.65	7.41	.18	.039	.381

JENSEN CATION AL2O3 - FEO+FE2O3+TIO2 - MGO
38.16 23.31 38.54

QUARTZ - FELDSPAR RATIOS
QUARTZ 89.06 ORTHOCLASE 9.51 PLAGIOCLASE 1.43
QUARTZ 89.10 ORTHOCLASE 9.52 ALBITE 1.39

CATION PROPORTIONS						
CA	1.13	FE	31.51	MG	67.35
CA	.40	MG	23.48	SI	76.12
SI	68.44	AL	10.45	MG	21.11
2MG	55.80	2FE	26.11	SI/5	18.09
CA	3.14	AL	92.31	NA+K	4.55

COORDINATES IN THE SYSTEM PLAGIOCLASE - OLIVINE - CLINOPYROXENE - QUARTZ (IN MOLE PERCENT)
PROPORTION OF ANALYSIS IN BASALT TETRAHEDRON IS 74.23 MOLE PERCENT

BASALT TETRAHEDRON	OL	43.11	CPX	.00	PLAG	.77	QTZ	56.12
CLINOPYROXENE PROJECTION		43.11		0.0		.77		56.12
QUARTZ PROJECTION		98.25		.00		1.75		0.0
PLAGIOCLASE PROJECTION		43.44		.00		0.0		56.56
OLIVINE PROJECTION		0.0		.00		.34	OPX+(4QTZ)	99.66

CMAS PROJECTIONS

TETRAHEDRON COORDINATES	C	.94	M	25.48	A	12.54	S	61.04
DIOPSIDE PROJECTION	C3A	24.26	M	17.94	S	57.81		
OLIVINE PROJECTION	CS	1.00	M	87.27	S	11.73		
ENSTATITE PROJECTION	M2S	*****	C2S3	*****	A2S3	*****		
QUARTZ PROJECTION	CAS2	*****	MS	*****	CMS2	*****		

SAMPLE NUMBER BG 156

ORIGINAL WEIGHT PERCENT OXIDES

SIO2	AL2O3	FE2O3	FEO	MNO	MGO	CAO	NA2O	K2O	TIO2	P2O5	CR2O3	TOTAL
66.79	12.54	3.31	7.45	.15	1.07	3.17	3.93	.16	1.02	.50	.00	100.08

WEIGHT PERCENT OXIDES RECALCULATED TO 100 PERCENT

SIO2	AL2O3	FE2O3	FEO	MNO	MGO	CAO	NA2O	K2O	TIO2	P2O5	CR2O3	TOTAL
66.73	12.53	3.31	7.44	.15	1.07	3.17	3.93	.16	1.02	.50	.00	100.00

CATION PROPORTIONS IN ANALYSIS

SI	AL	FE(3)	FE(2)	MN	MG	CA	NA	K	TI	P	CR
63.76	14.16	2.39	5.96	.12	1.53	3.25	7.30	.20	.73	.41	.00

CIPW NORM

	QTZ	COR	OR	AB	AN	LC	NE	KP
WEIGHT PERCENT	31.970	1.335	.945	33.219	12.450	.000	.000	.000
MOLE PERCENT	65.927	1.622	.313	15.676	5.544	.000	.000	.000
CATION PERCENT	33.643	1.508	.978	36.485	12.887	.000	.000	.000

	AC	NS	KS	DI	WO	HY	OL	CS
WEIGHT PERCENT	.000	.000	.000	.000	.000	12.187	.000	.000
MOLE PERCENT	.000	.000	.000	.000	.000	6.115	.000	.000
CATION PERCENT	.000	.000	.000	.000	.000	11.371	.000	.000

	MT	CM	IL	HM	TN	PF	RU	AP
WEIGHT PERCENT	4.796	.000	1.935	.000	.000	.000	.000	1.133
MOLE PERCENT	2.565	.000	1.590	.000	.000	.000	.000	.436
CATION PERCENT	3.573	.000	1.469	.000	.000	.000	.000	1.031

MAFIC INDEX = 20.102
NORM TOTAL = 100.019

OLIVINE COMPOSITION
FORSTERITE .000 FAYALITE .000

ORTHOPYROXENE COMPOSITION
ENSTATITE 21.850 FERROSILITE 78.150

CLINOPYROXENE COMPOSITION
WOLLASTONITE .000 ENSTATITE .000 FERROSILITE .000

FELDSPAR COMPOSITION
ORTHOCLASE 2.027 ALBITE 71.265 ANORTHITE 26.708
PLAGIOCLASE COMPOSITION (PERC AN) 27.261

THORNTON AND TUTTLE DIFFERENTIATION INDEX	= 66.133
SOLIDIFICATION INDEX (100*MGO/(MGO+FEO+FE2O3+NA2O+K2O))	= 6.723
CRYSTALLIZATION INDEX (AN+MG.DI+FO+FO EQIV OF EN)	= 14.316
LARSEN INDEX (1/3SI+K)-(CA+MG)	= 13.954
ALBITE RATIO (100*(AB+AB EQIV IN NE)/PLAG)	= 72.739
IRON RATIO ((FE2+MN)*100/(FE2+MN+MG))	= 90.146
MG NUMBER AS CATIONS MG/CATIONS (FE+MG)	= 20.388
OXIDATION RATIO ACCORDING TO LE MAITRE (FEO/FEO+FE2O3)	= .336
DENSITY OF DRY LIQUID OF THIS COMPOSITION (AT 1050 DEG)	= 2.500

AFM RATIO
TOTAL ALKALIS 26.25 TOTAL FE 66.39 MG 6.37

KOMATIITE PARAMETERS

FEO/(FEO+MGO)	CAO/AL2O3	SIO2/TIO2	AL2O3/TIO2	FEO*/TIO2	CAO/TIO2	NA2O/TIO2	K2O/TIO2
.9064	.25	65.47	12.29	10.22	3.11	3.853	.157

JENSEN CATION AL2O3 - FEO+FE2O3+TIO2 - MGO
57.16 36.68 6.17

QUARTZ - FELDSPAR RATIOS
QUARTZ 40.68 ORTHOCLASE 1.20 PLAGIOCLASE 58.11
QUARTZ 48.34 ORTHOCLASE 1.43 ALBITE 50.23

CATION PROPORTIONS						
	CA	27.25	FE	59.95	MG	12.80
	CA	4.73	MG	2.22	SI	93.05
	SI	89.14	AL	9.75	MG	2.10
	2MG	10.13	2FE	47.45	SI/5	42.42
	CA	23.11	AL	50.23	NA+K	26.61

COORDINATES IN THE SYSTEM PLAGIOCLASE - OLIVINE - CLINOPYROXENE - QUARTZ (IN MOLE PERCENT)

PROPORTION OF ANALYSIS IN BASALT TETRAHEDRON IS 91.39 MOLE PERCENT

BASALT TETRAHEDRON	OL	9.33	CPX	.00	PLAG	54.03	QTZ	36.64
CLINOPYROXENE PROJECTION		9.33		0.0		54.03		36.64
QUARTZ PROJECTION		14.73		.00		85.27		0.0
PLAGIOCLASE PROJECTION		20.30		.00		0.0		79.70
OLIVINE PROJECTION		0.0		.00		26.93	OPX+(4QTZ)	73.07

CMAS PROJECTIONS

TETRAHEDRON COORDINATES	C	11.69	M	7.98	A	14.80	S	65.53
DIOPSIDE PROJECTION	C3A	29.60	M	12.14	S	58.26		
OLIVINE PROJECTION	CS	10.54	M	77.74	S	11.71		
ENSTATITE PROJECTION	M2S	*****	C2S3	*****	A2S3	*****		
QUARTZ PROJECTION	CAS2	*****	MS	*****	CMS2	*****		

SAMPLE NUMBER 8G 157

ORIGINAL WEIGHT PERCENT OXIDES

SIO2	AL2O3	FE2O3	FEO	MNO	MGO	CAO	NA2O	K2O	TIO2	P2O5	CR2O3	TOTAL
53.29	16.30	4.36	13.09	.20	2.78	5.12	3.34	.36	1.30	.63	.00	100.47

WEIGHT PERCENT OXIDES RECALCULATED TO 100 PERCENT

SIO2	AL2O3	FE2O3	FEO	MNO	MGO	CAO	NA2O	K2O	TIO2	P2O5	CR2O3	TOTAL
53.04	15.93	4.34	13.02	.20	2.77	5.10	3.32	.36	1.29	.63	.00	100.00

CATION PROPORTIONS IN ANALYSIS

SI	AL	FE(3)	FE(2)	MN	MG	CA	NA	K	TI	P	CR
53.94	13.03	3.14	10.46	.16	3.95	5.24	6.19	.44	.93	.51	.00

CIPW NORM

	QTZ	COR	OR	AB	AN	LC	NE	KP
WEIGHT PERCENT	10.609	2.305	2.117	29.132	21.194	.000	.000	.000
MOLE PERCENT	32.440	4.133	1.704	19.703	13.989	.000	.000	.000
CATION PERCENT	10.198	2.609	2.195	30.945	21.970	.000	.000	.000

	AC	NS	KS	DI	WO	HY	OL	CS
WEIGHT PERCENT	.000	.000	.000	.000	.000	25.452	.000	.000
MOLE PERCENT	.000	.000	.000	.000	.000	19.228	.000	.000
CATION PERCENT	.000	.000	.000	.000	.000	24.137	.000	.000

	MT	CM	IL	HM	TN	PF	RU	AP
WEIGHT PERCENT	6.296	.000	2.458	.000	.000	.000	.000	1.435
MOLE PERCENT	4.996	.000	2.975	.000	.000	.000	.000	.312
CATION PERCENT	4.707	.000	1.469	.000	.000	.000	.000	1.360

MAFIC INDEX = 35.691
NORM TOTAL = 100.023

OLIVINE COMPOSITION
FORSTERITE .000 FAYALITE .000

ORTHOPYROXENE COMPOSITION
ENSTATITE 27.076 FERROSILITE 72.924

CLINOPYROXENE COMPOSITION
WOLLASTONITE .000 ENSTATITE .000 FERROSILITE .000

FELDSPAR COMPOSITION
ORTHOCLASE 4.118 ALBITE 54.687 ANORTHITE 41.196
PLAGIOCLASE COMPOSITION (PERC AN) 42.965

THORNTON AND TUTTLE DIFFERENTIATION INDEX	=	40.848
SOLIDIFICATION INDEX (100*MGO/(MGO+FEO+FE2O3+NA2O+K2O))	=	11.618
CRYSTALLIZATION INDEX (AN+MG,DI+FO+FO EQIV OF EN)	=	26.014
LARSEN INDEX (1/3SI+K)-(CA+MG)	=	9.313
ALBITE RATIO (100*(AB+AB EQIV IN NE)/PLAG)	=	57.039
IRON RATIO ((FE2+MN)*100/(FE2+MN+MG))	=	36.031
MG NUMBER AS CATIONS MG/CATIONS (FE+MG)	=	27.462
OXIDATION RATIO ACCORDING TO LE MAITRE (FEO/FEO+FE2O3)	=	.837
DENSITY OF DRY LIQUID OF THIS COMPOSITION (AT 1050 DEG)	=	2.677

AFM RATIO
TOTAL ALKALIS 15.75 TOTAL FE 72.41 MG 11.33

KOMATIITE PARAMETERS

FEO/(FEO+MGO)	CAO/AL2O3	SIO2/TIO2	AL2O3/TIO2	FEO*/TIO2	CAO/TIO2	NA2O/TIO2	K2O/TIO2
.3595	.32	40.99	12.31	13.09	3.94	2.569	.277

JENSEN CATION AL2O3 - FEO+FE2O3+TIO2 - MGO
49.36 39.79 10.84

QUARTZ - FELDSPAR RATIOS

QUARTZ	17.10	ORTHOCLASE	3.41	PLAGIOCLASE	79.48		
QUARTZ	25.97	ORTHOCLASE	5.18	ALBITE	68.34		
CATION PROPORTIONS	CA	24.70	FE	56.65	MG	18.65	
	CA	9.72	MG	6.59	SI	84.70	
	SI	79.70	AL	14.10	MG	6.20	
	2MG	18.79	2FE	57.05	SI/5	24.16	
	CA	29.84	AL	51.29	NA+K	18.86	

COORDINATES IN THE SYSTEM PLAGIOCLASE - OLIVINE - CLINOPYROXENE - QUARTZ (IN MOLE PERCENT)
PROPORTION OF ANALYSIS IN BASALT TETRAHEDRON IS 37.25 MOLE PERCENT

BASALT TETRAHEDRON	OL	20.76	CPX	.00	PLAG	60.64	QTZ	18.60
CLINOPYROXENE PROJECTION		20.76		0.0		60.64		18.60
QUARTZ PROJECTION		25.51		.00		74.49		0.0
PLAGIOCLASE PROJECTION		52.75		.00		0.0		47.25
OLIVINE PROJECTION		0.0		.00		44.91	OPX+(40TZ)	55.09

CMAS PROJECTIONS

TETRAHEDRON COORDINATES	C	13.15	M	16.28	A	17.69	S	52.87
DIOPSIDE PROJECTION	C3A	31.82	M	15.08	S	53.09		
OLIVINE PROJECTION	CS	15.79	M	65.56	S	18.65		
ENSTATITE PROJECTION	M2S	20.38	C2S3	28.77	A2S3	50.85		
QUARTZ PROJECTION	CAS2	*****	MS	*****	CMS2	*****		

SAMPLE NUMBER 8G 159

ORIGINAL WEIGHT PERCENT OXIDES

SIO2	AL2O3	FE2O3	FEO	MNO	MGO	CAO	NA2O	K2O	TIO2	P2O5	CR2O3	TOTAL
65.51	12.42	3.41	7.67	.18	1.13	5.09	3.75	.40	1.05	.52	.00	101.13

WEIGHT PERCENT OXIDES RECALCULATED TO 100 PERCENT

SIO2	AL2O3	FE2O3	FEO	MNO	MGO	CAO	NA2O	K2O	TIO2	P2O5	CR2O3	TOTAL
64.78	12.28	3.37	7.59	.18	1.12	5.03	3.71	.40	1.04	.51	.00	100.00

CATION PROPORTIONS IN ANALYSIS

SI	AL	FE(3)	FE(2)	MN	MG	CA	NA	K	TI	P	CR
62.13	13.89	2.43	6.09	.14	1.60	5.17	6.89	.48	.75	.42	.00

CIPW NORM

	QTZ	COR	OR	AB	AN	LC	NE	KP
WEIGHT PERCENT	27.530	.000	2.337	31.366	15.697	.000	.000	.000
MOLE PERCENT	61.613	.000	1.376	16.084	7.587	.000	.000	.000
CATION PERCENT	26.408	.000	2.420	34.476	16.261	.000	.000	.000

	AC	NS	KS	DI	WO	HY	OL	CS
WEIGHT PERCENT	.000	.000	.000	5.089	.000	9.922	.000	.000
MOLE PERCENT	.000	.000	.000	2.857	.000	5.409	.000	.000
CATION PERCENT	.000	.000	.000	4.899	.000	9.273	.000	.000

	MT	CM	IL	HM	TN	PF	RU	AP
WEIGHT PERCENT	4.890	.000	1.972	.000	.000	.000	.000	1.218
MOLE PERCENT	2.840	.000	1.747	.000	.000	.000	.000	.487
CATION PERCENT	3.651	.000	1.498	.000	.000	.000	.000	1.114

MAFIC INDEX = 23.090
NORM TOTAL = 100.021

OLIVINE COMPOSITION
FORSTERITE .000 FAYALITE .000

ORTHOPYROXENE COMPOSITION
ENSTATITE 22.187 FERROSILITE 77.813

CLINOPYROXENE COMPOSITION
WOLLASTONITE 48.502 ENSTATITE 11.426 FERROSILITE 40.072

FELDSPAR COMPOSITION
ORTHOCLASE 4.731 ALBITE 63.494 ANORTHITE 31.775
PLAGIOCLASE COMPOSITION (PERC AN) 33.353

THORNTON AND TUTTLE DIFFERENTIATION INDEX	=	61.234
SOLIDIFICATION INDEX (100*MGO/(MGO+FEO+FE2O3+NA2O+K2O))	=	6.905
CRYSTALLIZATION INDEX (AN+MG.DI+FO+FO EQIV OF EN)	=	18.494
LARSEN INDEX (1/3SI+K)-(CA+MG)	=	16.129
ALBITE RATIO (100*(AB+AB EQIV IN NE)/PLAG)	=	66.647
IRON RATIO ((FE2+MN)*100/(FE2+MN+MG))	=	89.955
MG NUMBER AS CATIONS MG/CATIONS (FE+MG)	=	20.790
OXIDATION RATIO ACCORDING TO LE MAITRE (FEO/FEO+FE2O3)	=	.835
DENSITY OF DRY LIQUID OF THIS COMPOSITION (AT 1050 DEG)	=	2.523

AFM RATIO
TOTAL ALKALIS 25.90 TOTAL FE 67.04 MG 7.05

KOMATIITE PARAMETERS

FEO/(FEO+MGO)	CAO/AL2O3	SIO2/TIO2	AL2O3/TIO2	FEO*/TIO2	CAO/TIO2	NA2O/TIO2	K2O/TIO2
.9043	.41	62.39	11.83	10.23	4.85	3.571	.381

JENSEN CATION AL2O3 - FEO+FE2O3+TIO2 - MGO
56.10 37.45 6.45

QUARTZ - FELDSPAR RATIOS
QUARTZ 35.79 ORTHOCLASE 3.04 PLAGIOCLASE 61.18
QUARTZ 44.96 ORTHOCLASE 3.82 ALBITE 51.22

CATION PROPORTIONS						
	CA	36.76	FE	51.89	MG	11.35
	CA	7.51	MG	2.32	SI	90.18
	SI	87.92	AL	9.82	MG	2.26
	2MG	10.57	2FE	48.32	SI/5	41.11
	CA	32.73	AL	43.92	NA+K	23.35

COORDINATES IN THE SYSTEM PLAGIOCLASE - OLIVINE - CLINOPYROXENE - QUARTZ (IN MOLE PERCENT)

PROPORTION OF ANALYSIS IN BASALT TETRAHEDRON IS 91.32 MOLE PERCENT

	OL		CPX		PLAG		QTZ	
BASALT TETRAHEDRON		7.62		5.36		55.56		31.46
CLINOPYROXENE PROJECTION		8.05		0.0		58.71		33.24
QUARTZ PROJECTION		11.11		7.83		81.06		0.0
PLAGIOCLASE PROJECTION		17.14		12.07		0.0		70.79
OLIVINE PROJECTION		0.0		2.87		29.75	OPX+(4QTZ)	67.38

CMAS PROJECTIONS

TETRAHEDRON COORDINATES	C	13.74	M	8.20	A	14.60	S	63.46
DIOPSIDE PROJECTION	C3A	30.55	M	11.94	S	57.51		
OLIVINE PROJECTION	CS	13.04	M	74.81	S	12.15		
ENSTATITE PROJECTION	M2S	*****	C2S3	*****	A2S3	*****		
QUARTZ PROJECTION	CAS2	*****	MS	*****	CMS2	*****		

SAMPLE NUMBER 8G 180

ORIGINAL WEIGHT PERCENT OXIDES

SIO2	AL2O3	FE2O3	FEO	MNO	MGO	CAO	NA2O	K2O	TIO2	P2O5	CR2O3	TOTAL
71.49	15.52	2.40	4.31	.11	1.12	.25	.19	4.42	1.03	.05	.00	100.88

WEIGHT PERCENT OXIDES RECALCULATED TO 100 PERCENT

SIO2	AL2O3	FE2O3	FEO	MNO	MGO	CAO	NA2O	K2O	TIO2	P2O5	CR2O3	TOTAL
70.87	15.38	2.38	4.27	.11	1.11	.25	.19	4.38	1.02	.05	.00	100.00

CATION PROPORTIONS IN ANALYSIS

SI	AL	FE(3)	FE(2)	MN	MG	CA	NA	K	TI	P	CR
68.72	17.59	1.73	3.47	.09	1.60	.26	.34	5.42	.74	.04	.00

CIPW NORM

	QTZ	COR	OR	AB	AN	LC	NE	KP
WEIGHT PERCENT	49.012	10.017	25.891	1.509	.906	.000	.000	.000
MOLE PERCENT	74.508	8.973	10.357	.526	.297	.000	.000	.000
CATION PERCENT	47.327	11.449	27.102	1.677	.948	.000	.000	.000

	AC	NS	KS	DI	WO	HY	OL	CS
WEIGHT PERCENT	.000	.000	.000	.000	.000	7.158	.000	.000
MOLE PERCENT	.000	.000	.000	.000	.000	2.782	.000	.000
CATION PERCENT	.000	.000	.000	.000	.000	7.099	.000	.000

	MT	CM	IL	HM	TN	PF	RU	AP
WEIGHT PERCENT	3.444	.000	1.939	.000	.000	.000	.000	.117
MOLE PERCENT	1.358	.000	1.167	.000	.000	.000	.000	.032
CATION PERCENT	2.600	.000	1.439	.000	.000	.000	.000	.109

MAFIC INDEX = 12.669
NORM TOTAL = 100.004

OLIVINE COMPOSITION
FORSTERITE .000 FAYALITE .000

ORTHOPYROXENE COMPOSITION
ENSTATITE 38.575 FERROSILITE 61.425

CLINOPYROXENE COMPOSITION
WOLLASTONITE .000 ENSTATITE .000 FERROSILITE .000

FELDSPAR COMPOSITION
ORTHOCLASE 91.468 ALBITE 5.332 ANORTHITE 3.199
PLAGIOCLASE COMPOSITION (PERC AN) 37.499

```
THORNTON AND TUTTLE DIFFERENTIATION INDEX                          =  76.412
SOLIDIFICATION INDEX (100*MGO/(MGO+FEO+FE2O3+NA2O+K2O))            =   9.012
CRYSTALLIZATION INDEX (AN+MG.DI+FO+FO EQIV OF EN)                  =   2.943
LARSEN INDEX (1/3SI+K)-(CA+MG)                                     =  27.167
ALBITE RATIO (100*(AB+AB EQIV IN NE)/PLAG)                         =  62.501
IRON RATIO ((FE2+MN)*100/(FE2+MN+MG))                              =  33.574
MG NUMBER AS CATIONS MG/CATIONS (FE+MG)                            =  31.641
OXIDATION RATIO ACCORDING TO LE MAITRE (FEO/FEO+FE2O3)             =    .825
DENSITY OF DRY LIQUID OF THIS COMPOSITION (AT 1050 DEG)            =   2.420
AFM RATIO
     TOTAL ALKALIS  37.74        TOTAL FE   53.07        MG          9.19
```

KOMATIITE PARAMETERS

FEO/(FEO+MGO)	CAO/AL2O3	SIO2/TIO2	AL2O3/TIO2	FEO*/TIO2	CAO/TIO2	NA2O/TIO2	K2O/TIO2
.8524	.02	69.41	15.07	6.26	.24	.175	4.291

JENSEN CATION AL2O3 - FEO+FE2O3+TIO2 - MGO
69.97 23.65 6.38

QUARTZ - FELDSPAR RATIOS
QUARTZ 63.39 ORTHOCLASE 33.49 PLAGIOCLASE 3.12
QUARTZ 64.14 ORTHOCLASE 33.88 ALBITE 1.98

CATION PROPORTIONS						
CA	4.16	FE	69.94	MG	25.90
CA	.36	MG	2.27	SI	97.36
SI	36.36	AL	11.11	MG	2.03
2MG	12.53	2FE	33.82	SI/5	53.65
CA	2.16	AL	73.71	NA+K	24.13

COORDINATES IN THE SYSTEM PLAGIOCLASE - OLIVINE - CLINOPYROXENE - QUARTZ (IN MOLE PERCENT)

PROPORTION OF ANALYSIS IN BASALT TETRAHEDRON IS 57.25 MOLE PERCENT

BASALT TETRAHEDRON	OL	9.30	CPX	.00	PLAG	4.59	QTZ	86.11
CLINOPYROXENE PROJECTION		9.30		0.0		4.59		86.11
QUARTZ PROJECTION		66.97		.00		33.03		0.0
PLAGIOCLASE PROJECTION		9.75		.00		0.0		90.25
OLIVINE PROJECTION		0.0		.00		1.31	OPX+(4QTZ)	98.69

CMAS PROJECTIONS

TETRAHEDRON COORDINATES	C	6.86	M	5.10	A	15.33	S	72.70
DIOPSIDE PROJECTION	C3A	27.62	M	11.89	S	60.49		
OLIVINE PROJECTION	CS	5.29	M	84.34	S	10.37		
ENSTATITE PROJECTION	M2S	*****	C2S3	*****	A2S3	*****		
QUARTZ PROJECTION	CAS2	*****	MS	*****	CMS2	*****		

SAMPLE NUMBER BG 183

ORIGINAL WEIGHT PERCENT OXIDES

SIO2	AL203	FE203	FEO	MNO	MGO	CAO	NA2O	K2O	TIO2	P2O5	CR2O3	TOTAL
61.60	14.73	2.46	5.52	.13	3.47	6.67	2.43	2.51	.76	.20	.00	100.48

WEIGHT PERCENT OXIDES RECALCULATED TO 100 PERCENT

SIO2	AL203	FE203	FEO	MNO	MGO	CAO	NA2O	K2O	TIO2	P2O5	CR2O3	TOTAL
61.31	14.66	2.44	5.50	.13	3.45	6.64	2.42	2.50	.76	.20	.00	100.00

CATION PROPORTIONS IN ANALYSIS

SI	AL	FE(3)	FE(2)	MN	MG	CA	NA	K	TI	P	CR
57.83	16.30	1.74	4.34	.10	4.86	6.71	4.42	3.01	.54	.16	.00

CIPW NORM

	QTZ	COR	OR	AB	AN	LC	NE	KP
WEIGHT PERCENT	17.784	.000	14.761	20.457	21.767	.000	.000	.000
MOLE PERCENT	46.952	.000	10.255	12.375	12.411	.000	.000	.000
CATION PERCENT	16.776	.000	15.032	22.113	22.176	.000	.000	.000

	AC	NS	KS	DI	WO	HY	OL	CS
WEIGHT PERCENT	.000	.000	.000	8.108	.000	11.679	.000	.000
MOLE PERCENT	.000	.000	.000	5.624	.000	9.231	.000	.000
CATION PERCENT	.000	.000	.000	8.038	.000	11.765	.000	.000

	MT	CM	IL	HM	TN	PF	RU	AP
WEIGHT PERCENT	3.544	.000	1.437	.000	.000	.000	.000	.471
MOLE PERCENT	2.428	.000	1.502	.000	.000	.000	.000	.222
CATION PERCENT	2.602	.000	1.073	.000	.000	.000	.000	.424

MAFIC INDEX = 25.238
NORM TOTAL = 100.007

OLIVINE COMPOSITION
FORSTERITE .000 FAYALITE .000

ORTHOPYROXENE COMPOSITION
ENSTATITE 54.894 FERROSILITE 45.106

CLINOPYROXENE COMPOSITION
WOLLASTONITE 50.794 ENSTATITE 27.011 FERROSILITE 22.195

FELDSPAR COMPOSITION
ORTHOCLASE 25.903 ALBITE 35.899 ANORTHITE 38.197
PLAGIOCLASE COMPOSITION (PERC AN) 51.551

THORNTON AND TUTTLE DIFFERENTIATION INDEX = 53.002
SOLIDIFICATION INDEX (100*MGO/(MGO+FEO+FE2O3+NA2O+K2O)) = 21.172
CRYSTALLIZATION INDEX (AN+MG.DI+FO+FO EQIV OF EN) = 30.983
LARSEN INDEX (1/3SI+K)-(CA+MG) = 10.571
ALBITE RATIO (100*(AB+AB EQIV IN NE)/PLAG) = 48.449
IRON RATIO ((FE2+MN)*100/(FE2+MN+MG)) = 67.741
MG NUMBER AS CATIONS MG/CATIONS (FE+MG) = 52.816
OXIDATION RATIO ACCORDING TO LE MAITRE (FEO/FEO+FE2O3) = .807
DENSITY OF DRY LIQUID OF THIS COMPOSITION (AT 1050 DEG) = 2.530
AFM RATIO
TOTAL ALKALIS 30.60 TOTAL FE 47.91 MG 21.49

KOMATIITE PARAMETERS

FEO/(FEO+MGO)	CAO/AL2O3	SIO2/TIO2	AL2O3/TIO2	FEO*/TIO2	CAO/TIO2	NA2O/TIO2	K2O/TIO2
.6903	.45	81.05	19.38	10.18	8.78	3.197	3.303

JENSEN CATION AL2O3 - FEO+FE2O3+TIO2 - MGO
58.71 23.80 17.49

QUARTZ - FELDSPAR RATIOS

QUARTZ 23.79		ORTHOCLASE 19.74		PLAGIOCLASE 56.47		
QUARTZ 33.55		ORTHOCLASE 27.85		ALBITE 38.60		
CATION PROPORTIONS	CA	40.01	FE	31.04	MG	28.96
	CA	9.67	MG	7.00	SI	83.34
	SI	81.64	AL	11.50	MG	6.85
	2MG	30.65	2FE	32.85	SI/5	36.50
	CA	36.12	AL	43.88	NA+K	20.00

COORDINATES IN THE SYSTEM PLAGIOCLASE - OLIVINE - CLINOPYROXENE - QUARTZ (IN MOLE PERCENT)

PROPORTION OF ANALYSIS IN BASALT TETRAHEDRON IS 80.87 MOLE PERCENT

BASALT TETRAHEDRON	OL	10.91	CPX	9.94	PLAG	54.77	QTZ	24.38
CLINOPYROXENE PROJECTION		12.12		0.0		60.81		27.07
QUARTZ PROJECTION		14.43		13.14		72.43		0.0
PLAGIOCLASE PROJECTION		24.12		21.97		0.0		53.90
OLIVINE PROJECTION		0.0		6.13		33.76	OPX+(4QTZ)	60.12

CMAS PROJECTIONS

TETRAHEDRON COORDINATES	C	16.07	M	10.15	A	15.37	S	58.40
DIOPSIDE PROJECTION	C3A	32.21	M	12.57	S	55.22		
OLIVINE PROJECTION	CS	17.11	M	68.54	S	14.36		
ENSTATITE PROJECTION	M2S	*****	C2S3	*****	A2S3	*****		
QUARTZ PROJECTION	CAS2	79.53	MS	17.64	CMS2	2.83		

SAMPLE NUMBER BG 184

ORIGINAL WEIGHT PERCENT OXIDES

SIO2	AL2O3	FE2O3	FEO	MNO	MGO	CAO	NA2O	K2O	TIO2	P2O5	CR2O3	TOTAL
62.34	13.03	2.36	5.32	.12	3.30	6.06	3.24	1.71	.78	.19	.00	101.05

WEIGHT PERCENT OXIDES RECALCULATED TO 100 PERCENT

SIO2	AL2O3	FE2O3	FEO	MNO	MGO	CAO	NA2O	K2O	TIO2	P2O5	CR2O3	TOTAL
61.69	14.87	2.34	5.26	.12	3.27	6.59	3.21	1.69	.77	.19	.00	100.00

CATION PROPORTIONS IN ANALYSIS

SI	AL	FE(3)	FE(2)	MN	MG	CA	NA	K	TI	P	CR
57.91	16.46	1.65	4.13	.09	4.57	6.63	5.83	2.03	.54	.15	.00

CIPW NORM

	QTZ	COR	OR	AB	AN	LC	NE	KP
WEIGHT PERCENT	17.296	.000	9.999	27.121	21.193	.000	.000	.000
MOLE PERCENT	40.328	.000	7.052	15.655	12.266	.000	.000	.000
CATION PERCENT	16.227	.000	10.133	29.173	21.485	.000	.000	.000

	AC	NS	KS	DI	WO	HY	OL	CS
WEIGHT PERCENT	.000	.000	.000	8.444	.000	10.656	.000	.000
MOLE PERCENT	.000	.000	.000	5.946	.000	7.625	.000	.000
CATION PERCENT	.000	.000	.000	5.331	.000	10.683	.000	.000

	MT	CM	IL	HM	TN	PF	RU	AP
WEIGHT PERCENT	3.393	.000	1.466	.000	.000	.000	.000	.445
MOLE PERCENT	2.359	.000	1.556	.000	.000	.000	.000	.213
CATION PERCENT	2.479	.000	1.090	.000	.000	.000	.000	.398

MAFIC INDEX = 24.404
NORM TOTAL = 100.005

OLIVINE COMPOSITION
FORSTERITE .000 FAYALITE .000

ORTHOPYROXENE COMPOSITION
ENSTATITE 54.912 FERROSILITE 45.089

CLINOPYROXENE COMPOSITION
WOLLASTONITE 50.795 ENSTATITE 27.019 FERROSILITE 22.186

FELDSPAR COMPOSITION
ORTHOCLASE 17.147 ALBITE 46.509 ANORTHITE 36.343
PLAGIOCLASE COMPOSITION (PERC AN) 43.865

THORNTON AND TUTTLE DIFFERENTIATION INDEX	=	54.407
SOLIDIFICATION INDEX (100*MGO/(MGO+FEO+FE2O3+NA2O+K2O))	=	20.711
CRYSTALLIZATION INDEX (AN+MG,DI+FO+FO EQIV OF EN)	=	30.215
LARSEN INDEX (1/3SI+K)-(CA+MG)	=	10.490
ALBITE RATIO (100*(AB+AB EQIV IN NE)/PLAG)	=	56.135
IRON RATIO ((FE2+MN)*100/(FE2+MN+MG))	=	67.991
MG NUMBER AS CATIONS MG/CATIONS (FE+MG)	=	52.506
OXIDATION RATIO ACCORDING TO LE MAITRE (FEO/FEO+FE2O3)	=	.809
DENSITY OF DRY LIQUID OF THIS COMPOSITION (AT 1050 DEG)	=	2.523

AFM RATIO
TOTAL ALKALIS 31.54 TOTAL FE 47.44 MG 21.02

KOMATIITE PARAMETERS

FEO/(FEO+MGO)	CAO/AL2O3	SIO2/TIO2	AL2O3/TIO2	FEO*/TIO2	CAO/TIO2	NA2O/TIO2	K2O/TIO2
.6929	.44	79.92	19.27	9.55	8.54	4.154	2.192

JENSEN CATION AL2O3 - FEO+FE2O3+TIO2 - MGO
60.15 23.14 16.70

QUARTZ - FELDSPAR RATIOS
QUARTZ 22.87 ORTHOCLASE 13.23 PLAGIOCLASE 63.91
QUARTZ 31.77 ORTHOCLASE 18.38 ALBITE 49.85

CATION PROPORTIONS						
	CA	41.03	FE	30.69	MG	28.28
	CA	9.59	MG	6.61	SI	83.80
	SI	81.90	AL	11.64	MG	6.46
	2MG	29.83	2FE	32.37	SI/5	37.80
	CA	35.28	AL	43.79	NA+K	20.92

COORDINATES IN THE SYSTEM PLAGIOCLASE - OLIVINE - CLINOPYROXENE - QUARTZ (IN MOLE PERCENT)

PROPORTION OF ANALYSIS IN BASALT TETRAHEDRON IS 85.90 MOLE PERCENT

BASALT TETRAHEDRON	OL	9.33	CPX	9.70	PLAG	58.97	QTZ	22.00
CLINOPYROXENE PROJECTION		10.33		0.0		65.31		24.36
QUARTZ PROJECTION		11.96		12.43		75.61		0.0
PLAGIOCLASE PROJECTION		22.74		23.64		0.0		53.62
OLIVINE PROJECTION		0.0		6.19		37.64	OPX+(4QTZ)	56.17

CMAS PROJECTIONS

TETRAHEDRON COORDINATES	C	16.55	M	9.59	A	15.72	S	58.15
DIOPSIDE PROJECTION	C3A	32.57	M	12.43	S	55.01		
OLIVINE PROJECTION	CS	17.61	M	67.72	S	14.68		
ENSTATITE PROJECTION	M2S	*****	C2S3	*****	A2S3	*****		
QUARTZ PROJECTION	CAS2	80.51	MS	16.19	CMS2	3.30		

SAMPLE NUMBER NK81-1 BR82

ORIGINAL WEIGHT PERCENT OXIDES

SIO2	AL2O3	FE2O3	FEO	MNO	MGO	CAO	NA2O	K2O	TIO2	P2O5	CR2O3	TOTAL
57.64	14.54	3.29	7.40	.13	4.61	6.00	3.51	1.69	.88	.32	.00	100.01

WEIGHT PERCENT OXIDES RECALCULATED TO 100 PERCENT

SIO2	AL2O3	FE2O3	FEO	MNO	MGO	CAO	NA2O	K2O	TIO2	P2O5	CR2O3	TOTAL
57.63	14.54	3.29	7.40	.13	4.61	6.00	3.51	1.69	.88	.32	.00	100.00

CATION PROPORTIONS IN ANALYSIS

SI	AL	FE(3)	FE(2)	MN	MG	CA	NA	K	TI	P	CR
54.00	16.05	2.32	5.80	.10	6.44	6.02	6.37	2.02	.62	.25	.00

CIPW NORM

	QTZ	COR	OR	AB	AN	LC	NE	KP
WEIGHT PERCENT	9.421	.000	9.985	29.687	18.924	.000	.000	.000
MOLE PERCENT	29.860	.000	8.327	21.558	12.953	.000	.000	.000
CATION PERCENT	8.827	.000	10.099	31.871	19.148	.000	.000	.000

	AC	NS	KS	DI	WO	HY	OL	CS
WEIGHT PERCENT	.000	.000	.000	7.195	.000	17.598	.000	.000
MOLE PERCENT	.000	.000	.000	5.986	.000	14.866	.000	.000
CATION PERCENT	.000	.000	.000	7.079	.000	17.580	.000	.000

	MT	CM	IL	HM	TN	PF	RU	AP
WEIGHT PERCENT	4.771	.000	1.671	.000	.000	.000	.000	.758
MOLE PERCENT	3.924	.000	2.097	.000	.000	.000	.000	.429
CATION PERCENT	3.480	.000	1.240	.003	.000	.000	.000	.677

MAFIC INDEX = 31.994
NORM TOTAL = 100.011

OLIVINE COMPOSITION
FORSTERITE .000 FAYALITE .000

ORTHOPYROXENE COMPOSITION
ENSTATITE 54.299 FERROSILITE 45.701

CLINOPYROXENE COMPOSITION
WOLLASTONITE 50.754 ENSTATITE 26.740 FERROSILITE 22.506

FELDSPAR COMPOSITION
ORTHOCLASE 17.040 ALBITE 50.664 ANORTHITE 32.296
PLAGIOCLASE COMPOSITION (PERC AN) 38.930

THORNTON AND TUTTLE DIFFERENTIATION INDEX = 49.093
SOLIDIFICATION INDEX (100*MGO/(MGO+FEO+FE2O3+NA2O+K2O)) = 22.483
CRYSTALLIZATION INDEX (AN+MG,DI+FO+FO EQIV OF EN) = 29.771
LARSEN INDEX (1/3SI+K)-(CA+MG) = 7.574
ALBITE RATIO (100*(AB+AB EQIV IN NE)/PLAG) = 61.070
IRON RATIO ((FE2+MN)*100/(FE2+MN+MG)) = 67.804
MG NUMBER AS CATIONS MG/CATIONS (FE+MG) = 52.598
OXIDATION RATIO ACCORDING TO LE MAITRE (FEO/FEO+FE2O3) = .796
DENSITY OF DRY LIQUID OF THIS COMPOSITION (AT 1050 DEG) = 2.579
AFM RATIO
TOTAL ALKALIS 25.77 TOTAL FE 51.37 MG 22.85

KOMATIITE PARAMETERS

FEO/(FEO+MGO)	CAO/AL2O3	SIO2/TIO2	AL2O3/TIO2	FEO*/TIO2	CAO/TIO2	NA2O/TIO2	K2O/TIO2
.6921	.41	65.50	16.52	11.78	6.82	3.989	1.920

JENSEN CATION AL2O3 - FEO+FE2O3+TIO2 - MGO
31.41 27.99 20.61

QUARTZ - FELDSPAR RATIOS
QUARTZ 13.85 ORTHOCLASE 14.68 PLAGIOCLASE 71.47
QUARTZ 19.19 ORTHOCLASE 20.34 ALBITE 60.47

CATION PROPORTIONS						
CA	31.01	FE	35.84	MG	33.15
CA	9.06	MG	9.69	SI	81.25
SI	78.87	AL	11.72	MG	9.40
2MG	34.25	2FE	37.03	SI/5	28.73
CA	33.00	AL	43.99	NA+K	23.00

COORDINATES IN THE SYSTEM PLAGIOCLASE - OLIVINE - CLINOPYROXENE - QUARTZ (IN MOLE PERCENT)

PROPORTION OF ANALYSIS IN BASALT TETRAHEDRON IS 84.50 MOLE PERCENT

BASALT TETRAHEDRON	OL	15.60	CPX	8.38	PLAG	60.37	QTZ	15.65
CLINOPYROXENE PROJECTION		17.03		0.0		65.89		17.08
QUARTZ PROJECTION		18.50		9.93		71.57		0.0
PLAGIOCLASE PROJECTION		39.37		21.14		0.0		39.49
OLIVINE PROJECTION		0.0		6.38		45.97	OPX+(4QTZ)	47.65

CMAS PROJECTIONS

TETRAHEDRON COORDINATES	C	16.40	M	13.74	A	16.41	S	53.45
DIOPSIDE PROJECTION	C3A	32.92	M	13.94	S	53.14		
OLIVINE PROJECTION	CS	19.77	M	62.88	S	17.36		
ENSTATITE PROJECTION	M2S	19.42	C2S3	34.81	A2S3	45.77		
QUARTZ PROJECTION	CAS2	*****	MS	*****	CMS2	*****		

SAMPLE NUMBER NK81-2 BR82

ORIGINAL WEIGHT PERCENT OXIDES

SIO2	AL2O3	FE2O3	FEO	MNO	MGO	CAO	NA2O	K2O	TIO2	P2O5	CR2O3	TOTAL
55.39	15.11	3.50	7.87	.17	5.17	5.63	3.23	2.59	.97	.20	.00	99.83

WEIGHT PERCENT OXIDES RECALCULATED TO 100 PERCENT

SIO2	AL2O3	FE2O3	FEO	MNO	MGO	CAO	NA2O	K2O	TIO2	P2O5	CR2O3	TOTAL
55.49	15.14	3.50	7.88	.17	5.18	5.64	3.24	2.59	.97	.20	.00	100.00

CATION PROPORTIONS IN ANALYSIS

SI	AL	FE(3)	FE(2)	MN	MG	CA	NA	K	TI	P	CR
51.89	16.68	2.47	6.16	.13	7.22	5.65	5.86	3.10	.68	.16	.00

CIPW NORM

	QTZ	COR	OR	AB	AN	LC	NE	KP
WEIGHT PERCENT	4.446	.000	15.331	27.370	19.114	.000	.000	.000
MOLE PERCENT	15.860	.000	14.392	22.372	14.726	.000	.000	.000
CATION PERCENT	4.157	.000	15.475	29.325	19.302	.000	.000	.000

	AC	NS	KS	DI	WO	HY	OL	CS
WEIGHT PERCENT	.000	.000	.000	6.204	.000	20.140	.000	.000
MOLE PERCENT	.000	.000	.000	5.820	.000	19.218	.000	.000
CATION PERCENT	.000	.000	.000	6.103	.000	20.150	.000	.000

	MT	CM	IL	HM	TN	PF	RU	AP
WEIGHT PERCENT	5.081	.000	1.845	.000	.000	.000	.000	.475
MOLE PERCENT	4.704	.000	2.606	.000	.000	.000	.000	.303
CATION PERCENT	3.699	.000	1.367	.000	.000	.000	.000	.423

MAFIC INDEX = 33.746
NORM TOTAL = 100.006

OLIVINE COMPOSITION
FORSTERITE .000 FAYALITE .000

ORTHOPYROXENE COMPOSITION
ENSTATITE 55.619 FERROSILITE 44.381

CLINOPYROXENE COMPOSITION
WOLLASTONITE 50.842 ENSTATITE 27.341 FERROSILITE 21.817

FELDSPAR COMPOSITION
ORTHOCLASE 24.802 ALBITE 44.277 ANORTHITE 30.921
PLAGIOCLASE COMPOSITION (PERC AN) 41.120

THORNTON AND TUTTLE DIFFERENTIATION INDEX = 47.146
SOLIDIFICATION INDEX (100*MGO/(MGO+FEO+FE2O3+NA2O+K2O)) = 23.123
CRYSTALLIZATION INDEX (AN+MG.DI+FO+FO EQIV OF EN) = 30.623
LARSEN INDEX (1/3SI+K)-(CA+MG) = 6.958
ALBITE RATIO (100*(AB+AB EQIV IN NE)/PLAG) = 58.880
IRON RATIO ((FE2+MN)*100/(FE2+MN+MG)) = 66.712
MG NUMBER AS CATIONS MG/CATIONS (FE+MG) = 53.931
OXIDATION RATIO ACCORDING TO LE MAITRE (FEO/FEO+FE2O3) = .780
DENSITY OF DRY LIQUID OF THIS COMPOSITION (AT 1050 DEG) = 2.598
AFM RATIO
TOTAL ALKALIS 26.45 TOTAL FE 50.06 MG 23.49

KOMATIITE PARAMETERS

FEO/(FEO+MGO)	CAO/AL2O3	SIO2/TIO2	AL2O3/TIO2	FEO*/TIO2	CAO/TIO2	NA2O/TIO2	K2O/TIO2
.6806	.37	57.10	15.58	11.36	5.80	3.330	2.670

JENSEN CATION AL2O3 - FEO+FE2O3+TIO2 - MGO
50.23 28.04 21.73

QUARTZ - FELDSPAR RATIOS
QUARTZ 6.71 ORTHOCLASE 23.14 PLAGIOCLASE 70.15
QUARTZ 9.43 ORTHOCLASE 32.52 ALBITE 58.05

CATION PROPORTIONS

CA	27.88	FE	36.50	MG	35.62
CA	8.73	MG	11.15	SI	80.13
SI	76.93	AL	12.37	MG	10.70
2MG	36.45	2FE	37.35	SI/5	26.20
CA	30.59	AL	45.15	NA+K	24.26

COORDINATES IN THE SYSTEM PLAGIOCLASE - OLIVINE - CLINOPYROXENE - QUARTZ (IN MOLE PERCENT)

PROPORTION OF ANALYSIS IN BASALT TETRAHEDRON IS 79.04 MOLE PERCENT

BASALT TETRAHEDRON	OL	19.12	CPX	7.72	PLAG	61.52	QTZ	11.63
CLINOPYROXENE PROJECTION		20.72		0.0		66.67		12.61
QUARTZ PROJECTION		21.64		8.74		69.62		0.0
PLAGIOCLASE PROJECTION		49.70		20.07		0.0		30.24
OLIVINE PROJECTION		0.0		6.67		53.14	OPX+(4QTZ)	40.19

CMAS PROJECTIONS

TETRAHEDRON COORDINATES	C	16.91	M	15.13	A	17.37	S	50.59
DIOPSIDE PROJECTION	C3A	33.54	M	14.50	S	51.96		
OLIVINE PROJECTION	CS	21.87	M	58.41	S	19.72		
ENSTATITE PROJECTION	M2S	27.87	C2S3	30.70	A2S3	41.43		
QUARTZ PROJECTION	CAS2	*****	MS	*****	CMS2	*****		

SAMPLE NUMBER NK81-6 BR82

ORIGINAL WEIGHT PERCENT OXIDES

SIO2	AL2O3	FE2O3	FEO	MNO	MGO	CAO	NA2O	K2O	TIO2	P2O5	CR2O3	TOTAL
57.62	15.14	2.69	6.05	.14	6.10	6.89	3.72	.78	.59	.29	.00	100.02

WEIGHT PERCENT OXIDES RECALCULATED TO 100 PERCENT

SIO2	AL2O3	FE2O3	FEO	MNO	MGO	CAO	NA2O	K2O	TIO2	P2O5	CR2O3	TOTAL
57.61	15.14	2.69	6.05	.14	6.10	6.89	3.72	.78	.59	.29	.00	100.00

CATION PROPORTIONS IN ANALYSIS

SI	AL	FE(3)	FE(2)	MN	MG	CA	NA	K	TI	P	CR
53.33	16.52	1.87	4.69	.11	8.41	6.83	6.67	.92	.41	.23	.00

CIPW NORM

	QTZ	COR	OR	AB	AN	LC	NE	KP
WEIGHT PERCENT	8.392	.000	4.608	31.463	22.305	.000	.000	.000
MOLE PERCENT	27.340	.000	3.951	23.487	15.694	.000	.000	.000
CATION PERCENT	7.768	.000	4.605	33.374	22.299	.000	.000	.000

	AC	NS	KS	DI	WO	HY	OL	CS
WEIGHT PERCENT	.000	.000	.000	8.093	.000	19.439	.000	.000
MOLE PERCENT	.000	.000	.000	7.018	.000	17.366	.000	.000
CATION PERCENT	.000	.000	.000	7.977	.000	19.737	.000	.000

	MT	CM	IL	HM	TN	PF	RU	AP
WEIGHT PERCENT	3.902	.000	1.120	.000	.000	.000	.000	.687
MOLE PERCENT	3.299	.000	1.445	.000	.000	.000	.000	.400
CATION PERCENT	2.812	.000	.821	.000	.000	.000	.000	.606

MAFIC INDEX = 33.241
NORM TOTAL = 100.009

OLIVINE COMPOSITION
FORSTERITE .000 FAYALITE .000

ORTHOPYROXENE COMPOSITION
ENSTATITE 65.004 FERROSILITE 34.996

CLINOPYROXENE COMPOSITION
WOLLASTONITE 51.462 ENSTATITE 31.552 FERROSILITE 16.986

FELDSPAR COMPOSITION
ORTHOCLASE 7.894 ALBITE 53.896 ANORTHITE 38.210
PLAGIOCLASE COMPOSITION (PERC AN) 41.484

THORNTON AND TUTTLE DIFFERENTIATION INDEX	= 44.463
SOLIDIFICATION INDEX (100*MGO/(MGO+FEO+FE2O3+NA2O+K2O))	= 31.532
CRYSTALLIZATION INDEX (AN+MG.DI+FO+FO EQIV OF EN)	= 36.669
LARSEN INDEX (1/3SI+K)-(CA+MG)	= 3.442
ALBITE RATIO (100*(AB+AB EQIV IN NE)/PLAG)	= 58.516
IRON RATIO ((FE2+MN)*100/(FE2+MN+MG))	= 56.684
MG NUMBER AS CATIONS MG/CATIONS (FE+MG)	= 64.228
OXIDATION RATIO ACCORDING TO LE MAITRE (FEO/FEO+FE2O3)	= .805
DENSITY OF DRY LIQUID OF THIS COMPOSITION (AT 1050 DEG)	= 2.577

AFM RATIO
TOTAL ALKALIS 23.59 TOTAL FE 44.43 MG 31.98

KOMATIITE PARAMETERS

FEO/(FEO+MGO)	CAO/AL2O3	SIO2/TIO2	AL2O3/TIO2	FEO*/TIO2	CAO/TIO2	NA2O/TIO2	K2O/TIO2
.5815	.46	97.66	25.66	14.37	11.68	6.305	1.322

JENSEN CATION AL2O3 - FEO+FE2O3+TIO2 - MGO
51.77 21.85 26.37

QUARTZ - FELDSPAR RATIOS

QUARTZ	12.57	ORTHOCLASE	6.90	PLAGIOCLASE	80.53	
QUARTZ	18.87	ORTHOCLASE	10.36	ALBITE	70.76	

CATION PROPORTIONS	CA	32.74	FE	26.94	MG	40.32
	CA	9.96	MG	12.27	SI	77.77
	SI	76.13	AL	11.80	MG	12.02
	2MG	43.44	2FE	29.03	SI/5	27.53
	CA	36.17	AL	43.72	NA+K	20.11

COORDINATES IN THE SYSTEM PLAGIOCLASE - OLIVINE - CLINOPYROXENE - QUARTZ (IN MOLE PERCENT)

PROPORTION OF ANALYSIS IN BASALT TETRAHEDRON IS 91.16 MOLE PERCENT

	OL	CPX	PLAG	QTZ
BASALT TETRAHEDRON	16.24	8.75	61.07	13.93
CLINOPYROXENE PROJECTION	17.80	0.0	66.93	15.27
QUARTZ PROJECTION	18.87	10.17	70.96	0.0
PLAGIOCLASE PROJECTION	41.72	22.48	0.0	35.80
OLIVINE PROJECTION	0.0	6.97	48.64	OPX+(4QTZ) 44.39

CMAS PROJECTIONS

TETRAHEDRON COORDINATES	C	16.34	M	14.89	A	15.59	S	53.19
DIOPSIDE PROJECTION	C3A	32.67	M	14.17	S	53.16		
OLIVINE PROJECTION	CS	20.21	M	62.87	S	16.92		
ENSTATITE PROJECTION	M2S	20.04	C2S3	35.49	A2S3	44.47		
QUARTZ PROJECTION	CAS2	73.27	MS	23.98	CMS2	2.75		

SAMPLE NUMBER NZ 7-4TN81

ORIGINAL WEIGHT PERCENT OXIDES

SIO2	AL203	FE203	FEO	MNO	MGO	CAO	NA2O	K2O	TIO2	P2O5	CR2O3	TOTAL
56.07	13.69	3.66	8.24	.20	6.12	7.11	3.34	.22	.99	.43	.00	100.08

WEIGHT PERCENT OXIDES RECALCULATED TO 100 PERCENT

SIO2	AL203	FE203	FEO	MNO	MGO	CAO	NA2O	K2O	TIO2	P2O5	CR2O3	TOTAL
56.03	13.68	3.66	8.24	.20	6.12	7.10	3.34	.22	.99	.43	.00	100.00

CATION PROPORTIONS IN ANALYSIS

SI	AL	FE(3)	FE(2)	MN	MG	CA	NA	K	TI	P	CR
52.58	15.13	2.59	6.47	.16	8.55	7.14	6.07	.26	.70	.34	.00

CIPW NORM

	QTZ	COR	OR	AB	AN	LC	NE	KP
WEIGHT PERCENT	10.034	.000	1.299	28.231	21.695	.000	.000	.000
MOLE PERCENT	31.339	.000	1.068	20.203	14.633	.000	.000	.000
CATION PERCENT	9.417	.000	1.316	30.361	21.990	.000	.000	.000

	AC	NS	KS	DI	WO	HY	OL	CS
WEIGHT PERCENT	.000	.000	.000	8.789	.000	21.764	.000	.000
MOLE PERCENT	.000	.000	.000	7.245	.000	18.319	.000	.000
CATION PERCENT	.000	.000	.000	8.709	.000	22.020	.000	.000

	MT	CM	IL	HM	TN	PF	RU	AP
WEIGHT PERCENT	5.310	.000	1.879	.000	.000	.000	.000	1.018
MOLE PERCENT	4.303	.000	2.323	.000	.000	.000	.000	.568
CATION PERCENT	3.880	.000	1.396	.000	.000	.000	.000	.910

MAFIC INDEX = 38.759
NORM TOTAL = 100.018

OLIVINE COMPOSITION
FORSTERITE .000 FAYALITE .000

ORTHOPYROXENE COMPOSITION
ENSTATITE 58.424 FERROSILITE 41.576

CLINOPYROXENE COMPOSITION
WOLLASTONITE 51.029 ENSTATITE 28.611 FERROSILITE 20.360

FELDSPAR COMPOSITION
ORTHOCLASE 2.536 ALBITE 55.112 ANORTHITE 42.352
PLAGIOCLASE COMPOSITION (PERC AN) 43.454

THORNTON AND TUTTLE DIFFERENTIATION INDEX	=	39.564
SOLIDIFICATION INDEX (100*MGO/(MGO+FEO+FE2O3+NA2O+K2O))	=	28.348
CRYSTALLIZATION INDEX (AN+MG.DI+FO+FO EQIV OF EN)	=	36.030
LARSEN INDEX (1/3SI+K)-(CA+MG)	=	2.234
ALBITE RATIO (100*(AB+AB EQIV IN NE)/PLAG)	=	56.546
IRON RATIO ((FE2=MN)*100/(FE2+MN+MG))	=	64.005
MG NUMBER AS CATIONS MG/CATIONS (FE+MG)	=	56.950
OXIDATION RATIO ACCORDING TO LE MAITRE (FEO/FEO+FE2O3)	=	.826
DENSITY OF DRY LIQUID OF THIS COMPOSITION (AT 1050 DEG)	=	2.627

AFM RATIO
TOTAL ALKALIS 16.78 TOTAL FE 54.39 MG 28.84

KOMATIITE PARAMETERS

FEO/(FEO+MGO)	CAO/AL2O3	SIO2/TIO2	AL2O3/TIO2	FEO*/TIO2	CAO/TIO2	NA2O/TIO2	K2O/TIO2
.6535	.52	56.64	13.83	11.66	7.18	3.374	.222

JENSEN CATION

AL2O3	- FEO+FE2O3+TIO2	- MGO
45.26	29.16	25.58

QUARTZ - FELDSPAR RATIOS
QUARTZ 16.38 ORTHOCLASE 2.12 PLAGIOCLASE 81.50
QUARTZ 25.36 ORTHOCLASE 3.28 ALBITE 71.36

CATION PROPORTIONS						
	CA	30.45	FE	33.08	MG	36.47
	CA	10.46	MG	12.53	SI	77.01
	SI	76.54	AL	11.01	MG	12.45
	2MG	39.66	2FE	35.97	SI/5	24.38
	CA	39.96	AL	42.32	NA+K	17.72

COORDINATES IN THE SYSTEM PLAGIOCLASE - OLIVINE - CLINOPYROXENE - QUARTZ (IN MOLE PERCENT)

PROPORTION OF ANALYSIS IN BASALT TETRAHEDRON IS 92.50 MOLE PERCENT

BASALT TETRAHEDRON	OL	17.85	CPX	9.42	PLAG	56.60	QTZ	16.13
CLINOPYROXENE PROJECTION		19.71		0.0		62.48		17.81
QUARTZ PROJECTION		21.29		11.23		67.48		0.0
PLAGIOCLASE PROJECTION		41.14		21.69		0.0		37.17
OLIVINE PROJECTION		0.0		7.21		43.35	OPX+(4QTZ)	49.43

CMAS PROJECTIONS

TETRAHEDRON COORDINATES	C	14.95	M	16.77	A	14.73	S	53.55
DIOPSIDE PROJECTION	C3A	31.67	M	14.76	S	53.57		
OLIVINE PROJECTION	CS	18.66	M	65.20	S	16.14		
ENSTATITE PROJECTION	M2S	17.84	C2S3	35.80	A2S3	46.36		
QUARTZ PROJECTION	CAS2	70.58	MS	28.62	CMS2	.80		

SAMPLE NUMBER NZ 7-STN81

ORIGINAL WEIGHT PERCENT OXIDES

SIO2	AL2O3	FE2O3	FEO	MNO	MGO	CAO	NA2O	K2O	TIO2	P2O5	CR2O3	TOTAL
59.65	13.06	3.28	7.39	.18	5.01	5.22	2.92	2.00	.94	.40	.00	100.05

WEIGHT PERCENT OXIDES RECALCULATED TO 100 PERCENT

SIO2	AL2O3	FE2O3	FEO	MNO	MGO	CAO	NA2O	K2O	TIO2	P2O5	CR2O3	TOTAL
59.62	13.05	3.28	7.39	.18	5.01	5.22	2.92	2.00	.94	.40	.00	100.00

CATION PROPORTIONS IN ANALYSIS

SI	AL	FE(3)	FE(2)	MN	MG	CA	NA	K	TI	P	CR
56.19	14.50	2.33	5.82	.14	7.03	5.27	5.33	2.40	.67	.32	.00

CIPW NORM

	QTZ	COR	OR	AB	AN	LC	NE	KP
WEIGHT PERCENT	14.533	.000	11.812	24.687	16.612	.000	.000	.000
MOLE PERCENT	40.777	.000	8.721	15.872	10.066	.000	.000	.000
CATION PERCENT	13.696	.000	12.017	26.660	16.908	.000	.000	.000

	AC	NS	KS	DI	WO	HY	OL	CS
WEIGHT PERCENT	.000	.000	.000	5.461	.000	19.420	.000	.000
MOLE PERCENT	.000	.000	.000	4.034	.000	14.607	.000	.000
CATION PERCENT	.000	.000	.000	5.420	.000	19.625	.000	.000

	MT	CM	IL	HM	TN	PF	RU	AP
WEIGHT PERCENT	4.760	.000	1.784	.000	.000	.000	.000	.947
MOLE PERCENT	3.466	.000	1.982	.000	.000	.000	.000	.475
CATION PERCENT	3.492	.000	1.332	.000	.000	.000	.000	.851

MAFIC INDEX = 32.373
NORM TOTAL = 100.017

OLIVINE COMPOSITION
FORSTERITE .000 FAYALITE .000

ORTHOPYROXENE COMPOSITION
ENSTATITE 56.424 FERROSILITE 43.576

CLINOPYROXENE COMPOSITION
WOLLASTONITE 50.896 ENSTATITE 27.706 FERROSILITE 21.398

FELDSPAR COMPOSITION
ORTHOCLASE 22.240 ALBITE 46.482 ANORTHITE 31.278
PLAGIOCLASE COMPOSITION (PERC AN) 40.224

THORNTON AND TUTTLE DIFFERENTIATION INDEX = 51.032
SOLIDIFICATION INDEX (100*MGO/(MGO+FEO+FE2O3+NA2O+K2O)) = 24.316
CRYSTALLIZATION INDEX (AN+MG.DI+FO+FO EQIV OF EN) = 27.556
LARSEN INDEX (1/3SI+K)-(CA+MG) = 8.713
ALBITE RATIO (100*(AB+AB EQIV IN NE)/PLAG) = 59.776
IRON RATIO ((FE2+MN)*100/(FE2+MN+MG)) = 66.067
MG NUMBER AS CATIONS MG/CATIONS (FE+MG) = 54.715
OXIDATION RATIO ACCORDING TO LE MAITRE (FEO/FEO+FE2O3) = .801
DENSITY OF DRY LIQUID OF THIS COMPOSITION (AT 1050 DEG) = 2.569
AFM RATIO
TOTAL ALKALIS 24.27 TOTAL FE 51.02 MG 24.71

KOMATIITE PARAMETERS

FEO/(FEO+MGO)	CAO/AL2O3	SIO2/TIO2	AL2O3/TIO2	FEO*/TIO2	CAO/TIO2	NA2O/TIO2	K2O/TIO2
.6737	.40	63.46	13.89	11.01	5.55	3.106	2.128

JENSEN CATION AL2O3 - FEO+FE2O3+TIO2 - MGO
47.78 29.05 23.17

QUARTZ - FELDSPAR RATIOS

QUARTZ	21.48	ORTHOCLASE	17.46	PLAGIOCLASE	61.05	
QUARTZ	28.48	ORTHOCLASE	23.15	ALBITE	48.38	

CATION PROPORTIONS						
CA	27.31	FE	36.21	MG	36.47
CA	7.69	MG	10.27	SI	82.04
SI	79.73	AL	10.29	MG	9.98
2MG	35.82	2FE	35.57	SI/5	28.61
CA	32.15	AL	44.24	NA+K	23.61

COORDINATES IN THE SYSTEM PLAGIOCLASE - OLIVINE - CLINOPYROXENE - QUARTZ (IN MOLE PERCENT)

PROPORTION OF ANALYSIS IN BASALT TETRAHEDRON IS 82.31 MOLE PERCENT

BASALT TETRAHEDRON	OL	17.88	CPX	6.58	PLAG	52.93	QTZ	22.60
CLINOPYROXENE PROJECTION		19.14		0.0		56.66		24.19
QUARTZ PROJECTION		23.10		8.51		68.39		0.0
PLAGIOCLASE PROJECTION		37.99		13.99		0.0		48.02
OLIVINE PROJECTION		0.0		4.39		35.31	OPX+(4QTZ)	60.30

CMAS PROJECTIONS

TETRAHEDRON COORDINATES	C	14.47	M	14.31	A	15.02	S	56.21
DIOPSIDE PROJECTION	C3A	31.41	M	14.01	S	54.59		
OLIVINE PROJECTION	CS	16.55	M	68.38	S	15.07		
ENSTATITE PROJECTION	M2S	6.15	C2S3	39.71	A2S3	54.15		
QUARTZ PROJECTION	CAS2	*****	MS	*****	CMS2	*****		

SAMPLE NUMBER NZ 7-7TN81

ORIGINAL WEIGHT PERCENT OXIDES

SIO2	AL203	FE203	FEO	MNO	MGO	CAO	NA2O	K2O	TIO2	P2O5	CR2O3	TOTAL
56.88	15.55	3.46	7.78	.15	3.80	7.32	2.83	.79	1.04	.45	.00	100.06

WEIGHT PERCENT OXIDES RECALCULATED TO 100 PERCENT

SIO2	AL203	FE203	FEO	MNO	MGO	CAO	NA2O	K2O	TIO2	P2O5	CR2O3	TOTAL
56.85	15.54	3.46	7.78	.15	3.80	7.32	2.83	.79	1.04	.45	.00	100.00

CATION PROPORTIONS IN ANALYSIS

SI	AL	FE(3)	FE(2)	MN	MG	CA	NA	K	TI	P	CR
53.86	17.35	2.47	6.16	.12	5.36	7.43	5.19	.95	.74	.36	.00

CIPW NORM

	QTZ	COR	OR	AB	AN	LC	NE	KP
WEIGHT PERCENT	14.050	.000	4.666	23.926	27.378	.000	.000	.000
MOLE PERCENT	40.495	.000	3.538	15.800	17.040	.000	.000	.000
CATION PERCENT	13.311	.000	4.771	25.973	28.010	.000	.000	.000

	AC	NS	KS	DI	WO	HY	OL	CS
WEIGHT PERCENT	.000	.000	.000	4.954	.000	16.991	.000	.000
MOLE PERCENT	.000	.000	.000	3.720	.000	12.854	.000	.000
CATION PERCENT	.000	.000	.000	4.892	.000	16.901	.000	.000

	MT	CM	IL	HM	TN	PF	RU	AP
WEIGHT PERCENT	5.015	.000	1.974	.000	.000	.000	.000	1.065
MOLE PERCENT	3.751	.000	2.253	.000	.000	.000	.000	.549
CATION PERCENT	3.699	.000	1.481	.000	.000	.000	.000	.962

MAFIC INDEX = 30.000
NORM TOTAL = 100.019

OLIVINE COMPOSITION
FORSTERITE .000 FAYALITE .000

ORTHOPYROXENE COMPOSITION
ENSTATITE 48.631 FERROSILITE 51.369

CLINOPYROXENE COMPOSITION
WOLLASTONITE 50.371 ENSTATITE 24.135 FERROSILITE 25.494

FELDSPAR COMPOSITION
ORTHOCLASE 8.336 ALBITE 42.748 ANORTHITE 48.916
PLAGIOCLASE COMPOSITION (PERC AN) 53.364

THORNTON AND TUTTLE DIFFERENTIATION INDEX = 42.642
SOLIDIFICATION INDEX (100*MGO/(MGO+FEO+FE2O3+NA2O+K2O)) = 20.358
CRYSTALLIZATION INDEX (AN+MG.DI+FO+FO EQIV OF EN) = 35.748
LARSEN INDEX (1/3SI+K)-(CA+MG) = 6.497
ALBITE RATIO (100*(AB+AB EQIV IN NE)/PLAG) = 46.636
IRON RATIO ((FE2+MN)*100/(FE2+MN+MG)) = 72.908
MG NUMBER AS CATIONS MG/CATIONS (FE+MG) = 46.520
OXIDATION RATIO ACCORDING TO LE MAITRE (FEO/FEO+FE2O3) = .834
DENSITY OF DRY LIQUID OF THIS COMPOSITION (AT 1050 DEG) = 2.600
AFM RATIO
TOTAL ALKALIS 19.76 TOTAL FE 59.50 MG 20.74

KOMATIITE PARAMETERS

FEO/(FEO+MGO)	CAO/AL2O3	SIO2/TIO2	AL2O3/TIO2	FEO*/TIO2	CAO/TIO2	NA2O/TIO2	K2O/TIO2
.7415	.47	54.69	14.95	10.48	7.04	2.721	.760

JENSEN CATION AL2O3 - FEO+FE2O3+TIO2 - MGO
54.08 29.20 16.71

QUARTZ - FELDSPAR RATIOS

QUARTZ	20.07	ORTHOCLASE	6.66	PLAGIOCLASE	73.27	
QUARTZ	32.95	ORTHOCLASE	10.94	ALBITE	56.11	

CATION PROPORTIONS

CA	36.79	FE	36.64	MG	26.57
CA	11.14	MG	8.05	SI	80.81
SI	79.32	AL	12.78	MG	7.90
2MG	29.55	2FE	40.76	SI/5	29.68
CA	38.72	AL	45.24	NA+K	16.03

COORDINATES IN THE SYSTEM PLAGIOCLASE - OLIVINE - CLINOPYROXENE - QUARTZ (IN MOLE PERCENT)

PROPORTION OF ANALYSIS IN BASALT TETRAHEDRON IS 89.09 MOLE PERCENT

BASALT TETRAHEDRON	OL	14.23	CPX	5.49	PLAG	60.60	QTZ	19.68
CLINOPYROXENE PROJECTION		15.06		0.0		64.12		20.83
QUARTZ PROJECTION		17.72		6.84		75.45		0.0
PLAGIOCLASE PROJECTION		36.11		13.93		0.0		49.96
OLIVINE PROJECTION		0.0		3.79		41.84	OPX+(4QTZ)	54.37

CMAS PROJECTIONS

TETRAHEDRON COORDINATES	C	15.21	M	12.78	A	16.09	S	55.92
DIOPSIDE PROJECTION	C3A	32.13	M	13.66	S	54.21		
OLIVINE PROJECTION	CS	17.15	M	66.93	S	15.92		
ENSTATITE PROJECTION	M2S	9.15	C2S3	38.02	A2S3	52.83		
QUARTZ PROJECTION	CAS2	*****	MS	*****	CMS2	*****		

SAMPLE NUMBER N27-9 TN81

ORIGINAL WEIGHT PERCENT OXIDES

SIO2	AL2O3	FE2O3	FEO	MNO	MGO	CAO	NA2O	K2O	TIO2	P2O5	CR2O3	TOTAL
53.52	14.96	2.99	8.98	.18	6.65	6.55	3.79	.28	1.10	.49	.00	99.47

WEIGHT PERCENT OXIDES RECALCULATED TO 100 PERCENT

SIO2	AL2O3	FE2O3	FEO	MNO	MGO	CAO	NA2O	K2O	TIO2	P2O5	CR2O3	TOTAL
53.81	15.04	3.01	9.02	.18	6.69	6.58	3.80	.28	1.11	.48	.00	100.00

CATION PROPORTIONS IN ANALYSIS

SI	AL	FE(3)	FE(2)	MN	MG	CA	NA	K	TI	P	CR
50.06	16.49	2.11	7.02	.14	9.27	6.56	6.85	.33	.77	.38	.00

CIPW NORM

	QTZ	COR	OR	AB	AN	LC	NE	KP
WEIGHT PERCENT	3.553	.000	1.663	32.146	23.148	.000	.000	.000
MOLE PERCENT	13.131	.000	1.617	27.218	13.473	.000	.000	.000
CATION PERCENT	3.306	.000	1.671	34.270	23.259	.000	.000	.000

	AC	NS	KS	DI	WO	HY	OL	CS
WEIGHT PERCENT	.000	.000	.000	5.219	.000	26.684	.000	.000
MOLE PERCENT	.000	.000	.000	5.080	.000	26.469	.000	.000
CATION PERCENT	.000	.000	.000	5.117	.000	26.657	.000	.000

	MT	CM	IL	HM	TN	PF	RU	AP
WEIGHT PERCENT	4.363	.000	2.100	.000	.000	.000	.000	1.143
MOLE PERCENT	4.183	.000	3.073	.000	.000	.000	.000	.755
CATION PERCENT	3.160	.000	1.548	.000	.000	.000	.000	1.014

MAFIC INDEX = 39.509
NORM TOTAL = 100.019

OLIVINE COMPOSITION
FORSTERITE .000 FAYALITE .000

ORTHOPYROXENE COMPOSITION
ENSTATITE 56.933 FERROSILITE 43.067

CLINOPYROXENE COMPOSITION
WOLLASTONITE 50.930 ENSTATITE 27.937 FERROSILITE 21.133

FELDSPAR COMPOSITION
ORTHOCLASE 2.920 ALBITE 56.439 ANORTHITE 40.641
PLAGIOCLASE COMPOSITION (PERC AN) 41.864

THORNTON AND TUTTLE DIFFERENTIATION INDEX	=	37.362
SOLIDIFICATION INDEX (100*MGO/(MGO+FEO+FE2O3+NA2O+K2O))	=	29.321
CRYSTALLIZATION INDEX (AN+MG.DI+FO+FO EQIV OF EN)	=	36.940
LARSEN INDEX (1/3SI+K)-(CA+MG)	=	1.173
ALBITE RATIO (100*(AB+AB EQIV IN NE)/PLAG)	=	58.136
IRON RATIO ((FE2*MN)*100/(FE2+MN+MG))	=	63.958
MG NUMBER AS CATIONS MG/CATIONS (FE+MG)	=	56.899
OXIDATION RATIO ACCORDING TO LE MAITRE (FEO/FEO+FE2O3)	=	.812
DENSITY OF DRY LIQUID OF THIS COMPOSITION (AT 1050 DEG)	=	2.647

AFM RATIO
TOTAL ALKALIS 18.14 TOTAL FE 52.14 MG 29.71

KOMATIITE PARAMETERS

FEO/(FEO+MGO)	CAO/AL2O3	SIO2/TIO2	AL2O3/TIO2	FEO*/TIO2	CAO/TIO2	NA2O/TIO2	K2O/TIO2
.6370	.44	48.65	13.60	10.61	5.95	3.436	.255

JENSEN CATION AL2O3 - FEO+FE2O3+TIO2 - MGO
46.24 - 27.76 - 25.99

QUARTZ - FELDSPAR RATIOS
QUARTZ 5.87 ORTHOCLASE 2.75 PLAGIOCLASE 91.38
QUARTZ 9.51 ORTHOCLASE 4.45 ALBITE 86.04

CATION PROPORTIONS	CA	27.45	FE	33.77	MG	38.78
	CA	9.96	MG	14.07	SI	75.97
	SI	74.08	AL	12.20	MG	13.72
	2MG	41.48	2FE	36.12	SI/5	22.40
	CA	35.67	AL	44.80	NA+K	19.53

COORDINATES IN THE SYSTEM PLAGIOCLASE - OLIVINE - CLINOPYROXENE - QUARTZ (IN MOLE PERCENT)

PROPORTION OF ANALYSIS IN BASALT TETRAHEDRON IS 92.61 MOLE PERCENT

BASALT TETRAHEDRON	OL	21.59	CPX	5.53	PLAG	62.12	QTZ	10.77
CLINOPYROXENE PROJECTION		22.85		0.0		65.75		11.40
QUARTZ PROJECTION		24.19		6.19		69.62		0.0
PLAGIOCLASE PROJECTION		56.99		14.59		0.0		28.42
OLIVINE PROJECTION		0.0		4.99		56.11	OPX+(4QTZ)	38.90

CMAS PROJECTIONS

TETRAHEDRON COORDINATES	C	15.38	M	18.36	A	16.02	S	50.25
DIOPSIDE PROJECTION	C3A	32.46	M	15.43	S	52.11		
OLIVINE PROJECTION	CS	20.82	M	60.15	S	19.03		
ENSTATITE PROJECTION	M2S	28.66	C2S3	30.12	A2S3	41.22		
QUARTZ PROJECTION	CAS2	*****	MS	*****	CMS2	*****		

SAMPLE NUMBER NZ 7-10TN81

ORIGINAL WEIGHT PERCENT OXIDES

SIO2	AL2O3	FE2O3	FEO	MNO	MGO	CAO	NA2O	K2O	TIO2	P2O5	CR2O3	TOTAL
54.82	14.87	2.52	8.38	.16	6.45	6.50	3.49	.17	1.16	.49	.00	99.01

WEIGHT PERCENT OXIDES RECALCULATED TO 100 PERCENT

SIO2	AL2O3	FE2O3	FEO	MNO	MGO	CAO	NA2O	K2O	TIO2	P2O5	CR2O3	TOTAL
55.37	15.02	2.54	8.47	.16	6.51	6.57	3.52	.17	1.17	.49	.00	100.00

CATION PROPORTIONS IN ANALYSIS

SI	AL	FE(3)	FE(2)	MN	MG	CA	NA	K	TI	P	CR
51.60	16.50	1.78	6.60	.13	9.05	6.56	6.37	.20	.82	.39	.00

CIPW NORM

	QTZ	COR	OR	AB	AN	LC	NE	KP
WEIGHT PERCENT	7.462	.000	1.015	29.818	24.650	.000	.000	.000
MOLE PERCENT	24.888	.000	.891	22.788	17.756	.000	.000	.000
CATION PERCENT	6.954	.000	1.021	31.843	24.811	.000	.000	.000

	AC	NS	KS	DI	WO	HY	OL	CS
WEIGHT PERCENT	.000	.000	.000	3.835	.000	26.160	.000	.000
MOLE PERCENT	.000	.000	.000	3.374	.000	23.479	.000	.000
CATION PERCENT	.000	.000	.000	3.771	.000	26.243	.000	.000

	MT	CM	IL	HM	TN	PF	RU	AP
WEIGHT PERCENT	3.683	.000	2.225	.000	.000	.000	.000	1.172
MOLE PERCENT	3.188	.000	2.938	.000	.000	.000	.000	.699
CATION PERCENT	2.672	.000	1.642	.000	.000	.000	.000	1.041

MAFIC INDEX = 37.076
NORM TOTAL = 100.020

OLIVINE COMPOSITION
FORSTERITE .000 FAYALITE .000

ORTHOPYROXENE COMPOSITION
ENSTATITE 57.863 FERROSILITE 42.137

CLINOPYROXENE COMPOSITION
WOLLASTONITE 50.992 ENSTATITE 28.358 FERROSILITE 20.651

FELDSPAR COMPOSITION
ORTHOCLASE 1.829 ALBITE 53.742 ANORTHITE 44.429
PLAGIOCLASE COMPOSITION (PERC AN) 45.257

THORNTON AND TUTTLE DIFFERENTIATION INDEX = 38.294
SOLIDIFICATION INDEX (100*MGO/(MGO+FEO+FE2O3+NA2O+K2O)) = 30.702
CRYSTALLIZATION INDEX (AN+MG DI+FO+FO EQIV OF EN) = 37.605
LARSEN INDEX (1/3SI+K)-(CA+MG) = 1.944
ALBITE RATIO (100*(AB+AB EQIV IN NE)/PLAG) = 54.743
IRON RATIO ((FE2=MN)*100/(FE2+MN+MG)) = 63.060
MG NUMBER AS CATIONS MG/CATIONS (FE+MG) = 57.823
OXIDATION RATIO ACCORDING TO LE MAITRE (FEO/FEO+FE2O3) = .821
DENSITY OF DRY LIQUID OF THIS COMPOSITION (AT 1050 DEG) = 2.630
AFM RATIO
TOTAL ALKALIS 17.63 TOTAL FE 51.29 MG 31.07

KOMATIITE PARAMETERS

FEO/(FEO+MGO)	CAO/AL2O3	SIO2/TIO2	AL2O3/TIO2	FEO*/TIO2	CAO/TIO2	NA2O/TIO2	K2O/TIO2
.6227	.44	47.26	12.82	9.18	5.60	3.009	.147

JENSEN CATION AL2O3 - FEO+FE2O3+TIO2 - MGO
47.48 26.48 26.04

QUARTZ - FELDSPAR RATIOS
QUARTZ 11.85 ORTHOCLASE 1.61 PLAGIOCLASE 86.53
QUARTZ 19.49 ORTHOCLASE 2.65 ALBITE 77.87

CATION PROPORTIONS						
	CA	28.38	FE	32.43	MG	39.18
	CA	9.75	MG	13.46	SI	76.78
	SI	74.90	AL	11.97	MG	13.13
	2MG	41.70	2FE	34.52	SI/5	23.78
	CA	36.24	AL	45.60	NA+K	18.17

COORDINATES IN THE SYSTEM PLAGIOCLASE - OLIVINE - CLINOPYROXENE - QUARTZ (IN MOLE PERCENT)
PROPORTION OF ANALYSIS IN BASALT TETRAHEDRON IS 93.62 MOLE PERCENT

BASALT TETRAHEDRON	OL	21.02	CPX	4.03	PLAG	60.51	QTZ	14.44
CLINOPYROXENE PROJECTION		21.91		0.0		63.05		15.04
QUARTZ PROJECTION		24.57		4.71		70.72		0.0
PLAGIOCLASE PROJECTION		53.24		10.20		0.0		36.56
OLIVINE PROJECTION		0.0		3.29		49.49	OPX+(4QTZ)	47.22

CMAS PROJECTIONS

TETRAHEDRON COORDINATES	C	14.56	M	17.45	A	15.46	S	52.54
DIOPSIDE PROJECTION	C3A	31.78	M	15.11	S	53.11		
OLIVINE PROJECTION	CS	18.50	M	64.27	S	17.23		
ENSTATITE PROJECTION	M2S	21.52	C2S3	32.78	A2S3	45.71		
QUARTZ PROJECTION	CAS2	*****	MS	*****	CMS2	*****		

SAMPLE NUMBER NZ 7-11TN81

ORIGINAL WEIGHT PERCENT OXIDES

SIO2	AL2O3	FE2O3	FEO	MNO	MGO	CAO	NA2O	K2O	TIO2	P2O5	CR2O3	TOTAL
57.60	14.23	3.26	7.33	.16	4.96	7.46	3.30	.13	1.02	.47	.00	100.11

WEIGHT PERCENT OXIDES RECALCULATED TO 100 PERCENT

SIO2	AL2O3	FE2O3	FEO	MNO	MGO	CAO	NA2O	K2O	TIO2	P2O5	CR2O3	TOTAL
57.54	14.21	3.25	7.32	.16	4.95	7.45	3.30	.13	1.02	.47	.00	100.00

CATION PROPORTIONS IN ANALYSIS

SI	AL	FE(3)	FE(2)	MN	MG	CA	NA	K	TI	P	CR
54.04	15.74	2.30	5.75	.13	6.94	7.50	6.37	.16	.72	.37	.00

CIPW NORM

	QTZ	COR	OR	AB	AN	LC	NE	KP
WEIGHT PERCENT	12.832	.000	.767	29.573	22.708	.000	.000	.000
MOLE PERCENT	37.813	.000	.595	19.968	14.451	.000	.000	.000
CATION PERCENT	12.053	.000	.778	31.829	23.034	.000	.000	.000

	AC	NS	KS	DI	WO	HY	OL	CS
WEIGHT PERCENT	.000	.000	.000	9.176	.000	17.199	.000	.000
MOLE PERCENT	.000	.000	.000	7.122	.000	13.602	.000	.000
CATION PERCENT	.000	.000	.000	9.081	.000	17.342	.000	.000

	MT	CM	IL	HM	TN	PF	RU	AP
WEIGHT PERCENT	4.717	.000	1.935	.000	.000	.000	.000	1.112
MOLE PERCENT	3.606	.000	2.258	.000	.000	.000	.000	.386
CATION PERCENT	3.449	.000	1.439	.000	.000	.000	.000	.996

MAFIC INDEX = 34.139
NORM TOTAL = 100.019

OLIVINE COMPOSITION
FORSTERITE .000 FAYALITE .000

ORTHOPYROXENE COMPOSITION
ENSTATITE 56.856 FERROSILITE 43.144

CLINOPYROXENE COMPOSITION
WOLLASTONITE 50.925 ENSTATITE 27.902 FERROSILITE 21.173

FELDSPAR COMPOSITION
ORTHOCLASE 1.446 ALBITE 55.748 ANORTHITE 42.805
PLAGIOCLASE COMPOSITION (PERC AN) 43.434

THORNTON AND TUTTLE DIFFERENTIATION INDEX = 43.173
SOLIDIFICATION INDEX (100*MGO/(MGO+FEO+FE2O3+NA2O+K2O)) = 25.871
CRYSTALLIZATION INDEX (AN+MG,DI+FO+FO EQIV OF EN) = 35.083
LARSEN INDEX (1/3SI+K)-(CA+MG) = 4.178
ALBITE RATIO (100*(AB+AB EQIV IN NE)/PLAG) = 56.566
IRON RATIO ((FE2+MN)*100/(FE2+MN+MG)) = 66.044
MG NUMBER AS CATIONS MG/CATIONS (FE+MG) = 54.681
OXIDATION RATIO ACCORDING TO LE MAITRE (FEO/FEO+FE2O3) = .829
DENSITY OF DRY LIQUID OF THIS COMPOSITION (AT 1050 DEG) = 2.599
AFM RATIO
TOTAL ALKALIS 19.26 TOTAL FE 54.42 MG 26.32

KOMATIITE PARAMETERS

FEO/(FEO+MGO)	CAO/AL2O3	SIO2/TIO2	AL2O3/TIO2	FEO*/TIO2	CAO/TIO2	NA2O/TIO2	K2O/TIO2
.6740	.52	56.47	13.95	10.05	7.31	3.431	.127

JENSEN CATION AL2O3 - FEO+FE2O3+TIO2 - MGO
50.05 27.89 22.06

QUARTZ - FELDSPAR RATIOS

QUARTZ	19.48		ORTHOCLASE	1.16		PLAGIOCLASE	79.36	
QUARTZ	29.72		ORTHOCLASE	1.78		ALBITE	68.50	

CATION PROPORTIONS

CA	35.15	FE	32.33	MG	32.52
CA	10.95	MG	10.13	SI	78.92
SI	78.50	AL	11.43	MG	10.07
2MG	36.06	2FE	35.85	SI/5	28.09
CA	40.26	AL	42.24	NA+K	17.51

COORDINATES IN THE SYSTEM PLAGIOCLASE - OLIVINE - CLINOPYROXENE - QUARTZ (IN MOLE PERCENT)

PROPORTION OF ANALYSIS IN BASALT TETRAHEDRON IS 93.34 MOLE PERCENT

BASALT TETRAHEDRON	OL	13.93	CPX	9.73	PLAG	58.78	QTZ	17.56
CLINOPYROXENE PROJECTION		15.44		0.0		65.11		19.45
QUARTZ PROJECTION		16.90		11.80		71.30		0.0
PLAGIOCLASE PROJECTION		33.80		23.60		0.0		42.59
OLIVINE PROJECTION		0.0		7.01		42.37	OPX+(4QTZ)	50.62

CMAS PROJECTIONS

TETRAHEDRON COORDINATES	C	15.58	M	14.06	A	15.11	S	55.25
DIOPSIDE PROJECTION	C3A	32.04	M	13.86	S	54.11		
OLIVINE PROJECTION	CS	18.27	M	66.18	S	15.55		
ENSTATITE PROJECTION	M2S	11.62	C2S3	38.86	A2S3	49.52		
QUARTZ PROJECTION	CAS2	74.15	MS	24.07	CMS2	1.78		

SAMPLE NUMBER NZ 7-12TN81

ORIGINAL WEIGHT PERCENT OXIDES

SIO2	AL2O3	FE2O3	FEO	MNO	MGO	CAO	NA2O	K2O	TIO2	P2O5	CR2O3	TOTAL
55.73	14.74	3.46	7.79	.18	5.06	7.08	3.85	.43	1.00	.46	.00	99.79

WEIGHT PERCENT OXIDES RECALCULATED TO 100 PERCENT

SIO2	AL2O3	FE2O3	FEO	MNO	MGO	CAO	NA2O	K2O	TIO2	P2O5	CR2O3	TOTAL
55.85	14.77	3.47	7.81	.18	5.07	7.10	3.86	.43	1.00	.46	.00	100.00

CATION PROPORTIONS IN ANALYSIS

SI	AL	FE(3)	FE(2)	MN	MG	CA	NA	K	TI	P	CR
52.25	16.29	2.44	6.11	.14	7.07	7.11	7.00	.51	.71	.37	.00

CIPW NORM

	QTZ	COR	OR	AB	AN	LC	NE	KP
WEIGHT PERCENT	7.940	.000	2.546	32.637	21.714	.000	.000	.000
MOLE PERCENT	26.245	.000	2.215	24.718	15.500	.000	.000	.000
CATION PERCENT	7.428	.000	2.572	34.988	21.939	.000	.000	.000

	AC	NS	KS	DI	WO	HY	OL	CS
WEIGHT PERCENT	.000	.000	.000	8.602	.000	18.550	.000	.000
MOLE PERCENT	.000	.000	.000	7.475	.000	16.393	.000	.000
CATION PERCENT	.000	.000	.000	8.464	.000	18.360	.000	.000

	MT	CM	IL	HM	TN	PF	RU	AP
WEIGHT PERCENT	5.033	.000	1.903	.000	.000	.000	.000	1.092
MOLE PERCENT	4.317	.000	2.491	.000	.000	.000	.000	.645
CATION PERCENT	3.666	.000	1.410	.000	.000	.000	.000	.974

MAFIC INDEX = 35.181
NORM TOTAL = 100.019

OLIVINE COMPOSITION
FORSTERITE .000 FAYALITE .000

ORTHOPYROXENE COMPOSITION
ENSTATITE 55.440 FERROSILITE 44.560

CLINOPYROXENE COMPOSITION
WOLLASTONITE 50.830 ENSTATITE 27.260 FERROSILITE 21.910

FELDSPAR COMPOSITION
ORTHOCLASE 4.475 ALBITE 57.361 ANORTHITE 38.163
PLAGIOCLASE COMPOSITION (PERC AN) 39.951

THORNTON AND TUTTLE DIFFERENTIATION INDEX	=	43.123
SOLIDIFICATION INDEX (100*MGO/(MGO+FEO+FE2O3+NA2O+K2O))	=	24.568
CRYSTALLIZATION INDEX (AN+MG.DI+FO+FO EQIV OF EN)	=	33.979
LARSEN INDEX (1/3SI+K)-(CA+MG)	=	4.028
ALBITE RATIO (100*(AB+AB EQIV IN NE)/PLAG)	=	60.049
IRON RATIO ((FE2+MN)*100/(FE2+MN+MG))	=	67.001
MG NUMBER AS CATIONS MG/CATIONS (FE+MG)	=	53.644
OXIDATION RATIO ACCORDING TO LE MAITRE (FEO/FEO+FE2O3)	=	.814
DENSITY OF DRY LIQUID OF THIS COMPOSITION (AT 1050 DEG)	=	2.611

AFM RATIO
TOTAL ALKALIS 21.14 TOTAL FE 53.87 MG 24.99

KOMATIITE PARAMETERS

FEO/(FEO+MGO)	CAO/AL2O3	SIO2/TIO2	AL2O3/TIO2	FEO*/TIO2	CAO/TIO2	NA2O/TIO2	K2O/TIO2
.6831	.48	55.73	14.74	10.91	7.08	3.850	.430

JENSEN CATION	AL2O3	- FEO+FE2O3+TIO2	- MGO
	49.94	28.39	21.68

QUARTZ - FELDSPAR RATIOS
QUARTZ 12.25 ORTHOCLASE 3.93 PLAGIOCLASE 83.83
QUARTZ 18.41 ORTHOCLASE 5.90 ALBITE 75.68

CATION PROPORTIONS						
CA	33.06	FE	34.08	MG	32.87
CA	10.70	MG	10.64	SI	78.65
SI	77.45	AL	12.07	MG	10.48
2MG	36.03	2FE	37.35	SI/5	26.62
CA	37.41	AL	42.83	NA+K	19.76

COORDINATES IN THE SYSTEM PLAGIOCLASE - OLIVINE - CLINOPYROXENE - QUARTZ (IN MOLE PERCENT)

PROPORTION OF ANALYSIS IN BASALT TETRAHEDRON IS 91.38 MOLE PERCENT

BASALT TETRAHEDRON	OL	15.23	CPX	9.26	PLAG	62.30	QTZ	13.21
CLINOPYROXENE PROJECTION		16.79		0.0		68.66		14.55
QUARTZ PROJECTION		17.55		10.67		71.78		0.0
PLAGIOCLASE PROJECTION		40.40		24.57		0.0		35.03
OLIVINE PROJECTION		0.0		7.45		50.09	OPX+(4QTZ)	42.47

CMAS PROJECTIONS

TETRAHEDRON COORDINATES	C	16.45	M	14.81	A	16.23	S	52.51
DIOPSIDE PROJECTION	C3A	32.94	M	14.25	S	52.81		
OLIVINE PROJECTION	CS	20.50	M	61.75	S	17.79		
ENSTATITE PROJECTION	M2S	22.38	C2S3	33.81	A2S3	43.81		
QUARTZ PROJECTION	CAS2	74.90	MS	24.30	CMS2	.80		

SAMPLE NUMBER NZ 7-13TN81

ORIGINAL WEIGHT PERCENT OXIDES

SIO2	AL2O3	FE2O3	FEO	MNO	MGO	CAO	NA2O	K2O	TIO2	P2O5	CR2O3	TOTAL
57.30	14.44	3.23	7.25	.16	4.55	7.49	3.77	.27	1.00	.44	.00	99.90

WEIGHT PERCENT OXIDES RECALCULATED TO 100 PERCENT

SIO2	AL2O3	FE2O3	FEO	MNO	MGO	CAO	NA2O	K2O	TIO2	P2O5	CR2O3	TOTAL
57.36	14.45	3.23	7.26	.16	4.55	7.50	3.77	.27	1.00	.44	.00	100.00

CATION PROPORTIONS IN ANALYSIS

SI	AL	FE(3)	FE(2)	MN	MG	CA	NA	K	TI	P	CR
53.79	15.98	2.28	5.70	.13	6.37	7.53	6.86	.32	.71	.35	.00

CIPW NORM

	QTZ	COR	OR	AB	AN	LC	NE	KP
WEIGHT PERCENT	11.248	.000	1.597	31.922	21.702	.000	.000	.000
MOLE PERCENT	34.397	.000	1.285	22.368	14.333	.000	.000	.000
CATION PERCENT	10.547	.000	1.617	34.301	21.978	.000	.000	.000

	AC	NS	KS	DI	WO	HY	OL	CS
WEIGHT PERCENT	.000	.000	.000	10.368	.000	15.554	.000	.000
MOLE PERCENT	.000	.000	.000	8.330	.000	12.699	.000	.000
CATION PERCENT	.000	.000	.000	10.218	.000	15.577	.000	.000

	MT	CM	IL	HM	TN	PF	RU	AP
WEIGHT PERCENT	4.681	.000	1.901	.000	.000	.000	.000	1.043
MOLE PERCENT	3.714	.000	2.302	.000	.000	.000	.000	.570
CATION PERCENT	3.417	.000	1.412	.000	.000	.000	.000	.932

MAFIC INDEX = 33.547
NORM TOTAL = 100.017

OLIVINE COMPOSITION
FORSTERITE .000 FAYALITE .000

ORTHOPYROXENE COMPOSITION
ENSTATITE 54.917 FERROSILITE 45.083

CLINOPYROXENE COMPOSITION
WOLLASTONITE 50.795 ENSTATITE 27.022 FERROSILITE 22.183

FELDSPAR COMPOSITION
ORTHOCLASE 2.892 ALBITE 57.808 ANORTHITE 39.300
PLAGIOCLASE COMPOSITION (PERC AN) 40.471

THORNTON AND TUTTLE DIFFERENTIATION INDEX = 44.767
SOLIDIFICATION INDEX (100*MGO/(MGO+FEO+FE2O3+NA2O+K2O)) = 23.859
CRYSTALLIZATION INDEX (AN+MG.DI+FO+FO EQIV OF EN) = 33.732
LARSEN INDEX (1/3SI+K)-(CA+MG) = 4.813
ALBITE RATIO (100*(AB+AB EQIV IN NE)/PLAG) = 59.529
IRON RATIO ((FE2+MN)*100/(FE2+MN+MG)) = 67.744
MG NUMBER AS CATIONS MG/CATIONS (FE+MG) = 52.777
OXIDATION RATIO ACCORDING TO LE MAITRE (FEO/FEO+FE2O3) = .822
DENSITY OF DRY LIQUID OF THIS COMPOSITION (AT 1050 DEG) = 2.594
AFM RATIO
TOTAL ALKALIS 21.55 TOTAL FE 54.18 MG 24.27

KOMATIITE PARAMETERS

FEO/(FEO+MGO)	CAO/AL2O3	SIO2/TIO2	AL2O3/TIO2	FEO*/TIO2	CAO/TIO2	NA2O/TIO2	K2O/TIO2
.6906	.52	57.30	14.44	10.16	7.49	3.770	.270

JENSEN CATION AL2O3 - FEO+FE2O3+TIO2 - MGO
51.50 27.98 20.52

QUARTZ - FELDSPAR RATIOS
QUARTZ 16.92 ORTHOCLASE 2.40 PLAGIOCLASE 80.68
QUARTZ 25.13 ORTHOCLASE 3.57 ALBITE 71.31

CATION PROPORTIONS	CA	36.33	FE	32.96	MG	30.71
	CA	11.13	MG	9.40	SI	79.47
	SI	78.94	AL	11.72	MG	9.34
	2MG	34.27	2FE	36.78	SI/5	28.95
	CA	39.41	AL	41.79	NA+K	18.80

COORDINATES IN THE SYSTEM PLAGIOCLASE - OLIVINE - CLINOPYROXENE - QUARTZ (IN MOLE PERCENT)

PROPORTION OF ANALYSIS IN BASALT TETRAHEDRON IS 92.62 MOLE PERCENT

	OL	CPX	PLAG	QTZ
BASALT TETRAHEDRON	12.61	11.03	60.76	15.59
CLINOPYROXENE PROJECTION	14.18	0.0	68.30	17.53
QUARTZ PROJECTION	14.94	13.07	71.99	0.0
PLAGIOCLASE PROJECTION	32.15	28.12	0.0	39.74
OLIVINE PROJECTION	0.0	8.22	45.29	OPX+(4QTZ) 46.49

CMAS PROJECTIONS

TETRAHEDRON COORDINATES	C	16.50	M	13.41	A	15.67	S	54.42
DIOPSIDE PROJECTION	C3A	32.72	M	13.68	S	53.60		
OLIVINE PROJECTION	CS	19.60	M	64.07	S	16.33		
ENSTATITE PROJECTION	M2S	15.85	C2S3	37.44	A2S3	46.71		
QUARTZ PROJECTION	CAS2	75.14	MS	21.76	CMS2	3.09		

SAMPLE NUMBER BG 116

ORIGINAL WEIGHT PERCENT OXIDES

SIO2	AL2O3	FE2O3	FEO	MNO	MGO	CAO	NA2O	K2O	TIO2	P2O5	CR2O3	TOTAL
50.72	5.03	1.34	12.09	.19	19.28	10.22	.28	.00	.52	.09	.00	99.77

WEIGHT PERCENT OXIDES RECALCULATED TO 100 PERCENT

SIO2	AL2O3	FE2O3	FEO	MNO	MGO	CAO	NA2O	K2O	TIO2	P2O5	CR2O3	TOTAL
50.84	5.04	1.35	12.12	.19	19.33	10.24	.28	.00	.52	.09	.00	100.00

CATION PROPORTIONS IN ANALYSIS

SI	AL	FE(3)	FE(2)	MN	MG	CA	NA	K	TI	P	CR
46.69	5.46	.93	9.31	.15	26.45	10.08	.50	.00	.36	.07	.00

CIPW NORM

	QTZ	COR	OR	AB	AN	LC	NE	KP
WEIGHT PERCENT	.000	.000	.000	2.374	12.497	.000	.000	.000
MOLE PERCENT	.000	.000	.000	1.989	9.866	.000	.000	.000
CATION PERCENT	.000	.000	.000	2.498	12.395	.000	.000	.000

	AC	NS	KS	DI	WO	HY	OL	CS
WEIGHT PERCENT	.000	.000	.000	30.422	.000	44.950	6.606	.000
MOLE PERCENT	.000	.000	.000	29.789	.000	45.644	9.288	.000
CATION PERCENT	.000	.000	.000	29.936	.000	45.868	7.000	.000

	MT	CM	IL	HM	TN	PF	RU	AP
WEIGHT PERCENT	1.953	.000	.990	.000	.000	.000	.000	.214
MOLE PERCENT	1.853	.000	1.433	.000	.000	.000	.000	.140
CATION PERCENT	1.396	.000	.720	.000	.000	.000	.000	.187

MAFIC INDEX = 85.136
NORM TOTAL = 100.006

OLIVINE COMPOSITION
FORSTERITE 67.911 FAYALITE 32.089

ORTHOPYROXENE COMPOSITION
ENSTATITE 69.991 FERROSILITE 30.009

CLINOPYROXENE COMPOSITION
WOLLASTONITE 51.784 ENSTATITE 33.747 FERROSILITE 14.469

FELDSPAR COMPOSITION
ORTHOCLASE .000 ALBITE 15.965 ANORTHITE 84.035
PLAGIOCLASE COMPOSITION (PERC AN) 84.035

THORNTON AND TUTTLE DIFFERENTIATION INDEX	=	2.374
SOLIDIFICATION INDEX (100*MGO/(MGO+FEO+FE2O3+NA2O+K2O))	=	58.431
CRYSTALLIZATION INDEX (AN+MG DI+FO+FO EQIV OF EN)	=	61.177
LARSEN INDEX (1/3SI+K)-(CA+MG)	=	-21.725
ALBITE RATIO (100*(AB+AB EQIV IN NE)/PLAG)	=	15.965
IRON RATIO ((FE2+MN)*100/(FE2+MN+MG))	=	45.086
MG NUMBER AS CATIONS MG/CATIONS (FE+MG)	=	73.966
OXIDATION RATIO ACCORDING TO LE MAITRE (FEO/FEO+FE2O3)	=	.843
DENSITY OF DRY LIQUID OF THIS COMPOSITION (AT 1050 DEG)	=	2.843

AFM RATIO
TOTAL ALKALIS .85 TOTAL FE 40.48 MG 58.67

KOMATIITE PARAMETERS

FEO/(FEO+MGO)	CAO/AL2O3	SIO2/TIO2	AL2O3/TIO2	FEO*/TIO2	CAO/TIO2	NA2O/TIO2	K2O/TIO2
.4083	2.03	97.54	9.67	25.58	19.65	.538	.000

JENSEN CATION AL2O3 - FEO+FE2O3+TIO2 - MGO
12.84 24.94 62.22

QUARTZ - FELDSPAR RATIOS

QUARTZ	.00	ORTHOCLASE	.00	PLAGIOCLASE	*****		
QUARTZ	.00	ORTHOCLASE	.00	ALBITE	*****		
CATION PROPORTIONS		CA	21.77	FE	21.11	MG	57.13
		CA	12.11	MG	31.79	SI	56.10
		SI	61.54	AL	3.60	MG	34.87
		2MG	64.68	2FE	23.90	SI/5	11.42
		CA	77.19	AL	20.90	NA+K	1.91

COORDINATES IN THE SYSTEM PLAGIOCLASE - OLIVINE - CLINOPYROXENE - QUARTZ (IN MOLE PERCENT)

PROPORTION OF ANALYSIS IN BASALT TETRAHEDRON IS 97.70 MOLE PERCENT

BASALT TETRAHEDRON	OL	42.38	CPX	30.64	PLAG	15.24	QTZ	11.74
CLINOPYROXENE PROJECTION		61.10		0.0		21.98		16.92
QUARTZ PROJECTION		48.01		34.72		17.27		0.0
PLAGIOCLASE PROJECTION		50.00		36.15		0.0		13.85
OLIVINE PROJECTION		0.0		33.01		16.42	OPX+(4QTZ)	50.57

CMAS PROJECTIONS

TETRAHEDRON COORDINATES	C	10.90	M	37.03	A	3.96	S	48.11
DIOPSIDE PROJECTION	C3A	19.07	M	27.30	S	53.62		
OLIVINE PROJECTION	CS	23.33	M	69.22	S	7.44		
ENSTATITE PROJECTION	M2S	40.11	C2S3	40.53	A2S3	19.36		
QUARTZ PROJECTION	CAS2	19.59	MS	53.71	CMS2	26.70		

SAMPLE NUMBER BG 121

ORIGINAL WEIGHT PERCENT OXIDES

SIO2	AL2O3	FE2O3	FEO	MNO	MGO	CAO	NA2O	K2O	TIO2	P2O5	CR2O3	TOTAL
50.18	4.78	1.29	11.58	.19	21.99	8.99	.00	.00	.35	.08	.66	100.09

WEIGHT PERCENT OXIDES RECALCULATED TO 100 PERCENT

SIO2	AL2O3	FE2O3	FEO	MNO	MGO	CAO	NA2O	K2O	TIO2	P2O5	CR2O3	TOTAL
50.14	4.78	1.29	11.57	.19	21.97	8.98	.00	.00	.35	.08	.66	100.0(

CATION PROPORTIONS IN ANALYSIS

SI	AL	FE(3)	FE(2)	MN	MG	CA	NA	K	TI	P	CR
45.66	5.13	.88	8.81	.15	29.82	8.77	.00	.00	.24	.06	.47

CIPW NORM

	QTZ	COR	OR	AB	AN	LC	NE	KP
WEIGHT PERCENT	.000	.000	.000	.000	13.031	.000	.000	.000
MOLE PERCENT	.000	.000	.000	.000	10.054	.000	.000	.000
CATION PERCENT	.000	.000	.000	.000	12.817	.000	.000	.000

	AC	NS	KS	DI	WO	HY	OL	CS
WEIGHT PERCENT	.000	.000	.000	24.880	.000	48.753	9.653	.000
MOLE PERCENT	.000	.000	.000	23.921	.000	48.859	13.446	.000
CATION PERCENT	.000	.000	.000	24.396	.000	49.825	10.284	.000

	MT	CM	IL	HM	TN	PF	RU	AP
WEIGHT PERCENT	1.865	.971	.664	.000	.000	.000	.000	.189
MOLE PERCENT	1.729	.931	.939	.000	.000	.000	.000	.121
CATION PERCENT	1.322	.712	.479	.000	.000	.000	.000	.164

MAFIC INDEX = 86.976
NORM TOTAL = 100.007

OLIVINE COMPOSITION
FORSTERITE 71.918 FAYALITE 28.082

ORTHOPYROXENE COMPOSITION
ENSTATITE 73.838 FERROSILITE 26.162

CLINOPYROXENE COMPOSITION
WOLLASTONITE 52.030 ENSTATITE 35.420 FERROSILITE 12.550

FELDSPAR COMPOSITION
ORTHOCLASE .000 ALBITE .000 ANORTHITE ******
PLAGIOCLASE COMPOSITION (PERC AN) ******

THORNTON AND TUTTLE DIFFERENTIATION INDEX = .000
SOLIDIFICATION INDEX (100*MGO/(MGO+FEO+FE2O3+NA2O+K2O)) = 63.083
CRYSTALLIZATION INDEX (AN+MG DI+FO+FO EQIV OF EN) = 64.211
LARSEN INDEX (1/3SI+K)-(CA+MG) = -24.160
ALBITE RATIO (100*(AB+AB EQIV IN NE)/PLAG) = .000
IRON RATIO ((FE2=MN)*100/(FE2+MN+MG)) = 40.825
MG NUMBER AS CATIONS MG/CATIONS (FE+MG) = 77.187
OXIDATION RATIO ACCORDING TO LE MAITRE (FEO/FEO+FE2O3) = .838
DENSITY OF DRY LIQUID OF THIS COMPOSITION (AT 1050 DEG) = 2.852
AFM RATIO
TOTAL ALKALIS .00 TOTAL FE 36.68 MG 63.32

KOMATIITE PARAMETERS

FEO/(FEO+MGO)	CAO/AL2O3	SIO2/TIO2	AL2O3/TIO2	FEO*/TIO2	CAO/TIO2	NA2O/TIO2	K2O/TIO2
.3668	1.88	143.37	13.66	36.40	25.69	.000	.000

JENSEN CATION AL2O3 - FEO+FE2O3+TIO2 - MGO
11.42 22.14 66.44

QUARTZ - FELDSPAR RATIOS

QUARTZ	.00	ORTHOCLASE	.00	PLAGIOCLASE	*****		
QUARTZ	.00	ORTHOCLASE	.00	ALBITE	.00		

CATION PROPORTIONS

CA	18.32	FE	19.34	MG	62.34
CA	10.40	MG	35.40	SI	54.20
SI	58.50	AL	3.28	MG	38.21
2MG	68.34	2FE	21.20	SI/5	10.46
CA	77.37	AL	22.63	NA+K	.00

COORDINATES IN THE SYSTEM PLAGIOCLASE - OLIVINE - CLINOPYROXENE - QUARTZ (IN MOLE PERCENT)

PROPORTION OF ANALYSIS IN BASALT TETRAHEDRON IS 97.32 MOLE PERCENT

BASALT TETRAHEDRON	OL	48.96	CPX	25.07	PLAG	13.17	QTZ	12.80
CLINOPYROXENE PROJECTION		65.34		0.0		17.58		17.08
QUARTZ PROJECTION		56.15		28.75		15.10		0.0
PLAGIOCLASE PROJECTION		56.39		28.87		0.0		14.74
OLIVINE PROJECTION		0.0		28.03		14.73	OPX+(4QTZ)	57.24

CMAS PROJECTIONS

TETRAHEDRON COORDINATES	C	8.99	M	40.00	A	3.61	S	47.39
DIOPSIDE PROJECTION	C3A	17.03	M	29.43	S	53.55		
OLIVINE PROJECTION	CS	20.45	M	72.34	S	7.21		
ENSTATITE PROJECTION	M2S	44.66	C2S3	36.22	A2S3	19.12		
QUARTZ PROJECTION	CAS2	17.80	MS	61.58	CMS2	20.62		

SAMPLE NUMBER BG 122

ORIGINAL WEIGHT PERCENT OXIDES

SIO2	AL2O3	FE2O3	FEO	MNO	MGO	CAO	NA2O	K2O	TIO2	P2O5	CR2O3	TOTAL
50.79	5.69	1.25	11.23	.27	20.64	9.92	.00	.02	.61	.09	.42	100.93

WEIGHT PERCENT OXIDES RECALCULATED TO 100 PERCENT

SIO2	AL2O3	FE2O3	FEO	MNO	MGO	CAO	NA2O	K2O	TIO2	P2O5	CR2O3	TOTAL
50.32	5.64	1.24	11.12	.27	20.45	9.83	.00	.02	.60	.09	.42	100.00

CATION PROPORTIONS IN ANALYSIS

SI	AL	FE(3)	FE(2)	MN	MG	CA	NA	K	TI	P	CR
46.03	6.08	.85	8.51	.21	27.88	9.63	.00	.02	.42	.07	.30

CIPW NORM

	QTZ	COR	OR	AB	AN	LC	NE	KP
WEIGHT PERCENT	.000	.000	.117	.000	15.324	.000	.000	.000
MOLE PERCENT	.000	.000	.112	.000	12.047	.000	.000	.000
CATION PERCENT	.000	.000	.116	.000	15.138	.000	.000	.000

	AC	NS	KS	DI	WO	HY	OL	CS
WEIGHT PERCENT	.000	.000	.000	26.380	.000	48.279	6.143	.000
MOLE PERCENT	.000	.000	.000	25.826	.000	49.230	8.702	.000
CATION PERCENT	.000	.000	.000	25.960	.000	49.484	6.559	.000

	MT	CM	IL	HM	TN	PF	RU	AP
WEIGHT PERCENT	1.793	.613	1.148	.000	.000	.000	.000	.211
MOLE PERCENT	1.693	.599	1.654	.000	.000	.000	.000	.137
CATION PERCENT	1.276	.451	.832	.000	.000	.000	.000	.184

MAFIC INDEX = 84.566
NORM TOTAL = 100.008

OLIVINE COMPOSITION
FORSTERITE 71.367 FAYALITE 28.633

ORTHOPYROXENE COMPOSITION
ENSTATITE 73.311 FERROSILITE 26.689

CLINOPYROXENE COMPOSITION
WOLLASTONITE 51.997 ENSTATITE 35.191 FERROSILITE 12.812

FELDSPAR COMPOSITION
ORTHOCLASE .758 ALBITE .000 ANORTHITE 99.242
PLAGIOCLASE COMPOSITION (PERC AN) ******

THORNTON AND TUTTLE DIFFERENTIATION INDEX = .117
SOLIDIFICATION INDEX (100*MGO/(MGO+FEO+FE2O3+NA2O+K2O)) = 62.291
CRYSTALLIZATION INDEX (AN+MG DI+FO+FO EQIV OF EN) = 64.538
LARSEN INDEX (1/3SI+K)-(CA+MG) = -23.000
ALBITE RATIO (100*(AB+AB EQIV IN NE)/PLAG) = .000
IRON RATIO ((FE2=MN)*100/(FE2+MN+MG)) = 41.789
MG NUMBER AS CATIONS MG/CATIONS (FE+MG) = 76.614
OXIDATION RATIO ACCORDING TO LE MAITRE (FEO/FEO+FE2O3) = .844
DENSITY OF DRY LIQUID OF THIS COMPOSITION (AT 1050 DEG) = 2.840
AFM RATIO
TOTAL ALKALIS .06 TOTAL FE 37.41 MG 62.53

KOMATIITE PARAMETERS

FEO/(FEO+MGO)	CAO/AL2O3	SIO2/TIO2	AL2O3/TIO2	FEO*/TIO2	CAO/TIO2	NA2O/TIO2	K2O/TIO2
.3744	1.74	83.26	9.33	20.25	16.26	.000	.033

JENSEN CATION AL2O3 - FEO+FE2O3+TIO2 - MGO
13.90 22.36 63.75

QUARTZ - FELDSPAR RATIOS

QUARTZ	.00		ORTHOCLASE	.76		PLAGIOCLASE	99.24	
QUARTZ	.00		ORTHOCLASE	*****		ALBITE	.00	
CATION PROPORTIONS		CA	20.74		FE	19.23	MG	60.03
		CA	11.53		MG	33.37	SI	55.10
		SI	59.82		AL	3.95	MG	36.23
		2MG	67.32		2FE	21.57	SI/5	11.11
		CA	75.95		AL	23.96	NA+K	.09

COORDINATES IN THE SYSTEM PLAGIOCLASE - OLIVINE - CLINOPYROXENE - QUARTZ (IN MOLE PERCENT)

PROPORTION OF ANALYSIS IN BASALT TETRAHEDRON IS 97.14 MOLE PERCENT

BASALT TETRAHEDRON	OL	44.96	CPX	26.72	PLAG	15.58	QTZ	12.74
CLINOPYROXENE PROJECTION		61.35		0.0		21.27		17.38
QUARTZ PROJECTION		51.52		30.62		17.86		0.0
PLAGIOCLASE PROJECTION		53.26		31.66		0.0		15.09
OLIVINE PROJECTION		0.0		28.66		16.71	OPX+(4QTZ)	54.63

CMAS PROJECTIONS

TETRAHEDRON COORDINATES	C	9.96	M	37.78	A	4.22	S	48.04
DIOPSIDE PROJECTION	C3A	19.06	M	27.27	S	53.67		
OLIVINE PROJECTION	CS	21.27	M	70.83	S	7.91		
ENSTATITE PROJECTION	M2S	40.60	C2S3	38.16	A2S3	21.24		
QUARTZ PROJECTION	CAS2	20.84	MS	57.09	CMS2	22.07		

SAMPLE NUMBER BG 123

ORIGINAL WEIGHT PERCENT OXIDES

SIO2	AL2O3	FE2O3	FEO	MNO	MGO	CAO	NA2O	K2O	TIO2	P2O5	CR2O3	TOTAL
44.94	9.37	1.45	13.01	.23	22.60	6.64	.29	.01	.39	.07	.00	99.00

WEIGHT PERCENT OXIDES RECALCULATED TO 100 PERCENT

SIO2	AL2O3	FE2O3	FEO	MNO	MGO	CAO	NA2O	K2O	TIO2	P2O5	CR2O3	TOTAL
45.40	9.47	1.46	13.14	.23	22.83	6.71	.29	.01	.39	.07	.00	100.00

CATION PROPORTIONS IN ANALYSIS

SI	AL	FE(3)	FE(2)	MN	MG	CA	NA	K	TI	P	CR
40.90	10.05	.99	9.90	.18	30.66	6.48	.51	.01	.27	.05	.00

CIPW NORM

	QTZ	COR	OR	AB	AN	LC	NE	KP
WEIGHT PERCENT	.000	.000	.060	2.478	24.481	.000	.000	.000
MOLE PERCENT	.000	.000	.053	1.903	17.724	.000	.000	.000
CATION PERCENT	.000	.000	.058	2.558	23.821	.000	.000	.000

	AC	NS	KS	DI	WO	HY	OL	CS
WEIGHT PERCENT	.000	.000	.000	6.705	.000	29.403	33.846	.000
MOLE PERCENT	.000	.000	.000	6.032	.000	27.484	43.868	.000
CATION PERCENT	.000	.000	.000	6.485	.000	29.547	35.368	.000

	MT	CM	IL	HM	TN	PF	RU	AP
WEIGHT PERCENT	2.118	.000	.748	.000	.000	.000	.000	.167
MOLE PERCENT	1.842	.000	.993	.000	.000	.000	.000	.100
CATION PERCENT	1.485	.000	.534	.000	.000	.000	.000	.144

MAFIC INDEX = 72.987
NORM TOTAL = 100.006

OLIVINE COMPOSITION
FORSTERITE 69.441 FAYALITE 30.559

ORTHOPYROXENE COMPOSITION
ENSTATITE 71.463 FERROSILITE 28.537

CLINOPYROXENE COMPOSITION
WOLLASTONITE 51.879 ENSTATITE 34.389 FERROSILITE 13.733

FELDSPAR COMPOSITION
ORTHOCLASE .221 ALBITE 9.171 ANORTHITE 90.608
PLAGIOCLASE COMPOSITION (PERC AN) 90.808

THORNTON AND TUTTLE DIFFERENTIATION INDEX = 2.538
SOLIDIFICATION INDEX (100*MGO/(MGO+FEO+FE2O3+NA2O+K2O)) = 60.500
CRYSTALLIZATION INDEX (AN+MG DI+FO+FO EQIV OF EN) = 67.683
LARSEN INDEX (1/3SI+K)-(CA+MG) = -24.942
ALBITE RATIO (100*(AB+AB EQIV IN NE)/PLAG) = 9.192
IRON RATIO ((FE2=MN)*100/(FE2+MN+MG)) = 43.020
MG NUMBER AS CATIONS MG/CATIONS (FE+MG) = 75.584
OXIDATION RATIO ACCORDING TO LE MAITRE (FEO/FEO+FE2O3) = .827
DENSITY OF DRY LIQUID OF THIS COMPOSITION (AT 1050 DEG) = 2.897
AFM RATIO
TOTAL ALKALIS .81 TOTAL FE 38.46 MG 60.74

KOMATIITE PARAMETERS

FEO/(FEO+MGO)	CAO/AL2O3	SIO2/TIO2	AL2O3/TIO2	FEO*/TIO2	CAO/TIO2	NA2O/TIO2	K2O/TIO2
.3877	.71	115.23	24.03	36.69	17.03	.744	.026

JENSEN CATION AL2O3 - FEO+FE2O3+TIO2 - MGO
19.38 21.52 59.10

QUARTZ - FELDSPAR RATIOS

QUARTZ	.00	ORTHOCLASE	.22	PLAGIOCLASE	99.78	
QUARTZ	.00	ORTHOCLASE	2.35	ALBITE	97.65	

CATION PROPORTIONS

CA	13.62	FE	21.87	MG	64.50
CA	8.30	MG	39.29	SI	52.42
SI	53.41	AL	6.56	MG	40.03
2MG	67.91	2FE	23.03	SI/5	9.06
CA	55.05	AL	42.73	NA+K	2.22

COORDINATES IN THE SYSTEM PLAGIOCLASE - OLIVINE - CLINOPYROXENE - QUARTZ (IN MOLE PERCENT)

PROPORTION OF ANALYSIS IN BASALT TETRAHEDRON IS 97.78 MOLE PERCENT

	OL	CPX	PLAG	QTZ
BASALT TETRAHEDRON	58.84	6.63	26.98	7.55
CLINOPYROXENE PROJECTION	63.01	0.0	28.89	8.09
QUARTZ PROJECTION	63.64	7.17	29.18	0.0
PLAGIOCLASE PROJECTION	80.57	9.08	0.0	10.35
OLIVINE PROJECTION	0.0	10.39	42.27	OPX+(4QTZ) 47.34

CMAS PROJECTIONS

TETRAHEDRON COORDINATES	C	7.36	M	43.14	A	6.45	S	43.05
DIOPSIDE PROJECTION	C3A	21.80	M	27.81	S	50.39		
OLIVINE PROJECTION	CS	19.68	M	65.19	S	15.12		
ENSTATITE PROJECTION	M2S	55.85	C2S3	20.53	A2S3	23.62		
QUARTZ PROJECTION	CAS2	28.78	MS	68.03	CMS2	3.18		

PLE NUMBER BG 124

GINAL WEIGHT PERCENT OXIDES

02	AL203	FE203	FEO	MNO	MGO	CAO	NA20	K20	TIO2	P205	CR203	TOTAL
.14	6.59	1.42	12.75	.18	21.36	8.37	.08	.00	.51	.09	.44	99.93

IGHT PERCENT OXIDES RECALCULATED TO 100 PERCENT

IO2	AL203	FE203	FEO	MNO	MGO	CAO	NA20	K20	TIO2	P205	CR203	TOTAL
.17	6.59	1.42	12.76	.18	21.37	8.38	.08	.00	.51	.09	.44	100.00

TION PROPORTIONS IN ANALYSIS

I	AL	FE(3)	FE(2)	MN	MG	CA	NA	K	TI	P	CR
.94	7.09	.97	9.74	.14	29.06	8.19	.14	.00	.35	.07	.32

PW NORM

	QTZ	COR	OR	AB	AN	LC	NE	KP
IGHT PERCENT	.000	.000	.000	.677	17.634	.000	.000	.000
LE PERCENT	.000	.000	.000	.546	13.406	.000	.000	.000.
TION PERCENT	.000	.000	.000	.708	17.370	.000	.000	.000

	AC	NS	KS	DI	WO	HY	OL	CS
EIGHT PERCENT	.000	.000	.000	18.777	.000	42.113	16.918	.000
LE PERCENT	.000	.000	.000	17.734	.000	41.322	23.016	.000
ATION PERCENT	.000	.000	.000	18.382	.000	42.828	17.890	.000

	MT	CM	IL	HM	TN	PF	RU	AP
EIGHT PERCENT	2.057	.648	.969	.000	.000	.000	.000	.213
OLE PERCENT	1.879	.613	1.351	.000	.000	.000	.000	.134
ATION PERCENT	1.460	.476	.700	.000	.000	.000	.000	.185

AFIC INDEX = 81.696
ORM TOTAL = 100.007

LIVINE COMPOSITION
FORSTERITE 69.326 FAYALITE 30.674

RTHOPYROXENE COMPOSITION
ENSTATITE 71.352 FERROSILITE 28.648

CLINOPYROXENE COMPOSITION
WOLLASTONITE 51.872 ENSTATITE 34.341 FERROSILITE 13.788

FELDSPAR COMPOSITION
ORTHOCLASE .000 ALBITE 3.698 ANORTHITE 96.302
PLAGIOCLASE COMPOSITION (PERC AN) 96.302

THORNTON AND TUTTLE DIFFERENTIATION INDEX	= .677
SOLIDIFICATION INDEX (100*MGO/(MGO+FEO+FE2O3+NA2O+K2O))	= 59.980
CRYSTALLIZATION INDEX (AN+MG DI+FO+FO EQIV OF EN)	= 64.330
LARSEN INDEX (1/3SI+K)-(CA+MG)	= -23.611
ALBITE RATIO (100*(AB+AB EQIV IN NE)/PLAG)	= 3.698
IRON RATIO ((FE2=MN)*100/(FE2+MN+MG))	= 43.834
MG NUMBER AS CATIONS MG/CATIONS (FE+MG)	= 74.901
OXIDATION RATIO ACCORDING TO LE MAITRE (FEO/FEO+FE2O3)	= .838
DENSITY OF DRY LIQUID OF THIS COMPOSITION (AT 1050 DEG)	= 2.876

AFM RATIO
TOTAL ALKALIS .23 TOTAL FE 39.55 MG 60.22

KOMATIITE PARAMETERS

FEO/(FEO+MGO)	CAO/AL203	SIO2/TIO2	AL203/TIO2	FEO*/TIO2	CAO/TIO2	NA2O/TIO2	K2O/TIO2
.3964	1.27	94.39	12.92	27.51	16.41	.157	.000

JENSEN CATION AL203 - FEO+FE203+TIO2 - MGO
15.02 23.43 61.55

QUARTZ - FELDSPAR RATIOS

QUARTZ	.00	ORTHOCLASE	.00	PLAGIOCLASE	*****	
QUARTZ	.00	ORTHOCLASE	.00	ALBITE	*****	

CATION PROPORTIONS

CA	17.24	FE	21.53	MG	61.22
CA	10.08	MG	35.79	SI	54.12
SI	57.41	AL	4.63	MG	37.96
2MG	66.54	2FE	23.40	SI/5	10.06
CA	69.36	AL	30.04	NA+K	.60

COORDINATES IN THE SYSTEM PLAGIOCLASE - OLIVINE - CLINOPYROXENE - QUARTZ (IN MOLE PERCENT)

PROPORTION OF ANALYSIS IN BASALT TETRAHEDRON IS 97.18 MOLE PERCENT

	OL	CPX	PLAG	QTZ
BASALT TETRAHEDRON	51.46	18.92	18.60	11.02
CLINOPYROXENE PROJECTION	63.47	0.0	22.94	13.59
QUARTZ PROJECTION	57.84	21.26	20.91	0.0
PLAGIOCLASE PROJECTION	63.23	23.24	0.0	13.54
OLIVINE PROJECTION	0.0	23.18	22.80	OPX+(4QTZ) 54.02

CMAS PROJECTIONS

TETRAHEDRON COORDINATES	C	8.62	M	40.53	A	4.84	S	46.01
DIOPSIDE PROJECTION	C3A	19.67	M	28.13	S	52.21		
OLIVINE PROJECTION	CS	20.31	M	69.68	S	10.01		
ENSTATITE PROJECTION	M2S	48.60	C2S3	29.58	A2S3	21.82		
QUARTZ PROJECTION	CAS2	23.01	MS	63.01	CMS2	13.98		

SAMPLE NUMBER BG 158

ORIGINAL WEIGHT PERCENT OXIDES

SIO2	AL2O3	FE2O3	FEO	MNO	MGO	CAO	NA2O	K2O	TIO2	P2O5	CR2O3	TOTAL
50.34	5.93	1.21	10.93	.20	20.87	9.47	.10	.00	.82	.11	.31	100.30

WEIGHT PERCENT OXIDES RECALCULATED TO 100 PERCENT

SIO2	AL2O3	FE2O3	FEO	MNO	MGO	CAO	NA2O	K2O	TIO2	P2O5	CR2O3	TOTAL
50.19	5.91	1.21	10.35	.20	20.81	9.44	.10	.00	.82	.11	.31	100.00

CATION PROPORTIONS IN ANALYSIS

SI	AL	FE(3)	FE(2)	MN	MG	CA	NA	K	TI	P	CR
45.78	6.36	.83	8.31	.15	28.29	9.23	.19	.00	.57	.08	.22

CIPW NORM

	QTZ	COR	OR	AB	AN	LC	NE	KP
WEIGHT PERCENT	.000	.000	.000	.843	15.634	.000	.000	.000
MOLE PERCENT	.000	.000	.000	.699	12.246	.000	.000	.000
CATION PERCENT	.000	.000	.000	.881	15.450	.000	.000	.000

	AC	NS	KS	DI	WO	HY	OL	CS
WEIGHT PERCENT	.000	.000	.000	24.409	.000	47.734	7.240	.000
MOLE PERCENT	.000	.000	.000	23.765	.000	48.554	10.230	.000
CATION PERCENT	.000	.000	.000	23.985	.000	49.000	7.742	.000

	MT	CM	IL	HM	TN	PF	RU	AP
WEIGHT PERCENT	1.756	.455	1.572	.000	.000	.000	.000	.260
MOLE PERCENT	1.647	.442	2.250	.000	.000	.000	.000	.168
CATION PERCENT	1.247	.334	1.135	.000	.000	.000	.000	.226

MAFIC INDEX = 83.481
NORM TOTAL = 100.008

OLIVINE COMPOSITION
FORSTERITE 72.608 FAYALITE 27.392

ORTHOPYROXENE COMPOSITION
ENSTATITE 74.498 FERROSILITE 25.502

CLINOPYROXENE COMPOSITION
WOLLASTONITE 52.072 ENSTATITE 35.705 FERROSILITE 12.223

FELDSPAR COMPOSITION
ORTHOCLASE .000 ALBITE 5.103 ANORTHITE 94.897
PLAGIOCLASE COMPOSITION (PERC AN) 94.897

THORNTON AND TUTTLE DIFFERENTIATION INDEX = .843
SOLIDIFICATION INDEX (100*MGO/(MGO+FEO+FE2O3+NA2O+K2O)) = 63.029
CRYSTALLIZATION INDEX (AN+MG.DI+FO+FO EQIV OF EN) = 64.690
LARSEN INDEX (1/3SI+K)-(CA+MG) = -23.143
ALBITE RATIO (100*(AB+AB EQIV IN NE)/PLAG) = 5.103
IRON RATIO ((FE2+MN)*100/(FE2+MN+MG)) = 40.728
MG NUMBER AS CATIONS MG/CATIONS (FE+MG) = 77.290
OXIDATION RATIO ACCORDING TO LE MAITRE (FEO/FEO+FE2O3) = .840
DENSITY OF DRY LIQUID OF THIS COMPOSITION (AT 1050 DEG) = 2.839
AFM RATIO
TOTAL ALKALIS .30 TOTAL FE 36.44 MG 63.26

KOMATIITE PARAMETERS

FEO/(FEO+MGO)	CAO/AL2O3	SIO2/TIO2	AL2O3/TIO2	FEO*/TIO2	CAO/TIO2	NA2O/TIO2	K2O/TIO2
.3655	1.60	60.65	7.14	14.48	11.41	.120	.000

JENSEN CATION AL2O3 - FEO+FE2O3+TIO2 - MGO
14.33 21.89 63.78

QUARTZ - FELDSPAR RATIOS

QUARTZ	.00		ORTHOCLASE	.00		PLAGIOCLASE	*****	
QUARTZ	.00		ORTHOCLASE	.00		ALBITE	*****	
CATION PROPORTIONS	CA	19.95	FE	18.87	MG	61.18		
	CA	11.08	MG	33.96	SI	54.96		
	SI	59.27	AL	4.11	MG	36.62		
	2MG	68.01	2FE	20.98	SI/5	11.01		
	CA	73.86	AL	25.44	NA+K	.71		

COORDINATES IN THE SYSTEM PLAGIOCLASE - OLIVINE - CLINOPYROXENE - QUARTZ (IN MOLE PERCENT)

PROPORTION OF ANALYSIS IN BASALT TETRAHEDRON IS 97.06 MOLE PERCENT

BASALT TETRAHEDRON	OL	45.84	CPX	24.71	PLAG	16.83	QTZ	12.62
CLINOPYROXENE PROJECTION		60.89		0.0		22.35		16.76
QUARTZ PROJECTION		52.46		28.28		19.26		0.0
PLAGIOCLASE PROJECTION		55.11		29.71		0.0		15.17
OLIVINE PROJECTION		0.0		26.85		18.29	CPX+(4QTZ)	54.86

CMAS PROJECTIONS

TETRAHEDRON COORDINATES	C	9.71	M	37.92	A	4.57	S	47.80
DIOPSIDE PROJECTION	C3A	19.67	M	26.92	S	53.41		
OLIVINE PROJECTION	CS	20.75	M	70.68	S	8.57		
ENSTATITE PROJECTION	M2S	41.42	C2S3	36.19	A2S3	22.38		
QUARTZ PROJECTION	CAS2	22.40	MS	58.00	CMS2	19.60		

SAMPLE NUMBER BG 173

ORIGINAL WEIGHT PERCENT OXIDES

SIO2	AL2O3	FE2O3	FEO	MNO	MGO	CAO	NA2O	K2O	TIO2	P2O5	CR2O3	TOTAL
47.65	8.21	1.05	9.42	.23	24.01	8.03	.24	-.02	.21	.03	.00	99.06

WEIGHT PERCENT OXIDES RECALCULATED TO 100 PERCENT

SIO2	AL2O3	FE2O3	FEO	MNO	MGO	CAO	NA2O	K2O	TIO2	P2O5	CR2O3	TOTAL
48.10	8.29	1.06	9.51	.23	24.24	8.11	.24	-.02	.21	.03	.00	100.00

CATION PROPORTIONS IN ANALYSIS

SI	AL	FE(3)	FE(2)	MN	MG	CA	NA	K	TI	P	CR
42.85	8.70	.71	7.09	.18	32.18	7.74	.42	-.02	.14	.02	.00

CIPW NORM

	QTZ	COR	OR	AB	AN	LC	NE	KP
WEIGHT PERCENT	.000	.000	-.119	2.049	21.586	.000	.000	.000
MOLE PERCENT	.000	.000	-.106	1.591	15.792	.000	.000	.000
CATION PERCENT	.000	.000	-.115	2.092	20.766	.000	.000	.000

	AC	NS	KS	DI	WO	HY	OL	CS
WEIGHT PERCENT	.000	.000	.000	14.708	.000	33.895	25.877	.000
MOLE PERCENT	.000	.000	.000	13.483	.000	32.582	34.728	.000
CATION PERCENT	.000	.000	.000	14.183	.000	34.271	27.395	.000

	MT	CM	IL	HM	TN	PF	RU	AP
WEIGHT PERCENT	1.533	.000	.403	.000	.000	.000	.000	.072
MOLE PERCENT	1.347	.000	.540	.000	.000	.000	.000	.043
CATION PERCENT	1.063	.000	.284	.000	.000	.000	.000	.061

MAFIC INDEX = 76.488
NORM TOTAL = 100.004

OLIVINE COMPOSITION
FORSTERITE 76.664 FAYALITE 23.336

ORTHOPYROXENE COMPOSITION
ENSTATITE 78.357 FERROSILITE 21.643

CLINOPYROXENE COMPOSITION
WOLLASTONITE 52.316 ENSTATITE 37.364 FERROSILITE 10.320

FELDSPAR COMPOSITION
ORTHOCLASE -.507 ALBITE 8.715 ANORTHITE 91.792
PLAGIOCLASE COMPOSITION (PERC AN) 91.329

THORNTON AND TUTTLE DIFFERENTIATION INDEX = 1.930
SOLIDIFICATION INDEX (100*MGO/(MGO+FEO+FE2O3+NA2O+K2O)) = 69.194
CRYSTALLIZATION INDEX (AN+MG DI+FO+FO EQIV OF EN) = 71.892
LARSEN INDEX (1/3SI+K)-(CA+MG) = -26.971
ALBITE RATIO (100*(AB+AB EQIV IN NE)/PLAG) = 8.671
IRON RATIO ((FE2=MN)*100/(FE2+MN+MG)) = 34.128
MG NUMBER AS CATIONS MG/CATIONS (FE+MG) = 81.952
OXIDATION RATIO ACCORDING TO LE MAITRE (FEO/FEO+FE2O3) = .823
DENSITY OF DRY LIQUID OF THIS COMPOSITION (AT 1050 DEG) = 2.840
AFM RATIO
TOTAL ALKALIS .64 TOTAL FE 29.96 MG 69.40

KOMATIITE PARAMETERS

FEO/(FEO+MGO)	CAO/AL2O3	SIO2/TIO2	AL2O3/TIO2	FEO*/TIO2	CAO/TIO2	NA2O/TIO2	K2O/TIO2
.3015	.98	226.90	39.10	49.36	38.24	1.143	-.095

JENSEN CATION	AL2O3	FEO+FE2O3+TIO2	MGO
	17.83	16.26	65.92

QUARTZ - FELDSPAR RATIOS
QUARTZ .00 ORTHOCLASE -.51 PLAGIOCLASE *****
QUARTZ .00 ORTHOCLASE -6.18 ALBITE *****

CATION PROPORTIONS						
	CA	16.34	FE	15.71	MG	67.95
	CA	9.35	MG	38.88	SI	51.77
	SI	53.98	AL	5.48	MG	40.54
	2MG	73.30	2FE	16.94	SI/5	9.76
	CA	62.98	AL	35.41	NA+K	1.61

COORDINATES IN THE SYSTEM PLAGIOCLASE - OLIVINE - CLINOPYROXENE - QUARTZ (IN MOLE PERCENT)

PROPORTION OF ANALYSIS IN BASALT TETRAHEDRON IS 98.71 MOLE PERCENT

	OL	CPX	PLAG	QTZ
BASALT TETRAHEDRON	53.79	14.37	23.16	8.68
CLINOPYROXENE PROJECTION	62.82	0.0	27.04	10.14
QUARTZ PROJECTION	58.91	15.73	25.36	0.0
PLAGIOCLASE PROJECTION	70.01	18.70	0.0	11.30
OLIVINE PROJECTION	0.0	19.89	32.05	OPX+(4QTZ) 48.06

CMAS PROJECTIONS

TETRAHEDRON COORDINATES	C	8.53	M	41.41	A	5.32	S	44.74
DIOPSIDE PROJECTION	C3A	20.56	M	28.18	S	51.25		
OLIVINE PROJECTION	CS	21.33	M	67.01	S	11.66		
ENSTATITE PROJECTION	M2S	51.97	C2S3	26.41	A2S3	21.62		
QUARTZ PROJECTION	CAS2	24.60	MS	63.82	CMS2	11.58		

SAMPLE NUMBER BG 175

ORIGINAL WEIGHT PERCENT OXIDES

SIO2	AL2O3	FE2O3	FEO	MNO	MGO	CAO	NA2O	K2O	TIO2	P2O5	CR2O3	TOTAL
51.04	7.45	.99	8.92	.16	25.95	4.34	.00	.00	.19	.04	.77	99.85

WEIGHT PERCENT OXIDES RECALCULATED TO 100 PERCENT

SIO2	AL2O3	FE2O3	FEO	MNO	MGO	CAO	NA2O	K2O	TIO2	P2O5	CR2O3	TOTAL
51.12	7.46	.99	8.93	.16	25.99	4.35	.00	.00	.19	.04	.77	100.00

CATION PROPORTIONS IN ANALYSIS

SI	AL	FE(3)	FE(2)	MN	MG	CA	NA	K	TI	P	CR
45.46	7.82	.66	6.64	.12	34.45	4.14	.00	.00	.13	.03	.54

CIPW NORM

	QTZ	COR	OR	AB	AN	LC	NE	KP
WEIGHT PERCENT	.000	.000	.000	.000	20.358	.000	.000	.000
MOLE PERCENT	.000	.000	.000	.000	15.648	.000	.000	.000
CATION PERCENT	.000	.000	.000	.000	19.553	.000	.000	.000

	AC	NS	KS	DI	WO	HY	OL	CS
WEIGHT PERCENT	.000	.000	.000	.749	.000	67.376	8.489	.000
MOLE PERCENT	.000	.000	.000	.724	.000	68.549	12.094	.000
CATION PERCENT	.000	.000	.000	.724	.000	68.513	9.065	.000

	MT	CM	IL	HM	TN	PF	RU	AP
WEIGHT PERCENT	1.439	1.136	.361	.000	.000	.000	.000	.095
MOLE PERCENT	1.329	1.085	.509	.000	.000	.000	.000	.060
CATION PERCENT	.996	.813	.255	.000	.000	.000	.000	.080

MAFIC INDEX = 79.646
NORM TOTAL = 100.004

OLIVINE COMPOSITION
FORSTERITE 79.771 FAYALITE 20.229

ORTHOPYROXENE COMPOSITION
ENSTATITE 81.294 FERROSILITE 18.706

CLINOPYROXENE COMPOSITION
WOLLASTONITE 52.500 ENSTATITE 38.614 FERROSILITE 8.885

FELDSPAR COMPOSITION
ORTHOCLASE .000 ALBITE .000 ANORTHITE ******
PLAGIOCLASE COMPOSITION (PERC AN) ******

THORNTON AND TUTTLE DIFFERENTIATION INDEX = .000
SOLIDIFICATION INDEX (100*MGO/(MGO+FEO+FE2O3+NA2O+K2O)) = 72.366
CRYSTALLIZATION INDEX (AN+MG DI+FO+FO EQIV OF EN) = 66.141
LARSEN INDEX (1/3SI+K)-(CA+MG) = -24.549
ALBITE RATIO (100*(AB+AB EQIV IN NE)/PLAG) = .000
IRON RATIO ((FE2=MN)*100/(FE2+MN+MG)) = 31.075
MG NUMBER AS CATIONS MG/CATIONS (FE+MG) = 83.832
OXIDATION RATIO ACCORDING TO LE MAITRE (FEO/FEO+FE2O3) = .821
DENSITY OF DRY LIQUID OF THIS COMPOSITION (AT 1050 DEG) = 2.800
AFM RATIO
TOTAL ALKALIS .00 TOTAL FE 27.43 MG 72.57

KOMATIITE PARAMETERS

FEO/(FEO+MGO)	CAO/AL2O3	SIO2/TIO2	AL2O3/TIO2	FEO*/TIO2	CAO/TIO2	NA2O/TIO2	K2O/TIO2
.2743	.58	268.63	39.21	51.63	22.84	.000	.000

JENSEN CATION AL2O3 - FEO+FE2O3+TIO2 - MGO
15.74 14.96 69.31

QUARTZ - FELDSPAR RATIOS
QUARTZ .00 ORTHOCLASE .00 PLAGIOCLASE *****
QUARTZ .00 ORTHOCLASE .00 ALBITE .00

CATION PROPORTIONS						
CA	9.09	FE	15.31	MG	75.60
CA	4.93	MG	40.99	SI	54.09
SI	54.24	AL	4.66	MG	41.10
2MG	74.94	2FE	15.17	SI/5	9.89
CA	51.44	AL	48.56	NA+K	.00

COORDINATES IN THE SYSTEM PLAGIOCLASE - OLIVINE - CLINOPYROXENE - QUARTZ (IN MOLE PERCENT)

PROPORTION OF ANALYSIS IN BASALT TETRAHEDRON IS 97.86 MOLE PERCENT

	OL	CPX	PLAG	QTZ
BASALT TETRAHEDRON	61.77	.74	19.98	17.50
CLINOPYROXENE PROJECTION	62.24	0.0	20.13	17.63
QUARTZ PROJECTION	74.88	.90	24.22	0.0
PLAGIOCLASE PROJECTION	77.20	.92	0.0	21.87
OLIVINE PROJECTION	0.0	.82	22.02	OPX+(4QTZ) 77.16

CMAS PROJECTIONS

TETRAHEDRON COORDINATES	C	4.29	M	43.12	A	4.87	S	47.71
DIOPSIDE PROJECTION	C3A	17.37	M	28.43	S	54.20		
OLIVINE PROJECTION	CS	9.26	M	81.52	S	9.22		
ENSTATITE PROJECTION	M2S	45.18	C2S3	22.02	A2S3	32.81		
QUARTZ PROJECTION	CAS2	*****	MS	*****	CMS2	*****		

SAMPLE NUMBER BG 192

ORIGINAL WEIGHT PERCENT OXIDES

SIO2	AL2O3	FE2O3	FEO	MNO	MGO	CAO	NA2O	K2O	TIO2	P2O5	CR2O3	TOTAL
53.49	15.64	.71	6.39	.15	8.97	11.69	1.76	.83	.34	.06	.00	100.03

WEIGHT PERCENT OXIDES RECALCULATED TO 100 PERCENT

SIO2	AL2O3	FE2O3	FEO	MNO	MGO	CAO	NA2O	K2O	TIO2	P2O5	CR2O3	TOTAL
53.47	15.63	.71	6.39	.15	8.97	11.69	1.76	.83	.34	.06	.00	100.00

CATION PROPORTIONS IN ANALYSIS

SI	AL	FE(3)	FE(2)	MN	MG	CA	NA	K	TI	P	CR
49.25	16.97	.49	4.92	.12	12.31	11.53	3.14	.98	.24	.05	.00

CIPW NORM

	QTZ	COR	OR	AB	AN	LC	NE	KP
WEIGHT PERCENT	2.338	.000	4.903	14.883	32.312	.000	.000	.000
MOLE PERCENT	8.841	.000	4.878	12.893	26.383	.000	.000	.000
CATION PERCENT	2.154	.000	4.875	15.708	32.141	.000	.000	.000

	AC	NS	KS	DI	WO	HY	OL	CS
WEIGHT PERCENT	.000	.000	.000	20.443	.000	23.305	.000	.000
MOLE PERCENT	.000	.000	.000	20.631	.000	24.302	.000	.000
CATION PERCENT	.000	.000	.000	20.106	.000	23.682	.000	.000

	MT	CM	IL	HM	TN	PF	RU	AP
WEIGHT PERCENT	1.030	.000	.646	.000	.000	.000	.000	.142
MOLE PERCENT	1.010	.000	.966	.000	.000	.000	.000	.096
CATION PERCENT	.738	.000	.471	.000	.000	.000	.000	.125

MAFIC INDEX = 45.565
NORM TOTAL = 100.001

OLIVINE COMPOSITION
FORSTERITE .000 FAYALITE .000

ORTHOPYROXENE COMPOSITION
ENSTATITE 67.272 FERROSILITE 32.728

CLINOPYROXENE COMPOSITION
WOLLASTONITE 51.609 ENSTATITE 32.554 FERROSILITE 15.837

FELDSPAR COMPOSITION
ORTHOCLASE 9.411 ALBITE 28.567 ANORTHITE 62.022
PLAGIOCLASE COMPOSITION (PERC AN) 68.465

THORNTON AND TUTTLE DIFFERENTIATION INDEX = 22.124
SOLIDIFICATION INDEX (100*MGO/(MGO+FEO+FE2O3+NA2O+K2O)) = 48.063
CRYSTALLIZATION INDEX (AN+MG DI+FO+FO EQIV OF EN) = 57.654
LARSEN INDEX (1/3SI+K)-(CA+MG) = -7.778
ALBITE RATIO (100*(AB+AB EQIV IN NE)/PLAG) = 31.535
IRON RATIO ((FE2=MN)*100/(FE2+MN+MG)) = 48.453
MG NUMBER AS CATIONS MG/CATIONS (FE+MG) = 71.432
OXIDATION RATIO ACCORDING TO LE MAITRE (FEO/FEO+FE2O3) = .835
DENSITY OF DRY LIQUID OF THIS COMPOSITION (AT 1050 DEG) = 2.654
AFM RATIO
TOTAL ALKALIS 13.93 TOTAL FE 37.82 MG 48.25

KOMATIITE PARAMETERS

FEO/(FEO+MGO)	CAO/AL2O3	SIO2/TIO2	AL2O3/TIO2	FEO*/TIO2	CAO/TIO2	NA2O/TIO2	K2O/TIO2
.4394	.75	157.32	46.00	20.68	34.38	5.176	2.441

JENSEN CATION AL2O3 - FEO+FE2O3+TIO2 - MGO
48.59 16.17 35.24

QUARTZ - FELDSPAR RATIOS
QUARTZ 4.30 ORTHOCLASE 9.01 PLAGIOCLASE 86.70
QUARTZ 10.57 ORTHOCLASE 22.16 ALBITE 67.27

CATION PROPORTIONS

CA	39.75	FE	17.81	MG	42.43
CA	15.78	MG	16.84	SI	67.38
SI	70.31	AL	12.11	MG	17.57
2MG	54.95	2FE	23.07	SI/5	21.98
CA	52.24	AL	38.44	NA+K	9.32

COORDINATES IN THE SYSTEM PLAGIOCLASE - OLIVINE - CLINOPYROXENE - QUARTZ (IN MOLE PERCENT)

PROPORTION OF ANALYSIS IN BASALT TETRAHEDRON IS 93.79 MOLE PERCENT

BASALT TETRAHEDRON	OL	18.94	CPX	21.44	PLAG	51.02	QTZ	8.61
CLINOPYROXENE PROJECTION		24.11		0.0		64.94		10.96
QUARTZ PROJECTION		20.72		23.46		55.82		0.0
PLAGIOCLASE PROJECTION		38.66		43.76		0.0		17.58
OLIVINE PROJECTION		0.0		20.06		47.73	OPX+(4QTZ)	32.22

CMAS PROJECTIONS

TETRAHEDRON COORDINATES	C	17.53	M	19.26	A	12.41	S	50.80
DIOPSIDE PROJECTION	C3A	32.41	M	15.18	S	52.40		
OLIVINE PROJECTION	CS	25.29	M	58.99	S	15.72		
ENSTATITE PROJECTION	M2S	27.55	C2S3	37.54	A2S3	34.92		
QUARTZ PROJECTION	CAS2	57.73	MS	23.75	CMS2	18.52		

HLAGOTHI COMPLEX

SAMPLE NUMBER BG 193

ORIGINAL WEIGHT PERCENT OXIDES

SIO2	AL2O3	FE2O3	FEO	MNO	MGO	CAO	NA2O	K2O	TIO2	P2O5	CR2O3	TOTAL
50.06	7.00	1.09	9.80	.20	25.51	5.38	.68	.24	.23	.05	.55	100.79

WEIGHT PERCENT OXIDES RECALCULATED TO 100 PERCENT

SIO2	AL2O3	FE2O3	FEO	MNO	MGO	CAO	NA2O	K2O	TIO2	P2O5	CR2O3	TOTAL
49.67	6.95	1.08	9.72	.20	25.31	5.34	.67	.24	.23	.05	.55	100.00

CATION PROPORTIONS IN ANALYSIS

SI	AL	FE(3)	FE(2)	MN	MG	CA	NA	K	TI	P	CR
44.09	7.27	.72	7.22	.15	33.48	5.08	1.16	.27	.15	.04	.38

CIPW NORM

	QTZ	COR	OR	AB	AN	LC	NE	KP
WEIGHT PERCENT	.000	.000	1.407	5.707	15.219	.000	.000	.000
MOLE PERCENT	.000	.000	1.252	4.422	11.113	.000	.000	.000
CATION PERCENT	.000	.000	1.348	5.804	14.588	.000	.000	.000

	AC	NS	KS	DI	WO	HY	OL	CS
WEIGHT PERCENT	.000	.000	.000	8.719	.000	42.553	23.477	.000
MOLE PERCENT	.000	.000	.000	7.987	.000	40.922	31.550	.000
CATION PERCENT	.000	.000	.000	8.387	.000	42.968	24.844	.000

	MT	CM	IL	HM	TN	PF	RU	AP
WEIGHT PERCENT	1.567	.804	.433	.000	.000	.000	.000	.118
MOLE PERCENT	1.375	.729	.580	.000	.000	.000	.000	.071
CATION PERCENT	1.083	.574	.305	.000	.000	.000	.000	.099

MAFIC INDEX = 77.671
NORM TOTAL = 100.004

OLIVINE COMPOSITION
FORSTERITE 77.634 FAYALITE 22.366

ORTHOPYROXENE COMPOSITION
ENSTATITE 79.275 FERROSILITE 20.725

CLINOPYROXENE COMPOSITION
WOLLASTONITE 52.374 ENSTATITE 37.756 FERROSILITE 9.870

FELDSPAR COMPOSITION
ORTHOCLASE 6.301 ALBITE 25.555 ANORTHITE 68.145
PLAGIOCLASE COMPOSITION (PERC AN) 72.727

THORNTON AND TUTTLE DIFFERENTIATION INDEX	= 7.114
SOLIDIFICATION INDEX (100*MGO/(MGO+FEO+FE2O3+NA2O+K2O))	= 68.356
CRYSTALLIZATION INDEX (AN+MG DI+FO+FO EQIV OF EN)	= 64.188
LARSEN INDEX (1/3SI+K)-(CA+MG)	= -24.957
ALBITE RATIO (100*(AB+AB EQIV IN NE)/PLAG)	= 27.273
IRON RATIO ((FE2=MN)*100/(FE2+MN+MG))	= 33.563
MG NUMBER AS CATIONS MG/CATIONS (FE+MG)	= 82.265
OXIDATION RATIO ACCORDING TO LE MAITRE (FEO/FEO+FE2O3)	= .804
DENSITY OF DRY LIQUID OF THIS COMPOSITION (AT 1050 DEG)	= 2.820

AFM RATIO
TOTAL ALKALIS 2.47 TOTAL FE 28.97 MG 68.56

KOMATIITE PARAMETERS

FEO/(FEO+MGO)	CAO/AL2O3	SIO2/TIO2	AL2O3/TIO2	FEO*/TIO2	CAO/TIO2	NA2O/TIO2	K2O/TIO2
.2971	.77	217.65	30.43	46.87	23.39	2.957	1.043

JENSEN CATION AL2O3 - FEO+FE2O3+TIO2 - MGO
14.88 16.57 68.55

QUARTZ - FELDSPAR RATIOS

QUARTZ	.00	ORTHOCLASE 6.30		PLAGIOCLASE 93.70		
QUARTZ	.00	ORTHOCLASE 19.78		ALBITE 80.22		
CATION PROPORTIONS	CA	11.00	FE	16.42	MG	72.57
	CA	6.14	MG	40.52	SI	53.34
	SI	54.29	AL	4.47	MG	41.24
	2MG	73.64	2FE	16.66	SI/5	9.70
	CA	53.86	AL	38.55	NA+K	7.59

COORDINATES IN THE SYSTEM PLAGIOCLASE - OLIVINE - CLINOPYROXENE - QUARTZ (IN MOLE PERCENT)

PROPORTION OF ANALYSIS IN BASALT TETRAHEDRON IS 96.59 MOLE PERCENT

BASALT TETRAHEDRON	OL	59.08	CPX	8.68	PLAG	21.11	QTZ	11.12
CLINOPYROXENE PROJECTION		64.70		0.[illegible]		23.12		12.18
QUARTZ PROJECTION		66.48		9.77		23.75		0.0
PLAGIOCLASE PROJECTION		74.90		11.01		0.0		14.10
OLIVINE PROJECTION		0.0		11.69		28.42	OPX+(4QTZ)	59.89

CMAS PROJECTIONS

TETRAHEDRON COORDINATES	C	6.79	M	42.91	A	5.33	S	44.97
DIOPSIDE PROJECTION	C3A	19.59	M	28.59	S	51.82		
OLIVINE PROJECTION	CS	16.83	M	71.60	S	11.58		
ENSTATITE PROJECTION	M2S	52.94	C2S3	23.18	A2S3	23.88		
QUARTZ PROJECTION	CAS2	24.86	MS	69.31	CMS2	5.33		

HLAGOTHI COMPLEX

SAMPLE NUMBER BG 196

ORIGINAL WEIGHT PERCENT OXIDES

SIO2	AL2O3	FE2O3	FEO	MNO	MGO	CAO	NA2O	K2O	TIO2	P2O5	CR2O3	TOTAL
47.76	6.74	1.14	10.25	.20	27.57	5.13	1.12	.31	.29	.07	.64	101.21

WEIGHT PERCENT OXIDES RECALCULATED TO 100 PERCENT

SIO2	AL2O3	FE2O3	FEO	MNO	MGO	CAO	NA2O	K2O	TIO2	P2O5	CR2O3	TOTAL
47.19	6.66	1.13	10.12	.20	27.24	5.07	1.11	.31	.29	.07	.63	100.00

CATION PROPORTIONS IN ANALYSIS

SI	AL	FE(3)	FE(2)	MN	MG	CA	NA	K	TI	P	CR
41.45	6.89	.74	7.44	.15	35.66	4.77	1.88	.34	.19	.05	.44

CIPW NORM

	QTZ	COR	OR	AB	AN	LC	NE	KP
WEIGHT PERCENT	.000	.000	1.810	9.360	12.298	.000	.000	.000
MOLE PERCENT	.000	.000	1.502	6.765	8.377	.000	.000	.000
CATION PERCENT	.000	.000	1.716	9.421	11.666	.000	.000	.000

	AC	NS	KS	DI	WO	HY	OL	CS
WEIGHT PERCENT	.000	.000	.000	9.872	.000	21.347	42.046	.000
MOLE PERCENT	.000	.000	.000	8.442	.000	19.183	52.835	.000
CATION PERCENT	.000	.000	.000	9.404	.000	21.367	44.137	.000

	MT	CM	IL	HM	TN	PF	RU	AP
WEIGHT PERCENT	1.631	.931	.544	.000	.000	.000	.000	.164
MOLE PERCENT	1.335	.788	.680	.000	.000	.000	.000	.092
CATION PERCENT	1.115	.659	.379	.000	.000	.000	.000	.137

MAFIC INDEX = 76.535
NORM TOTAL = 100.004

OLIVINE COMPOSITION
FORSTERITE 78.358 FAYALITE 21.642

ORTHOPYROXENE COMPOSITION
ENSTATITE 79.960 FERROSILITE 20.040

CLINOPYROXENE COMPOSITION
WOLLASTONITE 52.417 ENSTATITE 38.047 FERROSILITE 9.536

FELDSPAR COMPOSITION
ORTHOCLASE 7.712 ALBITE 39.885 ANORTHITE 52.403
PLAGIOCLASE COMPOSITION (PERC AN) 56.782

THORNTON AND TUTTLE DIFFERENTIATION INDEX = 11.170
SOLIDIFICATION INDEX (100*MGO/(MGO+FEO+FE2O3+NA2O+K2O)) = 68.269
CRYSTALLIZATION INDEX (AN+MG DI+FO+FO EQIV OF EN) = 65.309
LARSEN INDEX (1/3SI+K)-(CA+MG) = -27.885
ALBITE RATIO (100*(AB+AB EQIV IN NE)/PLAG) = 43.218
IRON RATIO ((FE2+MN)*100/(FE2+MN+MG)) = 32.808
MG NUMBER AS CATIONS MG/CATIONS (FE+MG) = 82.745
OXIDATION RATIO ACCORDING TO LE MAITRE (FEO/FEO+FE2O3) = .785
DENSITY OF DRY LIQUID OF THIS COMPOSITION (AT 1050 DEG) = 2.854
AFM RATIO
TOTAL ALKALIS 3.55 TOTAL FE 27.99 MG 68.46

KOMATIITE PARAMETERS

FEO/(FEO+MGO)	CAO/AL2O3	SIO2/TIO2	AL2O3/TIO2	FEO*/TIO2	CAO/TIO2	NA2O/TIO2	K2O/TIO2
.2902	.76	164.69	23.24	38.86	17.69	3.862	1.069

JENSEN CATION AL2O3 - FEO+FE2O3+TIO2 - MGO
13.54 16.44 70.03

QUARTZ - FELDSPAR RATIOS

QUARTZ	.00	ORTHOCLASE	7.71	PLAGIOCLASE	92.29		
QUARTZ	.00	ORTHOCLASE	16.20	ALBITE	83.80		

CATION PROPORTIONS

CA	9.89	FE	16.18	MG	73.93
CA	5.83	MG	43.55	SI	50.62
SI	51.45	AL	4.28	MG	44.27
2MG	74.90	2FE	16.40	SI/5	8.71
CA	51.12	AL	36.94	NA+K	11.94

COORDINATES IN THE SYSTEM PLAGIOCLASE - OLIVINE - CLINOPYROXENE - QUARTZ (IN MOLE PERCENT)

PROPORTION OF ANALYSIS IN BASALT TETRAHEDRON IS 95.99 MOLE PERCENT

BASALT TETRAHEDRON	OL	62.67	CPX	9.80	PLAG	21.97	QTZ	5.56
CLINOPYROXENE PROJECTION		69.48		0.[illegible]		24.35		6.17
QUARTZ PROJECTION		66.37		10.37		23.26		0.0
PLAGIOCLASE PROJECTION		80.31		12.55		0.0		7.13
OLIVINE PROJECTION		0.0		18.13		40.66	OPX+(4QTZ)	41.20

CMAS PROJECTIONS

TETRAHEDRON COORDINATES	C	7.31	M	45.55	A	5.65	S	41.49
DIOPSIDE PROJECTION	C3A	20.62	M	30.05	S	49.33		
OLIVINE PROJECTION	CS	22.86	M	61.64	S	15.50		
ENSTATITE PROJECTION	M2S	60.55	C2S3	19.58	A2S3	19.87		
QUARTZ PROJECTION	CAS2	24.80	MS	69.52	CMS2	5.68		

HLAGOTHI COMPLEX

SAMPLE NUMBER BG 212

ORIGINAL WEIGHT PERCENT OXIDES

SIO2	AL2O3	FE2O3	FEO	MNO	MGO	CAO	NA2O	K2O	TIO2	P2O5	CR2O3	TOTAL
48.34	7.00	1.08	9.68	.19	27.02	5.98	.08	.39	.29	.05	.57	100.67

WEIGHT PERCENT OXIDES RECALCULATED TO 100 PERCENT

SIO2	AL2O3	FE2O3	FEO	MNO	MGO	CAO	NA2O	K2O	TIO2	P2O5	CR2O3	TOTAL
48.02	6.95	1.07	9.62	.19	26.84	5.94	.08	.39	.29	.05	.57	100.00

CATION PROPORTIONS IN ANALYSIS

SI	AL	FE(3)	FE(2)	MN	MG	CA	NA	K	TI	P	CR
42.52	7.26	.71	7.12	.14	35.42	5.64	.14	.44	.19	.04	.40

CIPW NORM

	QTZ	COR	OR	AB	AN	LC	NE	KP
WEIGHT PERCENT	.000	.000	2.289	.672	17.472	.000	.000	.000
MOLE PERCENT	.000	.000	1.986	.508	12.438	.000	.000	.000
CATION PERCENT	.000	.000	2.188	.682	16.706	.000	.000	.000

	AC	NS	KS	DI	WO	HY	OL	CS
WEIGHT PERCENT	.000	.000	.000	9.291	.000	38.783	28.449	.000
MOLE PERCENT	.000	.000	.000	8.309	.000	36.475	37.437	.000
CATION PERCENT	.000	.000	.000	8.928	.000	39.187	30.164	.000

	MT	CM	IL	HM	TN	PF	RU	AP
WEIGHT PERCENT	1.550	.834	.547	.000	.000	.000	.000	.118
MOLE PERCENT	1.326	.738	.714	.000	.000	.000	.000	.069
CATION PERCENT	1.068	.595	.384	.000	.000	.000	.000	.099

MAFIC INDEX = 79.571
NORM TOTAL = 100.005

OLIVINE COMPOSITION
FORSTERITE 78.963 FAYALITE 21.037

ORTHOPYROXENE COMPOSITION
ENSTATITE 80.532 FERROSILITE 19.468

CLINOPYROXENE COMPOSITION
WOLLASTONITE 52.453 ENSTATITE 38.291 FERROSILITE 9.257

FELDSPAR COMPOSITION
ORTHOCLASE 11.203 ALBITE 3.290 ANORTHITE 85.507
PLAGIOCLASE COMPOSITION (PERC AN) 96.295

THORNTON AND TUTTLE DIFFERENTIATION INDEX = 2.962
SOLIDIFICATION INDEX (100*MGO/(MGO+FEO+FE2O3+NA2O+K2O)) = 70.645
CRYSTALLIZATION INDEX (AN+MG DI+FO+FO EQIV OF EN) = 69.499
LARSEN INDEX (1/3SI+K)-(CA+MG) = -27.917
ALBITE RATIO (100*(AB+AB EQIV IN NE)/PLAG) = 3.705
IRON RATIO ((FE2=MN)*100/(FE2+MN+MG)) = 32.012
MG NUMBER AS CATIONS MG/CATIONS (FE+MG) = 83.259
OXIDATION RATIO ACCORDING TO LE MAITRE (FEO/FEO+FE2O3) = .807
DENSITY OF DRY LIQUID OF THIS COMPOSITION (AT 1050 DEG) = 2.848
AFM RATIO
TOTAL ALKALIS 1.23 TOTAL FE 27.92 MG 70.84

KOMATIITE PARAMETERS

FEO/(FEO+MGO)	CAO/AL2O3	SIO2/TIO2	AL2O3/TIO2	FEO*/TIO2	CAO/TIO2	NA2O/TIO2	K2O/TIO2
.2827	.85	166.69	24.14	36.72	20.62	.276	1.345

JENSEN CATION AL2O3 - FEO+FE2O3+TIO2 - MGO
14.31 15.83 69.86

QUARTZ - FELDSPAR RATIOS
QUARTZ .00 ORTHOCLASE 11.20 PLAGIOCLASE 88.80
QUARTZ .00 ORTHOCLASE 77.30 ALBITE 22.70

CATION PROPORTIONS	CA 11.61		FE	15.41	MG	72.98
	CA 6.74		MG	42.38	SI	50.87
	SI 52.13		AL	4.45	MG	43.43
	2MG 75.12		2FE	15.86	SI/5	9.02
	CA 59.01		AL	37.99	NA+K	3.01

COORDINATES IN THE SYSTEM PLAGIOCLASE - OLIVINE - CLINOPYROXENE - QUARTZ (IN MOLE PERCENT)

PROPORTION OF ANALYSIS IN BASALT TETRAHEDRON IS 95.67 MOLE PERCENT

BASALT TETRAHEDRON	OL	62.25	CPX	9.33	PLAG	18.18	QTZ	10.24
CLINOPYROXENE PROJECTION		68.66		0.0		20.05		11.29
QUARTZ PROJECTION		69.35		10.40		20.25		0.0
PLAGIOCLASE PROJECTION		76.08		11.41		0.0		12.52
OLIVINE PROJECTION		0.0		13.63		26.55	OPX+(4QTZ)	59.82

CMAS PROJECTIONS

TETRAHEDRON COORDINATES	C	6.45	M	44.61	A	4.89	S	44.04
DIOPSIDE PROJECTION	C3A	18.66	M	30.05	S	51.29		
OLIVINE PROJECTION	CS	17.37	M	71.07	S	11.56		
ENSTATITE PROJECTION	M2S	56.80	C2S3	21.64	A2S3	21.56		
QUARTZ PROJECTION	CAS2	22.61	MS	71.78	CMS2	5.61		

HLAGOTHI COMPLEX

SAMPLE NUMBER BG 216

ORIGINAL WEIGHT PERCENT OXIDES

SIO2	AL2O3	FE2O3	FEO	MNO	MGO	CAO	NA2O	K2O	TIO2	P2O5	CR2O3	TOTAL
47.59	8.64	1.10	9.88	.22	23.42	8.04	.37	.02	.35	.06	.57	100.26

WEIGHT PERCENT OXIDES RECALCULATED TO 100 PERCENT

SIO2	AL2O3	FE2O3	FEO	MNO	MGO	CAO	NA2O	K2O	TIO2	P2O5	CR2O3	TOTAL
47.47	8.62	1.10	9.86	.22	23.36	8.02	.37	.02	.35	.06	.57	100.00

CATION PROPORTIONS IN ANALYSIS

SI	AL	FE(3)	FE(2)	MN	MG	CA	NA	K	TI	P	CR
42.46	9.09	.74	7.37	.17	31.14	7.69	.64	.02	.23	.05	.40

CIPW NORM

	QTZ	COR	OR	AB	AN	LC	NE	KP
WEIGHT PERCENT	.000	.000	.118	3.122	21.798	.000	.000	.000
MOLE PERCENT	.000	.000	.105	2.429	15.985	.000	.000	.000
CATION PERCENT	.000	.000	.114	3.200	21.058	.000	.000	.000

	AC	NS	KS	DI	WO	HY	OL	CS
WEIGHT PERCENT	.000	.000	.000	14.048	.000	31.609	26.080	.000
MOLE PERCENT	.000	.000	.000	12.901	.000	30.418	35.023	.000
CATION PERCENT	.000	.000	.000	13.595	.000	32.054	27.679	.000

	MT	CM	IL	HM	TN	PF	RU	AP
WEIGHT PERCENT	1.588	.837	.663	.000	.000	.000	.000	.142
MOLE PERCENT	1.399	.763	.891	.000	.000	.000	.000	.086
CATION PERCENT	1.106	.603	.470	.000	.000	.000	.000	.121

MAFIC INDEX = 74.968
NORM TOTAL = 100.005

OLIVINE COMPOSITION
FORSTERITE 76.154 FAYALITE 23.846

ORTHOPYROXENE COMPOSITION
ENSTATITE 77.873 FERROSILITE 22.127

CLINOPYROXENE COMPOSITION
WOLLASTONITE 52.286 ENSTATITE 37.156 FERROSILITE 10.558

FELDSPAR COMPOSITION
ORTHOCLASE .471 ALBITE 12.468 ANORTHITE 87.061
PLAGIOCLASE COMPOSITION (PERC AN) 87.473

THORNTON AND TUTTLE DIFFERENTIATION INDEX = 3.240
SOLIDIFICATION INDEX (100*MGO/(MGO+FEO+FE2O3+NA2O+K2O)) = 67.318
CRYSTALLIZATION INDEX (AN+MG DI+FO+FO EQIV OF EN) = 70.169
LARSEN INDEX (1/3SI+K)-(CA+MG) = -26.092
ALBITE RATIO (100*(AB+AB EQIV IN NE)/PLAG) = 12.527
IRON RATIO ((FE2=MN)*100/(FE2+MN+MG)) = 35.720
MG NUMBER AS CATIONS MG/CATIONS (FE+MG) = 80.855
OXIDATION RATIO ACCORDING TO LE MAITRE (FEO/FEO+FE2O3) = .823
DENSITY OF DRY LIQUID OF THIS COMPOSITION (AT 1050 DEG) = 2.843
AFM RATIO
TOTAL ALKALIS 1.12 TOTAL FE 31.34 MG 67.53

KOMATIITE PARAMETERS

FEO/(FEO+MGO)	CAO/AL2O3	SIO2/TIO2	AL2O3/TIO2	FEO*/TIO2	CAO/TIO2	NA2O/TIO2	K2O/TIO2
.3170	.93	135.97	24.69	31.06	22.97	1.057	.057

JENSEN CATION AL2O3 - FEO+FE2O3+TIO2 - MGO
18.71 17.18 64.11

QUARTZ - FELDSPAR RATIOS

QUARTZ	.00	ORTHOCLASE	.47	PLAGIOCLASE	99.53		
QUARTZ	.00	ORTHOCLASE	3.64	ALBITE	96.36		
CATION PROPORTIONS	CA	16.50	FE	16.62	MG	66.88	
	CA	9.45	MG	38.31	SI	52.23	
	SI	54.33	AL	5.81	MG	39.85	
	2MG	72.21	2FE	17.95	SI/5	9.84	
	CA	61.19	AL	36.17	NA+K	2.64	

COORDINATES IN THE SYSTEM PLAGIOCLASE - OLIVINE - CLINOPYROXENE - QUARTZ (IN MOLE PERCENT)

PROPORTION OF ANALYSIS IN BASALT TETRAHEDRON IS 97.59 MOLE PERCENT

BASALT TETRAHEDRON	OL	53.00	CPX	13.93	PLAG	24.86	QTZ	8.21
CLINOPYROXENE PROJECTION		61.58		0.0		28.88		9.54
QUARTZ PROJECTION		57.74		15.18		27.08		0.0
PLAGIOCLASE PROJECTION		70.53		18.54		0.0		10.93
OLIVINE PROJECTION		0.0		19.45		34.70	OPX+(4QTZ)	45.85

CMAS PROJECTIONS

TETRAHEDRON COORDINATES	C	8.78	M	40.82	A	6.03	S	44.37
DIOPSIDE PROJECTION	C3A	21.91	M	27.18	S	50.91		
OLIVINE PROJECTION	CS	21.78	M	65.10	S	13.12		
ENSTATITE PROJECTION	M2S	51.81	C2S3	25.34	A2S3	22.85		
QUARTZ PROJECTION	CAS2	27.51	MS	62.70	CMS2	9.78		

SAMPLE NUMBER BG 230

ORIGINAL WEIGHT PERCENT OXIDES

SIO2	AL2O3	FE2O3	FEO	MNO	MGO	CAO	NA2O	K2O	TIO2	P2O5	CR2O3	TOTAL
57.17	15.00	.95	8.55	.17	5.94	8.47	3.76	.66	.65	.13	.00	101.46

WEIGHT PERCENT OXIDES RECALCULATED TO 100 PERCENT

SIO2	AL2O3	FE2O3	FEO	MNO	MGO	CAO	NA2O	K2O	TIO2	P2O5	CR2O3	TOTAL
56.35	14.78	.94	8.43	.17	5.85	8.35	3.71	.65	.64	.13	.00	100.00

CATION PROPORTIONS IN ANALYSIS

SI	AL	FE(3)	FE(2)	MN	MG	CA	NA	K	TI	P	CR
52.20	16.14	.65	6.53	.13	8.08	8.29	6.65	.77	.45	.10	.00

CIPW NORM

	QTZ	COR	OR	AB	AN	LC	NE	KP
WEIGHT PERCENT	3.754	.000	3.844	31.350	21.785	.000	.000	.000
MOLE PERCENT	13.844	.000	3.731	26.493	17.352	.000	.000	.000
CATION PERCENT	3.477	.000	3.844	33.277	21.794	.000	.000	.000

	AC	NS	KS	DI	WO	HY	OL	CS
WEIGHT PERCENT	.000	.000	.000	15.527	.000	20.863	.000	.000
MOLE PERCENT	.000	.000	.000	14.969	.000	20.333	.000	.000
CATION PERCENT	.000	.000	.000	15.040	.000	20.428	.000	.000

	MT	CM	IL	HM	TN	PF	RU	AP
WEIGHT PERCENT	1.359	.000	1.217	.000	.000	.000	.000	.304
MOLE PERCENT	1.300	.000	1.777	.000	.000	.000	.000	.200
CATION PERCENT	.980	.000	.893	.000	.000	.000	.000	.268

MAFIC INDEX = 39.269
NORM TOTAL = 100.001

OLIVINE COMPOSITION
FORSTERITE .000 FAYALITE .000

ORTHOPYROXENE COMPOSITION
ENSTATITE 51.086 FERROSILITE 48.914

CLINOPYROXENE COMPOSITION
WOLLASTONITE 50.537 ENSTATITE 25.268 FERROSILITE 24.194

FELDSPAR COMPOSITION
ORTHOCLASE 6.747 ALBITE 55.020 ANORTHITE 38.233
PLAGIOCLASE COMPOSITION (PERC AN) 40.999

THORNTON AND TUTTLE DIFFERENTIATION INDEX = 38.947
SOLIDIFICATION INDEX (100*MGO/(MGO+FEO+FE2O3+NA2O+K2O)) = 29.901
CRYSTALLIZATION INDEX (AN+MG DI+FO+FO EQIV OF EN) = 37.717
LARSEN INDEX (1/3SI+K)-(CA+MG) = 1.611
ALBITE RATIO (100*(AB+AB EQIV IN NE)/PLAG) = 59.001
IRON RATIO ((FE2=MN)*100/(FE2+MN+MG)) = 65.433
MG NUMBER AS CATIONS MG/CATIONS (FE+MG) = 55.304
OXIDATION RATIO ACCORDING TO LE MAITRE (FEO/FEO+FE2O3) = .810
DENSITY OF DRY LIQUID OF THIS COMPOSITION (AT 1050 DEG) = 2.619
AFM RATIO
TOTAL ALKALIS 22.36 TOTAL FE 47.60 MG 30.05

KOMATIITE PARAMETERS

FEO/(FEO+MGO)	CAO/AL2O3	SIO2/TIO2	AL2O3/TIO2	FEO*/TIO2	CAO/TIO2	NA2O/TIO2	K2O/TIO2
.6130	.56	87.95	23.08	14.48	13.03	5.785	1.015

JENSEN CATION AL2O3 - FEO+FE2O3+TIO2 - MGO
50.67 23.96 25.37

QUARTZ - FELDSPAR RATIOS
QUARTZ 6.18 ORTHOCLASE 6.33 PLAGIOCLASE 87.49
QUARTZ 9.64 ORTHOCLASE 9.87 ALBITE 80.49

CATION PROPORTIONS						
CA	35.67	FE	29.53	MG	34.80
CA	12.08	MG	11.79	SI	76.13
SI	76.37	AL	11.81	MG	11.83
2MG	40.09	2FE	34.01	SI/5	25.89
CA	41.29	AL	40.22	NA+K	18.50

COORDINATES IN THE SYSTEM PLAGIOCLASE - OLIVINE - CLINOPYROXENE - QUARTZ (IN MOLE PERCENT)

PROPORTION OF ANALYSIS IN BASALT TETRAHEDRON IS 94.02 MOLE PERCENT

BASALT TETRAHEDRON	OL	16.30	CPX	16.00	PLAG	58.58	QTZ	9.13
CLINOPYROXENE PROJECTION		19.40		0.0		69.73		10.87
QUARTZ PROJECTION		17.93		17.60		64.46		0.0
PLAGIOCLASE PROJECTION		39.34		38.62		0.0		22.04
OLIVINE PROJECTION		0.0		14.40		52.73	OPX+(4QTZ)	32.87

CMAS PROJECTIONS

TETRAHEDRON COORDINATES	C	17.83	M	16.40	A	14.40	S	51.36
DIOPSIDE PROJECTION	C3A	33.23	M	14.38	S	52.39		
OLIVINE PROJECTION	CS	24.01	M	58.97	S	17.02		
ENSTATITE PROJECTION	M2S	25.96	C2S3	35.92	A2S3	38.12		
QUARTZ PROJECTION	CAS2	66.21	MS	21.53	CMS2	12.26		

HLAGOTHI COMPLEX

SAMPLE NUMBER BG222

ORIGINAL WEIGHT PERCENT OXIDES

SIO2	AL2O3	FE2O3	FEO	MNO	MGO	CAO	NA2O	K2O	TIO2	P2O5	CR2O3	TOTAL
55.43	15.03	.90	8.12	.16	6.65	10.52	2.19	.74	.55	.10	.00	100.39

WEIGHT PERCENT OXIDES RECALCULATED TO 100 PERCENT

SIO2	AL2O3	FE2O3	FEO	MNO	MGO	CAO	NA2O	K2O	TIO2	P2O5	CR2O3	TOTAL
55.21	14.97	.90	8.09	.16	6.62	10.48	2.18	.74	.55	.10	.00	100.00

CATION PROPORTIONS IN ANALYSIS

SI	AL	FE(3)	FE(2)	MN	MG	CA	NA	K	TI	P	CR
51.50	16.46	.63	6.31	.13	9.21	10.47	3.94	.88	.38	.08	.00

CIPW NORM

	QTZ	COR	OR	AB	AN	LC	NE	KP
WEIGHT PERCENT	6.362	.000	4.356	18.453	28.881	.000	.000	.000
MOLE PERCENT	21.789	.000	3.925	14.480	21.360	.000	.000	.000
CATION PERCENT	5.935	.000	4.386	19.724	29.095	.000	.000	.000

	AC	NS	KS	DI	WO	HY	OL	CS
WEIGHT PERCENT	.000	.000	.000	18.453	.000	20.917	.000	.000
MOLE PERCENT	.000	.000	.000	16.605	.000	19.129	.000	.000
CATION PERCENT	.000	.000	.000	18.093	.000	20.842	.000	.000

	MT	CM	IL	HM	TN	PF	RU	AP
WEIGHT PERCENT	1.303	.000	1.041	.000	.000	.000	.000	.236
MOLE PERCENT	1.158	.000	1.411	.000	.000	.000	.000	.144
CATION PERCENT	.946	.000	.769	.000	.000	.000	.000	.210

MAFIC INDEX = 41.950
NORM TOTAL = 100.003

OLIVINE COMPOSITION
FORSTERITE .000 FAYALITE .000

ORTHOPYROXENE COMPOSITION
ENSTATITE 54.999 FERROSILITE 45.001

CLINOPYROXENE COMPOSITION
WOLLASTONITE 50.801 ENSTATITE 27.059 FERROSILITE 22.140

FELDSPAR COMPOSITION
ORTHOCLASE 8.427 ALBITE 35.699 ANORTHITE 55.874
PLAGIOCLASE COMPOSITION (PERC AN) 61.016

THORNTON AND TUTTLE DIFFERENTIATION INDEX = 29.171
SOLIDIFICATION INDEX (100*MGO/(MGO+FEO+FE2O3+NA2O+K2O)) = 35.750
CRYSTALLIZATION INDEX (AN+MG DI+FO+FO EQIV OF EN) = 47.714
LARSEN INDEX (1/3SI+K)-(CA+MG) = -2.332
ALBITE RATIO (100*(AB+AB EQIV IN NE)/PLAG) = 38.984
IRON RATIO ((FE2=MN)*100/(FE2+MN+MG)) = 61.604
MG NUMBER AS CATIONS MG/CATIONS (FE+MG) = 59.343
OXIDATION RATIO ACCORDING TO LE MAITRE (FEO/FEO+FE2O3) = .838
DENSITY OF DRY LIQUID OF THIS COMPOSITION (AT 1050 DEG) = 2.645
AFM RATIO
TOTAL ALKALIS 15.83 TOTAL FE 48.25 MG 35.93

KOMATIITE PARAMETERS

FEO/(FEO+MGO)	CAO/AL2O3	SIO2/TIO2	AL2O3/TIO2	FEO*/TIO2	CAO/TIO2	NA2O/TIO2	K2O/TIO2
.5732	.70	100.78	27.33	16.24	19.13	3.982	1.345

JENSEN CATION AL2O3 - FEO+FE2O3+TIO2 - MGO
49.89 22.20 27.91

QUARTZ - FELDSPAR RATIOS
QUARTZ 10.96 ORTHOCLASE 7.50 PLAGIOCLASE 81.54
QUARTZ 21.81 ORTHOCLASE 14.93 ALBITE 63.26

CATION PROPORTIONS						
CA	39.81	FE	25.18	MG	35.01
CA	14.71	MG	12.94	SI	72.35
SI	74.71	AL	11.94	MG	13.36
2MG	43.89	2FE	31.57	SI/5	24.55
CA	49.60	AL	38.98	NA+K	11.42

COORDINATES IN THE SYSTEM PLAGIOCLASE - OLIVINE - CLINOPYROXENE - QUARTZ (IN MOLE PERCENT)

PROPORTION OF ANALYSIS IN BASALT TETRAHEDRON IS 93.69 MOLE PERCENT

BASALT TETRAHEDRON	OL	16.68	CPX	19.31	PLAG	52.11	QTZ	11.90
CLINOPYROXENE PROJECTION		20.68		0.0		64.58		14.74
QUARTZ PROJECTION		18.94		21.92		59.14		0.0
PLAGIOCLASE PROJECTION		34.84		40.32		0.0		24.84
OLIVINE PROJECTION		0.0		16.23		43.79	OPX+(4QTZ)	39.99

CMAS PROJECTIONS

TETRAHEDRON COORDINATES	C	17.14	M	17.25	A	12.82	S	52.78
DIOPSIDE PROJECTION	C3A	32.22	M	14.46	S	53.32		
OLIVINE PROJECTION	CS	22.83	M	62.18	S	14.98		
ENSTATITE PROJECTION	M2S	21.06	C2S3	39.82	A2S3	39.12		
QUARTZ PROJECTION	CAS2	61.48	MS	22.38	CMS2	16.14		

HLAGOTHI COMPLEX

SAMPLE NUMBER BG 223

ORIGINAL WEIGHT PERCENT OXIDES

SIO2	AL2O3	FE2O3	FEO	MNO	MGO	CAO	NA2O	K2O	TIO2	P2O5	CR2O3	TOTAL
54.97	12.98	.83	7.47	.16	10.57	9.20	2.77	.85	.46	.09	.00	100.35

WEIGHT PERCENT OXIDES RECALCULATED TO 100 PERCENT

SIO2	AL2O3	FE2O3	FEO	MNO	MGO	CAO	NA2O	K2O	TIO2	P2O5	CR2O3	TOTAL
54.78	12.93	.83	7.45	.16	10.53	9.17	2.76	.85	.46	.09	.00	100.00

CATION PROPORTIONS IN ANALYSIS

SI	AL	FE(3)	FE(2)	MN	MG	CA	NA	K	TI	P	CR
50.08	13.94	.57	5.69	.12	14.35	8.98	4.89	.99	.32	.07	.00

CIPW NORM

	QTZ	COR	OR	AB	AN	LC	NE	KP
WEIGHT PERCENT	.000	.000	5.005	23.349	20.401	.000	.000	.000
MOLE PERCENT	.000	.000	5.244	21.304	17.544	.000	.000	.000
CATION PERCENT	.000	.000	4.940	24.460	20.142	.000	.000	.000

	AC	NS	KS	DI	WO	HY	OL	CS
WEIGHT PERCENT	.000	.000	.000	19.805	.000	29.099	.059	.000
MOLE PERCENT	.000	.000	.000	21.062	.000	31.993	.090	.000
CATION PERCENT	.000	.000	.000	19.344	.000	29.382	.062	.000

	MT	CM	IL	HM	TN	PF	RU	AP
WEIGHT PERCENT	1.200	.000	.871	.000	.000	.000	.000	.212
MOLE PERCENT	1.240	.000	1.373	.000	.000	.000	.000	.151
CATION PERCENT	.854	.000	.630	.000	.000	.000	.000	.185

MAFIC INDEX = 51.246
NORM TOTAL = 100.001

OLIVINE COMPOSITION
FORSTERITE 65.520 FAYALITE 34.480

ORTHOPYROXENE COMPOSITION
ENSTATITE 67.680 FERROSILITE 32.320

CLINOPYROXENE COMPOSITION
WOLLASTONITE 51.635 ENSTATITE 32.733 FERROSILITE 15.631

FELDSPAR COMPOSITION
ORTHOCLASE 10.266 ALBITE 47.891 ANORTHITE 41.843
PLAGIOCLASE COMPOSITION (PERC AN) 46.630

THORNTON AND TUTTLE DIFFERENTIATION INDEX = 28.354
SOLIDIFICATION INDEX (100*MGO/(MGO+FEO+FE2O3+NA2O+K2O)) = 46.994
CRYSTALLIZATION INDEX (AN+MG DI+FO+FO EQIV OF EN) = 48.225
LARSEN INDEX (1/3SI+K)-(CA+MG) = -6.845
ALBITE RATIO (100*(AB+AB EQIV IN NE)/PLAG) = 53.370
IRON RATIO ((FE2=MN)*100/(FE2+MN+MG)) = 48.200
MG NUMBER AS CATIONS MG/CATIONS (FE+MG) = 71.599
OXIDATION RATIO ACCORDING TO LE MAITRE (FEO/FEO+FE2O3) = .806
DENSITY OF DRY LIQUID OF THIS COMPOSITION (AT 1050 DEG) = 2.654
AFM RATIO
TOTAL ALKALIS 16.15 TOTAL FE 36.68 MG 47.17

KOMATIITE PARAMETERS

FEO/(FEO+MGO)	CAO/AL2O3	SIO2/TIO2	AL2O3/TIO2	FEO*/TIO2	CAO/TIO2	NA2O/TIO2	K2O/TIO2
.4374	.71	119.50	28.22	17.87	20.00	6.022	1.848

JENSEN CATION AL2O3 - FEO+FE2O3+TIO2 - MGO
39.98 18.86 41.16

QUARTZ - FELDSPAR RATIOS
QUARTZ .00 ORTHOCLASE 10.27 PLAGIOCLASE 89.73
QUARTZ .00 ORTHOCLASE 17.65 ALBITE 82.35

CATION PROPORTIONS						
CA	30.64	FE	20.39	MG	48.97
CA	12.23	MG	19.55	SI	68.22
SI	70.14	AL	9.76	MG	20.10
2MG	56.65	2FE	23.59	SI/5	19.77
CA	47.54	AL	36.89	NA+K	15.57

COORDINATES IN THE SYSTEM PLAGIOCLASE - OLIVINE - CLINOPYROXENE - QUARTZ (IN MOLE PERCENT)

PROPORTION OF ANALYSIS IN BASALT TETRAHEDRON IS 93.39 MOLE PERCENT

	OL	CPX	PLAG	QTZ
BASALT TETRAHEDRON	23.66	20.71	47.76	7.87
CLINOPYROXENE PROJECTION	29.84	0.[illegible]	60.24	9.92
QUARTZ PROJECTION	25.68	22.48	51.84	0.0
PLAGIOCLASE PROJECTION	45.29	39.65	0.0	15.06
OLIVINE PROJECTION	0.0	20.73	47.79	OPX+(4QTZ) 31.48

CMAS PROJECTIONS

TETRAHEDRON COORDINATES	C	16.51	M	22.23	A	11.77	S	49.49
DIOPSIDE PROJECTION	C3A	31.59	M	16.43	S	51.98		
OLIVINE PROJECTION	CS	25.54	M	58.48	S	15.97		
ENSTATITE PROJECTION	M2S	31.33	C2S3	35.47	A2S3	33.21		
QUARTZ PROJECTION	CAS2	54.05	MS	28.99	CMS2	16.96		

HLAGOTHI COMPLEX

SAMPLE NUMBER BG 226

ORIGINAL WEIGHT PERCENT OXIDES

SIO2	AL2O3	FE2O3	FEO	MNO	MGO	CAO	NA2O	K2O	TIO2	P2O5	CR2O3	TOTAL
46.26	5.83	1.18	10.61	.19	30.97	3.85	.00	.13	.24	.04	.77	100.07

WEIGHT PERCENT OXIDES RECALCULATED TO 100 PERCENT

SIO2	AL2O3	FE2O3	FEO	MNO	MGO	CAO	NA2O	K2O	TIO2	P2O5	CR2O3	TOTAL
46.23	5.83	1.18	10.60	.19	30.95	3.85	.00	.13	.24	.04	.77	100.00

CATION PROPORTIONS IN ANALYSIS

SI	AL	FE(3)	FE(2)	MN	MG	CA	NA	K	TI	P	CR
40.46	6.01	.78	7.76	.14	40.37	3.61	.00	.15	.16	.03	.53

CIPW NORM

	QTZ	COR	OR	AB	AN	LC	NE	KP
WEIGHT PERCENT	.000	.000	.768	.000	15.513	.000	.000	.000
MOLE PERCENT	.000	.000	.632	.000	10.480	.000	.000	.000
CATION PERCENT	.000	.000	.725	.000	14.664	.000	.000	.000

	AC	NS	KS	DI	WO	HY	OL	CS
WEIGHT PERCENT	.000	.000	.000	2.634	.000	37.944	39.754	.000
MOLE PERCENT	.000	.000	.000	2.237	.000	33.926	49.769	.000
CATION PERCENT	.000	.000	.000	2.504	.000	37.972	41.777	.000

	MT	CM	IL	HM	TN	PF	RU	AP
WEIGHT PERCENT	1.708	1.133	.456	.000	.000	.000	.000	.095
MOLE PERCENT	1.387	.952	.564	.000	.000	.000	.000	.053
CATION PERCENT	1.164	.799	.316	.000	.000	.000	.000	.079

MAFIC INDEX = 83.724
NORM TOTAL = 100.005

OLIVINE COMPOSITION
FORSTERITE 79.730 FAYALITE 20.270

ORTHOPYROXENE COMPOSITION
ENSTATITE 81.254 FERROSILITE 18.746

CLINOPYROXENE COMPOSITION
WOLLASTONITE 52.498 ENSTATITE 38.598 FERROSILITE 8.905

FELDSPAR COMPOSITION
ORTHOCLASE 4.715 ALBITE .000 ANORTHITE 95.285
PLAGIOCLASE COMPOSITION (PERC AN) ******

THORNTON AND TUTTLE DIFFERENTIATION INDEX = .768
SOLIDIFICATION INDEX (100*MGO/(MGO+FEO+FE2O3+NA2O+K2O)) = 72.211
CRYSTALLIZATION INDEX (AN+MG DI+FO+FO EQIV OF EN) = 71.009
LARSEN INDEX (1/3SI+K)-(CA+MG) = -31.608
ALBITE RATIO (100*(AB+AB EQIV IN NE)/PLAG) = .000
IRON RATIO ((FE2=MN)*100/(FE2+MN+MG)) = 31.005
MG NUMBER AS CATIONS MG/CATIONS (FE+MG) = 83.876
OXIDATION RATIO ACCORDING TO LE MAITRE (FEO/FEO+FE2O3) = .797
DENSITY OF DRY LIQUID OF THIS COMPOSITION (AT 1050 DEG) = 2.898
AFM RATIO
TOTAL ALKALIS .30 TOTAL FE 27.29 MG 72.41

KOMATIITE PARAMETERS

FEO/(FEO+MGO)	CAO/AL2O3	SIO2/TIO2	AL2O3/TIO2	FEO*/TIO2	CAO/TIO2	NA2O/TIO2	K2O/TIO2
.2737	.66	192.75	24.29	48.62	16.04	.000	.542

JENSEN CATION AL2O3 - FEO+FE2O3+TIO2 - MGO
10.91 15.79 73.30

QUARTZ - FELDSPAR RATIOS
QUARTZ .00 ORTHOCLASE 4.72 PLAGIOCLASE 95.28
QUARTZ .00 ORTHOCLASE ***** ALBITE .00

CATION PROPORTIONS						
	CA	6.92	FE	15.63	MG	77.45
	CA	4.27	MG	47.81	SI	47.92
	SI	48.26	AL	3.58	MG	48.16
	2MG	76.80	2FE	15.50	SI/5	7.70
	CA	53.97	AL	44.95	NA+K	1.08

COORDINATES IN THE SYSTEM PLAGIOCLASE - OLIVINE - CLINOPYROXENE - QUARTZ (IN MOLE PERCENT)

PROPORTION OF ANALYSIS IN BASALT TETRAHEDRON IS 96.92 MOLE PERCENT

BASALT TETRAHEDRON	OL	72.49	CPX	2.58	PLAG	15.13	QTZ	9.79
CLINOPYROXENE PROJECTION		74.41		0.0		15.53		10.05
QUARTZ PROJECTION		80.36		2.86		16.77		0.0
PLAGIOCLASE PROJECTION		85.41		3.04		0.0		11.54
OLIVINE PROJECTION		0.0		4.54		26.59	OPX+(4QTZ)	68.86

CMAS PROJECTIONS

TETRAHEDRON COORDINATES	C	3.86	M	50.11	A	4.05	S	41.99
DIOPSIDE PROJECTION	C3A	15.71	M	33.78	S	50.51		
OLIVINE PROJECTION	CS	12.85	M	75.31	S	11.84		
ENSTATITE PROJECTION	M2S	67.70	C2S3	13.57	A2S3	18.73		
QUARTZ PROJECTION	CAS2	*****	MS	*****	CMS2	*****		

HLAGOTHI COMPLEX

SAMPLE NUMBER BC 227

ORIGINAL WEIGHT PERCENT OXIDES

SIO2	AL2O3	FE2O3	FEO	MNO	MGO	CAO	NA2O	K2O	TIO2	P2O5	CR2O3	TOTAL
55.75	8.02	.94	8.49	.19	18.45	7.47	.61	.04	.35	.06	.00	100.37

WEIGHT PERCENT OXIDES RECALCULATED TO 100 PERCENT

SIO2	AL2O3	FE2O3	FEO	MNO	MGO	CAO	NA2O	K2O	TIO2	P2O5	CR2O3	TOTAL
55.54	7.99	.94	8.46	.19	18.38	7.44	.61	.04	.35	.06	.00	100.00

CATION PROPORTIONS IN ANALYSIS

SI	AL	FE(3)	FE(2)	MN	MG	CA	NA	K	TI	P	CR
50.58	8.58	.64	6.44	.15	24.95	7.26	1.07	.05	.24	.05	.00

CIPW NORM

	QTZ	COR	OR	AB	AN	LC	NE	KP
WEIGHT PERCENT	5.862	.000	.235	5.141	18.956	.000	.000	.000
MOLE PERCENT	19.069	.000	.202	3.832	13.317	.000	.000	.000
CATION PERCENT	5.338	.000	.231	5.364	18.642	.000	.000	.000

	AC	NS	KS	DI	WO	HY	OL	CS
WEIGHT PERCENT	.000	.000	.000	14.066	.000	53.577	.000	.000
MOLE PERCENT	.000	.000	.000	12.346	.000	49.149	.000	.000
CATION PERCENT	.000	.000	.000	13.825	.000	55.033	.000	.000

	MT	CM	IL	HM	TN	PF	RU	AP
WEIGHT PERCENT	1.363	.000	.662	.000	.000	.000	.000	.142
MOLE PERCENT	1.150	.000	.853	.000	.000	.000	.000	.082
CATION PERCENT	.966	.000	.478	.000	.000	.000	.000	.123

MAFIC INDEX = 69.809
NORM TOTAL = 100.004

OLIVINE COMPOSITION
FORSTERITE .000 FAYALITE .000

ORTHOPYROXENE COMPOSITION
ENSTATITE 75.913 FERROSILITE 24.087

CLINOPYROXENE COMPOSITION
WOLLASTONITE 52.162 ENSTATITE 36.315 FERROSILITE 11.523

FELDSPAR COMPOSITION
ORTHOCLASE .968 ALBITE 21.128 ANORTHITE 77.905
PLAGIOCLASE COMPOSITION (PERC AN) 78.666

THORNTON AND TUTTLE DIFFERENTIATION INDEX = 11.238
SOLIDIFICATION INDEX (100*MGO/(MGO+FEO+FE2O3+NA2O+K2O)) = 64.668
CRYSTALLIZATION INDEX (AN+MG DI+FO+FO EQIV OF EN) = 58.479
LARSEN INDEX (1/3SI+K)-(CA+MG) = -16.166
ALBITE RATIO (100*(AB+AB EQIV IN NE)/PLAG) = 21.334
IRON RATIO ((FE2=MN)*100/(FE2+MN+MG)) = 37.737
MG NUMBER AS CATIONS MG/CATIONS (FE+MG) = 79.482
OXIDATION RATIO ACCORDING TO LE MAITRE (FEO/FEO+FE2O3) = .839
DENSITY OF DRY LIQUID OF THIS COMPOSITION (AT 1050 DEG) = 2.726
AFM RATIO
TOTAL ALKALIS 2.29 TOTAL FE 32.83 MG 64.88

KOMATIITE PARAMETERS

FEO/(FEO+MGO)	CAO/AL2O3	SIO2/TIO2	AL2O3/TIO2	FEO*/TIO2	CAO/TIO2	NA2O/TIO2	K2O/TIO2
.3360	.93	159.29	22.91	26.67	21.34	1.743	.114

JENSEN CATION AL2O3 - FEO+FE2O3+TIO2 - MGO
21.00 17.93 61.08

QUARTZ - FELDSPAR RATIOS
QUARTZ 19.41 ORTHOCLASE .78 PLAGIOCLASE 79.81
QUARTZ 52.16 ORTHOCLASE 2.10 ALBITE 45.74

CATION PROPORTIONS						
	CA	18.63	FE	17.35	MG	64.02
	CA	8.77	MG	30.14	SI	61.09
	SI	63.37	AL	5.37	MG	31.26
	2MG	67.86	2FE	18.39	SI/5	13.76
	CA	59.97	AL	35.41	NA+K	4.62

COORDINATES IN THE SYSTEM PLAGIOCLASE - OLIVINE - CLINOPYROXENE - QUARTZ (IN MOLE PERCENT)

PROPORTION OF ANALYSIS IN BASALT TETRAHEDRON IS 98.20 MOLE PERCENT

BASALT TETRAHEDRON	OL	42.03	CPX	14.08	PLAG	24.45	QTZ	19.45
CLINOPYROXENE PROJECTION		48.92		0.0		28.45		22.63
QUARTZ PROJECTION		52.18		17.48		30.35		0.0
PLAGIOCLASE PROJECTION		55.63		18.63		0.0		25.74
OLIVINE PROJECTION		0.0		12.10		21.02	OPX+(4QTZ)	66.88

CMAS PROJECTIONS

TETRAHEDRON COORDINATES	C	8.79	M	33.13	A	5.72	S	52.36
DIOPSIDE PROJECTION	C3A	20.98	M	22.69	S	56.33		
OLIVINE PROJECTION	CS	14.53	M	77.17	S	8.30		
ENSTATITE PROJECTION	M2S	13.04	C2S3	46.86	A2S3	40.10		
QUARTZ PROJECTION	CAS2	30.19	MS	57.23	CMS2	12.58		

HLAGOTHI COMPLEX

SAMPLE NUMBER BG 228

ORIGINAL WEIGHT PERCENT OXIDES

SIO2	AL2O3	FE2O3	FEO	MNO	MGO	CAO	NA2O	K2O	TIO2	P2O5	CR2O3	TOTAL
49.14	5.85	1.16	10.40	.20	26.22	5.11	.43	.36	.31	.07	.56	99.81

WEIGHT PERCENT OXIDES RECALCULATED TO 100 PERCENT

SIO2	AL2O3	FE2O3	FEO	MNO	MGO	CAO	NA2O	K2O	TIO2	P2O5	CR2O3	TOTAL
49.24	5.86	1.16	10.42	.20	26.27	5.12	.43	.36	.31	.07	.56	100.00

CATION PROPORTIONS IN ANALYSIS

SI	AL	FE(3)	FE(2)	MN	MG	CA	NA	K	TI	P	CR
43.74	6.14	.77	7.74	.15	34.78	4.87	.74	.41	.21	.05	.39

CIPW NORM

	QTZ	COR	OR	AB	AN	LC	NE	KP
WEIGHT PERCENT	.000	.000	2.131	3.644	12.994	.000	.000	.000
MOLE PERCENT	.000	.000	1.870	2.785	9.358	.000	.000	.000
CATION PERCENT	.000	.000	2.044	3.710	12.466	.000	.000	.000

	AC	NS	KS	DI	WO	HY	OL	CS
WEIGHT PERCENT	.000	.000	.000	9.529	.000	43.271	25.174	.000
MOLE PERCENT	.000	.000	.000	8.604	.000	40.997	33.316	.000
CATION PERCENT	.000	.000	.000	9.168	.000	43.682	26.623	.000

	MT	CM	IL	HM	TN	PF	RU	AP
WEIGHT PERCENT	1.679	.826	.590	.000	.000	.000	.000	.166
MOLE PERCENT	1.453	.740	.779	.000	.000	.000	.000	.099
CATION PERCENT	1.161	.591	.415	.000	.000	.000	.000	.141

MAFIC INDEX = 81.236
NORM TOTAL = 100.005

OLIVINE COMPOSITION
FORSTERITE 77.185 FAYALITE 22.815

ORTHOPYROXENE COMPOSITION
ENSTATITE 78.851 FERROSILITE 21.149

CLINOPYROXENE COMPOSITION
WOLLASTONITE 52.347 ENSTATITE 37.575 FERROSILITE 10.078

FELDSPAR COMPOSITION
ORTHOCLASE 11.356 ALBITE 19.417 ANORTHITE 69.228
PLAGIOCLASE COMPOSITION (PERC AN) 78.096

THORNTON AND TUTTLE DIFFERENTIATION INDEX = 5.776
SOLIDIFICATION INDEX (100*MGO/(MGO+FEO+FE2O3+NA2O+K2O)) = 67.988
CRYSTALLIZATION INDEX (AN+MG DI+FO+FO EQIV OF EN) = 64.060
LARSEN INDEX (1/3SI+K)-(CA+MG) = -25.977
ALBITE RATIO (100*(AB+AB EQIV IN NE)/PLAG) = 21.904
IRON RATIO ((FE2=MN)*100/(FE2+MN+MG)) = 34.254
MG NUMBER AS CATIONS MG/CATIONS (FE+MG) = 81.794
OXIDATION RATIO ACCORDING TO LE MAITRE (FEO/FEO+FE2O3) = .802
DENSITY OF DRY LIQUID OF THIS COMPOSITION (AT 1050 DEG) = 2.842
AFM RATIO
TOTAL ALKALIS 2.05 TOTAL FE 29.75 MG 68.19

KOMATIITE PARAMETERS

FEO/(FEO+MGO)	CAO/AL2O3	SIO2/TIO2	AL2O3/TIO2	FEO*/TIO2	CAO/TIO2	NA2O/TIO2	K2O/TIO2
.3038	.87	158.52	18.87	36.90	16.48	1.387	1.161

JENSEN CATION AL2O3 - FEO+FE2O3+TIO2 - MGO
12.36 17.57 70.06

QUARTZ - FELDSPAR RATIOS
QUARTZ .00 ORTHOCLASE 11.36 PLAGIOCLASE 88.64
QUARTZ .00 ORTHOCLASE 36.90 ALBITE 63.10

CATION PROPORTIONS						
CA	10.20	FE	17.01	MG	72.79
CA	5.84	MG	41.71	SI	52.45
SI	53.61	AL	3.76	MG	42.63
2MG	73.56	2FE	17.19	SI/5	9.25
CA	57.22	AL	36.03	NA+K	6.76

COORDINATES IN THE SYSTEM PLAGIOCLASE - OLIVINE - CLINOPYROXENE - QUARTZ (IN MOLE PERCENT)

PROPORTION OF ANALYSIS IN BASALT TETRAHEDRON IS 95.65 MOLE PERCENT

BASALT TETRAHEDRON	OL	62.09	CPX	9.59	PLAG	16.91	QTZ	11.42
CLINOPYROXENE PROJECTION		68.67		0 [illegible]		18.70		12.63
QUARTZ PROJECTION		70.09		10.82		19.09		0.0
PLAGIOCLASE PROJECTION		74.72		11.54		0.0		13.74
OLIVINE PROJECTION		0.0		13.28		23.43	OPX+(4QTZ)	63.28

CMAS PROJECTIONS

TETRAHEDRON COORDINATES	C	6.22	M	44.50	A	4.65	S	44.63
DIOPSIDE PROJECTION	C3A	18.01	M	30.20	S	51.79		
OLIVINE PROJECTION	CS	16.27	M	73.06	S	10.67		
ENSTATITE PROJECTION	M2S	55.81	C2S3	22.30	A2S3	21.89		
QUARTZ PROJECTION	CAS2	21.75	MS	72.52	CMS2	5.73		

SAMPLE NUMBER DG 229

ORIGINAL WEIGHT PERCENT OXIDES

SIO2	AL2O3	FE2O3	FEO	MNO	MGO	CAO	NA2O	K2O	TIO2	P2O5	CR2O3	TOTAL
55.58	6.80	.92	8.32	.21	20.00	6.64	.32	.59	.22	.03	.00	99.63

WEIGHT PERCENT OXIDES RECALCULATED TO 100 PERCENT

SIO2	AL2O3	FE2O3	FEO	MNO	MGO	CAO	NA2O	K2O	TIO2	P2O5	CR2O3	TOTAL
55.79	6.83	.93	8.35	.21	20.07	6.66	.32	.59	.22	.03	.00	100.00

CATION PROPORTIONS IN ANALYSIS

SI	AL	FE(3)	FE(2)	MN	MG	CA	NA	K	TI	P	CR
50.57	7.29	.63	6.33	.16	27.12	6.47	.56	.68	.15	.02	.00

CIPW NORM

	QTZ	COR	OR	AB	AN	LC	NE	KP
WEIGHT PERCENT	4.659	.000	3.499	2.717	15.432	.000	.000	.000
MOLE PERCENT	15.414	.000	3.046	2.060	11.026	.000	.000	.000
CATION PERCENT	4.223	.000	3.424	2.822	15.107	.000	.000	.000

	AC	NS	KS	DI	WO	HY	OL	CS
WEIGHT PERCENT	.000	.000	.000	13.929	.000	57.932	.000	.000
MOLE PERCENT	.000	.000	.000	12.455	.000	54.253	.000	.000
CATION PERCENT	.000	.000	.000	13.651	.000	59.460	.000	.000

	MT	CM	IL	HM	TN	PF	RU	AP
WEIGHT PERCENT	1.345	.000	.419	.000	.000	.000	.000	.071
MOLE PERCENT	1.155	.000	.549	.000	.000	.000	.000	.042
CATION PERCENT	.949	.000	.301	.000	.000	.000	.000	.062

MAFIC INDEX = 73.696
NORM TOTAL = 100.004

OLIVINE COMPOSITION
FORSTERITE .000 FAYALITE .000

ORTHOPYROXENE COMPOSITION
ENSTATITE 77.413 FERROSILITE 22.587

CLINOPYROXENE COMPOSITION
WOLLASTONITE 52.257 ENSTATITE 36.959 FERROSILITE 10.784

FELDSPAR COMPOSITION
ORTHOCLASE 16.164 ALBITE 12.550 ANORTHITE 71.285
PLAGIOCLASE COMPOSITION (PERC AN) 85.030

THORNTON AND TUTTLE DIFFERENTIATION INDEX = 10.875
SOLIDIFICATION INDEX (100*MGO/(MGO+FEO+FE2O3+NA2O+K2O)) = 66.334
CRYSTALLIZATION INDEX (AN+MG DI+FO+FO EQIV OF EN) = 57.967
LARSEN INDEX (1/3SI+K)-(CA+MG) = -17.186
ALBITE RATIO (100*(AB+AB EQIV IN NE)/PLAG) = 14.970
IRON RATIO ((FE2=MN)*100/(FE2+MN+MG)) = 35.459
MG NUMBER AS CATIONS MG/CATIONS (FE+MG) = 81.081
OXIDATION RATIO ACCORDING TO LE MAITRE (FEO/FEO+FE2O3) = .826
DENSITY OF DRY LIQUID OF THIS COMPOSITION (AT 1050 DEG) = 2.729
AFM RATIO
TOTAL ALKALIS 3.03 TOTAL FE 30.43 MG 66.54

KOMATIITE PARAMETERS

FEO/(FEO+MGO)	CAO/AL2O3	SIO2/TIO2	AL2O3/TIO2	FEO*/TIO2	CAO/TIO2	NA2O/TIO2	K2O/TIO2
.3138	.98	252.64	30.91	41.58	30.18	1.455	2.682

JENSEN CATION AL2O3 - FEO+FE2O3+TIO2 - MGO
17.56 17.13 65.31

QUARTZ - FELDSPAR RATIOS
QUARTZ 17.71 ORTHOCLASE 13.30 PLAGIOCLASE 68.99
QUARTZ 42.84 ORTHOCLASE 32.18 ALBITE 24.98

CATION PROPORTIONS						
CA	16.09	FE	16.51	MG	67.40
CA	7.69	MG	32.23	SI	60.08
SI	62.17	AL	4.48	MG	33.34
2MG	69.86	2FE	17.11	SI/5	13.03
CA	60.25	AL	33.94	NA+K	5.81

COORDINATES IN THE SYSTEM PLAGIOCLASE - OLIVINE - CLINOPYROXENE - QUARTZ (IN MOLE PERCENT)

PROPORTION OF ANALYSIS IN BASALT TETRAHEDRON IS 95.26 MOLE PERCENT

BASALT TETRAHEDRON	OL	46.81	CPX	14.33	PLAG	18.82	QTZ	20.04
CLINOPYROXENE PROJECTION		54.64		0.0		21.97		23.39
QUARTZ PROJECTION		58.54		17.92		23.54		0.0
PLAGIOCLASE PROJECTION		57.66		17.65		0.0		24.68
OLIVINE PROJECTION		0.0		12.65		16.61	OPX+(4QTZ)	70.74

CMAS PROJECTIONS

TETRAHEDRON COORDINATES	C	8.07	M	35.15	A	4.98	S	51.81
DIOPSIDE PROJECTION	C3A	19.28	M	24.28	S	56.45		
OLIVINE PROJECTION	CS	14.00	M	78.43	S	7.57		
ENSTATITE PROJECTION	M2S	16.09	C2S3	46.36	A2S3	37.55		
QUARTZ PROJECTION	CAS2	26.25	MS	61.04	CMS2	12.71		

HLAGOTHI COMPLEX

SAMPLE NUMBER BG 231

ORIGINAL WEIGHT PERCENT OXIDES

SIO2	AL2O3	FE2O3	FEO	MNO	MGO	CAO	NA2O	K2O	TIO2	P2O5	CR2O3	TOTAL
56.32	14.96	.91	8.23	.17	6.56	10.74	2.16	.78	.37	.06	.00	101.26

WEIGHT PERCENT OXIDES RECALCULATED TO 100 PERCENT

SIO2	AL2O3	FE2O3	FEO	MNO	MGO	CAO	NA2O	K2O	TIO2	P2O5	CR2O3	TOTAL
55.62	14.77	.90	8.12	.17	6.48	10.61	2.13	.77	.37	.06	.00	100.00

CATION PROPORTIONS IN ANALYSIS

SI	AL	FE(3)	FE(2)	MN	MG	CA	NA	K	TI	P	CR
51.93	16.26	.63	6.34	.13	9.01	10.61	3.86	.92	.26	.05	.00

CIPW NORM

	QTZ	COR	OR	AB	AN	LC	NE	KP
WEIGHT PERCENT	6.862	.000	4.552	18.044	28.461	.000	.000	.000
MOLE PERCENT	23.233	.000	4.055	13.998	20.811	.000	.000	.000
CATION PERCENT	6.406	.000	4.587	19.303	28.695	.000	.000	.000

	AC	NS	KS	DI	WO	HY	OL	CS
WEIGHT PERCENT	.000	.000	.000	19.566	.000	20.373	.000	.000
MOLE PERCENT	.000	.000	.000	17.378	.000	18.359	.000	.000
CATION PERCENT	.000	.000	.000	19.169	.000	20.249	.000	.000

	MT	CM	IL	HM	TN	PF	RU	AP
WEIGHT PERCENT	1.309	.000	.694	.000	.000	.000	.000	.140
MOLE PERCENT	1.150	.000	.930	.000	.000	.000	.000	.085
CATION PERCENT	.952	.000	.513	.000	.000	.000	.000	.125

MAFIC INDEX = 42.082
NORM TOTAL = 100.001

OLIVINE COMPOSITION
FORSTERITE .000 FAYALITE .000

ORTHOPYROXENE COMPOSITION
ENSTATITE 53.753 FERROSILITE 46.247

CLINOPYROXENE COMPOSITION
WOLLASTONITE 50.717 ENSTATITE 26.491 FERROSILITE 22.792

FELDSPAR COMPOSITION
ORTHOCLASE 8.915 ALBITE 35.341 ANORTHITE 55.744
PLAGIOCLASE COMPOSITION (PERC AN) 61.200

THORNTON AND TUTTLE DIFFERENTIATION INDEX = 29.457
SOLIDIFICATION INDEX (100*MGO/(MGO+FEO+FE2O3+NA2O+K2O)) = 35.190
CRYSTALLIZATION INDEX (AN+MG DI+FO+FO EQIV OF EN) = 47.316
LARSEN INDEX (1/3SI+K)-(CA+MG) = -2.082
ALBITE RATIO (100*(AB+AB EQIV IN NE)/PLAG) = 38.800
IRON RATIO ((FE2=MN)*100/(FE2+MN+MG)) = 62.260
MG NUMBER AS CATIONS MG/CATIONS (FE+MG) = 58.693
OXIDATION RATIO ACCORDING TO LE MAITRE (FEO/FEO+FE2O3) = .839
DENSITY OF DRY LIQUID OF THIS COMPOSITION (AT 1050 DEG) = 2.642
AFM RATIO
TOTAL ALKALIS 15.85 TOTAL FE 48.79 MG 35.36

KOMATIITE PARAMETERS

FEO/(FEO+MGO)	CAO/AL2O3	SIO2/TIO2	AL2O3/TIO2	FEO*/TIO2	CAO/TIO2	NA2O/TIO2	K2O/TIO2
.5798	.72	152.22	40.43	24.46	29.03	5.838	2.108

JENSEN CATION AL2O3 - FEO+FE2O3+TIO2 - MGO
50.01 22.26 27.73

QUARTZ - FELDSPAR RATIOS
QUARTZ 11.85 ORTHOCLASE 7.86 PLAGIOCLASE 80.29
QUARTZ 23.29 ORTHOCLASE 15.45 ALBITE 61.25

CATION PROPORTIONS						
CA	40.36	FE	25.34	MG	34.30
CA	14.83	MG	12.60	SI	72.57
SI	75.18	AL	11.77	MG	13.05
2MG	43.20	2FE	31.92	SI/5	24.88
CA	50.22	AL	38.47	NA+K	11.31

COORDINATES IN THE SYSTEM PLAGIOCLASE - OLIVINE - CLINOPYROXENE - QUARTZ (IN MOLE PERCENT)

PROPORTION OF ANALYSIS IN BASALT TETRAHEDRON IS 93.82 MOLE PERCENT

BASALT TETRAHEDRON	OL	16.19	CPX	20.43	PLAG	51.16	QTZ	12.22
CLINOPYROXENE PROJECTION		20.34		0.0		64.29		15.36
QUARTZ PROJECTION		18.44		23.28		58.28		0.0
PLAGIOCLASE PROJECTION		33.14		41.83		0.0		25.03
OLIVINE PROJECTION		0.0		16.96		42.46	OPX+(4QTZ)	40.58

CMAS PROJECTIONS

TETRAHEDRON COORDINATES	C	17.24	M	17.16	A	12.49	S	53.11
DIOPSIDE PROJECTION	C3A	32.13	M	14.35	S	53.52		
OLIVINE PROJECTION	CS	22.88	M	62.58	S	14.54		
ENSTATITE PROJECTION	M2S	19.84	C2S3	41.07	A2S3	39.09		
QUARTZ PROJECTION	CAS2	60.44	MS	21.67	CMS2	17.90		

HLAGOTHI COMPLEX

SAMPLE NUMBER BG 232

ORIGINAL WEIGHT PERCENT OXIDES

SIO2	AL2O3	FE2O3	FEO	MNO	MGO	CAO	NA2O	K2O	TIO2	P2O5	CR2O3	TOTAL
55.98	12.15	.96	8.64	.17	8.53	9.73	1.89	1.35	.67	.10	.00	100.17

WEIGHT PERCENT OXIDES RECALCULATED TO 100 PERCENT

SIO2	AL2O3	FE2O3	FEO	MNO	MGO	CAO	NA2O	K2O	TIO2	P2O5	CR2O3	TOTAL
55.88	12.13	.96	8.63	.17	8.52	9.71	1.89	1.35	.67	.10	.00	100.00

CATION PROPORTIONS IN ANALYSIS

SI	AL	FE(3)	FE(2)	MN	MG	CA	NA	K	TI	P	CR
52.07	13.32	.67	6.72	.13	11.82	9.70	3.41	1.60	.47	.08	.00

CIPW NORM

	QTZ	COR	OR	AB	AN	LC	NE	KP
WEIGHT PERCENT	5.845	.000	7.964	15.960	20.646	.000	.000	.000
MOLE PERCENT	19.843	.000	7.114	12.414	15.136	.000	.000	.000
CATION PERCENT	5.446	.000	8.010	17.040	20.775	.000	.000	.000

	AC	NS	KS	DI	WO	HY	OL	CS
WEIGHT PERCENT	.000	.000	.000	21.961	.000	24.730	.000	.000
MOLE PERCENT	.000	.000	.000	19.712	.000	22.706	.000	.000
CATION PERCENT	.000	.000	.000	21.643	.000	24.930	.000	.000

	MT	CM	IL	HM	TN	PF	RU	AP
WEIGHT PERCENT	1.390	.000	1.270	.000	.000	.000	.000	.236
MOLE PERCENT	1.224	.000	1.707	.000	.000	.000	.000	.143
CATION PERCENT	1.008	.000	.937	.000	.000	.000	.000	.210

MAFIC INDEX = 49.588
NORM TOTAL = 100.003

OLIVINE COMPOSITION
FORSTERITE .000 FAYALITE .000

ORTHOPYROXENE COMPOSITION
ENSTATITE 59.801 FERROSILITE 40.199

CLINOPYROXENE COMPOSITION
WOLLASTONITE 51.120 ENSTATITE 29.231 FERROSILITE 19.649

FELDSPAR COMPOSITION
ORTHOCLASE 17.868 ALBITE 35.809 ANORTHITE 46.323
PLAGIOCLASE COMPOSITION (PERC AN) 56.400

THORNTON AND TUTTLE DIFFERENTIATION INDEX = 29.770
SOLIDIFICATION INDEX (100*MGO/(MGO+FEO+FE2O3+NA2O+K2O)) = 39.916
CRYSTALLIZATION INDEX (AN+MG DI+FO+FO EQIV OF EN) = 44.857
LARSEN INDEX (1/3SI+K)-(CA+MG) = -3.719
ALBITE RATIO (100*(AB+AB EQIV IN NE)/PLAG) = 43.600
IRON RATIO ((FE2=MN)*100/(FE2+MN+MG)) = 57.100
MG NUMBER AS CATIONS MG/CATIONS (FE+MG) = 63.760
OXIDATION RATIO ACCORDING TO LE MAITRE (FEO/FEO+FE2O3) = .823
DENSITY OF DRY LIQUID OF THIS COMPOSITION (AT 1050 DEG) = 2.657
AFM RATIO
TOTAL ALKALIS 15.23 TOTAL FE 44.67 MG 40.10'

KOMATIITE PARAMETERS

FEO/(FEO+MGO)	CAO/AL2O3	SIO2/TIO2	AL2O3/TIO2	FEO*/TIO2	CAO/TIO2	NA2O/TIO2	K2O/TIO2
.5270	.80	83.55	18.13	14.18	14.52	2.821	2.015

JENSEN CATION AL2O3 - FEO+FE2O3+TIO2 - MGO
40.36 23.82 35.82

QUARTZ - FELDSPAR RATIOS
QUARTZ 11.59 ORTHOCLASE 15.80 PLAGIOCLASE 72.61
QUARTZ 19.64 ORTHOCLASE 26.75 ALBITE 53.61

CATION PROPORTIONS

CA	33.93	FE	24.69	MG	41.38
CA	13.18	MG	16.07	SI	70.76
SI	73.80	AL	9.44	MG	16.76
2MG	49.09	2FE	29.29	SI/5	21.62
CA	51.41	AL	35.31	NA+K	13.28

COORDINATES IN THE SYSTEM PLAGIOCLASE - OLIVINE - CLINOPYROXENE - QUARTZ (IN MOLE PERCENT)

PROPORTION OF ANALYSIS IN BASALT TETRAHEDRON IS 89.83 MOLE PERCENT

	OL	CPX	PLAG	QTZ
BASALT TETRAHEDRON	20.81	24.09	42.09	13.00
CLINOPYROXENE PROJECTION	27.42	0.0	55.45	17.13
QUARTZ PROJECTION	23.92	27.69	48.38	0.0
PLAGIOCLASE PROJECTION	35.94	41.61	0.0	22.45
OLIVINE PROJECTION	0.0	20.38	35.62	OPX+(4QTZ) 44.00

CMAS PROJECTIONS

TETRAHEDRON COORDINATES	C	16.23	M	20.28	A	11.10	S	52.40
DIOPSIDE PROJECTION	C3A	30.90	M	15.51	S	53.58		
OLIVINE PROJECTION	CS	22.87	M	63.41	S	13.72		
ENSTATITE PROJECTION	M2S	21.70	C2S3	41.24	A2S3	37.06		
QUARTZ PROJECTION	CAS2	53.99	MS	26.59	CMS2	19.42		

SAMPLE NUMBER BG 236

ORIGINAL WEIGHT PERCENT OXIDES

SIO2	AL2O3	FE2O3	FEO	MNO	MGO	CAO	NA2O	K2O	TIO2	P2O5	CR2O3	TOTAL
55.33	6.49	.94	8.50	.21	21.52	5.63	.63	.23	.17	.02	.00	99.67

WEIGHT PERCENT OXIDES RECALCULATED TO 100 PERCENT

SIO2	AL2O3	FE2O3	FEO	MNO	MGO	CAO	NA2O	K2O	TIO2	P2O5	CR2O3	TOTAL
55.51	6.51	.95	8.52	.21	21.59	5.65	.63	.23	.17	.02	.00	100.00

CATION PROPORTIONS IN ANALYSIS

SI	AL	FE(3)	FE(2)	MN	MG	CA	NA	K	TI	P	CR
49.96	6.91	.64	6.42	.16	28.96	5.45	1.10	.26	.12	.02	.00

CIPW NORM

	QTZ	COR	OR	AB	AN	LC	NE	KP
WEIGHT PERCENT	2.851	.000	1.364	5.347	14.248	.000	.000	.000
MOLE PERCENT	9.839	.000	1.238	4.227	10.618	.000	.000	.000
CATION PERCENT	2.566	.000	1.325	5.514	13.849	.000	.000	.000

	AC	NS	KS	DI	WO	HY	OL	CS
WEIGHT PERCENT	.000	.000	.000	10.890	.000	63.558	.000	.000
MOLE PERCENT	.000	.000	.000	10.166	.000	62.209	.000	.000
CATION PERCENT	.000	.000	.000	10.608	.000	64.904	.000	.000

	MT	CM	IL	HM	TN	PF	RU	AP
WEIGHT PERCENT	1.374	.000	.324	.000	.000	.000	.000	.048
MOLE PERCENT	1.230	.000	.443	.000	.000	.000	.000	.029
CATION PERCENT	.962	.000	.231	.000	.000	.000	.000	.041

MAFIC INDEX = 76.193
NORM TOTAL = 100.002

OLIVINE COMPOSITION
FORSTERITE .000 FAYALITE .000

ORTHOPYROXENE COMPOSITION
ENSTATITE 78.213 FERROSILITE 21.787

CLINOPYROXENE COMPOSITION
WOLLASTONITE 52.307 ENSTATITE 37.302 FERROSILITE 10.391

FELDSPAR COMPOSITION
ORTHOCLASE 6.506 ALBITE 25.511 ANORTHITE 67.982
PLAGIOCLASE COMPOSITION (PERC AN) 72.713

THORNTON AND TUTTLE DIFFERENTIATION INDEX = 9.562
SOLIDIFICATION INDEX (100*MGO/(MGO+FEO+FE2O3+NA2O+K2O)) = 67.630
CRYSTALLIZATION INDEX (AN+MG DI+FO+FO EQIV OF EN) = 57.849
LARSEN INDEX (1/3SI+K)-(CA+MG) = -18.448
ALBITE RATIO (100*(AB+AB EQIV IN NE)/PLAG) = 27.287
IRON RATIO ((FE2+MN)*100/(FE2+MN+MG)) = 34.270
MG NUMBER AS CATIONS MG/CATIONS (FE+MG) = 81.863
OXIDATION RATIO ACCORDING TO LE MAITRE (FEO/FEO+FE2O3) = .820
DENSITY OF DRY LIQUID OF THIS COMPOSITION (AT 1050 DEG) = 2.738
AFM RATIO
TOTAL ALKALIS 2.71 TOTAL FE 29.46 MG 67.83

KOMATIITE PARAMETERS

FEO/(FEO+MGO)	CAO/AL2O3	SIO2/TIO2	AL2O3/TIO2	FEO*/TIO2	CAO/TIO2	NA2O/TIO2	K2O/TIO2
.3028	.87	325.47	38.18	54.98	33.12	3.706	1.353

JENSEN CATION AL2O3 - FEO+FE2O3+TIO2 - MGO
16.05 16.67 67.29

QUARTZ - FELDSPAR RATIOS

QUARTZ	11.98	ORTHOCLASE	5.73	PLAGIOCLASE	82.30		
QUARTZ	29.82	ORTHOCLASE	14.26	ALBITE	55.92		

CATION PROPORTIONS

CA	13.24	FE	16.37	MG	70.39
CA	6.46	MG	34.33	SI	59.22
SI	60.65	AL	4.19	MG	35.16
2MG	71.17	2FE	16.55	SI/5	12.28
CA	56.83	AL	36.03	NA+K	7.14

COORDINATES IN THE SYSTEM PLAGIOCLASE - OLIVINE - CLINOPYROXENE - QUARTZ (IN MOLE PERCENT)

PROPORTION OF ANALYSIS IN BASALT TETRAHEDRON IS 97.44 MOLE PERCENT

BASALT TETRAHEDRON	OL	49.96	CPX	10.89	PLAG	19.87	QTZ	19.29
CLINOPYROXENE PROJECTION		56.06		0.0**		22.30		21.64
QUARTZ PROJECTION		61.89		13.49		24.62		0.0
PLAGIOCLASE PROJECTION		62.33		13.59		0.0		24.07
OLIVINE PROJECTION		0.0		10.09		18.42	OPX+(4QTZ)	71.49

CMAS PROJECTIONS

TETRAHEDRON COORDINATES	C	7.12	M	37.14	A	4.79	S	50.95
DIOPSIDE PROJECTION	C3A	18.45	M	25.50	S	56.05		
OLIVINE PROJECTION	CS	12.94	M	79.41	S	7.65		
ENSTATITE PROJECTION	M2S	22.55	C2S3	41.09	A2S3	36.36		
QUARTZ PROJECTION	CAS2	25.01	MS	65.55	CMS2	9.43		

HLAGOTHI COMPLEX

SAMPLE NUMBER BG 237

ORIGINAL WEIGHT PERCENT OXIDES

SIO2	AL2O3	FE2O3	FEO	MNO	MGO	CAO	NA2O	K2O	TIO2	P2O5	CR2O3	TOTAL
56.03	14.21	1.05	9.49	.19	5.35	10.74	2.15	.58	.45	.07	.00	100.31

WEIGHT PERCENT OXIDES RECALCULATED TO 100 PERCENT

SIO2	AL2O3	FE2O3	FEO	MNO	MGO	CAO	NA2O	K2O	TIO2	P2O5	CR2O3	TOTAL
55.86	14.17	1.05	9.46	.19	5.33	10.71	2.14	.58	.45	.07	.00	100.00

CATION PROPORTIONS IN ANALYSIS

SI	AL	FE(3)	FE(2)	MN	MG	CA	NA	K	TI	P	CR
52.63	15.73	.75	7.45	.15	7.49	10.81	3.91	.70	.32	.06	.00

CIPW NORM

	QTZ	COR	OR	AB	AN	LC	NE	KP
WEIGHT PERCENT	8.622	.000	3.417	18.131	27.324	.000	.000	.000
MOLE PERCENT	28.069	.000	2.927	13.525	19.212	.000	.000	.000
CATION PERCENT	8.124	.000	3.475	19.576	27.806	.000	.000	.000

	AC	NS	KS	DI	WO	HY	OL	CS
WEIGHT PERCENT	.000	.000	.000	21.098	.000	18.869	.000	.000
MOLE PERCENT	.000	.000	.000	17.812	.000	15.974	.000	.000
CATION PERCENT	.000	.000	.000	20.623	.000	18.494	.000	.000

	MT	CM	IL	HM	TN	PF	RU	AP
WEIGHT PERCENT	1.524	.000	.852	.000	.000	.000	.000	.165
MOLE PERCENT	1.287	.000	1.098	.000	.000	.000	.000	.096
CATION PERCENT	1.118	.000	.636	.000	.000	.000	.000	.148

MAFIC INDEX = 42.508
NORM TOTAL = 100.002

OLIVINE COMPOSITION
FORSTERITE .000 FAYALITE .000

ORTHOPYROXENE COMPOSITION
ENSTATITE 45.198 FERROSILITE 54.802

CLINOPYROXENE COMPOSITION
WOLLASTONITE 50.136 ENSTATITE 22.538 FERROSILITE 27.327

FELDSPAR COMPOSITION
ORTHOCLASE 6.991 ALBITE 37.099 ANORTHITE 55.910
PLAGIOCLASE COMPOSITION (PERC AN) 60.113

THORNTON AND TUTTLE DIFFERENTIATION INDEX = 30.169
SOLIDIFICATION INDEX (100*MGO/(MGO+FEO+FE2O3+NA2O+K2O)) = 28.733
CRYSTALLIZATION INDEX (AN+MG DI+FO+FO EQIV OF EN) = 43.558
LARSEN INDEX (1/3SI+K)-(CA+MG) = -.455
ALBITE RATIO (100*(AB+AB EQIV IN NE)/PLAG) = 39.887
IRON RATIO ((FE2=MN)*100/(FE2+MN+MG)) = 69.976
MG NUMBER AS CATIONS MG/CATIONS (FE+MG) = 50.127
OXIDATION RATIO ACCORDING TO LE MAITRE (FEO/FEO+FE2O3) = .848
DENSITY OF DRY LIQUID OF THIS COMPOSITION (AT 1050 DEG) = 2.653
AFM RATIO
TOTAL ALKALIS 14.75 TOTAL FE 56.36 MG 28.90

KOMATIITE PARAMETERS

FEO/(FEO+MGO)	CAO/AL2O3	SIO2/TIO2	AL2O3/TIO2	FEO*/TIO2	CAO/TIO2	NA2O/TIO2	K2O/TIO2
.6610	.76	124.51	31.50	23.19	23.87	4.778	1.289

JENSEN CATION AL2O3 - FEO+FE2O3+TIO2 - MGO
49.57 26.83 23.60

QUARTZ - FELDSPAR RATIOS

QUARTZ	15.00	ORTHOCLASE	5.94	PLAGIOCLASE	79.06	
QUARTZ	28.58	ORTHOCLASE	11.33	ALBITE	60.10	

CATION PROPORTIONS	CA	41.38	FE	29.95	MG	28.67
	CA	15.24	MG	10.56	SI	74.20
	SI	77.41	AL	11.57	MG	11.02
	2MG	36.40	2FE	38.02	SI/5	25.58
	CA	51.52	AL	37.49	NA+K	10.99

COORDINATES IN THE SYSTEM PLAGIOCLASE - OLIVINE - CLINOPYROXENE - QUARTZ (IN MOLE PERCENT)

PROPORTION OF ANALYSIS IN BASALT TETRAHEDRON IS 94.62 MOLE PERCENT

BASALT TETRAHEDRON	OL	14.66	CPX	21.80	PLAG	50.07	QTZ	13.47
CLINOPYROXENE PROJECTION		18.74		0.0		64.03		17.23
QUARTZ PROJECTION		16.94		25.19		57.87		0.0
PLAGIOCLASE PROJECTION		29.36		43.66		0.0		26.98
OLIVINE PROJECTION		0.0		17.33		39.82	OPX+(4QTZ)	42.35

CMAS PROJECTIONS

TETRAHEDRON COORDINATES	C	17.22	M	16.60	A	12.21	S	53.97
DIOPSIDE PROJECTION	C3A	31.95	M	14.06	S	53.99		
OLIVINE PROJECTION	CS	22.34	M	63.77	S	13.89		
ENSTATITE PROJECTION	M2S	16.40	C2S3	43.29	A2S3	40.30		
QUARTZ PROJECTION	CAS2	60.15	MS	20.61	CMS2	19.25		

HLAGOTHI COMPLEX

SAMPLE NUMBER BG 239

ORIGINAL WEIGHT PERCENT OXIDES

SIO2	AL2O3	FE2O3	FEO	MNO	MGO	CAO	NA2O	K2O	TIO2	P2O5	CR2O3	TOTAL
54.69	11.92	.96	8.60	.19	9.75	9.25	2.46	.73	.64	.11	.00	99.29

WEIGHT PERCENT OXIDES RECALCULATED TO 100 PERCENT

SIO2	AL2O3	FE2O3	FEO	MNO	MGO	CAO	NA2O	K2O	TIO2	P2O5	CR2O3	TOTAL
55.08	12.01	.96	8.66	.19	9.82	9.32	2.48	.74	.64	.11	.00	100.00

CATION PROPORTIONS IN ANALYSIS

SI	AL	FE(3)	FE(2)	MN	MG	CA	NA	K	TI	P	CR
58.86	13.07	.67	6.69	.15	13.51	9.22	4.43	.87	.45	.09	.00

CIPW NORM

	QTZ	COR	OR	AB	AN	LC	NE	KP
WEIGHT PERCENT	2.640	.000	4.344	20.958	19.464	.000	.000	.000
MOLE PERCENT	9.746	.000	4.220	17.728	15.518	.000	.000	.000
CATION PERCENT	2.438	.000	4.331	22.176	19.411	.000	.000	.000

	AC	NS	KS	DI	WO	HY	OL	CS
WEIGHT PERCENT	.000	.000	.000	21.172	.000	28.543	.000	.000
MOLE PERCENT	.000	.000	.000	20.750	.000	28.738	.000	.000
CATION PERCENT	.000	.000	.000	20.763	.000	28.754	.000	.000

	MT	CM	IL	HM	TN	PF	RU	AP
WEIGHT PERCENT	1.395	.000	1.224	.000	.000	.000	.000	.262
MOLE PERCENT	1.336	.000	1.789	.000	.000	.000	.000	.173
CATION PERCENT	1.003	.000	.895	.000	.000	.000	.000	.231

MAFIC INDEX = 52.596
NORM TOTAL = 100.003

OLIVINE COMPOSITION
FORSTERITE .000 FAYALITE .000

ORTHOPYROXENE COMPOSITION
ENSTATITE 62.954 FERROSILITE 37.046

CLINOPYROXENE COMPOSITION
WOLLASTONITE 51.328 ENSTATITE 30.641 FERROSILITE 18.031

FELDSPAR COMPOSITION
ORTHOCLASE 9.705 ALBITE 46.816 ANORTHITE 43.480
PLAGIOCLASE COMPOSITION (PERC AN) 48.153

THORNTON AND TUTTLE DIFFERENTIATION INDEX = 27.942
SOLIDIFICATION INDEX (100*MGO/(MGO+FEO+FE2O3+NA2O+K2O)) = 43.352
CRYSTALLIZATION INDEX (AN+MG DI+FO+FO EQIV OF EN) = 46.051
LARSEN INDEX (1/3SI+K)-(CA+MG) = -5.909
ALBITE RATIO (100*(AB+AB EQIV IN NE)/PLAG) = 51.847
IRON RATIO ((FE2=MN)*100/(FE2+MN+MG)) = 53.730
MG NUMBER AS CATIONS MG/CATIONS (FE+MG) = 66.903
OXIDATION RATIO ACCORDING TO LE MAITRE (FEO/FEO+FE2O3) = .818
DENSITY OF DRY LIQUID OF THIS COMPOSITION (AT 1050 DEG) = 2.670
AFM RATIO
TOTAL ALKALIS 14.24 TOTAL FE 42.22 MG 43.54

KOMATIITE PARAMETERS

FEO/(FEO+MGO)	CAO/AL2O3	SIO2/TIO2	AL2O3/TIO2	FEO*/TIO2	CAO/TIO2	NA2O/TIO2	K2O/TIO2
.4923	.78	85.45	18.62	14.77	14.45	3.844	1.141

JENSEN CATION AL2O3 - FEO+FE2O3+TIO2 - MGO
38.00 22.69 39.30

QUARTZ - FELDSPAR RATIOS

QUARTZ	5.57	ORTHOCLASE	9.16	PLAGIOCLASE	85.27		
QUARTZ	9.45	ORTHOCLASE	15.55	ALBITE	75.00		
CATION PROPORTIONS		CA	30.98	FE	23.59	MG	45.43
		CA	12.52	MG	18.36	SI	69.11
		SI	71.73	AL	9.21	MG	19.06
		2MG	52.75	2FE	27.39	SI/5	19.85
		CA	50.09	AL	35.50	NA+K	14.41

COORDINATES IN THE SYSTEM PLAGIOCLASE - OLIVINE - CLINOPYROXENE - QUARTZ (IN MOLE PERCENT)

PROPORTION OF ANALYSIS IN BASALT TETRAHEDRON IS 93.54 MOLE PERCENT

BASALT TETRAHEDRON	OL	23.05	CPX	22.20	PLAG	44.46	QTZ	10.29
CLINOPYROXENE PROJECTION		29.63		0.0		57.14		13.23
QUARTZ PROJECTION		25.70		24.74		49.56		0.0
PLAGIOCLASE PROJECTION		41.51		39.96		0.0		18.53
OLIVINE PROJECTION		0.0		20.59		41.23	OPX+(4QTZ)	38.18

CMAS PROJECTIONS

TETRAHEDRON COORDINATES	C	16.01	M	22.16	A	11.10	S	50.74
DIOPSIDE PROJECTION	C3A	30.86	M	16.37	S	52.77		
OLIVINE PROJECTION	CS	24.02	M	61.36	S	14.62		
ENSTATITE PROJECTION	M2S	27.54	C2S3	37.92	A2S3	34.54		
QUARTZ PROJECTION	CAS2	52.48	MS	29.45	CMS2	18.07		

HLAGOTHI COMPLEX

SAMPLE NUMBER BG 242

ORIGINAL WEIGHT PERCENT OXIDES

SIO2	AL2O3	FE2O3	FEO	MNO	MGO	CAO	NA2O	K2O	TIO2	P2O5	CR2O3	TOTAL
54.75	11.50	.98	8.84	.18	10.01	9.30	2.10	.96	.64	.10	.00	99.36

WEIGHT PERCENT OXIDES RECALCULATED TO 100 PERCENT

SIO2	AL2O3	FE2O3	FEO	MNO	MGO	CAO	NA2O	K2O	TIO2	P2O5	CR2O3	TOTAL
55.10	11.57	.99	8.89	.18	10.07	9.36	2.11	.97	.64	.10	.00	100.00

CATION PROPORTIONS IN ANALYSIS

SI	AL	FE(3)	FE(2)	MN	MG	CA	NA	K	TI	P	CR
51.01	12.63	.69	6.89	.14	13.90	9.28	3.79	1.14	.45	.08	.00

CIPW NORM

	QTZ	COR	OR	AB	AN	LC	NE	KP
WEIGHT PERCENT	3.322	.000	5.709	17.878	19.240	.000	.000	.000
MOLE PERCENT	11.986	.000	5.421	14.781	14.992	.000	.000	.000
CATION PERCENT	3.075	.000	5.705	18.964	19.235	.000	.000	.000

	AC	NS	KS	DI	WO	HY	OL	CS
WEIGHT PERCENT	.000	.000	.000	21.586	.000	29.372	.000	.000
MOLE PERCENT	.000	.000	.000	20.676	.000	28.901	.000	.000
CATION PERCENT	.000	.000	.000	21.221	.000	29.660	.000	.000

	MT	CM	IL	HM	TN	PF	RU	AP
WEIGHT PERCENT	1.433	.000	1.223	.000	.000	.000	.000	.238
MOLE PERCENT	1.342	.000	1.748	.000	.000	.000	.000	.154
CATION PERCENT	1.033	.000	.897	.000	.000	.000	.000	.210

MAFIC INDEX = 53.854
NORM TOTAL = 100.003

OLIVINE COMPOSITION
FORSTERITE .000 FAYALITE .000

ORTHOPYROXENE COMPOSITION
ENSTATITE 62.916 FERROSILITE 37.084

CLINOPYROXENE COMPOSITION
WOLLASTONITE 51.325 ENSTATITE 30.624 FERROSILITE 18.051

FELDSPAR COMPOSITION
ORTHOCLASE 13.331 ALBITE 41.745 ANORTHITE 44.924
PLAGIOCLASE COMPOSITION (PERC AN) 51.834

THORNTON AND TUTTLE DIFFERENTIATION INDEX = 26.910
SOLIDIFICATION INDEX (100*MGO/(MGO+FEO+FE2O3+NA2O+K2O)) = 43.731
CRYSTALLIZATION INDEX (AN+MG,DI+FO+FO EQIV OF EN) = 46.451
LARSEN INDEX (1/3SI+K)-(CA+MG) = -6.175
ALBITE RATIO (100*(AB+AB EQIV IN NE)/PLAG) = 48.166
IRON RATIO ((FE2=MN)*100/(FE2+MN+MG)) = 53.726
MG NUMBER AS CATIONS MG/CATIONS (FE+MG) = 66.869
OXIDATION RATIO ACCORDING TO LE MAITRE (FEO/FEO+FE2O3) = .820
DENSITY OF DRY LIQUID OF THIS COMPOSITION (AT 1050 DEG) = 2.676
AFM RATIO
TOTAL ALKALIS 13.43 TOTAL FE 42.65 MG 43.92

KOMATIITE PARAMETERS

FEO/(FEO+MGO)	CAO/AL2O3	SIO2/TIO2	AL2O3/TIO2	FEO*/TIO2	CAO/TIO2	NA2O/TIO2	K2O/TIO2
.4927	.81	85.55	17.97	15.19	14.53	3.281	1.500

JENSEN CATION AL2O3 - FEO+FE2O3+TIO2 - MGO
36.55 23.22 40.23

QUARTZ - FELDSPAR RATIOS
QUARTZ 7.20 ORTHOCLASE 12.37 PLAGIOCLASE 80.43
QUARTZ 12.34 ORTHOCLASE 21.22 ALBITE 66.44

CATION PROPORTIONS						
CA	30.52	FE	23.77	MG	45.71
CA	12.51	MG	18.74	SI	68.75
SI	71.62	AL	8.86	MG	19.52
2MG	52.99	2FE	27.56	SI/5	19.45
CA	51.39	AL	34.95	NA+K	13.66

COORDINATES IN THE SYSTEM PLAGIOCLASE - OLIVINE - CLINOPYROXENE - QUARTZ (IN MOLE PERCENT)

PROPORTION OF ANALYSIS IN BASALT TETRAHEDRON IS 92.15 MOLE PERCENT

	OL		CPX		PLAG		QTZ	
BASALT TETRAHEDRON		24.14		23.03		41.45		11.38
CLINOPYROXENE PROJECTION		31.36		0.0		53.85		14.79
QUARTZ PROJECTION		27.24		25.98		46.78		0.0
PLAGIOCLASE PROJECTION		41.23		39.33		0.0		19.44
OLIVINE PROJECTION		0.0		20.93		37.68	OPX+(4QTZ)	41.39

CMAS PROJECTIONS

TETRAHEDRON COORDINATES	C	15.61	M	22.70	A	10.61	S	51.07
DIOPSIDE PROJECTION	C3A	30.33	M	16.59	S	53.08		
OLIVINE PROJECTION	CS	23.44	M	62.58	S	13.98		
ENSTATITE PROJECTION	M2S	26.31	C2S3	38.93	A2S3	34.76		
QUARTZ PROJECTION	CAS2	50.79	MS	30.57	CMS2	18.64		

SAMPLE NUMBER BG 84

ORIGINAL WEIGHT PERCENT OXIDES

SIO2	AL2O3	FE2O3	FEO	MNO	MGO	CAO	NA2O	K2O	TIO2	P2O5	CR2O3	TOTAL
54.26	5.09	1.08	9.73	.18	13.35	13.28	1.55	.23	.79	.11	.00	99.64

WEIGHT PERCENT OXIDES RECALCULATED TO 100 PERCENT

SIO2	AL2O3	FE2O3	FEO	MNO	MGO	CAO	NA2O	K2O	TIO2	P2O5	CR2O3	TOTAL
54.46	5.11	1.09	9.76	.18	13.40	13.33	1.56	.23	.79	.11	.00	100.00

CATION PROPORTIONS IN ANALYSIS

SI	AL	FE(3)	FE(2)	MN	MG	CA	NA	K	TI	P	CR
50.49	5.58	.76	7.57	.14	18.51	13.24	2.30	.27	.55	.09	.00

CIPW NORM

	QTZ	COR	OR	AB	AN	LC	NE	KP
WEIGHT PERCENT	1.758	.000	1.364	13.159	6.274	.000	.000	.000
MOLE PERCENT	6.379	.000	1.302	10.940	4.917	.000	.000	.000
CATION PERCENT	1.630	.000	1.365	13.980	6.292	.000	.000	.000

	AC	NS	KS	DI	WO	HY	OL	CS
WEIGHT PERCENT	.000	.000	.000	47.818	.000	26.309	.000	.000
MOLE PERCENT	.000	.000	.000	46.329	.000	26.346	.000	.000
CATION PERCENT	.000	.000	.000	47.356	.000	26.928	.000	.000

	MT	CM	IL	HM	TN	PF	RU	AP
WEIGHT PERCENT	1.573	.000	1.487	.000	.000	.000	.000	.261
MOLE PERCENT	1.481	.000	2.136	.000	.000	.000	.000	.170
CATION PERCENT	1.136	.000	1.092	.000	.000	.000	.000	.231

MAFIC INDEX = 77.449
NORM TOTAL = 100.005

OLIVINE COMPOSITION
FORSTERITE .000 FAYALITE .000

ORTHOPYROXENE COMPOSITION
ENSTATITE 67.490 FERROSILITE 32.510

CLINOPYROXENE COMPOSITION
WOLLASTONITE 51.623 ENSTATITE 32.650 FERROSILITE 15.727

FELDSPAR COMPOSITION
ORTHOCLASE 6.559 ALBITE 63.272 ANORTHITE 30.169
PLAGIOCLASE COMPOSITION (PERC AN) 32.236

THORNTON AND TUTTLE DIFFERENTIATION INDEX = 16.281
SOLIDIFICATION INDEX (100*MGO/(MGO+FEO+FE2O3+NA2O+K2O)) = 51.467
CRYSTALLIZATION INDEX (AN+MG.DI+FO+FO EQIV OF EN) = 52.395
LARSEN INDEX (1/3SI+K)-(CA+MG) = -15.525
ALBITE RATIO (100*(AB+AB EQIV IN NE)/PLAG) = 67.714
IRON RATIO ((FE2+MN)*100/(FE2+MN+MG)) = 48.888
MG NUMBER AS CATIONS MG/CATIONS (FE+MG) = 70.977
OXIDATION RATIO ACCORDING TO LE MAITRE (FEO/FEO+FE2O3) = .834
DENSITY OF DRY LIQUID OF THIS COMPOSITION (AT 1050 DEG) = 2.753
AFM RATIO
TOTAL ALKALIS 6.59 TOTAL FE 41.43 MG 51.68

KOMATIITE PARAMETERS

FEO/(FEO+MGO)	CAO/AL2O3	SIO2/TIO2	AL2O3/TIO2	FEO*/TIO2	CAO/TIO2	NA2O/TIO2	K2O/TIO2
.4449	2.61	69.56	6.53	13.72	17.03	1.987	.295

JENSEN CATION AL2O3 - FEO+FE2O3+TIO2 - MGO
16.93 26.91 56.15

QUARTZ - FELDSPAR RATIOS
QUARTZ 7.79 ORTHOCLASE 6.05 PLAGIOCLASE 86.16
QUARTZ 10.80 ORTHOCLASE 8.38 ALBITE 80.82

CATION PROPORTIONS						
	CA	33.35	FE	20.02	MG	46.64
	CA	16.10	MG	22.51	SI	61.39
	SI	70.32	AL	3.89	MG	25.79
	2MG	58.76	2FE	25.22	SI/5	16.02
	CA	75.37	AL	15.89	NA+K	8.74

COORDINATES IN THE SYSTEM PLAGIOCLASE - OLIVINE - CLINOPYROXENE - QUARTZ (IN MOLE PERCENT)

PROPORTION OF ANALYSIS IN BASALT TETRAHEDRON IS 96.16 MOLE PERCENT

BASALT TETRAHEDRON	OL	21.00	CPX	49.24	PLAG	21.07	QTZ	8.69
CLINOPYROXENE PROJECTION		41.37		0.0		41.50		17.13
QUARTZ PROJECTION		23.00		53.93		23.07		0.0
PLAGIOCLASE PROJECTION		26.60		62.38		0.0		11.02
OLIVINE PROJECTION		0.0		46.96		20.05	OPX+(4QTZ)	33.10

CMAS PROJECTIONS

TETRAHEDRON COORDINATES	C	17.10	M	27.17	A	5.55	S	50.17
DIOPSIDE PROJECTION	C3A	27.09	M	19.45	S	53.46		
OLIVINE PROJECTION	CS	30.72	M	60.52	S	8.76		
ENSTATITE PROJECTION	M2S	30.23	C2S3	48.91	A2S3	20.87		
QUARTZ PROJECTION	CAS2	27.52	MS	27.94	CMS2	44.54		

SAMPLE NUMBER BG 125

ORIGINAL WEIGHT PERCENT OXIDES

SIO2	AL2O3	FE2O3	FEO	MNO	MGO	CAO	NA2O	K2O	TIO2	P2O5	CR2O3	TOTAL
52.00	14.97	.91	8.20	.17	9.81	10.73	1.81	1.02	.48	.08	.00	100.18

WEIGHT PERCENT OXIDES RECALCULATED TO 100 PERCENT

SIO2	AL2O3	FE2O3	FEO	MNO	MGO	CAO	NA2O	K2O	TIO2	P2O5	CR2O3	TOTAL
51.91	14.94	.91	8.18	.17	9.79	10.71	1.81	1.02	.48	.08	.00	100.00

CATION PROPORTIONS IN ANALYSIS

SI	AL	FE(3)	FE(2)	MN	MG	CA	NA	K	TI	P	CR
47.84	16.23	.63	6.31	.13	13.45	10.58	3.23	1.20	.33	.06	.00

CIPW NORM

	QTZ	COR	OR	AB	AN	LC	NE	KP
WEIGHT PERCENT	.000	.000	6.016	15.283	29.656	.000	.000	.000
MOLE PERCENT	.000	.000	6.296	13.927	25.470	.000	.000	.000
CATION PERCENT	.000	.000	5.986	16.141	29.519	.000	.000	.000

	AC	NS	KS	DI	WO	HY	OL	CS
WEIGHT PERCENT	.000	.000	.000	18.652	.000	24.935	3.043	.000
MOLE PERCENT	.000	.000	.000	19.716	.000	27.110	4.553	.000
CATION PERCENT	.000	.000	.000	18.279	.000	25.132	3.166	.000

	MT	CM	IL	HM	TN	PF	RU	AP
WEIGHT PERCENT	1.319	.000	.910	.000	.000	.000	.000	.189
MOLE PERCENT	1.361	.000	1.433	.000	.000	.000	.000	.134
CATION PERCENT	.946	.000	.664	.000	.000	.000	.000	.166

MAFIC INDEX = 49.847
NORM TOTAL = 100.002

OLIVINE COMPOSITION
FORSTERITE 61.589 FAYALITE 38.411

ORTHOPYROXENE COMPOSITION
ENSTATITE 63.860 FERROSILITE 36.140

CLINOPYROXENE COMPOSITION
WOLLASTONITE 51.387 ENSTATITE 31.044 FERROSILITE 17.569

FELDSPAR COMPOSITION
ORTHOCLASE 11.807 ALBITE 29.993 ANORTHITE 58.199
PLAGIOCLASE COMPOSITION (PERC AN) 65.991

THORNTON AND TUTTLE DIFFERENTIATION INDEX = 21.300
SOLIDIFICATION INDEX (100*MGO/(MGO+FEO+FE2O3+NA2O+K2O)) = 45.101
CRYSTALLIZATION INDEX (AN+MG DI+FO+FO EQIV OF EN) = 55.179
LARSEN INDEX (1/3SI+K)-(CA+MG) = -8.377
ALBITE RATIO (100*(AB+AB EQIV IN NE)/PLAG) = 34.009
IRON RATIO ((FE2=MN)*100/(FE2+MN+MG)) = 52.371
MG NUMBER AS CATIONS MG/CATIONS (FE+MG) = 68.071
OXIDATION RATIO ACCORDING TO LE MAITRE (FEO/FEO+FE2O3) = .827
DENSITY OF DRY LIQUID OF THIS COMPOSITION (AT 1050 DEG) = 2.689
AFM RATIO
TOTAL ALKALIS 13.07 TOTAL FE 41.64 MG 45.29

KOMATIITE PARAMETERS

FEO/(FEO+MGO)	CAO/AL2O3	SIO2/TIO2	AL2O3/TIO2	FEO*/TIO2	CAO/TIO2	NA2O/TIO2	K2O/TIO2
.4790	.72	108.33	31.19	18.79	22.35	3.771	2.125

JENSEN CATION AL2O3 - FEO+FE2O3+TIO2 - MGO
43.93 19.68 36.40

QUARTZ - FELDSPAR RATIOS
QUARTZ .00 ORTHOCLASE 11.81 PLAGIOCLASE 88.19
QUARTZ .00 ORTHOCLASE 28.25 ALBITE 71.75

CATION PROPORTIONS						
CA	34.50	FE	21.61	MG	43.89
CA	14.72	MG	18.72	SI	66.57
SI	68.93	AL	11.69	MG	19.38
2MG	54.11	2FE	26.64	SI/5	19.24
CA	50.59	AL	38.82	NA+K	10.58

COORDINATES IN THE SYSTEM PLAGIOCLASE - OLIVINE - CLINOPYROXENE - QUARTZ (IN MOLE PERCENT)

PROPORTION OF ANALYSIS IN BASALT TETRAHEDRON IS 92.24 MOLE PERCENT

BASALT TETRAHEDRON	OL	23.87	CPX	19.82	PLAG	49.50	QTZ	6.81
CLINOPYROXENE PROJECTION		29.77		0.0		61.74		8.50
QUARTZ PROJECTION		25.61		21.27		53.12		0.0
PLAGIOCLASE PROJECTION		47.27		39.24		0.0		13.49
OLIVINE PROJECTION		0.0		20.52		51.26	OPX+(4QTZ)	28.22

CMAS PROJECTIONS

TETRAHEDRON COORDINATES	C	16.77	M	22.02	A	12.35	S	48.86
DIOPSIDE PROJECTION	C3A	32.04	M	16.37	S	51.59		
OLIVINE PROJECTION	CS	26.17	M	56.91	S	16.92		
ENSTATITE PROJECTION	M2S	32.93	C2S3	34.08	A2S3	32.99		
QUARTZ PROJECTION	CAS2	55.79	MS	28.69	CMS2	15.52		

SAMPLE NUMBER BG 126

ORIGINAL WEIGHT PERCENT OXIDES

SIO2	AL2O3	FE2O3	FEO	MNO	MGO	CAO	NA2O	K2O	TIO2	P2O5	CR2O3	TOTAL
50.72	16.78	.78	6.99	.13	9.20	10.63	2.52	1.14	.39	.07	.00	99.34

WEIGHT PERCENT OXIDES RECALCULATED TO 100 PERCENT

SIO2	AL2O3	FE2O3	FEO	MNO	MGO	CAO	NA2O	K2O	TIO2	P2O5	CR2O3	TOTAL
51.06	16.89	.78	7.03	.13	9.26	10.70	2.54	1.15	.39	.07	.00	100.00

CATION PROPORTIONS IN ANALYSIS

SI	AL	FE(3)	FE(2)	MN	MG	CA	NA	K	TI	P	CR
46.61	18.17	.54	5.37	.10	12.60	10.47	4.49	1.34	.27	.05	.00

CIPW NORM

	QTZ	COR	OR	AB	AN	LC	NE	KP
WEIGHT PERCENT	.000	.000	6.781	21.458	31.313	.000	.000	.000
MOLE PERCENT	.000	.000	6.867	18.920	26.023	.000	.000	.000
CATION PERCENT	.000	.000	6.682	22.444	30.868	.000	.000	.000

	AC	NS	KS	DI	WO	HY	OL	CS
WEIGHT PERCENT	.000	.000	.000	17.266	.000	6.842	14.295	.000
MOLE PERCENT	.000	.000	.000	17.709	.000	7.239	20.859	.000
CATION PERCENT	.000	.000	.000	16.804	.000	6.868	14.844	.000

	MT	CM	IL	HM	TN	PF	RU	AP
WEIGHT PERCENT	1.133	.000	.746	.000	.000	.000	.000	.167
MOLE PERCENT	1.132	.000	1.136	.000	.000	.000	.000	.115
CATION PERCENT	.805	.000	.539	.000	.000	.000	.000	.143

MAFIC INDEX = 40.449
NORM TOTAL = 100.000

OLIVINE COMPOSITION
FORSTERITE 63.825 FAYALITE 36.175

ORTHOPYROXENE COMPOSITION
ENSTATITE 66.037 FERROSILITE 33.963

CLINOPYROXENE COMPOSITION
WOLLASTONITE 51.529 ENSTATITE 32.009 FERROSILITE 16.462

FELDSPAR COMPOSITION
ORTHOCLASE 11.387 ALBITE 36.032 ANORTHITE 52.581
PLAGIOCLASE COMPOSITION (PERC AN) 59.337

THORNTON AND TUTTLE DIFFERENTIATION INDEX	=	28.239
SOLIDIFICATION INDEX (100*MGO/(MGO+FEO+FE2O3+NA2O+K2O))	=	44.611
CRYSTALLIZATION INDEX (AN+MG DI+FO+FO EQIV OF EN)	=	55.524
LARSEN INDEX (1/3SI+K)-(CA+MG)	=	-7.823
ALBITE RATIO (100*(AB+AB EQIV IN NE)/PLAG)	=	40.663
IRON RATIO ((FE2+MN)*100/(FE2+MN+MG))	=	49.921
MG NUMBER AS CATIONS MG/CATIONS (FE+MG)	=	70.120
OXIDATION RATIO ACCORDING TO LE MAITRE (FEO/FEO+FE2O3)	=	.810
DENSITY OF DRY LIQUID OF THIS COMPOSITION (AT 1050 DEG)	=	2.668

AFM RATIO
TOTAL ALKALIS 17.81 TOTAL FE 37.41 MG 44.78

KOMATIITE PARAMETERS

FEO/(FEO+MGO)	CAO/AL2O3	SIO2/TIO2	AL2O3/TIO2	FEO*/TIO2	CAO/TIO2	NA2O/TIO2	K2O/TIO2
.4551	.63	130.05	43.03	19.70	27.26	6.462	2.923

JENSEN CATION AL2O3 - FEO+FE2O3+TIO2 - MGO
49.19 16.71 34.10

QUARTZ - FELDSPAR RATIOS

QUARTZ	.00		ORTHOCLASE 11.39		PLAGIOCLASE 88.61		
QUARTZ	.00		ORTHOCLASE 24.01		ALBITE 75.99		
CATION PROPORTIONS		CA	36.46	FE	19.64	MG	43.90
		CA	15.02	MG	18.09	SI	66.89
		SI	68.25	AL	13.30	MG	18.45
		2MG	55.03	2FE	24.62	SI/5	20.35
		CA	46.59	AL	40.45	NA+K	12.97

COORDINATES IN THE SYSTEM PLAGIOCLASE - OLIVINE - CLINOPYROXENE - QUARTZ (IN MOLE PERCENT)

PROPORTION OF ANALYSIS IN BASALT TETRAHEDRON IS 91.83 MOLE PERCENT

BASALT TETRAHEDRON	OL	21.77	CPX	18.30	PLAG	58.06	QTZ	1.87
CLINOPYROXENE PROJECTION		26.65		0.0		71.06		2.29
QUARTZ PROJECTION		22.19		18.65		59.16		0.0
PLAGIOCLASE PROJECTION		51.91		43.63		0.0		4.46
OLIVINE PROJECTION		0.0		21.83		69.25	OPX+(4QTZ)	8.92

CMAS PROJECTIONS

TETRAHEDRON COORDINATES	C	18.55	M	20.39	A	14.36	S	46.70
DIOPSIDE PROJECTION	C3A	33.90	M	15.82	S	50.28		
OLIVINE PROJECTION	CS	29.83	M	49.92	S	20.26		
ENSTATITE PROJECTION	M2S	37.22	C2S3	31.13	A2S3	31.65		
QUARTZ PROJECTION	CAS2	61.18	MS	24.90	CMS2	13.92		

SAMPLE NUMBER BG 141

ORIGINAL WEIGHT PERCENT OXIDES

SIO2	AL2O3	FE2O3	FEO	MNO	MGO	CAO	NA2O	K2O	TIO2	P2O5	CR2O3	TOTAL
52.76	18.85	.93	8.40	.20	7.60	2.94	.79	6.01	1.01	.15	.00	99.63

WEIGHT PERCENT OXIDES RECALCULATED TO 100 PERCENT

SIO2	AL2O3	FE2O3	FEO	MNO	MGO	CAO	NA2O	K2O	TIO2	P2O5	CR2O3	TOTAL
52.96	18.92	.94	8.43	.20	7.63	2.95	.78	6.03	1.01	.15	.00	100.00

CATION PROPORTIONS IN ANALYSIS

SI	AL	FE(3)	FE(2)	MN	MG	CA	NA	K	TI	P	CR
49.12	20.68	.65	6.54	.16	10.54	2.93	1.41	7.14	.71	.12	.00

CIPW NORM

	QTZ	COR	OR	AB	AN	LC	NE	KP
WEIGHT PERCENT	1.948	5.098	35.646	6.623	13.655	.000	.000	.000
MOLE PERCENT	6.648	12.263	32.011	5.179	10.064	.000	.000	.000
CATION PERCENT	1.807	6.667	35.688	7.038	13.678	.000	.000	.000

	AC	NS	KS	DI	WO	HY	OL	CS
WEIGHT PERCENT	.000	.000	.000	.000	.000	32.399	.000	.000
MOLE PERCENT	.000	.000	.000	.000	.000	25.814	.000	.000
CATION PERCENT	.000	.000	.000	.000	.000	32.412	.000	.000

	MT	CM	IL	HM	TN	PF	RU	AP
WEIGHT PERCENT	1.358	.000	1.925	.000	.000	.000	.000	.357
MOLE PERCENT	1.203	.000	2.601	.000	.000	.000	.000	.217
CATION PERCENT	.981	.000	1.414	.000	.000	.000	.000	.315

MAFIC INDEX = 36.039
NORM TOTAL = 100.009

OLIVINE COMPOSITION
FORSTERITE .000 FAYALITE .000

ORTHOPYROXENE COMPOSITION
ENSTATITE 58.638 FERROSILITE 41.362

CLINOPYROXENE COMPOSITION
WOLLASTONITE .000 ENSTATITE .000 FERROSILITE .000

FELDSPAR COMPOSITION
ORTHOCLASE 63.740 ALBITE 11.842 ANORTHITE 24.418
PLAGIOCLASE COMPOSITION (PERC AN) 67.341

THORNTON AND TUTTLE DIFFERENTIATION INDEX = 44.216
SOLIDIFICATION INDEX (100*MGO/(MGO+FEO+FE2O3+NA2O+K2O)) = 32.040
CRYSTALLIZATION INDEX (AN+MG.DI+FO+FO EQIV OF EN) = 26.970
LARSEN INDEX (1/3SI+K)-(CA+MG) = 7.604
ALBITE RATIO (100*(AB+AB EQIV IN NE)/PLAG) = 32.659
IRON RATIO ((FE2+MN)*100/(FE2+MN+MG)) = 59.313
MG NUMBER AS CATIONS MG/CATIONS (FE+MG) = 61.728
OXIDATION RATIO ACCORDING TO LE MAITRE (FEO/FEO+FE2O3) = .748
DENSITY OF DRY LIQUID OF THIS COMPOSITION (AT 1050 DEG) = 2.605
AFM RATIO
TOTAL ALKALIS 28.74 TOTAL FE 39.09 MG 32.17

KOMATIITE PARAMETERS

FEO/(FEO+MGO)	CAO/AL2O3	SIO2/TIO2	AL2O3/TIO2	FEO*/TIO2	CAO/TIO2	NA2O/TIO2	K2O/TIO2
.5486	.16	52.24	18.66	9.15	2.91	.772	5.950

JENSEN CATION AL2O3 - FEO+FE2O3+TIO2 - MGO
52.86 20.19 26.95

QUARTZ - FELDSPAR RATIOS
QUARTZ 3.37 ORTHOCLASE 61.59 PLAGIOCLASE 35.04
QUARTZ 4.41 ORTHOCLASE 80.62 ALBITE 14.98

CATION PROPORTIONS						
CA	14.42	FE	33.74	MG	51.84
CA	4.68	MG	16.85	SI	78.47
SI	70.16	AL	14.77	MG	15.06
2MG	47.24	2FE	30.75	SI/5	22.01
CA	16.71	AL	58.94	NA+K	24.35

COORDINATES IN THE SYSTEM PLAGIOCLASE - OLIVINE - CLINOPYROXENE - QUARTZ (IN MOLE PERCENT)

PROPORTION OF ANALYSIS IN BASALT TETRAHEDRON IS 54.93 MOLE PERCENT

BASALT TETRAHEDRON	OL	44.25	CPX	.00	PLAG	37.71	QTZ	18.04
CLINOPYROXENE PROJECTION		44.25		0.0		37.71		18.04
QUARTZ PROJECTION		53.99		.00		46.01		0.0
PLAGIOCLASE PROJECTION		71.04		.00		0.0		28.96
OLIVINE PROJECTION		0.0		.00		34.32	CPX+(4QTZ)	65.68

CMAS PROJECTIONS

TETRAHEDRON COORDINATES	C	13.42	M	19.67	A	18.62	S	48.28
DIOPSIDE PROJECTION	C3A	32.38	M	16.12	S	51.50		
OLIVINE PROJECTION	CS	18.38	M	59.24	S	22.38		
ENSTATITE PROJECTION	M2S	33.08	C2S3	23.71	A2S3	43.21		
QUARTZ PROJECTION	CAS2	*****	MS	*****	CMS2	*****		

SAMPLE NUMBER OG 164

ORIGINAL WEIGHT PERCENT OXIDES

SIO2	AL2O3	FE2O3	FEO	MNO	MGO	CAO	NA2O	K2O	TIO2	P2O5	CR2O3	TOTAL
51.79	13.43	1.57	14.14	.27	5.13	9.14	2.59	.48	1.39	.24	.00	100.67

WEIGHT PERCENT OXIDES RECALCULATED TO 100 PERCENT

SIO2	AL2O3	FE2O3	FEO	MNO	MGO	CAO	NA2O	K2O	TIO2	P2O5	CR2O3	TOTAL
51.44	13.34	1.56	14.05	.27	5.10	9.08	2.57	.49	1.38	.24	.00	100.00

CATION PROPORTIONS IN ANALYSIS

SI	AL	FE(3)	FE(2)	MN	MG	CA	NA	K	TI	P	CR
49.06	15.00	1.12	11.21	.22	7.24	9.28	4.76	.59	1.35	.19	.00

CIPW NORM

	QTZ	COR	OR	AB	AN	LC	NE	KP
WEIGHT PERCENT	2.634	.000	2.817	21.762	23.443	.000	.000	.000
MOLE PERCENT	9.949	.000	2.801	18.836	19.125	.000	.000	.000
CATION PERCENT	2.512	.000	2.901	23.733	24.146	.000	.000	.000

	AC	NS	KS	DI	WO	HY	OL	CS
WEIGHT PERCENT	.000	.000	.000	16.887	.000	26.073	.000	.000
MOLE PERCENT	.000	.000	.000	16.346	.000	25.011	.000	.000
CATION PERCENT	.000	.000	.000	16.510	.000	25.261	.000	.000

	MT	CM	IL	HM	TN	PF	RU	AP
WEIGHT PERCENT	2.264	.000	3.366	.000	.000	.000	.000	.565
MOLE PERCENT	2.219	.000	5.333	.000	.000	.000	.000	.381
CATION PERCENT	1.681	.000	2.693	.000	.000	.000	.000	.513

MAFIC INDEX = 49.354
NORM TOTAL = 100.010

OLIVINE COMPOSITION
FORSTERITE .000 FAYALITE .000

ORTHOPYROXENE COMPOSITION
ENSTATITE 36.686 FERROSILITE 63.314

CLINOPYROXENE COMPOSITION
WOLLASTONITE 49.543 ENSTATITE 18.510 FERROSILITE 31.946

FELDSPAR COMPOSITION
ORTHOCLASE 5.867 ALBITE 45.316 ANORTHITE 48.817
PLAGIOCLASE COMPOSITION (PERC AN) 51.859

THORNTON AND TUTTLE DIFFERENTIATION INDEX = 27.213
SOLIDIFICATION INDEX (100*MGO/(MGO+FEO+FE2O3+NA2O+K2O)) = 21.452
CRYSTALLIZATION INDEX (AN+MG.DI+FO+FO EQIV OF EN) = 36.889
LARSEN INDEX (1/3SI+K)-(CA+MG) = .140
ALBITE RATIO (100*(AB+AB EQIV IN NE)/PLAG) = 48.141
IRON RATIO ((FE2+MN)*100/(FE2+MN+MG)) = 78.353
MG NUMBER AS CATIONS MG/CATIONS (FE+MG) = 39.261
OXIDATION RATIO ACCORDING TO LE MAITRE (FEO/FEO+FE2O3) = .842
DENSITY OF DRY LIQUID OF THIS COMPOSITION (AT 1050 DEG) = 2.746
AFM RATIO
TOTAL ALKALIS 12.92 TOTAL FE 65.48 MG 21.59

KOMATIITE PARAMETERS

FEO/(FEO+MGO)	CAO/AL2O3	SIO2/TIO2	AL2O3/TIO2	FEO*/TIO2	CAO/TIO2	NA2O/TIO2	K2O/TIO2
.7520	.68	27.40	7.11	8.23	4.84	1.370	.254

JENSEN CATION AL2O3 - FEO+FE2O3+TIO2 - MGO
41.76 38.07 20.17

QUARTZ - FELDSPAR RATIOS
QUARTZ 5.20 ORTHOCLASE 5.56 PLAGIOCLASE 89.24
QUARTZ 9.68 ORTHOCLASE 10.35 ALBITE 79.97

CATION PROPORTIONS						
CA	32.80	FE	41.59	MG	25.61
CA	14.14	MG	11.04	SI	74.81
SI	76.90	AL	11.75	MG	11.35
2MG	30.29	2FE	49.19	SI/5	20.52
CA	47.71	AL	38.56	NA+K	13.73

COORDINATES IN THE SYSTEM PLAGIOCLASE - OLIVINE - CLINOPYROXENE - QUARTZ (IN MOLE PERCENT)

PROPORTION OF ANALYSIS IN BASALT TETRAHEDRON IS 92.21 MOLE PERCENT

BASALT TETRAHEDRON	OL	20.55	CPX	17.90	PLAG	51.98	QTZ	9.57
CLINOPYROXENE PROJECTION		25.03		0.0		63.31		11.66
QUARTZ PROJECTION		22.72		19.80		57.48		0.0
PLAGIOCLASE PROJECTION		42.78		37.28		0.0		19.93
OLIVINE PROJECTION		0.0		16.55		48.05	CPX+(4QTZ)	35.40

CMAS PROJECTIONS

TETRAHEDRON COORDINATES	C	16.35	M	19.81	A	13.81	S	50.03
DIOPSIDE PROJECTION	C3A	32.28	M	15.65	S	52.07		
OLIVINE PROJECTION	CS	23.51	M	59.07	S	17.42		
ENSTATITE PROJECTION	M2S	29.55	C2S3	33.40	A2S3	37.06		
QUARTZ PROJECTION	CAS2	62.71	MS	29.31	CMS2	9.98		

SAMPLE NUMBER BG 208

ORIGINAL WEIGHT PERCENT OXIDES

SIO2	AL2O3	FE2O3	FEO	MNO	MGO	CAO	NA2O	K2O	TIO2	P2O5	CR2O3	TOTAL
50.98	13.81	1.48	13.33	.25	5.38	8.77	2.43	1.06	1.52	.16	.00	99.18

WEIGHT PERCENT OXIDES RECALCULATED TO 100 PERCENT

SIO2	AL2O3	FE2O3	FEO	MNO	MGO	CAO	NA2O	K2O	TIO2	P2O5	CR2O3	TOTAL
51.40	13.92	1.49	13.44	.25	5.42	8.84	2.45	1.07	1.53	.16	.00	100.00

CATION PROPORTIONS IN ANALYSIS

SI	AL	FE(3)	FE(2)	MN	MG	CA	NA	K	TI	P	CR
48.79	15.58	1.07	10.67	.20	7.67	8.99	4.51	1.29	1.09	.13	.00

CIPW NORM

	QTZ	COR	OR	AB	AN	LC	NE	KP
WEIGHT PERCENT	.843	.000	6.316	20.726	23.840	.000	.000	.000
MOLE PERCENT	3.351	.000	6.609	18.885	20.474	.000	.000	.000
CATION PERCENT	.800	.000	6.471	22.541	24.436	.000	.000	.000

	AC	NS	KS	DI	WO	HY	OL	CS
WEIGHT PERCENT	.000	.000	.000	15.945	.000	26.877	.000	.000
MOLE PERCENT	.000	.000	.000	16.295	.000	27.296	.000	.000
CATION PERCENT	.000	.000	.000	15.558	.000	26.061	.000	.000

	MT	CM	IL	HM	TN	PF	RU	AP
WEIGHT PERCENT	2.166	.000	2.911	.000	.000	.000	.000	.382
MOLE PERCENT	2.235	.000	4.583	.000	.000	.000	.000	.272
CATION PERCENT	1.601	.000	2.188	.000	.000	.000	.000	.346

MAFIC INDEX = 48.282
NORM TOTAL = 100.006

OLIVINE COMPOSITION
FORSTERITE .000 FAYALITE .000

ORTHOPYROXENE COMPOSITION
ENSTATITE 38.712 FERROSILITE 61.288

CLINOPYROXENE COMPOSITION
WOLLASTONITE 49.686 ENSTATITE 19.478 FERROSILITE 30.836

FELDSPAR COMPOSITION
ORTHOCLASE 12.413 ALBITE 40.734 ANORTHITE 46.853
PLAGIOCLASE COMPOSITION (PERC AN) 53.493

THORNTON AND TUTTLE DIFFERENTIATION INDEX	= 27.885
SOLIDIFICATION INDEX (100*MGO/(MGO+FEO+FE2O3+NA2O+K2O))	= 22.715
CRYSTALLIZATION INDEX (AN+MG DI+FO+FO EQIV OF EN)	= 37.831
LARSEN INDEX (1/3SI+K)-(CA+MG)	= .275
ALBITE RATIO (100*(AB+AB EQIV IN NE)/PLAG)	= 46.507
IRON RATIO ((FE2=MN)*100/(FE2+MN+MG))	= 76.492
MG NUMBER AS CATIONS MG/CATIONS (FE+MG)	= 41.828
OXIDATION RATIO ACCORDING TO LE MAITRE (FEO/FEO+FE2O3)	= .830
DENSITY OF DRY LIQUID OF THIS COMPOSITION (AT 1050 DEG)	= 2.732

AFM RATIO
TOTAL ALKALIS 14.83 TOTAL FE 62.31 MG 22.86

KOMATIITE PARAMETERS

FEO/(FEO+MGO)	CAO/AL2O3	SIO2/TIO2	AL2O3/TIO2	FEO*/TIO2	CAO/TIO2	NA2O/TIO2	K2O/TIO2
.7316	.64	33.54	9.09	9.65	5.77	1.599	.697

JENSEN CATION AL2O3 - FEO+FE2O3+TIO2 - MGO
43.17 35.56 21.26

QUARTZ - FELDSPAR RATIOS
QUARTZ 1.63 ORTHOCLASE 12.21 PLAGIOCLASE 86.16
QUARTZ 3.02 ORTHOCLASE 22.65 ALBITE 74.33

CATION PROPORTIONS						
	CA	32.26	FE	40.20	MG	27.54
	CA	13.74	MG	11.72	SI	74.54
	SI	75.94	AL	12.12	MG	11.94
	2MG	32.30	2FE	47.16	SI/5	20.54
	CA	45.69	AL	39.57	NA+K	14.74

COORDINATES IN THE SYSTEM PLAGIOCLASE - OLIVINE - CLINOPYROXENE - QUARTZ (IN MOLE PERCENT)

PROPORTION OF ANALYSIS IN BASALT TETRAHEDRON IS 89.40 MOLE PERCENT

BASALT TETRAHEDRON	OL	21.86	CPX	17.40	PLAG	52.55	QTZ	8.18
CLINOPYROXENE PROJECTION		26.47		0.0		63.62		9.91
QUARTZ PROJECTION		23.81		18.95		57.23		0.0
PLAGIOCLASE PROJECTION		46.08		36.68		0.0		17.25
OLIVINE PROJECTION		0.0		16.95		51.18	OPX+(4QTZ)	31.88

CMAS PROJECTIONS

TETRAHEDRON COORDINATES	C	16.69	M	19.98	A	14.10	S	49.22
DIOPSIDE PROJECTION	C3A	32.61	M	15.73	S	51.66		
OLIVINE PROJECTION	CS	24.54	M	57.27	S	18.19		
ENSTATITE PROJECTION	M2S	31.67	C2S3	32.39	A2S3	35.95		
QUARTZ PROJECTION	CAS2	62.97	MS	28.03	CMS2	9.00		

MAP 2

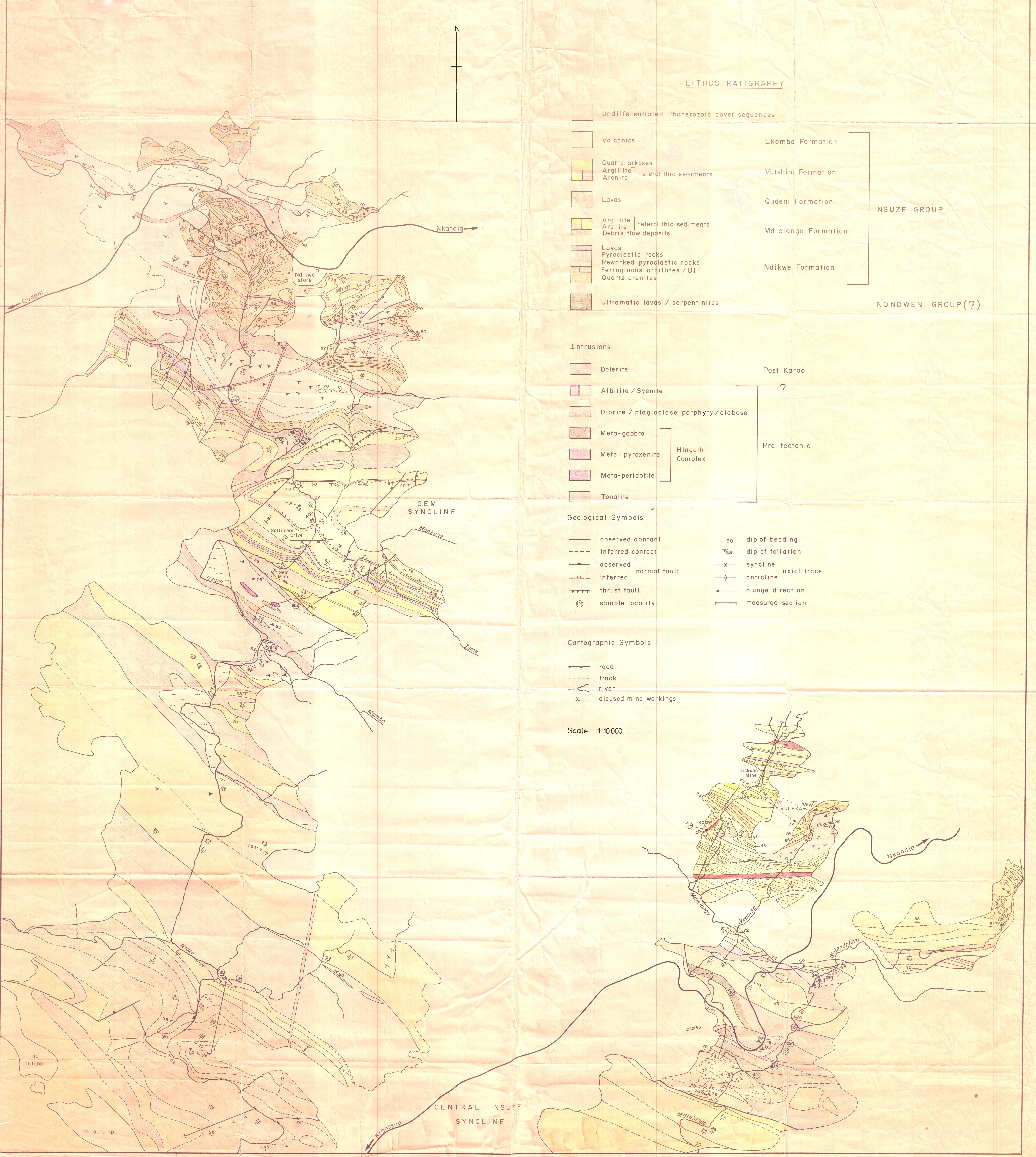
N
LITHOSTRATIGRAPHY
Undifferentiated Phanerozoic cover sequences
Volcanics
Ekombe Formation
Quartz arkoses
Argillite
Arenite
heterolithic sediments
Vutshini Formation
Lavas
Qudeni Formation
NSUZE GROUP
Argillite
Arenite
heterolithic sediments
Debris flow deposits
Mdlelanga Formation
Lavas
Pyroclastic rocks
Reworked pyroclastic rocks
Ferruginous argillites / BIF
Quartz arenites
Ndikwe Formation
Ultramafic lavas / serpentinites
NONDWENI GROUP(?)
Intrusions
Dolerite
Post Karoo
Albitite / Syenite
?
Diorite / plagioclase porphyry / diabase
Meta-gabbro
Meta - pyroxenite
Meta-peridotite
Hlagothi Complex
Pre-tectonic
Tonalite
Geological Symbols
observed contact
inferred contact
observed
inferred
normal fault
thrust fault
sample locality
dip of bedding
dip of foliation
syncline
anticline
axial trace
plunge direction
measured section
Cartographic Symbols
road
track
river
disused mine workings
Scale 1:10 000
Nsuze
Nkandla
Qudeni
Ndikwe store
Mhlazi
Ndikwe
GEM SYNCLINE
Galtimore Drive
Gem Mine
Mankane
Tume
Mamba
no outcrop
no outcrop
CENTRAL NSUZE SYNCLINE
Kranskop
Dickson Mine
VULEKA
Nkandla
Mdlelanga
Nkantsa
Mdlelanga